ANCHORAGE OF CONVENTIONAL AND HIGH-STRENGTH HEADED REINFORCING BARS

By

Yun Shao, David Darwin, Matthew O'Reilly,
Remy Lequesne, Krishna Ghimire, Muna Hano

Structural Engineering and Engineering Materials
SM Report No. 117
August 2016

THE UNIVERSITY OF KANSAS CENTER FOR RESEARCH, INC.
2385 Irving Hill Road, Lawrence, Kansas 66045-7563

ANCHORAGE OF CONVENTIONAL AND HIGH-STRENGTH HEADED REINFORCING BARS

By

Yun Shao

David Darwin

Matt O'Reilly

Remy D. Lequesne

Krishna Ghimire

Muna Hano

Structural Engineering and Engineering Materials
SM Report No. 117
THE UNIVERSITY OF KANSAS CENTER FOR RESEARCH, INC.
LAWRENCE, KANSAS
August 2016

ABSTRACT

Headed bars are often used to anchor reinforcing steel as a means of reducing congestion where member geometry precludes adequate anchorage with a straight bar. Currently, limited data on the behavior of headed bars are available, with no data on high-strength steel or high-strength concrete. Due to a lack of information, current design provisions for development length of headed reinforcing bars in ACI 318-14 limit the yield strength of headed reinforcing steel to 60,000 psi and the concrete compressive strength for calculating development length to 6,000 psi. Current design provisions for developing headed bars in ACI 349-13, which are based on ACI 318-08, apply the same limits on the material strengths (60,000 psi and 6,000 psi, respectively, for headed bars and concrete). These limits restrict the use of headed bars and prevent the full benefits of higher-strength reinforcing steel and concrete from being realized.

The purpose of this study was to establish the primary factors that affect the development length of headed bars and to develop new design guidelines for development length that allow higher strength steel and concrete to be utilized. A total of 233 specimens were tested, with four specimen types used to evaluate heads across a variety of applications. Two hundred two beam-column joint specimens, 10 beam specimens with headed bars anchored near the support in regions that are known as compression-compression-tension (CCT nodes, 15 shallow embedment specimens (each containing one to three headed bars for a total of 32 tests), and 6 splice specimens were evaluated. No. 5, No. 6, No. 8, and No. 11 bars were evaluated to cover the range of headed bar sizes commonly used in practice. Concrete compressive strengths ranged from 3,960 to 16,030 psi. A range of headed bar sizes, with net bearing areas between 3.8 and 14.9 times the area of the bar, were also investigated. Some of these heads had obstructions larger than allowed under current Code requirements. In addition, the amount of confining reinforcement, number of heads in a specimen, spacing between heads, and embedment length were evaluated in this study.

The results of this study show that provisions in ACI 318-14 and ACI 349-13 do not accurately account for the effect of bar size, compressive strength, or the spacing of headed bars in a joint. The effect of concrete compressive strength on the development length of headed bars is accurately represented by concrete strength raised to the 0.25 power, not the 0.5 power currently used in the ACI provisions. Confining reinforcement increases the anchorage strength of headed

i

bars in proportion to the amount of confining reinforcement per headed bar being developed. Headed bars with obstructions not meeting the Class HA head requirements of ASTM A970 (heads permitted by ACI 318-14 and ACI 349-13) perform similarly to HA heads, provided the unobstructed bearing area of the head is at least 4.5 times the area of the bar. Headed bars exhibit a reduction in capacity for values of center-to-center spacing less than eight bar diameters. These results are used to develop descriptive equations for anchorage strength that cover a broad range of material strengths and member properties. The equations are used to formulate design provisions for development length that safely allow for the use of headed reinforcing bars for steels with yield strengths up to 120,000 psi and concretes with compressive strengths up to 16,000 psi. Adoption of the proposed provisions will significantly improve the constructability and economy of nuclear power plants and other building structures.

ACKNOWLEDGEMENTS

iv

TABLE OF CONTENTS

viii

LIST OF FIGURES

xv

LIST OF TABLES

xxiii

CHAPTER 1: INTRODUCTION

1.1 GENERAL

Hooked and headed reinforcing bars are commonly used in reinforced concrete structures where member dimensions do not allow a straight length of reinforcement to fully develop its yield strength (a length referred to as the *development length*.) Both hooked and headed bars have shorter development lengths than straight reinforcing bars under current provisions in ACI 318; however, the ACI Code imposes much stricter limitations on the application of headed bars than on hooked bars. For headed bars, the yield strength is limited to 60,000 psi and the concrete compressive strength is limited to 6,000 psi when calculating the required development length, compared, respectively, to 80,000 and 10,000 psi for hooked bars. Headed bars are also required to have a clear spacing no less than four times the diameter of the bar ($4d_b$) and must conform to the Class HA head sizing requirements of ASTM A970 (requirements for HA heads are described in Section 1.2, and are also shown in the acronym list in Appendix A.) These limitations are the result of a lack of test data dealing with these parameters when the 2008 ACI 318 Code provisions for headed bars were developed, and are currently still in place. The current code provisions for use of headed bars in nuclear industry (ACI 349-13), which were developed on the basis of ACI 318-08, are also subjected to the limitations described above. Thus, it would be highly advantageous to develop an expanded experimental database that will not only improve the level of understanding of headed bar behavior, but also allow the development of improved Code provisions, removing many of the current restrictions on headed bars. This study serves as a good reference for engineers and researchers who work on development of headed bars in building structures or nuclear safety-related concrete structures.

In this chapter, a detailed discussion of the state-of-the-art for headed bars, including the historical background, relevant research work and code provisions, will be provided. Some of the relevant research work is used to compare with the test results in this study in Chapters 8 and 9. The chapter concludes with a summary of the objectives and scope of this study.

1.2 HEADED REINFORCING BARS

Headed reinforcing bars (headed bars) are a type of deformed bar with a round, elliptical, or rectangular shape attached to one or both ends. They achieve anchorage by a combination of bond along the bar length and direct bearing of the head on concrete (Figure 1.1).
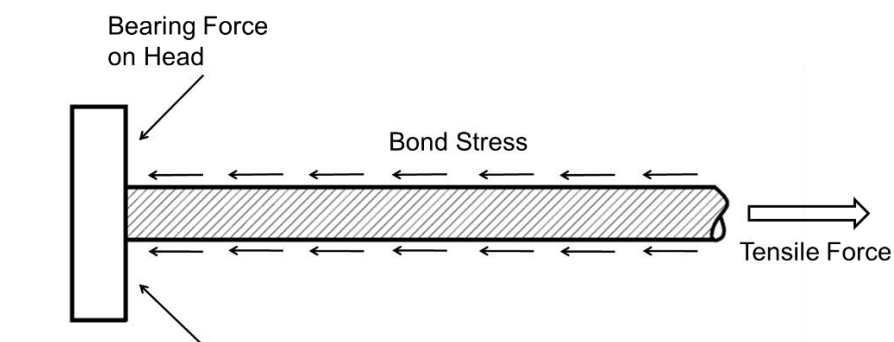
Figure 1.1 Force transfer on a headed bar

Headed bars do not have a bend or tail extension length as with hooks, so they ease construction and result in less steel congestion than hooked bars, especially in heavily reinforced regions such as beam-column joints. Heads may vary in size, shape and manufacturing process, but only those conforming to the Class HA requirements in ASTM A970 are allowed for use in reinforced concrete structures by ACI 318-14. A Class HA head must develop at least the minimum specified tensile strength of the reinforcing bar. According to Annex A1 of ASTM A970/M970-16, the net bearing area of head (A_{brg}) must be equal to or greater than four times the nominal cross-sectional area of the bar ($4A_b$). The net bearing area of head (A_{brg}) is the gross area of head minus the nominal area of the bar (A_b).

In addition to head size, the obstructions or interruptions generated from the manufacturing process also have to follow certain dimensional requirements in order for the headed bars to be "qualified". As shown in Figure 1.2, the obstructions or interruptions must be within a distance equal to twice the nominal bar diameter from the bearing face with a transverse dimension that may not exceed 1.5 times the nominal bar diameter. Qualified obstructions are not considered to detract from the net bearing area of the head. Headed bars not meeting Class HA head requirements may be used in concrete structures only if tests showing the adequacy of these devices are approved by the building official.
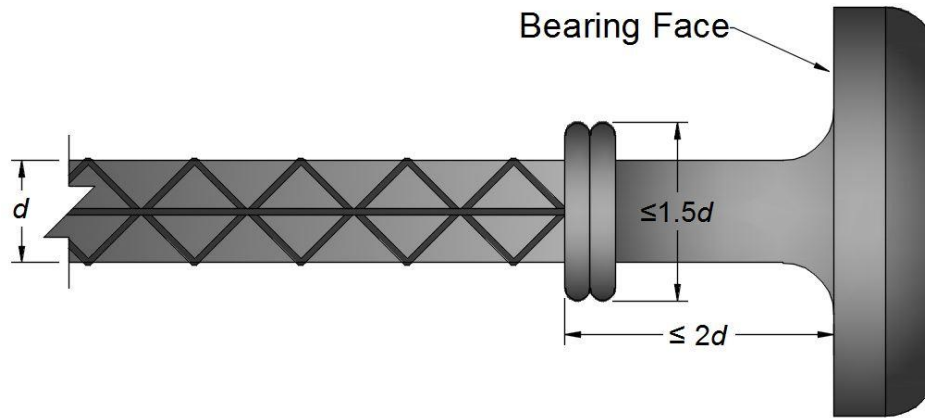
Figure 1.2 Dimensional requirements of obstructions or interruptions for headed bars (figure after ASTM A970/M970-16)

1.2.1 Previous Research on Headed Reinforcing Bar Anchorage

Although headed bars had been increasingly used in offshore platforms and bridges, only a few, if any, headed bars had been used in building structures by the late 20th century in the United States. This was mostly due to a lack of experimental data necessary to develop detailed design criteria. Therefore, researchers began to perform tests needed to develop code provisions for headed bar anchorage.

Wright and McCabe (1997) tested 70 beam-end specimens with friction-welded headed bars, as well as 180° hooked bars and straight bars, in accordance with ASTM A944-95. Some parameters remained constant throughout the program: test bar (No. 8 Grade 75 bars), head type (3 in. by 3 in. square head, concrete strength (4,500 to 5,000 psi), and embedment length (12 in.). Embedment length was measured from the bar end for straight bars, the centerline of the head for headed bars, and the centerline of the back portion of the hook for hooked bars, as shown in Figure 1.3.
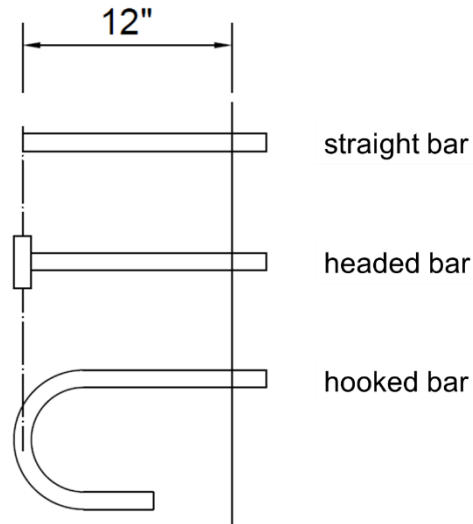
Figure 1.3 Embedment length definitions for different bars

The three primary variables investigated were:

Concrete Cover to the Bar: $2d_b$ or $3d_b$ (d_b = bar diameter);

Reinforcing Bar Exposure: A PVC tube was placed over the deformed bar in some specimens to eliminate the bond of the concrete to the test bar; and

Transverse Reinforcement: Specimens contained no confining transverse reinforcement or one of the four stirrup patterns shown in Figure 1.4.
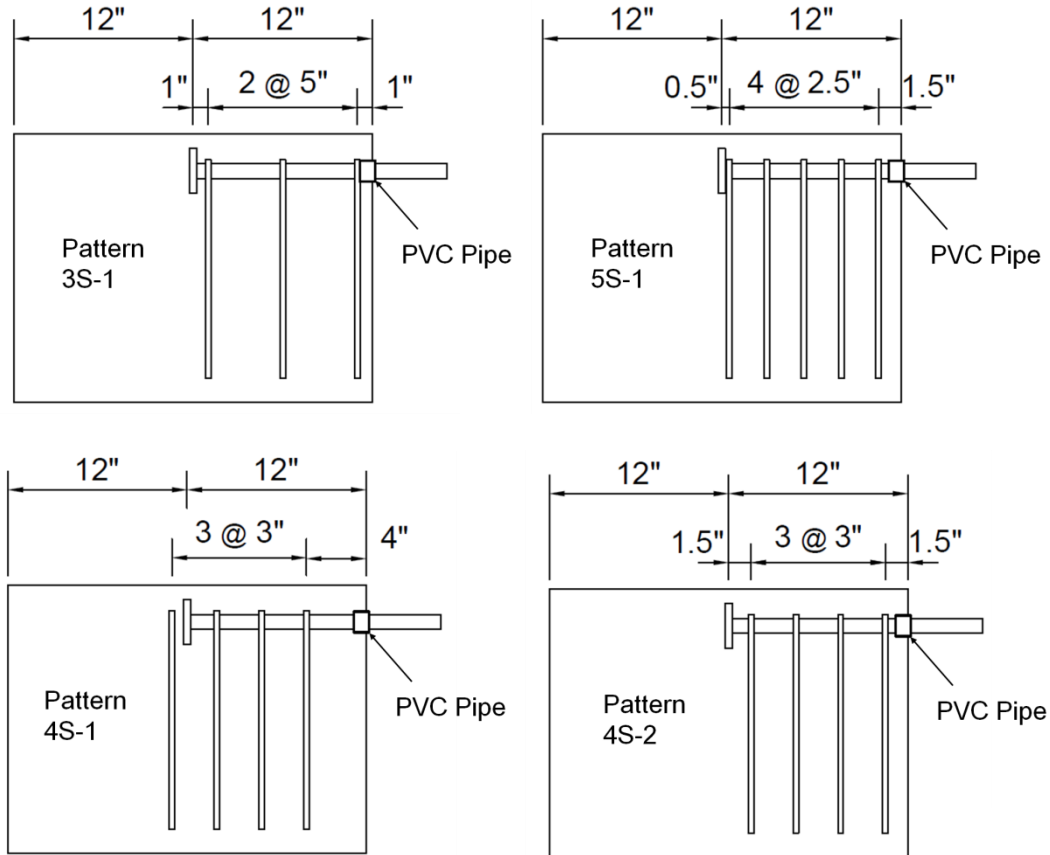
Figure 1.4 Stirrup configurations for beam-end specimens [figure after Wright and McCabe (1997)]

The test results showed that headed bars behaved similarly, and in many cases better than hooked bars, in terms of ultimate load, ductility, loaded-end slip, and the degree of cracking. The use of transverse reinforcement increased the ultimate loads for specimens both with and without PVC sheathing on the bars; additional concrete cover also increased the anchorage capacity, but the effect of cover decreased as the quantity of transverse reinforcement increased. It was found that confinement, either in the form of stirrups or additional cover, allowed the head to develop the bar "with no assistance from the deformations on the bar". In addition, specimens with PVC sheathing exhibited much less cracking and failed more abruptly than those without PVC sheathing because the PVC sheathing eliminated the splitting forces in the concrete created by the deformations on the bar.

An extensive study on the anchorage capacity of headed bars was published in 1996 by two Ph.D. students at the University of Texas at Austin and documented in their dissertations

5

(DeVries 1996, Bashandy 1996). DeVries (1996) conducted over 140 pullout tests, which were divided into shallow and deep embedment tests. The definitions of "shallow" and "deep" were based on the ratio of embedment depth to bar clear cover, with a ratio greater than 5 representing deep embedment. The variables examined in this research included embedment depth, development length, concrete clear cover, spacing of adjacent bars, head orientation and geometry, concrete strength (nominal concrete compressive strength ranging from 3,000 psi to 10,000 psi), transverse reinforcement, and bar size (No. 6, No. 8, and No. 11). Embedment depth was defined as the distance from the loaded surface (known as critical section) to the bearing face of the head; development length was the length along a deformed bar bonded to the concrete, excluding the unbonded portion provided by sheathing the bars with PVC tubes. Figure 1.5 illustrates the difference between embedment depth (h_d) and development length (l_d). Concrete clear cover was defined as the distance from the surface of the bar (not the head) to the closest face of concrete. To describe the geometry of the head, the term "head aspect ratio" was introduced, which was defined as the ratio of the largest head plan dimension to the smallest head plan dimension. For example, the aspect ratio for a square head is 1:1; a higher ratio represents a longer and narrower rectangular head. A rectangular head may have two orientations, with the long side placed in the horizontal or the vertical plane.
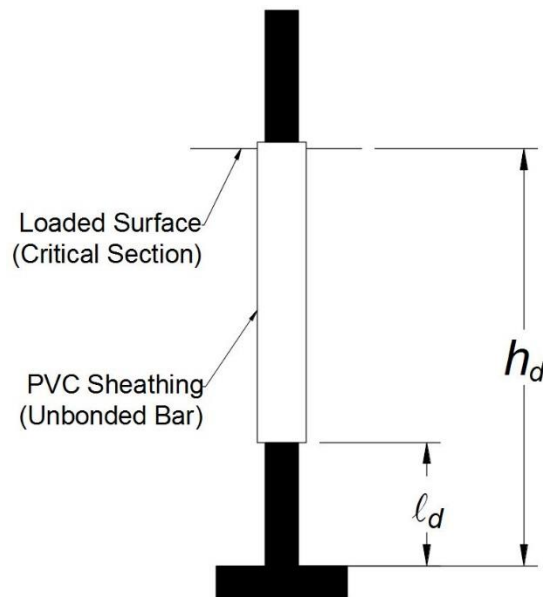
Figure 1.5 Difference between embedment depth and development length [figure after DeVries (1996)]

6

The test results revealed that the majority of the specimens failed in either pullout or side-blowout (Figure 1.6). Pullout failure was characterized by a cone-shaped section of concrete around the bar being pulled out of the surrounding concrete, and it was more likely to occur in shallow embedment specimens. Side-blowout failure was characterized by spalling of a portion of concrete cover off the head, and was associated with deep embedment specimens.

(a)   (b)
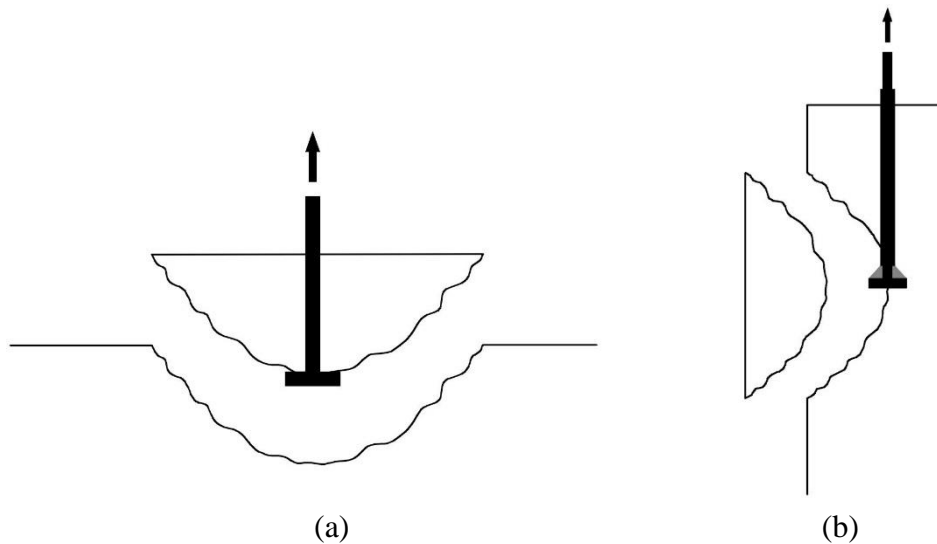
Figure 1.6 Pullout and side-blowout failure modes (a) pullout failure, (b) side-blowout failure [figure after DeVries (1996)]

The 21 shallow-embedment tests were performed on three concrete blocks. Three bar fractures were observed, and the remaining 18 tests resulted in pullout failures. The results of these tests indicated that head size and the amount of transverse reinforcement placed perpendicular to the headed bar had no effect on the anchorage behavior. Increasing embedment length and concrete strength increased the anchorage capacity. Concrete cover contributed to the anchorage capacity – bars placed away from all edges exhibited greater capacity than those near one edge, and bars placed at corners had the lowest capacity.

DeVries also conducted more than 120 deep-embedment tests on 18 concrete blocks, each with 4 to 12 headed bars cast around the perimeter. Most tests (108 tests on single bars and 6 tests on closely spaced paired bars) exhibited a side-blowout failure, but 15 tests exhibited an unexpected failure of the top bearing surface, which was characterized by the spalling of top edge of concrete under the applied load. From these tests, it was found that for a given embedment

length, development length provided a small increase in the anchorage capacity, and the increase could be predicted by the existing equations for straight anchorage in ACI 318-95. It was also found that transverse reinforcement did not increase the anchorage capacity, although large amounts of transverse reinforcement placed near the head improved the residual post-failure capacity; the orientation and shape of the head had no significant influence on the anchorage capacity, whereas increasing head area tended to provide a proportional increase in anchorage capacity; and corner placement and close spacing of bars caused a reduction of side-blowout capacity. DeVries found that many existing models of bearing or side-blowout capacity represented the test results fairly well. Based on a regression analysis and a physical model of the observed behavior, DeVries proposed a design procedure for side-blowout capacity, which covered the primary variables – close spacing and corner placement of headed bars. He also recommended that the head be thick enough to prevent yielding of the head at ultimate load.

Bashandy (1996) followed DeVries and performed an additional 25 pullout tests on No. 11 bars. Fourteen of the tests focused on the effects of cyclic loading as well as the anchorage of the head behind a crossing bar. The crossing bar, either No. 8 or No. 11 in size, was placed against the head bearing face perpendicular to the headed bar, simulating a longitudinal bar in front of a head. Bashandy observed that side-blowout capacity was not greatly affected by cyclic loading up to 15 cycles and that the addition of crossing bars greatly improved anchorage capacity. The remaining 11 tests investigated the use of interlocking headed bars as transverse reinforcement, which Bashandy found to be a promising alternative for traditional transverse reinforcement.

Bashandy also performed 32 tests on large scale specimens simulating exterior beam-column joints to evaluate the effects of bar size (No. 8 and No. 11), head size (ranging from $3A_b$ to $8.1A_b$), head orientation (the long side of a rectangular head in horizontal or vertical plane), embedment length (ranging from 9 in. to 18 in., including head thickness), concrete cover to the bar (1.5 in. and 3 in.), and confining transverse reinforcement within the joint region (no ties, No. 3 ties spaced at 2 in. or 4 in.). The specimens were 12 in. wide, with varying depths depending on the embedment length, and contained two headed bars with different spacings depending on the concrete cover. Three specimens had a 1.5-in. concrete cover on the bars; they contained two headed bars with a 9-in. outside-to-outside spacing, and were placed outside the column core that

was confined by the column longitudinal reinforcement. The balance of the specimens had a 3-in. concrete cover on the bars; they contained two headed bars with a 6-in. outside-to-outside spacing, and were placed inside the column core. Strain gauges were placed 1 in. from the head on the bar to determine the anchorage force provided by the head. The specimens had a similar design to those tested by Marques and Jirsa (1975), Pinc, Watkins, and Jirsa (1977), Hamad, Jirsa, and D'Abreu de Paulo (1993) on hooked bars, and by Burguieres (1974) on mechanical anchorages in beam-column joints. As shown in Figure 1.7, the headed bars embedded in the column simulated the top longitudinal reinforcement of a "beam", and the 51 mm (2 in.) thick plate below the headed bars simulated the compression zone of the virtual beam. No axial load was applied to these specimens.
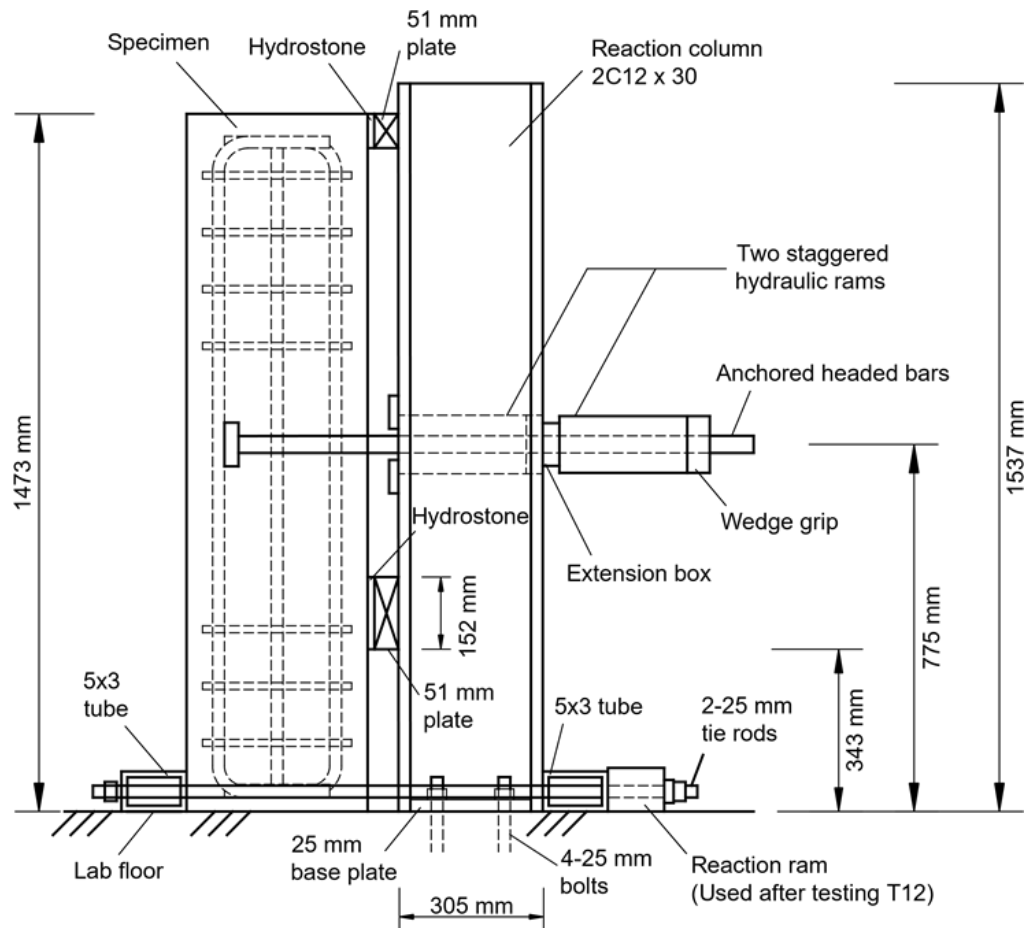
Figure 1.7 Test configuration for an exterior beam-column joint specimen [figure after Bashandy (1996)]

Bashandy reported two major failure types based on the test results, side blowout and shear related failure. Crack propagation for both failure types seemed to follow the same pattern. Initially, cracks appeared on the two sides of the column along the embedded bar. As load increased, some diagonal cracks initiating from the head extended towards the assumed compression beam zone within the joint region as well as toward the top of the column above the joint region. The specimens were severely cracked on both sides as the load increased to failure.

The test results showed that the anchorage capacity of headed bars in beam-column joints increased with increases in embedment length, head area, concrete cover, and confining transverse reinforcement within the joint region, whereas the effects of head aspect ratio, head orientation, and bar diameter were not as significant. Increasing embedment length increased the anchorage capacity, primarily through bond along the length of the bar with no increase in the contribution of the head due to bearing for embedment lengths greater than 12 in. It was also found that the anchorage capacity of headed bars in beam-column joint tests was significantly lower than that predicted by the design equations derived from DeVries' pullout tests.

Despite the efforts made and anchorage provisions proposed by Wright and McCabe (1997), DeVries (1996) and Bashandy (1996), neither the ACI 318-02 nor ACI 318-05 included design provisions for headed bar anchorage. It remained for the study by Thompson et al. (Thompson, Ziehl, Jirsa, and Breen 2005, Thompson, Jirsa, and Breen 2006a, Thompson, Ledesma, Jirsa, and Breen 2006b) to complete the foundation for the design provisions for headed bar anchorage, first incorporated in the 2008 edition of the ACI 318 Building Code. The details of that study are documented in Thompson's dissertation (Thompson 2002).

To capture the general anchorage behavior of headed reinforcement, Thompson et al. (2005, 2006a, 2006b) developed two test programs, compression-compression-tension (CCT) node tests and lap splice tests, as representatives for a variety of applications of headed bars used in practice. The CCT node tests provided experimental information on anchorage of a single headed bar at a CCT node in a deep beam; the lap splice tests explored how stress was transferred through multiple lapped headed bars anchored within a single layer. Specimens for the two types of tests were made as general as possible so that the test results could be extrapolated to other members where these two details are used.

10

The CCT node test involved a total of 64 specimens, with basic variables including bar size (No. 8 and No. 11), strut angle (30°, 45°, and 55°), head size (net head area ranging from 1.2 to 10.4A_b), and head orientation (horizontal and vertical). A few specimens were confined with No. 3 stirrups within the nodal zone to evaluate the effect of confining transverse reinforcement on the anchorage behavior. The typical unconfined and confined specimens are shown in figure 1.8. Companion specimens were also made with non-headed (straight and hooked) bars for comparison.

(a)

(b)
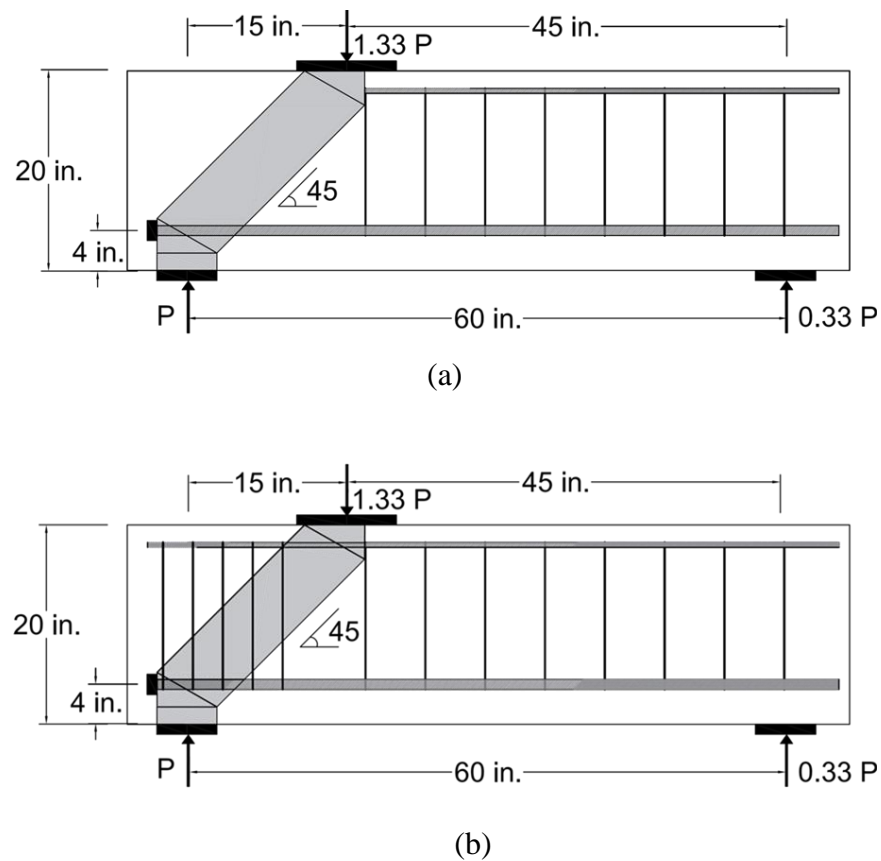
Figure 1.8 Typical CCT node specimens (a) unconfined specimen, (b) confined specimen [figure after Thompson (2002)]

Three failure modes were observed during the tests. All specimens anchored with straight bars exhibited pullout failure. All hooked-bar specimens and most headed-bar specimens experienced rupture failure in the strut and node region. A few headed bar specimens failed by yielding of the bars. The rupture failure was characterized by splitting of the diagonal compression strut along a transverse plane for smaller heads and vertically oriented rectangular heads; for larger

heads and rectangular heads with horizontal orientations, extensive crushing of the concrete near the bottom face of the strut was observed. Figure 1.9 shows the two rupture failure modes.

i. Strut Rupture with Splitting (vertical head orientation)

ii. Strut Rupture with Crushing (horizontal head orientation)

Crushed Concrete
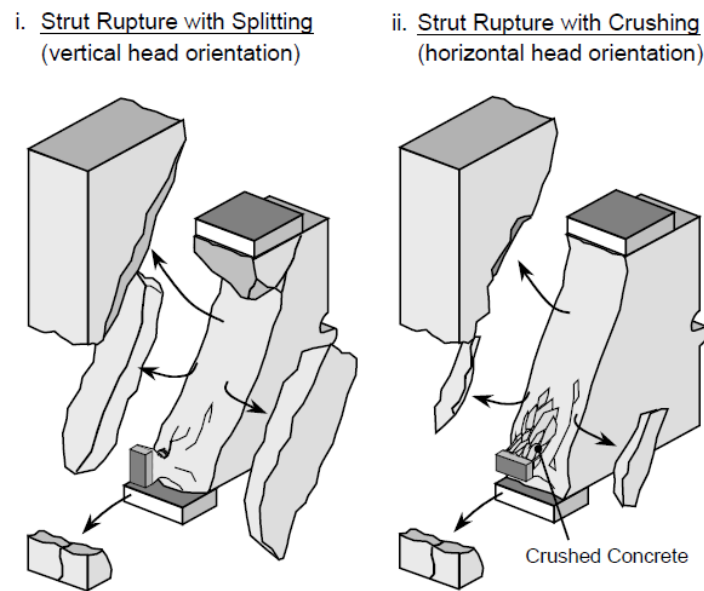
Figure 1.9 Rupture failure in the strut and node region [figure from Thompson (2002), reprinted with permission]

With strain gauges placed along the headed bar (tie bar) to trace the stress profile under different loading levels, it was found that bond force along the bar initially carried almost all of the anchorage force until achieving its peak (known as the first stage), and then decreased as the bar began to slip and the force was transferred to the bearing of the head (known as the second stage). The maximum anchorage capacity of the headed bar occurred when the bearing capacity of the head was at a maximum, after the bond between the bar and concrete decreased. The point where the maximum bar stress occurred was called the critical anchorage point, which occurred at the intersection of the tie bar and the boundary of the diagonal compression strut, or the edge of the "extended nodal zone" as defined by ACI 318-02 Appendix A. A decrease in strut angle increased the bonded length of the tie bar, and thus the contribution from bond to the total anchorage capacity was increased. The presence of confining stirrups did not significantly increase the head bearing capacity, but seemed to help sustain bond force during the second stage when the bar stress was transferred to the head. The use of a large head size decreased the bond force at failure and slip of the head.

For the 27 lap splice tests, Thompson et al. (2006b) investigated the effect of splice length (ranging from $3d_b$ to $14d_b$), head size (net head area ranging from 1.1 to $4.7A_b$) and shape (circular and rectangular), bar spacing ($10d_b$ and $6d_b$ center-to-center), lap configuration (contact and non-contact lapping; contact lapping means that the head of one bar touched the barrel of the adjacent bar), bonded bars versus debonded bars (debonded bars had a debonding sheath placed over bar deformations in lap zone; only one specimen had debonded bars), and confinement details (hairpin confinement and transverse tie-down, as shown in Figure 1.10). Some non-headed bars were also tested.
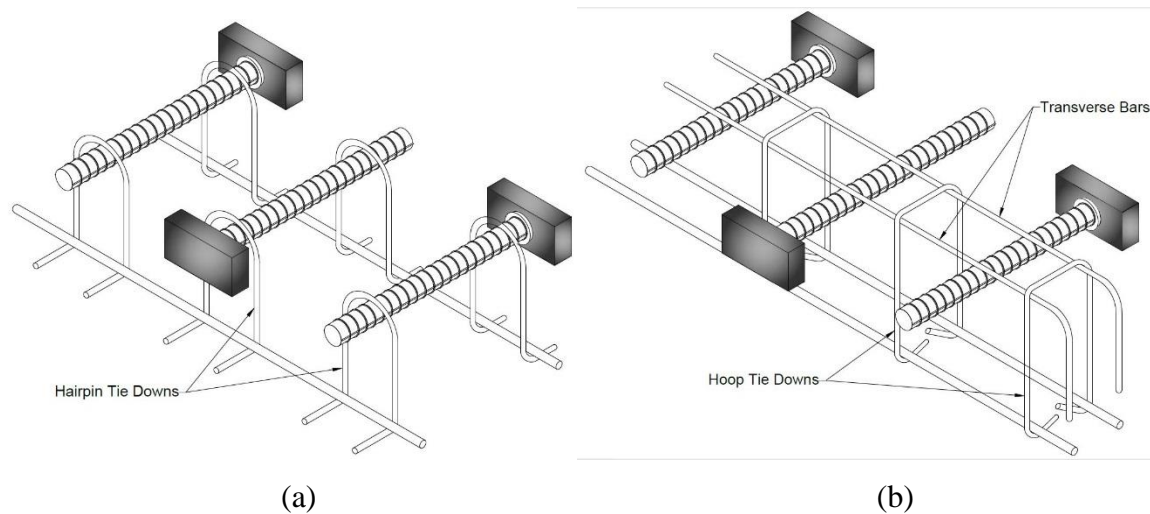
Figure 1.10 Two types of confinement details (a) hairpin confinement, (b) transverse tie-down detail [figure after Thompson (2002)]

Thompson et al. (2006b) found that the anchorage behavior of headed bars in lap splices, in general, was much the same as that observed in CCT nodes: anchorage was first carried by bond and then the force in the bar was gradually transferred to the head as the bond component along the bar declined. For non-contact lap splices, the force was transferred through struts extending from the head of one bar to the shaft of the opposing lapped bar acting at an angle of about 55° with respect to the direction of the bars. The intersection of the strut with the opposing bar determined the critical anchorage point (maximum bar force). The resulting anchorage length, which was shorter than the lap length, could be used to best describe the lap splice capacity. Head shape had no significant effect on the mechanism of stress transfer or the splice capacity. The

specimen with debonded bars exhibited fewer but wider surface cracks compared to the companion bonded specimen. Debonding greatly increased the portion of load carried by the head, but the overall capacity of the bar was decreased because of less contribution from bond along the bar length. Transverse bars over the top of the lap (Figure 1.10b) improved the struts between opposing bars, whereas tie-down confinement perpendicular to the splice plane (Figure 1.10a, b) did not greatly improve the lap splice behavior; it only provided residual capacity after the peak capacity was reached. Two specimens tested with short contact lap splice lengths showed slightly greater capacity than their non-contact splice companions, and more tests on contact splice with longer lap length were suggested to fully understand the performance of contact lap splice.

Based on the results from CCT node and lap splice tests on headed bars, Thompson concluded that headed reinforcement could provide anchorage superior to that provided by straight bars. Following the concept that the total anchorage capacity was a combination of peak head bearing and reduced bond, he proposed recommendations for headed bar design provisions to be included in the mechanical anchorage sections of both the ACI Code and the AASHTO Bridge Specifications.

1.2.2 Research on Beam-Column Joints Anchored with Headed Bars

In addition to the beam-column joint tests performed by Bashandy (1996) discussed in Section 1.4.2, Wallace, McConnell, Gupta, and Cote (1998) conducted tests on large-scale beam-column joint specimens. Two exterior beam-column joint specimens were anchored with taper-threaded headed bars – one was subjected to cyclic loading, and the other was subjected to monotonic loads. Three roof type corner joint specimens anchored with friction-welded headed bars and two specimens anchored with 90° hooks were subjected to cyclic loads. Examples of exterior and roof type corner joints are shown in Figure 1.11. Based on the test results, they found that the behavior of headed-bar specimens was equivalent to similarly constructed specimens with hooks. They also found that for corner joints, additional vertical transverse reinforcement is needed to provide adequate restraint to the heads.
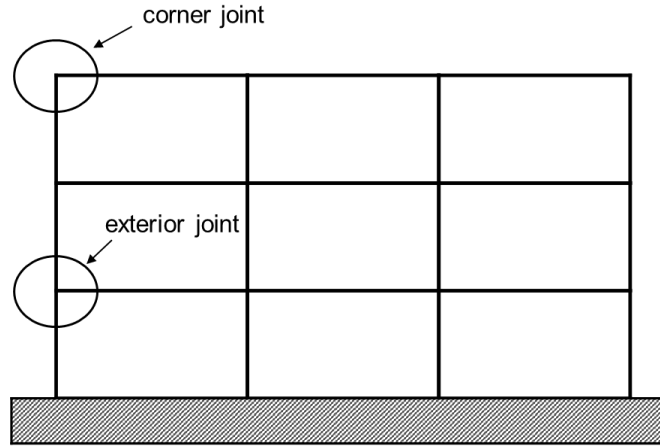
Figure 1.11 Exterior and corner joints [figure after Wallace et al. (1998)]

Hong, Chun, Lee, and Oh (2007) developed a strut-and-tie model to explain the stress transfer of a headed bar to an exterior beam-column joint. The model included a strut from the head to the compressive zone of the beam and a fan-shaped compression field along the interface of the headed bar and concrete, representing the bond component along the straight bar. The model took into account the head size, material strength, and structural configuration. To validate the proposed model, Hong et al. presented the test results for 24 full-scale simulated exterior beam-column joint specimens in which headed bars were anchored. The details of these tests are discussed by Chun, Oh, Lee, and Naito (2009). Comparisons between the experimental results and the proposed model showed that the ratios of predicted-to-test values ranged from 0.87 to 1.24, with a coefficient of variation of 10.6%.

Chun et al. (2009) examined 30 exterior beam-column joint specimens – 24 specimens contained headed bars, and the remaining six contained 90° hooked bars. The specimens were similar to those tested by Bashandy (1996). Each specimen contained a single bar and had a width of $6d_b$. The main variables included bar size (No. 8, No. 11, and No. 18) and embedment length (ranging from 6.3 in. to 35 in.). No transverse reinforcement was used within the joint region to investigate the contribution of the concrete alone to the anchorage capacity of the joint. The specimens were tested as shown in Figure 1.12. A compression/tension force couple was applied to the face of the column to simulate the forces generated from beam flexure. No axial load was applied. For each bar size, the column depth was fixed, with embedment length-to-column depth

15

ratios equal to 0.5, 0.7, and 0.9, respectively. Thus, some heads were anchored in the middle of the column.
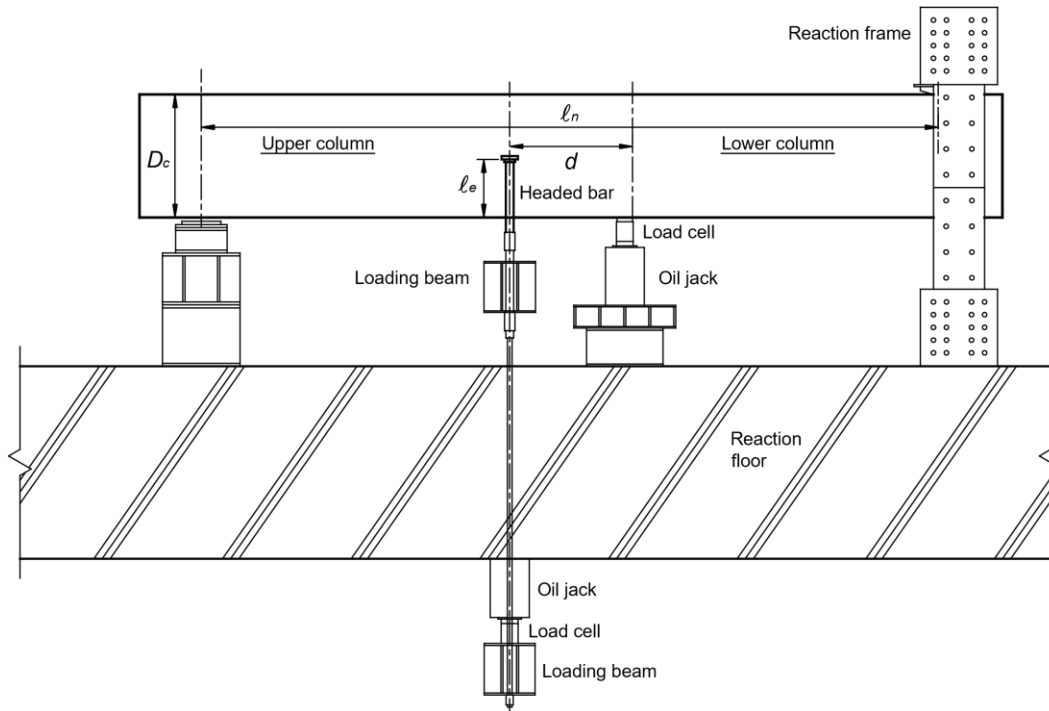
Figure 1.12 Test configuration for beam-column joints [figure after Chun et al. (2009)]

The test results showed that all of the specimens failed in either concrete breakout or joint shear, as shown in Figure 1.13. In a concrete breakout failure, diagonal cracks radiated from both sides of the head and a concrete cone was pulled out with the bar. In a joint shear failure, a diagonal crack formed within the joint and extended across the column.

(b)   (c)
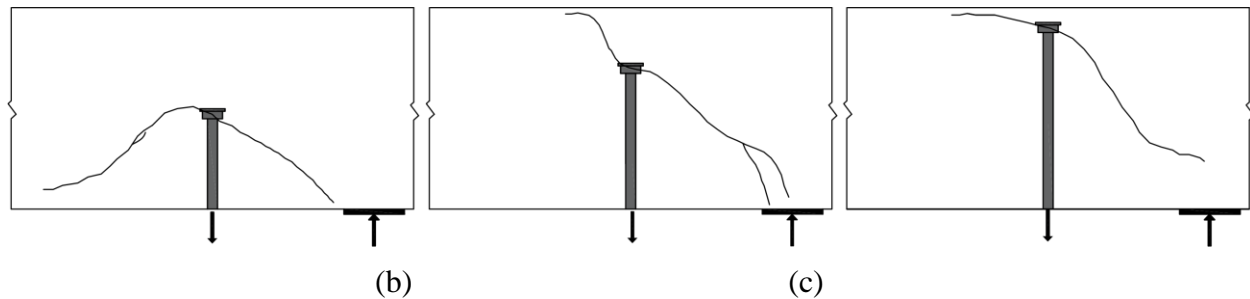
Figure 1.13 Failure Modes: (a) Concrete Breakout; (b) and (c) Joint Shear Failure [figure after Chun et al. (2009)]

Chun et al. (2009) also observed higher anchorage strengths for headed bars when a compressive force was applied at the surface near the head, perpendicular to the tensile force in

the bar (Figure 1.14a). Chun et al. felt that the surface load provided some confinement to the headed bar because of the compression in the surrounding concrete. The anchorage strengths of headed bars in beam-column joints were lower because confinement from a surface load was not present (Figure 1.14).
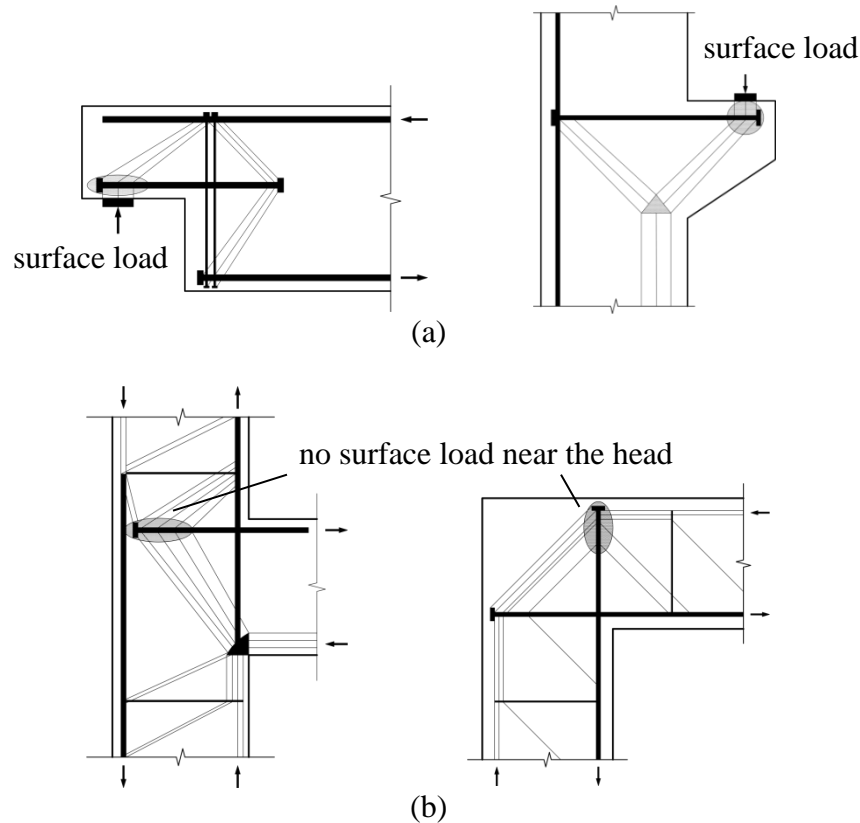
Figure 1.14 Anchorage of headed bars (a) surface load perpendicular to the bar, (b) no surface load [figure after Chun et al. (2009)]

Kang, Shin, Mitra, and Bonacci (2009) reviewed experimental data on the use of headed bars in beam-column joints subjected to cyclic loading. They found that the experimental data were reasonably well predicted by the expression for the development length ℓ_{dt} in ACI 352R-02, and that the expression for ℓ_{dt} in ACI 318-08 was more conservative. In addition, they suggested that for the design of beam-column joints, the net bearing area of a head be at least $3A_b$ (instead of $4A_b$ as currently required by ACI Code), the minimum clear spacing between the bars be reduced to $2d_b$ from $4d_b$, and that the concrete compressive strength f_c' and the yield strength of the bar f_y used to calculate ℓ_{dt} be expanded to 15,000 psi and 78,000 psi, respectively.

Kang, Ha, and Choi (2010) performed 12 anchorage tests of exterior beam-column joints to examine the effects of head type, head-attaching technique (welding versus threading), and loading condition (monotonic versus cyclic). Two specimens with straight bars were also tested for comparison. Each specimen contained a single bar; the embedment length was $10d_b$ for headed bars and $15d_b$ for straight bars. The test results showed that loading condition, head shape, and head-attaching technique did not have a large influence on the anchorage behavior, and that larger heads (net head area = $4.5A_b$) exhibited higher anchorage strengths than smaller heads (net head area = 2.6 to $2.8A_b$). In addition to monotonic loading, they conducted reversed cyclic tests on two full-scale exterior beam-column joints – one with small headed bars (net head area = $2.6A_b$), and the other with 90° hooked bars. The test results indicated that joints using the small headed bars exhibited greater energy dissipation, less strength degradation, and higher lateral drift capacity under cyclic loading than joints using hooked bars.

1.3 CODE PROVISIONS

1.3.1 Requirements in ACI 318 Building Code

The design provisions for development of headed deformed bars first appeared in the ACI 318-08 Building Code, with no significant changes in the current ACI 318-14 provisions. In accordance with Section 25.4.4.2 of ACI 318-14, the development length ℓ_{dt} required for anchoring headed bars in tension is given by

$$\ell_{dt} = \left(\frac{0.016 f_y \psi_e}{\sqrt{f_c'}} \right) d_b \tag{1.1}$$

with ℓ_{dt} not less than $8d_b$ or 6 in. In this equation, the yield strength of the bar, f_y, is limited to 60,000 psi; factor ψ_e is taken as 1.2 for epoxy-coated reinforcement and 1.0 elsewhere; and concrete compressive strength, f_c', has an upper limit of 6000 psi for calculating ℓ_{dt}. Additional limits are applied on bar size (not exceeding No. 11), concrete (normalweight), clear cover for bar and clear spacing between bars (not less than $2d_b$ and $4d_b$, respectively).

The development length of headed bars is measured from the critical section to the bearing face of the head. Figure 1.15 shows a typical exterior beam-column joint containing a headed bar satisfying the requirement for development length. The critical section, in this case, is at a point

where maximum stress is achieved, and usually refers to the face of the column for beam-column joints in non-seismic regions.
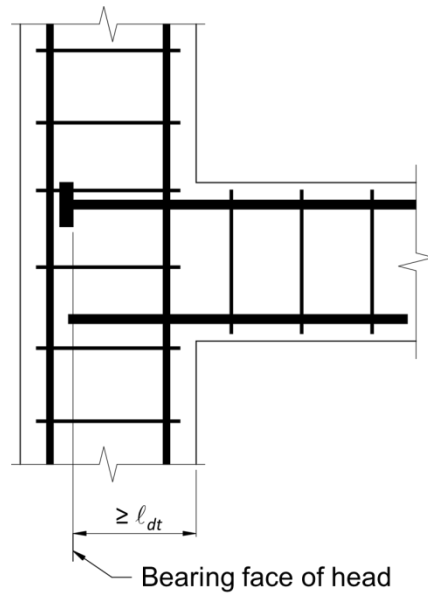
Figure 1.15 Exterior beam-column joint with headed bars satisfying the development length requirement of ACI 318-14 (figure after ACI 318-14)

1.3.2 Recommendations in ACI 352R-02

Before the ACI 318-08 code provisions were implemented, headed bars were often used in beam-column connections in accordance with the recommendations of Joint ACI-ASCE Committee 352 in ACI 352R-02. The ACI 352R-02 recommendations were reapproved in 2010, with only minor changes. ACI 352R-02 classifies connections into two categories: Type 1 in members designed without significant inelastic deformation and Type 2, which must maintain strength under deformation reversals into the inelastic range. The critical section is taken at the face of the column for Type 1 connections and at the outside edge of the confined column core for Type 2 connections based on research by Hawkins, Kobayashi, and Fourney (1975), who found that during seismic loading, concrete cover outside the column bars tends to spall off and is ineffective in developing the bar. According to the recommendations of ACI 352R-02, which are based on the research by DeVries (1996), Bashandy (1996), McConnell and Wallace (1994, 1995), Wallace et al. (1998), and Wright and McCabe (1997), the development length ℓ_{dt} of a headed bar for both Type 1 and Type 2 connections should be taken as $^3/_4$ of the development length required for hooked bars ℓ_{dh} used in Type 2 connections, and should be no less than $8d_b$ or 6 in.

19

The development length of hooked bars anchored in the confined core of a Type 2 connection is determined by

$$\ell_{dh} = \left(\frac{\alpha f_y}{75\sqrt{f_c'}} \right) d_b \tag{1.2}$$

where α is a stress multiplier for longitudinal reinforcement at a joint/member interface. For Type 2 connections, $\alpha \geq 1.25$. A value of $\alpha = 1.25$ should be regarded as the minimum for Type 2 connections using ASTM A706 or equivalent reinforcement; for other reinforcing steels, a value larger than the recommended minimum may be appropriate. If transverse joint reinforcement is provided along the full development length of a hooked bar, with a spacing not greater than $3d_b$, ℓ_{dh} as given in Eq. (1.2) can be multiplied by 0.8. Because the hook in a Type 2 connection should be enclosed within the confined concrete core, Eq. (1.2) incorporates a 0.7 factor that may be applied when side cover normal to the plane of the hook is at least 2.5 in. and cover on the bar extension beyond the hook is at least 2 in.

In accordance with ACI 352R-02, the development length of a headed bar ℓ_{dt} is taken as $^3/_4$ of the development length required for hooked bars, namely,

$$\ell_{dt} = \frac{3}{4} \left(\frac{\alpha f_y}{75\sqrt{f_c'}} \right) d_b \tag{1.3}$$

where α is the stress multiplier, and for Type 1 connections, $\alpha \geq 1.0$. If the headed bar has a side cover normal to the longitudinal axis of the bar less than $3d_b$, each head should be transversely restrained by a stirrup or hoop leg that is anchored in the joint. If the side cover is greater than $3d_b$, minimum transverse reinforcement should be provided through the joint region in accordance with Section 25.7 in ACI 318-14. In contrast to hooks, however, there is no reduction factor for side cover when calculating the development length for headed bars ℓ_{dt}.

In ACI 352R-02, the maximum concrete compressive strength f_c' that may be used for calculating ℓ_{dt} using Eq. (1.3) for headed bars in beam-column joints is 15,000 psi, much higher than the upper limit (6,000 psi) in ACI 318. This is in spite of the fact that no tests had been performed near the upper limit proposed in ACI 352R-02. In addition, ACI 352R-02 recommends that the bar heads be located in the confined core within 2 in. of the back of the core (Figure 1.16)
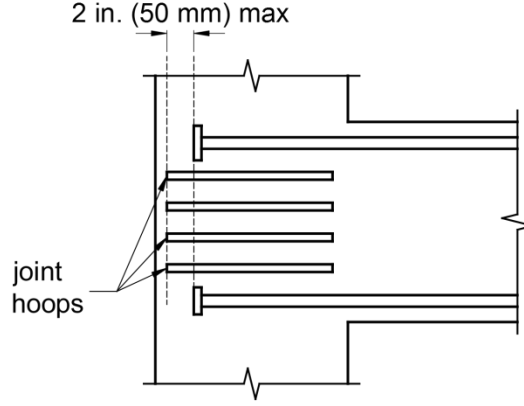
Figure 1.16 Location of headed bars (figure after ACI 352R-02)

1.3.3 Comparison between ACI 352R and ACI 318

The equations for the development length of headed bars in ACI 352R and ACI 318 have a similar form; both are a function of $f_y d_b / \sqrt{f_c'}$. Assuming that the stress multiplier has a minimal value $\alpha = 1.25$ in Eq. (1.3) and the bar is not epoxy-coated (namely, $\psi_e = 1$ in Eq. (1.1)), the development length equations, Eq. (1.3) and Eq. (1.1), respectively, can be simplified to

$$l_{dt} = \left(\frac{0.0125 f_y}{\sqrt{f_c'}} \right) d_b \qquad \text{(ACI 352R-02)} \qquad (1.4)$$

$$l_{dt} = \left(\frac{0.016 f_y}{\sqrt{f_c'}} \right) d_b \qquad \text{(ACI 318-14)} \qquad (1.5)$$

Comparing Eq. (1.4) and (1.5), it is observed that the development length recommended in ACI 352R-02 is 78% of that required in ACI 318-14, which indicates that the equation in ACI 318-14 is more conservative. The ACI 318-14 provisions are also more conservative in other aspects, such as specifying a lower limit on compressive strength (6,000 psi in ACI 318-14 versus 15,000 psi and ACI 352R-02) and specifying a minimum clear spacing of $4d_b$ for non-seismic applications. These limits prescribed on headed bar anchorage are based on the limited parameters used in the tests by Thompson et al. (2005, 2006a, 2006b), which did not include any beam-column joint specimens. In beam-column joints, however, the beam longitudinal bars are often more closely spaced than $4d_b$ (the typical bar clear spacing in practice ranges from $1d_b$ to $3d_b$ (Kang et al. 2009)). Therefore, the $4d_b$ clear spacing requirement tends to hinder the use of headed bars in some beam-column joint applications, even though headed bars provide the potential to alleviate steel congestion in joints when compared to hooked bars.

1.4 OBJECTIVE AND SCOPE

In the current ACI 318 Building Code, the development length provisions for headed reinforcing bars include limits on the compressive strength of concrete, the yield strength of bars, and spacing between the bars. These limits are due to a lack of experimental data when the Code provisions were developed. The objective of this study is to establish design criteria for the development of headed bars to cover a broader range of material and member properties.

For this study, a total of 233 specimens were tested: 202 beam-column joint specimens, 6 splice specimens, 15 shallow embedment specimens (each containing one to three headed bars for a total of 32 tests), and 10 CCT node specimens. The specimens are fully described in Chapter 2, with a summary of each specimen presented below.

The simulated beam-column joint specimens, which constituted the majority of the study, were used to investigate the behavior of headed bars in an external beam-column joint. The main variables were concrete compressive strength, embedment length, head size, bar size, group effects (number and spacing of headed bars), and confining transverse reinforcement within the joint region. Of the 202 simulated beam-column joint specimens, 122 contained two headed bars and 80 contained three or four headed bars. Three bar sizes were investigated – No. 5, No. 8 and No. 11. Concrete compressive strengths ranged from 3,960 to 16,030 psi. Bar stresses at failure ranged from 26,100 to 153,200 psi. Headed bars from several manufacturers were tested, which included heads with net bearing areas ranging from 3.8 to $14.9A_b$ and heads without and with obstructions, some of which did not meet the current code requirements. Specimens contained two, three, or four headed bars with center-to-center spacings ranging from $3d_b$ to $11.8d_b$

The CCT node specimens were used to investigate the behavior of headed bars at a compression-compression-tension (CCT) node, such as would be found at the end of a simply-supported or fixed-end beam. The main variables included the number of headed bars and the embedment length. The specimens contained two or three No. 8 headed bars with embedment lengths of 9 to 14 in. The specimens had concrete strengths ranging from 4,630 to 5,700 psi.

The shallow embedment specimens were used to investigate the behavior of headed bars embedded in concrete slabs with low amounts of confining concrete reinforcement and high concrete cover, such as would be used for column longitudinal steel embedded in a foundation.

The main variables were concrete compressive strength and head bearing area. No. 8 bars were investigated at concrete strengths ranging from 4,200 to 8,620 psi and net head bearing areas ranging from 4 to 14.9A_b, where A_b is the nominal cross-sectional area of the headed bar.

The splice specimens were used to investigate the behavior of headed bars in beam splices. The main variables included concrete compressive strength and splice spacing. Two sets of three specimens with spliced No. 6 headed bars were investigated at concrete strengths ranging from 6,330 to 11,070 psi and center-to-center splice spacings of 1.25, 1.75, and 2.625 in. A splice length of 12 in. was used for all specimens.

The test results are used to develop descriptive equations for headed bar anchorage, and design provisions are proposed. The design provisions are compared with the test results from the current and earlier studies.

CHAPTER 2: EXPERIMENTAL WORK

This chapter describes details of the specimens evaluated in this study: beam-column joint specimens, CCT node specimens, shallow embedment specimens, and splice specimens. Material properties for all specimens are described in Section 2.1. Test parameters, specimen fabrication, and testing procedures are described in Section 2.2 through 2.5 for the beam-column joint specimens, CCT node specimens, shallow embedment specimens, and splice specimens, respectively.

2.1 MATERIAL PROPERTIES

2.1.1 Headed bars

The headed bars evaluated in this study represent a variety of manufacturing processes: friction-forged, taper-threaded, and cold-swaged. Most of the headed bars conformed to Class HA requirements specified in ASTM A970. Class HA heads, as discussed in Section 1.2, must be able to develop the minimum specified tensile strength of the reinforcing bar with a head bearing area $A_{brg} \geq 4A_b$, and the obstructions or interruptions, if any, must follow certain dimensional requirements (Figure 1.2). Three versions of a type of bar, the "cold-swaged threaded coupling sleeve headed bar" that meets the requirements of ASTM A970 but does not satisfy the requirements of an HA head, were included in the study. In this case, a pre-threaded coupling sleeve is cold-swaged on the bar; the head is then screwed on the coupling sleeve. These headed bars do not meet the HA head requirements because the size of the coupling sleeve exceeds the allowable size of an obstruction. Thus these heads are described as non-HA heads in this report. Figure 2.1 shows the headed bars of all sizes investigated in this study with the different head-attachment methods.

Figure 2.1 Headed bars (a) No. 8 bars (left to right: cold-swaged threaded coupling sleeve, friction-forged, taper-threaded, and cold-swaged), (b) No. 5 (two on left) and No. 11 (two on right) friction-forged bars, (c) No. 11 cold-swaged bars (left one with threaded coupling sleeve), (d) No. 6 cold-swaged bars

Headed bars are designated by a letter (featuring the head type) and a number (representing the bearing area). The friction-forged, taper-threaded, and cold-swaged headed bars are represented by F, T, and S, respectively; the (non-HA) cold-swaged threaded coupling sleeve headed bars are represented by O in recognition of the sleeves serving as large obstructions. The diameter of the sleeve/obstruction on the non-HA O headed bars was not uniform along their lengths; the obstruction tapered to a smaller size adjacent to the head, providing a larger net bearing area than would be calculated based on the maximum diameter of the obstruction. The net bearing areas based on the size of obstruction adjacent to the head are used to represent the head size for data analysis in subsequent sections. A summary of head dimensions for all bar sizes is given in Table 2.1. Table 2.1 also provides the net bearing areas for the non-HA headed bars based on the difference between the gross area of the head and the maximum area of the obstruction. The net bearing areas of the headed bars ranged from 3.8 to 14.9A_b.

Table 2.1 Head dimensions
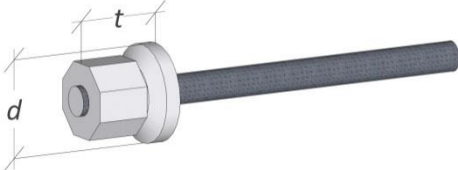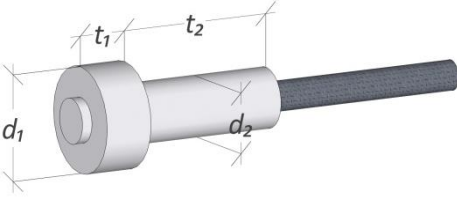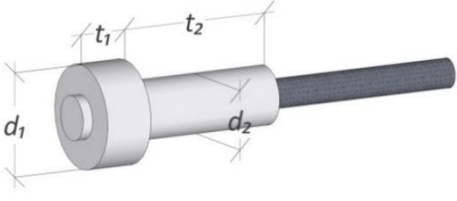
Friction-Forged Headed Bars						
	Designation	Bar Size	b (in.)	h (in.)	t (in.)	Net Bearing Area
	F4.0	No. 5	1.25	1.25	0.5	4.0A_b
	F4.1	No. 8	2	2	1	4.1A_b
	F3.8	No. 11	2.5	3	1.375	3.8A_b
	F13.1	No. 5	1.25	3.5	0.5	13.1A_b
	F9.1	No. 8	2	4	1	9.1A_b
	F8.6	No. 11	2.5	6	1.375	8.6A_b

Table 2.1 Cont. Head dimensions

Taper-Threaded Headed Bars					
	Designation	Bar Size	d (in.)	t (in.)	Net Bearing Area
	T4.0	No. 8	2.25	1.5	$4.0A_b$
	T9.5	No. 8	3.25	1.5	$9.5A_b$

Cold-Swaged Headed Bars					
	Designation	Bar Size	d (in.)	t (in.)	Net Bearing Area
	S4.0[1]	No. 6	1.5	0.69	$4.0A_b$
	S6.5[1]	No. 8	2.5	1.75	$6.5A_b$
	S5.5[1]	No. 11	3.5	2.75	$5.5A_b$
	S9.5	No. 8	3.25	2.75	$9.5A_b$
	S14.9	No. 8	4	2.75	$14.9A_b$

[1] Octagon-shape head

Table 2.1 Cont. Head dimensions

Cold-Swaged Threaded Coupling Sleeve Headed Bars							
	Designation	Bar Size	d_1 (in.)	t_1 (in.)	d_2 (in.)[2]	t_2 (in.)	Net Bearing Area[2]
	O4.5	No. 8	2.75	1.625	1.75	5.25	$4.5A_b$
	O4.5	No. 11	3.75	2.125	2.25	6.75	$4.5A_b$
	O9.1	No. 8	3.5	1.625	1.75	5.25	$9.1A_b$
	O12.9	No. 8	4	1.625	1.75	5.25	$12.9A_b$
	Designation	Bar Size	d_1 (in.)	t_1 (in.)	d_2 (in.)[3]	t_2 (in.)	Net Bearing Area[3]
	O4.5	No. 8	2.75	1.625	2	5.25	$3.5A_b$
	O4.5	No. 11	3.75	2.125	2.75	6.75	$3.3A_b$
	O9.1	No. 8	3.5	1.625	2	5.25	$8.2A_b$
	O12.9	No. 8	4	1.625	2	5.25	$11.9A_b$

[2] Based on size of obstruction adjacent to head
[3] Based on maximum size of obstruction

2.1.2 Concrete Properties

Non-air-entrained ready-mix concrete was used in this study, with the exception of one group of No. 11 headed-bar beam-column joint specimens that had air-entrained concrete. The air-entrained concrete is identified with "5a" as the nominal concrete compressive strength in the specimen designation. A mid-to-high range polycarboxylate-based water reducer was used as a water reducing agent for the 5,000 and 8,000-psi concrete mixtures, and a high-range polycarboxylate-based water reducer was used for the 12,000 and 15,000-psi concrete mixtures. The mixture proportions are given in Table 2.2. The specific gravity (SG) for cement and cementitious materials (fly ash and silica fume), and the bulk saturated surface dry specific gravity

BSG (SSD) of the aggregates are listed in the last column of Table 2.2. For one group of beam-column joint specimens constructed with 5,000-psi concrete, granite was used as coarse aggregate; these specimens are identified with "5g" following the nominal concrete compressive strength in the specimen designation. The maximum aggregate size was $^3/_4$ in.

Table 2.2 Concrete mixture proportions for different nominal strengths

Material	Quantity (SSD)				SG or BSD (SSD)
	5,000 psi $w/c = 0.44$	8,000 psi $w/c = 0.32$	12,000 psi $w/c = 0.29$	15,000 psi $w/cm = 0.23$	
Type I/II Cement, lb/yd^3	600	700	750	760	3.2
Type C Fly Ash, lb/yd^3	-	-	-	160	2.3
Silica Fume, lb/yd^3	-	-	-	100	2.2
Water, lb/yd^3	263	225	217	233	1.0
Kansas River Sand, lb/yd^3	1396	1375	1050	1138	2.63
Pea Gravel, lb/yd^3	-	-	316	-	2.60
Crushed Limestone, lb/yd^3	1735	1683	1796	-	2.59
Granite, lb/yd^3	-	-	-	1693	2.61
High-Range Water-Reducer, oz (US)	30 [1]	171 [1]	104 [2]	205 [2]	-

[1] Mid-to-high range polycarboxylate-based water reducer

[2] High-range polycarboxylate-based water reducer

2.1.3 Steel Properties

All headed bars tested were made of ASTM A1035 Grade 120 steel to help ensure that anchorage capacity was governed by the surrounding concrete and not the tensile strength of the headed bars. The confining reinforcement consisted of either No. 3 or No. 4 ASTM A615 Grade 60 bars. Most column longitudinal reinforcement was fabricated from ASTM A615 Grade 60 steel; in some specimens with a high flexural demand, ASTM A615 Grade 80 or ASTM A1035 Grade 120 steel was used. Physical properties of the headed bars are shown in Table 2.3.

Table 2.3: Headed Bar Physical Properties

Bar Size	Heads	Yield Strength (ksi)	Nominal Diameter (in.)	Average Rib Spacing (in.)	Average Rib Height		Average Gap Width (in.)	Relative Rib Area[2]
					A[1] (in.)	B[2] (in.)		
5	F4.0, F13.1	139.0	0.625	0.423	0.037	0.035	0.319	0.07
6	S4.0	119.8	0.75	0.475	0.053	0.052	0.293	0.096
8	F4.1, F9.1	129.0	1	0.633	0.065	0.060	0.347	0.084
8	T4.0, T9.5	120.0	1	0.590	0.067	0.062	0.287	0.095
8	S6.5, S9.5, S14.9, O4.5, O9.1, O12.9	115.9	1	0.580	0.069	0.063	0.280	0.099
11	F3.8, F8.6, S5.5, O4.5	135.0	1.41	0.838	0.097	0.092	0.394	0.099

[1] Per ASTM A615, A706. [2] Per ACI 408R-3

2.2 BEAM-COLUMN JOINT SPECIMENS

2.2.1 Specimen Design

The beam-column joint specimens were designed to simulate an exterior beam-column joint: the headed bars embedded in the column represented top longitudinal reinforcement of the beam and the bearing member below the headed bars simulated the compression zone of the virtual beam, as shown in Figure 2.2. During the test, a tensile force was applied to the headed bars and a compressive force was provided by the bearing member below the headed bars. The tensile and compressive forces at the face of the column simulated the negative bending moment acting at a beam-column joint.
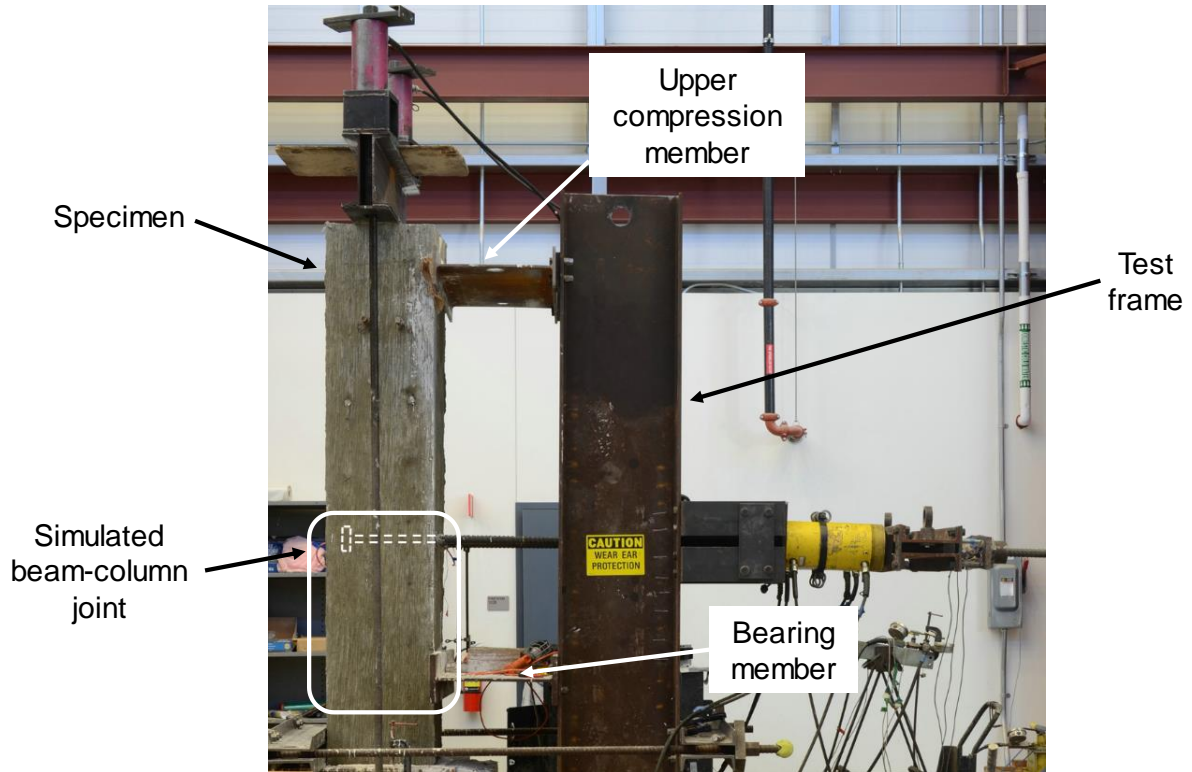
Figure 2.2 Test apparatus of a simulated exterior beam-column joint specimen

A typical beam-column joint specimen is illustrated in Figure 2.3. For all specimens, the embedment length ℓ_{eh} was chosen so that the specimens failed in anchorage (governed by concrete failure) rather than fracture of the headed bar. The embedment length ℓ_{eh} is defined as the distance from the bearing face of the head to the column front face (Figure 2.3b). Initially, the embedment length was chosen to be 80% of the development length that was required in the ACI Code (Eq. 25.4.4.2 in ACI 318-14) and, later, by extrapolating or interpolating trends from previous test results. The depth of the column h, thus, equaled the sum of embedment length, thickness of the head, and cover to the back of the head. The width of the column w was determined by the out-to-out spacing between the headed bars and the side cover to the bar. The height of the column was chosen to prevent interference from the upper support reaction of the test frame (Figure 2.). For the specimens containing No. 11 headed bars, the height of the column was 96 in.; for the specimens containing No. 5 or No. 8 headed bars, the height of the column was 54 in., with the exception of one test group of No. 8 headed bars (the columns were 96-in. high).
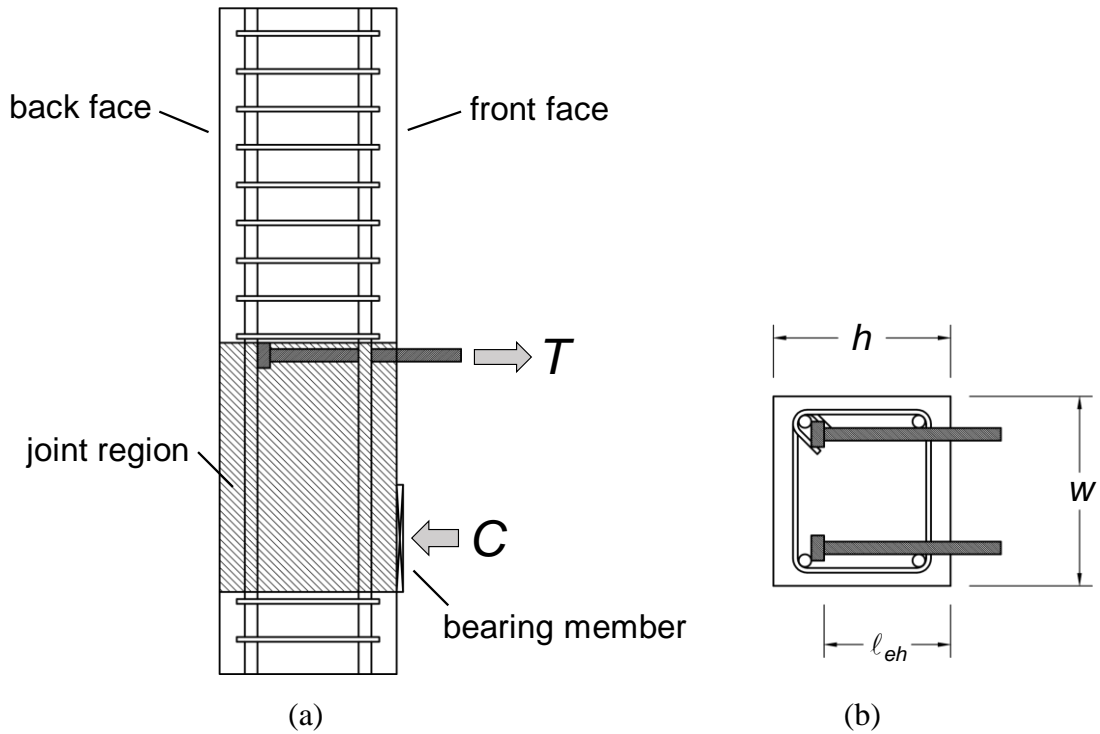
Figure 2.3 Typical beam-column joint specimen (a) side view, (b) top view

The longitudinal reinforcement and transverse reinforcement outside the joint region for the column were designed assuming the column was simply supported and that all headed bars in the joint would reach their expected failure stress simultaneously. Shear capacity within the joint region was provided by the concrete (and the confining reinforcement, if any). The amount of confining reinforcement within the joint region was one of the test parameters and will be discussed in the next section. Some specimens from the first three test groups had a joint shear demand that exceeded the shear capacity. For those specimens, crossties were placed in the middle of the column oriented in the direction of the headed bars with two No. 3 longitudinal bars used to hold the crossties, as shown in Figure 2.4. The use of crossties was discontinued for later specimens to avoid interference with the expected failure surface of the specimen.
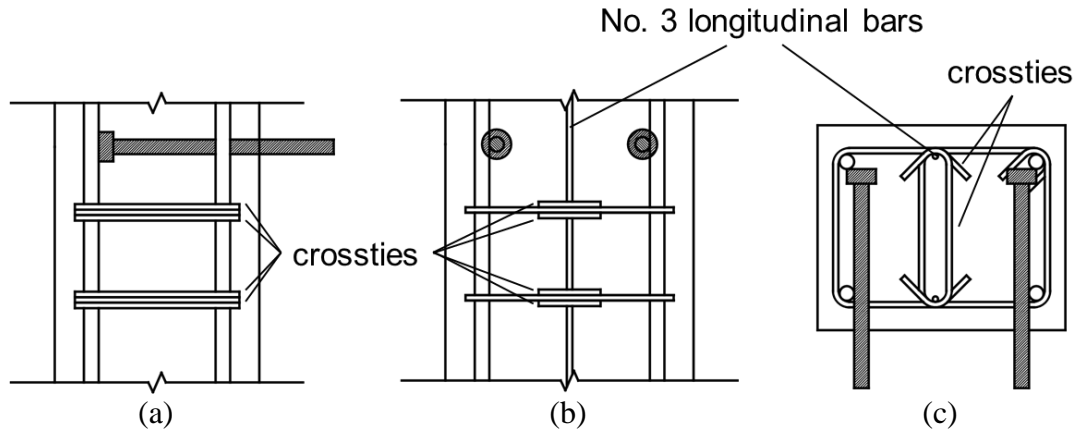
Figure 2.4 Specimen containing crossties within joint region
(a) side view, (b) front view, (c) top view

For some specimens in an early test group, *hairpin* reinforcement was used to better hold the middle headed bar in place for specimens containing three headed bars. Two sets, each containing two No. 3 bars, were placed perpendicular to the headed bars, spaced at 3 in. along the embedded bars, as shown in Figure 2.5. The specimens containing *hairpin* reinforcement are identified with HP at the end of the specimen designation described in Section 2.2.4.
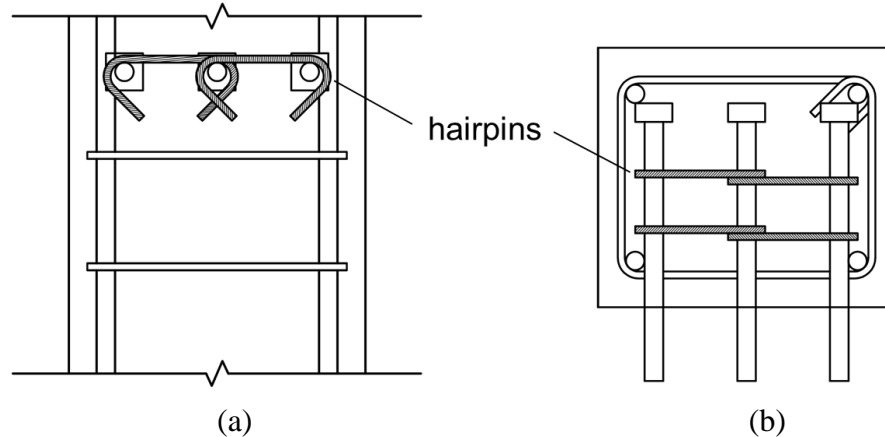
Figure 2.5 Specimen with hairpin reinforcement (a) front view, (b) top view

2.2.2 Test Parameters

The test parameters included in this study were bar size, compressive strength of concrete, embedment length, spacing between the bars, number of bars, side cover, type of headed bars, bar

placement within the joint, and quantity of confining reinforcement within the joint region. The ranges of these variables are described below:

Bar size: Three bar sizes were used – No. 5, No. 8, and No. 11 headed bars.

Concrete compressive strength: The target concrete compressive strengths were 5,000, 8,000, 12,000, and 15,000 psi, respectively. Actual concrete compressive strengths ranged from 3,960 to 16,030 psi. Concrete mixture proportions are given in Section 2.1.2.

Embedment length: Nominal embedment lengths ranged from 4 in. to 19.25 in. with 4 in. to 6 in., 6 in. to 14.5 in., and 12 in. to 19.25 in. for specimens containing No. 5, No. 8, and No. 11 bars, respectively.

Number and spacing of headed bars: Of the 202 specimens tested, 122 contained two headed bars and 80 contained three or four headed bars (hereafter referred to as multiple-headed-bar specimens). For the two-headed-bar specimens, the nominal center-to-center spacing between the bars ranged from $3d_b$ to $11.8d_b$ (where d_b is the bar diameter); for multiple-headed-bar specimens, the nominal center-to-center spacing between the adjacent bars ranged from $3d_b$ to $7d_b$. In this study, the term "closely spaced" was used to describe specimens with a center-to-center spacing between the bars of less than $8d_b$. Of all the two-headed-bar specimens tested, the majority had a fixed out-to-out spacing between the bars – 8 in. for No. 5 bars, 12 in. for No. 8 bars, and 16.5 in. for No. 11 bars (equal, respectively, to center-to-center spacings of $11.8d_b$, $11d_b$, and $10.7d_b$). These specimens are referred to as standard specimens and are shown in Figure 2.6.
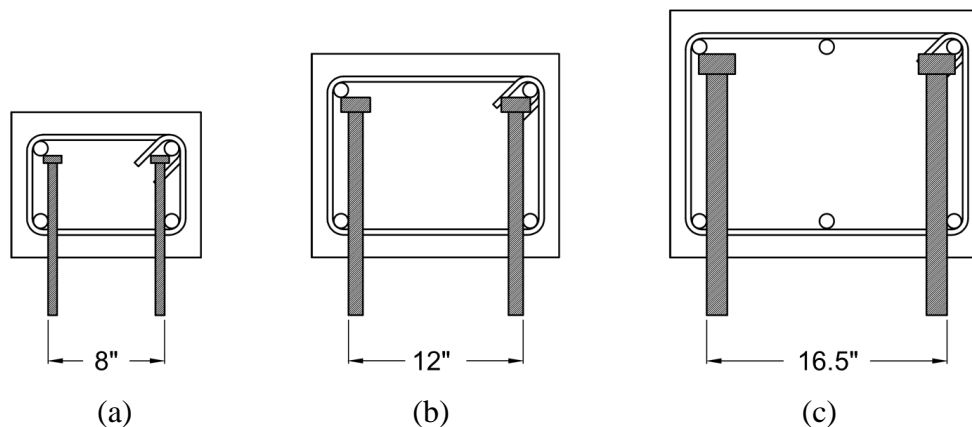
Figure 2.6 Cross sections of standard specimens (a) No. 5 headed bars, (b) No. 8 headed bars, (c) No. 11 headed bars

34

Side cover: Most specimens had a side cover of 2.5 in. A small number of the initial specimens had side covers of 3 in., 3.5 in., and 4 in. The test results showed that, within this range, side cover did not significantly influence anchorage strength; therefore, the side cover was kept at 2.5 in. in subsequent tests.

Type of headed bars: The full range of headed bars listed in Table 2.1 were evaluated in the beam-column joint specimens.

Bar placement within the joint: For the majority of the specimens, the headed bars were anchored near the far side of the column with the back of the head touching the column longitudinal bars, as shown in Figure 2.. For some specimens, the headed bars were anchored in the middle of the column, as shown in Figure 2.7. The nominal cover to the back of the head ranged from 3 to 7 in.
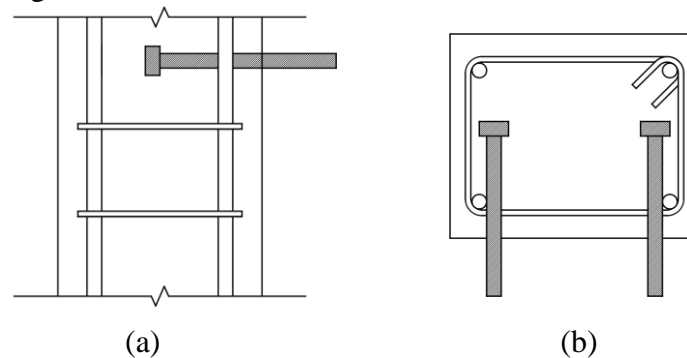
(a) (b)
Figure 2.7 Headed bars anchored in the middle of the column (a) side view, (b) top view

Confining reinforcement: Most specimens had one of the three levels of confining reinforcement placed parallel to the bar within the joint region: no confining reinforcement, two No. 3 hoops, or No. 3 hoops spaced at $3d_b$ (meeting the requirements for a 0.8 reduction factor for the development length calculation of 90° hooked bars, allowing comparisons to be made between hooked and headed bars at a constant joint reinforcement amount). Details of these three levels of confining reinforcement are shown in Figures 2.8 through 2.10. In these figures, ties outside the joint region are omitted for clarity, and the compression member attached to the test frame is drawn to show the location of the simulated beam compression zone. Some specimens had alternate stirrup patterns (four No. 3 hoops, five No. 3 hoops[1], three No. 4 hoops, and four No. 4 hoops within the joint region).

---

[1] The five No. 3 hoops for this pattern had a spacing of more than $3d_b$ and were used in one test group with No. 8 headed bars.
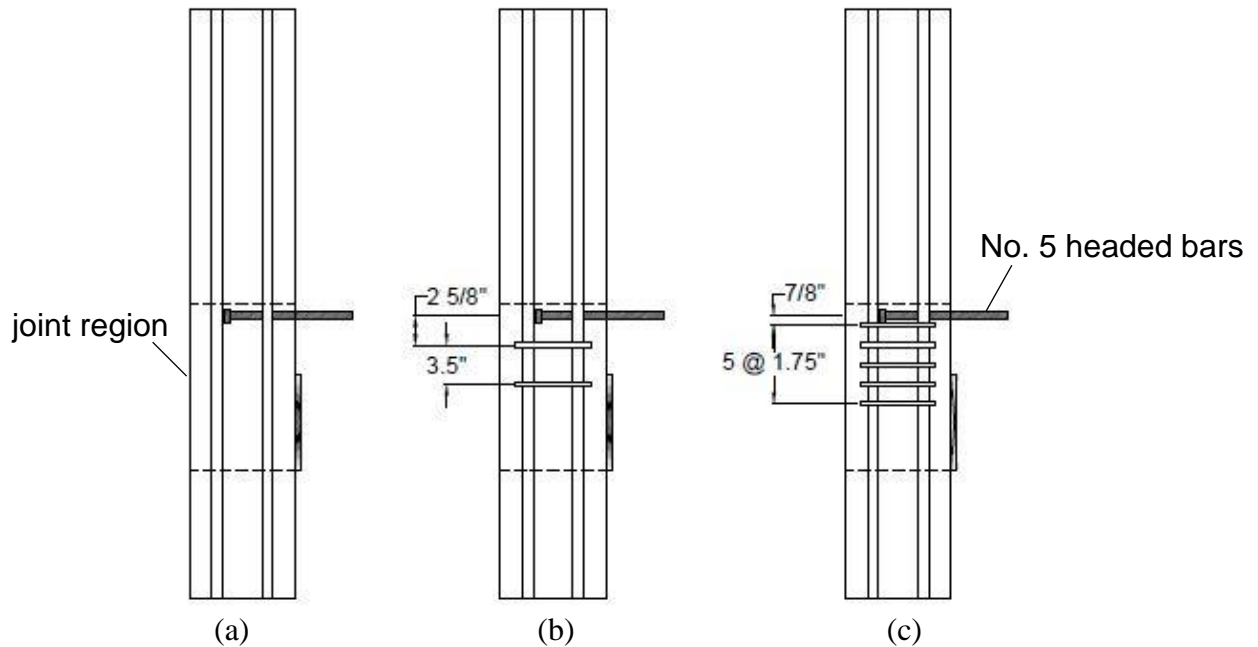
Figure 2.8 Confining reinforcement for No. 5 headed-bar specimens (a) no confining reinforcement, (b) two No. 3 hoops, (c) five No. 3 hoops
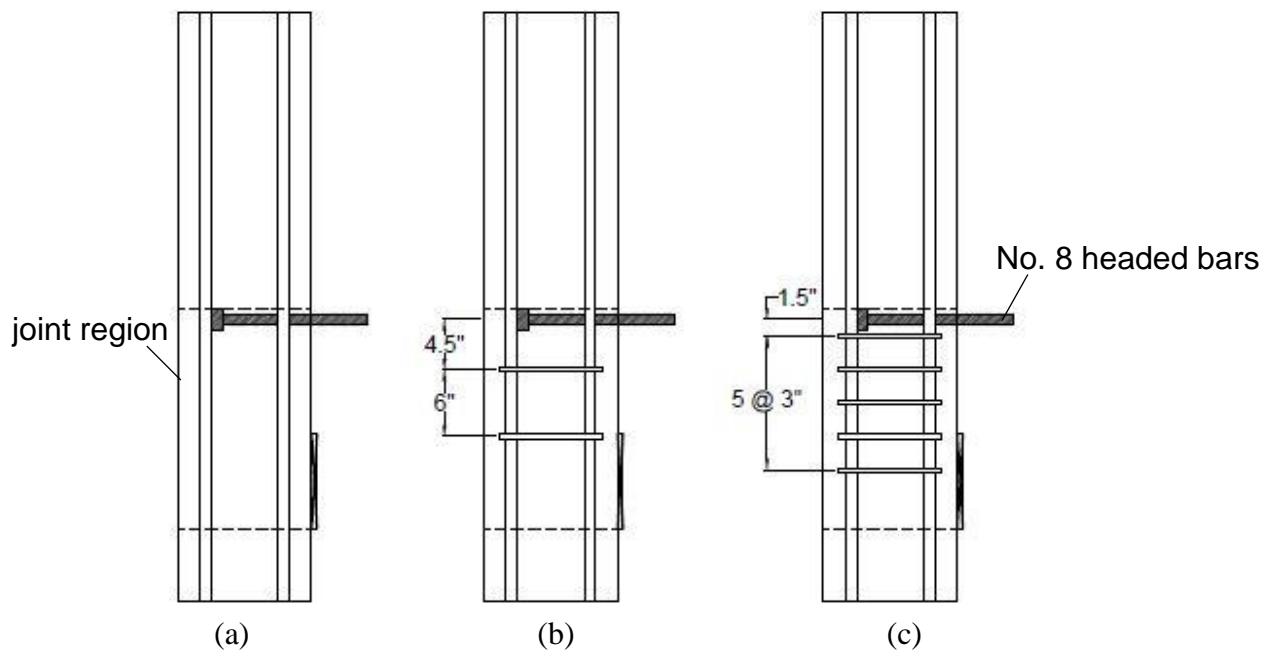
Figure 2.9 Confining reinforcement for No. 8 headed-bar specimens (a) no confining reinforcement, (b) two No. 3 hoops, (c) five No. 3 hoops
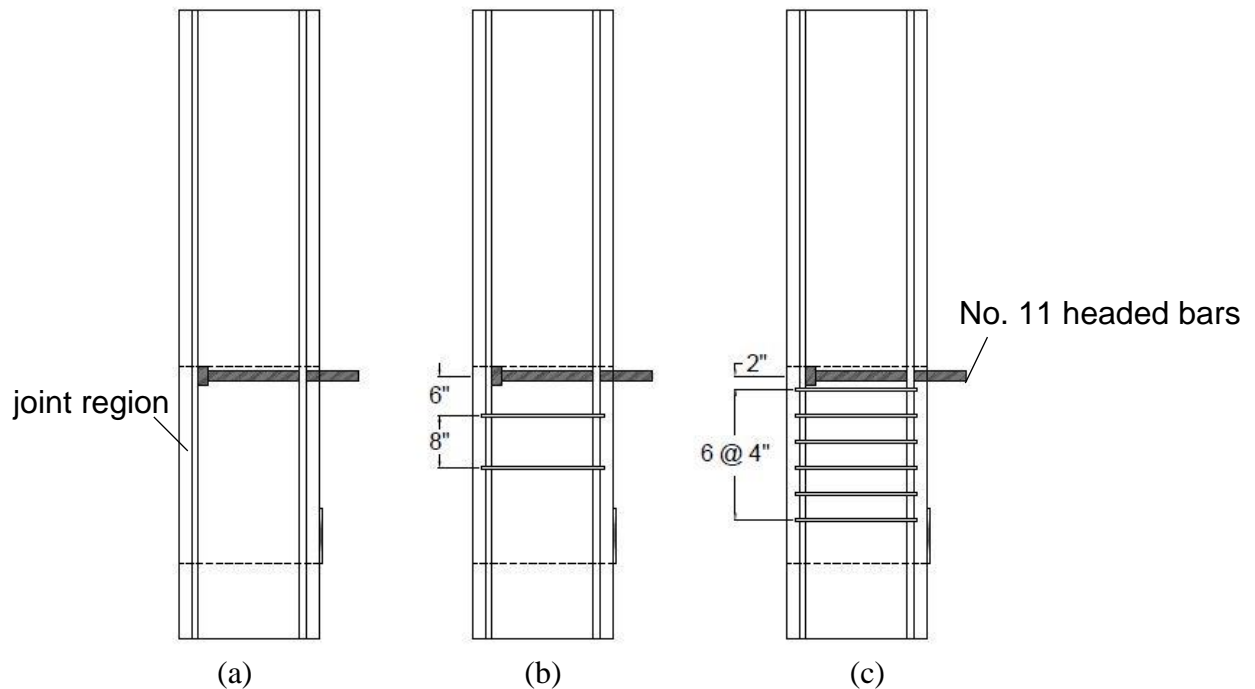
Figure 2.10 Confining reinforcement for No. 11 headed-bar specimens (a) no confining reinforcement, (b) two No. 3 hoops, (c) six No. 3 hoops

2.2.3 Specimen Designation

The variables described above are denoted in the specimen designation. An example is given in Figure 2.11, with dimensional variables shown in Figure 2.12. The example indicates a specimen that was cast with 12-ksi concrete and had three No. 8 headed bars (with friction-forged $4.1A_b$ heads) spaced at $3d_b$ center-to-center; the specimen had a 12-in. nominal embedment length and five No. 3 hoops as confining reinforcement within the joint region.
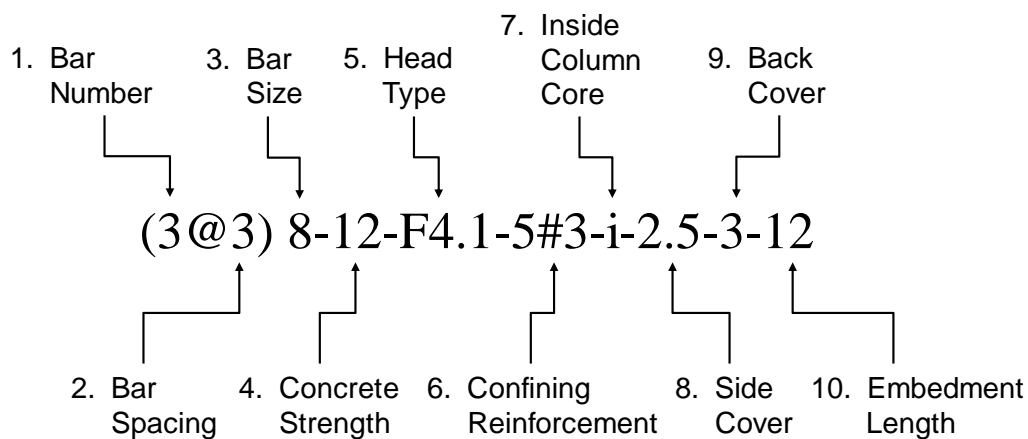
Figure 2.11 Specimen designation

37

1. Number of headed bars in the specimen

2. Center-to-center spacing between adjacent bars in terms of bar diameter, s (Figure 2.12) (lack of the term "A@B" indicates a standard specimen)

3. ASTM size of headed bar

4. Nominal compressive strength of concrete (ksi)

5. Type of headed bar (refer to Table 2.1)

6. The term "A#B" indicates the amount of confining reinforcement within joint region, with A representing the number of confining reinforcement, and B representing ASTM bar size of the confining reinforcement. If A#B = 0, no confining reinforcement was used within joint region

7. "i" means the headed bars of the specimen were placed inside the column core that was confined by the column longitudinal reinforcement. The headed bars were placed inside the column core for all the specimens in this study

8. Nominal value of side cover, c_{so} (in.) (Figure 2.12)

9. Nominal value of back cover to the head, c_{bc} (in.) (Figure 2.12)

10. Nominal value of embedment length, ℓ_{eh} (in.) (Figure 2.12)

Special note: Some specimens have a special designation after the nominal embedment length. "HP" indicates that hairpin reinforcement was used in the specimen to hold the middle headed bar (Figure 2.5), and "DB" indicates that No. 8 headed-bar specimens were tested in a manner that simulates a deep beam-column joint, as described in Section 2.2.5.
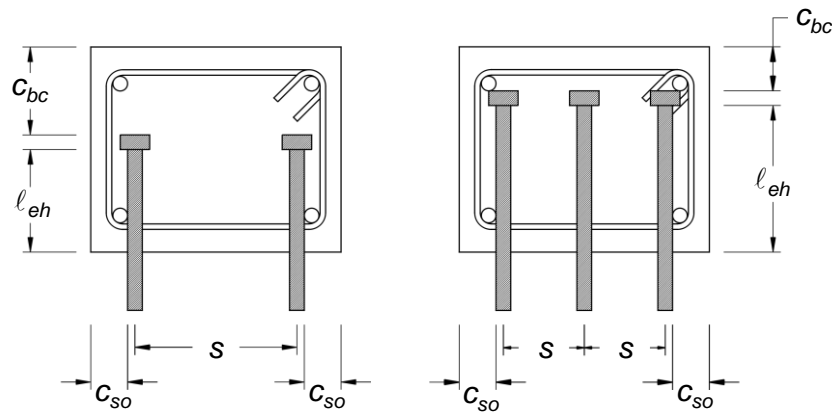
Figure 2.12 Dimensional variables of specimens

2.2.4 Specimen Fabrication

Reinforcement cages for the column were built in accordance with specimen design. Steel chairs with appropriate sizes were tied on the column longitudinal bars to control the concrete cover. Headed bars were tied to the column longitudinal reinforcement. The steel cages, together with the headed bars, were then placed in forms constructed using plywood and 2×4 lumber. Specimens were cast in three layers, with each layer consolidated using a spud vibrator. During placement, two samples of fresh concrete were combined to measure concrete temperature, slump, and unit weight. Concrete cylinders of two sizes, 4×8 in. and 6×12 in., were made and stored with the specimens. The concrete cylinders were used to keep track of concrete compressive strength. When the concrete strength reached 3,000 psi, the specimens were removed from the forms. For high-strength concrete (nominal strengths of 12,000 and 15,000 psi), the specimens were wet-cured immediately after demolding to allow concrete to continue to gain strength. When the concrete reached a strength approximately equal to the nominal strength, the specimens were ready for test.

2.2.5 Test Procedure

The test frame was a modified version of the test apparatus used by Marques and Jirsa (1975). Figure 2.13 schematically shows the applied loads and reactions on a typical specimen. Detailed descriptions of the test frame and test procedure are reported by Peckover and Darwin (2013).
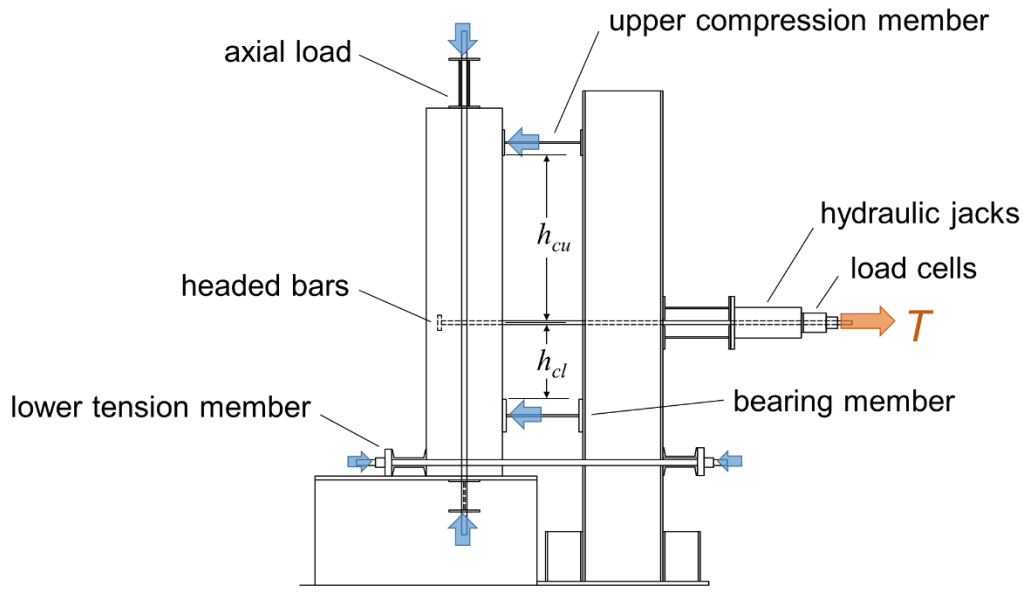
Figure 2.13 Loads and reactions on a typical specimen

As shown in Figure 2.13, the upper compression member, placed at the top of the specimen, and the lower tension member, placed at the bottom of the specimen, were used to prevent overturning of the specimen. The bearing member, placed below the headed bars, simulated the beam compression region on the front face of the column. The widths of the upper compression member and bearing member were $6^5/_8$ in. and $8^3/_8$ in., respectively. The positions of the bearing members were adjustable; the dimensions are shown in Table 2.4. One group of No. 8 headed-bar specimens was tested with the distance between the headed bar and top of the compression plate (h_{cl}) of 20 in. (as opposed to the standard 10.25 in.) to simulate a deep beam-column joint. These specimens are identified with "DB" at the end of the specimen designation.

Table 2.4 Position of bearing members

Headed bar size	No. 5	No. 8	No. 11
Specimen height	54 in.	54 in.	96 in.
Distance from the center of headed bar to the top edge of the lower compression plate, h_{cl} [1]	5.25 in.	10.25 in.	20 in.
Distance from the center of headed bar to the bottom edge of the upper compression plate, h_{cu} [1]	18.25 in.	18.25 in.	44.25 in.

[1] Refer to Figure 2.13

Before loading the headed bars, an axial load was applied to the column. For specimens that were 96 in. high (all No. 11 headed-bar specimens and one group of No. 8 headed bar specimens), an axial stress of 280 psi was applied; for specimens that were 54 in. high (all No. 5 headed-bar specimens and most No. 8 headed-bar specimens), an axial load of approximately 30,000 lb was applied (corresponding to a range in axial stress of 93 psi to 243 psi). This axial loading level was assumed to have no significant influence on the anchorage strength of headed bars, as Marques and Jirsa (1975) found that changes in axial load (with an axial stress of up to 3080 psi) did not have a significant effect on the anchorage strength of beam-column joint specimens containing hooked bars. Tensile loads were applied monotonically to the headed bars using hydraulic jacks at an interval of 5, 10, 15 or 20 kips per bar depending on the estimated failure load of the specimen. At each interval, loading was paused to allow cracks to be marked on the specimen. When the specimen approached its estimated failure load or had an obvious sign of failure (such as continuous bar slip or the load dropping during an interval), the specimen was then loaded to failure without marking additional cracks. After failure, loose concrete was removed from the specimen to expose internal cracks. Tests lasted about 30 minutes plus an additional 50 minutes for test preparation.

2.2.6 Specimen Instrumentation

In addition to the testing equipment described in Section 2.2.5, some specimens (listed in Table 2.5) had strain gauges installed to monitor the change in strain in the confining reinforcement within the joint region and in the headed bars throughout the test. For each specimen, strain gauges

were attached to one headed bar and all hoops on the same side of the column. If the specimen had three headed bars, strain gauges were also attached to the middle bar. Two strain gauges were mounted on the headed bars, with one gauge placed 1.5 in. from the head bearing face and the other gauge placed 1 in. from the front face of the column. One strain gauge was mounted on the hoops at the middle of the leg oriented parallel to the headed bar. Figure 2.14 shows the locations of the strain gauges.

Table 2.5 Specimens containing strain gauges

11-8-F3.8-0-i-2.5-3-14.5	(3@5.35)11-8-F3.8-0-i-2.5-3-14.5
11-8-F3.8-2#3-i-2.5-3-14.5	(3@5.35)11-8-F3.8-2#3-i-2.5-3-14.5
11-8-F3.8-6#3-i-2.5-3-14.5	(3@5.35)11-8-F3.8-6#3-i-2.5-3-14.5
11-5-F3.8-0-i-2.5-3-12	11-5-F3.8-0-i-2.5-3-17
11-5-F3.8-6#3-i-2.5-3-12	11-5-F3.8-6#3-i-2.5-3-17
11-5-F8.6-0-i-2.5-3-14.5	(3@5.35)11-5-F8.6-0-i-2.5-3-14.5
11-5-F8.6-6#3-i-2.5-3-14.5	(3@5.35)11-5-F8.6-6#3-i-2.5-3-14.5
11-5-S5.5-6#3-i-2.5-3-19.25[*]	11-12-S5.5-6#3-i-2.5-3-16.75[*]
8-8-S14.9-0-i-2.5-3-8.25	8-8-O12.9-5#3-i-2.5-3-9.5
8-8-S14.9-5#3-i-2.5-3-8.25	

[*]Strain gauges were attached only to hoops.

(a)   (b)
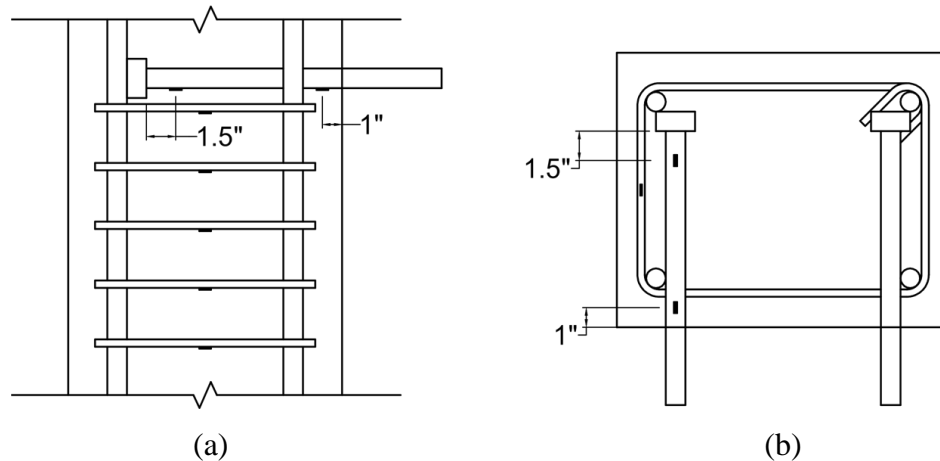
Figure 2.14 Strain gauge locations (a) side view, (b) top view

2.3 CCT NODE SPECIMENS

2.3.1 Specimen Design

CCT node specimens were designed to simulate the behavior of a headed bar anchored in a compression-compression-tension (CCT) node as defined for a strut-and-tie model (STM). The

use of a STM is preferred for the analysis of discontinuity regions (D-regions) in reinforced concrete structures, such as those found near supports, openings, and connections. Using a STM reduces the complicated state of stress in D-regions to the simple, uniaxial stress paths of a truss. The uniaxial stress paths are investigated as members within the truss, identified as struts, ties, and nodal zones. Struts are members under compressive stress while ties are the members subjected to tensile stresses. Ties coincide with the location of reinforcement. Nodal zones, or nodes, are formed where struts and ties intersect. Figure 2.15 illustrates a strut and tie model. The force in each member of the truss can be determined using equilibrium if forces acting on the boundary of the STM are known.
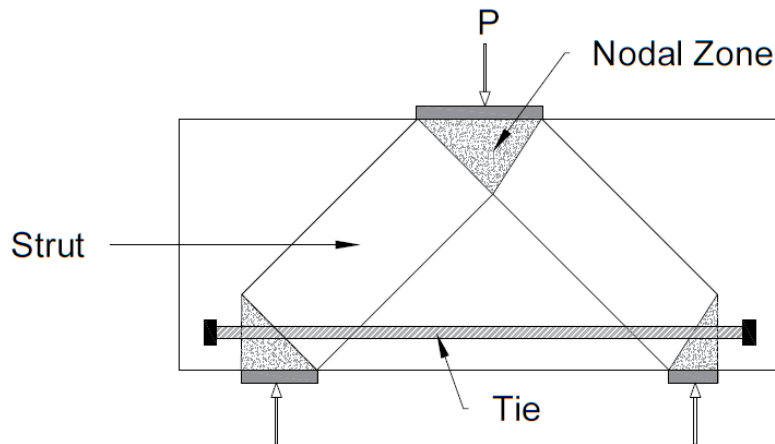
Figure 2.15 Strut and tie model

Two series of five beams were tested. For the specimens used in this study, no reinforcement was located within the nodal zone with the exception of the tensile tie reinforcement, which was provided by two or three bars. The two ends of the specimen were tested separately. At one end, the bars were terminated with a head, while at the other end the bars were straight. Figures 2.16a and b show the test configurations. The strut angle used in the design was 45°.

CCT node specimens were 20 in. deep and 18 in. wide, with a clear span of 60 in., and total length of 104 in. The tension tie consisted of No. 8 bars. Concrete with a nominal compressive strength of 5,000 psi was used for all specimens. No. 4 stirrups spaced 3.5 in. on center were used away from the strut and nodal zone to ensure that the specimens did not fail in shear. Figure 2.17 shows

the cross-sections of the specimens, and Figure 2.18 shows a CCT specimen in the testing frame (described in Section 2.3.5).

(a)

(b)
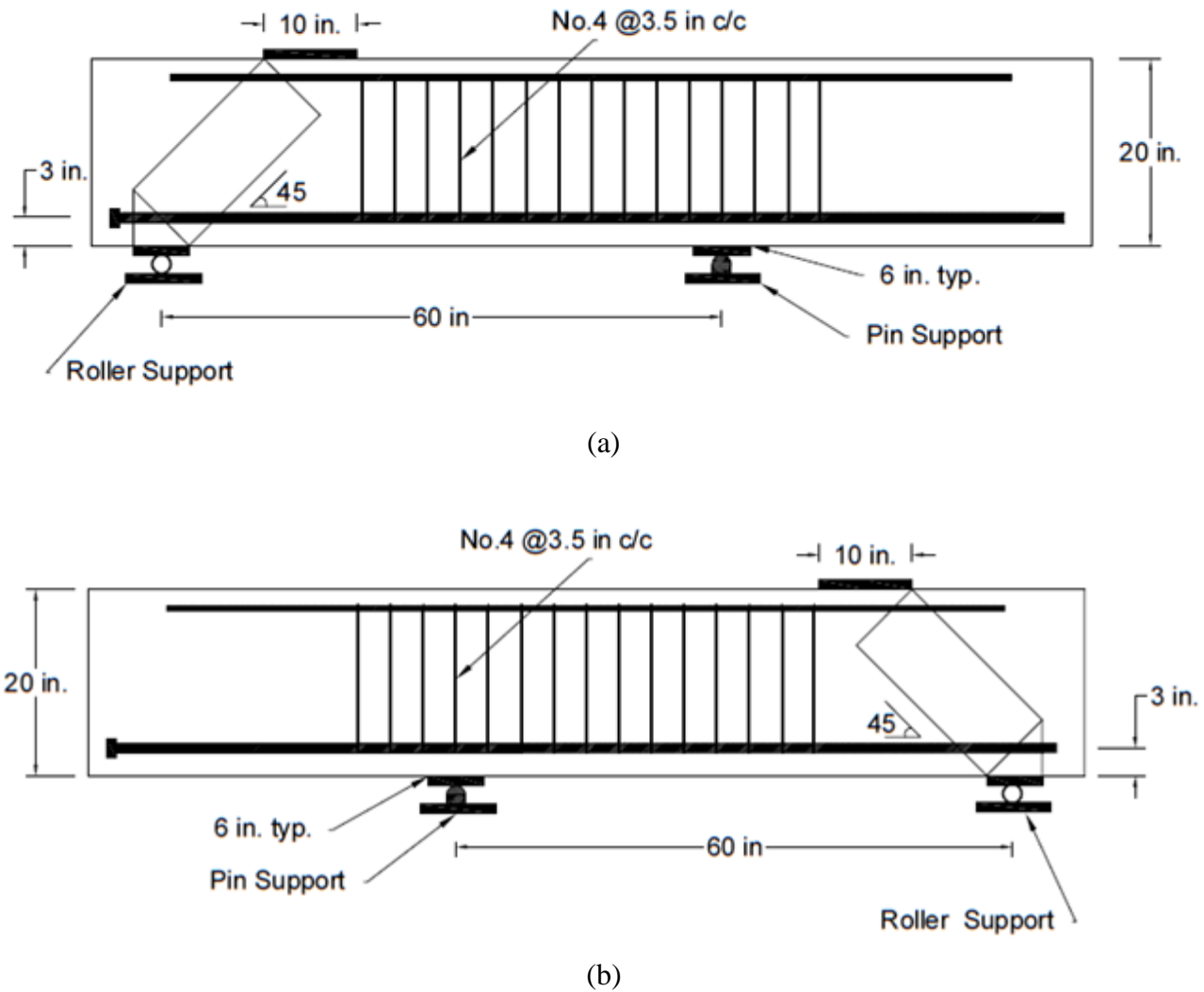
Figure 2.16 Testing configurations (a) headed end, (b) non-headed end
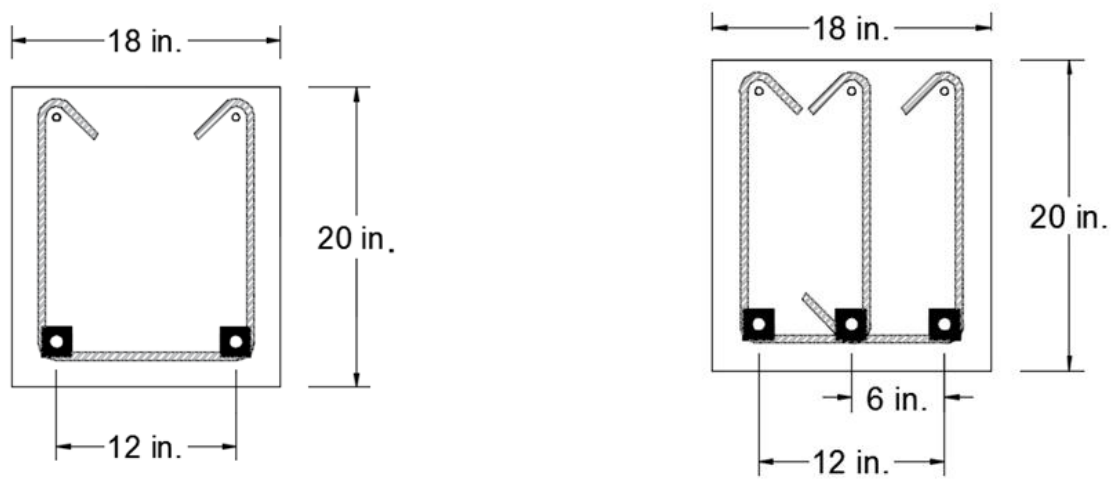
Figure 2.17 Cross-section of the specimens

Figure 2.18 A typical CCT node test

2.3.2 Test Parameters

Bar size: No. 8 bars were used in the study. The bars were fabricated using Grade 120 ASTM A1035 reinforcement.

Concrete compressive strength: The target concrete compressive strength was 5,000 psi. Concrete mixture proportions are given in Section 2.1.2.

Embedment length: Embedment lengths were measured from the face of the head to the intersection of the reinforcement with the extended nodal zone (ACI 318-14), as shown in Figure 2.19. For some of the specimens, the bearing face of the head aligned with the back edge of the bearing plate, providing a 9 in. embedment length. For the other specimens, the bearing face of the head was located beyond the edge of the bearing plate, providing an embedment length between 10 in. and 14 in., as shown in Figure 2.19. The same configurations were used for the non–headed end, with the embedment length measured from the end of the straight bar, as shown in Figure 2.20.

Number and spacing of headed bars: Two or three headed bars were used in each specimen. Two specimens in each group of five contained two headed bars with a center-to-center spacing of $12d_b$, while the rest of the specimens contained three headed bars with a center-to-center spacing of $6d_b$.

Type of headed bars: F4.1 (Friction-forged $4.1A_b$) headed bars were used in these specimens.
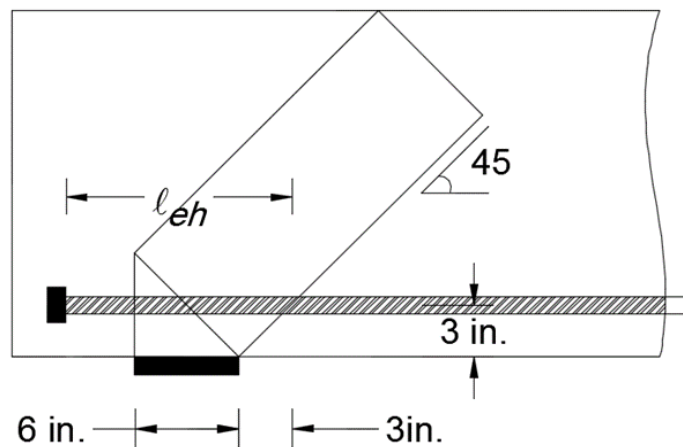
Figure 2.19 Position of heads with respect to bearing plate
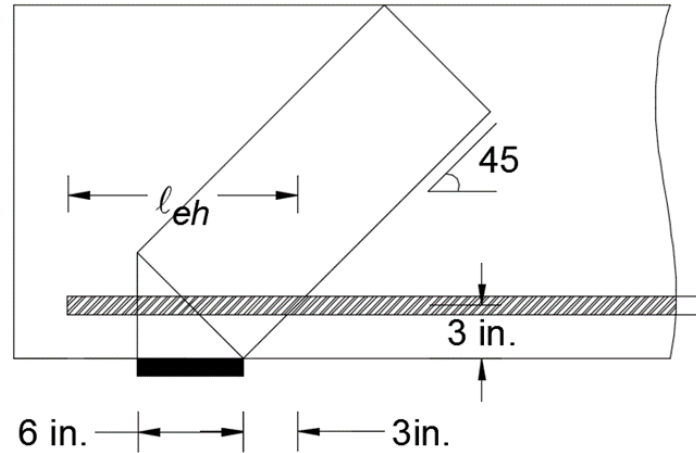
Figure 2.20 Position of non-headed end with respect to bearing plate

2.3.3 Specimen Designation

The specimens are identified based on the variables used in this study, as illustrated in Figure 2.21. The example identifies a specimen cast with concrete with a nominal compressive strength of 5,000 psi containing three No. 8 F4.1 headed bars with a 9 in. embedment length.
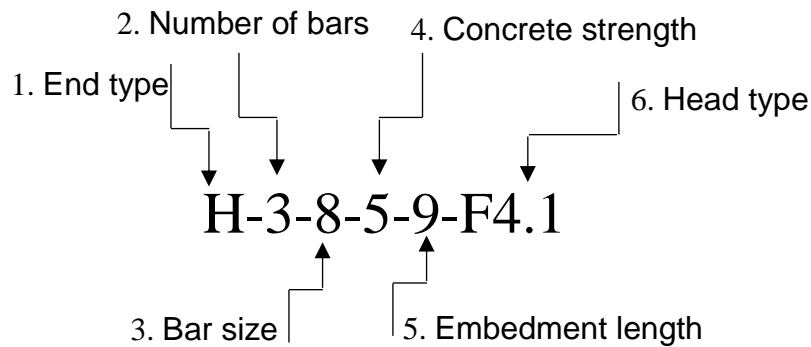
Figure 2.21 Specimen designation

The items in Figure 2.21 indicate: 1. Type of end (H for a headed end, NH for a non-headed end); 2. number of headed bars in the specimen; 3. size of headed bar (ASTM designation); 4. nominal compressive strength of concrete (ksi); 5. nominal value of embedment length, ℓ_{eh} (in.);

47

and 6. type of headed bar. Some specimens were duplicated between the two series; these specimens have a I or II after the head type to distinguish between the specimens.

2.3.4 Specimen Fabrication

Forms were fabricated from plywood and 2×4 lumber. The reinforcing cages, consisting of the longitudinal reinforcement and stirrups, were placed in the forms, using metal chairs to provide the required cover. The specimens were cast in two layers. For both layers, the concrete was first placed at the middle third of the specimen, followed by the two ends. Each layer was consolidated using a 1¾ in. spud vibrator. The upper surface was screeded, floated, and then covered with plastic. When the concrete compressive strength reached 3,000 psi the specimens were demolded.

2.3.5 Test Procedure

The frame, shown in Figures 2.22 and 2.23, was used to test the specimens. Load was applied using four hydraulic jacks and transferred by threaded rods through load cells to spreader beams bearing on the specimen. The load cells were located so as to measure the force transmitted to the spreader beam by the threaded rod. The spreader beams applied the load to the specimen through a steel plate. The beam itself was simply supported; the support close to the testing region was a roller, while the other support was a pin support.

During the test, the load was applied monotonically to the specimen using the hydraulic jacks in increments of 35 kips. Loading was paused in each interval to mark the cracks and measure crack widths. Specimens were loaded to failure without pausing once the load approached the estimated failure load.
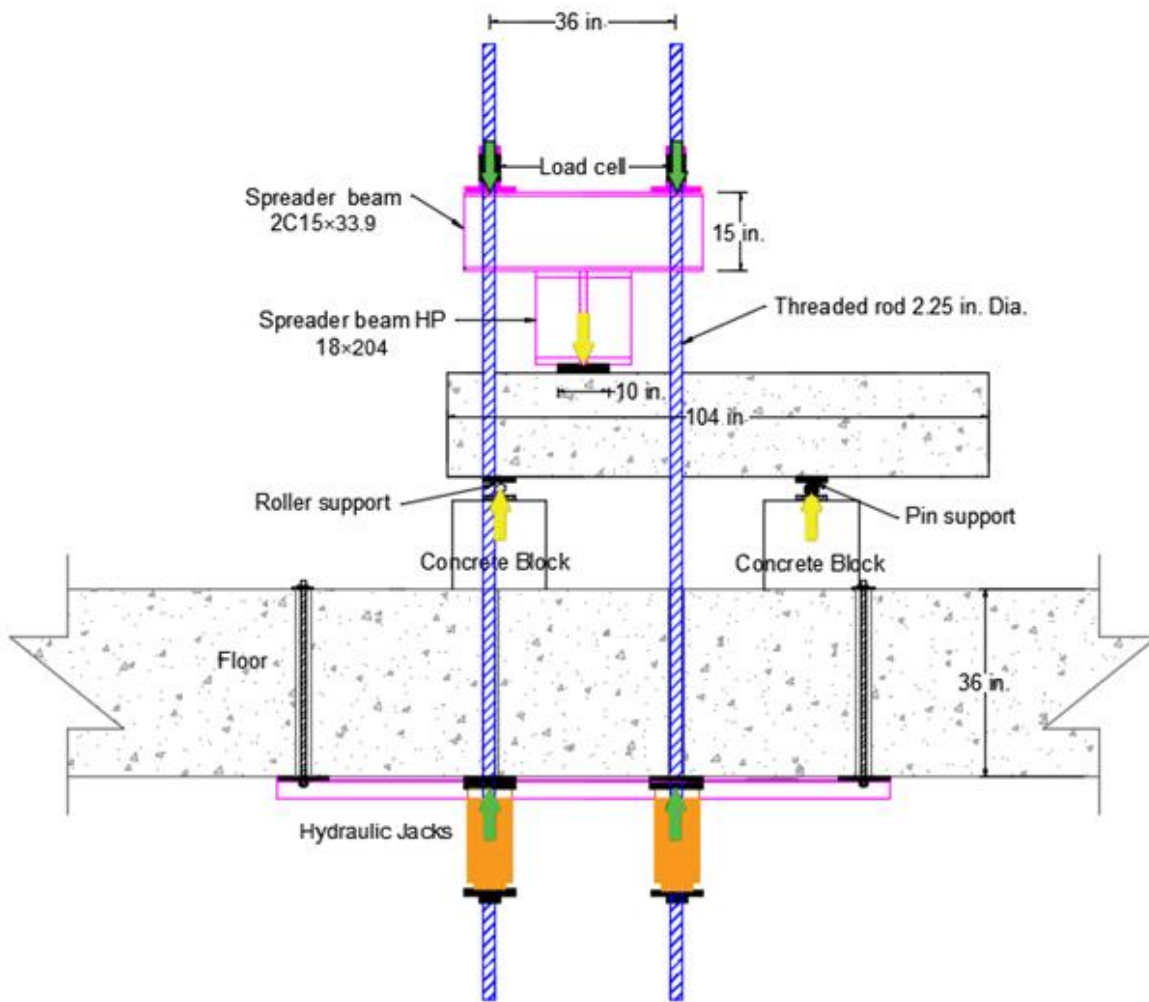
Figure 2.22 Front view of the loading system
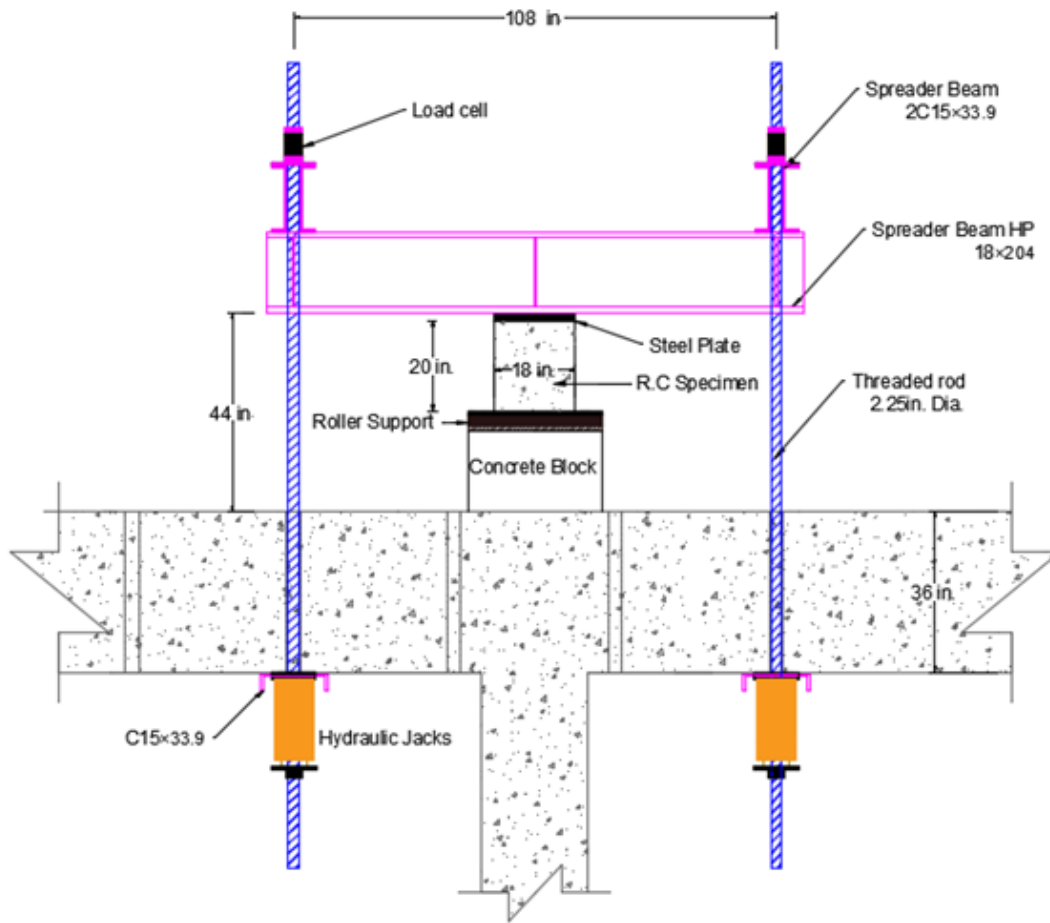
Figure 2.23 Side view of the loading system

2.3.6 Specimen Instrumentation

The following instrumentation was used in the tests:

Strain gages were mounted on the headed bar at both ends, as shown in Figure 2.24 to measured strains throughout the nodal zone and close to the head. For the headed end, four strain gauges were placed between the head and the point of applied load. The strain gauges were placed 1 in. from the face of the head, at the support, where the bar crossed the extended nodal zone, and under the applied load point. For the non-headed end, three strain gauges were installed between the end of the bar and the point of applied load. The strain gauges were placed at the support, where the bar crossed the extended nodal zone, and under the applied load point.
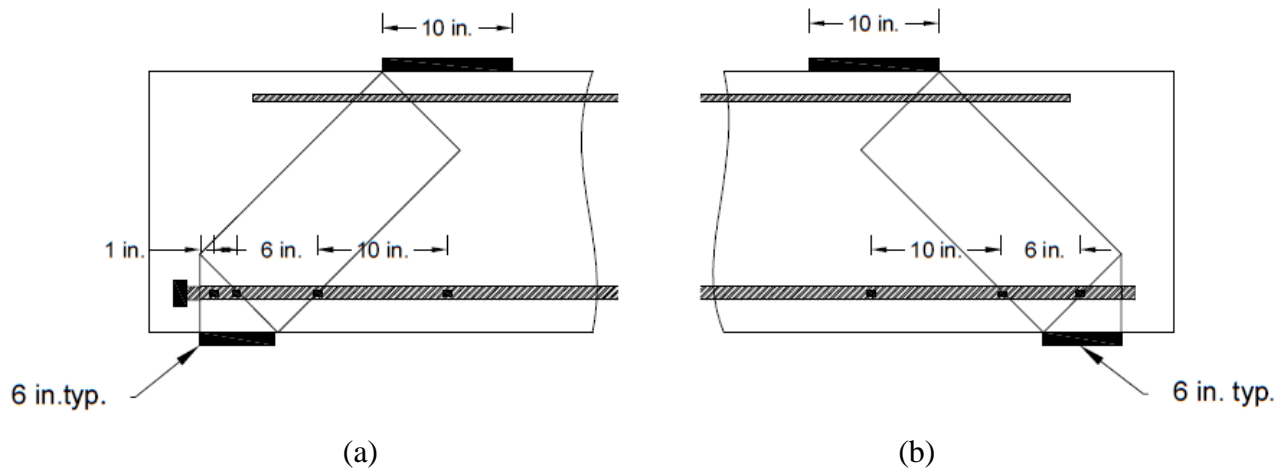
Figure 2.24 Placement of strain gauges for a typical specimen (a) headed end, (b) non-headed end

A non-contact infrared-based system was used to measure displacements. Figure 2.25 shows the infrared markers that were installed on the specimen near midspan and at the supports to provide information on the deflection, slip, and crack widths.

Figure 2.25 Placement of markers for a typical specimen

Linear potentiometers with displacement ranges of 2 in. and 4 in. were used to measure the horizontal slip at the headed and non-headed end relative to the outside face of the concrete beam, as shown in Figure 2.26. The potentiometers were connected to the headed end bar using a wire that passed through a plastic tube cast into the concrete. Displacement of the concrete was measured using a non-contact infrared based system. The displacement of the linear potentiometers

was subtracted from the displacement measured using the non-contact infrared based system to find the slip on the bar.
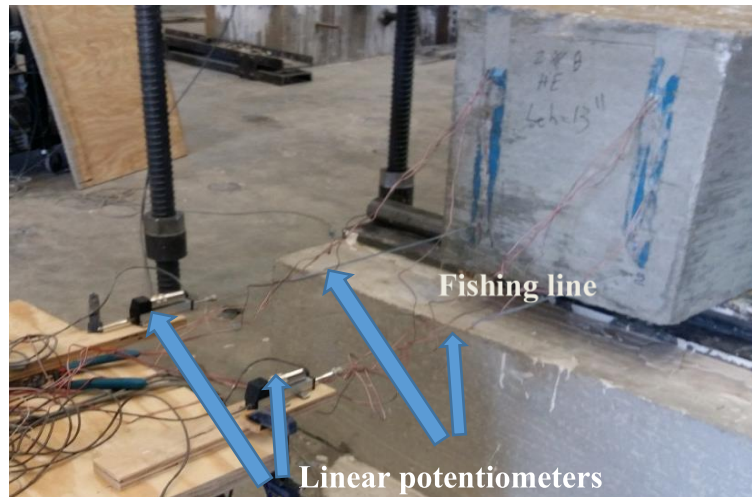
Figure 2.26 Linear potentiometers

2.4 SHALLOW EMBEDMENT SPECIMENS

2.4.1 Specimen Design

The shallow embedment pullout tests investigated the anchorage behavior of headed bars in a simulated column-foundation joint. A total of 32 headed bars with 6 in. nominal embedment length were tested to study the effects of the distance between the headed bar and compression reaction, head type and bearing area, and the effect of reinforcement oriented perpendicular to the headed bar.

Headed bars simulating column longitudinal reinforcement were embedded in a concrete slab, as shown in Figure 2.27. The slabs were designed as simply-supported beams (neglecting self-weight) to resist bending and shear at the maximum anticipated load on the anchored bar. The specimens contained two or three headed bars, which were loaded one at a time and embedded sufficiently far apart so that an anchorage failure of one bar did not interfere with the anchorage capacity of the others. The width of the specimen was chosen so that it was greater than the diameter of the anticipated concrete breakout failure surface. The depth of the specimens was sufficient to provide flexural and shear strength; only the minimum required flexural reinforcement

52

was provided. In the first five test series, the clear distance between the nearest support and the headed bar was 10 in., while the clear distance between the farthest support and the headed bar was 44.5 in. This configuration was intended to simulate a column anchored in the foundation and subjected to bending, with the reaction support nearest to the anchored headed bar representing the compression zone of the column and the headed bar representing anchored tension reinforcement. The other reaction support was placed sufficiently far away from the anchored bar to avoid interference with the concrete breakout failure surface. In the final test series, both supports were outside the anticipated failure region. The clear distance between the supports and the headed bar was 14.5 or 16.5 in., which is greater than the radius of the anticipated failure surface, which, using the provisions for anchors in ACI 318-14 (Section 17.4.2.1 and Figure R17.4.2.1), would be located $1.5\ell_{eh}$ from the center of the headed bar.

Load was applied using a hydraulic jack supported by two spreader beams, which were selected based on the moment and shear strength demands at the maximum anticipated load applied to the specimens, so that the maximum deflection of the spreader beams was less than the thickness of the plates that served as support plates to prevent the beam from touching the slab.
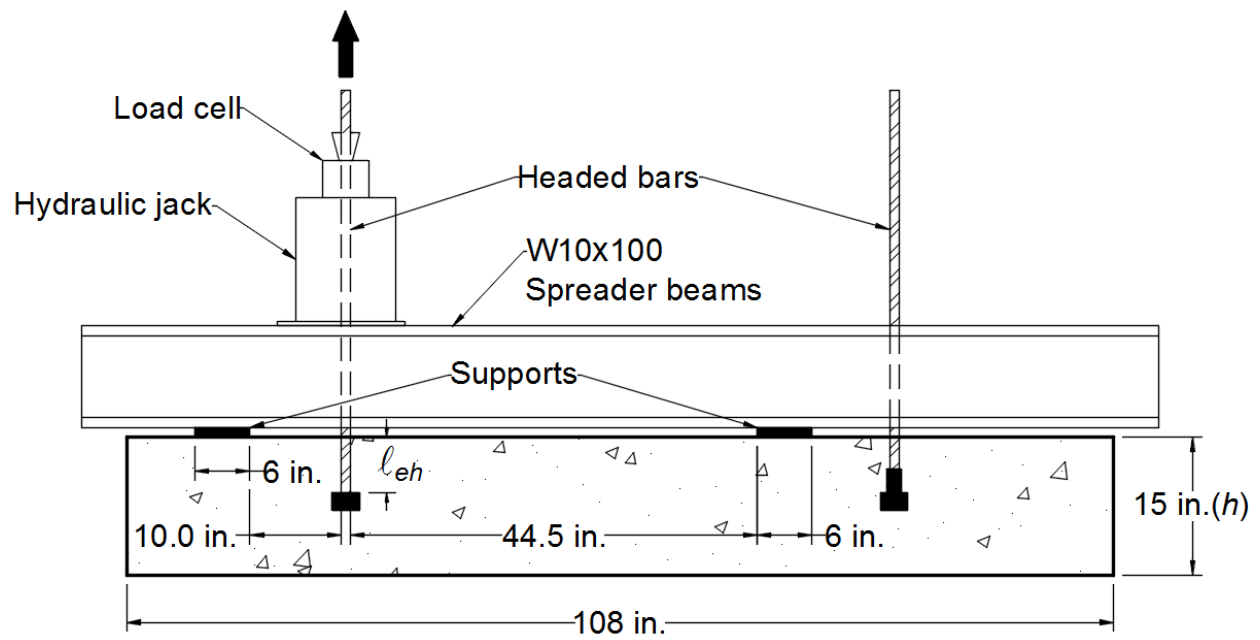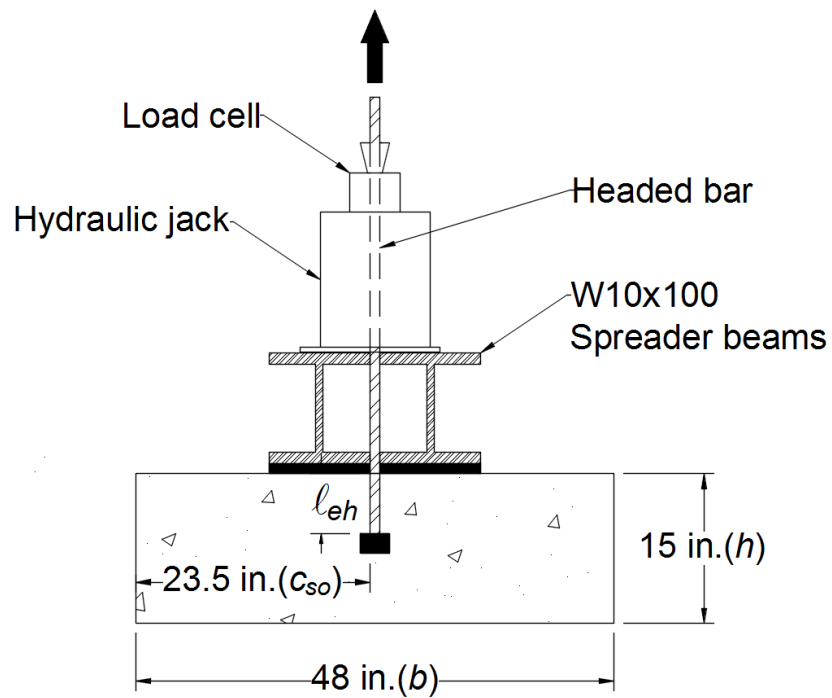
Figure 2.27 Schematic view of shallow embedment pullout test (a) front view, (b) side view

2.4.2 Test Parameters

Bar size: No. 8 bars were used in the study. The bars were fabricated using Grade 120 ASTM A1035 reinforcement.

Concrete compressive strength: The target concrete compressive strengths were 5,000 and 8,000 psi. Concrete mixture proportions are given in Section 2.1.2.

Embedment length: The nominal embedment length was 6 in. for all specimens.

Type of headed bar: All head types listed in Table 2.1 were evaluated with these specimens.

Reaction force placement: The placement of the nearest reaction force varied from 10 to 16.5 in.

Amount of flexural reinforcement: The amount of flexural reinforcement in the slab ranged from none to eight No. 5 bars.

2.4.3 Specimen Designation

The shallow embedment specimen designation followed the convention shown in Figure 2.28. The first and second terms indicate the bar size and the nominal concrete compressive strength, respectively. The third term represents the head type (Table 2.1). The fourth and final terms represent the amount of flexural reinforcement the embedment length in in., respectively. For example, 8-5-S6.5-2#8-6, indicates that the specimen contained No. 8 headed bars cast in concrete with a nominal compressive strength of 5 ksi, a cold-swaged head with a net bearing area of 6.5 times the area of the embedded bar, two No. 8 bars as flexural reinforcement, and a nominal embedment length of 6 in.
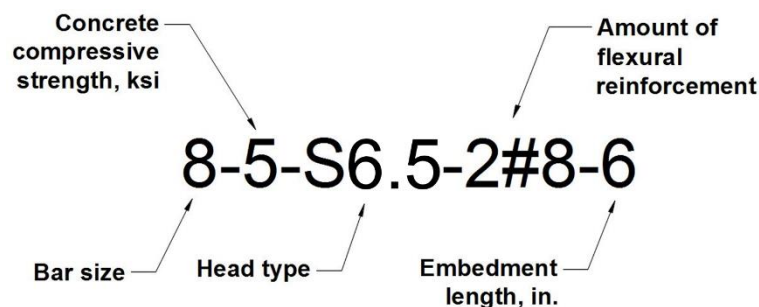
Figure 2.28 Shallow embedment pullout specimen designation

2.4.4 Specimen Fabrication

Formwork for the shallow embedment specimens was constructed from plywood and timber with nominal dimensions of 2×4 in. and are shown in Figure 2.29. Headed bars were supported from underneath the head with a small PVC pipe; a wooden truss above the form kept the bar upright until the concrete had set. Concrete was placed in two layers; each layer was consolidated with a spud vibrator. Specimens were wet cured with burlap and plastic covering the top surface until the compressive strength of the concrete reached 3,000 psi. The forms were then removed and the specimen allowed to dry until testing.

Figure 2.29 Shallow embedment specimen formwork

2.4.5 Test Procedure

The shallow embedment pullout specimens were tested using the self-reacting frame shown in Figure 2.27, which consisted of two steel spreader beams placed along the longest dimension of the pullout specimen on either side of the anchored headed bar. An upward force was applied on the anchored bar using a hydraulic jack placed on top of the spreader beams. A load cell was

mounted on top of the jack to measure the tensile force applied on the bar. Load was applied monotonically, pausing at regular intervals for marking cracks. The tensile load applied to the headed bar was recorded during the test using a load cell placed between the hydraulic jack and the bar grips.

2.5 SPLICE SPECIMENS

2.5.1 Specimen Design

The splice specimens were beams tested using four-point loading to evaluate the splice strength of headed bars. The specimens were designed to ensure a bond failure in the splice region. The test parameters included in this study were the spacing between the lapped bars and the compressive strength of the concrete. Six specimens containing No. 6 headed bars (Figure 2.30) were used to investigate lap splice performance. The 18×20 in. beams contained three bottom cast lapped bars at mid-span with a lap length of $16d_b$ (12 in.). The tension splice length ℓ_{st} (equal to the distance between the bearing faces of adjacent headed bars) was chosen based on the results from headed bar anchorage tests in beam-column joints so that the anticipated failure stress on the bar was above 60 ksi but below the strength of the bar. None of the specimens had confining reinforcement within the splice region.
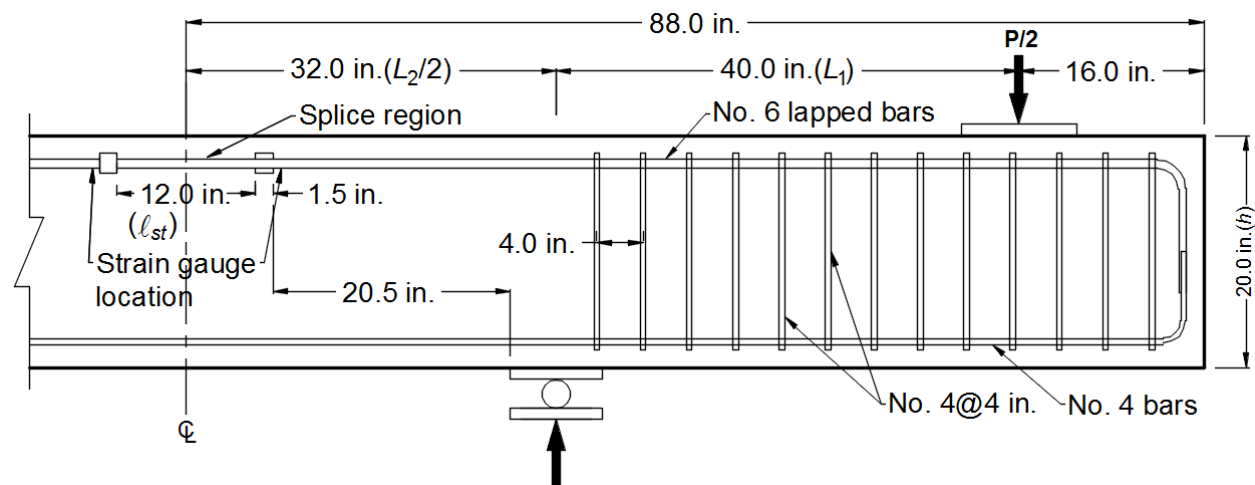
Figure 2.30 Splice test specimen detail and test configuration

Figure 2.30 shows a side view of the specimen and the test configuration. A four-point loading configuration was used to provide a uniform moment and zero shear within the splice

57

region. Sufficient shear reinforcement was provided outside the constant moment region to prevent shear failure. The specimens were inverted (with the splice on top) and loaded symmetrically during the test.

2.5.2 Test Parameters

Bar size: No. 6 bars were used in the study. The bars were fabricated using Grade 120 ASTM A1035 reinforcement.

Concrete compressive strength: The target concrete compressive strengths were 5,000 and 12,000 psi. Concrete mixture proportions are given in Section 2.1.2.

Lap length: The nominal embedment length was 6 in. for all specimens.

Type of headed bar: All specimens had No. 6 S4.0 heads (See Table 2.1).

Splice spacing: Three configurations of splice spacings were used, as shown in Figure 2.31: (i) lapped bars placed with the heads in contact with the adjacent bar, giving a clear spacing of $^1/_2$ in. ($0.67d_b$) and a center-to-center spacing of $1^1/_4$ in. between the lapped bars; (ii) lapped bars with a clear spacing of 1 in. ($1.33d_b$) (center-to-center spacing of $1^3/_4$ in.), the minimum clear distance between the parallel bars in a layer required by ACI 318 for the ¾-in. maximum size aggregate used in the concrete; and (iii) lapped bars spaced equally along the width of the beam giving a clear spacing of $1^7/_8$ in. ($2.55d_b$) and a center-to-center spacing of $2^5/_8$ in.
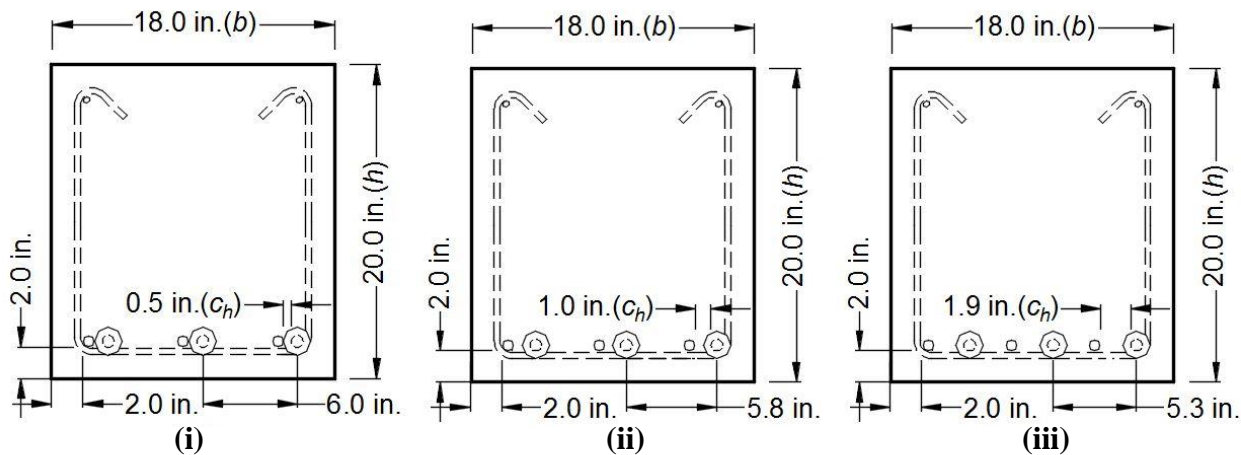
Figure 2.31: Splice configurations investigated in this study

58

2.5.3 Specimen Designation

The designation for the splice specimens was chosen so as to describe the key test parameters (Figure 2.32), as follows. The first number (in parenthesis) represents the number of lapped bars. The second and third numbers indicate the ASTM size designation for the bars and nominal concrete compressive strength in ksi, respectively. The fourth and fifth terms show the head type (Table 2.1) and the nominal lap length, in in., respectively. The last term indicates the clear spacing between the bars in inches. For instance, specimen (3)-6-5-S4.0-12-0.5 contained three No. 6 headed lapped bars in 5 ksi nominal compressive strength concrete. The headed bars had cold-swaged heads with a net bearing area equal to four times the bar area, a lap length of 12 in., and a clear spacing between the lapped bars of 0.5 in.
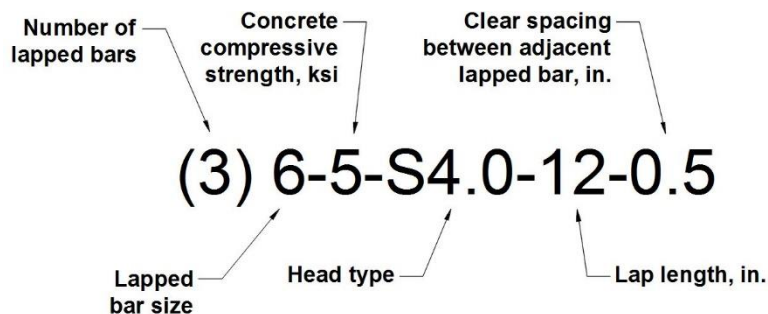
Figure 2.32 Splice specimen designation

2.5.4 Specimen Fabrication

The specimens were cast in wooden forms. The bottom-cast, headed-bar splices were placed symmetrically at the midspan of the beam. The concrete was placed in two lifts, with internal vibration after each lift. After finishing, the specimens were covered with wet burlap and plastic to cure. Forms were removed once the concrete compressive strength reached 3,000 psi. Specimens with a target concrete compressive strength of 5,000 psi were allowed to air dry; specimens with a target compressive strength of 12,000 psi were wrapped in wet burlap and wet-cured for approximately one month before drying and testing.

2.5.5 Test Procedure

Splice specimens were inverted and placed on supports prior to testing (pin and roller supports spaced at 64 in.). Placing the splices on top facilitated inspection and marking of cracks in the splice region during tests. The specimens were then leveled, and the location of the loading

points from the supports and the span length were measured. Loads were applied symmetrically at the ends of the specimen using spreader beams, each connected by two threaded rods to dual-acting center-hole hydraulic jacks mounted under the strong floor in the laboratory, as shown in Figure 2.33. The hydraulic jacks were mounted directly to the strong floor and were not supported by the spreader beams. The loading frame was designed to transfer the maximum anticipated load to the specimen without undergoing significant deflection during the test. Two concrete blocks were placed symmetrically in between the two loading frames to serve as the middle supports (Figure 2.33a). High-strength gypsum cement paste used to level the blocks and prevent sliding during the test. A 2.5 in. diameter steel roller was placed on a $1\times10\times24$ in. steel base plate (also leveled using the gypsum cement) and mounted on each block. The roller on one of the concrete blocks was fixed against motion, simulating a pinned support. The roller on the other concrete block was free to roll, simulating a roller support. The supports were placed at least the depth of the beam away from the splice region. Specimens were placed symmetrically on the supports; the nominal distance between the loading point and nearest support was 40 in., and the nominal length of the central span was 64 in. The actual span measurements were recorded before each test; in all cases, actual measurements were within 0.5 in. of the nominal measurements.

Prior to testing, a small load was initially applied to the beam to ensure free motion of all portions of the test apparatus. During testing, load was applied monotonically with periodic pauses for marking cracks. Crack marking was continued until the load reached about 70% of the expected failure load, after which the specimen was loaded until failure.
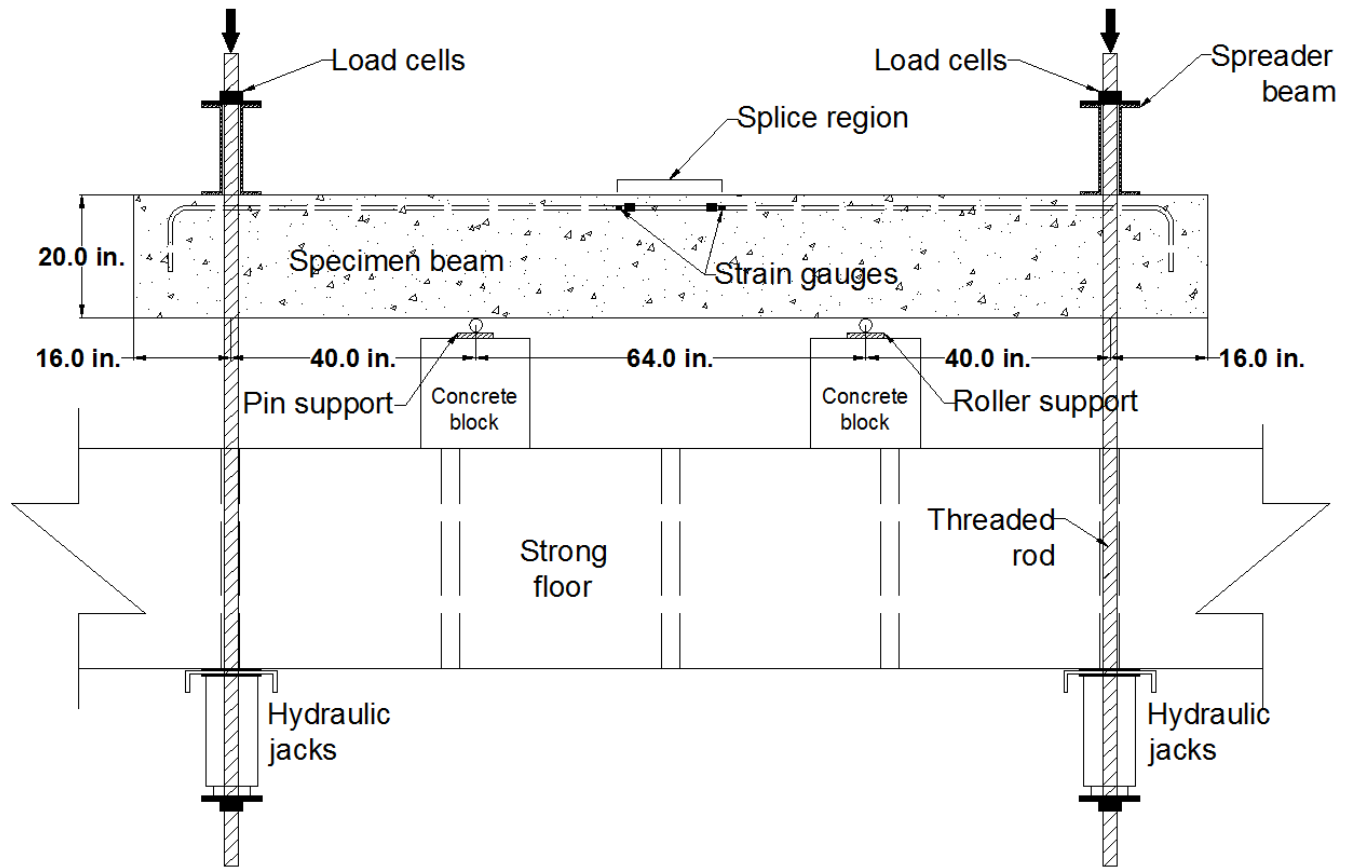
Figure 2.33a Schematic view of splice test (front view)
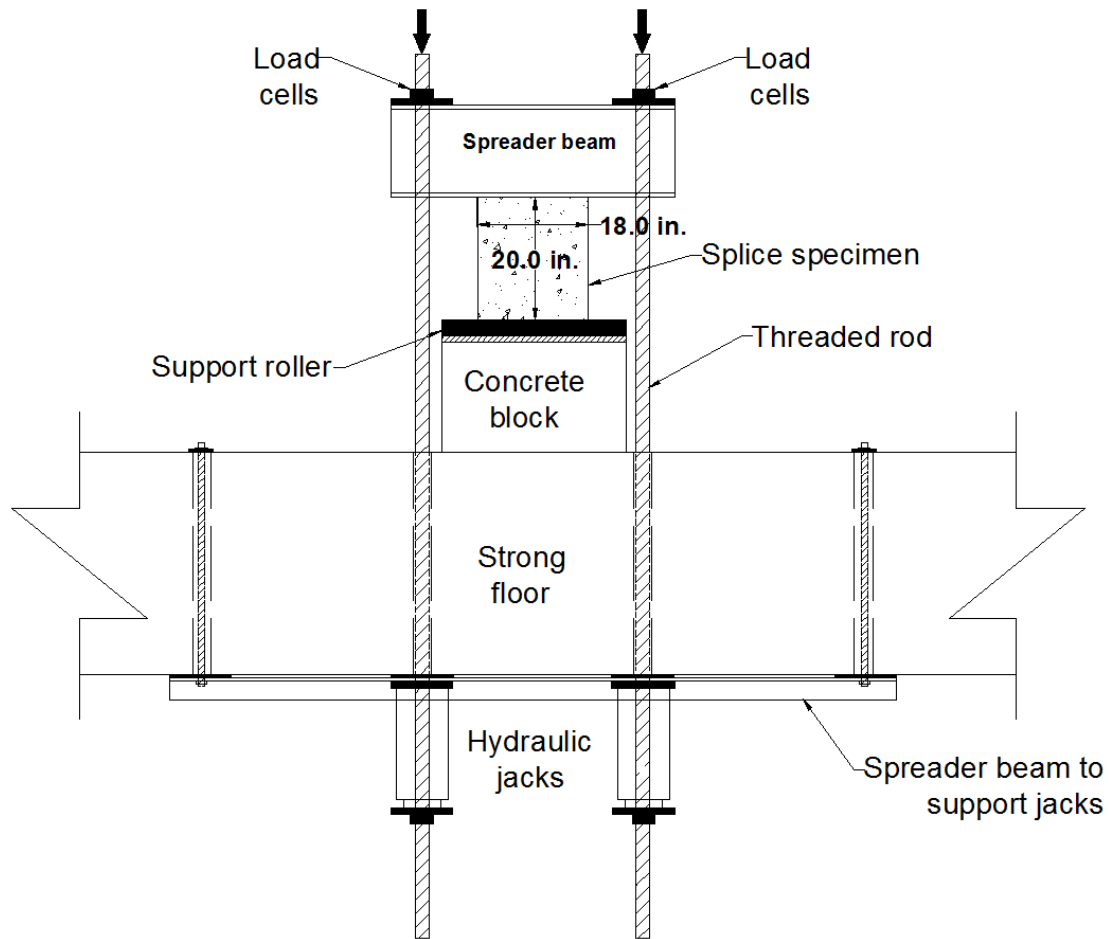
Figure 2.33b Schematic view of splice test (side view*)*

2.5.6 Specimen Instrumentation

Specimens were instrumented to measure the load, displacement, rotation, and maximum crack width on the beam, as well as the strain on the spliced bars. The loads applied through the hydraulic jacks were measured using center-hole load cells installed above the spreader beams on each threaded rod. An infrared tracking system was used to measure the displacement, rotation, and crack width during testing. Infrared markers (as shown in Figure 2.25) were installed along one of the vertical faces of the specimen so that the displacement and rotation at the loaded ends and midspan could be measured. In the first series of splice test specimens, strains in the lapped bars were measured using strain gauges mounted 1 in. outside the splice region (one on an edge bar and another on the middle bar). In the second series, a strain gauge was mounted 1 in. outside the splice region on each of the lapped bars. Load and strain measurements were recorded using a single data acquisition system. Displacements and rotations were recorded using the separate

optical tracking system. An effort was made to start both systems simultaneously to avoid mismatch of load/strain and corresponding displacement data from the tests. The data were synchronized by aligning the load and displacement values at failure (the sudden drop in load after the specimen fails also causes an abrupt change in deflection). The data sampling rate for both systems was 2 Hz. Prior to testing, the beam was centered on the loading system and all measurement systems connected. To avoid interference with the displacement readings, infrared markers were installed on the vertical face of the specimen opposite to the face where cracks were marked.

2.6 SUMMARY OF TEST PROGRAM

This section presents a summary of the test program for this study. Detailed information about the beam-column joint specimens, CCT node specimens, shallow embedment specimens, and splice specimens are presented in Chapters 3, 4, 5, and 6, respectively.

2.6.1 Beam-Column Joint Specimens

A total of 202 beam-column joint specimens were tested, with nominal embedment lengths ranging from 4.0 to 19.25 in. Actual concrete compressive strengths ranged from 3,960 to 16,030 psi, and bar stresses at failure ranged from 26,100 to 153,200 psi. Table 2.6 gives the number of specimens tested with each bar size.

Table 2.6: Test Program for Beam-Column Joint Specimens

Bar size	Confining Reinforcement	# of Specimens	
		Two Head	Multiple Head
No. 5	Without	8	2
	With	11	4
No. 8	Without	35	30
	With	43	31
No. 11	Without	11	6
	With	14	7

2.6.2 CCT Node Specimens

A total of 10 CCT node specimens were tested, with nominal embedment lengths ranging from 9.0 to 14.0 in. Actual concrete compressive strengths ranged from 4,630 to 5,750 psi, and bar

stresses at failure ranged from 101,300 to 160,700 psi. Table 2.7 gives the number of specimens tested in terms of number of headed bars in the node.

Table 2.7 Test Program for CCT Node Specimens

Bar size	Number of Headed Bars	# of Specimens
No. 8	2	4
	3	6

2.6.3 Shallow Embedment Specimens

A total of 32 shallow embedment specimens were tested, all with nominal embedment lengths of 6.0 in. Actual concrete compressive strengths ranged from 4,200 to 8,620 psi, and bar stresses at failure ranged from 49,500 to 117,000 psi. Table 2.8 gives the number of specimens tested in terms of amount of flexural reinforcement in the slab.

Table 2.8: Test Program for Shallow Embedment Specimens

Bar size	Amount of Reinforcement	# of Specimens
	0	2
	2 No. 8	4
	2 No. 5	1
No. 8	4 No. 5	3
	6 No. 5	14
	8 No. 5	8

2.6.4 Splice Specimens

A total of six splice specimens were tested, all with nominal lap lengths of 12 in. Actual concrete compressive strengths ranged from 6,330 to 11,070 psi, and bar stresses at failure ranged from 75,000 to 83,600 psi. Table 2.9 gives the number of specimens tested in terms of spacing between spliced bars.

Table 2.9: Test Program for Splice Specimens

Bar size	Clear Spacing Between Spliced Bars[1], in.	# of Specimens
	0.5	2
No. 6	1	2
	1.9	2

[1]See Figure 2.31

CHAPTER 3: TEST RESULTS FOR BEAM-COLUMN JOINT SPECIMENS

The general behavior of the beam-column joint specimens as observed during the test is discussed in this chapter, including cracking patterns, failure types, and strain/stress development in headed bars and confining reinforcement within the joint region. Test results for 202 specimens from 20 test groups are summarized at the end of the chapter. The effects of test parameters, including head size, side cover, embedment length, confining reinforcement, bar size, concrete compressive strength, and spacing between the bars, will be discussed in Chapter 7 along with the development of descriptive equations that capture the anchorage strength of headed bars.

3.1 CRACKING PATTERNS

Although cracking differed in terms of quantity and shape in different specimens, overall crack propagation followed similar patterns. First, a horizontal crack initiated on the front face of the column at the level of the headed bars, extending slightly towards both sides of the column (Figure 3.1a). As the load increased, the horizontal cracks on the column front face connected between the bars, occasionally accompanied by small radial cracks extending from the bars. In the meantime, the horizontal crack on the side of the column continued to grow towards the position of the head, with diagonal cracks branching from the horizontal crack towards the front face (Figure 3.1b). With increasing load, more horizontal cracks due to column flexure began to appear on the front face below and/or above the level of the headed bars, extending slightly around the side of the column. On the side of the column, a large diagonal crack occurred within the joint region, extending from the position of the head towards the bearing member (the compression region of the virtual beam); the crack above the joint region extended diagonally towards the upper compression member or upward towards the top of the column (Figure 3.1c). As load further increased, the existing cracks on the side became wider and continued growing towards the front face of the column, with new cracks branching from the existing cracks on both side and front faces (Figure 3.1d). The amount of cracking was directly related to the confining reinforcement level within the joint region: specimens with confining reinforcement generally exhibited more cracks prior to failure than those without confining reinforcement.

(a)   (b)

(c)   (d)
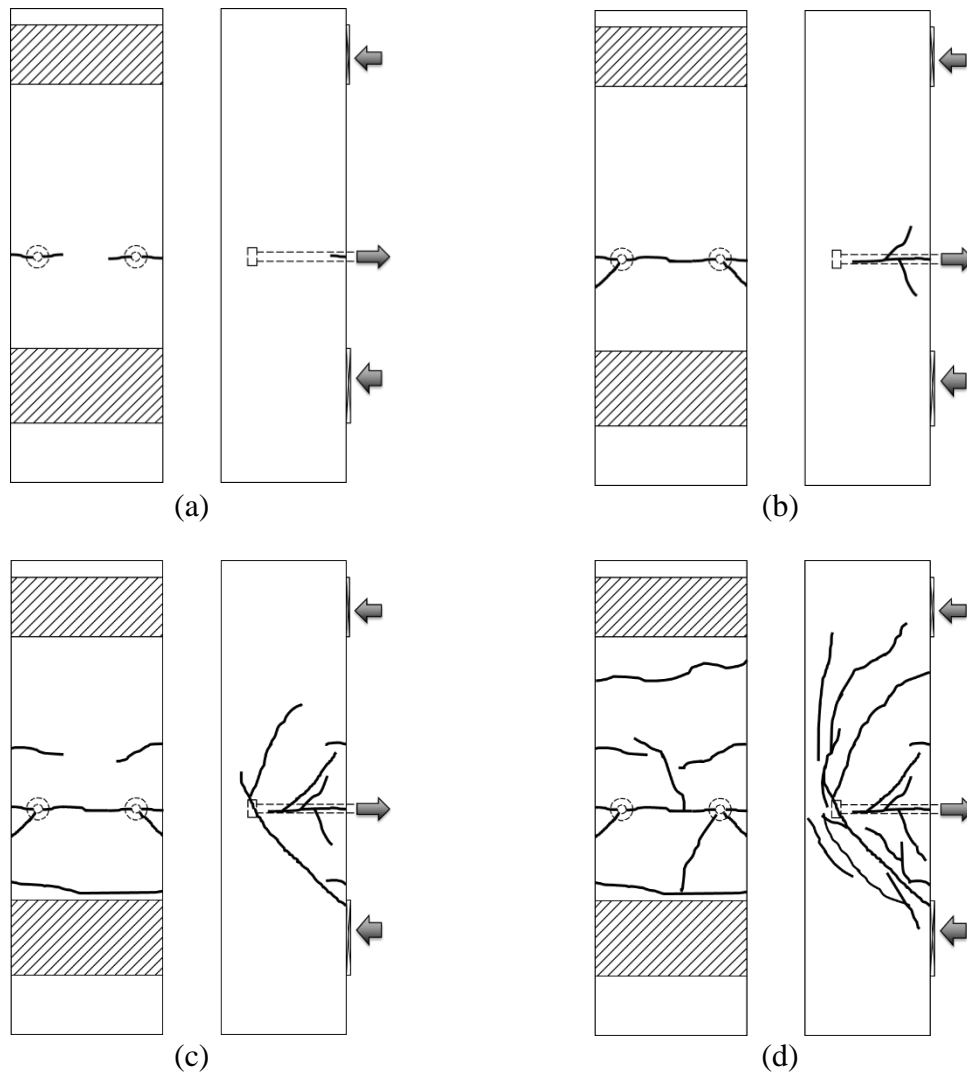
Figure 3.1 Typical crack propagation (front and side views)

The cracking patterns for deep-beam specimens (which had relatively short embedment lengths compared to the distance from the center of the headed bar to the top of the bearing member) were slightly different from those of the conventional specimens shown above, with a large diagonal crack extending at an angle of about 35° with respect to the direction of the column longitudinal bars, from the bearing head towards the top of the bearing member for specimens both without and with confining reinforcement. For the conventional specimens, the large diagonal crack connected between the bearing head and the top of the bearing member, with an angle usually flatter than the large diagonal crack observed in deep-beam specimens (that is, greater than 35° with respect to the direction of column longitudinal bars). A description of deep-beam specimens, along with the associated cracking patterns, is presented in Section 7.4.4.

3.2 FAILURE TYPES

The different types of anchorage failure observed are discussed in this section. Of the 202 beam-column joint specimens tested, 196 exhibited an anchorage failure, as designed. An anchorage failure is defined as failure of the concrete around the head, accompanied by slip and loss of capacity of the headed bar. Two modes of failure were observed, concrete breakout and side-face blowout. Headed bars with large obstructions (O4.5, O9.1, and O12.9) that did not meet the requirement in ASTM A970 for HA heads exhibited similar failure types as those with HA heads. Deep-beam specimens all exhibited concrete breakout failure.

Six specimens were not loaded to failure because of safety concerns; either the bar was loaded to near its fracture strength or the testing equipment had reached its capacity. In this study, "bar yielding" is used to describe the specimens that did not fail in anchorage, although some specimens with anchorage failure had bars loaded beyond the nominal yield strength (120 ksi).

3.2.1 Concrete Breakout

Concrete breakout was observed in the majority (149) of the specimens. It occurred when concrete in front of the head was pulled out and separated from the specimen. Two types of failure surface were observed: the first type was cone-shaped, as shown in Figure 3.2a; the second type was similar to the first within the joint region, but above the joint region, a crack extended from

the head towards the top of the column, as shown in Figure 3.2b, which resulted in various degrees of splitting of the column back cover. Occasionally, the longitudinal splitting crack (Figure 3.2b) did not appear until the joint was near failure; in these instances, the longitudinal crack appeared suddenly and grew rapidly. However, it was more common for the longitudinal crack to propagate slowly throughout the test.

(a)   (b)
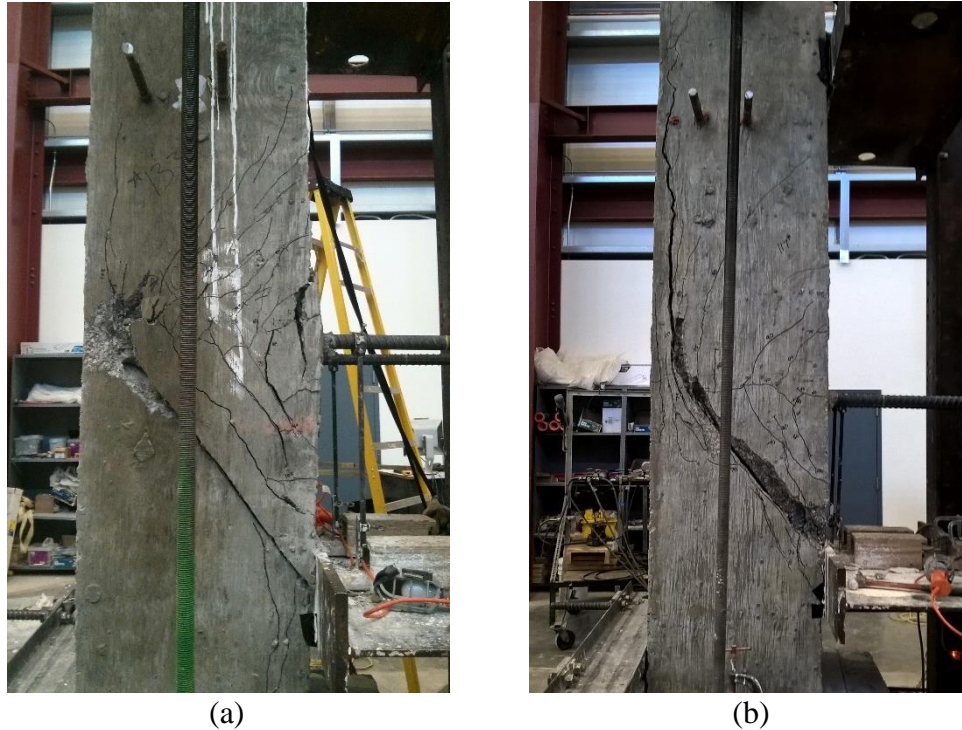
Figure 3.2 Two types of breakout failure (a) cone-shaped (b) back cover splitting

Table 3.1 summarizes the number of specimens exhibiting each of the two types of breakout failure. Specimens exhibiting side-face blowout failure are not included in the table. If a specimen with breakout failure exhibited both types of cracking above the joint region, the maximum crack width was used to determine the category of the failure surface. The table is based on the available record for the test specimens. The failure type of a specimen (breakout failure or side-face blowout) was recorded at the time of the test, while the type of breakout failure (cone-shaped failure surface or back cover splitting) was determined after the test and based on the photo records. One early specimen that was recorded as breakout failure but lacked relevant photo records is not included in Table 3.1.

Table 3.1 Summary of Specimens with Different Types of Breakout Failure

Specimen details		Number with cone-shaped failure surface	Number with back cover splitting
Confining reinforcement level	Spacing[*]		
Without confining reinforcement	Closely-spaced	12	29
	Widely-spaced	21	12
With confining reinforcement	Closely-spaced	17	21
	Widely-spaced	25	11
All		75	73

[*] "Closely-spaced" refers to specimens with a center-to-center bar spacing less than $8d_b$; "widely-spaced" refers to specimens with a center-to-center bar spacing greater than or equal to $8d_b$.

As shown in Table 3.1, about half (75 out of 148) of the specimens exhibiting a breakout failure had a cone-shaped failure surface. Cone-shaped failure surfaces were more likely to occur in specimens with widely-spaced bars, while back cover splitting tended to occur in specimens with closely-spaced bars and no confining reinforcement within the joint region. A closer look into the test data reveals no direct relationship between the shape of the failure surface and the anchorage strength of headed bars exhibiting a concrete breakout failure.

3.2.2 Side-Face Blowout

Of the 196 specimens that had an anchorage failure, 47 exhibited side-face blowout. Side-face blowout occurred when the movement of the head resulted in local damage to the side cover around the head, as shown in Figures 3.3 and 3.4. The damage was often characterized by separation of the cracked concrete cover (Figure 3.3). Sometimes, the failure was so sudden and explosive that the side cover was blown out, thus exposing the head (and confining reinforcement if any), as shown in Figure 3.4.

(a)   (b)

Figure 3.3 Side-face blowout (a) side view, (b) back view

(a)   (b)

Figure 3.4 Explosive side-face blowout (a) side view, (b) back view

Specimens with a concrete breakout failure might also exhibit damage on the side, especially along the dominant crack within the joint region. In such cases, however, failure was

characterized as side-face blowout only if the failure appeared to be the direct result of local damage of side cover around the head. Specimens with side-face blowout did not exhibit splitting cracks above the joint region.

3.2.3 Secondary Failures

Often, a secondary failure occurred in conjunction with concrete breakout or side-face blowout failure. Secondary failures tended to be one of two types – local front breakout or back cover spalling. Local front breakout (Figure 3.5a) was characterized by a small portion of concrete cover near the bar being pulled out of the column front face. Back cover spalling occurred when the splitting crack above the joint region (Figure 3.5b) widened, with the concrete cover from the back of the column separating from the column.

(a)   (b)
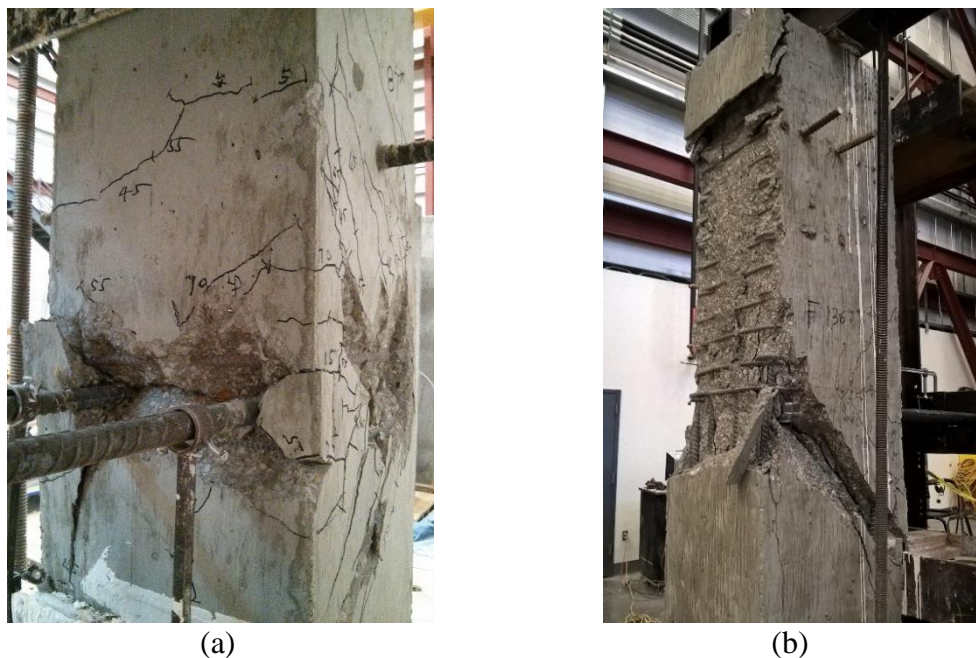
Figure 3.5 Secondary failure types (a) local front breakout, (b) back cover spalling

3.3 STRAIN DEVELOPMENT IN HEADED BARS AND CONFINING HOOPS

As described in Section 2.2.6, strain gauges were used to monitor the change in strain in the headed bars and confining reinforcement within the joint region for the specimens listed in Table 2.5. For the two-bar specimens, strain gauges were mounted on one headed bar and all confining hoops on the same side of the column as the instrumented headed bar. For the three-bar

specimens, strain gauges were also attached to the middle bar. Two strain gauges were mounted on each headed bar, one 1.5 in. from the bearing face of the head (identified as the "head" gauge) and the other 1 in. from the front face of the column (identified as the "bar" gauge). For the confining hoops, one strain gauge was mounted in the middle of the leg parallel to the headed bar. In this section, the strain in the headed bars and confining hoops is discussed. The maximum strain and the corresponding stress for all specimens listed in Table 2.5 are summarized.

3.3.1 Strain Development in Headed Bars and Hoops for Specimens with Confining Reinforcement

Figure 3.6 shows the strain development for a specimen containing two No. 8 headed bars confined by five No. 3 hoops spaced at $3d_b$ (8-8-S14.9-5#3-i-2.5-3-8.25) within the joint region. The locations of the strain gauges are shown in Figure 3.6a. Figures 3.6b and 3.6c show the increase in strain with the increase in average load (total load applied on the specimen divided by the number of headed bars), respectively, for the headed bar and the five hoops.

As shown in Figure 3.6b, the strain in the headed bar 1 in. from the front face of the column increased almost linearly with increasing load during the test. The strain in the headed bar 1.5 in. from the bearing face of the head increased slowly at loads below 20 kips, as indicated by the nearly vertical slope of the curve. The strain increased faster at loads above 20 kips, but the strain remained below the value near the front face of the column. As the specimen approached failure, the strain near the head increased rapidly from 0.003 to 0.005, decreasing the difference in strain at the two locations along the length of the bar. At the peak load, the strain in the bar near the head was only 0.0006 less than that near the column front face. The difference in strain along the length of the bar reflects the force transferred by bond along the bar. The rapid decrease in this difference observed near the peak load indicates a sudden loss of bond and the transfer of load from the front of the bar to the head.

head   bar

S1
S2
S3
S4
S5

(a)

(b)   (c)
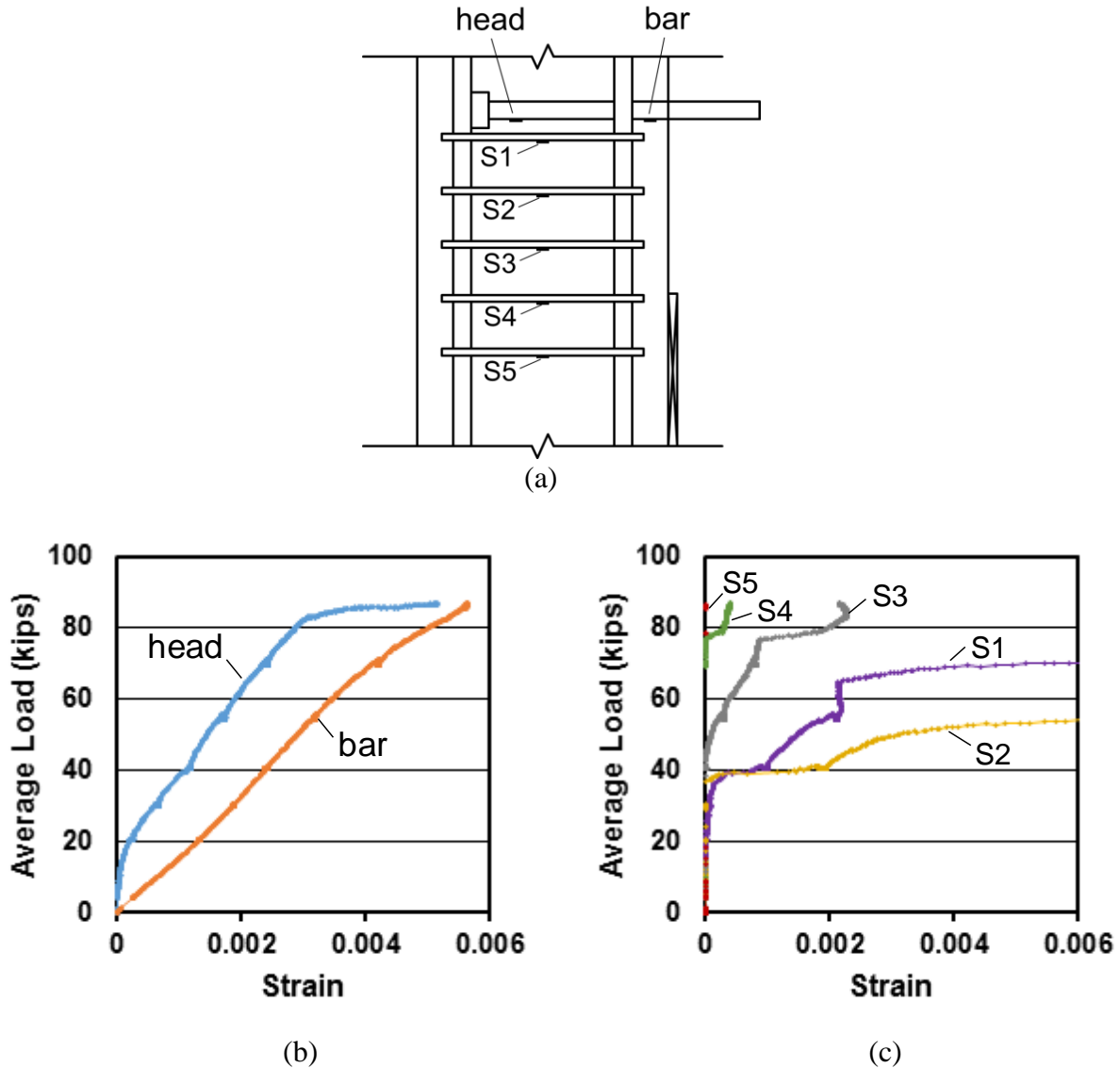
Figure 3.6 Average load per headed bar versus strain in headed bar and confining reinforcement for specimen 8-8-S14.9-5#3-i-2.5-3-8.25 (a) strain gauge location, (b) strain in headed bar, (c) strain in confining reinforcement

The load-strain curves for the hoops shown in Figure 3.6c differ depending on hoop location. The top two hoops (S1 and S2) exhibited a sudden increase in strain at an applied load of about 40 kips, increasing from 0.0002 to 0.0011 and 0.0020, respectively. The strain at S1 and S2 continued to increase as the applied load increased, and reached as much as 0.022 and 0.027 during the test (not shown in the figure). The third hoop (S3) did not experience strain until the load reached 50 kips, after which the strain increased gradually until the specimen approached failure, ultimately reaching 0.0021 at the peak load. The bottom two hoops (S4 and S5, located in the

compression region of the simulated joint), however, exhibited minimal strain increase throughout the test. Although the strain gauges only recorded strain at the middle of each hoop and that the strain in the hoops may vary depending upon the cracking pattern, the overall difference in the strains observed for the hoops indicates that hoops placed close to a headed bar are more effective in confining cracks (and thus improving anchorage strength) than hoops located further from the bars.

Figure 3.7 shows the strain for a specimen containing two No. 11 headed bars confined by six No. 3 hoops spaced at $3d_b$ (11-5-F3.8-6#3-i-2.5-3-17), with the locations of the strain gauges shown in Figure 3.7a. Figures 3.7b and 3.7c, respectively, show the increase in strain with an increase in average load for the headed bar and the six hoops.

The load-strain curves in Figure 3.7b show that the strain in the headed bar near the front face of the column had a nearly linear relationship with an increase in applied load, the same trend observed for No. 8 bars in Figure 3.6b. The strain in the bar near the head began to increase once the load reached about 50 kips, reaching a value of 0.0018 at the peak load. In contrast to the observations for No. 8 bars (Figure 3.6b), the bond force along the bar, represented by the difference between the two strain readings, continued to grow throughout the test; the difference in strain between the two gauges was 0.002 at the peak load, much greater than the value (0.0006) observed for No. 8 bars (Figure 3.6b).

The load-strain curves for the hoops shown in Figure 3.7c are again a function of the hoop location. The hoop closest to the head (S1) started to exhibit strain at an applied load of about 65 kips, with a steady increase in strain up to 0.0022 at the peak load. Hoops S2, S3, and S4 experienced a sudden increase in strain at a load of about 100 kips, increasing to values of about 0.001, 0.002, and 0.001, respectively, and ultimately to maximum strains of 0.017, 0.014, and 0.002 at the peak load (the maximum strains for S2 and S3 are not shown in the figure). The two bottom hoops (S5 and S6, located near the top of the compression member) exhibited minimal strain throughout the test. Once again, the strain development for the six hoops indicates that the effectiveness of confining hoops is directly related to their locations – hoops became less effective when located further from headed bars.
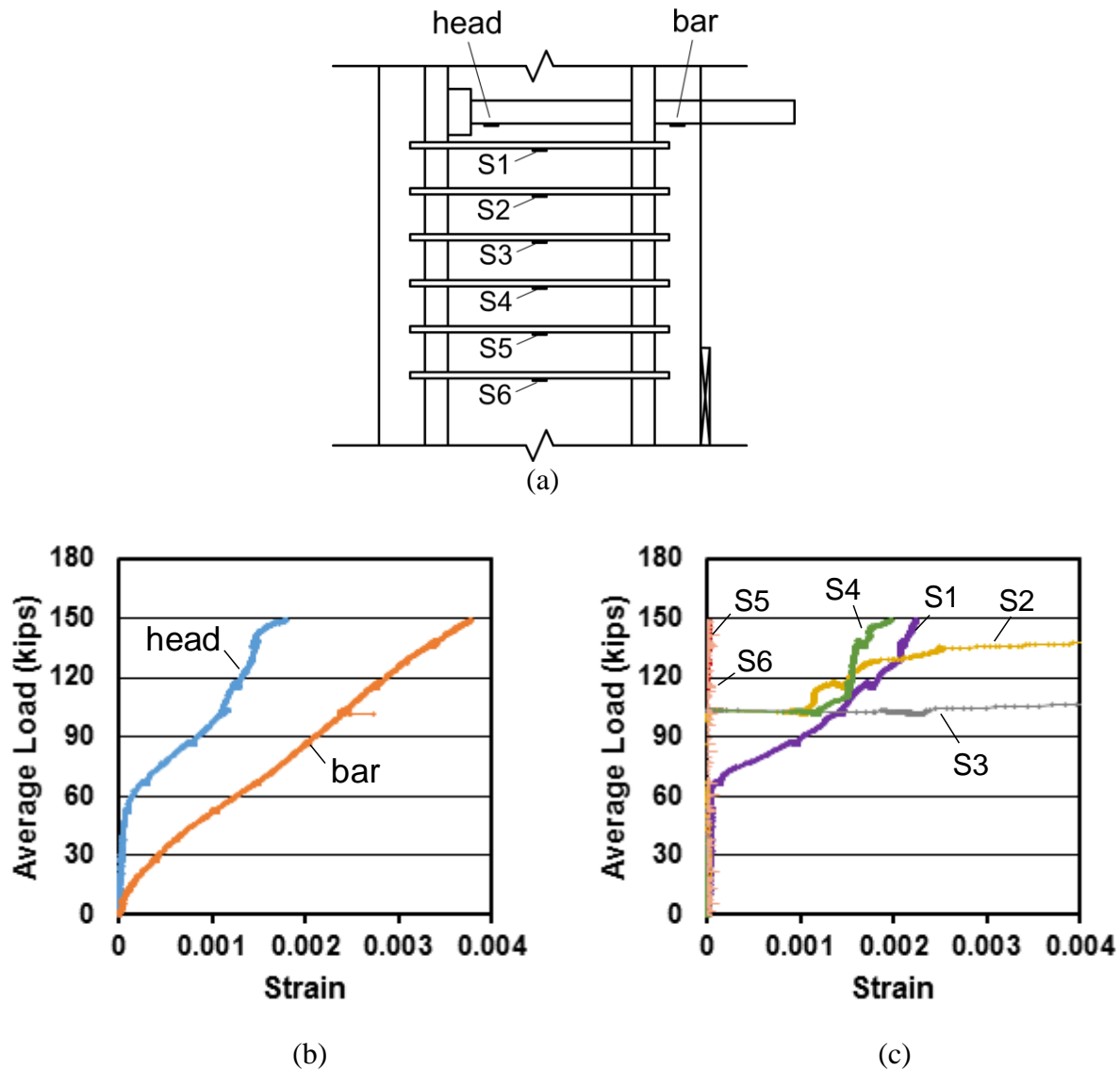
Figure 3.7 Average load per headed bar versus strain in headed bar and confining reinforcement for specimen 11-5-F3.8-6#3-i-2.5-3-17 (a) strain gauge location, (b) strain in headed bar, (c) strain in confining reinforcement

3.3.2 Strain Development in Headed Bars for Specimens without Confining Reinforcement

Figure 3.8 shows the load-strain curves for two specimens without confining reinforcement, one containing No. 8 headed bars (Figure 3.8a) and the other containing No. 11 headed bars (Figure

75

3.8b). As in the other specimens, the strain gauges were placed 1.5 in. from the bearing head and 1 in. from the front face of the column.

8-8-S14.9-0-i-2.5-3-8.25

(a)

11-5-F8.6-0-i-2.5-3-14.5

(b)
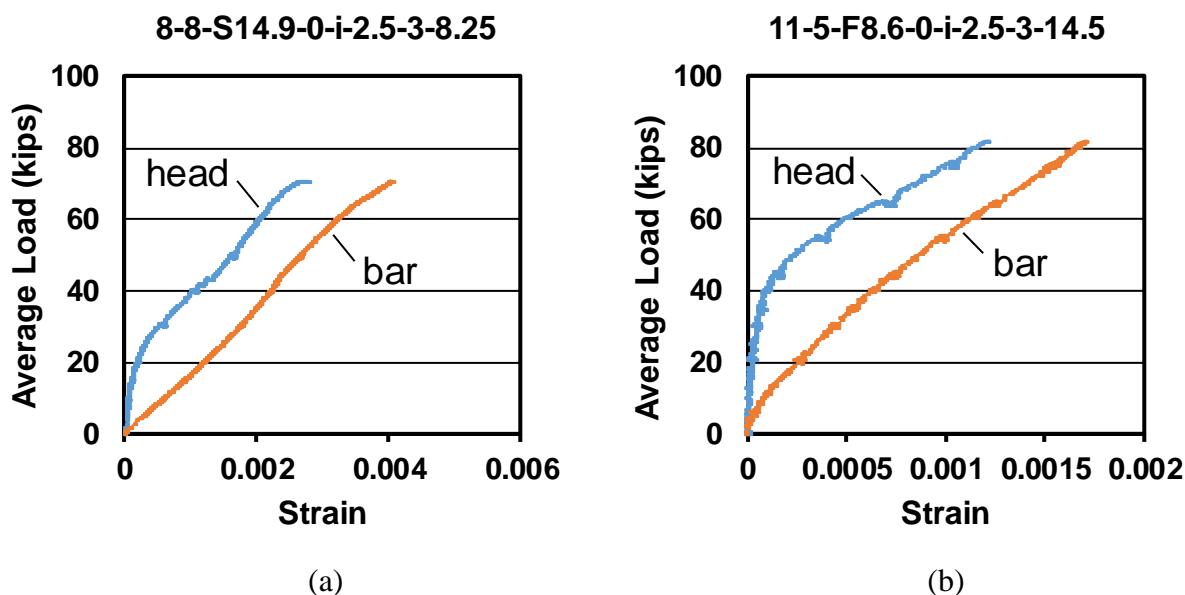
Figure 3.8 Average load per headed bar versus strain in headed bars for specimens without confining reinforcement (a) specimen 8-8-S14.9-0-i-2.5-3-8.25, (b) specimen 11-5-F8.6-0-i-2.5-3-14.5

The load-strain curves in Figure 3.8 are generally similar to those for the headed bars with confining reinforcement. The strains in headed bars near the front face of the column exhibited a nearly linear relationship with the applied load for both specimens. The strains in the No. 11 headed bars were less than one-half of the values for the No. 8 and bars. For the strains in the headed bars near the head, the changing slope indicates that the strain development was slow initially (below loads of 20 and 40 kips for the No. 8 and No. 11 bars, respectively), but increased more rapidly as the load increased. Once strain was recorded by both strain gauges on the bars, the difference in strain measured by the two gauges remained approximately constant (about 0.0013 for the No. 8 bar and about 0.0005 for the No. 11 bar), indicating that the portion of the applied load carried by bond remained nearly constant up to failure and that the increase in the applied load was carried by the head.

3.3.3 Maximum Strain Measured and Corresponding Stress

Tables 3.2 and 3.3 summarize the maximum strain measured during the test and the corresponding stress obtained from stress-strain curves for the reinforcing steel used in the study. The stress-strain curves are shown in Appendix B. Table 3.2 gives the strain and stress results for the headed bars. The gauge locations, "head" and "bar", are illustrated in Figures 3.6a and 3.7a, with "(middle)" following in "head" or "bar" in Table 3.2 to indicate a middle bar. For comparison, Table 3.2 also shows the ratio of the stress in the bar near the head to the stress in the bar near the front face of the column. Table 3.3 gives the strain and stress results in the confining reinforcement. The first two specimens listed in Table 3.3 contained two No. 3 hoops as confining reinforcement, and the two hoops were placed at locations corresponding to the second and fourth hoops in a specimen with No. 3 hoops spaced at $3d_b$ (referred to as S2 and S4 in Figure 3.7a). Results for strain gauges that were damaged during casting or testing are not shown in the tables.

The values of the ratio (stress in the bar near the head to stress in the bar near front face) shown in Table 3.2 indicate that the stress in the bar near the head was 4% to 64% less than the stress in the bar near the front face of the specimen, with the exception of the middle bar in specimen (3@5.35)11-5-F8.6-0-i-2.5-3-14.5, which had a stress near the head 19% greater than the stress near the front face at the peak load. For that middle bar, the bar stress based on the strain gauge reading near the front face of the specimen was 26.3 ksi, much less than the average value 39.6 ksi (based on the applied load on the bar divided by the nominal area of the bar). It is likely that the greater stress in the bar near the head than the stress near the front face was due to a malfunction of the strain gauge attached near the front face. For the three-bar specimens without confining reinforcement, the stresses in the side bar and middle bar were approximately the same at the peak load for both locations (with the exception of specimen (3@5.35)11-5-F8.6-0-i-2.5-3-14.5). For the three-bar specimens with confining reinforcement, the middle bar tended to experience higher stress than the side bar near the front face, while the stresses near the head for the middle bar and side bar were similar in magnitude. Given the small number of test specimens and the variation in the test data, the trend is not clear as to differences between side bar and middle bar in load transfer along the bar.

Table 3.2 Maximum strain and stress in headed bars

Specimen	Gauge Location[‡]	Strain	Stress (ksi)	Ratio[†]
8-8-S14.9-0-i-2.5-3-8.25	Head	0.00279	73.5	0.72
	Bar	0.00406	102.2	
11-8-F3.8-0-i-2.5-3-14.5	Head	0.00090	24.4	0.49
	Bar	0.00182	49.3	
11-5-F3.8-0-i-2.5-3-12	Head	0.00097	26.3	0.68
	Bar	0.00143	38.8	
11-5-F3.8-0-i-2.5-3-17[‡]	Head	0.00149	40.4	N/A
11-5-F8.6-0-i-2.5-3-14.5	Head	0.00122	33.1	0.71
	Bar	0.00171	46.4	
(3@5.35)11-5-F8.6-0-i-2.5-3-14.5	Head	0.00116	31.5	0.87
	Bar	0.00133	36.1	
	Head (middle)	0.00115	31.2	1.19
	Bar (middle)	0.00097	26.3	
(3@5.35)11-8-F3.8-0-i-2.5-3-14.5	Head	0.00053	14.4	0.41
	Bar	0.00130	35.3	
	Head (middle)	0.00051	13.8	0.38
	Bar (middle)	0.00133	36.1	
8-8-S14.9-5#3-i-2.5-3-8.25	Head	0.00517	105.4	0.96
	Bar	0.00564	109.3	
8-8-O12.9-5#3-i-2.5-3-9.5[*]	Head	0.00039	11.2	N/A[*]
	Bar	0.00489	107.2	
11-8-F3.8-2#3-i-2.5-3-14.5	Head	0.00156	42.3	0.67
	Bar	0.00234	63.5	
11-8-F3.8-6#3-i-2.5-3-14.5	Head	0.00129	35.0	0.54
	Bar	0.00237	64.3	
11-5-F3.8-6#3-i-2.5-3-12	Head	0.00138	37.4	0.94
	Bar	0.00147	39.9	
11-5-F3.8-6#3-i-2.5-3-17	Head	0.00179	48.5	0.47
	Bar	0.00378	102.5	
11-5-F8.6-6#3-i-2.5-3-14.5	Head	0.00168	45.6	0.95
	Bar	0.00177	48.0	
(3@5.35)11-5-F8.6-6#3-i-2.5-3-14.5	Head	0.00119	32.3	0.79
	Bar	0.00151	40.9	
	Head (middle)	0.00134	36.3	0.66
	Bar (middle)	0.00203	55.0	
(3@5.35)11-8-F3.8-2#3-i-2.5-3-14.5	Head	0.00078	21.2	0.48
	Bar	0.00162	43.9	
	Head (middle)	0.00084	22.8	0.45
	Bar (middle)	0.00188	51.0	
(3@5.35)11-8-F3.8-6#3-i-2.5-3-14.5[‡]	Head	0.00069	18.7	0.36
	Bar	0.00193	52.3	
	Head (middle)	0.00057	15.5	N/A

[‡] Refer to Figure 3.6a or Figure 3.7a
[†] Ratio of stress in the bar near the head to the stress in the bar near the front face of the column
[‡] Specimen had a missing strain gauge
[*] One strain gauge was attached on the obstruction of the head; stresses at the two locations are not comparable

Table 3.3 Maximum strain and stress in confining reinforcement

Specimen	Gauge Location[†]	Strain	Stress (ksi)	Note
11-8-F3.8-2#3-i-2.5-3-14.5	S2	0.0134	72.1	yielded
	S4	0.0005	15.3	-
(3@5.35)11-8-F3.8-2#3-i-2.5-3-14.5[‡]	S4	0.0002	6.1	-
11-8-F3.8-6#3-i-2.5-3-14.5	S1	0.0038	68.8	yielded
	S2	0.0097	69.1	yielded
	S3	0.0046	68.8	yielded
	S4	0.0004	12.2	-
	S5	0.0000	0	-
	S6	0.0002	6.1	-
(3@5.35)11-8-F3.8-6#3-i-2.5-3-14.5	S1	0.0023	68.7	yielded
	S2	0.0107	69.1	yielded
	S3	0.0126	71.2	yielded
	S4	0.0022	65.9	-
	S5	0.0002	6.1	-
	S6	0.0000	0	-
11-5-F3.8-6#3-i-2.5-3-12[‡]	S1	0.0025	68.6	yielded
	S2	0.0266	84.0	yielded
	S3	0.0186	77.3	yielded
	S5	0.0001	3.1	-
	S6	0.0000	0	-
11-5-F3.8-6#3-i-2.5-3-17	S1	0.0022	65.9	-
	S2	0.0173	76.1	yielded
	S3	0.0140	72.3	yielded
	S4	0.0020	61.4	-
	S5	0.0000	0	-
	S6	0.0001	3.1	-
11-5-F8.6-6#3-i-2.5-3-14.5	S1	0.0018	53.3	-
	S2	0.0280	85.2	yielded
	S3	0.0290	85.8	yielded
	S4	0.0018	53.3	-
	S5	0.0000	0	-
	S6	0.0002	6.1	-
(3@5.35)11-5-F8.6-6#3-i-2.5-3-14.5	S1	0.0024	68.4	yielded
	S2	0.0294	86.0	yielded
	S3	0.0289	85.7	yielded
	S4	0.0029	68.6	yielded
	S5	0.0001	3.1	-
	S6	0.0000	0	-
11-12-S5.5-6#3-i-2.5-3-16.75[‡]	S1	0.0027	68.6	yielded
	S2	0.0272	84.9	yielded
	S3	0.0169	75.5	yielded
	S4	0.0026	68.6	yielded
	S5	0.0001	3.1	-

[†] Refer to Figure 3.6a and Figure 3.7a for specimens containing No. 8 and No. 11 bars, respectively

[‡] Specimen had missing strain gauge(s)

Table 3.3 Cont. Maximum strain and stress in confining reinforcement

Specimen	Gauge Location[†]	Strain	Stress (ksi)	Note
11-5-S5.5-6#3-i-2.5-3-19.25[‡]	S1	0.0040	69.1	yielded
	S2	0.0064	69.0	yielded
	S3	0.0188	69.3	yielded
8-8-S14.9-5#3-i-2.5-3-8.25	S1	0.0222	80.5	yielded
	S2	0.0266	84.0	yielded
	S3	0.0023	69.0	yielded
	S4	0.0004	12.2	-
	S5	0.0000	0	-
8-8-O12.9-5#3-i-2.5-3-9.5	S1	0.0156	74.4	yielded
	S2	0.0162	75.0	yielded
	S3	0.0036	69.0	yielded
	S4	0.0003	9.2	-
	S5	0.0000	0	-

[†] Refer to Figure 3.6a and Figure 3.7a for specimens containing No. 8 and No. 11 bars, respectively
[‡] Specimen had missing strain gauge(s)

Table 3.3 shows the values of maximum strain and stress in the hoops providing confinement within the joint region. For the two specimens with No. 8 bars and five No. 3 hoops as confining reinforcement, the three top hoops yielded, with significant increases in strain observed during the test, while the two bottom hoops exhibited only small or no strain increase. For the specimens with No. 11 bars and six No. 3 hoops spaced at $3d_b$, the three top hoops yielded, with the exception of two specimens (11-5-F3.8-6#3-i-2.5-3-17 and 11-5-F8.6-6#3-i-2.5-3-14.5), in which the first hoop had a maximum stress close to the yield strength. The lower maximum strain exhibited in the first hoop may result from the fact that the diagonal cracks in the joint region (Figure 3.1d) were relatively far from the center the first hoop (gauge location). Strains were negligible throughout the test for the two bottom hoops (S5 and S6). The strain in the remaining hoop (S4) was below yield in four out of six specimens. In addition, for the two specimens containing two No. 3 hoops, the second hoop (corresponding to the fourth hoop S4 in a specimen containing six hoops) was far below yielding, while the first hoop yielded with a large increase in strain.

Based on the analysis of strain and stress in the headed bars and confining reinforcement, it can be concluded that (1) the difference in bar stress along the length of the bar is due to the portion of the load carried by bond, a difference that decreases as the peak load is attained, and (2) the effectiveness of confining reinforcement is directly related to the location of the hoops: hoops

located closer to the headed bars are more effective in confining the joint and thus improving the anchorage strength than those placed further from the headed bars.

3.4 ANCHORAGE STRENGTH

This section summarizes the headed bar anchorage strength results measured in the beam-column joint tests. The effects of the test parameters, including head size, side cover, embedment length, confining reinforcement, bar size, concrete compressive strength, and spacing between the bars, on the anchorage strength of headed bars are analyzed in Chapter 7.

A summary of the 20 beam-column joint specimen test groups is given in Table 3.4. As shown in the table, the majority of the specimens (139 out of 202) contained No. 8 headed bars, 25 specimens contained No. 5 headed bars, and 38 specimens contained No. 11 headed bars. Nominal concrete strengths ranged from 5 to 15 ksi for No. 8 bars, and from 5 to 12 ksi for No. 5 and No. 11 bars.

Table 3.4 Summary of beam-column joint test groups

Group	Test Date	Bar Size	Nominal Concrete Strength, ksi	Number of Specimens
1	September, 2013	No. 8	5	6
2	December, 2013	No. 8	5	6
3	January, 2014	No. 8	5	6
4	April, 2014	No. 8	8	13
5	July, 2014	No. 8	12	8
6	September, 2014	No. 8	5	12
7	November, 2014	No. 8	5	12
8	December, 2014	No. 8	15	9
9	December, 2014	No. 8	8	15
10	December, 2014	No. 8	12	12
11	February, 2015	No. 8	8	13
12	March, 2015	No. 8	5	14
13	April, 2015	No. 5	5	11
14	June, 2015	No. 5	12	14
15	July, 2015	No. 11	5	8
16	August – September, 2015	No. 8	5 / 8	6 / 3
17	October, 2015	No. 8 / No. 11	8	4 / 6
18	November, 2015	No. 11	5	8
19	March, 2016	No. 11	12	8
20	March, 2016	No. 11	5	8

The test results of the 202 beam-column joint specimens are given in Table 3.5, including number of bars in each specimen n, center-to-center spacing between the bars in terms of bar diameter s/d_b, measured concrete compressive strength f_{cm}, net bearing area of head in terms of nominal bar area A_{brg}/A_b, average of measured embedment length $\ell_{eh,\text{avg}}$, average peak load T (total peak load applied on the specimen divided by the number of headed bars), and failure type (described in Section 3.2). Comprehensive test results are given in Table B.1 in Appendix B.

Table 3.5 Test results for beam-column joint specimens

Group	Specimen	n	s/d_b	f_{cm} psi	A_{brg}/A_b	$\ell_{eh,\text{avg}}$ in.	T kips	Failure Type[†]
1	8-5-T4.0-0-i-3-3-15.5	2	11	4850	4.0	15.75	80.4	SB/FP
	8-5-T4.0-0-i-4-3-15.5	2	11	5070	4.0	15.28	95.4	SB/FP
	8-5-T4.0-4#3-i-3-3-12.5[*]	2	11	5070	4.0	12.38	87.5	SB/FP
	8-5-T4.0-4#3-i-4-3-12.5	2	11	5380	4.0	12.06	96.2	SB/FP
	8-5-T4.0-4#4-i-3-3-12.5	2	11	5070	4.0	12.44	109.0	SB/FP
	8-5-T4.0-4#4-i-4-3-12.5	2	11	4850	4.0	12.19	101.5	SB/FP
2	8-5g-T4.0-0-i-2.5-3-12.5	2	11	5910	4.0	12.56	97.7	SB/FP
	8-5g-T4.0-0-i-3.5-3-12.5	2	11	6320	4.0	12.50	93.4	SB/FP
	8-5g-T4.0-5#3-i-2.5-3-9.5	2	11	5090	4.0	9.56	78.7	SB
	8-5g-T4.0-5#3-i-3.5-3-9.5	2	11	5910	4.0	9.56	79.5	SB
	8-5g-T4.0-4#4-i-2.5-3-9.5	2	11	5180	4.0	9.19	90.7	SB
	8-5g-T4.0-4#4-i-3.5-3-9.5	2	11	5910	4.0	9.50	96.7	SB
3	8-5-T4.0-0-i-2.5-3-12.5	2	11	6210	4.0	12.59	83.3	SB/FP
	8-5-T4.0-0-i-3.5-3-12.5	2	11	6440	4.0	12.66	91.9	SB/FP
	8-5-T4.0-5#3-i-2.5-3-9.5	2	11	5960	4.0	9.31	74.2	SB
	8-5-T4.0-5#3-i-3.5-3-9.5	2	11	6440	4.0	9.06	80.6	SB/FP
	8-5-T4.0-4#4-i-2.5-3-9.5	2	11	6440	4.0	9.25	90.5	SB/FP
	8-5-T4.0-4#4-i-3.5-3-9.5	2	11	6210	4.0	9.25	85.6	SB/FP
4	8-8-F4.1-0-i-2.5-3-10.5	2	11	8450	4.1	10.50	77.1	CB
	8-8-F4.1-2#3-i-2.5-3-10	2	11	8450	4.1	9.88	73.4	CB
	(3@3)8-8-F4.1-0-i-2.5-3-10.5	3	3	8450	4.1	10.58	54.8	CB
	(3@3)8-8-F4.1-0-i-2.5-3-10.5-HP	3	3	8450	4.1	10.33	50.5	CB/FP
	(3@3)8-8-F4.1-2#3-i-2.5-3-10	3	3	8260	4.1	10.08	61.9	CB
	(3@3)8-8-F4.1-2#3-i-2.5-3-10-HP	3	3	8260	4.1	10.29	56.7	CB
	(3@4)8-8-F4.1-0-i-2.5-3-10.5	3	4	8450	4.1	10.83	58.7	CB
	(3@4)8-8-F4.1-2#3-i-2.5-3-10	3	4	8050	4.1	9.88	55.5	CB
	(3@4)8-8-F4.1-2#3-i-2.5-3-10-HP	3	4	8050	4.1	10.33	69.8	CB
	(3@5)8-8-F4.1-0-i-2.5-3-10.5	3	5	8050	4.1	10.35	64.0	CB
	(3@5)8-8-F4.1-0-i-2.5-3-10.5-HP	3	5	8260	4.1	10.25	59.9	CB
	(3@5)8-8-F4.1-2#3-i-2.5-3-10.5	3	5	8260	4.1	9.79	56.1	CB
	(3@5)8-8-F4.1-2#3-i-2.5-3-10.5-HP	3	5	8260	4.1	10.00	65.5	CB

[†] CB – concrete breakout; SB – side blowout; FP – local front pullout; BS – back cover spalling; and Y – bar yielding
[*] Specimen with only one bar failed

Table 3.5 Cont. Test results for beam-column joint specimens

Group	Specimen	n	s/d_b	f_{cm} psi	A_{brg}/A_b	$\ell_{eh,\text{avg}}$ in.	T kips	Failure Type[†]
5	8-12-F4.1-0-i-2.5-3-10	2	11	11760	4.1	9.69	71.8	CB
	8-12-F4.1-5#3-i-2.5-3-10	2	11	11760	4.1	10.00	87.2	SB/FP
	(3@3)8-12-F4.1-0-i-2.5-3-10	3	3	11040	4.1	9.90	42.2	CB
	(3@3)8-12-F4.1-5#3-i-2.5-3-10	3	3	11040	4.1	10.00	61.6	CB
	(3@4)8-12-F4.1-0-i-2.5-3-10	3	4	11440	4.1	9.92	48.9	CB
	(3@4)8-12-F4.1-5#3-i-2.5-3-10	3	4	11440	4.1	9.77	65.7	CB/FP
	(3@5)8-12-F4.1-0-i-2.5-3-10	3	5	11460	4.1	9.92	55.1	CB
	(3@5)8-12-F4.1-5#3-i-2.5-3-10	3	5	11460	4.1	9.60	69.7	CB/FP
6	8-5-S6.5-0-i-2.5-3-11.25	2	11	5500	6.5	11.06	75.6	SB/FP
	8-5-S6.5-0-i-2.5-3-14.25	2	11	5500	6.5	14.25	87.7	SB/FP
	8-5-O4.5-0-i-2.5-3-11.25	2	11	5500	4.5[‡]	11.25	67.4	SB/FP
	8-5-O4.5-0-i-2.5-3-14.25	2	11	5500	4.5[‡]	14.13	85.0	SB/FP
	8-5-S6.5-2#3-i-2.5-3-9.25	2	11	5750	6.5	9.13	63.4	CB
	8-5-S6.5-2#3-i-2.5-3-12.25	2	11	5750	6.5	12.31	86.0	SB/FP
	8-5-O4.5-2#3-i-2.5-3-9.25	2	11	5750	4.5[‡]	9.38	67.9	SB/FP
	8-5-O4.5-2#3-i-2.5-3-12.25	2	11	5750	4.5[‡]	12.00	78.5	SB/FP
	8-5-S6.5-5#3-i-2.5-3-8.25	2	11	5900	6.5	8.31	62.0	CB/FP
	8-5-S6.5-5#3-i-2.5-3-11.25	2	11	5900	6.5	10.94	84.5	SB/FP
	8-5-O4.5-5#3-i-2.5-3-8.25	2	11	5900	4.5[‡]	8.00	68.4	SB/FP
	8-5-O4.5-5#3-i-2.5-3-11.25	2	11	5900	4.5[‡]	11.13	82.2	SB/FP
7	8-5-T9.5-0-i-2.5-3-14.5	2	11	4970	9.5	14.38	91.7	SB/FP
	8-5-O9.1-0-i-2.5-3-14.5	2	11	4970	9.1[‡]	14.38	94.8	SB/FP
	8-5-T9.5-5#3-i-2.5-3-14.5[*]	2	11	5420	9.5	14.38	121.0	SB/FP
	8-5-O9.1-5#3-i-2.5-3-14.5	2	11	4970	9.1[‡]	14.09	119.3	Y
	(3@5.5)8-5-T9.5-0-i-2.5-3-14.5	3	5.5	4960	9.5	14.25	73.4	CB
	(3@5.5)8-5-O9.1-0-i-2.5-3-14.5	3	5.5	4960	9.1[‡]	14.35	75.7	CB
	(3@5.5)8-5-T9.5-5#3-i-2.5-3-14.5	3	5.5	5370	9.5	14.42	94.6	CB
	(3@5.5)8-5-O9.1-5#3-i-2.5-3-14.5	3	5.5	5420	9.1[‡]	14.27	102.2	Y
	(4@3.7)8-5-T9.5-0-i-2.5-3-14.5	4	3.7	5570	9.5	14.27	60.8	CB
	(4@3.7)8-5-O9.1-0-i-2.5-3-14.5	4	3.7	5570	9.1[‡]	14.06	61.2	CB
	(4@3.7)8-5-T9.5-5#3-i-2.5-3-14.5	4	3.7	5570	9.5	14.50	76.9	CB
	(4@3.7)8-5-O9.1-5#3-i-2.5-3-14.5	4	3.7	5570	9.1[‡]	14.50	89.1	Y

[†] CB – concrete breakout; SB – side blowout; FP – local front pullout; BS – back cover spalling; and Y – bar yielding
[*] Specimen with only one bar failed
[‡] Head had large obstruction, with net bearing area taken as the difference between the gross area of the head and the area of the obstruction adjacent to the head

Table 3.5 Cont. Test results for beam-column joint specimens

Group	Specimen	n	s/d_b	f_{cm} psi	A_{brg}/A_b	$\ell_{eh,\text{avg}}$ in.	T kips	Failure Type[†]
8	8-15-T4.0-0-i-2.5-4.5-9.5	2	11	16030	4.0	9.50	83.3	CB
	8-15-S9.5-0-i-2.5-3-9.5	2	11	16030	9.5	9.50	81.7	CB
	8-15-S14.9-0-i-2.5-3-9.5	2	11	16030	14.9	9.69	87.1	CB
	8-15-T4.0-2#3-i-2.5-4.5-7	2	11	16030	4.0	7.06	59.0	CB
	8-15-S9.5-2#3-i-2.5-3-7	2	11	16030	9.5	7.06	67.1	CB
	8-15-S14.9-2#3-i-2.5-3-7	2	11	16030	14.9	7.00	79.3	CB
	8-15-T4.0-5#3-i-2.5-4.5-5.5	2	11	16030	4.0	5.50	63.3	CB
	8-15-S9.5-5#3-i-2.5-3-5.5	2	11	16030	9.5	5.63	75.8	CB
	8-15-S14.9-5#3-i-2.5-3-5.5	2	11	16030	14.9	5.50	81.4	CB
9	8-8-T9.5-0-i-2.5-3-9.5	2	11	9040	9.5	9.38	65.2	CB
	8-8-T9.5-2#3-i-2.5-3-9.5	2	11	9040	9.5	9.19	68.7	CB
	(3@4)8-8-T9.5-0-i-2.5-3-9.5	3	4	9040	9.5	9.25	40.3	CB
	(3@4)8-8-T9.5-2#3-i-2.5-3-9.5	3	4	9040	9.5	9.58	51.8	CB
	(3@5)8-8-T9.5-0-i-2.5-3-9.5	3	5	9940	9.5	9.50	44.5	CB
	(3@5)8-8-T9.5-2#3-i-2.5-3-9.5	3	5	9940	9.5	9.42	55.9	CB
	(3@7)8-8-T9.5-0-i-2.5-3-9.5	3	7	10180	9.5	9.50	68.7	CB
	(3@7)8-8-T9.5-2#3-i-2.5-3-9.5	3	7	10180	9.5	9.58	67.6	CB
	8-8-T9.5-0-i-2.5-3-14.5	2	11	10180	9.5	14.38	118.8	Y
	(3@4)8-8-T9.5-0-i-2.5-3-14.5	3	4	9040	9.5	14.58	76.6	CB
	(3@4)8-8-T9.5-2#3-i-2.5-3-14.5	3	4	9040	9.5	14.42	85.4	CB
	(3@5)8-8-T9.5-0-i-2.5-3-14.5	3	5	9940	9.5	14.58	93.2	CB
	(3@5)8-8-T9.5-2#3-i-2.5-3-14.5	3	5	9940	9.5	14.08	105.2	CB
	(3@7)8-8-T9.5-0-i-2.5-3-14.5	3	7	10180	9.5	14.54	104.0	CB/BS
	(3@7)8-8-T9.5-2#3-i-2.5-3-14.5	3	7	10180	9.5	14.54	113.4	CB
10	(2@9)8-12-F4.1-0-i-2.5-3-12	2	9	12080	4.1	12.06	79.1	CB/FP
	(2@9)8-12-F9.1-0-i-2.5-3-12	2	9	12080	9.1	11.88	76.5	CB/BS
	(2@9)8-12-F4.1-5#3-i-2.5-3-12[*]	2	9	12080	4.1	11.97	111.9	SB/FP
	(2@9)8-12-F9.1-5#3-i-2.5-3-12	2	9	12080	9.1	12.13	121.2	Y
	(3@4.5)8-12-F4.1-0-i-2.5-3-12	3	4.5	12040	4.1	12.21	75.2	CB
	(3@4.5)8-12-F9.1-0-i-2.5-3-12	3	4.5	12040	9.1	12.04	75.4	CB
	(3@4.5)8-12-F4.1-5#3-i-2.5-3-12	3	4.5	12040	4.1	12.17	87.7	CB
	(3@4.5)8-12-F9.1-5#3-i-2.5-3-12	3	4.5	12040	9.1	11.90	108.6	CB
	(4@3)8-12-F4.1-0-i-2.5-3-12	4	3	12040	4.1	12.00	49.3	CB
	(4@3)8-12-F9.1-0-i-2.5-3-12	4	3	12360	9.1	12.17	50.3	CB
	(4@3)8-12-F4.1-5#3-i-2.5-3-12	4	3	12360	4.1	12.03	64.2	CB
	(4@3)8-12-F9.1-5#3-i-2.5-3-12	4	3	12360	9.1	11.95	87.8	CB

[†] CB – concrete breakout; SB – side blowout; FP – local front pullout; BS – back cover spalling; and Y – bar yielding
[*] Specimen with only one bar failed

Table 3.5 Cont. Test results for beam-column joint specimens

Group	Specimen	n	s/d_b	f_{cm} psi	A_{brg}/A_b	$\ell_{eh,\text{avg}}$ in.	T kips	Failure Type[†]
11	8-8-O4.5-0-i-2.5-3-9.5	2	11	6710	4.5[‡]	9.19	58.4	CB/FP
	(2@9)8-8-O4.5-0-i-2.5-3-9.5	2	9	6710	4.5[‡]	9.00	58.8	CB
	(2@7)8-8-O4.5-0-i-2.5-3-9.5	2	7	6710	4.5[‡]	9.25	54.5	CB
	(2@5)8-8-O4.5-0-i-2.5-3-9.5	2	5	6710	4.5[‡]	9.00	51.2	CB
	(2@3)8-8-O4.5-0-i-2.5-3-9.5	2	3	6710	4.5[‡]	9.00	47.7	CB
	(2@9)8-8-T4.0-0-i-2.5-3-9.5	2	9	6790	4.0	9.38	61.8	CB
	(2@9)8-8-T4.0-5#3-i-2.5-3-9.5	2	9	6790	4.0	9.50	76.7	SB/FP
	(3@4.5)8-8-T4.0-0-i-2.5-3-9.5	3	4.5	6790	4.0	9.33	40.7	CB
	(3@4.5)8-8-T4.0-5#3-i-2.5-3-9.5	3	4.5	6650	4.0	9.17	62.5	CB/FP
	(4@3)8-8-T4.0-0-i-2.5-3-9.5	4	3	6650	4.0	9.47	26.2	CB
	(4@3)8-8-T4.0-5#3-i-2.5-3-9.5	4	3	6650	4.0	9.66	48.6	CB
	(3@3)8-8-T4.0-0-i-2.5-3-9.5	3	3	6790	4.0	9.46	39.4	CB
	(3@3)8-8-T4.0-5#3-i-2.5-3-9.5	3	3	6650	4.0	9.33	56.5	CB
12	8-5-F4.1-0-i-2.5-7-6	2	11	4930	4.1	6.09	28.7	CB
	8-5-F4.1-5#3-i-2.5-7-6	2	11	4930	4.1	6.25	50.7	CB
	(3@3)8-5-F4.1-0-i-2.5-7-6	3	3	4930	4.1	6.19	20.6	CB
	(3@3)8-5-F4.1-5#3-i-2.5-7-6	3	3	4930	4.1	6.00	32.1	CB
	(3@5)8-5-F4.1-0-i-2.5-7-6	3	5	4930	4.1	6.33	23.9	CB
	(3@5)8-5-F4.1-5#3-i-2.5-7-6	3	5	4930	4.1	6.29	37.5	CB
	(3@7)8-5-F4.1-0-i-2.5-7-6	3	7	4940	4.1	6.25	27.1	CB
	(3@7)8-5-F4.1-5#3-i-2.5-7-6	3	7	4940	4.1	6.10	42.3	CB
	8-5-F9.1-0-i-2.5-7-6	2	11	4940	9.1	6.13	33.4	CB
	8-5-F9.1-5#3-i-2.5-7-6	2	11	4940	9.1	6.16	53.8	CB
	(3@5.5)8-5-F9.1-0-i-2.5-7-6	3	5.5	5160	9.1	6.21	23.0	CB
	(3@5.5)8-5-F9.1-5#3-i-2.5-7-6	3	5.5	5160	9.1	6.25	43.1	CB
	(4@3.7)8-5-T9.5-0-i-2.5-6.5-6	4	3.7	5160	9.5	6.13	21.7	CB
	(4@3.7)8-5-F9.1-5#3-i-2.5-7-6	4	3.7	5160	9.1	6.03	31.6	CB
13	5-5-F4.0-0-i-2.5-5-4	2	11.8	4810	4.0	4.06	24.5	CB
	5-5-F13.1-0-i-2.5-5-4	2	11.8	4810	13.1	4.41	28.2	CB
	5-5-F4.0-2#3-i-2.5-5-4	2	11.8	4810	4.0	3.81	19.7	CB
	5-5-F13.1-2#3-i-2.5-5-4	2	11.8	4810	13.1	4.09	28.9	CB
	5-5-F4.0-5#3-i-2.5-5-4[*]	2	11.8	4810	4.0	4.16	26.5	CB
	5-5-F13.1-5#3-i-2.5-5-4	2	11.8	4690	13.1	4.19	35.2	CB
	5-5-F4.0-0-i-2.5-3-6[*]	2	11.8	4690	4.0	6.00	32.7	SB
	5-5-F13.1-0-i-2.5-3-6[*]	2	11.8	4690	13.1	6.22	35.3	SB/FP
	5-5-F4.0-2#3-i-2.5-3-6	2	11.8	4690	4.0	6.00	37.9	SB/FP
	5-5-F13.1-2#3-i-2.5-3-6[*]	2	11.8	4690	13.1	5.94	46.4	SB/FP
	5-5-F4.0-5#3-i-2.5-3-6	2	11.8	4690	4.0	6.06	43.5	SB/FP

[†] CB – concrete breakout; SB – side blowout; FP – local front pullout; BS – back cover spalling; and Y – bar yielding

[*] Specimen with only one bar failed

[‡] Head had large obstruction, with net bearing area taken as the difference between the gross area of the head and the area of the obstruction adjacent to the head

Table 3.5 Cont. Test results for beam-column joint specimens

Group	Specimen	n	s/d_b	f_{cm} psi	A_{brg}/A_b	$\ell_{eh,\mathrm{avg}}$ in.	T kips	Failure Type[†]
14	5-12-F4.0-0-i-2.5-5-4	2	11.8	11030	4.0	4.06	28.3	CB
	5-12-F13.1-0-i-2.5-5-4	2	11.8	11030	13.1	4.13	31.4	CB
	5-12-F4.0-2#3-i-2.5-5-4	2	11.8	11030	4.0	4.13	32.7	CB
	5-12-F13.1-2#3-i-2.5-5-4	2	11.8	11030	13.1	4.09	36.3	CB
	5-12-F4.0-5#3-i-2.5-5-4	2	11.8	11030	4.0	4.22	38.9	CB
	5-12-F13.1-5#3-i-2.5-5-4	2	11.8	11030	13.1	4.13	40.3	CB
	5-12-F4.0-0-i-2.5-3-6	2	11.8	11030	4.0	6.00	41.7	SB
	5-12-F13.1-0-i-2.5-3-6	2	11.8	11030	13.1	6.03	44.2	CB
	(3@5.9)5-12-F4.0-0-i-2.5-4-5	3	5.9	11030	4.0	5.04	28.0	CB
	(3@5.9)5-12-F4.0-2#3-i-2.5-4-5	3	5.9	11030	4.0	5.15	35.1	CB
	(3@5.9)5-12-F4.0-5#3-i-2.5-4-5	3	5.9	11030	4.0	5.02	38.6	CB
	(4@3.9)5-12-F4.0-0-i-2.5-4-5	4	3.9	11030	4.0	5.19	25.6	CB
	(4@3.9)5-12-F4.0-2#3-i-2.5-4-5	4	3.9	11030	4.0	5.03	30.9	CB
	(4@3.9)5-12-F4.0-5#3-i-2.5-4-5	4	3.9	11030	4.0	5.19	48.1	Y
15	11-5a-F3.8-0-i-2.5-3-17	2	10.7	4050	3.8	16.56	97.5	CB/FP
	11-5a-F3.8-2#3-i-2.5-3-17	2	10.7	4050	3.8	17.44	118.2	SB/FP
	11-5a-F3.8-6#3-i-2.5-3-17	2	10.7	4050	3.8	16.72	116.2	SB/FP
	11-5a-F3.8-0-i-2.5-3-12	2	10.7	3960	3.8	12.00	56.8	CB
	11-5a-F3.8-2#3-i-2.5-3-12	2	10.7	3960	3.8	12.00	67.3	CB
	11-5a-F3.8-6#3-i-2.5-3-12	2	10.7	3960	3.8	12.09	78.0	CB/FP
	11-5a-F8.6-0-i-2.5-3-12	2	10.7	3960	8.6	12.13	63.8	CB
	11-5a-F8.6-6#3-i-2.5-3-12	2	10.7	4050	8.6	12.56	79.2	CB
16	8-8-F4.1-0-i-2.5-3-10-DB	2	11	7410	4.1	9.88	50.2	CB
	8-8-F9.1-0-i-2.5-3-10-DB	2	11	7410	9.1	9.81	51.8	CB
	8-8-F9.1-5#3-i-2.5-3-10-DB	2	11	7410	9.1	9.63	68.2	CB
	8-5-F4.1-0-i-2.5-3-10-DB	2	11	4880	4.1	9.88	40.6	CB/FP
	8-5-F9.1-0-i-2.5-3-10-DB	2	11	4880	9.1	9.75	44.4	CB
	8-5-F4.1-3#4-i-2.5-3-10-DB	2	11	4880	4.1	10.13	64.6	CB
	8-5-F9.1-3#4-i-2.5-3-10-DB	2	11	4880	9.1	9.75	65.8	CB
	8-5-F4.1-5#3-i-2.5-3-10-DB	2	11	4880	4.1	10.19	70.2	CB
	8-5-F9.1-5#3-i-2.5-3-10-DB	2	11	4880	9.1	9.94	70.5	CB

[†] CB – concrete breakout; SB – side blowout; FP – local front pullout; BS – back cover spalling; and Y – bar yielding

Table 3.5 Cont. Test results for beam-column joint specimens

Group	Specimen	n	s/d_b	f_{cm} psi	A_{brg}/A_b	$\ell_{eh,\text{avg}}$ in.	T kips	Failure Type[†]
17	11-8-F3.8-0-i-2.5-3-14.5	2	10.7	8660	3.8	14.50	79.1	CB
	11-8-F3.8-2#3-i-2.5-3-14.5	2	10.7	8660	3.8	14.69	88.4	CB
	11-8-F3.8-6#3-i-2.5-3-14.5	2	10.7	8660	3.8	14.69	112.7	CB
	(3@5.35)11-8-F3.8-0-i-2.5-3-14.5	3	5.35	8720	3.8	14.63	52.9	CB
	(3@5.35)11-8-F3.8-2#3-i-2.5-3-14.5	3	5.35	8720	3.8	14.54	72.6	CB
	(3@5.35)11-8-F3.8-6#3-i-2.5-3-14.5	3	5.35	8720	3.8	14.92	83.7	CB
	8-8-O12.9-0-i-2.5-3-9.5	2	11	8800	12.9[‡]	9.69	85.2	CB
	8-8-S14.9-0-i-2.5-3-8.25	2	11	8800	14.9	8.25	70.9	CB
	8-8-O12.9-5#3-i-2.5-3-9.5	2	11	8800	12.9[‡]	9.38	83.5	CB
	8-8-S14.9-5#3-i-2.5-3-8.25	2	11	8800	14.9	8.25	87.0	CB
18	11-5-F3.8-0-i-2.5-3-12	2	10.7	5760	3.8	12.13	66.5	CB
	11-5-F3.8-6#3-i-2.5-3-12	2	10.7	5760	3.8	12.50	88.3	CB
	11-5-F3.8-0-i-2.5-3-17	2	10.7	5760	3.8	17.25	132.7	CB/FP
	11-5-F3.8-6#3-i-2.5-3-17	2	10.7	5970	3.8	16.94	151.9	CB
	11-5-F8.6-0-i-2.5-3-14.5	2	10.7	5970	8.6	14.50	82.8	CB
	11-5-F8.6-6#3-i-2.5-3-14.5	2	10.7	5970	8.6	14.63	112.3	CB
	(3@5.35)11-5-F8.6-0-i-2.5-3-14.5	3	5.35	6240	8.6	14.71	65.1	CB
	(3@5.35)11-5-F8.6-6#3-i-2.5-3-14.5	3	5.35	6240	8.6	14.54	75.6	CB
19	11-12-O4.5-0-i-2.5-3-16.75	2	10.7	10860	4.5[‡]	17.13	169.6	CB
	11-12-S5.5-0-i-2.5-3-16.75	2	10.7	10120	5.5	16.94	175.9	CB
	11-12-O4.5-6#3-i-2.5-3-16.75[*]	2	10.7	10860	4.5[‡]	16.81	201.5	SB/FP
	11-12-S5.5-6#3-i-2.5-3-16.75	2	10.7	10120	5.5	16.81	197.4	CB
	(3@5.35)11-12-O4.5-0-i-2.5-3-16.75	3	5.35	10860	4.5[‡]	16.92	106.8	CB
	(3@5.35)11-12-S5.5-0-i-2.5-3-16.75	3	5.35	10120	5.5	16.92	109.0	CB
	(3@5.35)11-12-O4.5-6#3-i-2.5-3-16.75	3	5.35	10860	4.5[‡]	17.00	135.8	CB
	(3@5.35)11-12-S5.5-6#3-i-2.5-3-16.75	3	5.35	10120	5.5	16.75	153.8	CB
20	11-5-O4.5-0-i-2.5-3-19.25	2	10.7	5430	4.5[‡]	19.44	157.9	SB/FP
	11-5-S5.5-0-i-2.5-3-19.25[*]	2	10.7	6320	5.5	19.38	176.8	SB/FP
	11-5-O4.5-6#3-i-2.5-3-19.25[*]	2	10.7	5430	4.5[‡]	19.63	181.4	SB/FP
	11-5-S5.5-6#3-i-2.5-3-19.25[*]	2	10.7	6320	5.5	19.13	189.6	SB/FP
	(3@5.35)11-5-O4.5-0-i-2.5-3-19.25	3	5.35	5430	4.5[‡]	19.50	128.7	CB
	(3@5.35)11-5-S5.5-0-i-2.5-3-19.25	3	5.35	6320	5.5	19.29	137.4	CB/BS
	(3@5.35)11-5-O4.5-6#3-i-2.5-3-19.25	3	5.35	5430	4.5[‡]	19.38	141.7	CB
	(3@5.35)11-5-S5.5-6#3-i-2.5-3-19.25	3	5.35	6320	5.5	19.25	152.9	CB

[†] CB – concrete breakout; SB – side blowout; FP – local front pullout; BS – back cover spalling; and Y – bar yielding
[*] Specimen with only one bar failed
[‡] Head had large obstruction, with net bearing area taken as the difference between the gross area of the head and the area of the obstruction adjacent to the head

As shown in the table, the ranges of measured concrete compressive strengths were 4690 to 11,030 psi, 4850 to 16,030 psi, and 3960 to 10,860 psi, respectively, for specimens containing No. 5, No. 8, and No. 11 headed bars. At anchorage failure, the average peak loads T for the three

bar sizes ranged from 19.7 to 46.4 kips, 20.6 to 121.0 kips, and 52.9 to 201.5 kips, respectively, corresponding to bar stresses ranging from 63.5 to 149.7 ksi, 26.1 to 153.2 ksi, and 33.9 to 129.2 ksi. A detailed analysis of these results will be presented in Chapter 7.

CHAPTER 4: TEST RESULTS AND ANALYSIS FOR CCT NODE SPECIMENS

This chapter describes the behavior of the CCTnode specimens during testing. Specimen behavior is reported in terms of crack development, anchorage strength, deflection, strain of the longitudinal reinforcement, and slip of the headed and non-headed ends of the reinforcing bars relative to the surrounding concrete. Detailed specimen data are presented in Table C.1 of Appendix C.

4.1 CRACKING BEHAVIOR AND MODE OF FAILURE

4.1.1 Cracking Behavior

The specimens with headed reinforcement had similar cracking patterns, likely because the specimens had similar cover, bar size, head size, and compressive strength. (The bars had square heads with a net bearing area of $4.1A_b$ at one end and no head at the other end. The concrete compressive strength was 4,900 psi at the time of testing.) The first crack was observed at a load of approximately 80 kips for all specimens, largely because the specimens had the same width and similar concrete compressive (and thus, tensile) strengths. The first crack was located under the applied load and oriented vertically, as shown for Specimen H-3-8-5-13-F4.1-II in Figure 4.1a, which had three No. 8 bars as longitudinal reinforcement.

As the force was increased, existing cracks propagated towards the loading point and additional vertical cracks developed. As illustrated in Figures 4.1b and 4.1c, vertical cracks that developed close to the roller support tended to become inclined as they propagated towards the region where a compressive strut was assumed to be active. Upon further loading, an inclined crack extended from the edge of the support plate up towards the load point at an angle of approximately 45 degrees from horizontal (Figure 4.1d). This inclined crack was typically observed at about 50% of the peak load. As the load continued to increase and the specimen neared failure, existing cracks tended to widen and propagate towards the load point (Figure 4.1e).

(a)

(b)

Assumed strut

(c)

(d)

(e)
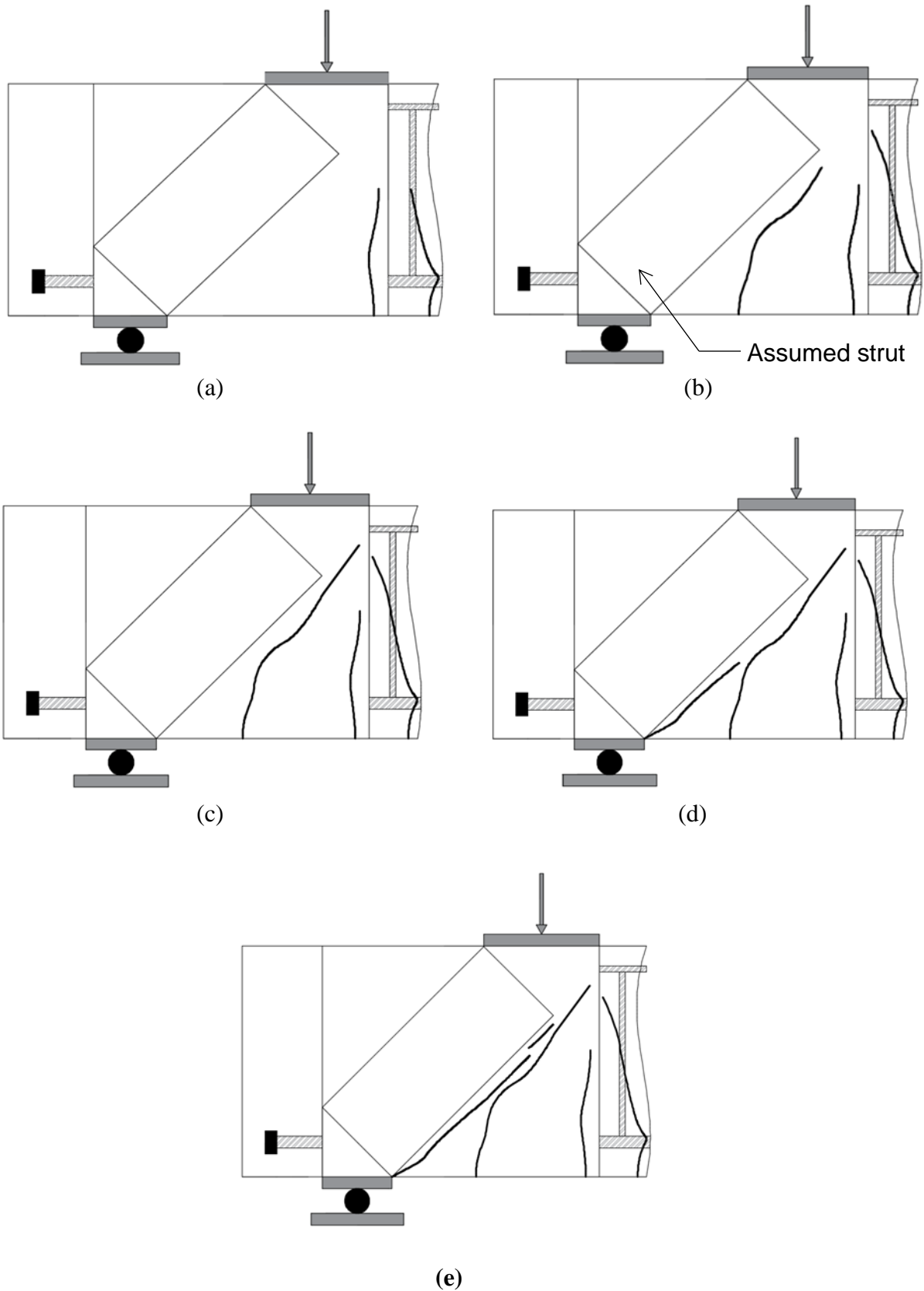
Figure 4.1 Observed crack growth of Specimen H-3-8-5-13-F4.1-II

The observed failure modes varied slightly among the specimens, as will be described in Section 4.1.2. Failures were sudden and led to a total loss of strength. Figure 4.2 shows Specimen H-3-8-5-13-F4.1-II after failure. The wide inclined crack extending from the face of the support towards the load point and the dislodged side cover were typical for specimens with headed reinforcing bars.

Figure 4.2 Specimen H-3-8-5-13-F4.1-II after failure

Figure 4.3 illustrates the typical pattern of cracking in specimens with longitudinal reinforcement terminated without a head (specimen NH-3-8-5-13-F4.1-II, the non-headed end of specimen H-3-8-5-13-F4.1-II, is pictured). The first crack was typically oriented vertically and located under the applied load. As was seen in the tests where the reinforcement was terminated with a head, this crack was first observed at a load of approximately 80 kips. Unlike the specimens with headed longitudinal bars, specimens with straight bar anchorage exhibited prominent inclined cracks near and over the support, as shown in Figure 4.3b. As the specimen neared failure, the inclined cracks widened and propagated towards the top bearing plate. The very wide inclined cracks are believed to result from the longitudinal bars pulling out of their anchorage. As explained in Chapter 2, the anchorage length of the straight (non-headed) bars was the same as for the headed bars to obtain a measure of the contribution from the heads and, as such, was known to be insufficient to develop the bars.

Figure 4.4 shows a photo of Specimen NH-3-8-5-13-F4.1 after failure. The failure, which was dominated by opening of the inclined crack located near or over the support, occurred suddenly.

a.

b.

c.
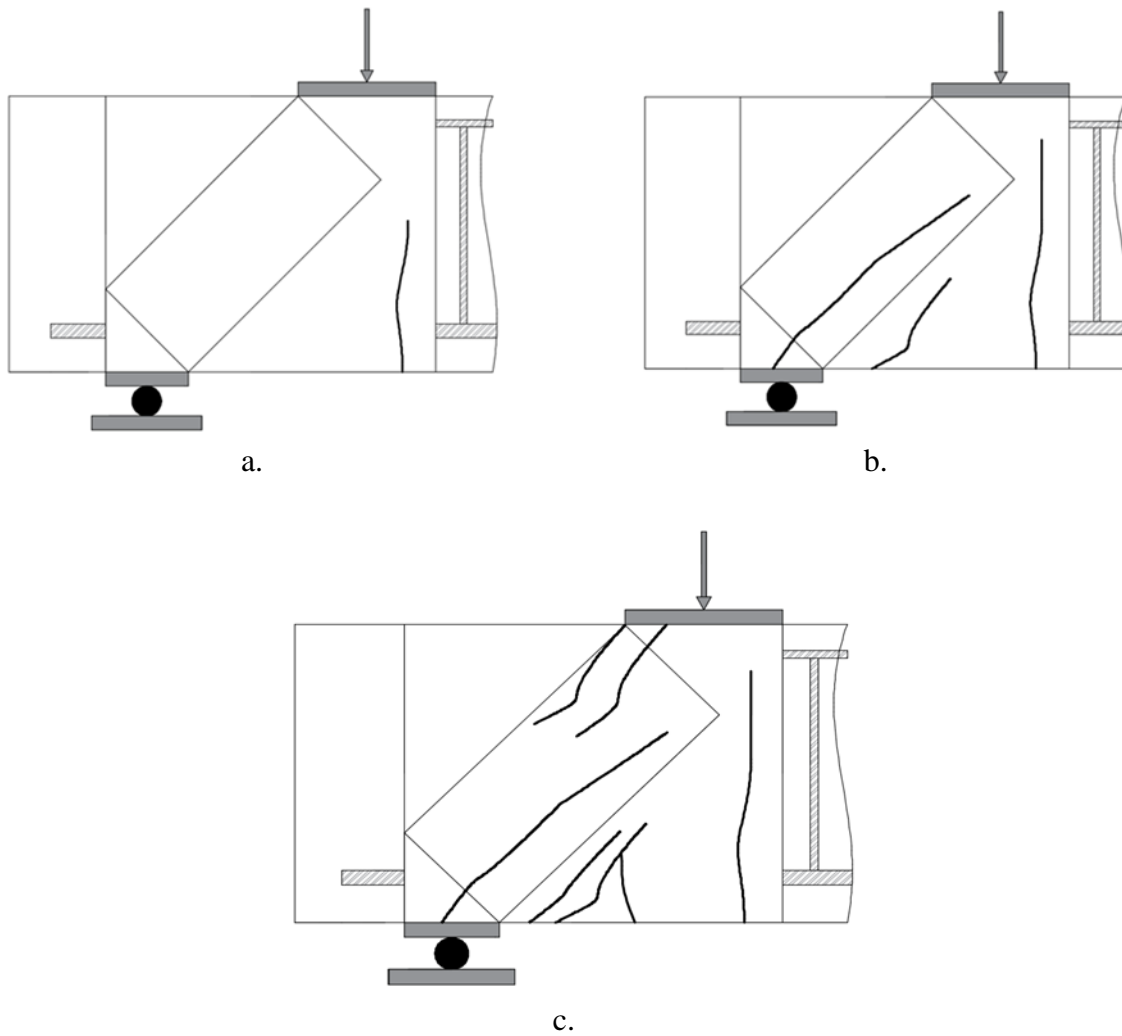
Figure 4.3 Observed crack growth of Specimen NH-3-8-5-13-F4.1-II

Figure 4.4 Specimen NH-3-8-5-13-F4.1-II after failure

4.1.2 Modes of Failure

Three failure modes were observed during this series of tests. Table 4.1 indicates which mode dominated in each test.

Side blowout: The majority of the headed-end tests failed in a manner dominated by side blowout, which is characterized by a sudden separation of the side cover along a plane intersecting the outermost longitudinal reinforcing bar (Figure 4.5). This mode of failure is associated with a sudden and complete loss of strength.

Concrete crushing: In one case, pronounced crushing of concrete was observed parallel to the assumed compressive strut in front of the head and within the assumed nodal zone, as shown in Figure 4.6. This occurred in Specimen H-3-8-5-9-F4.1-II, which had three No. 8 bars and an embedment length ℓ_{eh} of 9 in. measured from the boundary of the extended nodal zone. In this specimen, the bearing face of the head was aligned with the back of the support plate.

Figure 4.5 Side blowout failure – Specimen H-3-8-5-13-F4.1-II

a. Side view   b. Bottom of the specimen

Figure 4.6 Concrete crushing failure – Specimen H-3-8-5-9-F4.1-II

Pullout failure: All non-headed end tests failed due to pullout of the longitudinal reinforcing bar (Figure 4.7). Prior to failure, slip of the bar relative to the surrounding concrete resulted in formation of cracks wider than 0.2 in. at the level of the longitudinal reinforcement. This crack can also be seen along the side and bottom of the specimen after failure (Figure 4.7).

| a. Side view | b. Bottom of the specimen |

Figure 4.7 Pullout failure – Specimen H-3-8-5-11-F4.1-II

Table 4.1 Failure Modes

Series 1		Series 2	
Beam Type	**Failure Type**	**Beam Type**	**Failure Type**
H-2-8-5-9-F4.1-I	Side blowout	H-2-8-5-9-F4.1-II	Side blowout
H-2-8-5-10.4-F4.1-I	Side blowout	H-2-8-5-13-F4.1-II	Side blowout
H-3-8-5-9-F4.1-I	Side blowout	H-3-8-5-9-F4.1-II	Concrete crushing
H-3-8-5-11.4-F4.1-I	Side blowout	H-3-8-5-11-F4.1-II	Side blowout
H-3-8-5-14-F4.1-I	Side blowout	H-3-8-5-13-F4.1-II	Side blowout
NH-2-8-5-9-F4.1-I	Pullout	NH-2-8-5-9-F4.1-II	Pullout
NH-2-8-5-10.4-F4.1-I	Pullout	NH-2-8-5-13-F4.1-II	Pullout
NH-3-8-5-9-F4.1-I	Pullout	NH-3-8-5-9-F4.1-II	Pullout
NH-3-8-5-11.4-F4.1-I	Pullout	NH-3-8-5-11-F4.1-II	Pullout
NH-3-8-5-14-F4.1-I	Pullout	NH-3-8-5-13-F4.1-II	Pullout

4.2 PEAK LOAD AND EMBEDMENT LENGTH

Table 4.2 summarizes the test results, including the concrete compressive strength on the day of testing, the peak force applied to each specimen, and the maximum deflection of the specimen prior to loss of load-carrying capacity. Deflection, described in Section 4.3, was calculated using results from the non-contact infrared based system described in Chapter 2 as the vertical displacement of the beam directly under the applied load corrected for movement of the

supports. For specimens with equivalent amounts of longitudinal reinforcement, both force and deflection at failure increased as embedment length increased.

The peak force applied to each specimen is plotted for the beams in Series 1 and Series 2 in Figures 4.8 and 4.9, respectively. In general, the peak force increased with an increase in embedment length for both the headed and non-headed bar tests. As expected, the peak load in the specimens containing three bars was greater than in those containing two bars. Deflections at failure for both headed and non-headed bar tests also increased with increases in embedment length and increases number of longitudinal bars.

Table 4.2 Summary of Test Results

Beam Type	Embedment Length (in.)	Concrete Compressive Strength (psi)	Peak Load (kips)	Deflection (in.)
Series 1 / Headed end				
H-2-8-5-9-F4.1-I	9.0	5740	278	0.20
H-2-8-5-10.4-F4.1-I	10.4	4490	346	0.30
H-3-8-5-9-F4.1-I	9.0	5800	446	*
H-3-8-5-11.4-F4.1-I	11.4	5750	386	0.33
H-3-8-5-14-F4.1-I	14.0	5750	495	*
Series 1 / Non-headed end				
NH-2-8-5-9-F4.1-I	9.0	5740	158	0.05
NH-2-8-5-10.4-F4.1-I	10.4	5330	236	0.13
NH-3-8-5-9-F4.1-I	9.0	5800	255	0.10
NH-3-8-5-11.4-F4.1-I	11.4	5750	245	*
NH-3-8-5-14-F4.1-I	14.0	5750	356	0.18
Series 2 / Headed end				
H-2-8-5-9-F4.1-II	9.0	4630	218	0.10
H-2-8-5-13-F4.1-II	13.0	4760	250	0.11
H-3-8-5-9-F4.1-II	9.0	4770	355	0.14
H-3-8-5-11-F4.1-II	11.0	4820	403	0.19
H-3-8-5-13-F4.1-II	13.0	4900	499	0.37
Series 2 / Non-headed end				
NH-2-8-5-9-F4.1-II	9.0	4630	218	*
NH-2-8-5-13-F4.1-II	13.0	4760	234	0.08
NH-3-8-5-9-F4.1-II	9.0	4770	205	0.08
NH-3-8-5-11-F4.1-II	11.0	4820	316	0.13
NH-3-8-5-13-F4.1-II	13.0	4900	365	0.14

*Data not available
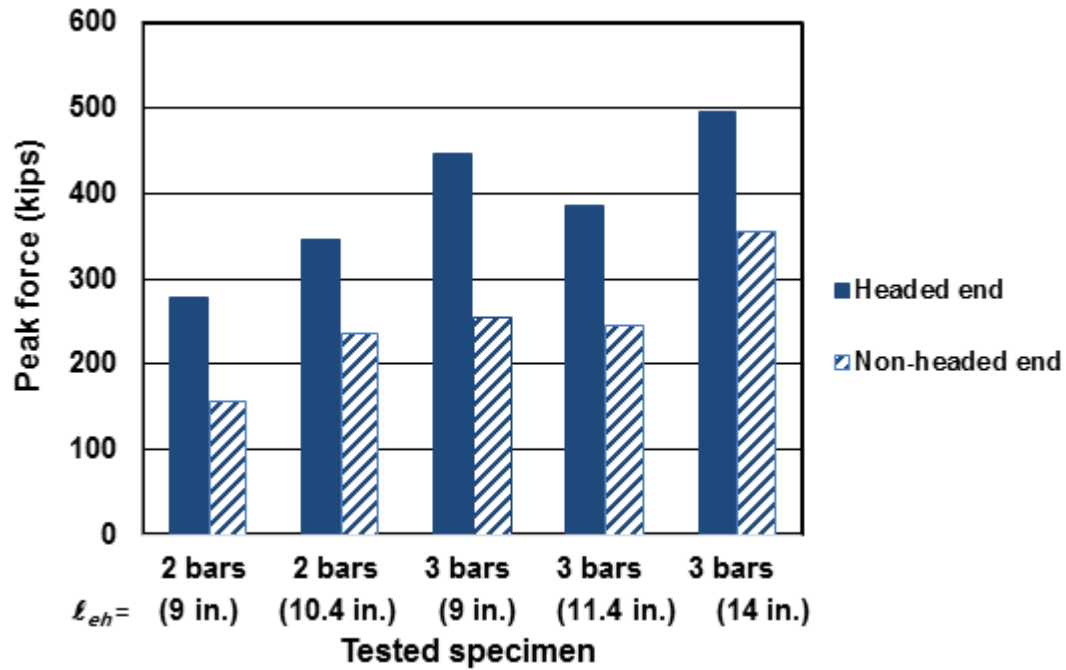
Figure 4.8 Peak force recorded for headed and non-headed end (Series 1)
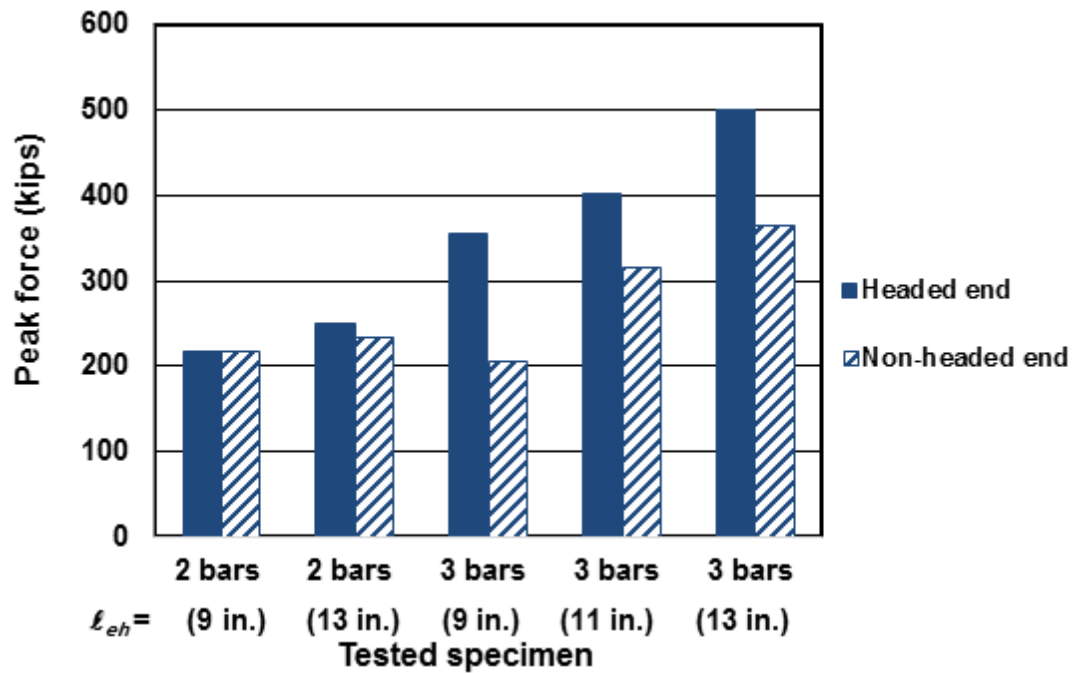
Figure 4.9 Peak force recorded for headed and non-head end (Series 2)

4.3 LOAD-DEFLECTION RESPONSE

Figure 4.10 shows applied force versus deflection under the loading point for the five specimens in Series 2 with headed bar anchorages (H-2-8-5-9-F4.1-II, H-2-8-5-13-F4.1-II, H-3-8-5-9-F4.1-II, H-3-8-5-11-F4.1-II, and H-3-8-5-13-F4.1-II). The specimens in Series 1, not shown here, exhibited similar behavior. Upon initial loading, the specimens had similar stiffness until the load reached approximately 80 kips, at which point all five specimens exhibited a reduction in stiffness due to formation of the first flexural crack. After cracking, the three specimens with three longitudinal bars exhibited similar force-displacement behavior, stiffer than the specimens with two longitudinal bars, as expected. The similarity between the behavior of the specimens with three longitudinal bars shows that differences in embedment length did not result in notable differences in response, with the exception of the peak load. This differs from the response of the two specimens in Series 2 with two longitudinal bars, in which the specimen with the longer embedment length exhibited greater post-cracking stiffness.

Figure 4.11 shows applied force plotted versus deflection under the loading point for Specimens H-3-8-5-13-F4.1-II and NH-3-8-5-13-F4.1-II. These two specimens, which were nominally identical except for the anchorage used for the longitudinal reinforcing bar (headed versus non-headed), illustrate the effect of the headed end on beam behavior. Upon initial loading, both specimens had similar stiffness until the first crack formed at a load of approximately 80 kips. After cracking, both specimens exhibited similar force-displacement behavior until the specimen with the non-headed bar end failed by bar pullout due to insufficient development length. The specimen with the headed bar end continued to gain strength until it failed at a deflection that was more than double that of the beam with the non-headed reinforcement. The similarity between the behavior of the specimens with headed and non-headed bar ends shows that, like the headed bar specimens with different embedment lengths, differences in anchorage type did not result in notable differences in beam stiffness. Because Specimens H-3-8-5-13-F4.1-II and NH-3-8-5-13-F4.1-II are part of the same test specimen, the similarity in responses shown in Figure 4.11 also indicates that the test of the headed bar end of the specimen (which was tested first) did not negatively affect the non-headed end of the specimen.
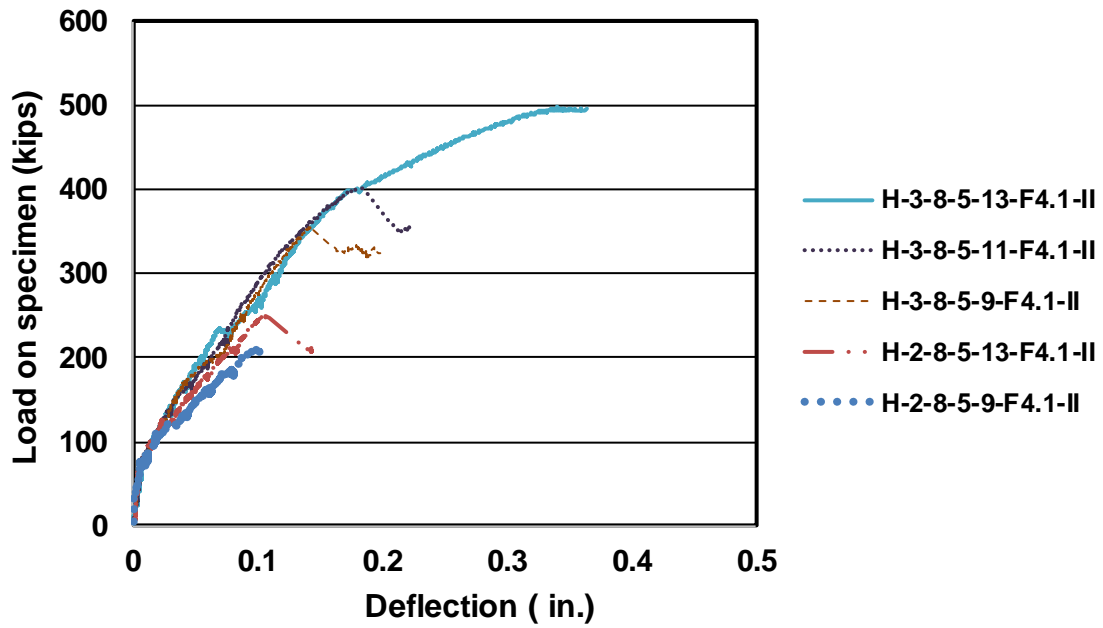
Figure 4.10 Force versus deflection results for the Series 2 headed-end tests
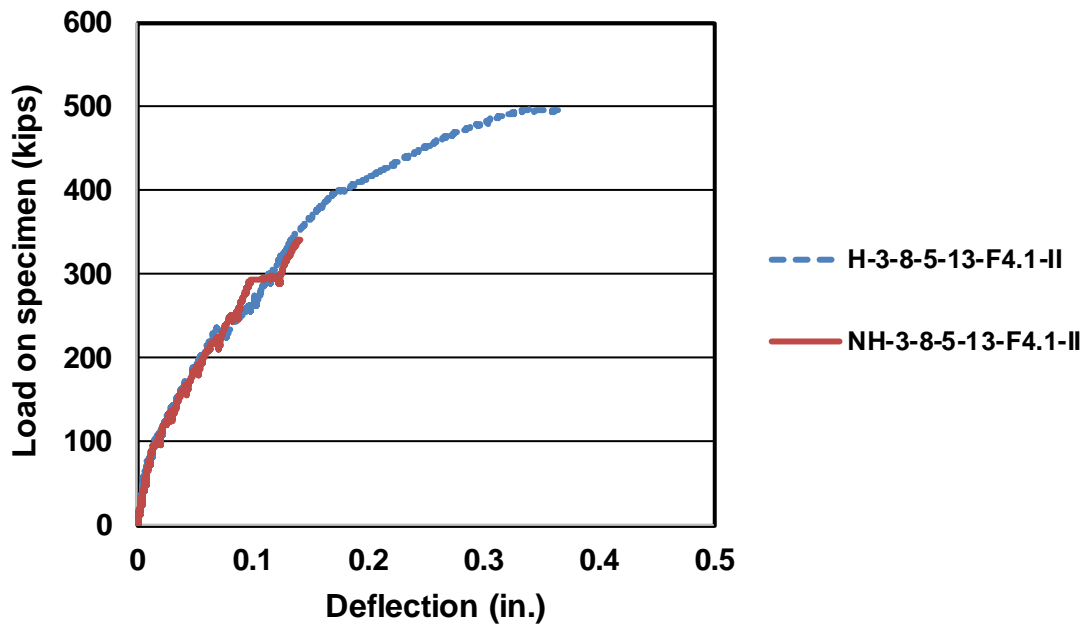
Figure 4.11 Force versus deflection results for Specimens H-3-8-5-13-F4.1 and NH-3-8-5-13-F4.1

99

4.4 REINFORCEMENT STRAIN

Strain gauges were placed along the reinforcing bars to measure the strain in both headed and non-headed end tests. As described in Section 2.3.6, for bars with heads, four strain gauges were placed between the head and the point of applied load. The strain gauges were placed 1 in. from the face of the head, at the center of the support, where the bar intersected the front of the assumed extended nodal zone, and under the applied load point (Figure 4.12). For the non-headed end, three strain gauges were installed between the end of the bar and the point of applied load. The strain gauges were placed at the center of the support, where the bar intersected the front of the assumed extended nodal zone, and under the applied load point (Figure 4.12). This layout of strain gauges was used for all reinforcing bars within each specimen. For specimens in Series 1, the location of gauges varied somewhat from this intended layout. For that reason, discussion of strain gauge data will be focused on Series 2.

Headed end   Non-headed end
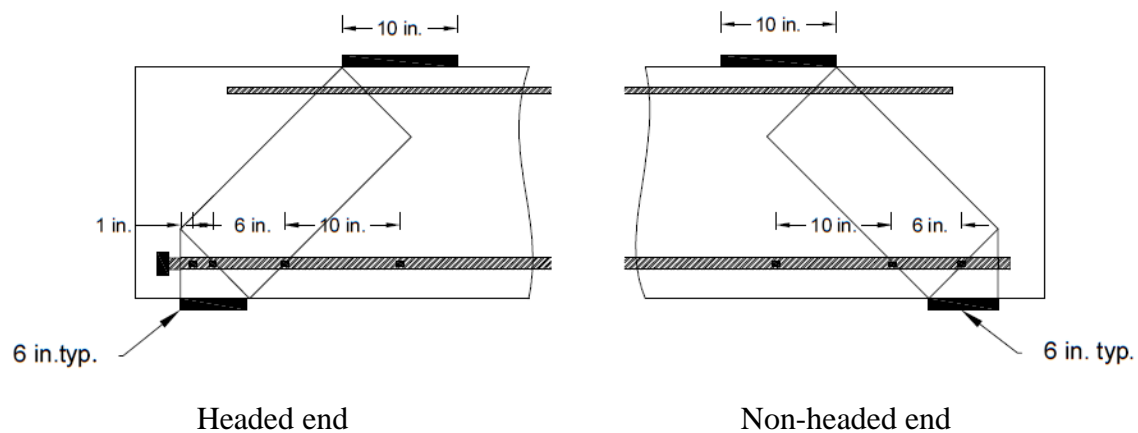
Figure 4.12 Position of strain gauges on longitudinal reinforcement

Figures 4.13 through 4.15 show a summary of the strain gauge results for three pairs of specimens: H-3-8-5-9-F4.1-II and NH-3-8-5-9-F4.1-II; H-3-8-5-11-F4.1-II and NH-3-8-5-11-F4.1-II; and H-3-8-5-13-F4.1-II and NH-3-8-5-13-F4.1-II. Each figure shows recorded strain versus strain gauge location for various levels of imposed force on the specimen. The strain values represent an average of the strain recorded in the longitudinal bars at each location. The position

of the support plate is illustrated at the bottom of each figure. Plots for nominally identical specimens with and without headed ends are placed on the same page to facilitate comparison.
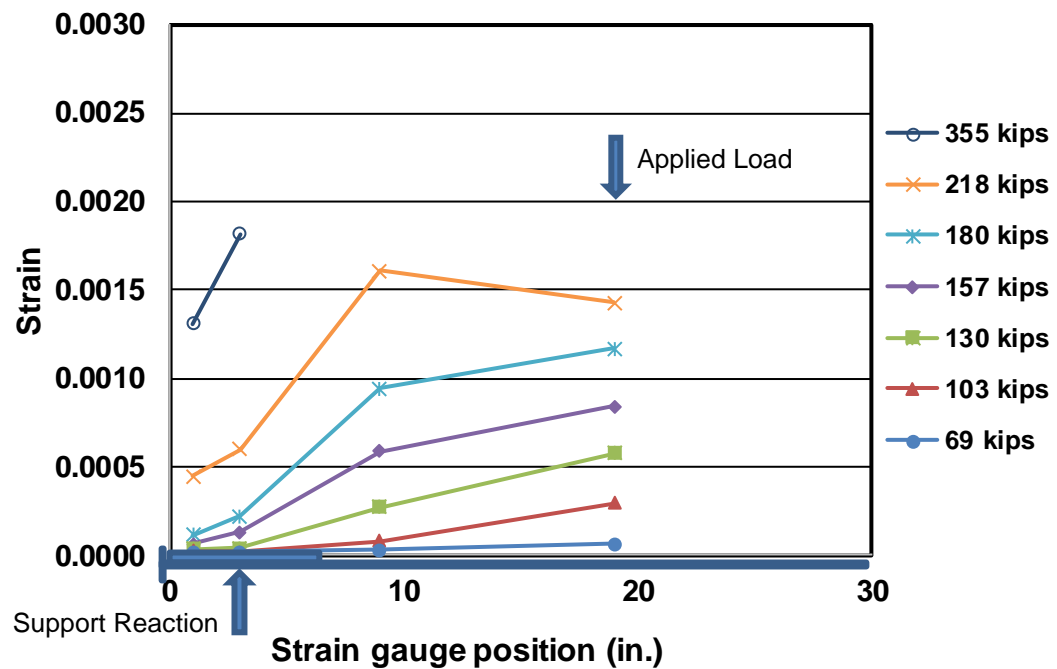
(a)
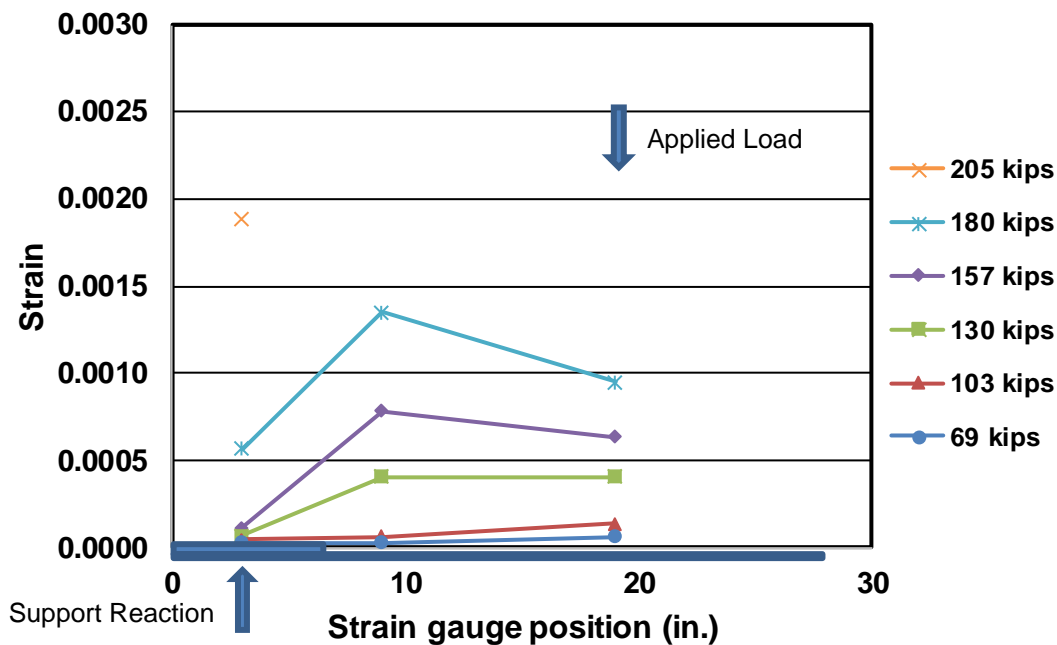
(b)

Figure 4.13 Strain along the longitudinal bars (a) Specimen H-3-8-5-9-F4.1-II, (b) Specimen NH-3-8-5-9-F4.1-II

(a)

(b)
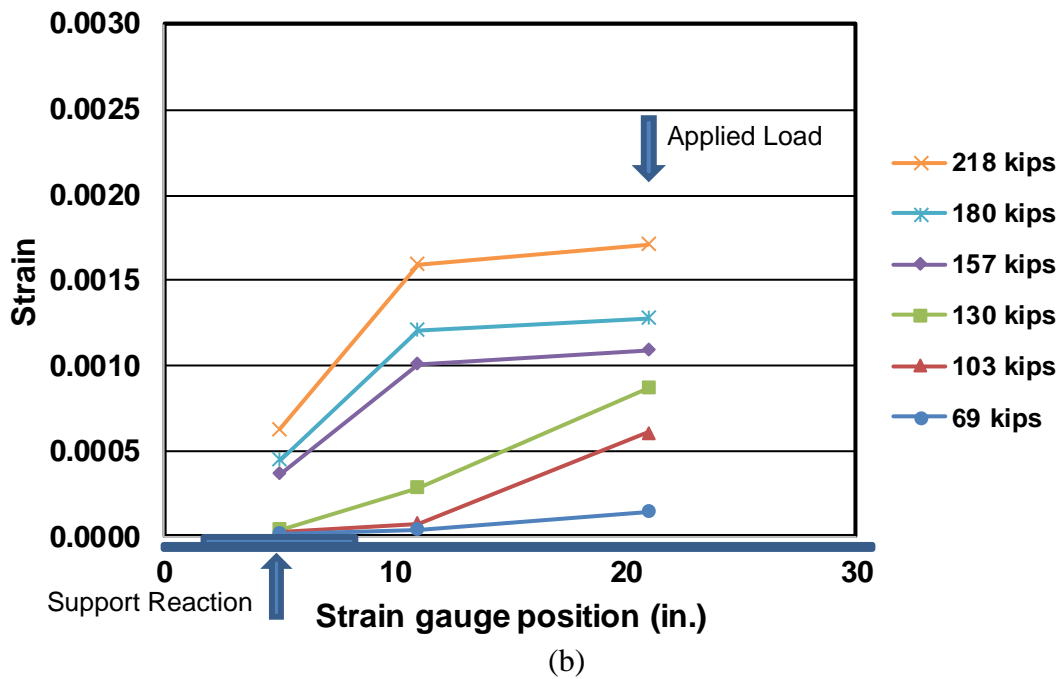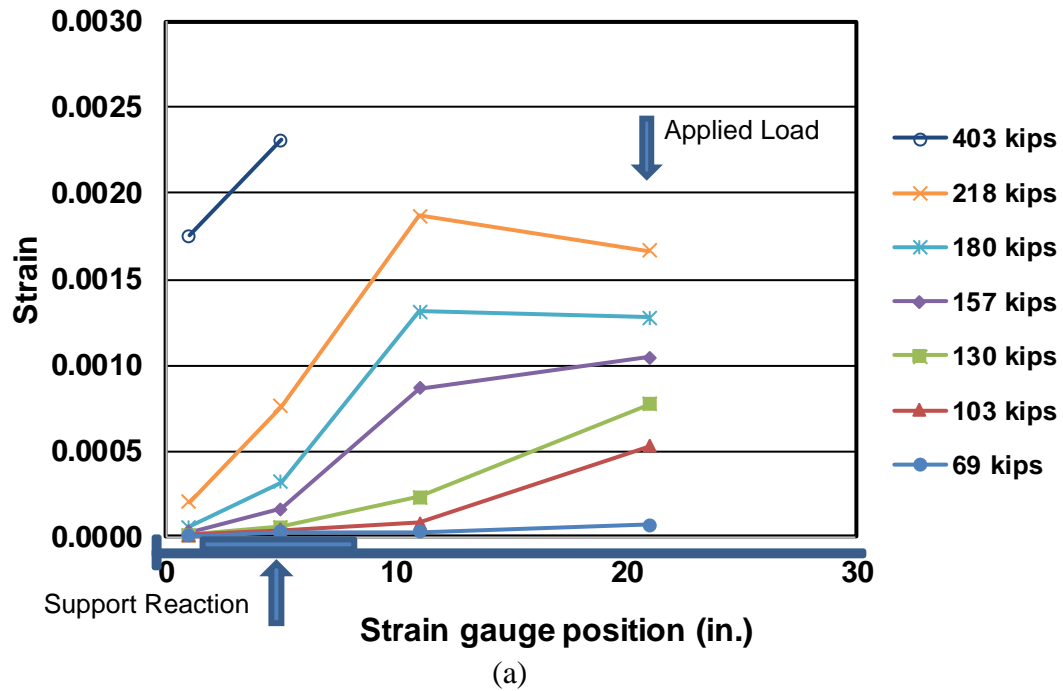
Figure 4.14 Strain along the longitudinal bars (a) Specimen H-3-8-5-11-F4.1-II, (b) Specimen NH-3-8-5-11-F4.1-II

102

(a)

(b)
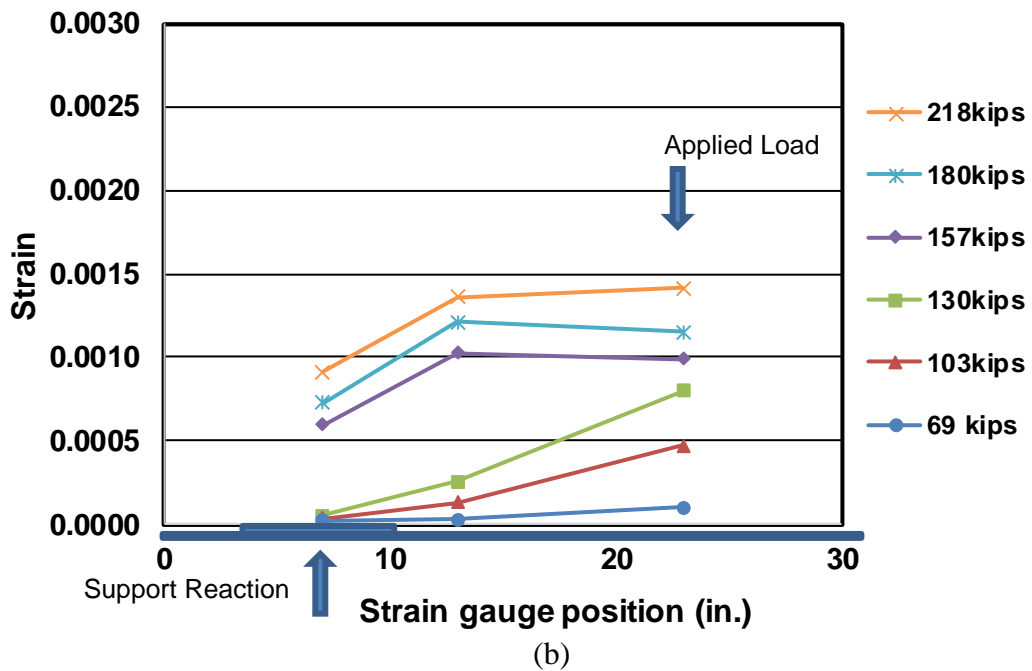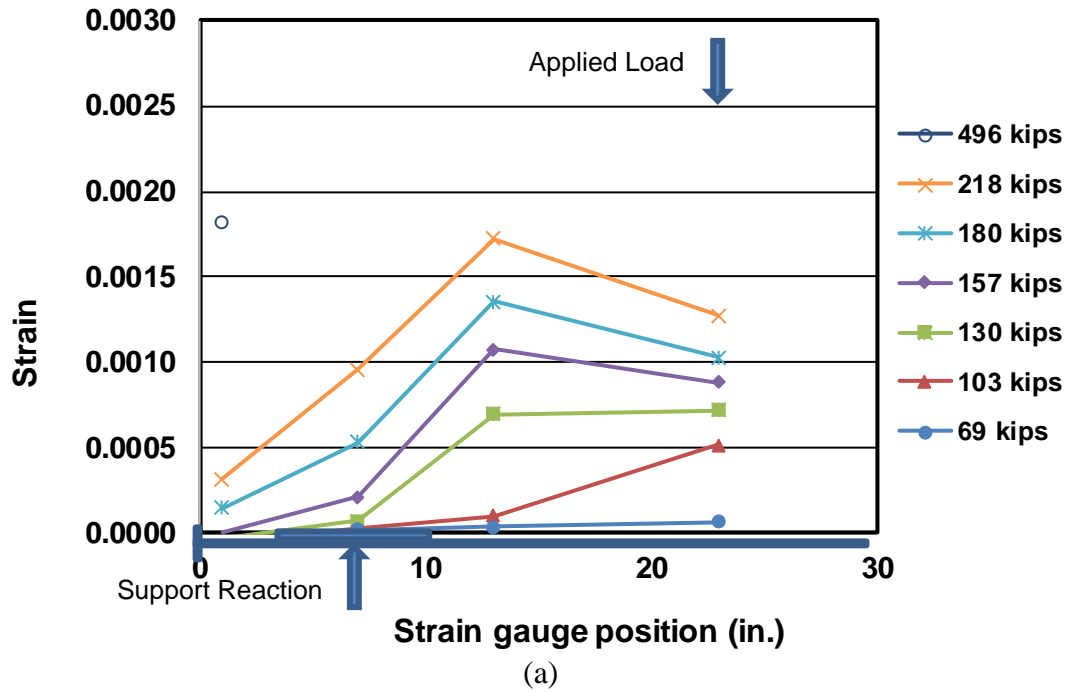
Figure 4.15 Strain along the longitudinal bars (a) Specimen H-3-8-5-13-F4.1-II, (b) Specimen
NH-3-8-5-13-F4.1-II

Figures 4.13 through 4.15 show that, as expected, reinforcement strains were near zero
until after cracking. After the first crack formed, strains varied gradually from approximately zero
at the center of the support plate to a peak located under the applied load. This distribution was

observed up to a load of approximately 130 kips, when nearly equal strain was observed at the face of the assumed extended nodal zone and under the load point. The gradient of strain observed between the face of the extended nodal zone and the end of the bar is consistent with the assumption that a portion of the force in the bar is transferred from the bar to the concrete via bond over this length. The strain reading in the gauge placed on the bar 1 in. from the face of the head remained less than 0.0001 until the applied force reached between approximately 130 and 180 kips.

4.5 HEAD SLIP

Slip of both headed and non-headed ends relative to the surrounding concrete was measured using a combination of linear potentiometers and a non-contact position-monitoring system. While the non-contact position-monitoring system recorded the movement of the concrete near the end of the beam, the potentiometers recorded movement of the reinforcing bars. The potentiometers were connected to the reinforcing bars with wires that passed freely through tubes cast into the concrete cover. Slip was then calculated as the difference between the displacement of the reinforcing bar ends and the surrounding concrete. As illustrated in Figure 4.16, a separate potentiometer was used to record slip of each of the longitudinal bars individually.

Figure 4.17 shows the slip at the headed end for the three longitudinal bars in Specimen H-3-8-5-13-F4.1-II. For most of the test, slip of the middle bar was greater than the outer bars (by approximately 50% greater at a load of 250 kips). These differences diminished as the specimen neared failure; near the peak load, the recorded slip values were within 10%. This pattern, with the middle bar exhibiting greater slip throughout much of the test, was observed for all of the specimens with three longitudinal bars for which slip was recorded.

For comparison between specimens, recorded bar slip was averaged for the bars within a specimen. Figure 4.18 shows the average slip at the headed ends for Specimens H-2-8-5-9-F4.1-II, H-2-8-5-13-F4.1-II, H-3-8-5-9-F4.1-II, and H-3-8-5-13-F4.1-II. The bars did not slip until the applied load reached about 80 kips, coinciding with the initiation of the first crack. Bar slip at the peak load was 0.020 in. for Specimen-2-8-5-9-F4.1-II, 0.03 in. for Specimen H-2-8-5-13-F4.1-II,

0.025 in. for Specimen H-3-8-5-9-F4.1-II, and 0.037 in. for Specimen H-3-8-5-13-F4.1-II. For the non-headed end tests, technical problems during testing prevented recording of slip.
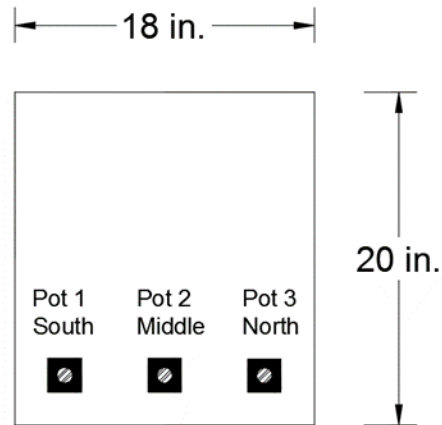
Figure 4.16 Position of linear potentiometers
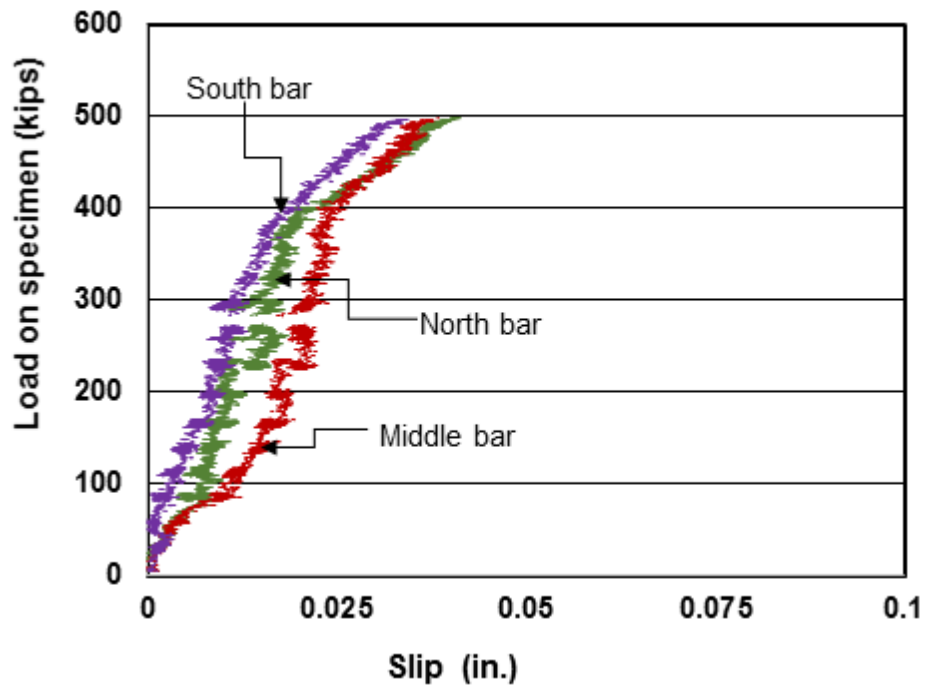
Figure 4.17 Load versus slip of the three headed bar ends in Specimen H-3-8-5-13-F4.1-II
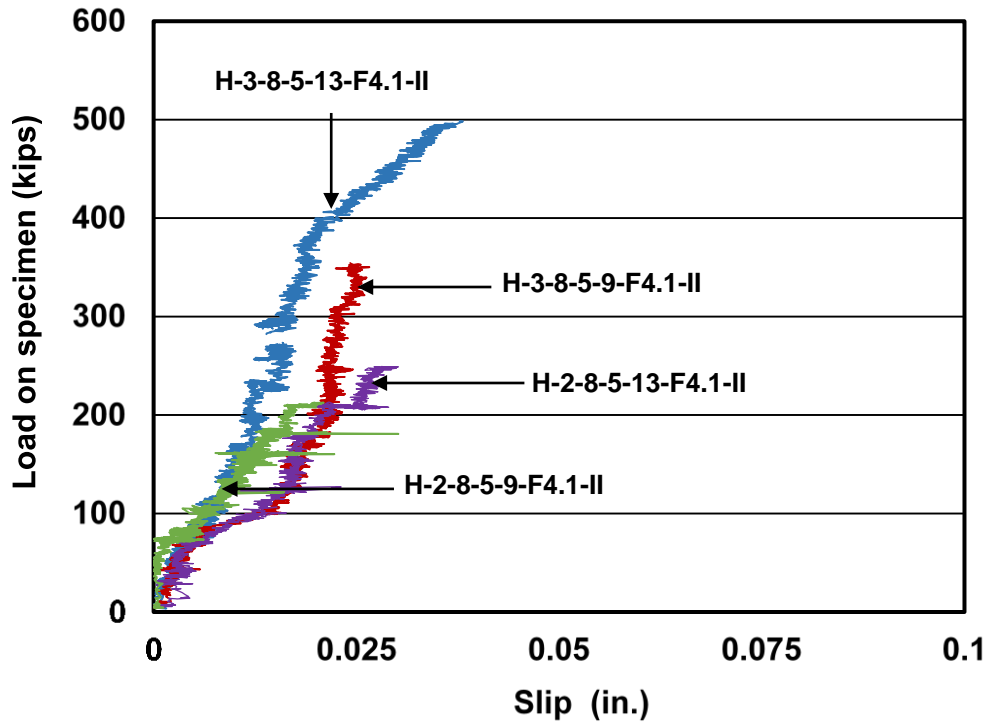
Figure 4.18 Load versus average slip of headed bars for Specimens H-2-8-5-9-F4.1-II, H-2-8-5-13-F4.1-II, H-3-8-5-9-F4.1-II, and H-3-8-5-13-F4.1-II

4.6 ANALYSIS OF INTERNAL ACTIONS

4.6.1 Strut and Tie Forces

The forces in the strut and tie that comprised the model shown in Figure 4.19 were estimated and compared to limits prescribed in the ACI Building Code to corroborate observations that strength of the specimens was limited by anchorage failures (discussed in Section 4.1.2). Internal forces were estimated using equilibrium and assuming that the strut was oriented at an angle of 45° with horizontal. Values calculated based on the peak force resisted by the specimens are listed in Table 4.3.
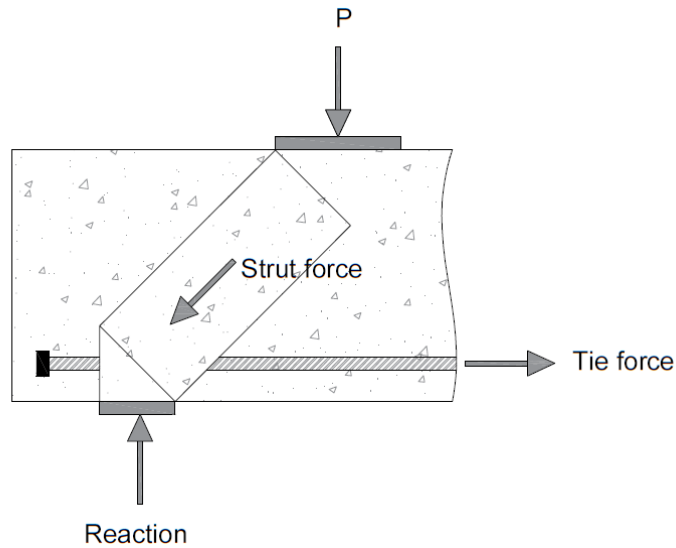
Figure 4.19 Partial strut-and-tie model

Table 4.3 Estimated strut and tie forces

Specimen	Concrete Compressive Strength (psi)	Peak Load (kips)	Strut Force (kips)	Tie Force (kips)
Series 1				
H-2-8-5-9-F4.1-I	5740	278	288	204
H-2-8-5-10.4-F4.1-I	4490	346	359	254
H-3-8-5-9-F4.1-I	5800	446	463	327
H-3-8-5-11.4-F4.1-I	5750	387	401	284
H-3-8-5-14-F4.1-I	5750	495	513	363
Series 2				
H-2-8-5-9-F4.1-II	4630	218	226	160
H-2-8-5-13-F4.1-II	4760	250	259	183
H-3-8-5-9-F4.1-II	4770	355	368	260
H-3-8-5-11-F4.1-II	4820	403	418	296
H-3-8-5-13-F4.1-II	4900	499	518	366

4.6.2 Comparison of Capacity and Demand for Struts and Nodes

The nominal strut capacity (in kips) was calculated according to ACI Building Code (318-14) provisions [Eq. (4.1)].

$$\text{Strut Capacity} = 0.85\beta_s f_{cm} A_{cs} \tag{4.1}$$

where β_s = 0.6, as required by ACI 318-14 for struts with no transverse reinforcement; f_{cm} = the measured concrete compressive strength; and A_{cs} = area of the strut. The area of the strut was assumed to be the product of the beam thickness (18 in.) and the width of the strut, which was limited by the node over the support (Figure 4.20). As illustrated in Figure 4.20, the horizontal and vertical sides of the node were taken as 6 in., resulting in a length of the hypotenuse, and thus strut width, of 8.5 in. The strength of the node was estimated using Eq. (4.1) with β_s replaced by β_n = 0.8 in accordance with ACI Building Code provisions. The calculated nodal capacity was, therefore, greater than the strut capacity by one-third (β_n / β_s = 4/3) Calculated strut and node capacities are compared to demand in Table 4.4.
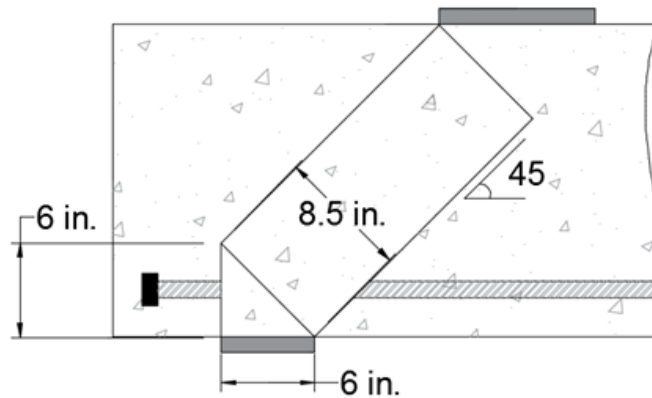
Figure 4.20 Assumed dimensions of the strut and node

Table 4.4 Estimated strut and node capacity and demand

Beam type	Strut demand (kips)	Strut capacity (kips)	Strut capacity/ demand	Node capacity/ demand[1]
Series 1				
H-2-8-5-9-F4.1-I	288	448	1.6	2.0
H-2-8-5-10.4-F4.1-I	359	350	1.0	1.3
H-3-8-5-9-F4.1-I	463	452	1.0	1.3
H-3-8-5-11.4-F4.1-I	401	448	1.1	1.5
H-3-8-5-14-F4.1-I	513	448	0.9	1.2
Series 2				
H-2-8-5-9-F4.1-II	226	361	1.6	2.1
H-2-8-5-13-F4.1-II	259	371	1.4	1.9
H-3-8-5-9-F4.1-II	368	372	1.0	1.4
H-3-8-5-11-F4.1-II	418	376	0.9	1.2
H-3-8-5-13-F4.1-II	518	382	0.7	1.0

[1] For these specimens, node capacity/demand ratios are always 4/3 of the ratios calculated for the struts because the demand was equivalent and the calculated capacity of the node was 4/3 that of the strut.

As shown in Table 4.4, the strut capacity-to-demand ratio is no less than 1.0 for the majority of specimens, indicating that strut failure likely did not govern the strength of the specimens. For the three specimens with a strut capacity-to-demand ratio less than 1.0 (H-3-8-5-14-F4.1-I, H-3-8-5-11-F4.1-II, and H-3-8-5-13-F4.1-II), observations during testing strongly indicated that specimen strength was limited by side blowout (anchorage) and not strut failure.

Table 4.4 shows that node capacity-to-demand ratios are no less than 1.0 for all specimens. Observations made after testing, however, indicate that H-3-8-5-9-F4.1-II may have failed due to crushing of concrete within the node despite having a node capacity-to-demand ratio of 1.4. It is therefore not clear whether anchorage controlled the capacity of this specimen. For this reason, results from H-3-8-5-9-F4.1-II are omitted from comparisons of measured to calculated anchorage strengths.

4.6.3 Stresses, Forces and Embedment Length

Observations and calculations indicate that anchorage failures limited the strength of the CCT-node specimens, with the possible exception of Specimen H-3-8-5-9-F4.1-II in Series 2, which exhibited crushing of concrete within the node. Estimated forces in the longitudinal bars at

peak load can, therefore, be used to evaluate the adequacy of equations proposed for calculation of required embedment length. For this purpose, bar forces were estimated using two means, the strain measurements described in Section 4.4 and the strut-and-tie model described in Section 4.6.2.

Bar force estimated from measured strain: Results from tensile tests of coupons were used to develop relations between measured strain and bar force. The force in the longitudinal bars at peak load was then estimated from bar strains recorded at the face of the extended nodal zone just prior to failure. The bar forces estimated for the four specimens that had strain gauge data recorded until the end of the test are listed in Table 4.5.

Table 4.5 Estimated forces per using strain gauge results and strut-and-tie model

| Beam Type | Force per Bar (kips) | | Ratio |
	From strain gauges	From strut-and-tie	Strut-and-tie/ strain gauge
Series 1			
H-2-8-5-9-F4.1-I	*	102	
H-2-8-5-10.4-F4.1-I	105	127	1.2
H-3-8-5-9-F4.1-I	*	109	
H-3-8-5-11.4-F4.1-I	84	95	1.1
H-3-8-5-14-F4.1-I	102	121	1.2
Series 2			
H-2-8-5-9-F4.1-II	*	80	
H-2-8-5-13-F4.1-II	*	92	
H-3-8-5-9-F4.1-II	72	87	1.2
H-3-8-5-11-F4.1-II	*	99	
H-3-8-5-13-F4.1-II	*	122	

*Data at failure not available

Bar force estimated using strut-and-tie model: Because the longitudinal bars serve as the tie in the strut-and-tie model, the average force per bar at failure can be calculated by dividing the tie force (Table 4.3) by the number of longitudinal bars. The calculated average force per bar is listed in Table 4.5. For specimens that had bar force estimated from both strain gauge data and the strut-and-tie model, the strut-and-tie model tended to result in a 10 to 20% greater bar force than was estimated based on strain gauge data.

110

Figure 4.21 shows the force per bar estimated from the strut-and-tie model for both Series 1 and 2 versus the embedment length measured from the face of the extended nodal zone to the face of the head. This figure shows that there is little difference between specimens with two and three longitudinal bars in the force per bar at failure. For specimens with three longitudinal bars, there appears to be a modest trend of greater force per bar. For specimens with two bars, there does not appear to be a trend within the range of embedment lengths considered.
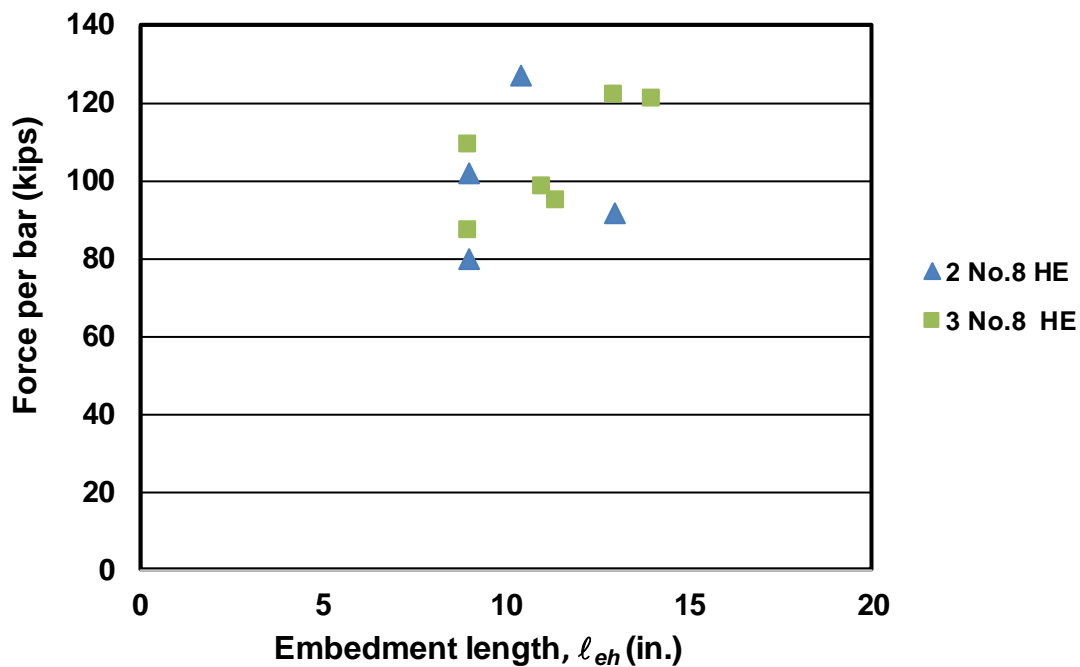
Figure 4.21 Force per bar estimated using a strut-and-tie model versus embedment length

CHAPTER 5: TEST RESULTS FOR SHALLOW EMBEDMENT SPECIMENS

In this chapter, test results from shallow embedment specimens are presented. It includes failure modes and the effects of test parameters on headed bar anchorage strength.

5.1 SHALLOW EMBEDMENT TESTS

Six series of shallow embedment pullout tests were conducted to investigate the effects of concrete compressive strength, net bearing area of the head, and flexural reinforcement running perpendicular to the headed bar on the anchorage capacity of a headed bar. Table 5.1 shows the details of specimens tested. The 32 headed bars in this portion of the study had a 6 in. nominal embedment length ℓ_{eh}. Concrete compressive strength f_{cm} ranged from 4,200 to 8,620 psi and stress in the bars at failure ranged from 49,500 to 117,000 psi.

5.1.1 Failure Modes

The shallow embedment pullout specimens contained two or three headed bars, except for one specimen that had a single bar anchored in the middle. Only one headed bar was loaded at a time; the spacing between the bars was chosen to ensure that the failure of one headed bar would not interfere with the anchorage strength of adjacent bars. All specimens exhibited breakout failure in which a region of concrete was pulled out of the slab along with the anchored bar, forming a cone-shaped failure surface. The exact failure pattern depended on the placement of the test frame supports, as shown in Figure 5.1. In Figure 5.1a, one of the supports is within the anticipated failure region and the other is away from it, while in Figure 5.1b both supports are outside the anticipated failure region. When the support was close to the bar it confined, the concrete and the failure surface extended towards the unconfined region away from the supports. The effect of support locations on anchorage strength is described in Section 5.1.4.

Table 5.1 Detail of shallow embedment pullout specimens[1]

	Specimen[2]			ℓ_{eh}	f_{cm}	b	h	h_{cl}	c_{so}	c_{th}	A_{brg}/A_b	A_{st}	T	f_{su}
	SN	Designation	Head	in.	psi	in.	in.	in.	in.	in.		in.^{2}	kips	ksi
Series 1	1	8-5-T9.5-8#5-6	A	8.0	7040	48	15	10.5	23.5	7.0	9.5	2.48	65.6	83.0
		8-5-T9.5-8#5-6	B	8.3	7040	48	15	10.5	23.5	6.8	9.5	2.48	67.8	85.8
	2	8-5-T4.0-8#5-6	A	8.5	7040	48	15	10.5	23.5	6.5	4.0	2.48	61.8	78.2
		8-5-T4.0-8#5-6	B	7.5	7040	48	15	10.5	23.5	7.5	4.0	2.48	56.3	71.3
Series 2	3	8-5-F4.1-8#5-6	A	7.4	5220	48	15	10.5	23.5	7.6	4.1	2.48	68.9	87.2
		8-5-F4.1-8#5-6	B	7.4	5220	48	15	10.5	23.5	7.6	4.1	2.48	64.4	81.5
	4	8-5-F9.1-8#5-6	A	7.1	5220	48	15	10.5	23.5	7.9	9.1	2.48	69.9	88.5
		8-5-F9.1-8#5-6	B	7.0	5220	48	15	10.5	23.5	8.0	9.1	2.48	54.9	69.5
Series 3	5	8-5-F4.1-2#8-6	A	6.0	7390	48	15	10.5	23.5	9.0	4.1	1.58	64.4	81.5
		8-5-F9.1-2#8-6	B	6.0	7390	48	15	10.5	23.5	9.0	9.1	1.58	65.0	82.3
	6	8-5-T4.0-2#8-6	A	6.1	7390	48	15	10.5	23.5	8.9	4.0	1.58	60.5	76.6
		8-5-T9.5-2#8-6	B	6.1	7390	48	15	10.5	23.5	8.9	9.5	1.58	57.7	73.0
Series 4	7	8-8-O12.9-6#5-6	A	6.3	8620	48	15	9.8	23.5	8.8	12.9	1.86	79.0	100.0
		8-8-O9.1-6#5-6	B	6.3	8620	48	15	10.5	23.5	8.8	9.1	1.86	70.9	89.7
	8	8-8-S6.5-6#5-6	A	6.4	8620	48	15	10.0	23.5	8.6	6.5	1.86	92.4	117.0
		8-8-O4.5-6#5-6	B	6.5	8620	48	15	10.8	23.5	8.5	4.5	1.86	74.0	93.7
Series 5	9	8-5-S14.9-6#5-6	A	6.5	4200	48	15	10.3	23.5	8.5	14.9	1.86	61.8	78.2
		8-5-S6.5-6#5-6	B	6.5	4200	48	15	10.0	23.5	8.5	6.5	1.86	49.2	62.3
	10	8-5-O12.9-6#5-6	A	6.6	4200	48	15	10.0	23.5	8.4	12.9	1.86	52.4	66.3
		8-5-O4.5-6#5-6	B	6.5	4200	48	15	10.1	23.5	8.5	4.5	1.86	50.1	63.4
	11	8-5-S9.5-6#5-6	A	6.5	4200	48	15	10.3	23.5	8.5	9.5	1.86	48.9	61.9
		8-5-S9.5-6#5-6	B	6.4	4200	48	15	10.1	23.5	8.6	9.5	1.86	54.5	69.0
	12	8-5-F4.1-6#5-6[3]	-	8.4	4200	48	15	47.3	23.5	6.6	4.1	1.86	39.1	49.5
Series 6	13	8-5-F4.1-0-6	A	6.5	5180	60	19	15.0	30.3	12.0	4.1	0	50.5	63.9
		8-5-F4.1-0-6	B	6.3	5180	60	19	17.0	30.5	12.0	4.1	0	48.9	61.9
		8-5-F4.1-2#5-6	C	6.8	5180	60	19	17.0	30.3	12.0	4.1	0.62	61.5	77.8
	14	8-5-F4.1-4#5-6	A	6.0	5180	60	19	16.8	30.0	12.0	4.1	1.24	53.4	67.6
		8-5-F4.1-4#5-6	B	6.1	5180	60	19	17.0	30.3	12.0	4.1	1.24	52.4	66.3
		8-5-F4.1-4#5-6	C	6.8	5460	60	19	17.0	30.3	12.0	4.1	1.24	53.5	67.7
	15	8-5-F4.1-6#5-6	A	6.3	5460	60	19	17.3	30.5	12.0	4.1	1.86	47.3	59.8
		8-5-F4.1-6#5-6	B	6.6	5460	60	19	16.8	30.0	12.0	4.1	1.86	55.9	70.8
		8-5-F4.1-6#5-6	C	6.9	5460	60	19	17.0	30.3	12.0	4.1	1.86	52.6	66.6

[1] SN = specimen number; ℓ_{eh} = embedment length; b and h_{slab} = width and height of slab, respectively; h_{cl} = clear distance between the center of headed bar to the inner face of the nearest support plate; c_{so} = clear side concrete cover to the headed bar; c_{th} = bottom clear concrete cover to the head; A_{brg} = net bearing area of head; A_b = area of bar; A_{st} = total area of flexural reinforcement; T = peak tensile load; f_{su} = peak stress on headed bar

[2] Multiple headed bars in a single specimen are denoted by letters A, B, and C.

[3] Specimen contained a single centrally placed headed bar.

113
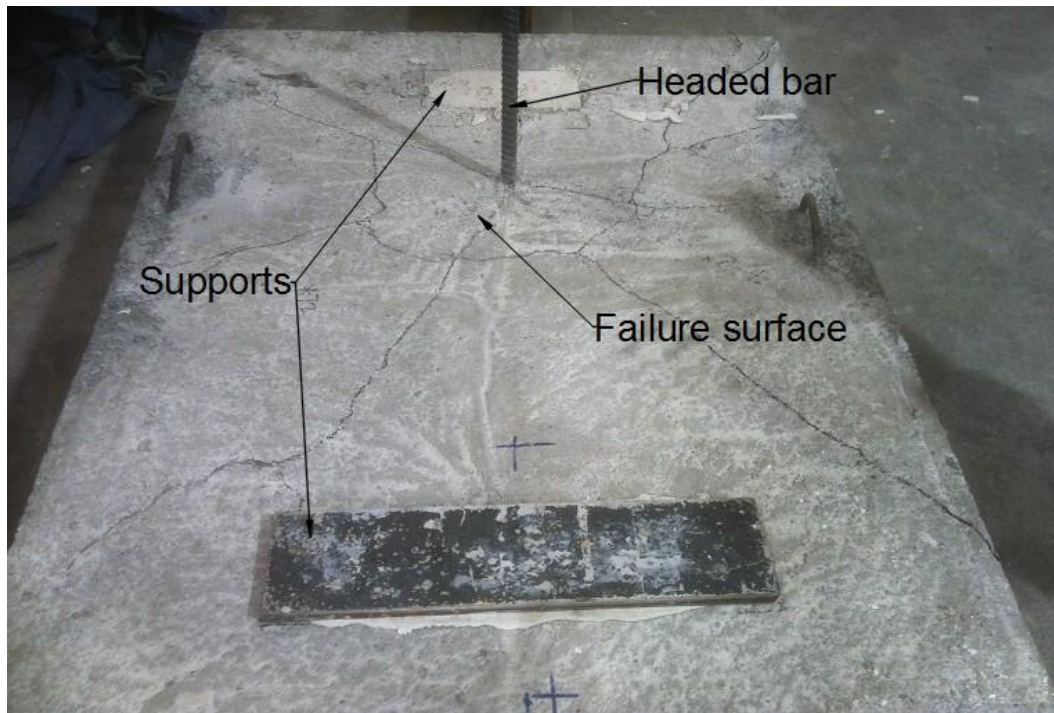
Figure 5.1a Breakout failure of shallow embedment pullout specimens from test Series 1 to 5.
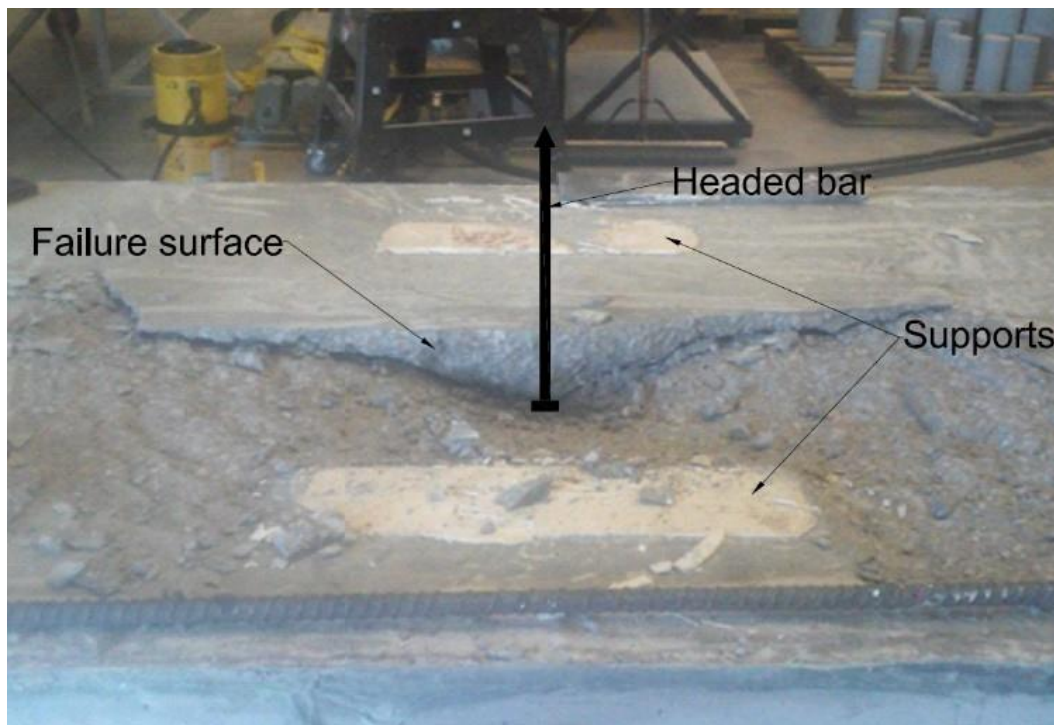
Figure 5.1b Breakout failure of shallow embedment pullout specimens from Series 6

5.1.2 Effect of Reinforcement in a Plane Perpendicular to Headed Bar

Reinforcement in a plane perpendicular to the headed bar (flexural reinforcement), as shown in Figure 5.2, was provided symmetrically on both sides of the bar. The amount of total flexural reinforcement A_{st} provided is presented in Table 5.1. In the first five series, an equal amount of reinforcement was provided close to the edge of the slab with 1.5-in. concrete clear cover (Figures 5.2a and b), with the exception of one specimen in Series 1 that contained No. 5 bars at 6-in. spacing in the long direction and 12-in. spacing in the short direction with 1.5-in concrete clear cover on the top. In Series 6, for the headed bar that contained flexural reinforcement, the reinforcement was provided close to the bar on both sides (Figures 5.2c and d).
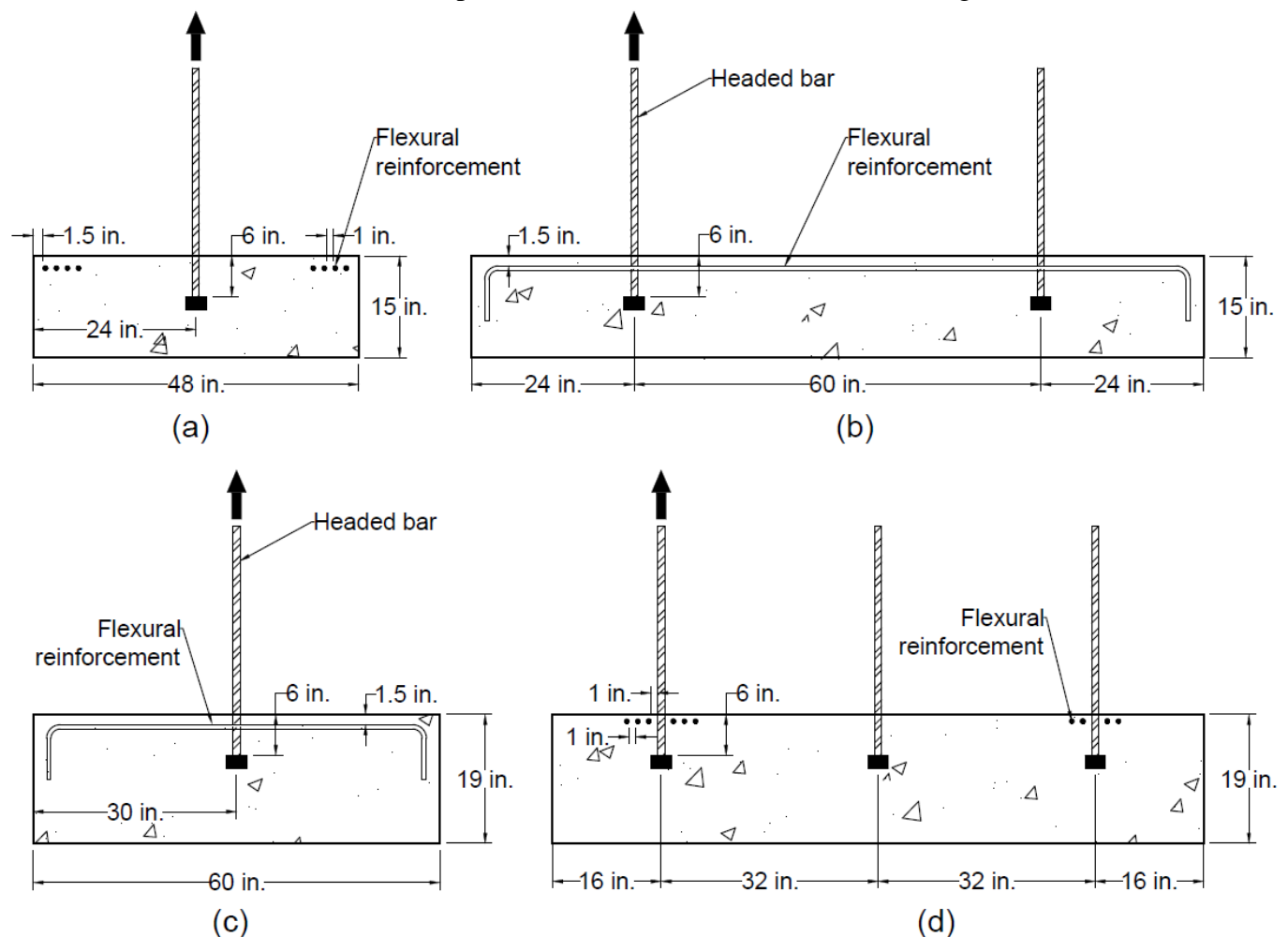
Figure 5.2 Location of headed bars and flexural reinforcement: (a) front and (b) side views of specimens in first five series, (c) front and (d) side views of specimens in Series 6

Figure 5.3 shows the relationship between bar force normalized with respect to concrete compressive strength T_N and amount of flexural reinforcement A_{st}. The force in the headed bar plotted in vertical axis is normalized with respect to 5000 psi concrete compressive strength using Eq. (5.1).

$$T_N = T \left(\frac{5000}{f_{cm}} \right)^{1/4}$$
(5.1)

where T is the measured tensile force in the headed bar in kips, and f_{cm} is the measured concrete compressive strength in psi (pounds per square inch). The trend line (specimens without the flexural reinforcement are not included) suggests a positive relationship between anchorage strength and amount of flexural reinforcement. Based on the trend line, increasing the flexural reinforcement from 0.62 to 2.5 in.^{2} increased the anchorage strength by 13% on average, although the single strength for 0.62 in.^{2} closely matches the normalized force for 2.5 in.^{2} flexural reinforcement.
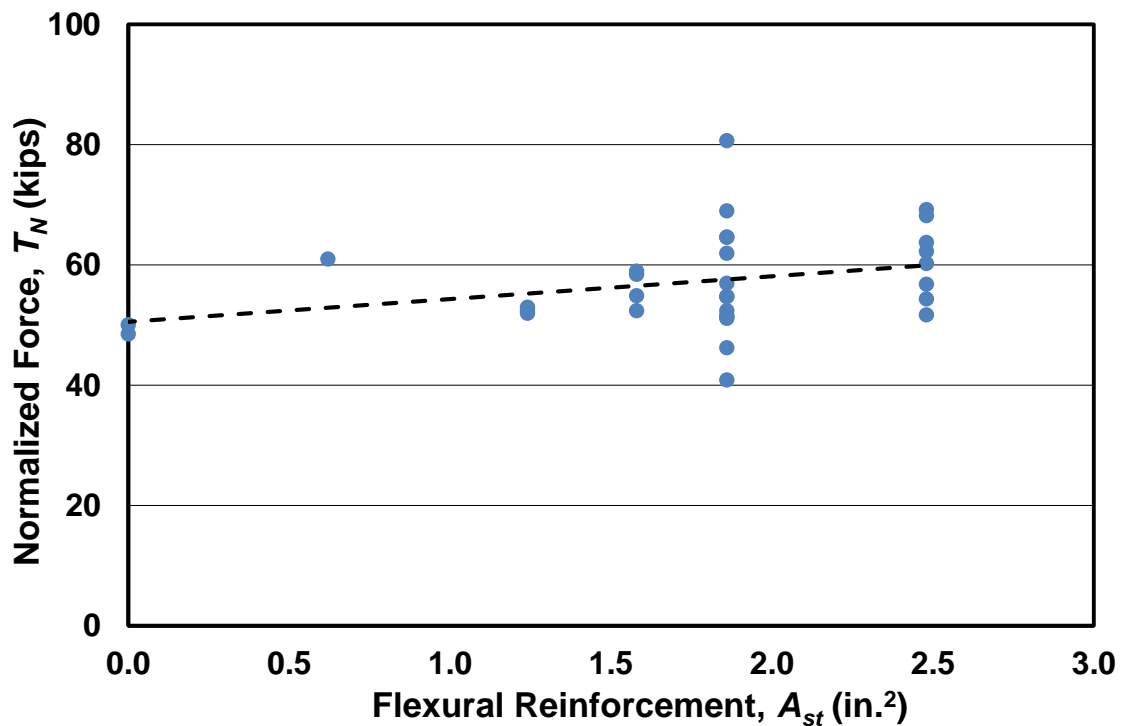
Figure 5.3 Normalized maximum bar force in shallow embedment pullout tests T as a function of flexural reinforcement

5.1.3 Effect of Net Bearing Area of Head

The effect of net bearing area on the anchorage strength of headed bar is shown in Figure 5.4. In general, increasing the net bearing area of the head increased the anchorage strength. However, increasing the net bearing area head A_{brg} from 4 to 14.9A_b resulted in only an 18% average increase in the anchorage strength.
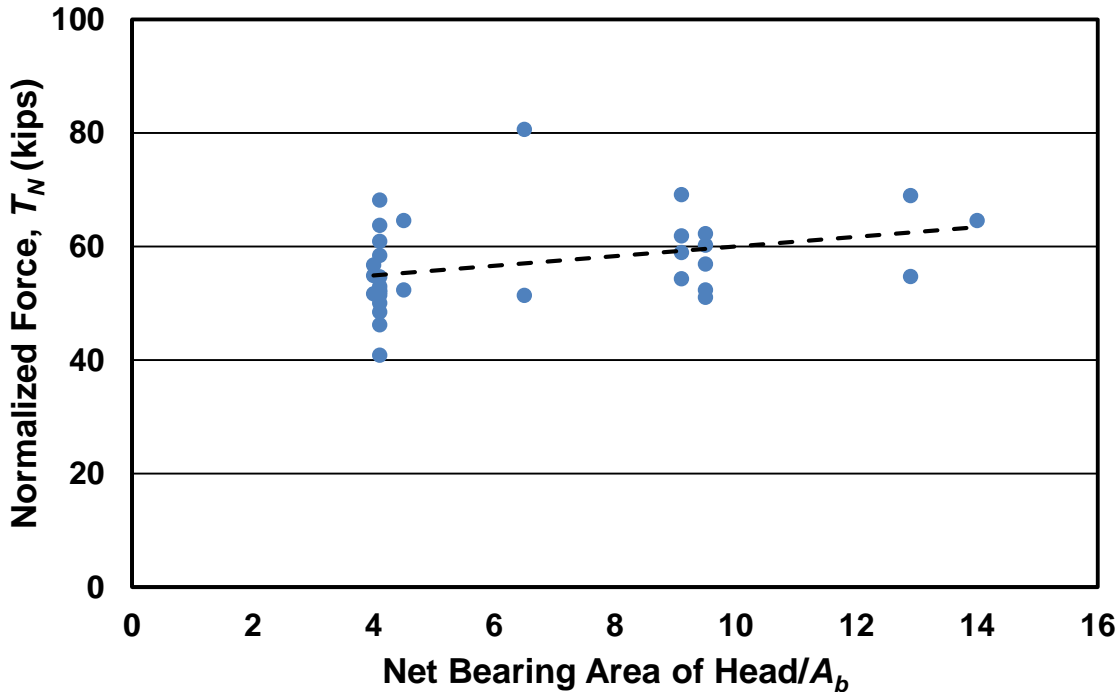
Figure 5.4 Normalized maximum bar force in shallow embedment pullout tests T as a function of net bearing area of head

5.1.4 Effect of Strut Angle

The anchorage strength of a headed bar is dependent on the angle of the strut between the head and the compressive reaction (Figure 5.5). The flatter the angle, the lower the strength. To limit the angle, Section R25.4.4.2 of the Commentary to ACI 318-14 suggests that the effective depth of the beam d at a beam-column joint not exceed $1.5\ell_{dt}$. To determine if this behavior is observable in the shallow embedment pullout tests, the normalized anchorage strengths of the shallow embedment specimens are compared with the ratio h_{cl}/ℓ_{eh} for the specimens, where h_{cl} is distance from the center of the headed bar to the inside face of the bearing plate (Figure 5.5). This angle is somewhat higher than the actual strut angle (measured from the headed bar to the centroid of the reaction) but is representative of the region susceptible to a breakout failure. As shown in

Figure 5.6, increasing h_{cl}/ℓ_{eh} from 1.24 to 5.6 resulted in a decrease in anchorage strength. Figure 5.6 also shows that Specimen 8-5-F4.1-6#5-6, which contained a single headed bar in the middle of the concrete with $h_{cl}/\ell_{eh} = 5.6$, had the lowest strength of the shallow embedment specimens. In this case, $h_{cl} = 47.3$ in. for both supports. $h_{cl}/\ell_{eh} = 5.6$ is much higher than the maximum ratio of 1.5 suggested by Commentary Section R25.4.4.2 of ACI 318-14. As a result, the headed bar in Specimen 8-5-F4.1-6#5-6 exhibited a low strength relative to that of the other shallow embedment pullout specimens.
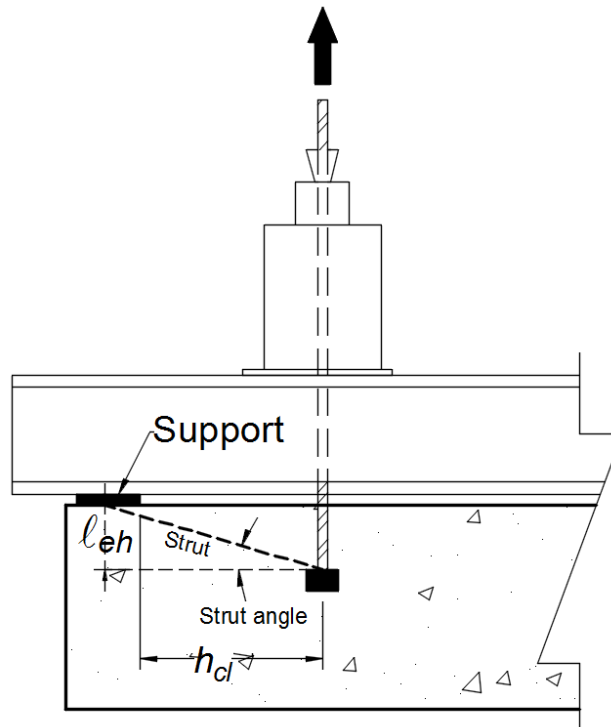
Figure 5.5 Compression region between anchored headed bar and nearest support
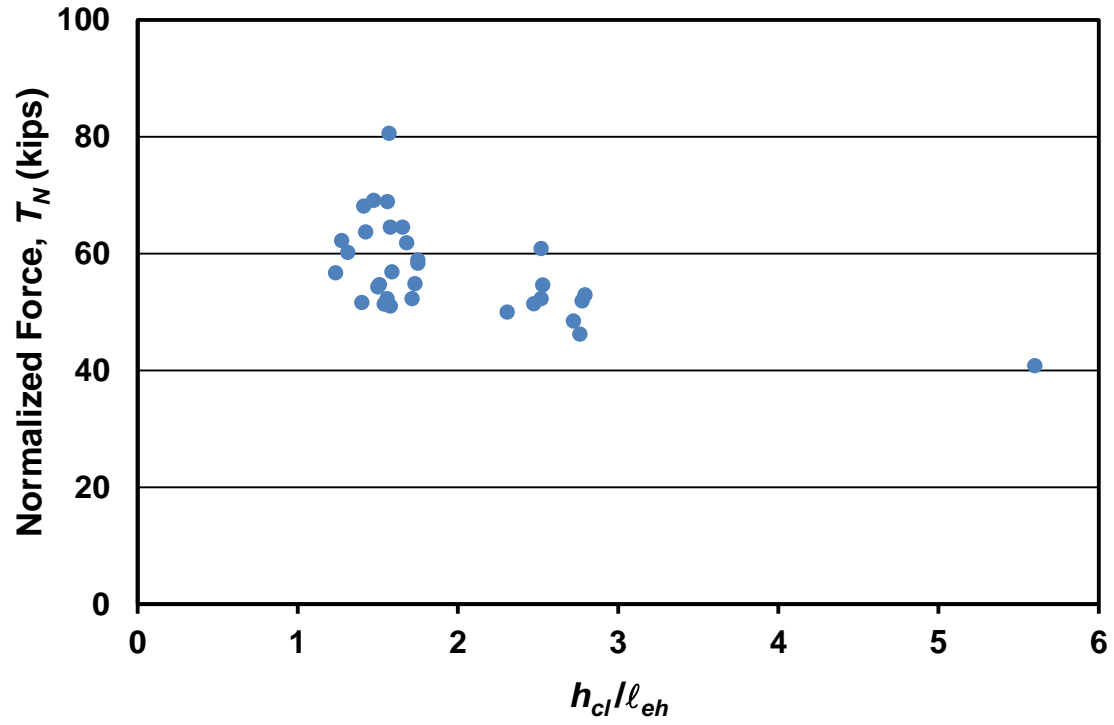
Figure 5.6 Normalized maximum bar force in shallow embedment pullout tests T as a function of the ratio of the distance from the center of the headed bar to the inside face of the bearing plate h_{cl} to the embedment length ℓ_{eh}

CHAPTER 6: TEST RESULTS FOR SPLICE SPECIMENS

In this chapter, test results from headed bar splice specimens are presented. It includes failure modes, effects of test parameters on headed bar anchorage strength, and a comparison of splice test results with the results from other studies.

6.1   HEADED BAR SPLICE TESTS

A total of six specimens with headed bar splices were tested in two series of three specimens each. The heads with a net bearing area A_{brg} equal to four times the area of the lapped bar A_b (Figure 2.2). The specimens had a lap splice length ℓ_{st} of 12 in., with center-to-center spacing between the bars being spliced of $1^1/_4$, $1^3/_4$, or $2^5/_8$ in., corresponding to clear spacing between bars of $^1/_2$ in. ($0.67d_b$), 1 in. ($1.33d_b$), and $1^7/_8$ in. ($2.55d_b$), respectively. The lowest spacing corresponds to lapped bars with the heads in contact with the adjacent bar. The concrete compressive strengths f_{cm} averaged 6,360 and 10,950 psi for the first and second series, respectively. Table 6.1 summarizes the details of the specimens tested. Specimens with clear spacing between the spliced bars c_h of 1 in. and $1^7/_8$ in. complied with the minimum clear spacing requirements in accordance with Section 25.2.1 of ACI 318-14; the specimens with $c_h = {}^1/_2$ in. did not comply with these requirements. (The maximum aggregate size was $^3/_4$ in.)

Table 6.1 Detail of headed bar splice specimens tested[1]

Specimen	N	d_b	A_b	f_{cm}	ℓ_{st}	c_h	b	h	L_1	L_2	f_{su}	P	M
		in.	in^2	psi	in.	in.	in.	in.	in.	in.	ksi	kips	kip-in
(3) 6-5-S4.0-12-0.5	3	0.75	0.44	6330	12	$^1/_2$	18.0	20.3	40.1	64.0	77.2	83.2	1669.2
(3) 6-5-S4.0-12-1.0	3	0.75	0.44	6380	12	1	18.1	20.3	40.1	64.0	83.6	90.1	1804.8
(3) 6-5-S4.0-12-1.9	3	0.75	0.44	6380	12	$1^7/_8$	18.0	20.1	40.1	64.0	76.3	82.2	1649.1
(3) 6-12-S4.0-12-0.5	3	0.75	0.44	10890	12	$^1/_2$	18.0	20.1	40.0	64.1	81.9	89.1	1782.8
(3) 6-12-S4.0-12-1.0	3	0.75	0.44	10890	12	1	18.0	20.5	40.1	64.0	75.0	81.5	1635.9
(3) 6-12-S4.0-12-1.9	3	0.75	0.44	11070	12	$1^7/_8$	18.0	20.5	40.0	64.0	82.8	90.1	1802.4

[1]N = number of lapped bars; A_b = cross-sectional area of lapped bar; b and h = width and depth of specimen, respectively; L_1 = average distance between loading points and the nearest supports; L_2 = distance between two supports (span length); f_{su} = stress on lapped bar at failure calculated from moment-curvature analysis; P = total load applied on specimen; M = average bending moment in splice region.

6.1.1 Failure Modes

The first flexural cracks were observed at about 40% of the ultimate load in the vicinity of the splice. Increasing the load resulted in new flexural cracks near the supports as the existing cracks widened. Specimens failed at widened flexural cracks in the vicinity of the splice; in most cases exposing the head of the lapped bar (as shown in Figure 6.1). All specimens exhibited a side splitting failure in which the lapped bars closest to the side faces of the beam (edge bars) pushed the cover concrete out while the middle bar remained confined by concrete. This resulted in a greater strain at failure in the middle bar compared to the edge bars. Strain in the lapped bars is discussed in detail in Section 6.1.2. In five out of six specimens, side splitting occurred predominantly at the end of the splice region closer to the pinned support (described in Section 2.5.5), while one specimen exhibited side splitting at the end of the splice region closer to the roller support.
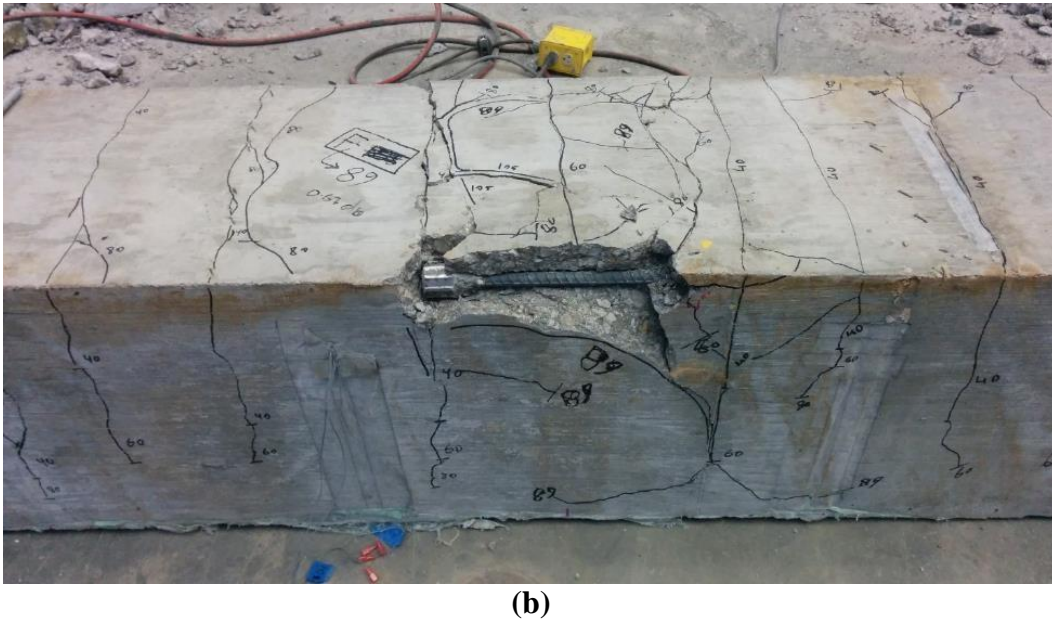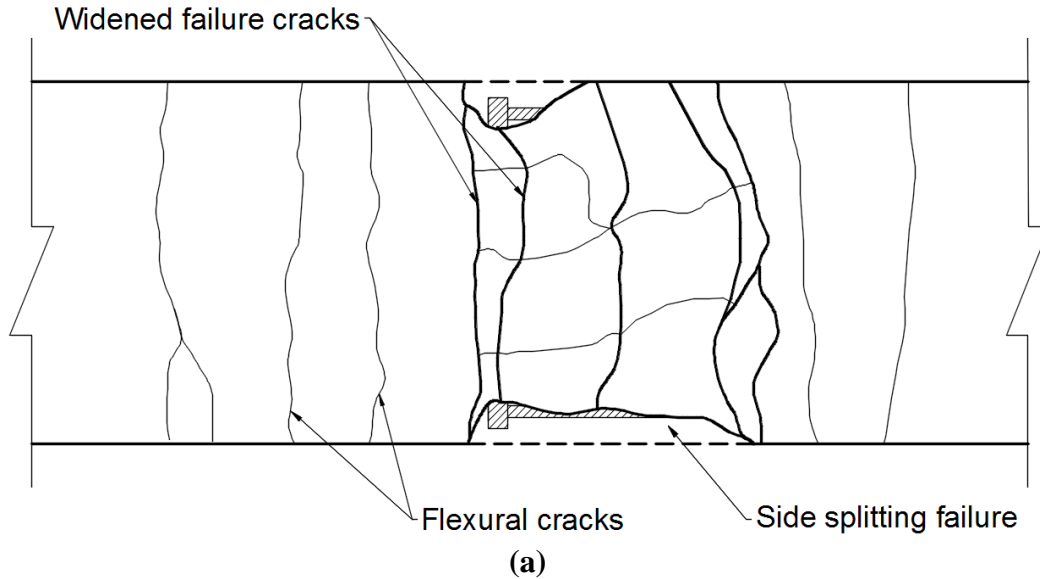
Figure 6.1 (a) Schematic diagram of general cracking patterns and failure modes of headed splice specimens (top view) (b) cracking patterns and failure mode of Specimen (3) 6-12-S4.0-12-0.5

6.1.2 Effect of Lapped Bar Spacing and Concrete Compressive Strength

The center-to-center spacing between the spliced headed bars was $1\frac{1}{4}$, $1\frac{3}{4}$, or $2\frac{5}{8}$ in. The concrete compressive strengths averaged 6,360 and 10,950 psi for the first and second series, respectively. Figures 6.2 and 6.3 compare the average maximum forces and average stresses, respectively, in the spliced bars in the specimens as a function of center-to-center spacing. The

average forces in the headed bars plotted in the vertical axis were determined using moment-curvature analysis, as described in ACI 408R-03. The moment-curvature analysis takes into account both concrete and steel stress-strain characteristics to determine the stress on the bar. In this analysis, the stress-strain behavior for concrete was assumed to follow the model proposed by Hognestad (1951); the stress-strain behavior of the headed bar was obtained from tensile tests (Figure 6.4). The moment M in the splice region is determined by multiplying one-half of the total load applied on the specimen P by the average distance between the loading point and the support L_1. The moment-curvature analysis converted the moment in the beam to a strain in the bars due to bending. Results from tensile tests of headed bars (Figure 6.4) were used to convert the bar strain to stress.

Figures 6.2 and 6.3 show that the spacing between the bars being spliced did not have a significant effect on the splice strength of headed bars. Furthermore, Student's t-test was used to determine the statistical significance of differences between the splice strength for different concrete compressive strengths. Based on the average maximum force in the spliced bars in each of the two test series (with average concrete compressive strengths of 6,360 and 10,950 psi), Student's t-test indicates that the differences in splice strength as a function of concrete compressive strength are not statically significant (level of significance $p = 0.8$).
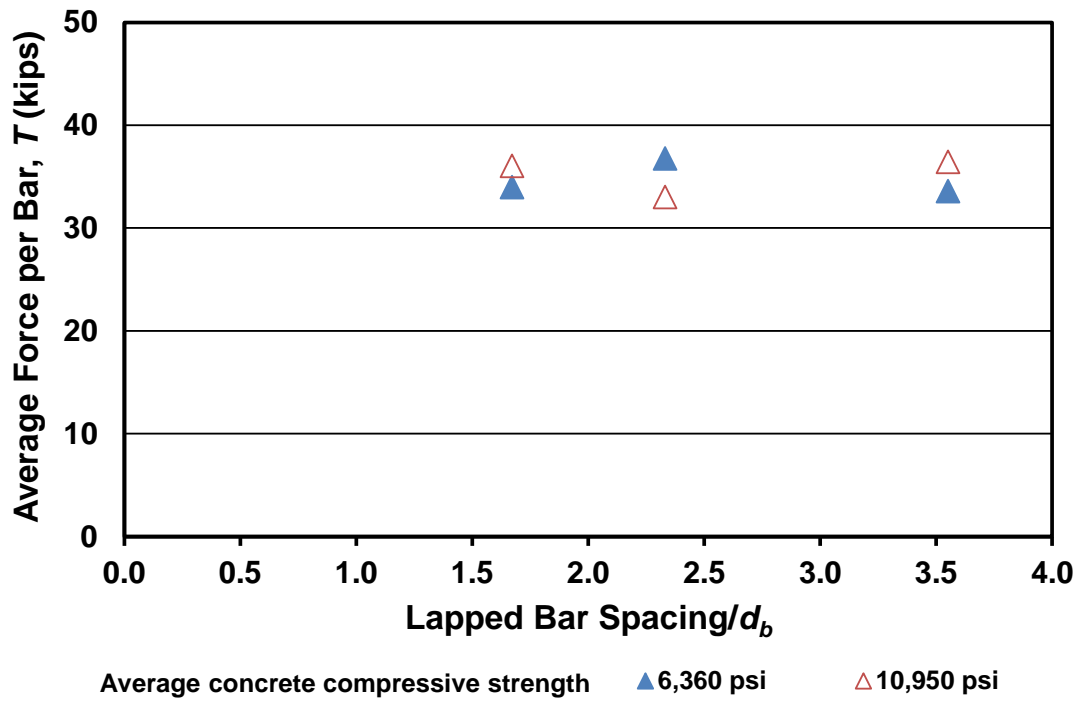
Figure 6.2 Average maximum force in spliced headed bars *T* as a function of center-to-center spacing and concrete compressive strength
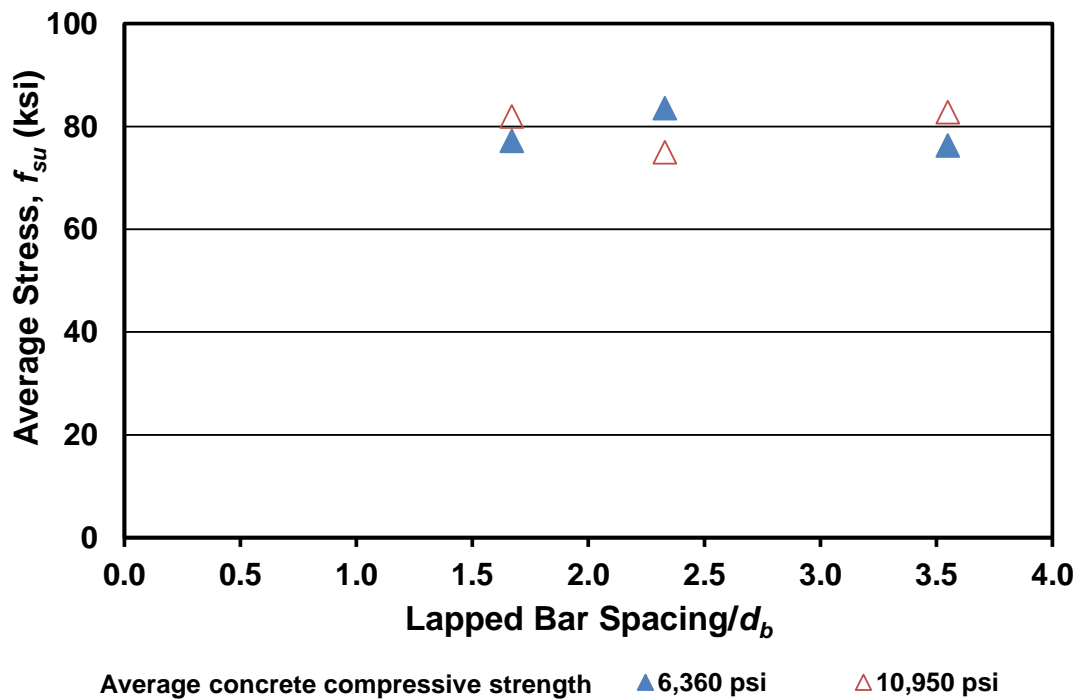
Figure 6.3 Average maximum stress f_{su} in spliced headed bars as a function of center-to-center spacing and concrete compressive strength
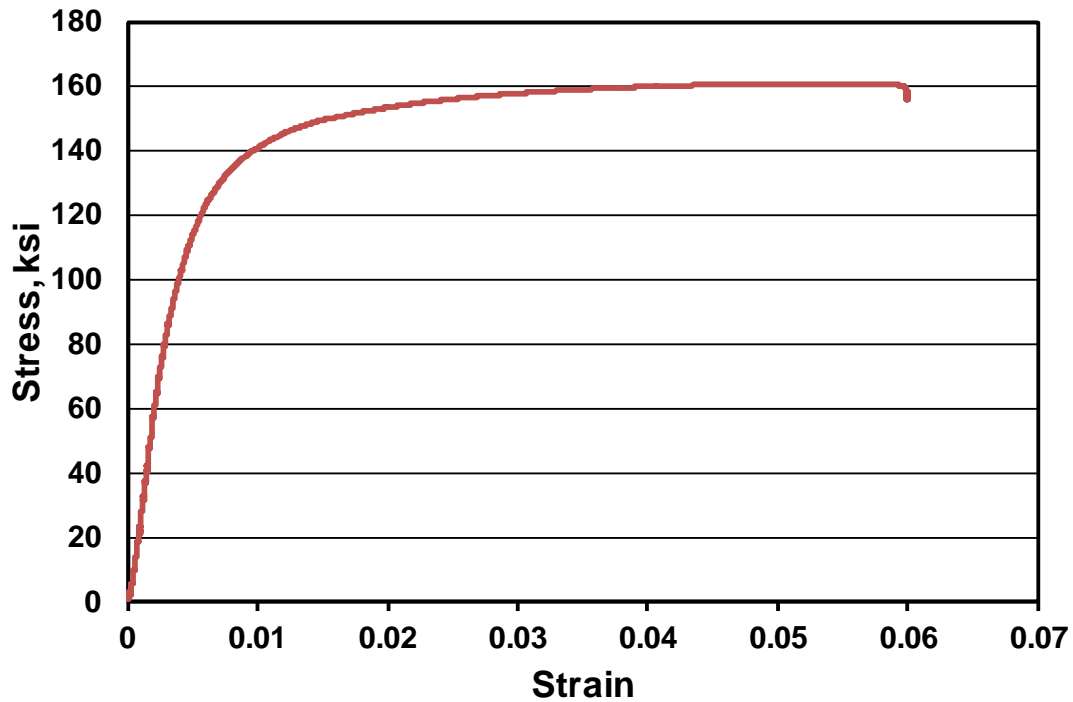
Figure 6.4 Stress-strain behavior for headed bars used in splice specimens

6.1.3 Load-Deflection and Strain in Lapped Bars

The deflection of each specimen was measured using infrared markers. Markers mounted at the loading points and at midspan were used to calculate the maximum deflection of the beam. The load-deflection diagram for Specimen (3) 6-12-4Ab-12-0.5 is presented in Figure 6.5. The decrease in stiffness of the beam (marked by the change in slope of the load-deflection curve at about 40% of the maximum load) corresponds with the formation of flexural cracks.
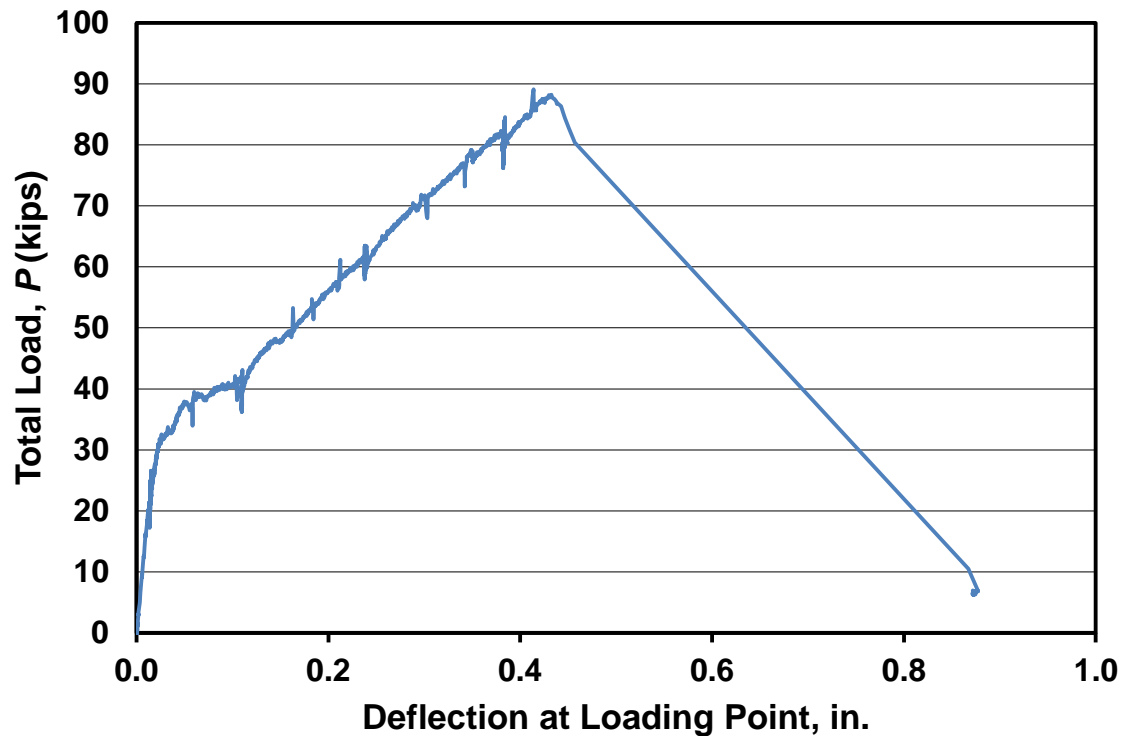
Figure 6.5 Load-deflection diagram for Specimen (3) 6-12-S4.0-12-0.5

The strain on the headed bars was measured using strain gauges mounted 1 in. outside the splice region. The strain results were used to evaluate the stress distribution between the middle and edge spliced bars. The gauge readings were highly dependent on the location of the gauges with respect to the flexural cracks; when cracks crossed the gauge, the strain readings were higher than when the cracks did not cross the gauge. Therefore, the results from the strain gauges were not reliable and were not used to determine the average stress in the lapped bars, which were calculated using a moment-curvature analysis.

Figure 6.6 shows the load-strain curves for the three lapped bars in Specimen (3) 6-12-S4.0-12-0.5. In this specimen (and in five of the six specimens tested), the middle bar exhibited greater strain than the edge bars. As discussed earlier, when specimens failed due to splitting of concrete at the edge bars, the middle bar was still well confined by the concrete. This likely explains the greater strain in the middle bar. The sudden increase in strains at about 40% of the maximum load marks the formation of flexural cracks within the splice region, as reflected in the load-deflection diagram in Figure 6.5.
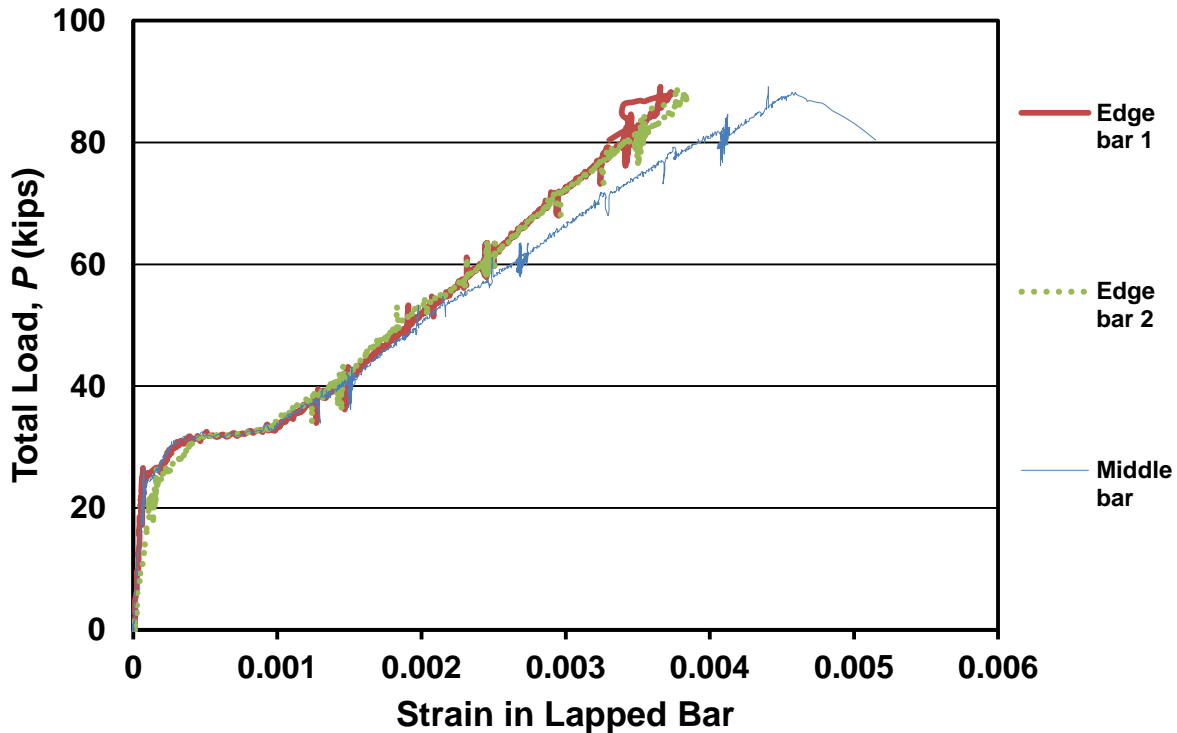
Figure 6.6 Strain in lapped bars in Specimen (3) 6-12-S4.0-12-0.5 as a function of total applied load

6.2   COMPARISON WITH OTHER HEADED SPLICE TEST RESULTS

A comparison of the splice test results with the results of similar tests conducted by Thompson (2002) and Chun (2015) is made to investigate the effects of spacing of lapped bars. The specimens tested by Thompson (2002) contained No. 8 headed bars with a lap length of $3d_b$ or $5d_b$, center-to-center spacing between bars of $2d_b$, $3d_b$, or $5d_b$, and concrete compressive strengths between 3,200 and 4,200 psi. The clear concrete cover was 2 in. for all specimens. Only specimens containing headed bars with a net bearing area of at least $4A_b$ are used in the comparison. The specimens tested by Chun (2015) contained No. 9 headed bars with lap lengths of $15d_b$ or $20d_b$, center-to-center spacing between the bars of $2d_b$ or $3d_b$, and concrete compressive strengths between 2,940 and 9,120 psi. Figure 6.7 shows the effect of lapped bar spacing on splice strength. The stress in the lapped bar plotted in vertical axis is normalized with respect to 5000 psi concrete compressive strength using Eq. (6.1).

127

$$f_N = f_{su} \left(\frac{5000}{f_{cm}} \right)^{1/4}$$

<div align="right">(6.1)</div>

where f_{su} is stress in the lapped bar in ksi (kilopounds per square inch) calculated from moment-curvature analysis, and f_{cm} is the measured concrete compressive strength in psi (pounds per square inch). The power of $^1/_4$ is close to the value of 0.24 obtained in the analysis of headed bars anchored in beam-column joint specimens described in Chapter 8 and matches the proposed value for use in design proposed in Chapter 9. Lap lengths varied between studies; therefore, comparisons between studies in Figure 6.7 are of little value. However, results within a study can be compared. The results from the current study and Thompson (2002) show no significant effect of lapped bar spacing on splice strength; results from Chun (2015), however, show a slight increase (5% on average) in splice strength as the spacing increases from $2d_b$ to $3d_b$.
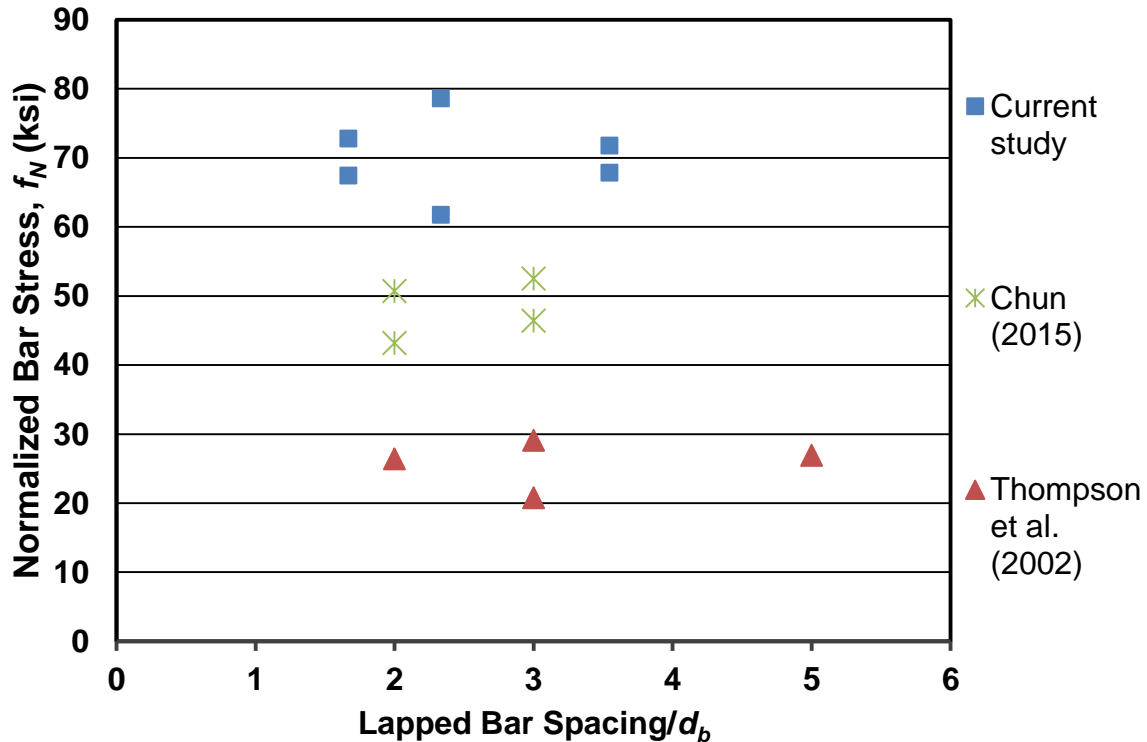
Figure 6.7 Normalized maximum bar stresses as a function of lapped bar spacing for tests in the current study and by Chun (2015) and Thompson (2002)

CHAPTER 7: ANALYSIS AND DISCUSSION

This chapter focuses on the analysis of the test results of the beam-column joint specimens. The test results are initially compared with the development length equation for headed bars in the ACI 318-14 Building Code. The comparisons reveal the limitations of the current code equation. Parameters that affect the anchorage strength of the headed bars are then analyzed, and descriptive equations are developed to capture the key factors affecting the anchorage strength. This chapter ends with evaluations of the effects of confining reinforcement within and above the joint region, headed bars with large heads, heads with large obstructions, headed bars in specimens simulating deep beam-column joints, and headed bars in CCT node, shallow embedment, and splice specimens.

Two analysis techniques are used throughout the chapter – dummy variable analysis and Student's t-test. Dummy variables are numerical variables used in regression analysis to distinguish multiple subgroups within a sample. For example, assuming that the anchorage strength of a headed bar T is linearly related to embedment length ℓ_{eh} and that the effect of *changes* in ℓ_{eh} on *changes* in T are the same for bars of different size, but that T will be different for bars of different sizes, the anchorage strength with dummy variables representing bars of different sizes can be expressed as

$$T = \beta_0 \ell_{eh} + \beta_1 Z_1 + \beta_2 Z_2 + \beta_3 Z_3 + ... + \beta_i Z_i \qquad (7.1)$$

where β_0 represents the slope of the regression line for bars of all sizes; β_i are factors representing changes in anchorage strength that depend on bar size; and Z_i are dummy variables, with a value of 0 or 1 acting as switches to turn off/on the effect of bar size. Dummy variable lines of T have the same slope β_0 but different intercepts for bars of different size, which allows the common trend in ℓ_{eh} to be observed while showing the difference in T as a function of bar size.

Student's t-test is used to determine if differences between two sets of data (populations) for a certain test parameter (such as the difference in failure load for headed bars with different sizes of heads) are statistically significant. In this report, a level of $\alpha = 0.05$ is used as the threshold; $\alpha = 0.05$ means that there is a 5% probability that the observed difference between the sets is due to random variation and not a meaningful difference in behavior. Smaller values of α indicate a greater probability of statistical significance.

7.1 COMPARISON WITH ACI 318-14

In Section 25.4.4.2(a) of ACI 318-14, the development length of a headed bar ℓ_{dt} is given by

$$\ell_{dt} = \left(\frac{0.016 f_y \psi_e}{\sqrt{f_c'}}\right) d_b \tag{7.2}$$

where f_y = yield strength of the bar; f_c' = compressive strength of concrete; d_b = bar diameter; and ψ_e = modification factor for epoxy-coated or zinc and epoxy dual-coated bars. The value of f_c' used to calculate ℓ_{dt} has an upper limit of 6,000 psi. The development length ℓ_{dt} represents the minimum embedment length required to develop the yield strength of the bar, and may be no less than the larger of $8d_b$ or 6 in. To evaluate the test results, however, it is more useful to know the anchorage stress $f_{s,\text{ACI}}$ predicted for a given development length. $f_{s,\text{ACI}}$, as given by Eq. (7.3), is derived from Eq. (7.2) by replacing f_y with $f_{s,\text{ACI}}$, replacing ℓ_{dt} with ℓ_{eh} (measured embedment length), and replacing f_c' with f_{cm} (measured concrete compressive strength). All headed bars in this study were uncoated, so ψ_e equals 1 and is omitted in Eq. (7.3).

$$f_{s,\text{ACI}} = \frac{\ell_{eh}\sqrt{f_{cm}}}{0.016 d_b} \tag{7.3}$$

The ratio of test to calculated bar stress at failure $f_{su}/f_{s,\text{ACI}}$ is used to compare the test results with the ACI equation. f_{su} is taken as the total peak load applied on a specimen divided by the total area of the headed bars in the specimen. $f_{s,\text{ACI}}$ is calculated using Eq. (7.3), in which ℓ_{eh} is the average measured embedment length (corresponding to $\ell_{eh,\text{avg}}$ in Table B.1) and f_{cm} is the measured concrete compressive strength without applying the 6,000 psi limit. The 6,000 psi limit on f_{cm} was not applied so that the effect of f_{cm} raised to the 0.5 power could be accurately evaluated across all concrete strengths and to determine if the limit could be raised or eliminated.

For the comparison, test results are grouped based on bar size and head size. In some cases, heads with similar but not identical bearing areas are combined to obtain a sufficient number of data points for analysis. For example, the results for the two specimens with No. 8 bars with $12.9A_b$ heads and the five specimens with No. 8 bars with $14.9A_b$ heads are combined. With the exception of the example given above, combined heads differed in area by less than $1A_b$.

7.1.1 Widely-Spaced Bars

Figures 7.1 through 7.3 compare the ratio $f_{su}/f_{s,\text{ACI}}$ to the measured concrete compressive strength f_{cm} for the specimens in this study with two widely-spaced headed bars and different levels of confining reinforcement (in the form of hoops) within the joint region. The different levels of confining reinforcement are shown in Figures 2.8 through 2.10. Figure 7.1 includes 46 specimens without confining reinforcement, Figure 7.2 includes 18 specimens with two No. 3 hoops as confining reinforcement, and Figure 7.3 includes 35 specimens with No. 3 hoops spaced at $3d_b$. The trend lines in the figures are obtained using dummy variable analyses. The order of the lines from highest to lowest is listed in the legend.
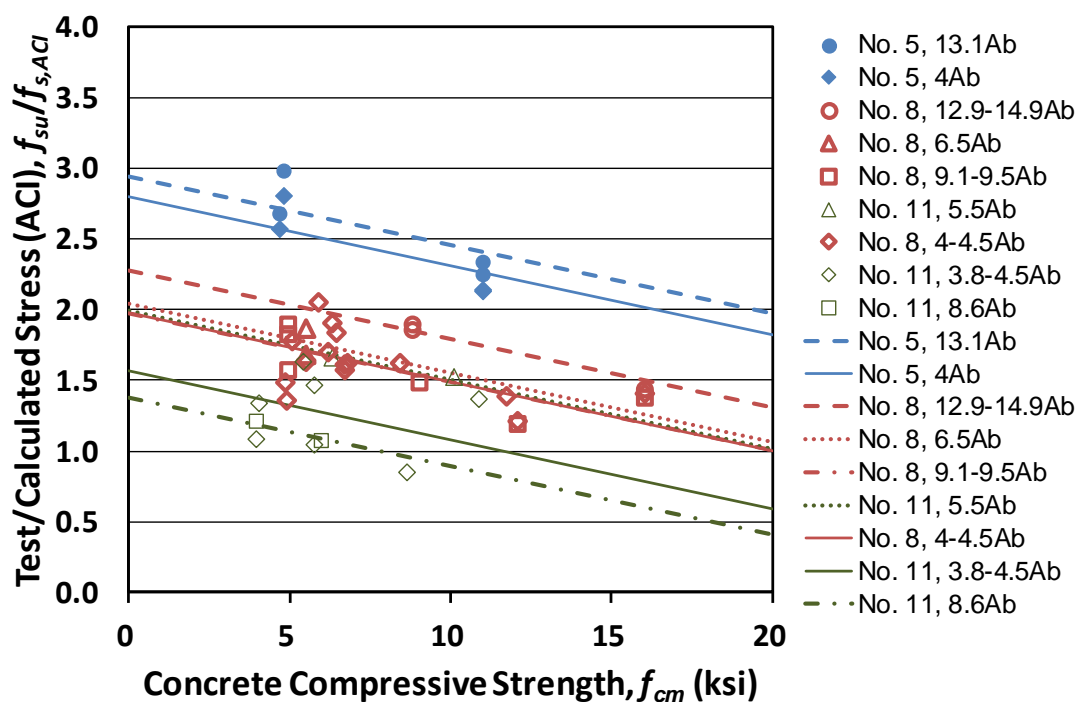
Figure 7.1 Ratio of test-to-calculated stress $f_{su}/f_{s,\text{ACI}}$ versus concrete compressive strength f_{cm} for specimens without confining reinforcement in the joint region
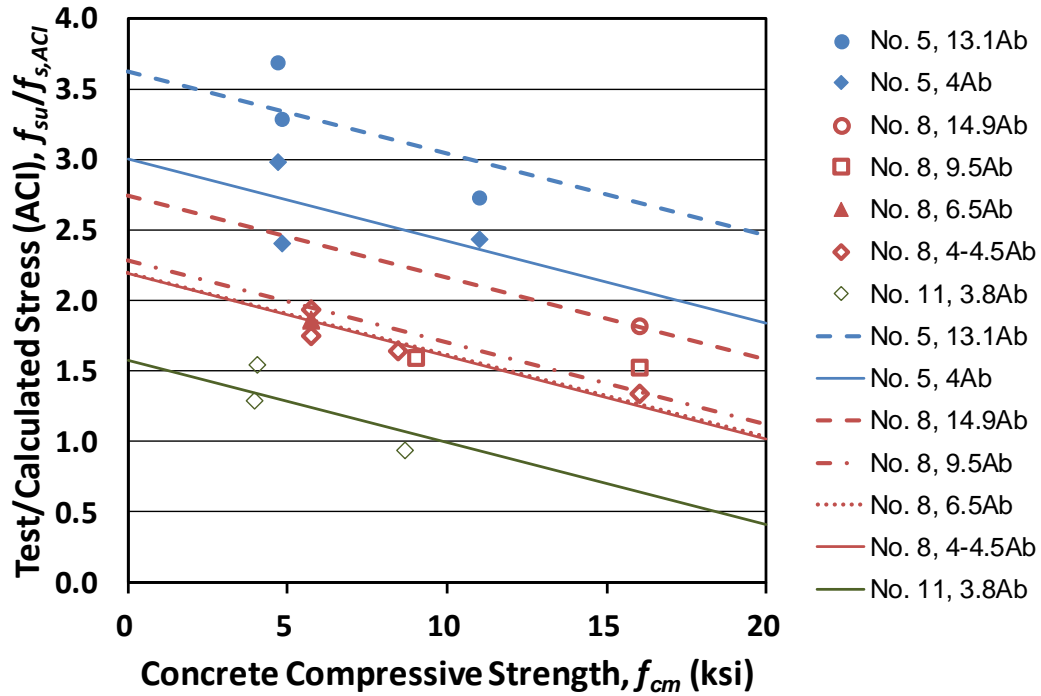
Figure 7.2 Ratio of test-to-calculated stress $f_{su}/f_{s,\text{ACI}}$ versus concrete compressive strength f_{cm} for specimens with two No. 3 hoops in the joint region
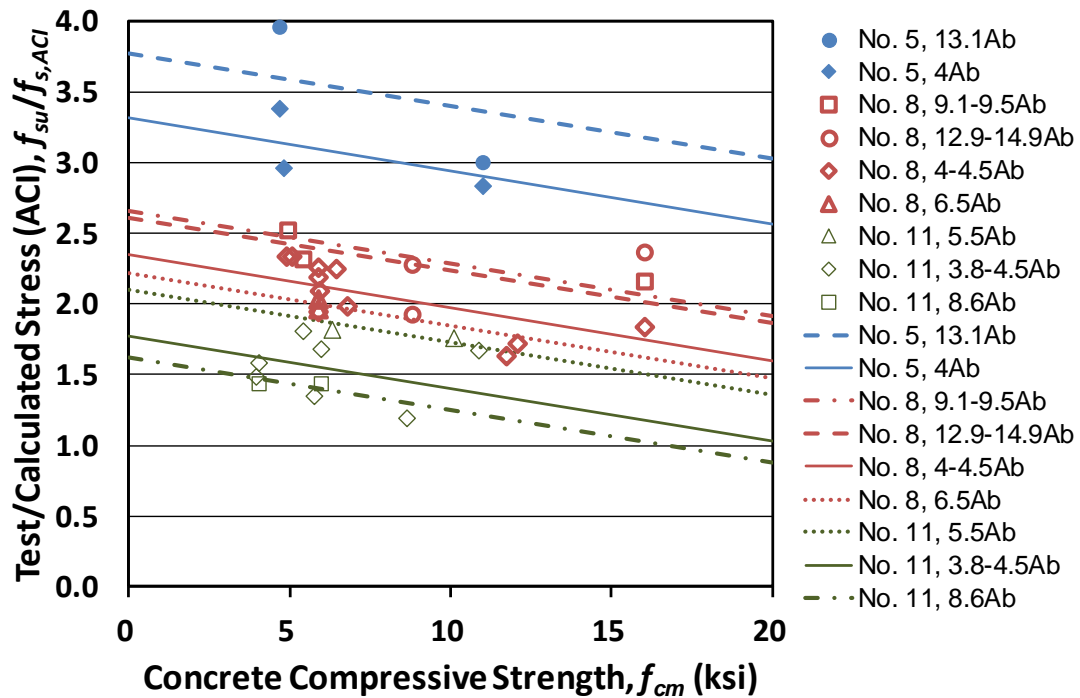
Figure 7.3 Ratio of test-to-calculated stress $f_{su}/f_{s,\text{ACI}}$ versus concrete compressive strength f_{cm} for specimens with No. 3 hoops spaced at $3d_b$ in the joint region

132

The trend lines in the three figures have negative slopes, indicating that the effect of concrete compressive strength is overestimated by the 0.5 power in the ACI equation. The values of $f_{su}/f_{s,ACI}$ are greater than 1.0 with the exception of two specimens containing No. 11 bars, one without confining reinforcement (Figure 7.1) and the other with two No. 3 hoops as confining reinforcement (Figure 7.2). This indicates that the ACI equation is generally conservative. The ACI equation is most conservative for No. 5 bars and becomes less conservative as bar size increases.

The order of the trend lines also reflects the effect of head size. For the No. 5 bars at all levels of confinement, the $f_{su}/f_{s,ACI}$ values for the $13.1A_b$ heads are consistently greater than those for the $4A_b$ heads. For the No. 8 bars, the $f_{su}/f_{s,ACI}$ values for 12.9-$14.9A_b$ heads are far greater than those for the smaller heads for specimens without confining reinforcement or with two No. 3 hoops as confinement. For No. 8 bar specimens with No. 3 hoops spaced at $3d_b$, the $f_{su}/f_{s,ACI}$ values are similar for $9A_b$ heads and larger, while heads with 4 to $6.5A_b$ bearing area exhibit lower values. While a trend is observed for No. 5 and No. 8 bars that larger heads tended to result in greater $f_{su}/f_{s,ACI}$ values, the No. 11-bar specimens did not show this trend for heads ranging from 3.8 to $8.6A_b$. In addition to bar and head size, Figures 7.1 through 7.3 show that the presence of confining reinforcement within the joint region results in an increase in $f_{su}/f_{s,ACI}$. This indicates that confining reinforcement improves the anchorage strength of headed bars, a factor that is not accounted for in the ACI provisions for the development of headed bars.

7.1.2 Closely-Spaced Bars

Figures 7.4 through 7.6 compare the ratio $f_{su}/f_{s,ACI}$ for specimens from test groups 4, 5, 7, 9 to 12, 14, and 17 to 20 (Table B.1 in Appendix B), groups that included specimens with three or four closely-spaced headed bars (multiple bars) and specimens with two widely-spaced headed bars. Specimens with a center-to-center spacing less than $5d_b$ ($5d_b$ is indicated by the vertical lines in Figures 7.4 to 7.6) did not meet the minimum $4d_b$ clear spacing requirement in ACI 318 (although it should be noted that a $3d_b$ clear spacing is permitted for use in beam-column joints of special moment frames in seismic-resisting systems). Like Figures 7.1 through 7.3, Figures 7.4 through 7.6 represent results for specimens with different amounts of confining reinforcement in the joint region.
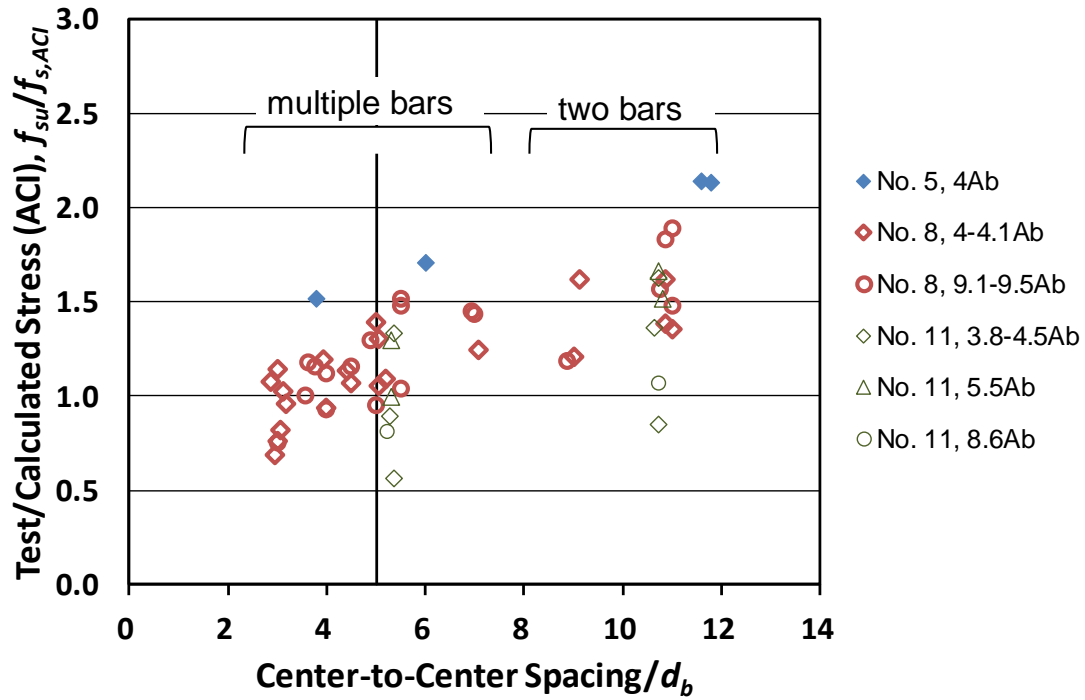
Figure 7.4 Ratio of test-to-calculated stress $f_{su}/f_{s,\mathrm{ACI}}$ versus center-to-center spacing for headed bars without confining reinforcement in the joint region
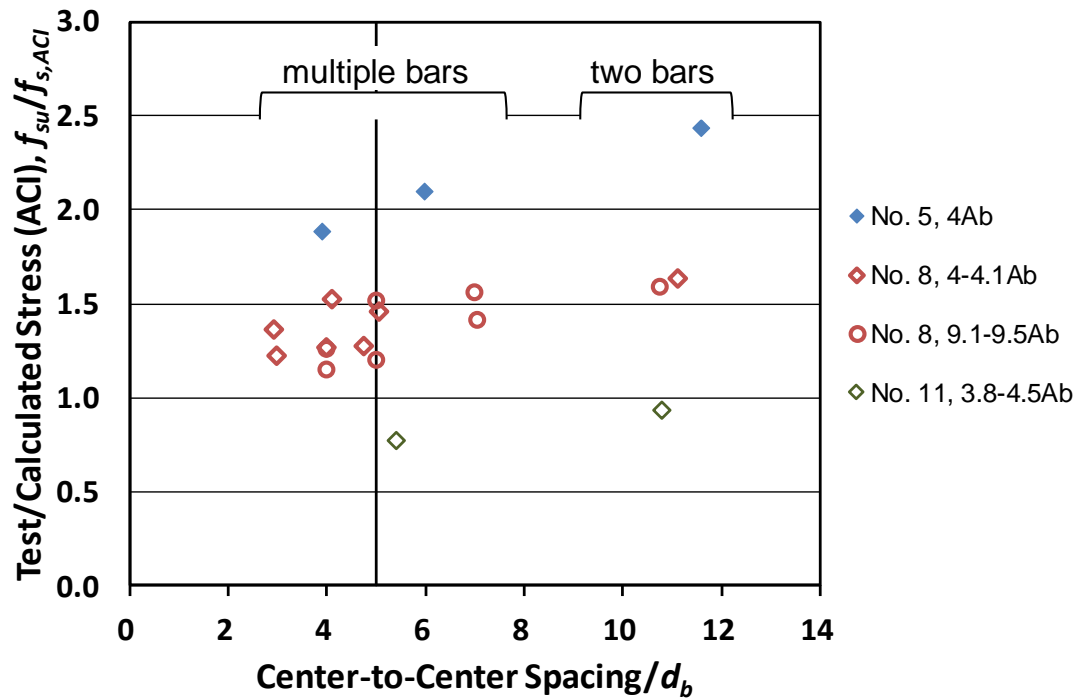
Figure 7.5 Ratio of test-to-calculated stress $f_{su}/f_{s,\mathrm{ACI}}$ versus center-to-center spacing for headed bars with two No. 3 hoops in the joint region

134
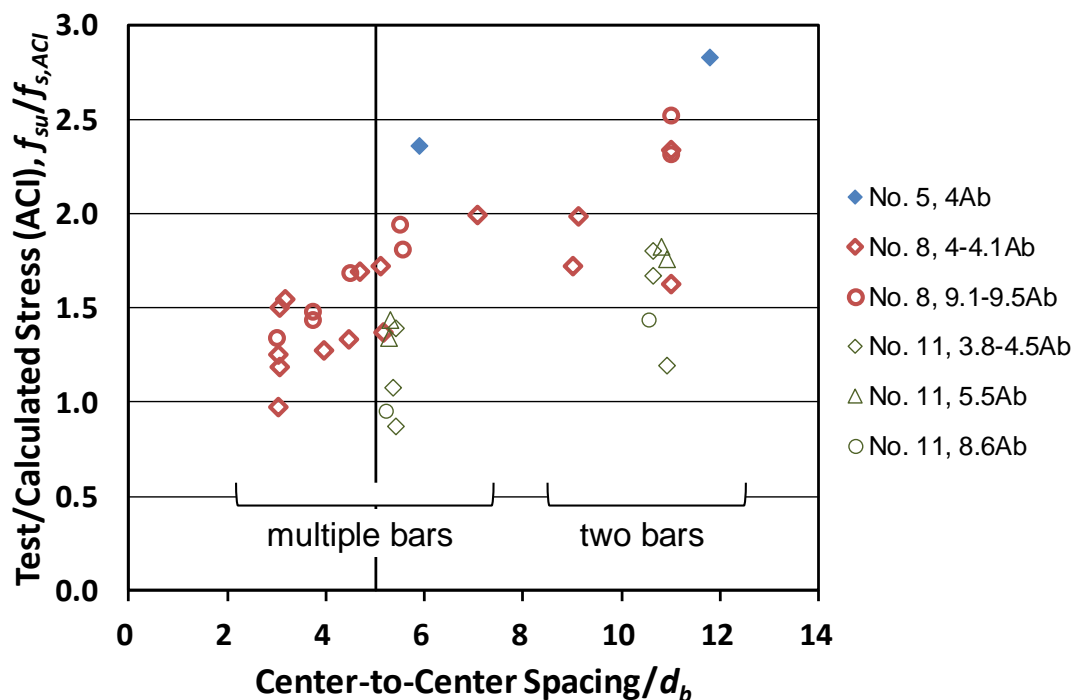
Figure 7.6 Ratio of test-to-calculated stress $f_{su}/f_{s,ACI}$ versus center-to-center spacing for headed bars with No. 3 hoops spaced at $3d_b$ in the joint region

The three figures show that, relative to the current ACI Code provisions, closely-spaced headed bars generally have lower anchorage strengths than widely-spaced bars. The overall upward trend of $f_{su}/f_{s,ACI}$ as bar spacing increases indicates that bar spacing has an effect on anchorage strength that the current Code provisions do not account for. Most headed bars with less than $5d_b$ center-to-center spacing (below the ACI $4d_b$ clear spacing requirement), had $f_{su}/f_{s,ACI}$ values greater than 1; of the specimens with $f_{su}/f_{s,ACI}$ values less than 1, all but one had no confining reinforcement within the joint region. Therefore, it appears that the current limit on bar spacing could be safely reduced to allow for use of more closely spaced headed bars, provided that confining reinforcement is added to the joint.

For both widely-spaced and closely-spaced bars, the ACI provisions are most conservative for No. 5 bars, becoming less conservative as the bar size increases. Of the ten specimens that had at least $5d_b$ center-to-center spacing (meeting the ACI requirement) and $f_{su}/f_{s,ACI}$ values less than 1, nine specimens contained No. 11 bars and one specimen contained No. 8 bars.

135

The comparisons with ACI 318 reveal that the current code provisions for headed bar development do not accurately capture the effects of concrete compressive strength, bar spacing, or bar size on the anchorage strength of headed bars.

7.2 EFFECTS OF HEAD SIZE AND SIDE COVER

The effects of head size and side cover are evaluated in this section. Other parameters, including concrete compressive strength, confining reinforcement within the joint region, embedment length, bar size, and bar spacing, are addressed in the development of descriptive equations in Section 7.3.

7.2.1 Head Size

The anchorage strengths of headed bars with different head sizes are compared for each bar size. As described in Chapter 2, three types of heads (O4.5, O9.1, and O12.9) had large obstructions and, thus, did not meet the requirements in ASTM A970 for HA heads. For a non-HA head, the difference between the gross area of the head and the area of the obstruction adjacent to the head is used in this study to represent the net bearing area. As will be shown in Section 7.4.3, non-HA and HA heads had similar anchorage strengths. Thus, for the current analysis, the results for non-HA and HA headed bars are combined to study the effect of head size. A full description of all head types is given in Table 2.1.

For No. 5 headed bars, only two types of heads were tested – F4.0 and F13.1. These specimens were tested in pairs, with the only difference between the two specimens in a pair being the net bearing area of the head. Table 7.1 gives specimen properties and test results for these specimens, including the net bearing area of the head as a multiple of the bar area A_b, the average measured embedment length ℓ_{eh} ($\ell_{eh,\text{avg}}$ in Table B.1 in Appendix B), the concrete compressive strength f_{cm}, average peak load T (the total peak load divided by the number of headed bars), and the ratio of the average peak load for the specimen containing $13A_b$ heads to the specimen containing $4A_b$ heads.

Table 7.1 Test results for No. 5 bars with different head sizes

Specimen	Net Bearing Area	ℓ_{eh} (in.)	f_{cm} (psi)	T (kips)	Ratio[*]
5-5-F4.0-0-i-2.5-5-4	$4.0A_b$	4.06	4810	24.5	1.15
5-5-F13.1-0-i-2.5-5-4	$13.1A_b$	4.41	4810	28.2	
5-5-F4.0-0-i-2.5-5-6	$4.0A_b$	6.00	4690	32.7	1.08
5-5-F13.1-0-i-2.5-5-6	$13.1A_b$	6.22	4690	35.3	
5-12-F4.0-0-i-2.5-5-4	$4.0A_b$	4.06	11030	28.3	1.11
5-12-F13.1-0-i-2.5-5-4	$13.1A_b$	4.13	11030	31.4	
5-12-F4.0-0-i-2.5-5-6	$4.0A_b$	6.00	11030	41.7	1.06
5-12-F13.1-0-i-2.5-5-6	$13.1A_b$	6.03	11030	44.2	
5-5-F4.0-2#3-i-2.5-5-4	$4.0A_b$	3.81	4810	19.7	1.47
5-5-F13.1-2#3-i-2.5-5-4	$13.1A_b$	4.09	4810	28.9	
5-5-F4.0-2#3-i-2.5-5-6	$4.0A_b$	6.00	4690	37.9	1.22
5-5-F13.1-2#3-i-2.5-5-6	$13.1A_b$	5.94	4690	46.4	
5-5-F4.0-5#3-i-2.5-5-4	$4.0A_b$	4.16	4810	26.5	1.33
5-5-F13.1-5#3-i-2.5-5-4	$13.1A_b$	4.19	4690	35.2	
5-12-F4.0-2#3-i-2.5-5-4	$4.0A_b$	4.13	11030	32.7	1.11
5-12-F13.1-2#3-i-2.5-5-4	$13.1A_b$	4.09	11030	36.3	
5-12-F4.0-5#3-i-2.5-5-4	$4.0A_b$	4.22	11030	38.9	1.04
5-12-F13.1-5#3-i-2.5-5-4	$13.1A_b$	4.13	11030	40.3	

[*] Ratio of T for the specimen containing $13A_b$ heads to T for the specimen containing $4A_b$ heads

For the specimens without confining reinforcement shown in Table 7.1, bars with F13.1 heads exhibited a 6% to 15% (average of 10%) increase in anchorage strength compared to bars with F4.0 heads. With confining reinforcement, the percentage increase was greater but more scattered, ranging from 4% to 47% (average of 23%). Student's t-test indicates that these differences in anchorage strength are statistically significant: $p = 0.002$ for the specimens without confining reinforcement and $p = 0.017$ for the specimens with confining reinforcement, with both values of p much less than the threshold of $\alpha = 0.05$ that indicates statistical significance.

For No. 8 headed bars, ten types of heads with net bearing areas ranging from 4.0 to $14.9A_b$ were tested. The wide variety of head sizes and test specimens and the fact that most specimens were not paired prevent a direct comparison of specimens, as was done with No. 5 bars. To allow for comparisons to be made, it is necessary to eliminate the effect of concrete compressive strength. To accomplish this, the average peak load T is normalized with respect to 5,000-psi concrete using the 0.24 power [Eq. (7.4)], as 0.24 is found to be a suitable power for concrete compressive strength based on the test results on beam-column joint specimens, as will be shown in Section 7.3.1. The

effect of head size on the anchorage strength of No. 8 headed bars is evaluated using both dummy variable analysis and Student's t-test, separately for specimens without confining reinforcement and specimens with No. 3 hoops spaced at $3d_b$. Headed bars with other confinement levels are not analyzed due to the small number of specimens tested.

$$T_N = T \times \left(\frac{5000}{f_{cm}} \right)^{0.24} \tag{7.4}$$

The test results for the specimens containing widely-spaced No. 8 bars without confining reinforcement are given in Table 7.2. Figure 7.7 shows the normalized failure load as a function of embedment length for these specimens, with dummy variable lines separated by head size.
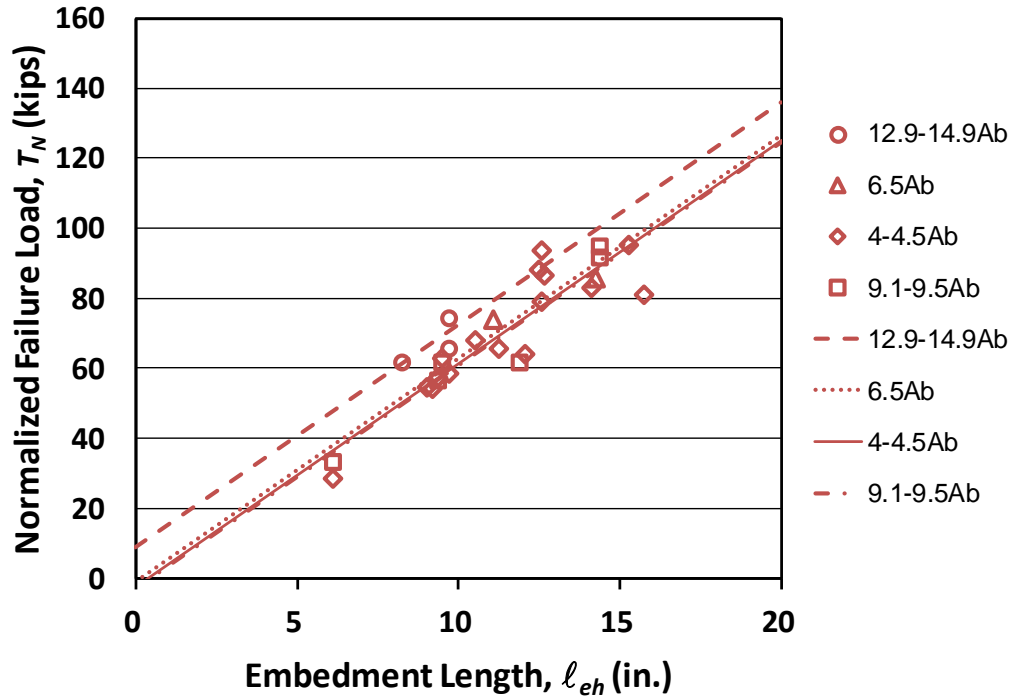
Figure 7.7 Normalized bar force at failure T_N versus embedment length ℓ_{eh} for widely-spaced No. 8 bars with different head sizes and no confining reinforcement

Table 7.2 Test results for specimens containing widely-spaced No. 8 bars and no confining reinforcement

Specimen	Net Bearing Area	ℓ_{eh} (in.)	f_{cm} (psi)	T (kips)	T_N (kips)
8-5g-T4.0-0-i-2.5-3-12.5	$4.0A_b$	12.56	5910	97.7	93.9
8-5g-T4.0-0-i-3.5-3-12.5	$4.0A_b$	12.50	6320	93.4	88.3
8-5-T4.0-i-0-3-3-15.5	$4.0A_b$	15.75	4850	80.4	81.0
8-5-T4.0-i-0-4-3-15.5	$4.0A_b$	15.28	5070	95.4	95.1
8-5-T4.0-0-i-2.5-3-12.5	$4.0A_b$	12.59	6210	83.3	79.1
8-5-T4.0-0-i-3.5-3-12.5	$4.0A_b$	12.66	6440	91.9	86.5
8-8-F4.1-0-i-2.5-3-10.5	$4.1A_b$	10.50	8450	77.1	68.0
8-12-F4.1-0-i-2.5-3-10	$4.1A_b$	9.69	11760	71.8	58.5
8-5-F4.1-0-i-2.5-7-6	$4.1A_b$	6.09	4930	28.7	28.8
8-15-T4.0-0-i-2.5-4.5-9.5	$4.0A_b$	9.50	16030	83.3	63.0
(2@9)8-12-F4.1-0-i-2.5-3-12	$4.1A_b$	12.06	12080	79.1	64.0
(2@9)8-8-T4.0-0-i-2.5-3-9.5	$4.0A_b$	9.38	6790	61.8	57.4
8-5-O4.5-0-i-2.5-3-11.25	$4.5A_b$	11.25	5500	67.4	65.9
8-5-O4.5-0-i-2.5-3-14.25	$4.5A_b$	14.13	5500	85.0	83.1
8-8-O4.5-0-i-2.5-3-9.5	$4.5A_b$	9.19	6710	58.4	54.4
(2@9)8-8-O4.5-0-i-2.5-3-9.5	$4.5A_b$	9.00	6710	58.8	54.8
8-5-S6.5-0-i-2.5-3-11.25	$6.5A_b$	11.06	5500	75.6	73.8
8-5-S6.5-0-i-2.5-3-14.25	$6.5A_b$	14.25	5500	87.7	85.7
8-5-T9.5-0-i-2.5-3-14.5	$9.5A_b$	14.38	4970	91.7	91.8
8-15-S9.5-0-i-2.5-3-9.5	$9.5A_b$	9.50	16030	81.7	61.7
8-8-T9.5-0-i-2.5-3-9.5	$9.5A_b$	9.38	9040	65.2	56.6
(2@9)8-12-F9.1-0-i-2.5-3-12	$9.1A_b$	11.88	12080	76.5	61.9
8-5-F9.1-0-i-2.5-7-6	$9.1A_b$	6.13	4940	33.4	33.5
8-5-O9.1-0-i-2.5-3-14.5	$9.1A_b$	14.38	4970	94.8	94.9
8-8-O12.9-0-i-2.5-3-9.5	$12.9A_b$	9.69	8800	85.2	74.4
8-8-S14.9-0-i-2.5-3-8.25	$14.9A_b$	8.25	8800	70.9	61.9
8-15-S14.9-0-i-2.5-3-9.5	$14.9A_b$	9.69	16030	87.1	65.9

As indicated by the dummy variable lines in the figure, the No. 8 bars with 12.9 through 14.9A_b (12.9-14.9A_b) heads exhibited higher anchorage strengths than those with smaller heads (4 through 9.5A_b). The lines for the bars with 9.5A_b and smaller heads are close together and not in the order of head size, indicating no effect of head size on anchorage strength for the smaller heads. To evaluate the difference in normalized failure load associated with head size for these results, Student's t-test is used to compare the intercepts with the T_N axis obtained by extending lines through each data point parallel to the dummy variable trend lines. The values of p obtained from

Student's t-test for each comparison between the strengths of the bars with different head sizes are given in Table 7.3. The number in parenthesis shows the number of the specimens tested with a given head size.

Table 7.3 Student's t-test significance level p comparing effect of head size on anchorage strength of No. 8 headed bars without confining reinforcement[*]

Head Size (number of specimens)	**4-4.5A_b** (16)	**6.5A_b** (2)	**9.1-9.5A_b** (6)
6.5A_b (2)	0.79	-	-
9.1-9.5A_b (6)	0.89	0.69	-
12.9-14.9A_b (3)	0.036	0.12	0.023

[*] Values of p above $\alpha = 0.05$ indicate differences in anchorage strength are not statistically significant

The values shown in Table 7.3 indicate that the differences in anchorage strength between bars with 4-4.5A_b heads or bars with 9.1-9.5A_b heads and those with 12.9-14.9A_b heads are statistically significant, using $\alpha = 0.05$ as the threshold. The value of p for the comparison between bars with 6.5A_b heads and those with 12.9-14.9A_b heads is 0.12; although not indicating statistical significance using the $\alpha = 0.05$, $p = 0.12$ is much lower than the values (0.79, 0.89, and 0.69) obtained for the comparisons between the smaller heads (4 through 9.5A_b). If the anchorage strengths for bars with 4 through 9.5A_b heads are combined and compared to the strengths for the bars with 12.9-14.9A_b heads, Student's t-test shows that the difference in anchorage strength between bars with the smaller and larger heads is statistically significant, with $p = 0.016$. The average difference shown in Figure 7.7 between the normalized failure loads T_N of the bars with 12.9-14.9A_b heads and those with smaller heads was 11.1 kips, equal about 18% for $\ell_{eh} = 10$ in. and 12% for $\ell_{eh} = 15$ in.

The test results for the specimens containing widely-spaced No. 8 bars confined by No. 3 hoops spaced at $3d_b$ are given in Table 7.4. Figure 7.8 shows the normalized failure load as a function of embedment length for these specimens, with dummy variable lines separated by head size.

Table 7.4 Test results for specimens containing widely-spaced No. 8 bars and No. 3 hoops spaced at $3d_b$

Specimen	Net Bearing Area	ℓ_{eh} (in.)	f_{cm} (psi)	T (kips)	T_N (kips)
8-5g-T4.0-5#3-i-2.5-3-9.5	$4.0A_b$	9.56	5090	78.7	78.4
8-5g-T4.0-5#3-i-3.5-3-9.5	$4.0A_b$	9.56	5910	79.5	76.4
8-5-T4.0-5#3-i-2.5-3-9.5	$4.0A_b$	9.31	5960	74.2	71.1
8-5-T4.0-5#3-i-3.5-3-9.5	$4.0A_b$	9.06	6440	80.6	75.8
8-12-F4.1-5#3-i-2.5-3-10	$4.1A_b$	10.00	11760	87.2	71.0
8-5-F4.1-5#3-i-2.5-7-6	$4.1A_b$	6.25	4930	50.7	50.8
8-15-T4.0-5#3-i-2.5-4.5-5.5	$4.0A_b$	5.5	16030	63.3	47.9
(2@9)8-12-F4.1-5#3-i-2.5-3-12	$4.1A_b$	11.97	12080	111.9	90.5
(2@9)8-8-T4.0-5#3-i-2.5-3-9.5	$4.0A_b$	9.5	6790	76.7	71.3
8-5-O4.5-5#3-i-2.5-3-8.25	$4.5A_b$	8.00	5900	68.4	65.7
8-5-O4.5-5#3-i-2.5-3-11.25	$4.5A_b$	11.13	5900	82.2	79.0
8-5-S6.5-5#3-i-2.5-3-8.25	$6.5A_b$	8.31	5900	62.0	59.6
8-5-S6.5-5#3-i-2.5-3-11.25	$6.5A_b$	10.94	5900	84.5	81.2
8-5-T9.5-5#3-i-2.5-3-14.5	$9.5A_b$	14.38	5420	121.0	118.7
8-15-S9.5-5#3-i-2.5-3-5.5	$9.5A_b$	5.63	16030	75.8	57.3
8-5-F9.1-5#3-i-2.5-7-6	$9.1A_b$	6.16	4940	53.8	54.0
8-8-O12.9-5#3-i-2.5-3-9.5	$12.9A_b$	9.38	8800	83.5	72.9
8-8-S14.9-5#3-i-2.5-3-8.25	$14.9A_b$	8.25	8800	87.0	76.0
8-15-S14.9-5#3-i-2.5-3-5.5	$14.9A_b$	5.50	16030	81.4	61.5
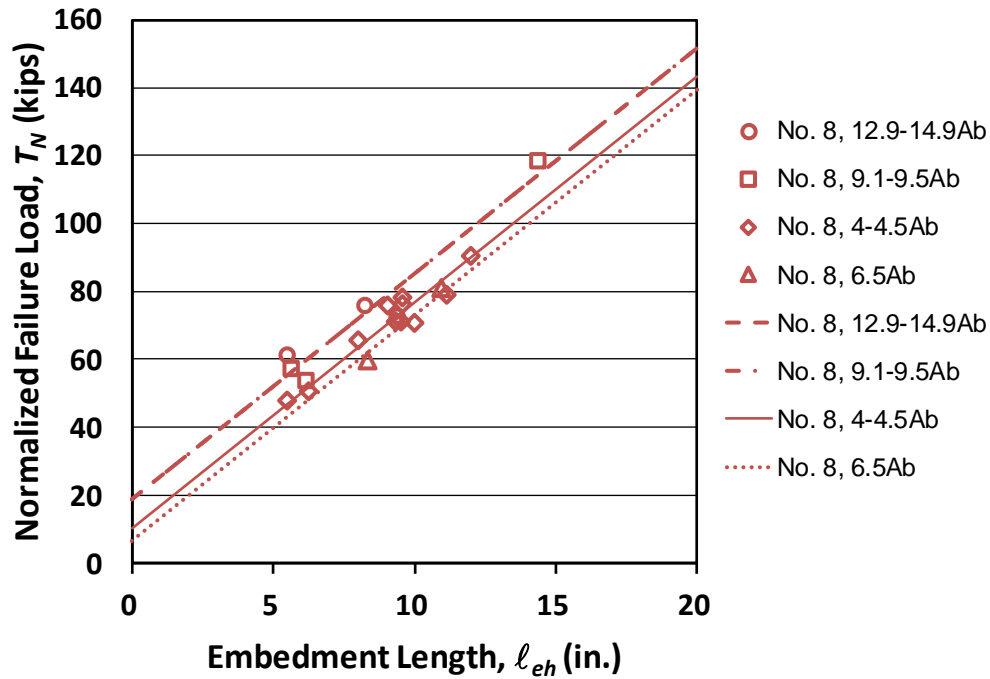
Figure 7.8 Normalized bar force at failure T_N versus embedment length ℓ_{eh} for widely-spaced No. 8 bars with different head sizes and No. 3 hoops spaced at $3d_b$

As indicated by the dummy variable lines in Figure 7.8, the anchorage strengths for the bars with 12.9-14.9A_b and 9.1-9.5A_b heads were similar, both higher than those with 4-4.5A_b heads. The bars with 6.5A_b heads exhibited the lowest anchorage strength.

Table 7.5 shows the values of p obtained from Student's t-test for each comparison between the strengths of the bars with different head sizes. Using $\alpha = 0.05$ as the threshold, the lower strengths exhibited by the bars with 4-4.5A_b heads in comparison to the bars with 9.1-9.5A_b and 12.9-14.9A_b heads represents a statistically significant difference with values of $p = 0.006$ and 0.013, respectively. The respective values of p for the bars with 6.5A_b heads, 0.059 and 0.12 are relatively low, but above $\alpha = 0.05$. The value of $p = 0.97$ for the comparison between bars with 9.1-9.5A_b heads and bars with 12.9-14.9A_b heads is much greater than the value (0.023) observed from the comparison for bars with the same head sizes without confining reinforcement (Table 7.3), indicating no appreciable difference in anchorage strengths. The average difference shown in Figure 7.8 between the normalized failure loads T_N of the bars with 9.1-9.5A_b and 12.9-14.9A_b heads and those with 4-4.5A_b heads and 6.5A_b heads was 12.8 kips, equal about 20% for $\ell_{eh} = 10$ in. and 12% for $\ell_{eh} = 15$ in.

Table 7.5 Student's t-test significance level p comparing effect of head size on anchorage strength of No. 8 headed bars with confining reinforcement[*]

Head Size (number of specimens)	4-4.5A_b (11)	6.5A_b (2)	9.1-9.5A_b (3)
6.5A_b (2)	0.18	-	-
9.1-9.5A_b (3)	0.006	0.059	-
12.9-14.9A_b (3)	0.013	0.12	0.97

[*] Values of p above $\alpha = 0.05$ indicate differences in anchorage strength are not statistically significant

For No. 11 headed bars, four types of heads with net bearing areas ranging from 3.8 to 8.6A_b were tested. Specimens were tested in pairs to compare the anchorage strengths obtained with 3.8A_b and 8.6A_b heads, and with 4.5A_b and 5.5A_b heads. The comparison between 4.5A_b and 5.5A_b heads also reflects the effect of large obstructions: The 4.5A_b heads (O4.5) had a slightly smaller bearing area than the 5.5A_b heads (S5.5), but also had a large obstruction, beyond the dimensional limits for HA heads in ASTM A970. The effect of large obstructions is discussed separately in Section 7.4.3. Table 7.6 gives the test results for these specimens, including the net

bearing area, measured embedment length ℓ_{eh}, concrete compressive strength f_{cm}, average peak load T, and the ratio of the average peak load for the specimen containing larger heads to the specimen containing smaller heads within each pair.

Table 7.6 Test results for No. 11 bars with different head sizes

Specimen	Net Bearing Area	ℓ_{eh} (in.)	f_{cm} (psi)	T (kips)	Ratio[*]
11-5a-F3.8-0-i-2.5-3-12	$3.8A_b$	12.00	3960	56.8	1.12
11-5a-F8.6-0-i-2.5-3-12	$8.6A_b$	12.13	3960	63.8	
11-5a-F3.8-6#3-i-2.5-3-12	$3.8A_b$	12.09	3960	78.0	1.02
11-5a-F8.6-6#3-i-2.5-3-12	$8.6A_b$	12.56	4050	79.2	
11-12-O4.5-0-i-2.5-3-16.75	$4.5A_b$	17.13	10860	169.6	1.04
11-12-S5.5-0-i-2.5-3-16.75	$5.5A_b$	16.94	10120	175.9	
11-5-O4.5-0-i-2.5-3-19.25	$4.5A_b$	19.44	5430	157.9	1.12
11-5-S5.5-0-i-2.5-3-19.25	$5.5A_b$	19.38	6320	176.8	
(3@5.35)11-12-O4.5-0-i-2.5-3-16.75	$4.5A_b$	16.92	10860	106.8	1.02
(3@5.35)11-12-S5.5-0-i-2.5-3-16.75	$5.5A_b$	16.92	10120	109.0	
(3@5.35)11-5-O4.5-0-i-2.5-3-19.25	$4.5A_b$	19.50	5430	128.7	1.07
(3@5.35)11-5-S5.5-0-i-2.5-3-19.25	$5.5A_b$	19.29	6320	137.4	
11-12-O4.5-6#3-i-2.5-3-16.75	$4.5A_b$	16.81	10860	201.5	0.98
11-12-S5.5-6#3-i-2.5-3-16.75	$5.5A_b$	16.81	10120	197.4	
(3@5.35)11-12-O4.5-6#3-i-2.5-3-16.75	$4.5A_b$	17.00	10860	135.8	1.13
(3@5.35)11-12-S5.5-6#3-i-2.5-3-16.75	$5.5A_b$	16.75	10120	153.8	
11-5-O4.5-6#3-i-2.5-3-19.25	$4.5A_b$	19.63	5430	181.4	1.05
11-5-S5.5-6#3-i-2.5-3-19.25	$5.5A_b$	19.13	6320	189.6	
(3@5.35)11-5-O4.5-6#3-i-2.5-3-19.25	$4.5A_b$	19.38	5430	141.7	1.08
(3@5.35)11-5-S5.5-6#3-i-2.5-3-19.25	$5.5A_b$	19.25	6320	152.9	

[*] Ratio of T for the specimen containing larger heads to T for specimen containing smaller heads

For the specimens shown in Table 7.6, the No. 11 bars with $8.6A_b$ heads, without and with confining reinforcement, respectively, exhibited a 12% and 2% greater anchorage strength, than the bars with $3.8A_b$ heads. Since there is only one pair of bars each without and with confining reinforcement, the statistical significance of these differences cannot be evaluated. Of the eight pairs of specimens with $4.5A_b$ and $5.5A_b$ heads, the ratios of peak load (for the specimen containing $5.5A_b$ heads to the specimen containing $4.5A_b$ heads) range from 1.02 to 1.12 for the bars without confining reinforcement and from 0.98 to 1.13 for the bars with confining reinforcement. Student's t-test shows that the differences in anchorage strength of the No. 11 bars with $4.5A_b$ and $5.5A_b$

heads are not statistically significant, with $p = 0.08$ for the bars without confining reinforcement and $p = 0.17$ for the bars with confining reinforcement.

The analyses of the effect of head size on anchorage strength for the No. 5 and No. 11 bars are based on Student's t-test for paired specimens. For No. 5 bars, those with $13.1A_b$ heads had higher anchorage strengths than the bars with $4A_b$ heads, differences that are statistically significant. For the No. 11 bars, the differences in anchorage strength between bars with $3.8A_b$ and $8.6A_b$ heads were small, but could not be evaluated for statistical significance because of the small sample size. For the No. 11 bars with $4.5A_b$ and $5.5A_b$ heads, the differences in anchorage strength are not statistically significant. The analysis of head size for No. 8 bars is based on both dummy variable analysis and Student's t-test. The dummy variable trend lines show that, without confining reinforcement, the bars with 12.9-$14.9A_b$ heads exhibited higher anchorage strengths than the bars with smaller heads (4-$9.5A_b$), differences that are statistically significant when analyzed using Student's t-test. For bars without confining reinforcement, there appears to be no effect of head size on the anchorage strength for bars with bearing areas in the range of 4-$9.5A_b$. For bars with confining reinforcement, the dummy variable trend lines show that the bars with 9.1-$9.5A_b$ heads had similar anchorage strengths to those with 12.9-$14.9A_b$ heads, and both 9.1-$9.5A_b$ and 12.9-$14.9A_b$ heads provided the bars with higher anchorage strengths than those with smaller heads. The comparisons for No. 8 bars are based on a small number of specimens with widely-spaced bars either with no confining reinforcement or confined by No. 3 hoops spaced at $3d_b$.

In all cases, bars with heads with net bearing areas in the range of 12.9 to $14.9A_b$ consistently exhibited higher anchorage strengths than those with smaller heads, while no clear trend is observed as for differences in anchorage strength associated with head size ranging from 3.8 to $9.5A_b$. The single exception to this statement involves the higher strengths exhibited by three specimens containing No. 8 bars with 9.1-$9.5A_b$ heads with confining reinforcement. Based on the overall observations, bars with 3.8 to $9.5A_b$ heads are used to develop the descriptive equations; this combination will be further justified in Section 7.3, where the full database is compared with the descriptive equations (best-fit equations for the beam-column specimens) as a function of head size. The anchorage strengths of bars with large heads (12.9 to $14.9A_b$) are compared with the descriptive equations in Section 7.4.2.

7.2.2 Side Cover

The effect of side cover on anchorage strength was studied only in the first three test groups using paired specimens. The paired specimens containing No. 8 bars with $4A_b$ heads (Table 2.1) were tested both without and with confining reinforcement (four or five No. 3 hoops or four No. 4 hoops within the joint region). Side covers to the bar for the specimens ranged from 2.5 to 4 in. Table 7.7 summarizes the measured side cover c_{so} ($c_{so,\text{avg}}$ in Table B.1 in Appendix B), embedment length ℓ_{eh} ($\ell_{eh,\text{avg}}$ in Table B.1 in Appendix B), concrete compressive strength f_{cm}, average peak load T, normalized failure load T_N, and the ratio of T_N for the specimen with the greater cover to that with the lower cover.

Table 7.7 Comparisons for specimens with different side covers

Specimen	c_{so} (in.)	ℓ_{eh} (in.)	f_{cm} (psi)	T (kips)	T_N (kips)	Ratio
8-5-T4.0-0-i-3-3-15.5	2.97	15.75	4850	80.4	81.0	1.17
8-5-T4.0-0-i-4-3-15.5	3.81	15.28	5070	95.4	95.1	
8-5g-T4.0-0-i-2.5-3-12.5	2.50	12.56	5910	97.7	93.9	0.94
8-5g-T4.0-0-i-3.5-3-12.5	3.31	12.50	6320	93.4	88.3	
8-5-T4.0-0-i-2.5-3-12.5	2.44	12.59	6210	83.3	79.1	1.09
8-5-T4.0-0-i-3.5-3-12.5	3.56	12.66	6440	91.9	86.5	
8-5-T4.0-4#3-i-3-3-12.5	2.88	12.38	5070	87.5	87.2	1.08
8-5-T4.0-4#3-i-4-3-12.5	4.00	12.06	5380	96.2	94.5	
8-5-T4.0-4#4-i-3-3-12.5	2.94	12.44	5070	109.0	108.6	0.94
8-5-T4.0-4#4-i-4-3-12.5	3.97	12.19	4850	101.5	102.2	
8-5g-T4.0-5#3-i-2.5-3-9.5	2.75	9.56	5090	78.7	78.4	0.97
8-5g-T4.0-5#3-i-3.5-3-9.5	3.31	9.56	5910	79.5	76.4	
8-5g-T4.0-4#4-i-2.5-3-9.5	2.50	9.19	5180	90.7	89.9	1.03
8-5g-T4.0-4#4-i-3.5-3-9.5	3.88	9.50	5910	96.7	92.9	
8-5-T4.0-5#3-i-2.5-3-9.5	2.50	9.31	5960	74.2	71.1	1.07
8-5-T4.0-5#3-i-3.5-3-9.5	3.44	9.06	6440	80.6	75.8	
8-5-T4.0-4#4-i-2.5-3-9.5	2.56	9.25	6440	90.5	85.2	0.95
8-5-T4.0-4#4-i-3.5-3-9.5	3.44	9.25	6210	85.6	81.3	

[*] Ratio of T_N for the specimen with greater cover to T_N for the specimen with lower cover

The results in Table 7.7 indicate that a 1 in. increase in nominal side cover does not necessarily result in an increase in the anchorage strength for specimens both without and with confining reinforcement; of the nine pairs of specimens, four exhibited a greater failure load in the specimen with lower side cover. Without confining reinforcement, the ratio of normalized failure loads ranged from 0.94 to 1.17, with an average of 1.07; with confining reinforcement, the ratio

ranged from 0.94 to 1.08, with an average of 1.01. Student's t-test shows that the differences in anchorage strength between headed bars with higher and lower side covers are not statistically significant (p values equal to 0.45 and 0.84, respectively, for specimens without and with confining reinforcement). The ratios of normalized failure loads and the results from Student's t-test indicate that the anchorage strength of No. 8 headed bars was not affected by difference in side cover with a range of 2.5 to 4 in. Therefore, the test results of the specimens with this range of side cover are combined to develop the descriptive equations, described next.

7.3 DESCRIPTIVE EQUATIONS

To develop equations that characterize the behavior of headed bars without and with confining reinforcement in simulated beam-column joints, a series of iterative analyses are performed. This section summarizes the results of those analyses.

Development of the descriptive equations first requires a selection of a set of specimens that include the key factors affecting the anchorage strength of headed bars. Based on the discussion in Section 7.2, specimens with bars containing 3.8 to 9.5A_b heads and 2.5 to 4 in. side cover are selected as the data set used to develop the descriptive equations. Specimens with large heads (12.9 to 14.9A_b) are not included in the development of the descriptive equations, as bars with large heads exhibited higher anchorage strengths than bars with 9.5A_b and smaller heads (as discussed in Section 7.2.1); large heads are addressed in Section 7.4.2. As will be demonstrated in Section 7.4.4, some headed bars with a relatively short embedment length ℓ_{eh} relative to h_{cl} (distance from the center of the bar to the top of bearing member) tended to exhibit low anchorage strengths, and are also not used to develop the descriptive equations. Finally, two specimens from Group 1 had no confining reinforcement above or within the joint region, and served as trial specimens to provide information for the design of subsequent beam-column joint specimens. Because the lack of confining reinforcement above the joint is inconsistent with design requirements for reinforced concrete columns (ACI 318-14), these specimens were also not used to develop the descriptive equations.

7.3.1 Anchorage Strength of Headed Bars Without Confining Reinforcement

The descriptive equation for the anchorage strength of headed bars without confining reinforcement is based on test results of 30 specimens with *widely-spaced* bars (center-to-center spacing $\geq 8d_b$). The equation is obtained using iterative analyses and is given by

$$T_c = 781 f_{cm}^{0.24} \ell_{eh}^{1.03} d_b^{0.35} \tag{7.5}$$

where T_c = anchorage strength of headed bars without confining reinforcement (lb); f_{cm} = concrete compressive strength (psi); ℓ_{eh} = embedment length (in.); and d_b = diameter of headed bar (in.). Figure 7.9 compares the ratio T/T_c to the concrete compressive strength for the 30 specimens. T is the average peak load. The maximum, minimum, mean, STD, and COV values for T/T_c are given in Table 7.8. The dummy variable lines in Figure 7.9 are almost horizontal, indicating that the effect of concrete compressive strength is accurately captured by the 0.24 power. Compared with Figure 7.1, the T/T_c values are less scattered, with no bar size bias present. The values of T/T_c range from 0.80 to 1.18, with a coefficient of variation of 0.100.
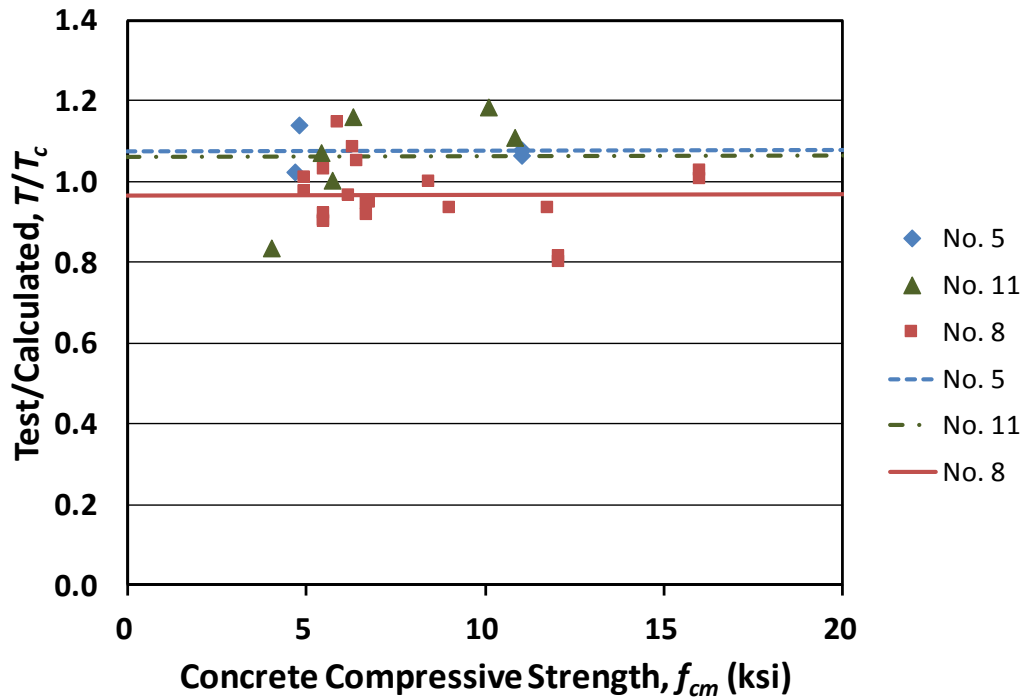
Figure 7.9 Ratio of test-to-calculated failure load T/T_c versus concrete compressive strength f_{cm} for specimens with widely-spaced bars and no confining reinforcement

Table 7.8 Statistical parameters of T/T_c values for specimens with widely-spaced bars and no confining reinforcement

(Number of specimens)	**All** (30)	**No. 5** (4)	**No. 8** (20)	**No. 11** (6)
Max	1.18	1.14	1.15	1.18
Min	0.80	1.03	0.80	0.84
Mean	1.00	1.08	0.97	1.06
STD	0.100	0.048	0.083	0.127
COV	0.100	0.045	0.086	0.120

The 0.24 power used to represent the effect of concrete compressive strength on anchorage strength is considerably below the value of 0.5 used for calculating the development length of straight, hooked, and headed bars in ACI 318-14. This lower value, however, closely matches results from tests on the development and splice strength of straight reinforcement (Darwin et al. 1996, Zuo and Darwin 1998, 2000) and the anchorage strength of hooked bars (Sperry et al. 2015a, 2015b). The 0.24 power was also found to provide the best fit with the data for spliced reinforcement by Zuo and Darwin (1998). Justification for the lower power of compressive strength is provided by the fact that both the bond strength of straight reinforcement and the anchorage strength of hooked and headed bars are governed by the combined effects of concrete tensile strength, which controls initial crack formation and increases with the compressive strength to a power between $\frac{1}{2}$ and $\frac{2}{3}$, and fracture energy, which controls crack propagation and is independent of compressive strength (Darwin et al. 2001). The overall effect is a power between 0.5 and zero.

For 34 specimens with *closely-spaced* bars (center-to-center spacing $< 8d_b$), the ratios of anchorage strengths T/T_c [T_c based on Eq. (7.5)] are plotted versus the center-to-center spacing between the bars in Figure 7.10. For comparison, the 30 specimens used to develop Eq. (7.5) are also shown in the figure, represented by open symbols.
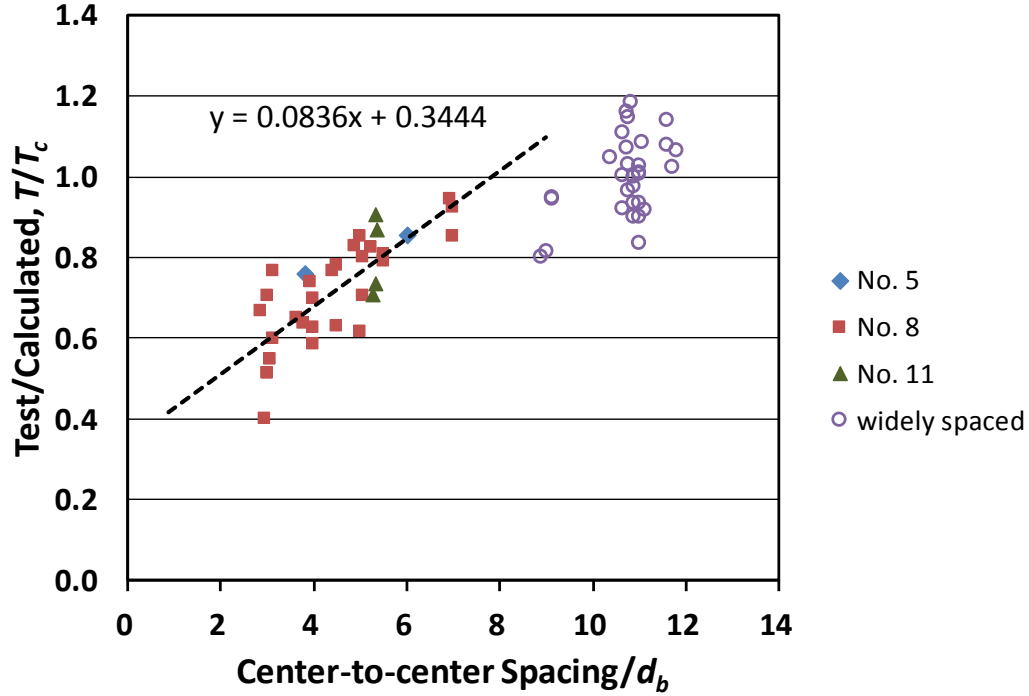
Figure 7.10 Ratio of test-to-calculated failure load T/T_c versus center-to-center spacing for headed bars without confining reinforcement

As shown in Figure 7.10, the closely-spaced headed bars, regardless of bar size, were generally weaker than those with widely-spaced bars. The trend line for the closely-spaced bars shows an increase in anchorage strength with an increase in bar spacing. The value of T/T_c equals 1.0 at a center-to-center spacing of about $8d_b$, which is greater than the value of $7d_b$ observed for closely-spaced hooked bars tested in simulated beam-column joint specimens by Sperry et al. (2015a).[2] The difference in critical bar spacing between headed and hooked bars is likely due to the geometry of the head; the larger size of the head relative to the bar reduces the effective clear spacing between heads and may result in interaction between headed bars at slightly greater spacings than was observed for hooked bars. Modifying Eq. (7.5) to account for the effect of closely spaced headed bars results in Eq. (7.6).

$$T_c = \left(781 f_{cm}^{0.24} \ell_{eh}^{1.03} d_b^{0.35}\right)\left(0.0836\frac{s}{d_b} + 0.3444\right) \qquad (4.6)$$

with $0.0836\dfrac{s}{d_b} + 0.3444 \leq 1.0$

where s = center-to-center spacing between the bars (in.).

---

[2] Recent unpublished work at the University of Kansas suggests that a value of $6d_b$ is more appropriate for hooked bars.

Figure 7.11 compares the ratio T/T_c to the concrete compressive strength for the headed bars (both widely-spaced and closely-spaced) without confining reinforcement with T_c based on Eq. (7.6). The maximum, minimum, mean, STD, and COV values for T/T_c are given in Table 7.9. The slope of the dummy variable lines in the figure indicates that the effect of concrete compressive strength is slightly overestimated by Eq. (7.6). A slightly lower value for the power of f_{cm} might be more suitable for the combined widely-spaced and closely-spaced bars, but for simplicity, the 0.24 power for f_{cm} is retained. The ratio T/T_c ranges from 0.68 to 1.27, with a coefficient of variation of 0.111.
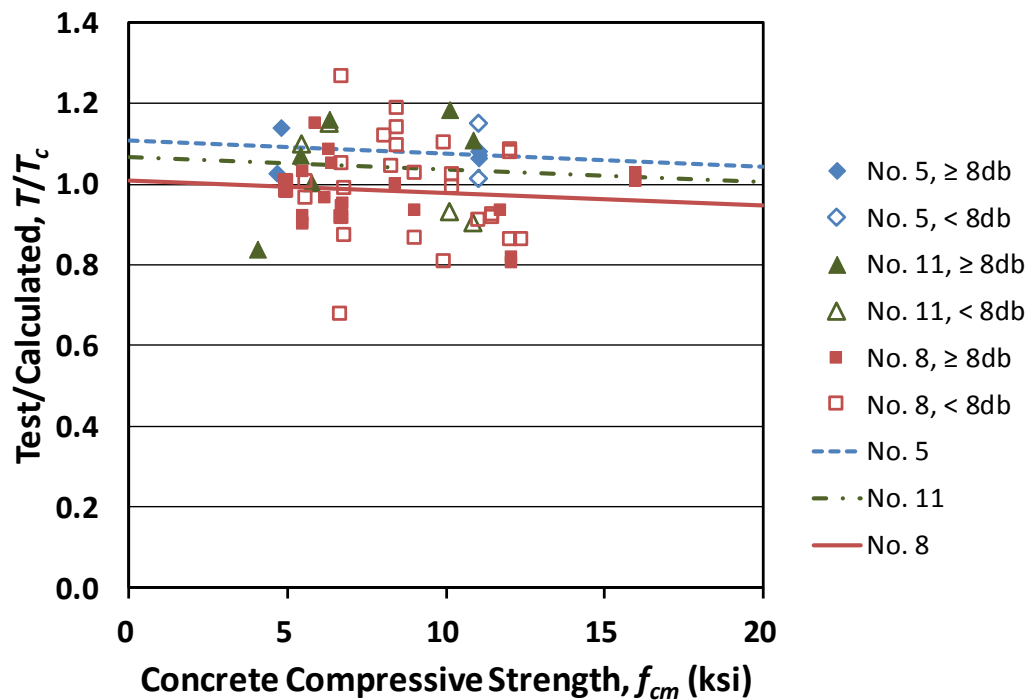
Figure 7.11 Ratio of test-to-calculated failure load T/T_c versus concrete compressive strength f_{cm} for specimens without confining reinforcement

Table 7.9 Statistical parameters of T/T_c values for headed bars without confining reinforcement

(Number of specimens)	All	Widely spaced			Closely spaced		
		No. 5	No. 8	No. 11	No. 5	No. 8	No. 11
	(64)	(4)	(20)	(6)	(2)	(28)	(4)
Max	1.27	1.14	1.15	1.18	1.15	1.27	1.15
Min	0.68	1.03	0.80	0.84	1.01	0.68	0.90
Mean	1.00	1.08	0.97	1.06	1.08	0.99	1.02
STD	0.111	0.048	0.083	0.127	0.096	0.125	0.122
COV	0.111	0.045	0.086	0.120	0.089	0.126	0.119

150

With the descriptive equations [Eq. (7.5) and (7.6)] developed for headed bars without confining reinforcement, the ratios of test-to-calculated failure load T/T_c are plotted versus head size (net bearing area with respect to bar area) in Figure 7.12 for the specimens used to develop the descriptive equations.
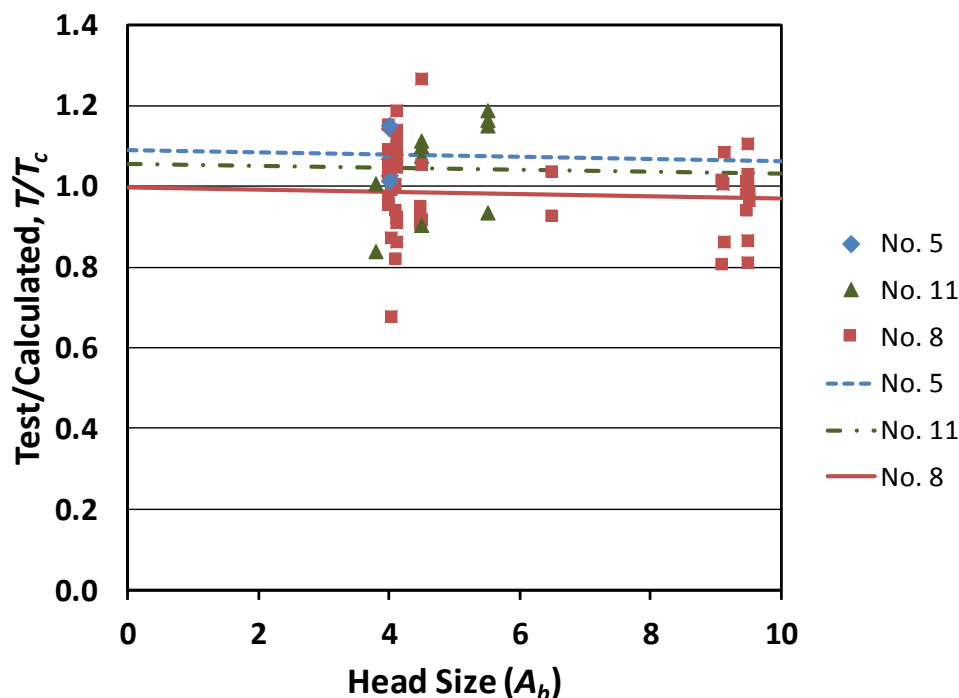
Figure 7.12 Ratio of test-to-calculated failure load T/T_c versus head size for specimens without confining reinforcement

The slightly negative slope of the trend lines shown in Figure 7.12, primarily based on the range of head size for No. 8 bars, indicates that the anchorage strength for headed bars without confining reinforcement has a minimal correlation with the head size for bars with 3.8 to 9.5A_b heads. This, in turn, justifies grouping headed bars with 3.8 to 9.5A_b heads as a single series for the development of the descriptive equations.

7.3.2 Anchorage Strength of Headed Bars With Confining Reinforcement

For 43 specimens with widely-spaced bars and confining reinforcement within the joint region, the development of a descriptive equation is based on two assumptions:

1) The anchorage strength (T_h) is the sum of a concrete contribution T_c, given by Eq. (7.5), and a contribution from the confining reinforcement within the joint region T_s;

2) The contribution from confining reinforcement is directly related to an effective quantity of confining reinforcement. Confining reinforcement is considered to be effective if it is fully anchored, in the form of closed hoops, and is located close to the top of the headed bar – within $8d_b$ for No. 3 through No. 8 bars and within $10d_b$ for No. 9 through No. 11 bars. These regions match those observed for hooked bars anchored in simulated beam-column joints (Sperry et al. 2015a, 2015b).

The second assumption (dealing with the location of the effective confining reinforcement) is supported by the strain measurements in the confining reinforcement for 12 specimens, as described in Section 3.3.3. The results indicate that the hoops located within the appropriate region ($8d_b$ or $10d_b$) experienced a significant strain increase at failure (almost all yielded), while the hoops outside this region exhibited much less or a negligible increase in strain. This assumption is also supported by observations of specimens after failure. Most cracks at failure were confined by the hoops that were close to the headed bars, rather than by all of the hoops provided in the joint region. Figure 7.13 shows cracks for a specimen with No. 3 hoops spaced at $3d_b$. The photo was taken after the loose concrete had been removed from the specimen following failure. The specimen contained six hoops within the joint region, but only the top four hoops crossed the major diagonal crack that propagated from the bottom of the head toward the bearing member. The bottom two hoops, one slightly above the top of the bearing member, another slightly below the top of the bearing member (within the compression region), were below the cracked region.

Figure 7.13 Cracks confined by effective confining reinforcement (specimen 11-5-F3.8-6#3-i-2.5-3-12)

Based on these assumptions and the analysis of the 43 specimens with confining reinforcement, the contribution of confining reinforcement can be expressed as

$$T_s = 48,800 \frac{A_{tt}}{n} d_b^{0.88} \tag{7.7}$$

where T_s = contribution of confining reinforcement to the anchorage strength of a headed bar (lb); A_{tt} = total cross-sectional area of effective confining reinforcement parallel to the headed bars being developed (in.²), which is the product of the cross-sectional area of the confining reinforcement and the total number of single legs parallel to the headed bars; n = number of headed bars; and d_b = diameter of headed bar (in.). The term A_{tt}/n is the area of confining reinforcement per headed bar.

Combining Eq. (7.5) with Eq. (7.7), the anchorage strength for widely-spaced headed bars with confining reinforcement can expressed as

$$T_h = 781 f_{cm}^{0.24} \ell_{eh}^{1.03} d_b^{0.35} + 48,800 \frac{A_{tt}}{n} d_b^{0.88} \tag{7.8}$$

Figure 7.14 compares the ratio T/T_h to the concrete compressive strength f_{cm} for the 43 specimens. T is the average peak load. T_h is based on Eq. (7.8). The maximum, minimum, mean, STD, and COV values of T/T_h are given in Table 7.10. The slope of dummy variable lines in the

153

figure indicates that the effect of concrete compressive strength is slightly underestimated by Eq. (7.8). Compared with Figures 7.2 and 7.3, the values of T/T_h are much less scattered. The values of T/T_h range from 0.81 to 1.20, with a coefficient of variation of 0.095.
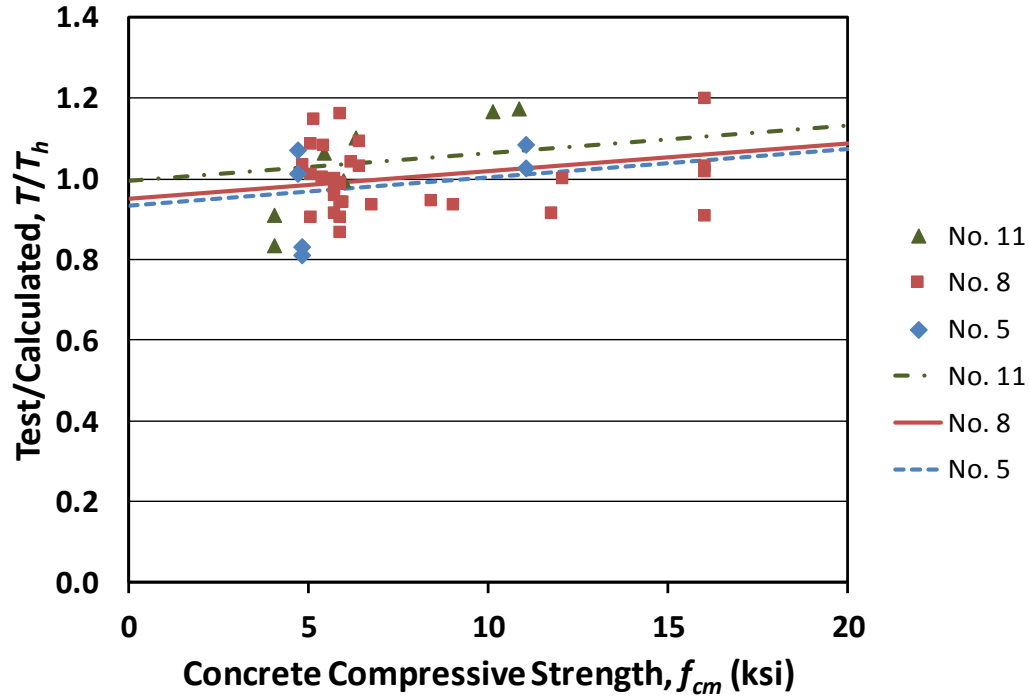
Figure 7.14 Ratio of test-to-calculated failure load T/T_h versus concrete compressive strength f_{cm} for specimens with widely-spaced bars and confining reinforcement

Table 7.10 Statistical parameters of T/T_h values for widely-spaced bars with confining reinforcement

(Number of specimens)	**All** (43)	**No. 5** (6)	**No. 8** (30)	**No. 11** (7)
Max	1.20	1.08	1.20	1.17
Min	0.81	0.81	0.87	0.83
Mean	1.00	0.97	1.00	1.03
STD	0.095	0.120	0.082	0.129
COV	0.095	0.123	0.082	0.125

For 31 specimens with closely-spaced bars and confining reinforcement, the ratios of anchorage strengths T/T_h, with T_h based on Eq. (7.8), are plotted versus the center-to-center spacing between the bars in Figure 7.15. The 43 specimens with widely-space headed bars used to develop Eq. (7.8) are also shown in the figure, represented by open symbols.
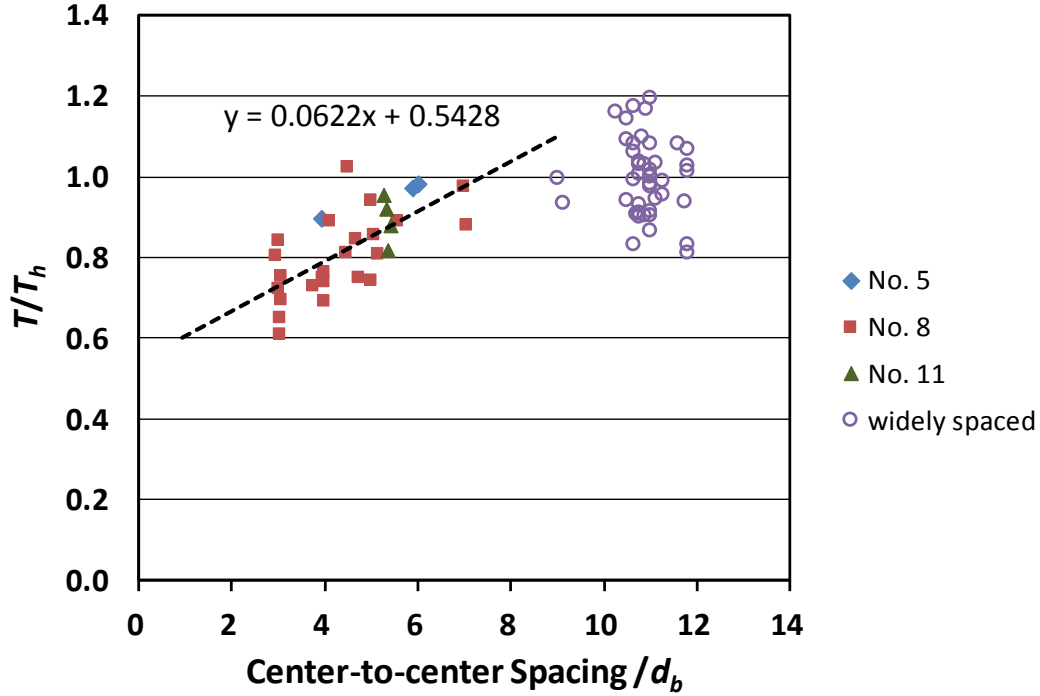
Figure 7.15 Ratio of test-to-calculated failure load T/T_h versus center-to-center spacing for headed bars with confining reinforcement

As shown in Figure 7.15, the closely-spaced bars with confining reinforcement generally exhibited lower anchorage strengths than the widely-spaced bars, as was observed for the bars without confining reinforcement. The trend line, however, is flatter than that shown in Figure 7.10, indicating that the anchorage strength of headed bars with confining reinforcement is affected less by close bar spacing than that of headed bars without confining reinforcement. Of the 31 specimens with closely-spaced bars and confining reinforcement, 14 had two No. 3 hoops, and 17 had No. 3 hoops at $3d_b$. Based on the trend line, the anchorage strength for both closely and widely spaced headed bars with confining reinforcement can be expressed as

$$T_h = \left(781 f_{cm}^{0.24} \ell_{eh}^{1.03} d_b^{0.35} + 48{,}800 \frac{A_{tt}}{n} d_b^{0.88}\right)\left(0.0622 \frac{s}{d_b} + 0.5428\right) \tag{7.9}$$

with $0.0622 \dfrac{s}{d_b} + 0.5428 \le 1.0$

Figure 7.16 compares the ratio T/T_h to concrete compressive strength for the headed bars (both widely-spaced and closely-spaced) with confining reinforcement, with T_h based on Eq. (7.9). The maximum, minimum, mean, STD, and COV values for T/T_h are given in Table 7.11. The slope

155

of dummy variable lines in the figure indicates that the effect of concrete compressive strength is slightly underestimated by Eq. (7.9). The ratio T/T_h ranges from 0.81 to 1.24, with a coefficient of variation of 0.095.
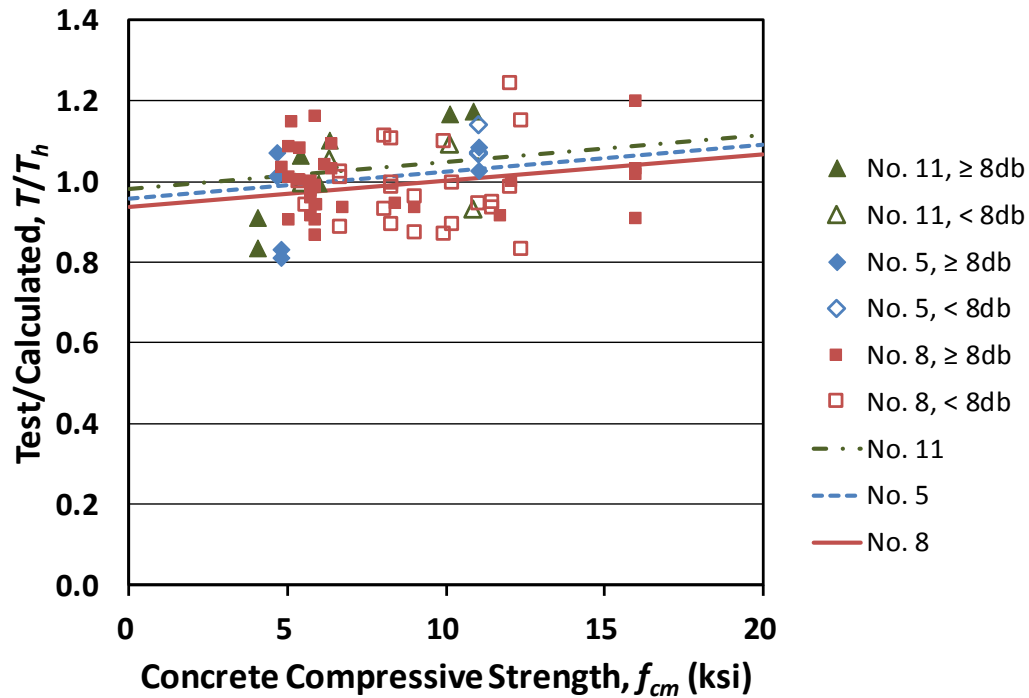
Figure 7.16 Ratio of test-to-calculated load T/T_h versus concrete compressive strength f_{cm} for specimens with confining reinforcement

Table 7.11 Statistical parameters of T/T_h values for specimens with confining reinforcement

(Number of specimens)	All	Widely spaced			Closely spaced		
		No. 5	No. 8	No. 11	No. 5	No. 8	No. 11
	(74)	(6)	(30)	(7)	(3)	(24)	(4)
Max	1.24	1.08	1.20	1.17	1.14	1.24	1.09
Min	0.81	0.81	0.87	0.83	1.07	0.83	0.93
Mean	1.00	0.97	1.00	1.03	1.09	0.98	1.02
STD	0.095	0.120	0.082	0.129	0.040	0.099	0.070
COV	0.095	0.123	0.082	0.125	0.036	0.101	0.069

With the descriptive equations [Eq. (7.8) and (7.9)] developed for headed bars with confining reinforcement, the ratios of test-to-calculated failure load T/T_h are plotted versus head size in Figure 7.17 for the specimens used to develop the descriptive equations.

156
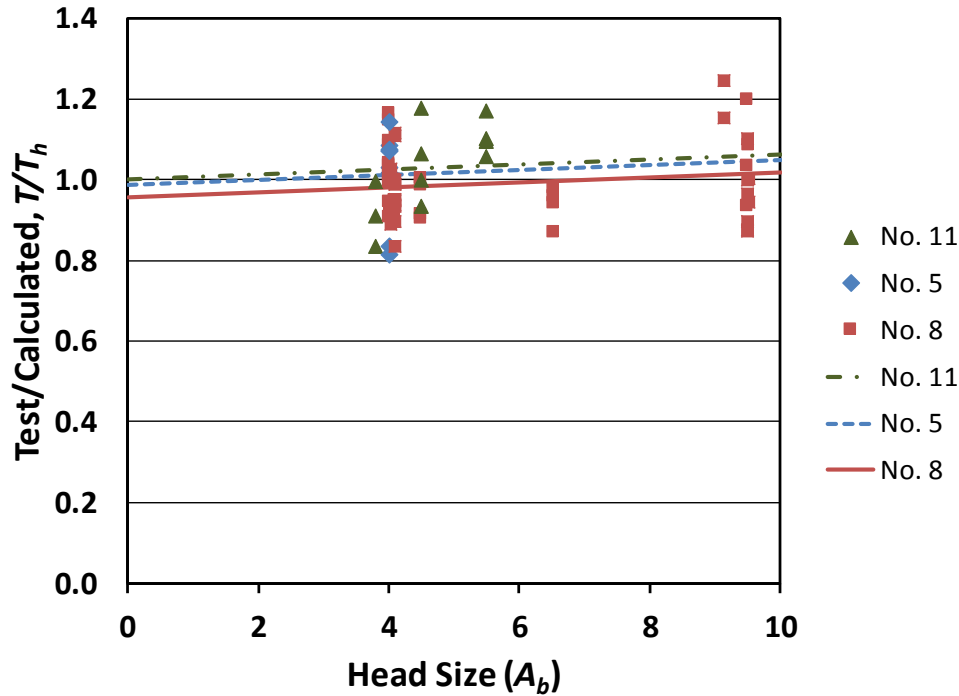
Figure 7.17 Ratio of test-to-calculated failure load T/T_h versus head size for specimens with confining reinforcement

The closely spaced, slightly upward trend lines shown in Figure 7.17 indicate that within a range of 3.8 to 9.5A_b, head size has a minimal influence on the anchorage strength for headed bars with confining reinforcement. As was found for specimens without confining reinforcement, this result justifies treating headed bars with 3.8 to 9.5A_b heads as a single series for the development of the descriptive equations.

7.3.3 Summary

In the development of the descriptive equations, Eq. (7.5) is based on test results of widely-spaced bars without confining reinforcement within the joint region, and serves as the basis of the other equations. Equation (7.8) applies to widely-spaced headed bars with confining reinforcement within the joint region, and equals Eq. (7.5) when no confining reinforcement is present. Equations (7.6) and (7.9) take into account the effect of spacing between the bars, and were developed by applying a modification factor to Eq. (7.5) and (7.8), respectively.

157

The failure loads T for all specimens are compared with the values of T_h obtained using the descriptive equations in Figure 7.18. As shown in the figure, the descriptive equations slightly overestimate the anchorage strength for No. 5 bars and slightly underestimate the anchorage strength for No. 11 bars. The variation, however, is small given the range of data.
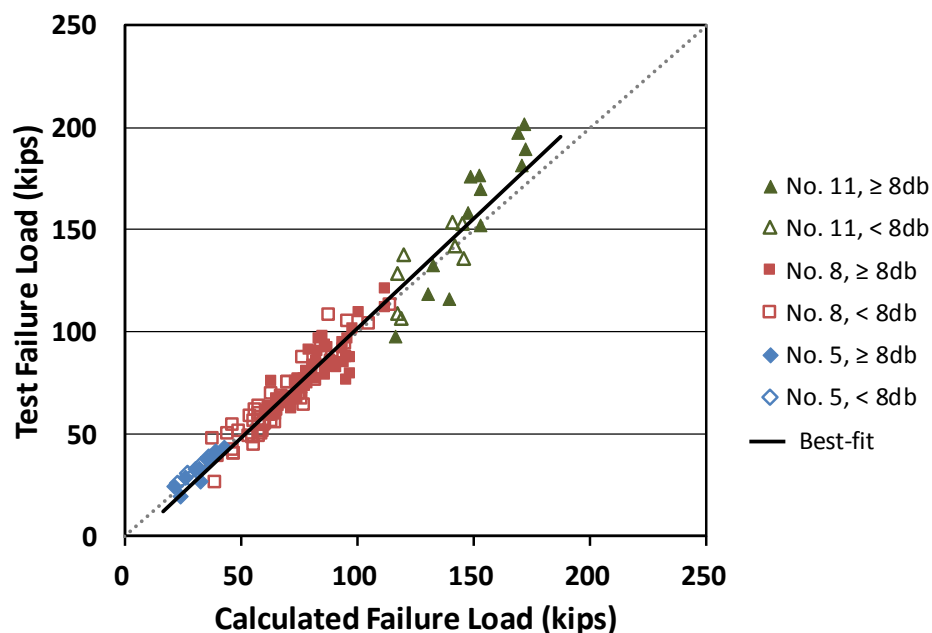
Figure 7.18 Test versus calculated failure load for specimens without and with confining reinforcement

7.4 EFFECT OF OTHER TEST PARAMETERS

7.4.1 Confining Reinforcement Within/Above Joint Region

In the development of the descriptive equations, it was assumed that only confining reinforcement, in the form of hoops, within a certain distance ($8d_b$ for No. 3 through No. 8 bars and $10d_b$ for No. 9 through No. 11 bars) from the headed bar *within the joint region* is effective as confining reinforcement. In this section, the effectiveness of hoops within and above the joint region is evaluated.

For each evaluation, the ratios of test-to-calculated failure load T/T_h (or T/T_c), with T_h (or T_c) based on the descriptive equations, are plotted versus the value of the *normalized confining reinforcement*, equal to the ratio of the total cross-sectional area of effective confining reinforcement to the total area of the headed bars being developed. The total cross-sectional area

of effective confining reinforcement *within the joint region* A_{tt} is as used in Eq. (7.7) through (7.9); the total cross-sectional area of the effective confining reinforcement *above the joint region* is notated by A_{ab}, and is determined based on the same rule as used for A_{tt}. The total area of headed bars being developed A_{hs} is the product of the nominal area of the headed bar A_b and the number of headed bars being developed *n*. The values of A_{tt}, A_{ab}, and A_{hs} for each specimen are given in Table B.1 in Appendix B.

For specimens with confining reinforcement, the effect of hoops *within* and *above the joint region* are evaluated separately; for specimens without confining reinforcement, the effective hoops *above* the joint region are evaluated. The location of the effective hoops that are illustrated in Figure 7.19 to Figure 7.21, with horizontal dashed lines representing the boundaries of the joint region.

7.4.1.1 Effectiveness of hoops within joint region for specimens with confining reinforcement

Figure 7.19 shows the ratio T/T_h as a function of the normalized confining reinforcement *within the joint region* A_{tt}/A_{hs} for the specimens with confining reinforcement. T_h is calculated based on Eq. (7.9). The closely spaced, nearly horizontal trend lines in the figure indicate that the effect of confining reinforcement *within the joint region* is well captured by the descriptive equation.
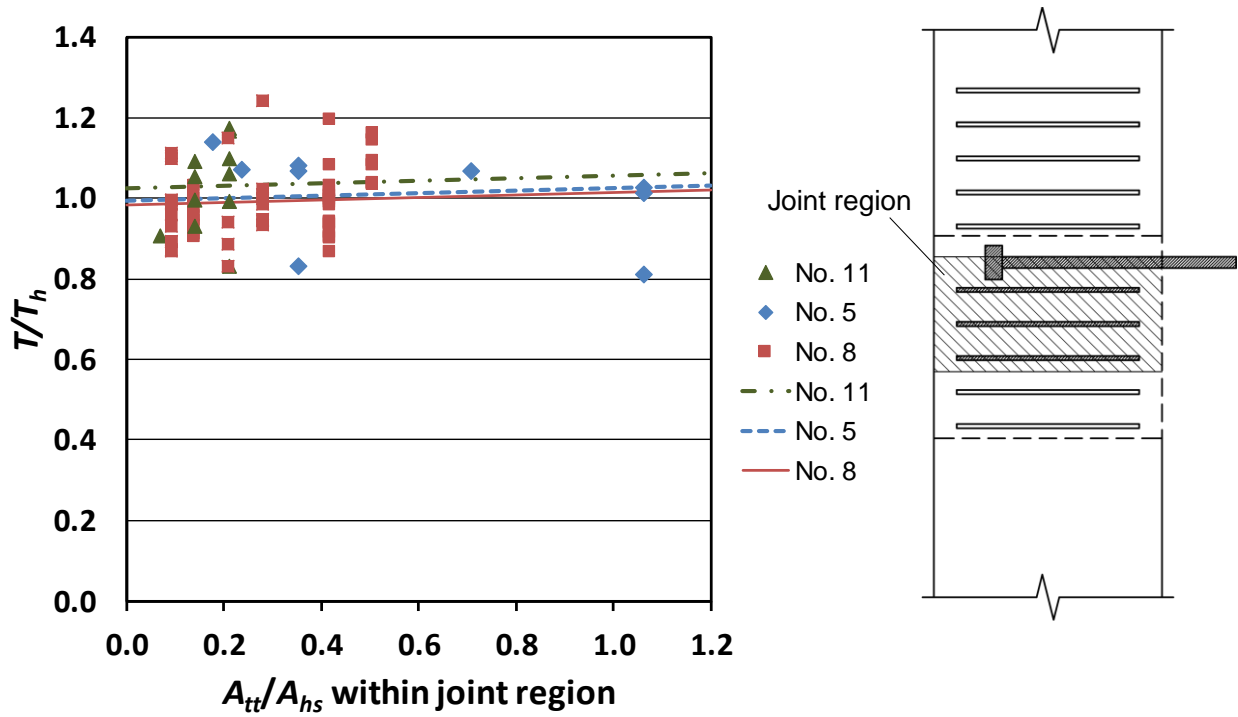
Figure 7.19 Ratio of test-to-calculated failure load T/T_h versus normalized confining reinforcement within joint region A_{tt}/A_{hs} for specimens with confining reinforcement

7.4.1.2 Effectiveness of hoops above joint region for specimens with confining reinforcement

Figure 7.20 shows the ratio T/T_h as a function of the normalized confining reinforcement *above the joint region* A_{ab}/A_{hs}. T_h is, again, calculated based on Eq. (7.9), which does not account for the effect of confining reinforcement above the joint region. The values of A_{ab}/A_{hs} vary significantly, from 0.18 to 0.76, and are different from A_{tt}/A_{hs}. The trend lines are, however, nearly horizontal, indicating that the amount of confining reinforcement *above the joint region* had no influence on the anchorage strength of headed bars in beam-column joints. If the hoops above the joint region contributed to the anchorage strength of headed bars, the trend line in Figure 7.20 would slope upward, because Eq. (7.9) does not account for this reinforcement. These comparisons, therefore, indicate that only the confining reinforcement *within the joint region* affected the anchorage strength of the headed bars, and the effect of that confining reinforcement is well captured by Eq. (7.9), as demonstrated in Section 7.4.1.1.

160
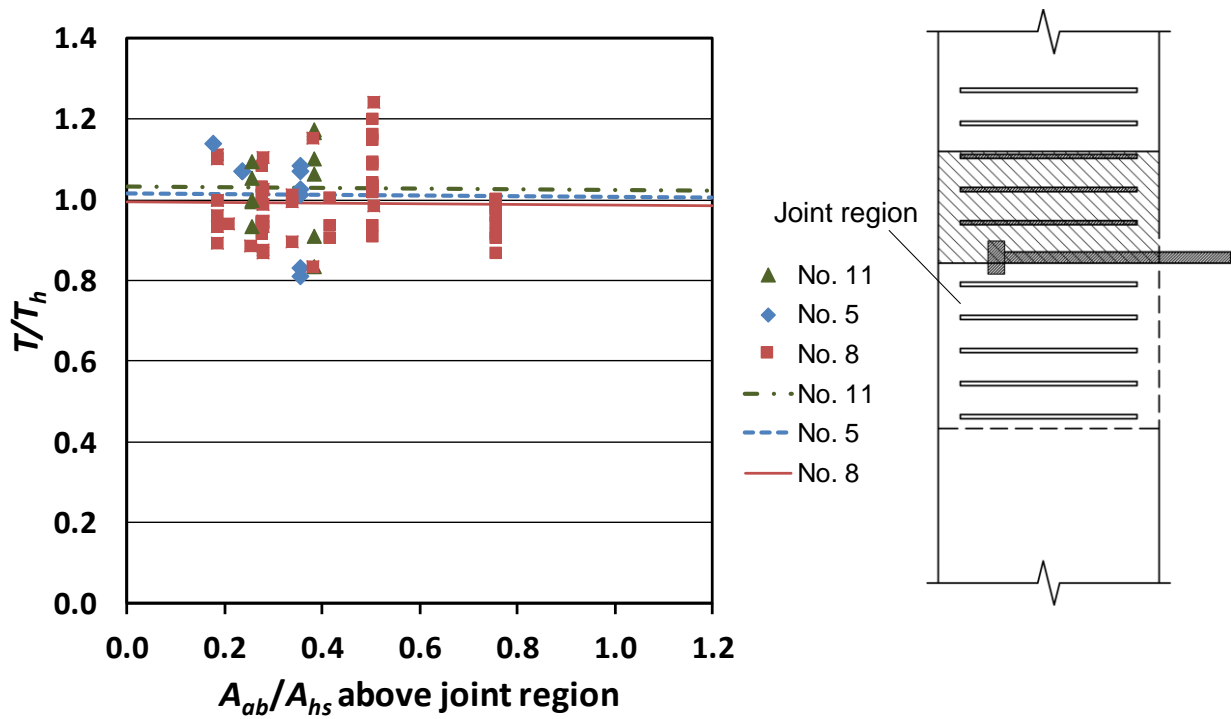
Figure 7.20 Ratio of test-to-calculated failure load T/T_h versus normalized confining reinforcement above joint region A_{ab}/A_{hs} for specimens with confining reinforcement

7.4.1.3 Effectiveness of hoops above joint region for specimens without confining reinforcement

Figure 7.21 shows the ratio T/T_c as a function of the normalized confining reinforcement *above the joint region A_{ab}/A_{hs}* for the specimens without confining reinforcement in the joint region. T_c is calculated based on Eq. (7.6).
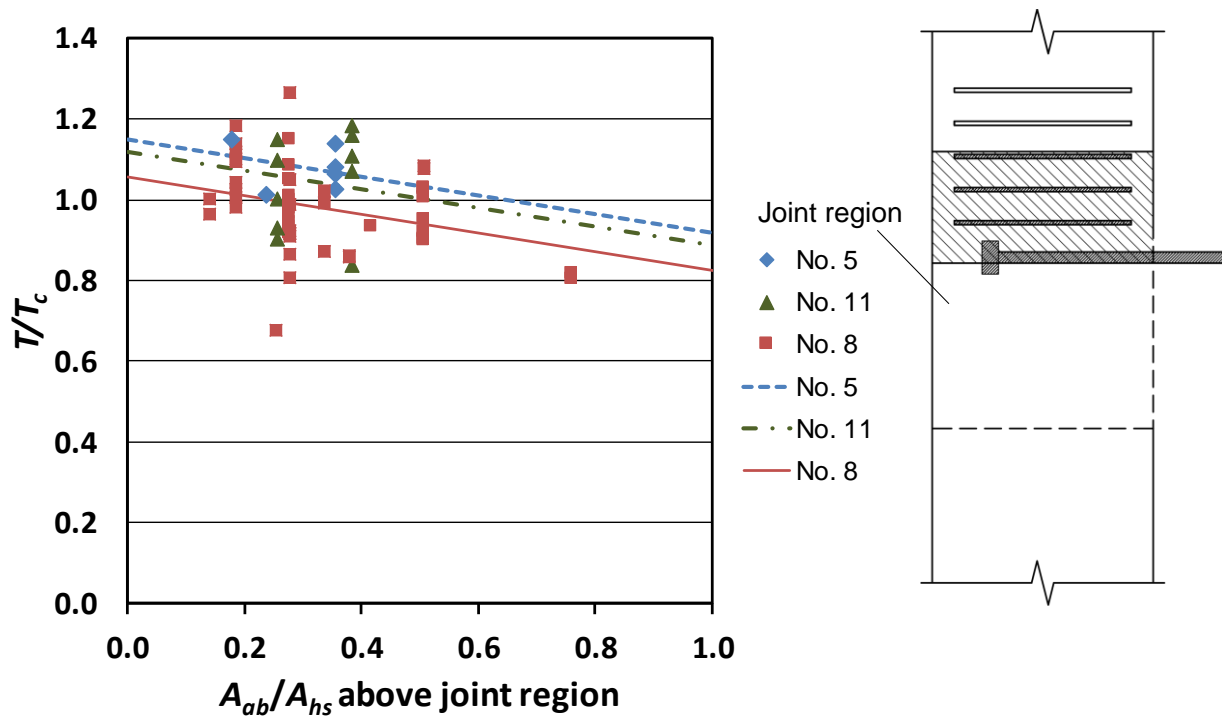
Figure 7.21 Ratio of test-to-calculated failure load T/T_c versus normalized confining reinforcement above joint region A_{ab}/A_{hs} for specimens without confining reinforcement

In contrast to Figure 7.19 and Figure 7.20, the trend lines in Figure 7.21 have a negative slope. This would seem to indicate that an increase in confining reinforcement above the joint region results in a lower anchorage strength. It is likely, however, that the downward trend shown in Figure 7.21 is simply due to the random distribution of the strength T with respect to T_c for the test specimens; trends for specimens with confining reinforcement (Section 7.4.1.2) indicated no trend.

7.4.2 Headed Bars with Large Heads

As discussed in Section 7.2.1, headed bars with 12.9 through $14.9A_b$ heads exhibited higher anchorage strengths than the headed bars with smaller heads. For simplicity, the term "large heads" will be used to describe the heads with a net bearing area greater than $12A_b$. In this study, it refers to the No. 5 F13.1, No. 8 S14.9, and No. 8 O12.9 headed bars with net bearing areas of $13.1A_b$, $14.9A_b$, and $12.9A_b$, respectively. Table 7.12 summarizes the test results for the 16 test specimens with these large heads, including the net bearing area of the head, expressed as a multiple of bar area A_b, the measured embedment length ℓ_{eh}, concrete compressive strength f_{cm}, average peak load

T, and the ratio of test-to-calculated failure load T/T_c or T/T_h, with T_c and T_h based on descriptive Eq. (7.6) and Eq. (7.9), respectively.

Table 7.12 Test results for specimens containing large heads

Specimen	Net Bearing Area[*]	ℓ_{eh} (in.)	f_{cm} (psi)	T (kips)	T/T_c[†] T/T_h[†]
8-15-S14.9-0-i-2.5-3-9.5	14.9A_b	9.69	16030	87.1	1.05
8-8-O12.9-0-i-2.5-3-9.5	12.9A_b	9.69	8800	85.2	1.19
8-8-S14.9-0-i-2.5-3-8.25	14.9A_b	8.25	8800	70.9	1.17
5-5-F13.1-0-i-2.5-5-4	13.1A_b	4.41	4810	28.2	1.21
5-5-F13.1-0-i-2.5-3-6	13.1A_b	6.22	4690	35.3	1.07
5-12-F13.1-0-i-2.5-5-4	13.1A_b	4.13	11030	31.4	1.18
5-12-F13.1-0-i-2.5-3-6	13.1A_b	6.03	11030	44.2	1.12
8-15-S14.9-2#3-i-2.5-3-7	14.9A_b	7.00	16030	79.3	1.23
8-15-S14.9-5#3-i-2.5-3-5.5	14.9A_b	5.50	16030	81.4	1.31
8-8-O12.9-5#3-i-2.5-3-9.5	12.9A_b	9.38	8800	83.5	0.98
8-8-S14.9-5#3-i-2.5-3-8.25	14.9A_b	8.25	8800	87.0	1.13
5-5-F13.1-2#3-i-2.5-5-4	13.1A_b	4.09	4810	28.9	1.15
5-5-F13.1-5#3-i-2.5-5-4	13.1A_b	4.19	4690	35.2	1.08
5-5-F13.1-2#3-i-2.5-3-6	13.1A_b	5.94	4690	46.4	1.32
5-12-F13.1-2#3-i-2.5-5-4	13.1A_b	4.09	11030	36.3	1.21
5-12-F13.1-5#3-i-2.5-5-4	13.1A_b	4.13	11030	40.3	1.08

[*] Net bearing area of O12.9 is taken as the difference between the gross area of the head and the area of obstruction closest to the head. Refer to Table 2.1
[†] T_c is based on Eq. (7.6) for specimens without confining reinforcement; T_h is based on Eq. (7.9) for specimens with confining reinforcement

As shown in Table 7.12, only one specimen out of 16 had a T/T_c or T/T_h value below 1.0. For the seven specimens without confining reinforcement, the average value of T/T_c is 1.14, with a coefficient of variation of 0.059. For the nine specimens with confining reinforcement, the average value of T/T_h is 1.17, slightly greater but with more scatter, with a coefficient of variation of 0.115. This indicates that headed bars with large heads provided approximately 15% higher anchorage strengths than the headed bars with smaller heads. The advantage in strength obtained with large heads could be included in Code provisions for development length, which will be discussed in Chapter 9.

7.4.3 Headed Bars with Large Obstructions

O4.5, O9.1, and O12.9, the three types of heads with obstructions exceeding the dimensional limits for HA heads in ASTM A970, are referred to in this study as non-HA heads. The test results for the non-HA heads are summarized in Table 7.13, including the net bearing area of the head, expressed as a multiple of bar area A_b, embedment length ℓ_{eh}, concrete compressive strength f_{cm}, average peak load T, and the ratio of test-to-calculated failure load T/T_c or T/T_h, with T_c and T_h based on descriptive Eq. (7.6) and Eq. (7.9), respectively. The net bearing area of the non-HA heads is taken as the difference between the gross area of head and the area of the obstruction adjacent to the head. The dimensions of the heads and obstructions are shown in Table 2.1.

Table 7.13 Test results for specimens containing non-HA heads

Specimen	Net Bearing Area	ℓ_{eh} (in.)	f_{cm} (psi)	T (kips)	$T/T_c^\dagger$ $T/T_h^\dagger$
(2@9)8-8-O4.5-0-i-2.5-3-9.5		9.00	6710	58.8	0.94
(2@7)8-8-O4.5-0-i-2.5-3-9.5		9.25	6710	54.5	0.92
(2@5)8-8-O4.5-0-i-2.5-3-9.5		9.00	6710	51.2	1.05
(2@3)8-8-O4.5-0-i-2.5-3-9.5		9.00	6710	47.7	1.27
8-5-O4.5-0-i-2.5-3-11.25		11.25	5500	67.4	0.90
8-5-O4.5-0-i-2.5-3-14.25	$4.5A_b$	14.13	5500	85.0	0.90
8-8-O4.5-0-i-2.5-3-9.5		9.19	6710	58.4	0.92
(3@5.35)11-12-O4.5-0-i-2.5-3-16.75		16.92	10860	106.8	0.90
(3@5.35)11-5-O4.5-0-i-2.5-3-19.25		19.50	5430	128.7	1.10
11-12-O4.5-0-i-2.5-3-16.75		17.13	10860	169.6	1.11
11-5-O4.5-0-i-2.5-3-19.25		19.44	5430	157.9	1.07
8-5-O9.1-0-i-2.5-3-14.5		14.38	4970	94.8	1.01
(3@5.5)8-5-O9.1-0-i-2.5-3-14.5	$9.1A_b$	14.35	4960	75.7	1.01
(4@3.7)8-5-O9.1-0-i-2.5-3-14.5		14.06	5570	61.2	1.00
8-8-O12.9-0-i-2.5-3-9.5	$12.9A_b$	9.69	8800	85.2	1.19
8-5-O4.5-2#3-i-2.5-3-9.25		9.38	5750	67.9	1.00
8-5-O4.5-2#3-i-2.5-3-12.25		12.00	5750	78.5	0.91
8-5-O4.5-5#3-i-2.5-3-8.25		8.00	5900	68.4	0.98
8-5-O4.5-5#3-i-2.5-3-11.25		11.13	5900	82.2	0.90
(3@5.35)11-12-O4.5-6#3-i-2.5-3-16.75	$4.5A_b$	17.00	10860	135.8	0.93
(3@5.35)11-5-O4.5-6#3-i-2.5-3-19.25		19.38	5430	141.7	1.00
11-12-O4.5-6#3-i-2.5-3-16.75		16.81	10860	201.5	1.17
11-5-O4.5-6#3-i-2.5-3-19.25		19.63	5430	181.4	1.06
8-8-O12.9-5#3-i-2.5-3-9.5	$12.9A_b$	9.38	8800	83.5	0.98

† T_c is based on Eq. (7.6) for specimens without confining reinforcement; T_h is based on Eq. (7.9) for specimens with confining reinforcement

As shown in Table 7.13, for the 15 specimens without confining reinforcement, T/T_c ranges from 0.90 to 1.27, with an average of 1.02. For the nine specimens with confining reinforcement, T/T_h ranges from 0.90 to 1.17, with an average of 0.99. This indicates that the bars with non-HA heads had similar anchorage strengths to those with HA heads. It is thus suggested that the use of non-HA heads that fall within the sizes of those tested in this study can be safely used in design.

7.4.4 Headed Bars with Large h_{cl}/ℓ_{eh} Ratio

7.4.4.1 Ratio of h_{cl}/ℓ_{eh}

During the initial analysis for the development of the descriptive equations, it was found that the headed bars in this study with a net bearing area (A_{brg}) $\leq 9.5A_b$ tended to exhibit lower anchorage strengths as the ratio h_{cl}/ℓ_{eh} increased above 1.33. h_{cl}, as illustrated in Figure 2.13, is the distance from the center of the bar to the top of bearing member. For headed bars terminating at the far side of the column (representing the vast majority of the test specimens in this study), a small embedment length ℓ_{eh} relative to h_{cl} indicates a deeper beam-column joint.

The specimens with $h_{cl}/\ell_{eh} \geq 1.33$ and low failure loads included those with No. 8 bars from Group 12 ($h_{cl} = 10.25$ in. and $\ell_{eh} = 6$ in.) and Group 16 ($h_{cl} = 20$ in. and $\ell_{eh} = 10$ in.), and No 11 bars from Groups 15, 17, and 18 ($h_{cl} = 20$ in. and $\ell_{eh} = 12$ or 14.5 in.); the specimens from Group 12 which had headed bars terminating in the middle of the column (illustrated in Figure 2.7); and the specimens from Group 16, with $h_{cl} = 20$ in. (as opposed to the standard 10.25 in. for No. 8 bars), that were intentionally designed to simulate a deep beam-column joint. For this reason, the specimens in Group 16 are referred to as "deep-beam specimens" and identified with "DB" at the end of the specimen designation. As will be demonstrated in Table 7.14 and Figures 7.22 and 7.23, the low anchorage strengths of the headed bars associated with large h_{cl}/ℓ_{eh} ratios led to the decision to exclude these specimens from the development of the descriptive equations.

In addition to the specimens listed above, five specimens with $h_{cl}/\ell_{eh} \geq 1.33$ (one with No. 5 bars and four with No. 8 bars; the first five specimens listed in Table 7.14) were used in the development of the descriptive equation. All five had confining reinforcement. The No. 5-bar specimen with $h_{cl}/\ell_{eh} =1.38$ had a nominal embedment length of 4 in., the shortest embedment length used in this study. It was included in the development of the descriptive equation because

very little data from this study were available for specimens with short embedment lengths, although when compared to T_h obtained using Eq. (7.9), T/T_h was 0.83. The four specimens with No. 8 bars have values of h_{cl}/ℓ_{eh} equal to 1.42, 1.42, 1.78, and 1.82. These bars were cast in concrete with a nominal strength of 15 ksi, the highest used in this study. Due to the relatively small amount of data obtained with high strength concrete (only nine specimens had 15-ksi concrete), these four specimens were used to develop the descriptive equations. Of the four specimens, three had values of T/T_h greater than 1.0 (one specimen had $T/T_h = 1.20$, above the values for the majority of the specimens used to develop the descriptive equations), and the other specimen had $T/T_h = 0.91$.

The test results for the specimens with $A_{brg} \leq 9.5A_b$ and $h_{cl}/\ell_{eh} \geq 1.33$ are given in Table 7.14, including the ratio h_{cl}/ℓ_{eh} (with ℓ_{eh} corresponding to $\ell_{eh,avg}$ in Table B.1 in Appendix B), the measured concrete compressive strength f_{cm}, average peak load T, and the ratio of test-to-calculated failure load T/T_c or T/T_h, with T_c and T_h based on descriptive equations Eq. (7.6) and Eq. (7.9), respectively. The vast majority of the specimens listed in Table 7.14 have values of T/T_c (or T/T_h) below 1.0. Excluding the five specimens that were used to develop the descriptive equations, the specimens in Table 7.14 have values of T/T_c (or T/T_h) ranging from 0.54 to 0.97, with average values of 0.73 and 0.82, respectively, for headed bars without and with confining reinforcement.

Table 7.14 Test results for specimens with $A_{brg} \leq 9.5A_b$ and $h_{cl}/\ell_{eh} \geq 1.33$

	Specimen	h_{cl}/ℓ_{eh}	f_{cm} (psi)	T (kips)	T/T_c[†] T/T_h[†]
Group 8	8-15-T4.0-2#3-i-2.5-4.5-7	1.42	16030	59.0	0.91
	8-15-T4.0-5#3-i-2.5-4.5-5.5	1.82	16030	63.3	1.02
	8-15-S9.5-2#3-i-2.5-3.25-7	1.42	16030	67.1	1.03
	8-15-S9.5-5#3-i-2.5-3.25-5.5	1.78	16030	75.8	1.20
Group 13	5-5-F4.0-2#3-i-2.5-5-4	1.38	4810	19.7	0.83
Group 12[*]	(3@3)8-5-F4.1-0-i-2.5-7-6	1.62	4930	20.6	0.86
	(3@5)8-5-F4.1-0-i-2.5-7-6	1.58	4930	23.9	0.76
	(3@7)8-5-F4.1-0-i-2.5-7-6	1.60	4940	27.1	0.73
	(3@5.5)8-5-F9.1-0-i-2.5-7-6	1.61	5160	23.0	0.72
	(4@3.7)8-5-T9.5-0-i-2.5-7-6	1.63	5160	21.7	0.86
	8-5-F4.1-0-i-2.5-7-6	1.64	4930	28.7	0.74
	8-5-F9.1-0-i-2.5-7-6	1.63	4940	33.4	0.86

[†] T_c is based on Eq. (7.6) for specimens without confining reinforcement; T_h is based on Eq. (7.9) for specimens with confining reinforcement

[*] Specimens were not used to develop the descriptive equations

Table 7.14 Cont. Test results for specimens with $A_{brg} \leq 9.5A_b$ and $h_{cl}/\ell_{eh} \geq 1.33$

	Specimen	h_{cl}/ℓ_{eh}	f_{cm} (psi)	T (kips)	T/T_c[†] T/T_h[†]
Group 12[*]	(3@3)8-5-F4.1-5#3-i-2.5-7-6	1.67	4930	32.1	0.89
	(3@5)8-5-F4.1-5#3-i-2.5-7-6	1.59	4930	37.5	0.86
	(3@7)8-5-F4.1-5#3-i-2.5-7-6	1.64	4940	42.3	0.87
	(3@5.5)8-5-F9.1-5#3-i-2.5-7-6	1.60	5160	43.1	0.96
	(4@3.7)8-5-F9.1-5#3-i-2.5-7-6	1.66	5160	31.6	0.87
	8-5-F4.1-5#3-i-2.5-7-6	1.60	4930	50.7	0.91
	8-5-F9.1-5#3-i-2.5-7-6	1.62	4940	53.8	0.97
Group 15[*]	11-5a-F3.8-0-i-2.5-3-12	1.63	3960	56.8	0.68
	11-5a-F8.6-0-i-2.5-3-12	1.61	3960	63.8	0.76
	11-5a-F3.8-2#3-i-2.5-3-12	1.63	3960	67.3	0.74
	11-5a-F3.8-6#3-i-2.5-3-12	1.61	3960	78.0	0.74
	11-5a-F8.6-6#3-i-2.5-3-12	1.55	4050	79.2	0.72
Group 16[*]	8-8-F4.1-0-i-2.5-3-10-DB	1.97	7410	50.2	0.72
	8-8-F9.1-0-i-2.5-3-10-DB	1.99	7410	51.8	0.74
	8-5-F4.1-0-i-2.5-3-10-DB	1.97	4880	40.6	0.64
	8-5-F9.1-0-i-2.5-3-10-DB	2.00	4880	44.4	0.71
	8-8-F9.1-5#3-i-2.5-3-10-DB	2.03	7410	68.2	0.86
	8-5-F4.1-3#4-i-2.5-3-10-DB	1.93	4880	64.6	0.86
	8-5-F9.1-3#4-i-2.5-3-10-DB	2.00	4880	65.8	0.91
	8-5-F4.1-5#3-i-2.5-3-10-DB	1.91	4880	70.2	0.92
	8-5-F9.1-5#3-i-2.5-3-10-DB	1.96	4880	70.5	0.95
Group 17[*]	11-8-F3.8-0-i-2.5-3-14.5	1.34	8660	79.1	0.65
	(3@5.35)11-8-F3.8-0-i-2.5-3-14.5	1.33	8720	52.9	0.54
	11-8-F3.8-2#3-i-2.5-3-14.5	1.33	8660	88.4	0.68
	(3@5.35)11-8-F3.8-2#3-i-2.5-3-14.5	1.34	8720	72.6	0.65
	11-8-F3.8-6#3-i-2.5-3-14.5	1.33	8660	112.7	0.78
	(3@5.35)11-8-F3.8-6#3-i-2.5-3-14.5	1.31	8720	83.7	0.68
Group 18[*]	11-5-F3.8-0-i-2.5-3-12	1.61	5760	66.5	0.72
	11-5-F8.6-0-i-2.5-3-14.5	1.34	5970	82.8	0.74
	(3@5.35)11-5-F8.6-0-i-2.5-3-14.5	1.33	6240	65.1	0.73
	11-5-F3.8-6#3-i-2.5-3-12	1.56	5760	88.3	0.76
	11-5-F8.6-6#3-i-2.5-3-14.5	1.33	5970	112.3	0.84
	(3@5.35)11-5-F8.6-6#3-i-2.5-3-14.5	1.34	6240	75.6	0.68

[†] T_c is based on Eq. (7.6) for specimens without confining reinforcement; T_h is based on Eq. (7.9) for specimens with confining reinforcement

[*] Specimens were not used to develop the descriptive equations

The values of T/T_c are plotted versus h_{cl}/ℓ_{eh} for all specimens with $A_{brg} \leq 9.5A_b$ without confining reinforcement in Figure 7.22. The specimens that were not used to develop the descriptive equations are represented by open symbols. As shown in Figure 7.22, the specimens

with $h_{cl}/\ell_{eh} \geq 1.33$ exhibited much lower failure loads than predicted by Eq. (7.6); for No. 8 bars, the anchorage strengths equal approximately 75% of the strengths predicted by Eq. (7.6); for No. 11 bars, the anchorage strengths equal approximately 70% of the predicted strengths, with one value as low as 54%.
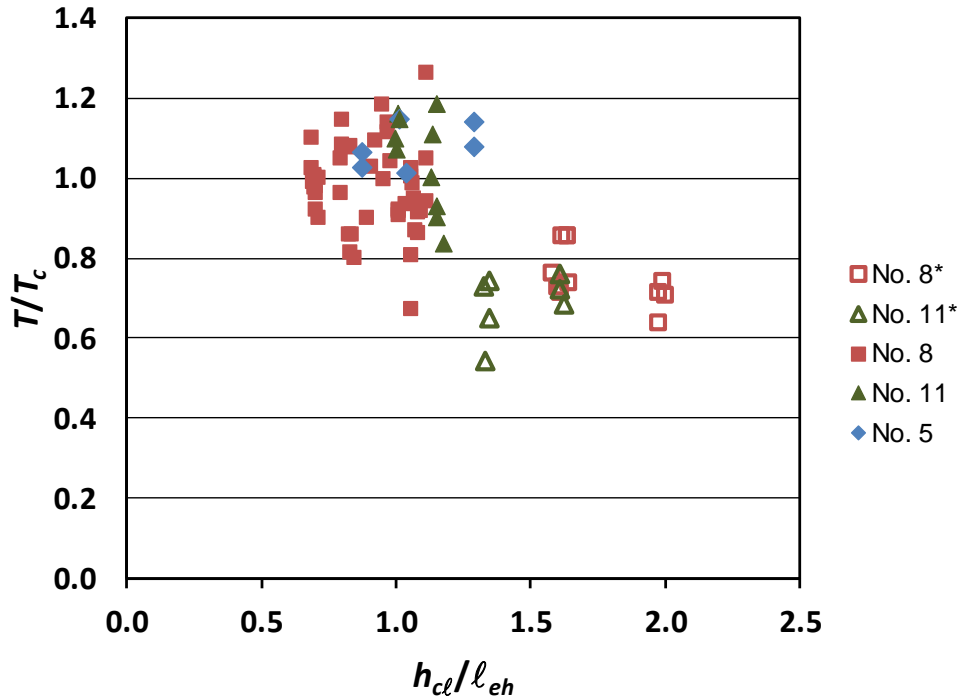
*Specimens not used to develop the descriptive equations

Figure 7.22 Ratio of test-to-calculated failure load T/T_c versus ratio of h_{cl}/ℓ_{eh} for specimens with $A_{brg} \leq 9.5A_b$ and no confining reinforcement

For the specimens with $A_{brg} \leq 9.5A_b$ with confining reinforcement, Figure 7.23 shows the ratios of T/T_h as a function of h_{cl}/ℓ_{eh}. The five specimens with solid symbols and with $h_{cl}/\ell_{eh} \geq 1.33$ represent specimens that were included in the development of the descriptive equation, as described above. As was shown in Figure 7.22, with the exception of three out of five of the specimens used to develop Eq. (7.9), the specimens with $h_{cl}/\ell_{eh} \geq 1.33$ exhibited lower failure loads than predicted by Eq. (7.9).
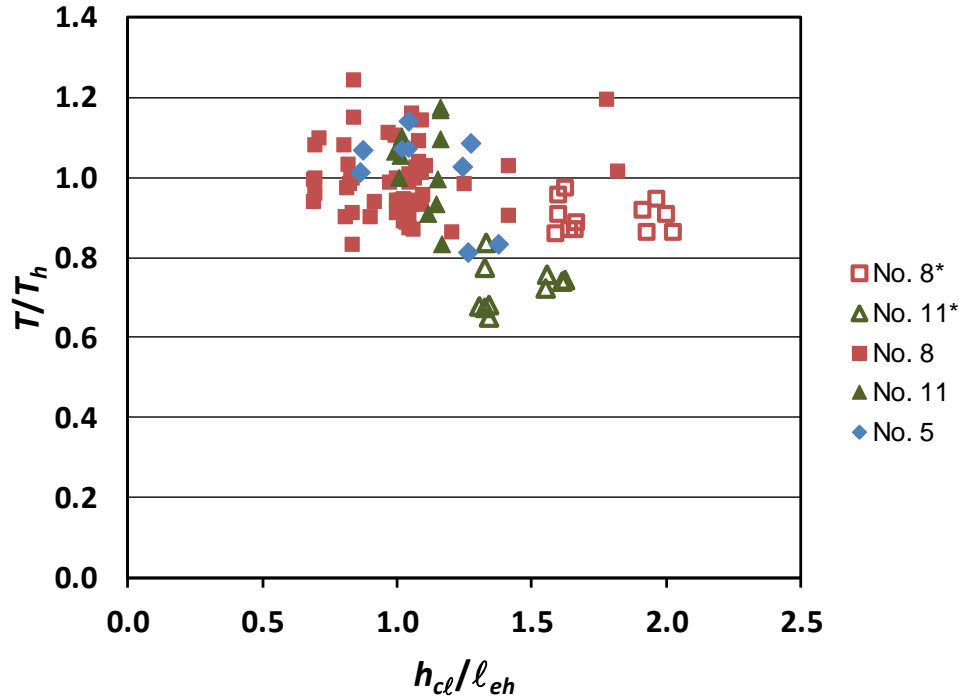
*Specimens not used to develop the descriptive equations

Figure 7.23 Ratio of test-to-calculated failure load T/T_h versus ratio of h_{cl}/ℓ_{eh} for specimens with $A_{brg} \leq 9.5A_b$ and confining reinforcement

For the specimens not used to develop the descriptive equations, the values of T/T_h (Figure 7.23) relative to the values of T/T_c (Figure 7.22) indicate that, with the addition of confining reinforcement, the decrease in anchorage strength for the No. 8 bars is not as great as the decrease for the specimens without confining reinforcement [an average of 90% of the strengths calculated using Eq. (7.9), compared to 75% for specimens without confining reinforcement]. For the No. 11 bars with confining reinforcement, however, the anchorage strengths were 73% of the calculated strengths, only a small increase compared to the 70% as observed in the specimens without confining reinforcement.

To evaluate the effectiveness of confining reinforcement provided within the joint region for the specimens not used to develop the descriptive equations, the ratio T/T_h [with T_h based on Eq. (7.9)] is plotted as a function of the normalized confining reinforcement within joint region A_{tt}/A_{hs} in Figure 7.24. The values of A_{tt} and A_{hs} are given in Table B.1 in Appendix B.

169
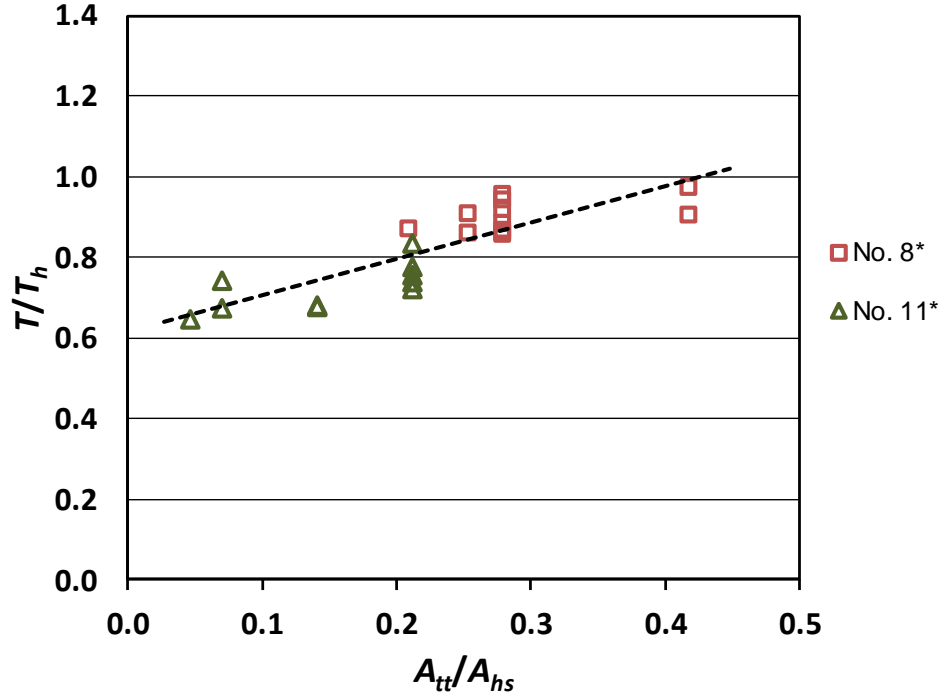
*Specimens not used to develop the descriptive equations

Figure 7.24 Ratio of test-to-calculated failure load T/T_h versus normalized confining reinforcement A_{tt}/A_{hs} for specimens with $h_{cl}/\ell_{eh} \geq 1.33$ from Groups 12, and 15 to 18

The upward sloping of the trend line in Figure 7.24 indicates that, relative to the strength calculated using the descriptive equation, the negative effect on anchorage strength associated with a large h_{cl}/ℓ_{eh} ratio (≥ 1.33) is reduced as the amount of confining reinforcement increases.

7.4.4.2 Ratio of d_{eff}/ℓ_{eh}

As discussed in Section 7.4.4.1, the headed bars with $h_{cl}/\ell_{eh} \geq 1.33$ generally exhibited lower anchorage strengths than the headed bars with $h_{cl}/\ell_{eh} < 1.33$. h_{cl}, the distance from the center of the bar to the top of bearing member, simulates the approximate depth of the neutral axis of a beam measured from the centroid of the tension reinforcement. For use in design, it would be desirable to correlate h_{cl} to d, the distance from the centroid of the tension bar to the extreme compression fiber of the beam, as d is a readily known value. Since the beam-column joint specimens in this study had the beam simulated with a bearing member, d can only be approximated for these specimens. The value of d could be taken as the sum of h_{cl} and the height

of the bearing member ($8^3/_8$ in., as illustrated in Figure 2.12); however, using the full height of the bearing member tends to overestimate the value of d, since in beam-column joint tests the compressive force of the assumed beam is concentrated at the top of the bearing member rather than evenly distributed along its full height.

As an alternative approach, the reaction from the bearing member can be assumed to represent the equivalent rectangular stress block often assumed for reinforced concrete beams in flexure. The upper edge of the bearing member is assumed to represent the neutral axis of the concrete beam, with the extreme compressive fiber located some distance c (effective depth of neutral axis) below this point. The effective value of d, d_{eff}, is taken as the sum of h_{cl} and c, as shown in Figure 7.25.
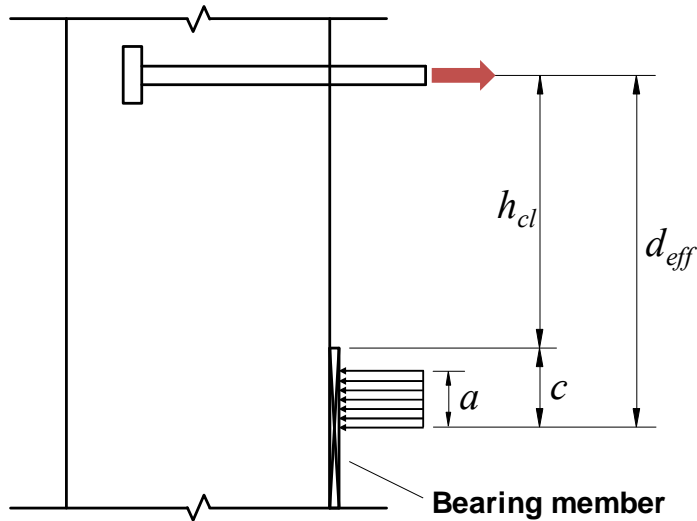
Figure 7.25 Effective depth d_{eff}

The distance c is calculated by:

$$c = a/\beta_1 \tag{7.10}$$

where $\beta_1 = 0.85 - \dfrac{0.05(f_{cm} - 4000)}{1000}$, $0.65 \leq \beta_1 \leq 0.85$; c = effective depth of neutral axis (in.); a = depth of equivalent rectangular compressive stress block (in.); β_1 = factor relating depth of equivalent rectangular compressive stress block a to depth of neutral axis c, as described in Section 22.2.2.4.3 of ACI 318-14; and f_{cm} = measured concrete compressive strength (psi).

171

The depth of equivalent rectangular compressive stress block a is calculated using Eq. (7.11), based on the assumptions that the peak load applied on a specimen T_{total} (values given in Table B.1 in Appendix B) equals the compressive force on the compressive stress block (lb), and that the concrete within the depth of a is crushed at the failure of the specimen.

$$a = T_{total} / (0.85 f_{cm} b) \qquad (7.11)$$

where b = width of the column in a beam-column joint specimen (in.).

With this approach, d_{eff} is calculated for each specimen, and given in Table B.1 in Appendix B. Figure 7.26 and Figure 7.27 show the ratios T/T_c (or T/T_h, as appropriate) as a function of d_{eff}/ℓ_{eh} for the specimens without and with confining reinforcement, respectively. As in Figure 7.22 and Figure 7.23, the specimens that are not used to develop the descriptive equations are represented by open symbols.
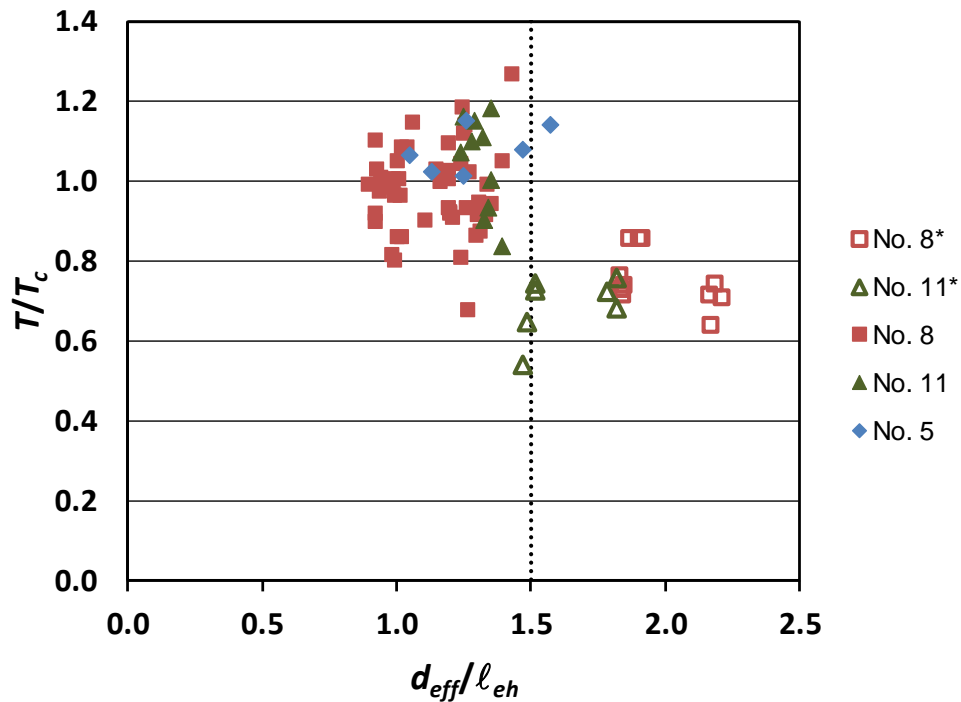
*Specimens not used to develop the descriptive equations

Figure 7.26 Ratio of test-to-calculated failure load T/T_c versus ratio of d_{eff}/ℓ_{eh} for specimens with $A_{brg} \leq 9.5 A_b$ and no confining reinforcement

172
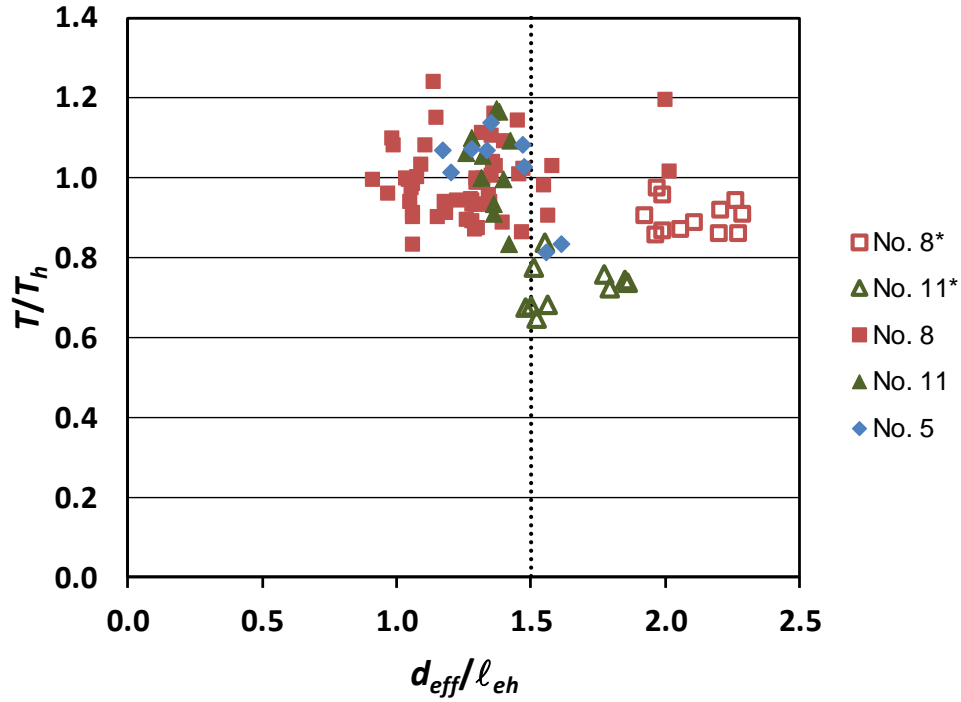
*Specimens not used to develop the descriptive equations

Figure 7.27 Ratio of test-to-calculated failure load T/T_h versus ratio of d_{eff}/ℓ_{eh} for specimens with $A_{brg} \leq 9.5A_b$ and confining reinforcement

As shown in Figures 7.26 and 7.27, the headed bars began to exhibit low anchorage strengths as the ratio d_{eff}/ℓ_{eh} increased above 1.5 (see dotted lines in Figures 7.26 and 7.27). This value of d_{eff}/ℓ_{eh} matches the Commentary in ACI 318-14 regarding the potential of a breakout failure when $\ell_{dt} < d/1.5$. Commentary Section R25.4.4.2 of ACI 318-14 states that for headed bars used as the top longitudinal reinforcement of a beam terminating at an exterior beam-column joint, in cases where the development length ℓ_{dt} is less than $d/1.5$, a concrete breakout failure can be precluded by "providing reinforcement in the form of hoops and ties to establish a load path in accordance with strut-and-tie modeling principles." As will be shown in Section 9.2.1.3, these recommendations appear appropriate based on the results presented in this section.

7.4.4.3 Cracking pattern

All specimens with $d_{eff}/\ell_{eh} \geq 1.5$ exhibited a crack within the joint region that tended to grow from the bottom of bearing head, extending at an angle of about 35° with respect to the direction of the column longitudinal bars, towards the front face of the column above the bearing

member. Figure 7.28 shows the cracks for two specimens without confining reinforcement. The photos were taken following failure after the loose concrete had been removed from the specimens.
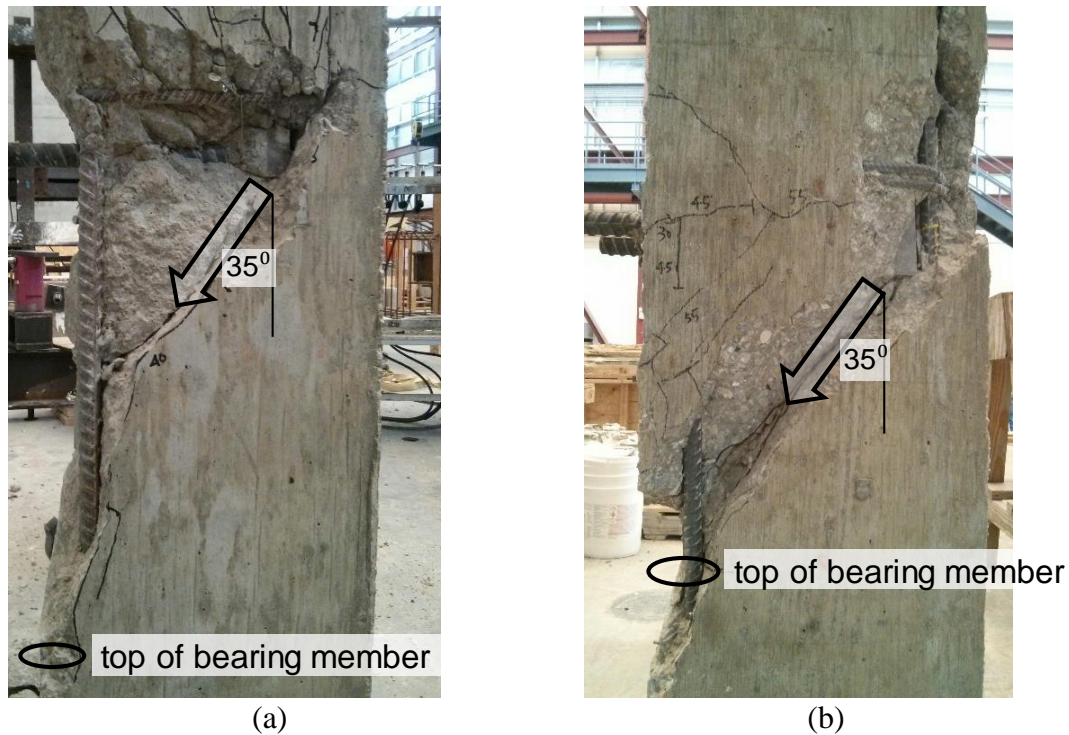
Figure 7.28 Cracks for specimens with large h_{cl}/ℓ_{eh} ratio and no confining reinforcement (a) specimen 8-5-F4.1-0-i-2.5-3-10-DB (b) specimen (3@5.35)11-5-F8.6-0-i-2.5-3-14.5

For specimens with confining reinforcement, more cracking was exhibited within the joint region than in the specimens without confining reinforcement, as shown in Figure 7.29. The additional cracks tended to grow from the bearing head and extend at a flatter angle than the cracks observed in specimens without confining reinforcement, indicating that one (or more) struts had formed within the joint.
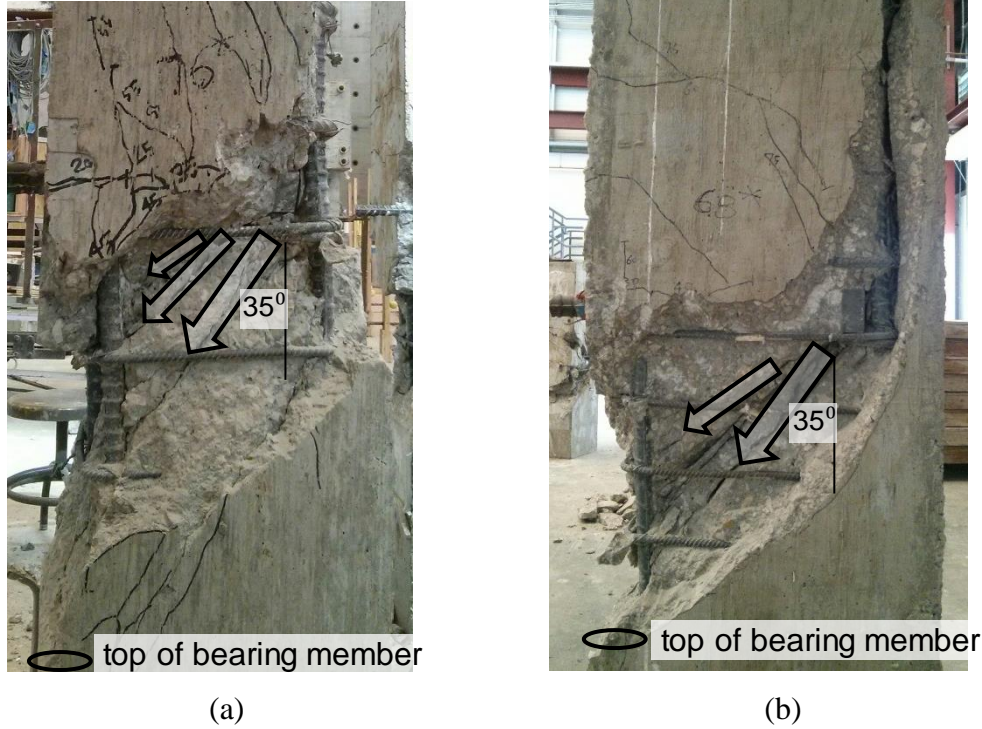
Figure 7.29 Cracks for specimens with large h_{cl}/ℓ_{eh} ratio and confining reinforcement (a) specimen 8-5-F4.1-5#3-i-2.5-3-10-DB (b) specimen (3@5.35)11-8-F3.8-6#3-i-2.5-3-14.5

7.4.4.4 Summary

The headed bars with $h_{cl}/\ell_{eh} \geq 1.33$ generally exhibited lower anchorage strengths compared to headed bars with $h_{cl}/\ell_{eh} < 1.33$. The threshold of $h_{cl}/\ell_{eh} = 1.33$ corresponds to d_{eff}/ℓ_{eh} of approximately 1.5; a value seen as increasing the potential of breakout failure in Commentary Section R25.4.4.2 of ACI 318-14.

Commentary Section R25.4.4.2 suggests that for cases of $\ell_{dt} < d/1.5$ in beam-column joints, transverse reinforcement should be provided to enable a strut-and-tie mechanism to preclude breakout failure. As will be shown in Section 9.2.1.3, strut-and-tie modeling provides a conservative estimate of the anchorage strength of headed bars in the specimens with a large ratio of h_{cl}/ℓ_{eh} (or d_{eff}/ℓ_{eh}) discussed in this section. Though not used to develop the descriptive equations, these specimens are helpful in developing guidance on the use of headed bars in deep beam-column joints, which will also be discussed in Chapter 9.

7.5 EFFECT OF BAR LOCATION

The headed bars in the beam-column joint specimens in this study were placed inside the column core (for this reason, the specimens are identified with "i" in the specimen designation). The specimens had a 2.5-in. minimum side cover to the bar, with this value used for the vast majority of the specimens, as described in Section 2.2. In practice, however, the headed bars are used in many applications, other than in column cores. As part of a study on hooked bars anchored in simulated beam-column joints by Sperry et al. (2015a), the effect of placing hooked bars outside the column core was examined. These specimens were used to evaluate cases, such as beams, where vertical confining steel is not present. Sperry et al. (2015a) used paired specimens containing No. 8 or No. 11 hooks that were cast with the same concrete with the only variable being hook location (inside or outside the column core). These specimens had either no confining reinforcement or No. 3 hoops spaced at $3d_b$ within the joint region (corresponding to five No. 3 hoops for No. 8 bars and six No. 3 hoops for No. 11 bars). Test results showed that hooked bars cast outside the confined column core exhibited lower anchorage strength than hooked bars placed within the confined column core.

Figure 7.30 shows the ratio of failure load of the hooked bars placed outside the column core to the failure load of the hooked bars placed inside the column core $T_{outside}/T_{inside}$, plotted versus concrete compressive strength f_{cm}. In the figure, "no conf." represents no confining reinforcement, and "5 No. 3" and "6 No. 3" represent No. 3 hoops spaced at $3d_b$.

As shown in Figure 7.30, the hooked bars cast outside the column core generally exhibited lower failure loads than those cast inside the column core. The reduction in anchorage strength due to bar location outside rather than inside the column core can be conservatively represented by a strength modification factor of 0.8.
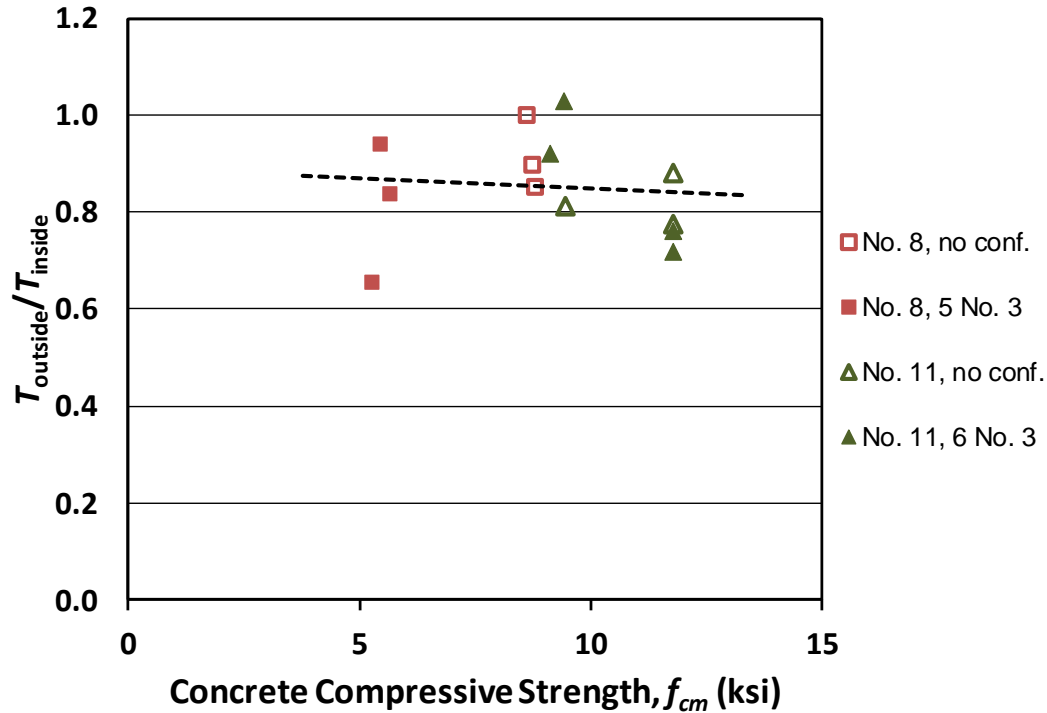
Figure 7.30 Ratio of failure load for hooked bars cast outside column core to that for hooked bars cast inside column core $T_{\text{outside}}/T_{\text{inside}}$ versus concrete compressive strength f_{cm}

In cases where the headed bars terminate in members other than beam-column joints, a wide concrete cover is likely to be present (such as walls and foundations). In the study on hooked bars, Sperry et al. (2015a) compared the failure loads of the hooked bars in wall specimens tested by Johnson and Jirsa (1981) to those in the simulated beam-column joint specimens, and found that high side cover was adequate to confine the hooked bars in a similar manner as the column core. For design, Sperry et al. (2015a) suggested that wide side cover be defined as clear cover greater than $7d_b$, the center-to-center spacing seen as the critical value for the effect of close spacing on the anchorage strength of hooked bars.

For headed bars, it is reasonable to assume that high concrete cover can also act as a confined column core to provide adequate confinement. As discussed in Section 7.3.1, the critical value for the effect of bar spacing for headed bars is $8d_b$ (rather than the $7d_b$ seen in hooked-bar specimens). Following the approach used by Sperry et al. (2015a), it is suggested that for headed bars terminating in members other than beam-column joints, a side cover of at least $8d_b$ is needed

to allow for the headed bars to be treated as being anchored within a region that is equivalent to a confined column core.

Based on the discussions above, it is suggested that a 0.8 modification factor be applied to the anchorage strength calculated using the descriptive equations except in cases where: (1) headed bars terminate *inside a confined column core with a side cover to the bar of at least 2.5 in.* (this is based on the range of the beam-column joint tests in this study) or (2) headed bars terminate in supporting members with *a side cover to the bar of at least $8d_b$.*

7.6 COMPARISON OF DESCRIPTIVE EQUATIONS FOR OTHER SPECIMEN TYPES

The descriptive equations [Eq. (7.5), (7.6), (7.8) and (7.9)] developed in Section 7.3 are based solely on the beam-column joint specimens tested as part of this study. In this section, the anchorage strengths predicted using these equations are compared with the anchorage strengths measured in tests of CCT node, shallow embedment, and splice specimens in this study. A comparison with specimens tested by other researchers is provided in Chapter 8. Results of these comparisons are summarized in Appendix F.

7.6.1 CCT Node Tests

The CCT node specimens investigated in this study contained No. 8 bars with a 2.5 in. side cover to the bar, as described in Section 2.3.1. Each specimen had either two bars spaced at $12d_b$ or three bars spaced at $6d_b$ center-to-center. No confining reinforcement was provided in the nodal zone. Because the headed bars were placed at the end of a beam specimen (rather than inside a confined column core) with a $2.5d_b$ (less than $8d_b$) side cover, the modification factor 0.8 is applied to the calculated anchorage strength using the descriptive equation [Eq. (7.6)]. Table 7.15 shows comparisons of the anchorage forces measured in the CCT node tests T (as described in Section 4.6) with those calculated using the descriptive equation [Eq. (7.6)] T_c, along with the embedment length ℓ_{eh} (distance from the bearing face of the head to the end of the extended nodal zone), measured concrete compressive strength f_{cm}, and center-to-center spacing between the bars in terms of bar diameter s/d_b.

Table 7.15 Test results for headed bars in CCT node specimens in current study and comparisons with descriptive equation [Eq. (7.6)] with 0.8 modification factor applied

Specimen	ℓ_{eh} (in.)	f_{cm} (psi)	s/d_b	T (kips)†	T_c (kips)*	$T/T_c{}^*$
H-2-8-5-10.4-F4.1	10.4	4490	12	126.9	52.5	2.42
H-2-8-5-9-F4.1	9	5740	12	101.9	47.9	2.13
H-3-8-5-11.4-F4.1	11.4	5750	6	94.6	51.8	1.83
H-3-8-5-9-F4.1	9	5800	6	109.0	40.7	2.68
H-3-8-5-14-F4.1	14	5750	6	121.0	64.0	1.89
H-2-8-5-9-F4.1	9	4630	12	79.9	45.5	1.76
H-2-8-5-13-F4.1	13	4760	12	91.7	66.9	1.37
H-3-8-5-9-F4.1	9	4770	6	86.8	38.8	2.24
H-3-8-5-11-F4.1	11	4820	6	98.5	47.8	2.06
H-3-8-5-13-F4.1	13	4900	6	122.0	57.0	2.14

† T is based on strut-and-tie model
* T_c is based on Eq. (7.6) with a 0.8 modification factor applied

As shown in Table 7.15, all headed bars in the CCT node specimens exhibited much higher anchorage strengths than the strengths calculated using Eq. (7.6) with the 0.8 modification factor applied. The values of T/T_c range from 1.37 to 2.68, with an average of 2.05. Because the values of T/T_c are very high, the measured anchorage forces T are compared with the anchorage strengths calculated using Eq. (7.6), but without the application of the 0.8 modification factor. The comparisons are shown in Table 7.16.

Table 7.16 Test results for headed bars in CCT node specimens in current study and comparisons with descriptive equation [Eq. (7.6)]

Specimen	T (kips)†	T_c (kips)*	$T/T_c{}^*$
H-2-8-5-10.4-F4.1	126.9	65.6	1.93
H-2-8-5-9-F4.1	101.9	59.9	1.70
H-3-8-5-11.4-F4.1	94.6	64.7	1.46
H-3-8-5-9-F4.1	109.0	50.8	2.14
H-3-8-5-14-F4.1	121.0	80.0	1.51
H-2-8-5-9-F4.1	79.9	56.9	1.40
H-2-8-5-13-F4.1	91.7	83.7	1.10
H-3-8-5-9-F4.1	86.8	48.5	1.79
H-3-8-5-11-F4.1	98.5	59.8	1.65
H-3-8-5-13-F4.1	122.0	71.3	1.71

† T is based on strut-and-tie model
* T_c is based on Eq. (7.6) without the 0.8 modification factor

The comparisons in Table 7.16 indicate that, even without the 0.8 modification factor, the headed bars in the CCT node specimens exhibited higher anchorage strengths than the strengths predicted by Eq. (7.6). The values of T/T_c range from 1.10 to 2.14, with an average of 1.64. The

high anchorage strengths of headed bars at CCT nodes are likely due to the direct compressive force perpendicular to the bar from the support reaction, a force that is not present in beam-column joints. In practice, CCT nodes normally occur within a column core, rather than at the end of a simply-supported beam as investigated in this study and would not justify the use of the 0.8 modification factor.

7.6.2 Shallow Embedment Pullout Tests

The shallow embedment pullout specimens described in Section 2.4 and Section 5.1 contained No. 8 headed bars without confining reinforcement. The headed bars were the same types used for the beam-column joint tests in this study, with net bearing areas A_{brg} ranging from 4.0 to 14.9A_b. Three specimens had large heads ($A_{brg} > 12A_b$), one with S14.9 (14.9A_b) and two with O12.9 (12.9A_b). The O12.9 heads had large obstructions that did not meet the dimensional requirements for HA head in ASTM A970. In addition to O12.9, three specimens also had large obstructions, two with O4.5 and one with O9.1. A full description of these head types are given in Table 2.1.

The headed bars were tested individually. Based on the high concrete side cover (at least 23.5d_b to the bar), the anchorage strength T_c is calculated using the descriptive equation for widely-spaced bars ($s \geq 8d_b$) without confining reinforcement [Eq. (7.5)], and the 0.8 modification factor is not applied. The calculated anchorage strength T_c for each headed bar is compared with the measured failure load T in Table 7.17, along with the measured embedment length ℓ_{eh}, the ratio h_{cl}/ℓ_{eh} (where h_{cl} is the distance from the center of the bar to the nearest edge of bearing plate, similar to h_{cl} as defined for beam-column joint tests), and the measured concrete compressive strength f_{cm}. Figure 7.31 shows the ratio T/T_c as a function of the ratio h_{cl}/ℓ_{eh} for the 32 headed bars with shallow embedment. In the figure, solid symbols represent HA heads, open symbols represent non-HA heads (those with large obstructions), squares represent smaller heads ($A_{brg} \leq 9.5A_b$), and triangles represent large heads ($A_{brg} > 12A_b$).

Table 7.17 Test results for headed bars with shallow embedment in current study and comparisons with descriptive equation [Eq. (7.5)]

Specimen	ℓ_{eh} (in.)	h_{cl}/ℓ_{eh}	f_{cm} (psi)	T (kips)	T_c (kips)	T/T_c
8-5-T9.5-8#5-6	8.0	1.31	7040	65.6	55.8	1.18
8-5-T9.5-8#5-6	8.3	1.27	7040	67.8	57.5	1.18
8-5-T4.0-8#5-6	8.5	1.24	7040	61.8	59.3	1.04
8-5-T4.0-8#5-6	7.5	1.40	7040	56.3	52.2	1.08
8-5-F4.1-8#5-6	7.4	1.41	5220	68.9	48.1	1.43
8-5-F4.1-8#5-6	7.4	1.42	5220	64.4	47.7	1.35
8-5-F9.1-8#5-6	7.1	1.47	5220	69.9	46.1	1.52
8-5-F9.1-8#5-6	7.0	1.50	5220	54.9	45.2	1.21
8-5-F4.1-2#8-6	6.0	1.75	7390	64.4	41.9	1.54
8-5-F9.1-2#8-6	6.0	1.75	7390	65.0	41.9	1.55
8-5-T4.0-2#8-6	6.1	1.73	7390	60.5	42.4	1.43
8-5-T9.5-2#8-6	6.1	1.71	7390	57.7	42.8	1.35
8-8-O12.9-6#5-6[*][‡]	6.3	1.56	8620	79.0	45.4	1.74
8-8-O9.1-6#5-6[*]	6.3	1.68	8620	70.9	45.4	1.56
8-8-S6.5-6#5-6	6.4	1.57	8620	92.4	46.3	1.99
8-8-O4.5-6#5-6[*]	6.5	1.65	8620	74.0	47.3	1.57
8-5-S14.9-6#5-6[‡]	6.5	1.58	4200	61.8	39.8	1.55
8-5-S6.5-6#5-6	6.5	1.54	4200	49.2	39.8	1.24
8-5-O12.9-6#5-6[*][‡]	6.6	1.51	4200	52.4	40.6	1.29
8-5-O4.5-6#5-6[*]	6.5	1.56	4200	50.1	39.8	1.26
8-5-S9.5-6#5-6	6.5	1.58	4200	48.9	39.8	1.23
8-5-S9.5-6#5-6	6.4	1.59	4200	54.5	39.0	1.40
8-5-F4.1-6#5-6	8.4	5.60	4200	39.1	52.0	0.75
8-5-F4.1-0-6	6.5	2.31	5180	50.5	41.8	1.21
8-5-F4.1-0-6	6.3	2.72	5180	48.9	40.2	1.22
8-5-F4.1-2#5-6	6.8	2.52	5180	61.5	43.5	1.41
8-5-F4.1-4#5-6	6.0	2.79	5180	53.4	38.5	1.39
8-5-F4.1-4#5-6	6.1	2.78	5180	52.4	39.3	1.33
8-5-F4.1-4#5-6	6.8	2.52	5460	53.5	44.0	1.21
8-5-F4.1-6#5-6	6.3	2.76	5460	47.3	40.7	1.16
8-5-F4.1-6#5-6	6.6	2.53	5460	55.9	43.2	1.29
8-5-F4.1-6#5-6	6.9	2.47	5460	52.6	44.9	1.17

[*] Headed bars with large obstructions exceeding the dimensional limits for HA heads in ASTM A970 (Figure 2.1)
[‡] Bars with large heads ($A_{brg} > 12A_b$)

Figure 7.31 Ratio of test-to-calculated failure load T/T_c versus ratio of h_{cl}/ℓ_{eh} for shallow embedment pullout specimens

As shown in Figure 7.31, the ratios T/T_c for non-HA heads (identified with open symbols) are similar to those with HA heads. This indicates that for headed bars with shallow embedment, those with non-HA heads exhibited similar anchorage strengths to those with HA heads, as was observed for beam-column joint tests (Section 7.4.3). For the three headed bars with large heads (identified with triangles in Figure 7.31), the values T/T_c equal 1.74, 1.55, and 1.29, respectively, two of which are above the average (1.36) for those with $h_{cl}/\ell_{eh} \leq 2.79$.

The values of T/T_c shown in Table 7.17 and Figure 7.31 indicate that the headed bars with shallow embedment exhibited 4% to 99% (with an average of 36%) higher anchorage strengths than predicted by Eq. (7.5), with the exception of Specimen 8-5-F4.1-6#5-6, for which the headed bar exhibited 25% lower anchorage strength than predicted. The low anchorage strength of this headed bar may result from a difference in loading mechanism, with the support reaction placed relatively far from the headed bar, compared with that of the other headed bars. This specimen had a ratio $h_{cl}/\ell_{eh} = 5.6$, while the other headed bars exhibiting higher anchorage strengths ($T/T_c > 1.0$)

correspond to $h_{cl}/\ell_{eh} \leq 2.79$. This indicates that the h_{cl}/ℓ_{eh} ratio has a qualitatively similar effect on anchorage strength in shallow embedment tests as it did in beam-column joint tests.

Following the approach used for the beam-column joint specimens (Section 7.4.4.2), the effective depth d_{eff} is calculated for these shallow embedment pullout specimens to provide a design guidance. The values of effective depth d_{eff} are shown in Table 7.18, along with the embedment length ℓ_{eh}, and the ratios d_{eff}/ℓ_{eh} and T/T_c [with T_c based on Eq. (7.5)]. As shown in the table, the headed bars with T/T_c above 1.0 had $d_{eff}/\ell_{eh} \leq 3.00$, while the only specimen with T/T_c below 1.0 ($T/T_c = 0.75$) had d_{eff}/ℓ_{eh} equal to 5.73. Based on this observation, it is suggested that the descriptive equations could be used to provide an estimate of the anchorage strength of headed bars terminating in a foundation from a column with an effective depth d_{eff} not exceeding three times the embedment length ℓ_{eh}.

Table 7.18 Test results for headed bars with shallow embedment in current study and ratio T/T_c, with T_c based on descriptive equation [Eq. (7.5)]

Specimen	ℓ_{eh} (in.)	d_{eff} (in.)	d_{eff}/ℓ_{eh}	T/T_c
8-5-T9.5-8#5-6	8.0	11.8	1.48	1.18
8-5-T9.5-8#5-6	8.3	11.9	1.44	1.18
8-5-T4.0-8#5-6	8.5	11.7	1.38	1.04
8-5-T4.0-8#5-6	7.5	11.6	1.55	1.08
8-5-F4.1-8#5-6	7.4	12.1	1.63	1.43
8-5-F4.1-8#5-6	7.4	12.0	1.63	1.35
8-5-F9.1-8#5-6	7.1	12.2	1.71	1.52
8-5-F9.1-8#5-6	7.0	11.8	1.69	1.21
8-5-F4.1-2#8-6	6.0	11.8	1.96	1.54
8-5-F9.1-2#8-6	6.0	11.8	1.96	1.55
8-5-T4.0-2#8-6	6.1	11.7	1.93	1.43
8-5-T9.5-2#8-6	6.1	11.6	1.90	1.35
8-8-O12.9-6#5-6[*][‡]	6.3	11.2	1.79	1.74
8-8-O9.1-6#5-6[*]	6.3	11.8	1.89	1.56
8-8-S6.5-6#5-6	6.4	11.7	1.83	1.99
8-8-O4.5-6#5-6[*]	6.5	12.1	1.86	1.57
8-5-S14.9-6#5-6[‡]	6.5	12.0	1.84	1.55
8-5-S6.5-6#5-6	6.5	11.4	1.75	1.24
8-5-O12.9-6#5-6[*][‡]	6.6	11.5	1.73	1.29
8-5-O4.5-6#5-6[*]	6.5	11.5	1.77	1.26

[*] Headed bars with large obstructions exceeding the dimensional limits for HA heads in ASTM A970 (Figure 2.1)
[‡] Bars with large heads ($A_{brg} > 12A_b$)

Table 7.18 Cont. Test results for headed bars with shallow embedment in current study and ratio T/T_c, with T_c based on descriptive equation [Eq. (7.5)]

Specimen	ℓ_{eh} (in.)	d_{eff} (in.)	d_{eff}/ℓ_{eh}	T/T_c
8-5-S9.5-6#5-6	6.5	11.6	1.79	1.23
8-5-S9.5-6#5-6	6.4	11.6	1.83	1.40
8-5-F4.1-6#5-6	8.4	48.3	5.73	0.75
8-5-F4.1-0-6	6.5	16.2	2.49	1.21
8-5-F4.1-0-6	6.3	18.2	2.91	1.22
8-5-F4.1-2#5-6	6.8	18.5	2.74	1.41
8-5-F4.1-4#5-6	6.0	18.0	3.00	1.39
8-5-F4.1-4#5-6	6.1	18.3	2.98	1.33
8-5-F4.1-4#5-6	6.8	18.2	2.70	1.21
8-5-F4.1-6#5-6	6.3	18.3	2.93	1.16
8-5-F4.1-6#5-6	6.6	18.0	2.72	1.29
8-5-F4.1-6#5-6	6.9	18.2	2.65	1.17

7.6.3 Lap Splice Tests

The six lap splice specimens tested in this study contained No. 6 headed bars with 2 in. bottom and side covers to the bar and different spacings between the adjacent bars. No confining reinforcement was used in the lap zone. Based on the discussion in Section 7.5, the 2 in. side cover ($2.67d_b$) for the splice specimens is less than the $8d_b$ required to be treated as anchorage inside a column core; therefore, the strength T_c calculated using the descriptive equation is multiplied by a modification factor 0.8. Table 7.19 compares the splice strengths measured in the lap splice tests T (as described in Section 6.1) with the calculated strengths T_c, along with the splice length ℓ_{st}, measured concrete compressive strength f_{cm}, and the smallest center-to-center spacing between adjacent bars in terms of bar diameter s/d_b.

Table 7.19 Test results for headed bars in lap splice specimens in current study and comparisons with descriptive equation [Eq. (7.6)] with 0.8 modification factor applied

Specimen	ℓ_{st} (in.)	f_{cm} (psi)	s/d_b	T (kips)[†]	T_c (kips)	T/T_c
(3)6-5-S4.0-12-0.5	12	6330	1.67	34.0	28.9	1.18
(3)6-5-S4.0-12-1.0	12	6380	2.33	36.8	32.3	1.14
(3)6-5-S4.0-12-1.9	12	6380	3.55	33.6	38.3	0.88
(3)6-12-S4.0-12-0.5	12	10890	1.67	36.1	32.9	1.10
(3)6-12-S4.0-12-1.0	12	10890	2.33	33.0	36.7	0.90
(3)6-12-S4.0-12-1.9	12	11070	3.55	36.4	43.7	0.83

[†] T based on moment-curvature method
[*] T_c is based on Eq. (7.6) with a 0.8 modification factor applied

As shown in Table 7.19, the headed bars in the lap splice specimens have values of T/T_c ranging from 0.83 to 1.18, with an average of 1.0. This indicates that the descriptive equation [Eq. (7.6)] along with the 0.8 modification factor accounting for bar location would be appropriate to characterize the splice strength of the headed bars in this study. The descriptive equation alone would be unconservative.

CHAPTER 8: COMPARISON OF DESCRIPTIVE EQUATIONS FOR PREVIOUS RESEARCH

In Chapter 7, the anchorage strengths for the CCT node, shallow embedment, and lap splice specimens tested as a part of this study are compared with the anchorage strengths predicted by the descriptive equations developed in Section 7.3. In this chapter, test results from previous studies are compared with the same equations to evaluate their applicability to all headed bar applications. Detailed data for the specimens from previous studies and the comparisons are given in Appendix F. These comparisons serve as a foundation for the development of design provisions for headed bars proposed in Chapter 9.

8.1 INTRODUCTION

The two descriptive equations developed in Chapter 7, Eq. (7.6) and (7.9), apply to headed bars without and with confining reinforcement, respectively.

$$T_c = \left(781 f_{cm}^{0.24} \ell_{eh}^{1.03} d_b^{0.35}\right)\left(0.0836\frac{s}{d_b} + 0.3444\right) \tag{7.6}$$

with $0.0836\dfrac{s}{d_b} + 0.3444 \leq 1.0$

$$T_h = \left(781 f_{cm}^{0.24} \ell_{eh}^{1.03} d_b^{0.35} + 48{,}800\frac{A_{tt}}{n} d_b^{0.88}\right)\left(0.0622\frac{s}{d_b} + 0.5428\right) \tag{7.9}$$

with $0.0622\dfrac{s}{d_b} + 0.5428 \leq 1.0$

where T_c = anchorage strength of a headed bar without confining reinforcement (lb); T_h = anchorage strength of a headed bar with confining reinforcement (lb); f_{cm} = compressive strength of concrete (psi); ℓ_{eh} = embedment length (in.); d_b = diameter of headed bar (in.); s = center-to-center spacing between the bars (in.); A_{tt} = total cross-sectional area of all confining reinforcement parallel to the headed bars being developed in beam-column joints and located within $8d_b$ of the headed bars in direction of the interior of the joint for No. 3 through No. 8 bars and within $10d_b$ of the bar in direction of the interior of the joint for No. 9 through No. 11 bars (in.^{2}); and n = number of headed bars being developed.

As suggested in Section 7.5, a 0.8 modification factor is applied to the calculated strength (T_c or T_h based on the presence of confining reinforcement) except in cases where headed bars (1)

terminate inside a confined column core with at least 2.5-in. side cover to the bar or (2) terminate in supporting members with at least $8d_b$ side cover to the bar.

In Eq. (7.9), the definition of A_{tt} is based on the analysis of the effect of confining reinforcement in beam-column joint specimens in this study. To allow for the descriptive equation [Eq. (7.9)] to be evaluated for members other than beam-column joints, the definition of A_{tt} needs to be modified.

The discussions in Sections 7.3.2 and 7.4.1 show that confining reinforcement located near headed bars *within* the joint region contribute most to the anchorage strength of headed bars, while the confining reinforcement located *above* the joint region does not. In structural members other than beam-column joints, anchorage strength would be governed by one side of a headed bar where less confining reinforcement is provided, assuming that the confining reinforcement layout is not symmetric about the bar and that the contribution of concrete on the anchorage strength is the same on all sides of the headed bar. Therefore, for headed bars terminating in members other beam-column joints, it is suggested that A_{tt} is defined as the minimum total cross-sectional area of all confining reinforcement parallel to headed bars being developed within $7\frac{1}{2}d_b$ on one side of the bar centerline for No. 3 through No. 8 headed bars or within $9\frac{1}{2}d_b$ on one side of the bar centerline for No. 9 through No. 11 headed bars. This is equivalent to the $8d_b$ and $10d_b$ limits for beam-column joints, which are measured from the far side of the bar.

8.2 BEAM-COLUMN JOINT TESTS

8.2.1 Bashandy (1996)

The specimens tested by Bashandy (1996) contained two headed bars without or with confining reinforcement. The location of the nearest confining reinforcement within the joint region, however, was not reported, which does not allow the amount of effective confining reinforcement A_{tt} to be determined. Therefore, only specimens without confining reinforcement are compared with the descriptive equation [Eq. (7.6)]. The headed bars with net bearing areas less than $4A_b$ (not in accordance with the required minimum bearing area of $4A_b$ for HA heads) are excluded from the comparisons. This leaves five specimens for comparison.

The five specimens used for comparison had headed bars placed inside the column core with a 3-in. side cover to the bar (greater than the required 2.5-in. cover); therefore, the 0.8 modification factor accounting for bar location need not be applied to the calculated anchorage strength T_c obtained using Eq. (7.6). The failure loads measured on the bar T are compared with the calculated failure loads T_c in Table 8.1, along with the bar size, embedment length ℓ_{eh}, the ratio h_{cl}/ℓ_{eh} (where h_{cl} is the distance from the center of the bar to the top of the bearing member), the ratio d_{eff}/ℓ_{eh} (with d_{eff} calculated based on the approach described in Section 7.4.4.2), concrete compressive strength f_{cm}, and the center-to-center spacing in terms of bar diameter s/d_b. The embedment lengths reported by Bashandy (1996) were measured from the back of the head; the embedment lengths ℓ_{eh} in Table 8.1 are measured from the bearing face of the head in accordance with the definition of development length ℓ_{dt} in ACI 318-14.

Table 8.1 Test results for beam-column joint specimens tested by Bashandy (1996) and comparisons with descriptive equation [Eq. (7.6)]

Specimen	Bar Size	ℓ_{eh}^* (in.)	h_{cl}/ℓ_{eh}	d_{eff}/ℓ_{eh}	f_{cm}^* (psi)	s/d_b	T^* (kips)	T_c (kips)	T/T_c
T1	No. 11	11.0	1.00	1.27	3870	3.3	51.0	46.7	1.09
T2	No. 11	11.0	1.00	1.25	4260	3.3	49.9	47.8	1.04
T3	No. 11	11.2	0.98	1.24	4260	3.3	52.2	48.7	1.07
T4	No. 8	8.3	1.32	1.47	3870	5.0	21.1	38.3	0.55
T5	No. 11	11.0	1.00	1.23	3260	3.3	37.5	44.8	0.84

* Values are converted SI (1 in. = 25.4 mm; 1 psi = 1/145 MPa; and 1 kip = 4.44822 kN)

Of the five specimens shown in Table 8.1, four specimens (T1 to T3, and T5) had values of T/T_c ranging from 0.84 to 1.09, within the range (0.68 to 1.27) for the data that were used to develop Eq. (7.6). The average value of T/T_c for these four specimens equals 1.01. Specimen T4 had a low value of T/T_c (0.55) relative to the values for the other four specimens. An examination of the data for the five specimens shows that the low anchorage strength obtained with T4 may be related to the h_{cl}/ℓ_{eh} (or d_{eff}/ℓ_{eh}) ratio. Specimen T4 had $h_{cl}/\ell_{eh} = 1.32$ and $d_{eff}/\ell_{eh} = 1.47$, approximately the threshold values of $h_{cl}/\ell_{eh} = 1.33$ and $d_{eff}/\ell_{eh} = 1.5$ found to result in a reduction in anchorage strength for the beam-column joint specimens in the current study (demonstrated in Section 7.4.4), while the other four specimens had $h_{cl}/\ell_{eh} \le 1.0$ and $d_{eff}/\ell_{eh} \le 1.27$, below the

threshold values. The values, $h_{cl}/\ell_{eh} = 1.33$ and $d_{eff}/\ell_{eh} = 1.5$, however, are not precise and somewhat smaller values may be appropriate.

8.2.2 Chun et al. (2009)

Chun et al. (2009) tested 24 beam-column joint specimens with the columns cast and tested in a horizontal position (Figure 1.12), rather than in a vertical position as in the current study. The heads used in the specimens met the requirements to be classified as HA heads, but as shown in Figure 8.1, they differ significantly in shape from the heads used in the U.S. (Figure 2.1) or contemplated for use in ASTM A970 (Figure 1.2). The head used by Chun et al. (2009) had an obstruction that reduces the actual bearing area of the head to values between 2.7 and 2.8A_b.

Bar Size	d_b	d_h	d_c	t_h	t_o
No. 8	1.0	2.24	1.50	0.35	0.79
No. 11	1.41	3.15	2.13	0.47	1.03
No. 18	2.26	5.04	3.31	0.79	1.65

(Unit: in.)
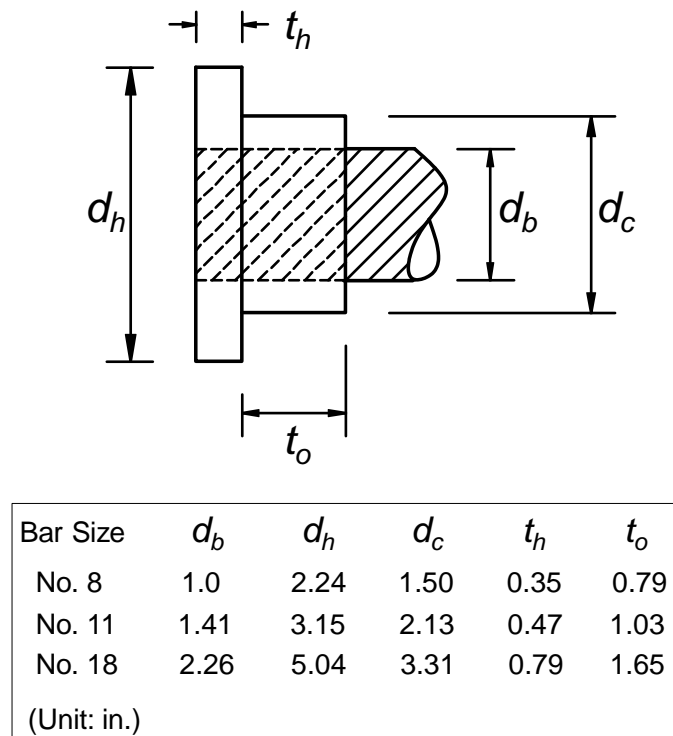
Figure 8.1 Dimensions of heads used in beam-column joint tests by Chun et al. (2009) [figure after Hong et al. (2007)]

The beam-column joint specimens tested by Chun et al. (2009) contained a single headed bar (No. 8, No. 11, or No. 18) with a 2.5d_b side cover to the bar. No confining reinforcement was used within the joint region. Since the 2.5d_b side cover meets the 2.5-in. side cover requirement described in Section 7.5, no modification factor is applied when calculating the anchorage strength T_c using Eq. (7.6). The center-to-center bar spacing s for use in Eq. (7.6) is taken as the width of the specimen (6d_b). The specimens had three values of *embedment length relative to column depth*,

0.9, 0.7, and 0.5. The values (0.7 and 0.5) indicate that the headed bars were not placed to the far face of the column core. Based on this observation, the ratios h_{cl}/ℓ_{eh} and d_{eff}/ℓ_{eh} are calculated and listed in Table 8.2 for each specimen. In the calculation of d_{eff} using the approach described in Section 7.4.4.2, it was found that the calculated effective depth of neutral axis c (illustrated in Figure 7.25) for some specimens exceeded the width of the bearing member, which may suggest that the bearing was inadequate for these specimens. For these specimens, c is taken as the width of the bearing member, and thus, d_{eff} is the distance from the center of the bar to the far side of the bearing member. Table 8.2 shows the bar size, embedment length ℓ_{eh}, the ratios h_{cl}/ℓ_{eh} and d_{eff}/ℓ_{eh}, concrete compressive strength f_{cm}, failure load measured on the bar T, calculated failure load T_c using Eq. (7.6), and the ratio T/T_c.

Table 8.2 Test results for beam-column joint specimens tested by Chun et al. (2009) and comparisons with descriptive equation [Eq. (7.6)]

Specimen	Bar Size	ℓ_{eh} (in.)	h_{cl}/ℓ_{eh}	d_{eff}/ℓ_{eh}	f_{cm} (psi)	T (kips)	T_c (kips)	T/T_c
No. 8-M-0.9L-(1)		10.4	1.05	1.21	3640	27.9	52.8	0.53
No. 8-M-0.9L-(2)		10.4	1.05	1.22	3640	28.6	52.8	0.54
No. 8-M-0.7L-(1)		8.3	1.31	1.52	3640	27.4	41.8	0.66
No. 8-M-0.7L-(2)	No. 8	8.3	1.31	1.53	3640	28.5	41.8	0.68
No. 8-M-0.7L-2R-(1)		8.3	1.31	1.53	3640	31.8	41.8	0.76
No. 8-M-0.7L-2R-(2)		8.3	1.31	1.53	3640	32.6	41.8	0.78
No. 8-M-0.5L-(1)		6.3	1.73	1.89	3640	16.4	31.5	0.52
No. 8-M-0.5L-(2)		6.3	1.73	1.94	3640	21.1	31.5	0.67
No. 11-M-0.9L-(1)		14.6	0.99	1.15	3570	51.4	84.0	0.61
No. 11-M-0.9L-(2)		14.6	0.99	1.15	3570	52.4	84.0	0.62
No. 11-M-0.7L-(1)		11.6	1.25	1.42	3570	43.3	66.3	0.65
No. 11-M-0.7L-(2)	No. 11	11.6	1.25	1.41	3570	41.6	66.3	0.63
No. 11-M-0.7L-2R-(1)		11.6	1.25	1.47	3570	59.1	66.3	0.89
No. 11-M-0.7L-2R-(2)		11.6	1.25	1.45	3570	51.1	66.3	0.77
No. 11-M-0.5L-(1)		8.5	1.71	1.94	3570	43.7	48.1	0.91
No. 11-M-0.5L-(2)		8.5	1.71	1.89	3570	34.3	48.1	0.71
No. 18-M-0.9L-(1)		35.0	0.96	1.08	3510	157.7	242.7	0.65
No. 18-M-0.9L-(2)		35.0	0.96	1.08	3510	155.8	242.7	0.64
No. 18-M-0.7L-(1)		26.9	1.25	1.35	3510	97.6	185.0	0.53
No. 18-M-0.7L-(2)	No. 18	26.9	1.25	1.35	3510	99.8	185.0	0.54
No. 18-M-0.7L-2R-(1)		26.9	1.25	1.37	3510	110.6	185.0	0.60
No. 18-M-0.7L-2R-(2)		26.9	1.25	1.37	3510	115.8	185.0	0.63
No. 18-M-0.5L-(1)		18.9	1.78	1.88	3510	69.6	128.6	0.54
No. 18-M-0.5L-(2)		18.9	1.78	1.88	3510	69.5	128.6	0.54

As shown in Table 8.2, the specimens tested by Chun et al. (2009) failed with lower loads than predicted by the descriptive equation. The ratios of T/T_c range from 0.52 to 0.91, with an average of 0.65. Of the 24 specimens investigated, 10 specimens with $d_{eff}/\ell_{eh} > 1.5$ ($h_{cl}/\ell_{eh} \geq 1.31$) had an average value of T/T_c equal to 0.68, and the remaining 14 specimens with $d_{eff}/\ell_{eh} < 1.5$ ($h_{cl}/\ell_{eh} \leq 1.25$) had an average value of T/T_c equal to 0.63. The similar values of the average T/T_c (0.68 and 0.63) for the specimens with $d_{eff}/\ell_{eh} > 1.5$ and those with $d_{eff}/\ell_{eh} < 1.5$ is unexpected, because it has been demonstrated in Section 7.4.4.2 that the headed bars exhibit low anchorage strengths as the ratio d_{eff}/ℓ_{eh} increases above 1.5. The low values of T/T_c for both groups with $d_{eff}/\ell_{eh} > 1.5$ and $d_{eff}/\ell_{eh} < 1.5$ suggest that the descriptive equations, which were developed based on the test results of beam-column joint specimens containing at least two headed bars along with the actual value of center-to-center bar spacing (s = column width) may not apply to members of the type tested by Chun et al. (2009) that include a single headed bar.

There is some concern, however, that although these heads just meet the requirements for HA heads in ASTM A970, the shape of the heads on the bars used by Chun et al. (2009) may have been responsible for the low failure loads of these specimens. As shown in Figure 8.1, the obstruction, which is in contact with the head, has a constant area over its full length. The diameter of the obstruction equals approximately 1.5 times the bar diameter. Currently, ASTM A970 defines "net bearing area" as the difference between the gross area of the head and the bar area, while ignoring the area of the obstructions if "obstructions or interruptions of the bar deformations and non-planar features on the bearing face of the head" do "not extend more than two nominal bar diameters from the bearing face and" do "not have a diameter greater than 1.5 nominal bar diameters." If, however, the net bearing areas of the heads tested by Chun et al. (2009) are taken as the difference between the gross area of the head and the area of the obstruction adjacent to the head (as done for the non-HA heads with large obstructions investigated in this study), the head areas would be $2.8A_b$, $2.7A_b$, and $2.8A_b$, respectively, for the No. 8, No. 11, and No. 18 bars, less than the required minimum head size ($4A_b$) in the ACI provisions. Compared to $2.7A_b$ and $2.8A_b$, the net bearing areas of the non-HA heads used in this study are much larger, with the smallest equal to $4.5A_b$. More tests are suggested to validate the anchorage strength of headed bars with heads of the type used by Chun et al. (2009), but in the interim, it is suggested that definition of an

acceptable head with an obstruction be modified to require a minimum bearing area adjacent to the head of at least $4A_b$, the current requirement for HA heads.

8.3 CCT NODE TESTS

The CCT node specimens tested by Thompson et al. (2006a) contained a single bar with $2.5d_b$ side cover to the bar. Following the same approach used for the beam-column joint specimens tested by Chun et al. (2009) (Section 8.2.2), the bar spacing s is taken as the width of the specimen ($6d_b$). Two specimens (CCT-08-45-04.70(V)-1-C0.006 and CCT-08-45-04.70(V)-1-C0.012) had No. 3 stirrups placed perpendicular to the bar within the nodal zone, rather than parallel to the bar as required for determining A_{tt} in Eq. (7.9). Therefore, the stirrups in these two specimens are assumed to be ineffective, and Eq. (7.6) (for the case of no confining reinforcement) is used to calculate the anchorage strength T_c.

For the CCT node specimens tested by Thompson et al. (2006a), the anchorage forces T were measured based on strain gauges located at $7d_b$ from the bearing face of the head, as $7d_b$ was the approximate location of the end of the extended nodal zone for most of these specimens. For consistency, the embedment length ℓ_{eh} for calculating T_c is also taken as $7d_b$. As discussed in Section 7.6.1, CCT nodes most often form at the end of a beam within a column core; therefore, the 0.8 modification factor is not applied to T_c, although it could be argued that the 0.8 factor is appropriate for these tests because the bars were not anchored within a confined column core. Comparisons of the measured anchorage forces T to the calculated anchorage forces T_c without applying the 0.8 modification factor are shown in Table 8.3, along with the bar size, embedment length ℓ_{eh}, and concrete compressive strength f_{cm}. Tests by Thompson et al. (2006a) of headed bars with net bearing areas less than $4A_b$ are excluded from the comparisons.

Table 8.3 Test results for CCT node specimens tested by Thompson et al. (2006a) and comparisons with descriptive equation [Eq. (7.6)]

Specimen	Bar Size	ℓ_{eh} (in.)	f_{cm} (psi)	T (kips)[a]	T_c (kips)	T/T_c
CCT-08-55-04.70(H)-1[b][d]		7	4000	54.0[b]	35.9	1.51
CCT-08-55-04.70(V)-1[d]		7	3900	54.0	35.7	1.51
CCT-08-55-10.39-1[b]		7	4000	54.0[b]	35.9	1.51
CCT-08-45-04.04-1[b]		7	4000	48.2[b]	35.9	1.34
CCT-08-45-04.70(V)-1[d]		7	3900	54.0	35.7	1.51
CCT-08-30-04.04-1[b]	No. 8	7	4100	48.2[b]	36.1	1.33
CCT-08-30-04.06-1[b]		7	4100	54.0[b]	36.1	1.50
CCT-08-30-10.39-1[b]		7	4100	54.0[b]	36.1	1.50
CCT-08-45-04.70(H)-1-S3[d]		7	3800	52.1	35.5	1.47
CCT-08-45-04.70(V)-1-C0.006[c][d]		7	3800	50.6	35.5	1.43
CCT-08-45-04.70(V)-1-C0.012[c][d]		7	3800	51.8	35.5	1.46
CCT-11-45-04.13(V)-1[d]		9.87	4000	88.9	57.7	1.54
CCT-11-45-06.69(H)-1[b][d]	No. 11	9.87	4000	98.0[b]	57.7	1.70
CCT-11-45-06.69(V)-1[b][d]		9.87	4000	98.0[b]	57.7	1.70
CCT-11-45-09.26-1[b]		9.87	4000	98.0[b]	57.7	1.70

[a] T is based on strain gauges located at $7d_b$ from the face of the head (the approximate location of the end of the extended nodal zone in most specimens)
[b] Specimen exhibited bar yielding before failure of the node
[c] Specimen had transverse stirrups perpendicular to the headed bars within the nodal zone
[d] "H" represents a rectangular head with the long side orientated horizontally; "V" represents a rectangular head with the long side orientated vertically

As shown in Table 8.3, the headed bars in the CCT node specimens exhibited higher anchorage strengths than calculated using the descriptive equation, even without the 0.8 modification factor. The values of T/T_c range from 1.33 to 1.70 with an average of 1.51, matching those in the current study (T/T_c from 1.10 to 2.14 with an average of 1.64; Section 7.6.1). The comparisons for the CCT node specimens from both sources indicate that headed bars in CCT node applications, even when not within a column core, exhibit higher anchorage strengths than headed bars in beam-column joints, probably due to the compressive force from the reaction acting perpendicular to the bar in the anchorage region, as discussed in Section 7.6.1.

The two specimens tested by Thompson et al. (2006a) with confining reinforcement perpendicular to the bar, CCT-08-45-04.70(V)-1-C0.006 and CCT-08-45-04.70(V)-1-C0.012, had values of T/T_c equal to 1.43 and 1.46, respectively, slightly below the average T/T_c value of 1.51 for all specimens in Table 8.3, suggesting that the presence of transverse reinforcement

perpendicular to the bar within a nodal zone does not result in an increase in anchorage strength of headed bars in the CCT nodes.

8.4 SHALLOW EMBEDMENT PULLOUT TESTS

DeVries et al. (1999) tested 18 headed bars with shallow embedment. The 18 headed bars can be divided into three groups based on the location of the bar – eight center bars, five edge bars, and five corner bars. The center bars had an 18-in. concrete cover to the *center* of the bar. The edge bars had a 2-in. concrete cover from the closest edge to the *center* of the bar, and an 18-in. cover from the orthogonal edge to the *center* of the bar. The corner bars had a 2-in. cover from the nearest two edges to the *center* of the bar. Due to the low concrete cover provided for the edge and corner bars (1.6 in. or $2d_b$ to the *side* of the bar, less than the required $8d_b$), the 0.8 modification factor is applied to the calculated failure load. The 2-in. side cover to the *center* of the bar corresponds to 1-in. clear cover to the head. The bars were tested individually, and the bar spacing s is taken as twice of the minimum concrete cover to the center of the bar.

Of the 18 specimens investigated, four specimens (T2B3, T2B4, T2B7, and T2B8) had transverse reinforcement placed perpendicular to the headed bars and is considered as having no confining reinforcement for this analysis. This is also in agreement with the anchorage design provisions in the ACI Code, which do not account for reinforcement perpendicular to the bars (Section 17.4 in ACI 318-14).

In 14 of the tests, the straight length of the bar was covered by PVC sheathing to prevent any bond between the straight portion of the bar and the surrounding concrete. As this is not done in design, it is expected that the behavior of these specimens will differ from that of fully bonded bars. For the debonded bars, ℓ_{eh} in the descriptive equation is taken as the actual embedment length, although this may result in an overestimation of the anchorage strength.

Table 8.4 shows the comparisons of the measured failure load T on the headed bar with the calculated failure load T_c [based on Eq. (7.6), with the 0.8 modification factor applied as appropriate], along with the bar diameter d_b, embedment length ℓ_{eh}, concrete compressive strength f_{cm}, and the bar spacing in terms of bar diameter s/d_b.

Table 8.4 Test results for headed bars with shallow embedment tested by DeVries et al. (1999) and comparisons with descriptive equation [Eq. (7.6)] with the application of 0.8 modification factor as appropriate

Specimen	d_b (in.)[a]	ℓ_{eh} (in.)[a]	f_{cm} (psi)[a]	s/d_b[c]	T (kips)[a]	T_c (kips)[g]	T/T_c[g]	Note[e]
T1B1[b]	0.79	1.4	12040	45.7	17.3	9.8	1.76	
T1B2[b]	0.79	1.4	12040	45.7	13.9	9.8	1.42	
T1B3[b d]	0.79	4.4	12040	45.7	46.1[d]	31.9	1.45	
T1B4[b d]	0.79	4.4	12040	45.7	46.8[d]	31.9	1.47	
T1B5[b]	1.38	3.1	12040	26.1	48.3	27.2	1.78	Center bar
T1B6[b]	1.38	3.1	12040	26.1	50.6	27.2	1.86	
T1B7[b]	1.38	8.2	12040	26.1	110.2	73.0	1.51	
T3B11[b d]	0.79	9.0	3920	45.7	47.7[d]	50.4	0.95	
T2B1[b]	0.79	9.0	4790	5.1	41.4	32.6	1.27	
T2B2	0.79	9.0	4790	5.1	33.3	32.6	1.02	
T2B3[b f]	0.79	9.0	4790	5.1	36.0	32.6	1.10	Edge bar
T2B4[f]	0.79	9.0	4790	5.1	38.7	32.6	1.19	
T3B4[b]	0.79	9.0	3920	5.1	33.5	31.1	1.08	
T2B5[b]	0.79	9.0	4790	5.1	19.8	32.6	0.61	
T2B6	0.79	9.0	4790	5.1	27.4	32.6	0.84	
T2B7[b f]	0.79	9.0	4790	5.1	20.0	32.6	0.61	Corner bar
T2B8[f]	0.79	9.0	4790	5.1	28.1	32.6	0.86	
T3B8[b]	0.79	9.0	3920	5.1	12.8	31.1	0.41	

[a] Values are converted SI (1 in. = 25.4 mm; 1 psi = 1/145 MPa; and 1 kip = 4.44822 kN)

[b] Headed bar was covered with PVC sheathing to eliminate bond force along the bar; the actual embedment length rather than the bonded length was used to calculate T_c

[c] Bar spacing s is taken as twice of the minimum concrete cover to the center of the bar

[d] Specimen failed with bar fracture

[e] Center bar: 18 in. from center of the bar to each edge; edge bar: 2 in. from center of the bar to the nearest edge and 18 in. to the orthogonal edge; corner bar: 2 in. from center of the bar to the nearest two edges

[f] Specimen had transverse reinforcement perpendicular to the headed bar

[g] T_c is based on Eq. (7.6) with a 0.8 modification factor applied for edge and corner bars

The values of T/T_c in Table 8.4 show that the addition of concrete cover tended to increase the anchorage strength of the headed bars. For the eight center bars (all debonded by the PVC sheathing), the values of T/T_c range from 0.95 to 1.86, with an average of 1.52; only one bar exhibited a lower anchorage strength than predicted by Eq. (7.6) ($T/T_c = 0.95$). That bar (with $T/T_c = 0.95$) fractured, indicating that T/T_c would have been greater than 0.95 had the bar been stronger. For the five edge bars (three debonded), the values of T/T_c are less scattered but smaller on average compared to the values for the center bars – T/T_c ranges from 1.02 to 1.27 with an average of 1.13. For the five corner bars (three debonded), the values of T/T_c are all below 1.0, with a range of 0.41 to 0.86 and an average of 0.67. Of these five corner bars, the two bars that were not debonded

exhibited higher anchorage strengths (T/T_c = 0.84 and 0.86) than the strengths of the three debonded bars (T/T_c = 0.61, 0.61, and 0.41, respectively). Overall, all of the headed bars, except for the three debonded corners bars, had values of T/T_c within or above the range of 0.68 to 1.27 for the beam-column joint specimens used to develop the descriptive equation [Eq. (7.6)]. Excluding the 14 headed bars debonded by the PVC sheathing, the remaining four bars had values of T/T_c ranging from 0.84 to 1.19, with an average of 0.98. This indicates that the descriptive equation, combined with the additional 0.8 modification factor to account for bar location, is suitable in predicting the anchorage strength for these headed bars in the shallow embedment pullout tests. Without the 0.8 modification factor, the descriptive equation would have produced an unconservative estimate of anchorage strength.

In the calculation of T_c, four specimens (T2B3, T2B4, T2B7, and T2B8) with transverse reinforcement were assumed to have no confining reinforcement. The values of T/T_c for these four bars are, respectively, 1.10, 1.19, 0.61, and 0.86, while the corresponding specimens without transverse reinforcement (T2B1, T2B2, T2B5, and T2B6) have values of 1.27, 1.02, 0.61, and 0.84. A comparison of these values shows that, relative to the calculated failure load based on Eq. (7.6), the anchorage strengths of the headed bars with transverse reinforcement were not higher than those without transverse reinforcement. This reinforces the observation by DeVries et al. (1999) that transverse reinforcement placed perpendicular to the headed bars with shallow embedment is not effective in confining the headed bars.

As suggested in Section 7.6.2, the descriptive equations could be used to provide an estimate of the anchorage strength of headed bars terminating in a foundation from a column with $h_{cl}/\ell_{eh} \leq 2.79$ or $d_{eff}/\ell_{eh} \leq 3$ (based on the data for the shallow embedment pullout tests in this study). The headed bars with shallow embedment tested by DeVries et al. (1999) had bearing reactions located at a distance from the center of the bar to the nearest edge of the bearing member at least twice of the embedment length ($h_{cl}/\ell_{eh} > 2$) to allow for the assumed failure surface to develop without interference from the loading apparatus. Although the location of the bearing reaction was not reported, the bonded headed bars (those without PVC sheathing) with a ratio $h_{cl}/\ell_{eh} > 2$ exhibited similar anchorage strengths to the strengths predicted by the descriptive equation,

indicating that a value of h_{cl}/ℓ_{eh} greater than 2 as the threshold for column-foundation connections is justifiable.

8.5 LAP SPLICE TESTS

8.5.1 Thompson et al. (2006b)

The lap splice specimens tested by Thompson et al. (2006b) contained No. 8 bars with a 2-in. clear side cover c_{so} to the bar, with the exception of the first specimen listed in Table 8.6, LS-08-04.70-03-06(N)-1, which had a 1-in. clear side cover. The clear concrete cover on top of the bar was 2 in. for all but one specimen, LS-08-04.04-14-10(N)-1-DB, which had a 4.5-in. clear top cover to the bar. As the top and side cover provided for these specimens is less than the required $8d_b$ to be treated as anchorage within a region equivalent to a column core, the calculated strengths based on the descriptive equation are multiplied by the 0.8 modification factor. Specimen LS-08-04.04-14-10(N)-1-DB also had a debonding sheath placed over the bar deformations in the lap zone, and the actual lap length (rather than the bonded length) is used to calculate the strength. The last five specimens in Table 8.5 had confining reinforcement in the form of hairpins or transverse tie-down reinforcement placed perpendicular to the headed bars (the two confinement details are illustrated in Figure 1.13). Because the confining reinforcement is not parallel to the bar as required for calculating A_{tt} in the descriptive equation [Eq. (7.9)], these five specimens are treated as unconfined specimens for this analysis. Headed bars with net bearing areas less than $4A_b$ are excluded from the comparisons. Table 8.5 compares the splice strengths measured in the lap splice tests T (based on strain gauge readings) with those calculated using descriptive Eq. (7.6), along with the splice length ℓ_{st}, concrete compressive strength f_{cm}, and the smallest center-to-center spacing between adjacent bars and clear side cover to the bar, s/d_b and c_{so}/d_b, both in terms of bar diameter.

Table 8.5 Test results for lap splice specimens tested by Thompson et al. (2006b) and comparisons with descriptive equation [Eq. (7.6)] with 0.8 modification factor applied

Specimen	ℓ_{st} (in.)	f_{cm} (psi)	s/d_b	c_{so}/d_b	T [b] (kips)	T_c [d] (kips)	T/T_c [d]
LS-08-04.70-03-06(N)-1	3	3200	3	1	14.7	8.0	1.84
LS-08-04.70-05-06(N)-1	5	3700	3	2	21.3	14.0	1.52
LS-08-04.70-05-10(N)-1	5	3200	5	2	19.0	17.3	1.10
LS-08-04.70-05-10(C)-1	5	3700	2	2	19.4	12.0	1.61
LS-08-04.70-08-10(N)-1	8	4000	5	2	34.4	29.7	1.16
LS-08-04.70-12-10(N)-1	12	4200	5	2	52.4	45.6	1.15
LS-08-04.04-08-10(N)-1	8	4000	5	2	35.1	29.7	1.18
LS-08-04.04-12-10(N)-1	12	3800	5	2	40.3	44.5	0.90
LS-08-04.04-14-10(N)-1	14	3500	5	2	51.4	51.2	1.00
LS-08-04.04-14-10(N)-1-DB[a]	14	3500	5	2	43.0	51.2	0.84
LS-08-04.70-08-10(N)-1-H0.25[c]	8	4200	5	2	43.3	30.0	1.44
LS-08-04.04-08-10(N)-1-H0.56[c]	8	3500	5	2	42.7	28.8	1.49
LS-08-04.04-08-10(N)-1-H1.01[c]	8	3500	5	2	44.8	28.8	1.56
LS-08-04.04-12-10(N)-1-H0.56[c]	12	3800	5	2	42.5	44.5	0.95
LS-08-04.04-12-10(N)-1-TTD[c]	12	3800	5	2	44.7	44.5	1.00

[a] Specimen had a debonding sheath placed over bar deformations in lap splice region
[b] T is based on strain gauge readings
[c] Specimen had confining reinforcement perpendicular to the headed bars
[d] T_c is based on Eq. (7.6) with a 0.8 modification factor applied

As shown in Table 8.5, the values of T/T_c for the lap splice specimens tested by Thompson et al. (2006b) range from 0.84 to 1.84, with an average of 1.25. Three out of 15 specimens exhibited lower splice strengths than predicted by the descriptive equation, with T/T_c equal 0.90, 0.84, and 0.95, respectively. The smallest value $T/T_c = 0.84$ is obtained with Specimen LS-08-04.04-14-10(N)-1-DB, for which the headed bars were debonded in the lap zone. Without the debonded specimen, the average value of T/T_c is 1.28. Although the average value of T/T_c might indicate that the 0.8 factor applied to T_c is too conservative, an inspection of values of T/T_c shows that without the 0.8 factor, nine of these 15 specimens would have had $T/T_c < 1.0$, with two equal to 0.80 and three below 0.8.

For the five specimens with confining reinforcement placed in the lap zone, the values of T/T_c range from 0.95 to 1.56, with an average of 1.29, approximating the value 1.28 for all specimens with fully bonded bars. These values indicate that the type of confining reinforcement studied by Thompson et al. (2006b) has a minimal effect on the anchorage strength of headed bar splices, which is in accordance with conclusion by Thompson (2002) that the "tie-down or tie-

back confinement perpendicular to the plane of the lap splice did not significantly improve lap splice performance", and for the "transverse confining bars parallel to the plane of the lap splice and placed within the cover concrete over the splices", "the data from this study is not sufficient to draw general conclusions or develop design guidelines." Therefore, the confining reinforcement placed perpendicular to the spliced bars in these tests are considered as not effective for comparison with the design equation, which will be presented in Chapter 9.

8.5.2 Chun (2015)

Chun (2015) tested 24 lap splice specimens containing No. 8 or No. 9 headed bars. The headed bars were similar in type to those used in the beam-column joint tests by Chun et al. (2009) (Figure 8.1), with an obstruction reducing the actual bearing area of the head to a value below $3A_b$ ($4A_b$ is the minimum required area in ACI 318). The specimens were tested with the spliced headed bars located at the bottom of the specimen, rather than at the top as was done in the current study and in the splice tests by Thompson et al. (2006b). The clear bottom cover to the bar was $2d_b$.[3] Twenty-two of the specimens had a $2d_b$ center-to-center spacing ($1d_b$ clear spacing), and the other two specimens had a $3d_b$ center-to-center spacing. Of the 24 specimens, 19 had only $1d_b$ side cover to the bar, providing clear cover of only $0.38d_b$ (0.37 or 0.43 in. depending on bar size) to the head, and the other five specimens had either $2d_b$ or $3.5d_b$ side cover to the bar (corresponding to, respectively, 1.58 in. and 3.29 in. cover to the head). Because the concrete cover was much less than the required $8d_b$ to be treated as anchorage in a region equivalent to a column core, the 0.8 modification factor is applied to the calculated strength based on the descriptive equation.

The last eight specimens listed in Table 8.6 were confined by stirrups placed perpendicular to the spliced bars. Two types of confinement details were used: No. 3 stirrups placed along the full splice length at a constant spacing, and two No. 3 stirrups placed at the ends of the lap splice region. Chun (2015) represented the amount of confinement using the transverse reinforcement index for the development length of straight reinforcing bars K_{tr}, calculated in accordance with Section 12.2.3 of ACI 318-11, where $K_{tr} = 40A_{tr}/sn$, s = center-to-center spacing between transverse reinforcement (not equal to s in the descriptive equations); A_{tr} = total cross-sectional

---

[3] Bottom cover was provided by the author through personal communication.

area of all transverse reinforcement within spacing s; and n = number of headed bars being spliced along the plane of splitting. For this analysis, the stirrups, which are perpendicular to the bars, are assumed to be ineffective in confining the headed bars, and descriptive equation, Eq. (7.6), is used to calculate the failure load on the bar T_c. Table 8.6 compares the measured splice strengths T [T calculated by Chun (2015) using the moment-curvature method, as used for the splice specimens in this study] with the calculated strengths T_c based on Eq. (7.6) for the 24 specimens, along with the bar diameter d_b, splice length ℓ_{st}, concrete compressive strength f_{cm}, center-to-center spacing between adjacent spliced bars in terms of bar diameter s/d_b, side cover to the bar in terms of bar diameter c_{so}/d_b, and the transverse reinforcement index K_{tr}.

Table 8.6 Test results for lap splice specimens tested by Chun (2015) and comparisons with descriptive equation [Eq. (7.6)] with 0.8 modification factor applied

Specimen	d_b [a] (in.)	ℓ_{st} [a] (in.)	f_{cm} [a] (psi)	s/d_b	c_{so}/d_b	K_{tr}	T [b] (kips)	T_c [c] (kips)	T/T_c
D29-S2-F42-L15	1.14	17.1	6000	2	1	-	45.0	50.4	0.89
D29-S2-F42-L20	1.14	22.8	6000	2	1	-	52.9	67.8	0.78
D29-S2-F42-L25	1.14	28.5	6000	2	1	-	62.6	85.3	0.73
D29-S2-F42-L30	1.14	34.3	5820	2	1	-	66.2	102.1	0.65
D29-S4-F42-L15	1.14	17.1	6000	3	2	-	48.4	58.6	0.83
D29-S4-F42-L20	1.14	22.8	6000	3	2	-	54.8	78.8	0.69
D29-S2-C3.5-F42-L15	1.14	17.1	5820	2	3.5	-	52.9	50.0	1.06
D29-S2-C3.5-F42-L20	1.14	22.8	5820	2	3.5	-	63.8	67.2	0.95
D29-S2-C3.5-F42-L25	1.14	28.5	5820	2	3.5	-	72.4	84.6	0.86
D25-S2-F42-L20	0.98	19.7	6000	2	1	-	37.1	55.2	0.67
D25-S2-F42-L25	0.98	24.6	6000	2	1	-	46.5	69.5	0.67
D29-S2-F21-L20	1.14	22.8	2940	2	1	-	34.0	57.1	0.59
D29-S2-F21-L25	1.14	28.5	2940	2	1	-	40.7	71.9	0.57
D29-S2-F70-L15	1.14	17.1	9120	2	1	-	49.8	55.7	0.89
D29-S2-F70-L20	1.14	22.8	9120	2	1	-	62.3	74.9	0.83
D29-S2-F70-L25	1.14	28.5	9120	2	1	-	67.0	94.3	0.71
D29-S2-F42-L15-Con.[d]	1.14	17.1	6000	2	1	1.51	69.9	50.4	1.39
D29-S2-F42-L20-Con.[d]	1.14	22.8	6000	2	1	1.51	84.4	67.8	1.25
D29-S2-F42-L20-LCon.[d]	1.14	22.8	6000	2	1	0.57	70.6	67.8	1.04
D29-S2-F42-L25-Lcon.[d]	1.14	28.5	5820	2	1	0.46	82.2	84.6	0.97
D29-S2-F42-L15-Con.2 [d]	1.14	17.1	5820	2	1	2.50	75.4	50.0	1.51
D29-S2-F42-L20-Con.2 [d]	1.14	22.8	5820	2	1	2.50	98.3	67.2	1.46
D29-S2-F70-L15-Con.[d]	1.14	17.1	9120	2	1	1.51	81.2	55.7	1.46
D29-S2-F70-L20-Con.[d e]	1.14	22.8	9120	2	1	1.51	105.4[d]	74.9	1.41

[a] Values are converted SI (1 in. = 25.4 mm; 1 psi = 1/145 MPa)
[b] T is based on moment-curvature method
[c] T_c is based on Eq. (7.6) with a 0.8 modification factor applied
[d] Specimen was confined by transverse stirrups perpendicular to the spliced bars
[e] Specimen failed with yielding of spliced bars

200

As shown in Table 8.6, 16 specimens out of 24 exhibited lower splice strengths than predicted by the descriptive equation, even with the 0.8 modification factor applied. Nine specimens had values of T/T_c below 0.8, with a value as low as 0.57. The low splice strengths relative to the strengths predicted by the descriptive equation do not match the comparisons for the splice tests by Thompson et al. (2006b) or those from the current study. For the specimens tested by Thompson et al. (2006b), only three specimens (out of 15) have $T/T_c < 1.0$, with the smallest T/T_c equal to 0.84 (corresponding to the specimen with debonded bars in the lap zone). For the six splice specimens in the current study (Section 7.6.3), the values of T/T_c are within the range for the beam-column joint specimens used to develop the descriptive equation, with the smallest $T/T_c = 0.83$ and an average $T/T_c = 1.0$.

The low values of T/T_c observed for these splice specimens, however, do match those for the beam-column joint specimens tested by Chun et al. (2009). In both types of test, heads with obstructions that just met the upper dimensional (diameter) limit for HA heads were used. As discussed in Section 8.2.2, the obstruction for these heads had a constant area over its full length, reducing the actual net bearing area to approximately $2.8A_b$, if "net bearing area" is defined as the difference between the gross area of the head and the area of the obstruction adjacent to the head. In the current version of ASTM A970, the definition of net bearing area (gross area of the head minus bar area) ignores the area of the obstructions that are within the required dimensional limits. There is cause for concern, however, if full advantage is taken of the definition, because a head with a diameter of $\sqrt{5}d_b$ with an obstruction with a diameter of $1.5d_b$ qualifies as an HA head while providing a bearing area of only $2.75A_b$. Such is the case for the heads used by Chun et al. (2009) and Chun (2015) that exhibited low anchorage strengths. The non-HA heads in this study, with obstructions exceeding the dimensional limits in the current ASTM A970 but with actual bearing areas at the face of the head $\geq 4.5A_b$, however, have been demonstrated to provide similar anchorage strengths to those of HA heads. Based on these observations for heads with obstructions, it is suggested that the "net bearing area" A_{brg} for heads with obstructions be the bearing area adjacent to the head and that $A_{brg} \geq 4A_b$.

The low splice strengths for the specimens tested by Chun (2015) are also possibly due to the low concrete side cover used − $1d_b$ to the bar and $0.38d_b$ to the head for most specimens, with

d_b = 1.14 in. or 0.98 in. As a comparison, the specimens tested by Thompson et al. (2006b), in all but one case, had a clear side cover of 2 in. ($2d_b$), and the specimens in the current study had a side cover of 2 in. ($2.67d_b$), both much greater than the $1d_b$ cover to the bar. The 24 specimens tested by Chun (2015) were cast in concrete with 1 in. maximum aggregate size[4], while the $0.38d_b$ cover to the head (corresponding to 0.43 in. for 17 specimens and 0.37 in. for two specimens) is even less than half of the maximum aggregate size, which could cause honeycombing and prevent the proper encasement of the headed bars. The $0.38d_b$ cover to the head also violates the specified concrete cover requirements in Section 20.6.1.3 of ACI 318-14, and thus, the configurations in these tests would not be used in practice.

The eight specimens listed at the end of Table 8.6 with transverse stirrups placed perpendicular to the spliced bars also had $1d_b$ side cover to the bar; as opposed to the low values of T/T_c for the splice specimens without confining reinforcement, these eight specimens exhibited higher or similar splice strengths to that predicted by the descriptive equation (the stirrups were not considered as effective confining reinforcement in calculating T_c). The values of T/T_c for these eight specimens range from 0.97 to 1.51, with an average of 1.31. This indicates that the transverse stirrups used in the tests were effective in confining these spliced headed bars, and might also be effective in reducing the adverse effects of low side cover. The effectiveness of the transverse stirrups for these splice specimens might be dependent upon the type of headed bars used and side cover provided – it is possible that the increase in splice strength resulting from the transverse stirrups would be less if another type of headed bars (without obstructions) had been used and more side cover had been provided. More tests are needed to evaluate the effectiveness of the confining reinforcement (in the form of the transverse stirrups used in these tests or in other forms) for spliced headed bars.

---

[4] Maximum aggregate size was provided by the author through personal communication.

CHAPTER 9: DESIGN PROVISIONS

The descriptive equations developed in Chapter 7 characterize the anchorage strength of headed bars. Design provisions for development length ℓ_{dt} are needed that are not only reasonably accurate, but also conservative and easy to apply. Based on the analysis and descriptive equations in Chapter 7, a design equation and supporting provisions for the development length of headed bars are proposed in this chapter. Test results of headed bars in beam-column joints, CCT nodes, shallow-embedment specimens, and lap splices from the current study and test results from previous studies are compared with the proposed design equation to establish its applicability across all uses of headed bars. These comparisons are presented in detail in this chapter and summarized in Appendix F. Proposed code provisions for the development of headed bars are presented at the end of this chapter.

9.1 DESIGN EQUATION

In the current Building Code (ACI 318-14), the development length for headed bars is given by

$$\ell_{dt} = \left(\frac{0.016 f_y \psi_e}{\sqrt{f_c'}} \right) d_b \tag{7.2}$$

which indicates that the development length is proportional to the yield strength of the bar f_y, diameter of the bar d_b, and concrete compressive strength raised to 0.5 power $\sqrt{f_c'}$.

The analysis in Chapter 7, however, shows that the current design provisions do not accurately capture the effects of concrete compressive strength or bar size on the anchorage strength of headed bars, giving conservative results for lower strength concrete and smaller diameter bars – results that become progressively less conservative as both concrete strength and bar diameter increase. The analysis indicates that the effect of concrete compressive strength is overestimated by the 0.5 power and that ℓ_{dt} should increase more rapidly than the bar diameter d_b. In addition, the current provisions do not account for the effects of confining reinforcement and spacing between the bars, which were demonstrated in Chapter 7 to affect the anchorage strength of headed bars.

Based on the analysis and descriptive equations developed in Chapter 7 that were compared with test results in Chapters 7 and 8, a new design equation for the development length of headed bars is proposed:

$$\ell_{dt} = \left(0.0024 \frac{f_y \Psi_e \Psi_{cs} \Psi_o}{f_c'^{0.25}} \right) d_b^{1.5} \tag{9.1}$$

where ℓ_{dt} = development length of a headed bar in tension (in.), but not less than $8d_b$ or 6 in.; f_y = yield strength of the headed bar (psi); Ψ_e = modification factor for epoxy-coated or zinc and epoxy dual-coated bars; Ψ_{cs} = modification factor for confining reinforcement and bar spacing; Ψ_o = modification factor for bar location; f_c' = compressive strength of concrete (psi); and d_b = diameter of the headed bar (in.). The minimum values of development length and the modification factor Ψ_e are retained from the current ACI Code.

Equation (9.1) was developed using the descriptive equations presented in Chapter 7 for widely-spaced headed bars that are simplified, as described in Section 9.1.1. The equation includes an embedded strength reduction factor.

9.1.1 Simplified Descriptive Equations

9.1.1.1 Widely-spaced bars

The descriptive equation for widely-spaced headed bars (center-to-center spacing $\geq 8d_b$) developed in Chapter 7 is

$$T_h = 781 f_{cm}^{0.24} \ell_{eh}^{1.03} d_b^{0.35} + 48,800 \frac{A_{tt}}{n} d_b^{0.88} \tag{7.8}$$

where T_h = anchorage strength of a headed bar (lb); f_{cm} = compressive strength of concrete (psi); ℓ_{eh} = embedment length (in.); d_b = diameter of headed bar (in.); A_{tt} = total cross-sectional area of all confining reinforcement parallel to the headed bars being developed in beam-column joints and located within $8d_b$ of the top (bottom) of the headed bars in direction of the interior of the joint for No. 3 through No. 8 bars and within $10d_b$ of the top (bottom) of the bar in direction of the interior of the joint for No. 9 through No. 11 bars, or minimum total cross-sectional area of all confining reinforcement parallel to headed bars being developed in members other than beam-column joints within $7\frac{1}{2}d_b$ on one side of the bar centerline for No. 3 through No. 8 headed bars or within $9\frac{1}{2}d_b$

on one side of the bar centerline for No. 9 through No. 11 headed bars (in.^{2}); and n = number of headed bars being developed.

Following the approach used by Sperry et al. (2015b) to simplify the descriptive equation, the powers of f_{cm} and ℓ_{eh} are changed to 0.25 and 1.0, respectively, and the power of d_b is increased to 0.5 for the first term and decreased to 0.75 in the second term, giving

$$T_h = C_1 f_{cm}^{0.25} \ell_{eh} d_b^{0.5} + C_2 \frac{A_{tt}}{n} d_b^{0.75} \tag{9.2}$$

The value of C_1 is selected so that the ratio of test-to-calculated failure load T/T_h has an average value of 1.0 for specimens without confining reinforcement. With C_1 fixed, the value of C_2 is then selected so that the ratio of test-to-calculated failure load T/T_h has an average value of 1.0 for specimens with confining reinforcement. With the values of C_1 and C_2 determined, Eq. (9.2) becomes

$$T_h = 768 f_{cm}^{0.25} \ell_{eh} d_b^{0.5} + 48,000 \frac{A_{tt}}{n} d_b^{0.75} \tag{9.3}$$

Figures 9.1 and 9.2, respectively, show the ratio T/T_h as a function of f_{cm} for the specimens without and with confining reinforcement used to develop Eq. (9.3). The trend lines in the figures are based on dummy variable analysis. Table 9.1 gives the maximum, minimum, mean, STD, and COV values of T/T_h for the specimens included in the two figures.
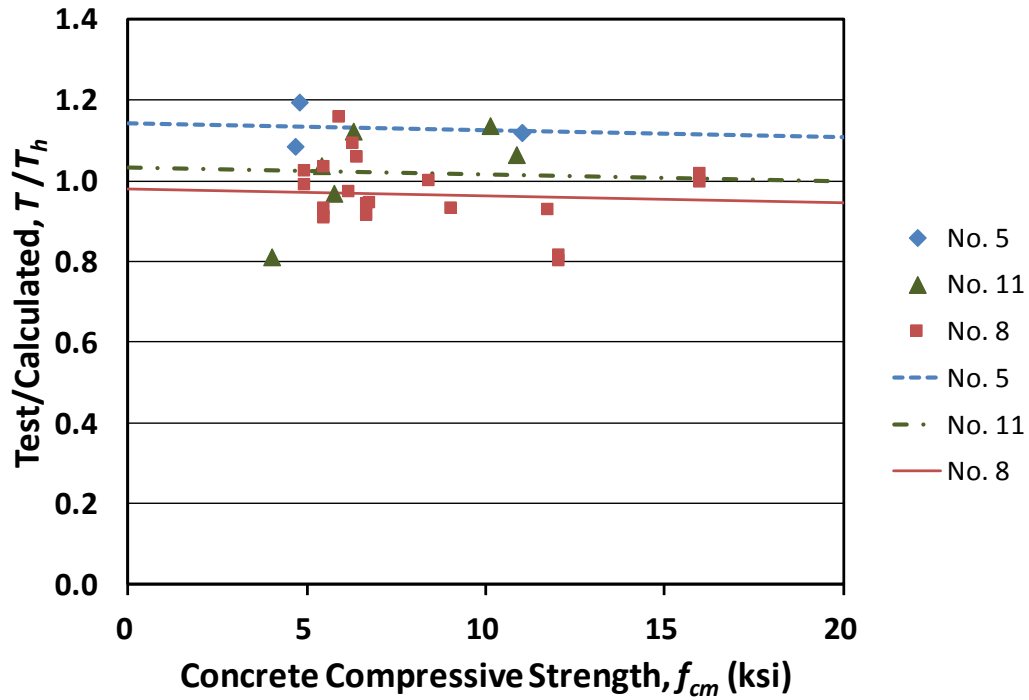
Figure 9.1 Ratio of test to calculated failure load T/T_h versus concrete compressive strength f_{cm} for widely-spaced bars without confining reinforcement, with T_h based on Eq. (9.3)
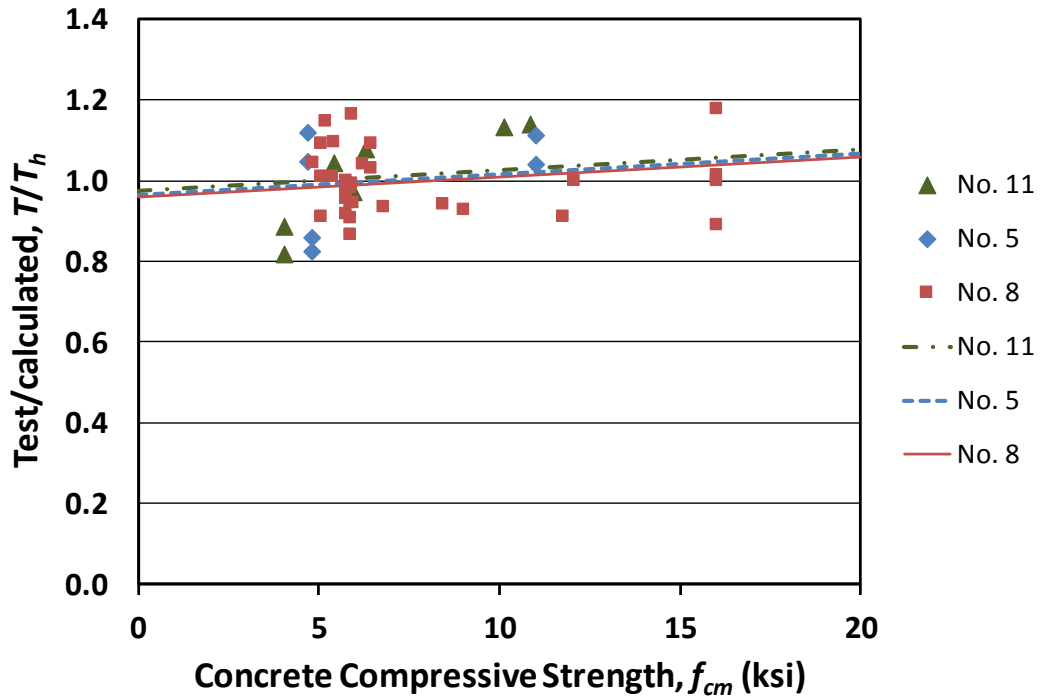
Figure 9.2 Ratio of test to calculated failure load T/T_h versus concrete compressive strength f_{cm} for widely-spaced bars with confining reinforcement, with T_h based on Eq. (9.3)

Table 9.1 Statistical parameters of T/T_h for widely-spaced headed bars, with T_h based on Eq. (9.3)

(Number of specimens)	Without Confining Reinforcement				With Confining Reinforcement			
	No. 5	No. 8	No. 11	All	No. 5	No. 8	No. 11	All
	(4)	(20)	(6)	(30)	(6)	(30)	(7)	(43)
Max	1.19	1.15	1.14	1.19	1.12	1.18	1.14	1.18
Min	1.08	0.80	0.81	0.80	0.82	0.86	0.82	0.82
Mean	1.13	0.97	1.02	1.00	1.00	1.00	1.01	1.00
STD	0.046	0.085	0.121	0.103	0.128	0.082	0.123	0.094
COV	0.040	0.088	0.118	0.103	0.128	0.082	0.122	0.094

In Figure 9.1, the slightly downward sloping trend lines indicate that the 0.25 power for f_{cm} slightly overestimates the effect of concrete compressive strength for the specimens without confining reinforcement. This is expected, as the descriptive equation (Section 7.3.1) included the power 0.24 for f_{cm}. There is also a greater spread in the dummy variable lines for No. 5 and No. 11 bars as a result of increasing the power of d_b for the first term of the simplified descriptive equation [Eq. (9.2)]. In contrast to the results in Figure 9.1, the slightly upward sloping trend lines in Figure 9.2 show that the 0.25 power for f_{cm} slightly underestimates the effect of concrete compressive strength for the specimens with confining reinforcement, suggesting that the effect of higher strength concrete is greater for headed bars with confining reinforcement. The sign of the slopes of the dummy variable lines in Figures 9.1 and 9.2 match those for the descriptive equations shown in Figures 7.9 and 7.14. The dummy variable lines have similar intercepts, indicating that the two powers of d_b in the simplified descriptive equation capture the effect of bar size with reasonable accuracy.

For the specimens without and with confining reinforcement, the values of the coefficient of variation in Table 9.1 for the simplified equation [Eq. (9.3)] are 0.103 and 0.094, respectively, which compare favorably to the values for the descriptive equation [Eq. (7.8)], 0.100 and 0.095.

9.1.1.2 Closely-spaced bars

For closely-spaced bars (center-to-center spacing $< 8d_b$), the test results for specimens are compared with the simplified descriptive equation, Eq. (9.3), and plotted versus the center-to-center spacing between the bars in Figures 9.3 and 9.4 for the closely-spaced bars without and with

confining reinforcement, respectively. The specimens with widely-spaced bars are also shown in the figures for comparison and are represented by open symbols.
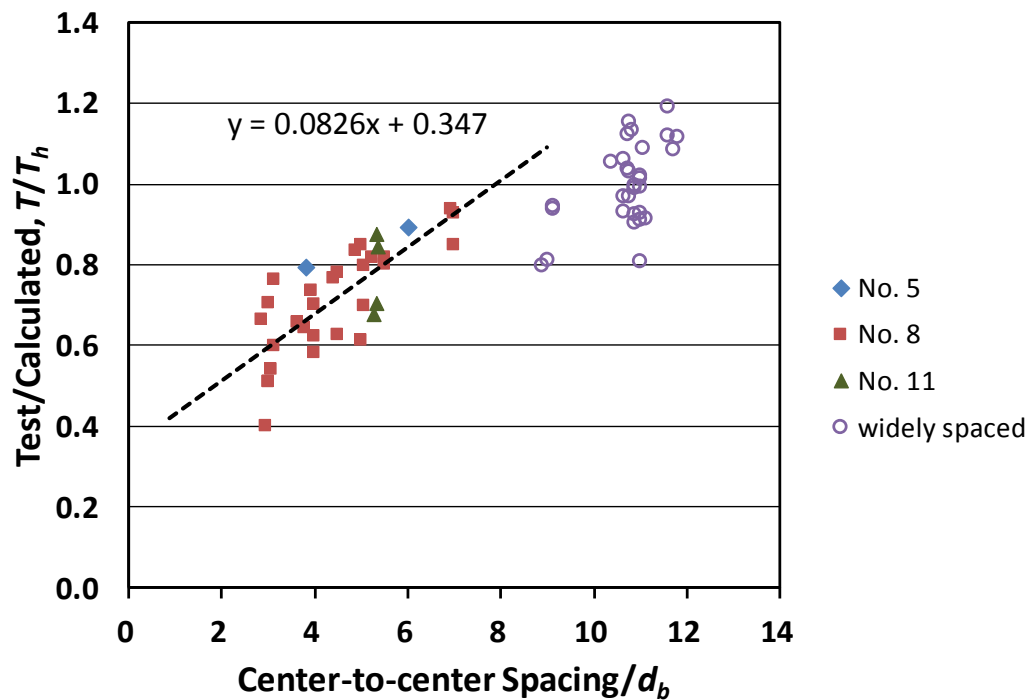
Figure 9.3 Ratio of test-to-calculated failure load T/T_h versus center-to-center spacing for headed bars without confining reinforcement, with T_h based on Eq. (9.3)
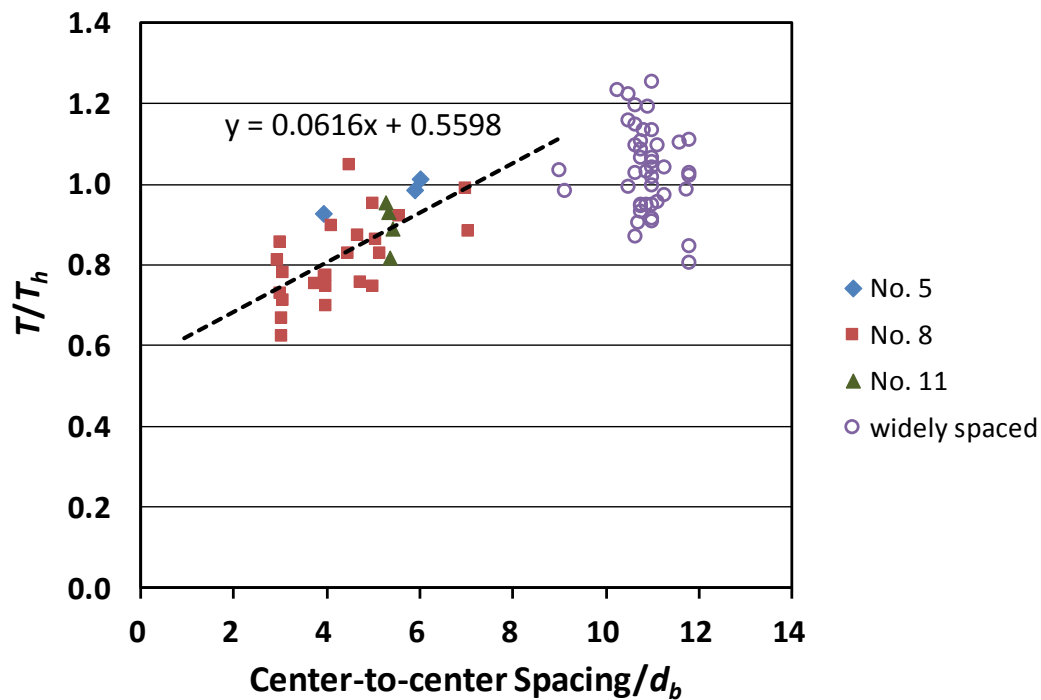
Figure 9.4 Ratio of test-to-calculated failure load T/T_h versus center-to-center spacing for headed bars with confining reinforcement, with T_h based on Eq. (9.3)

208

As indicated by the trend lines in the two figures, the anchorage strengths for closely-spaced headed bars can be calculated by applying a modification factor to the simplified descriptive equation for widely-spaced bars Eq. (9.3). For the bars without and with confining reinforcement, the anchorage strengths are expressed by Eq. (9.4) and (9.5), respectively. The second term $48,000\frac{A_{tt}}{n}d_b^{0.75}$ in Eq. (9.3) equals 0 when no confining reinforcement is present and is omitted in Eq. (9.4).

$$T_c = \left(768 f_{cm}^{0.25}\ell_{eh}d_b^{0.5}\right)\left(0.0826\frac{s}{d_b}+0.347\right) \tag{9.4}$$

with $\left(0.0826\dfrac{s}{d_b}+0.347\right)\le 1.0$

$$T_h = \left(768 f_{cm}^{0.25}\ell_{eh}d_b^{0.5}+48,000\frac{A_{tt}}{n}d_b^{0.75}\right)\left(0.0616\frac{s}{d_b}+0.5598\right) \tag{9.5}$$

with $\left(0.0616\dfrac{s}{d_b}+0.5598\right)\le 1.0$

where s = center-to-center spacing between the bars (in.).

For the next step, the terms for bar spacing in parenthesis are not incorporated directly into an expression for development length, but rather are used to develop a simplified representation for the effect of headed bar spacing.

9.1.2 Development Length Equation

9.1.2.1 Widely-spaced bars

To develop an expression for development length, the simplified descriptive equation, Eq. (9.3) for widely-spaced headed bars, is solved for embedment length ℓ_{eh}, substituting $A_b f_s = \pi f_s d_b^2/4$ for T_h. The resulting equation is

$$\ell_{eh} = 0.001\frac{f_s\psi_r}{f_{cm}^{0.25}}d_b^{1.5} \tag{9.6}$$

where $\psi_r = 1 - \dfrac{48,000}{f_s}\dfrac{A_{tt}}{A_{hs}}d_b^{0.75}$ = modification factor to account for the contribution of confining reinforcement to the anchorage strength of headed bars, with a value of 1.0 for no confining reinforcement; f_s = stress in headed bar at anchorage failure (psi); A_{tt} = total cross-sectional area of all confining reinforcement parallel to the headed bars being developed in beam-column joints

and located within $8d_b$ of the top (bottom) of the headed bars in direction of the interior of the joint for No. 3 through No. 8 bars and within $10d_b$ of the top (bottom) of the bar in direction of the interior of the joint for No. 9 through No. 11 bars (in.^{2}); A_{hs} = total cross-sectional area of headed bars being developed (in.^{2}); d_b = diameter of headed bar (in.); and f_{cm} = measured compressive strength of concrete (psi).

For use in design, Eq. (9.6) is modified by replacing ℓ_{eh} with development length ℓ_{dt}, replacing f_s with the specified yield strength of the headed bar f_y, and replacing f_{cm} with the specified compressive strength of concrete f'_c, giving

$$\ell_{dt} = 0.001 \frac{f_y \psi_r}{f'^{0.25}_c} d_b^{1.5} \tag{9.7}$$

where $\psi_r = 1 - \dfrac{48,000}{f_y} \dfrac{A_{tt}}{A_{hs}} d_b^{0.75}$, as given following Eq. (9.6).

As indicated by the expression for ψ_r, an increase in A_{tt}/A_{hs} results in a decrease in ψ_r. An upper limit on A_{tt}/A_{hs} is selected for calculating ψ_r based on the range of the test results. For the specimens used to develop the descriptive equations, the values of A_{tt}/A_{hs} ranged from 0.07 to 1.07, highest for No. 5 bars and lowest for No. 11 bars, with an average of 0.3. For the No. 11 bars, the maximum value of A_{tt}/A_{hs} is 0.21, below the average value 0.3. Given this range of data, 0.3 is set as the upper limit of A_{tt}/A_{hs} for calculating ψ_r.

To evaluate the 0.3 limit on A_{tt}/A_{hs}, the ratio T/T_h for specimens with confining reinforcement is plotted versus A_{tt}/A_{hs} in Figures 9.5 and 9.6. T_h in Figure 9.5 is based on descriptive Eq. (7.9) using the actual value of A_{tt}/A_{hs} (without any limit); T_h in Figure 9.6 is based on descriptive Eq. (7.9) with the limit $A_{tt}/A_{hs} \leq 0.3$.
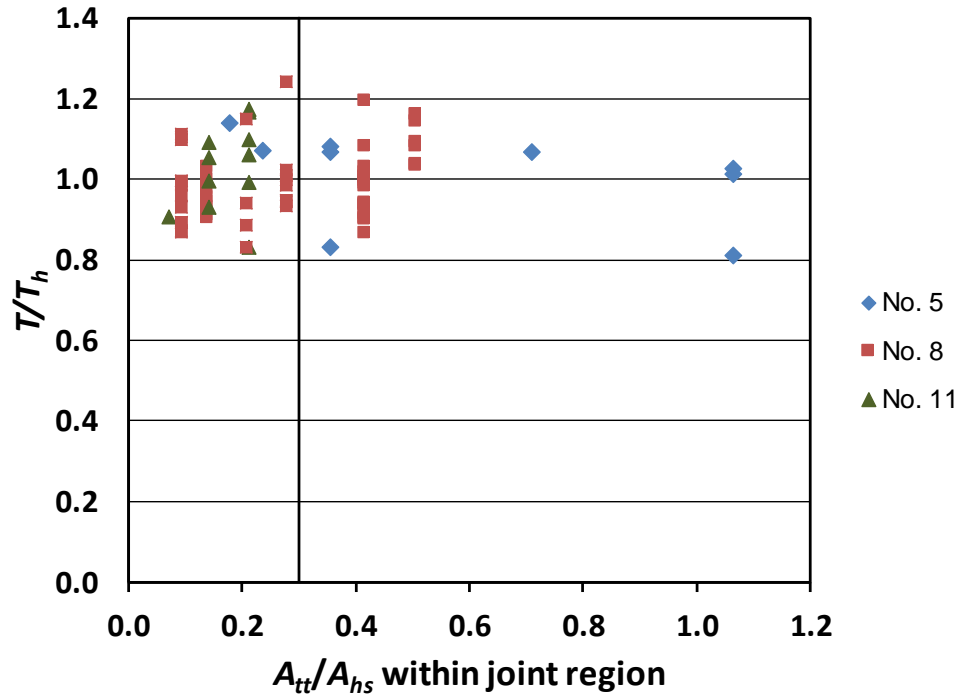
Figure 9.5 Ratio of T/T_h versus A_{tt}/A_{hs}, with T_h based on Eq. (7.9)
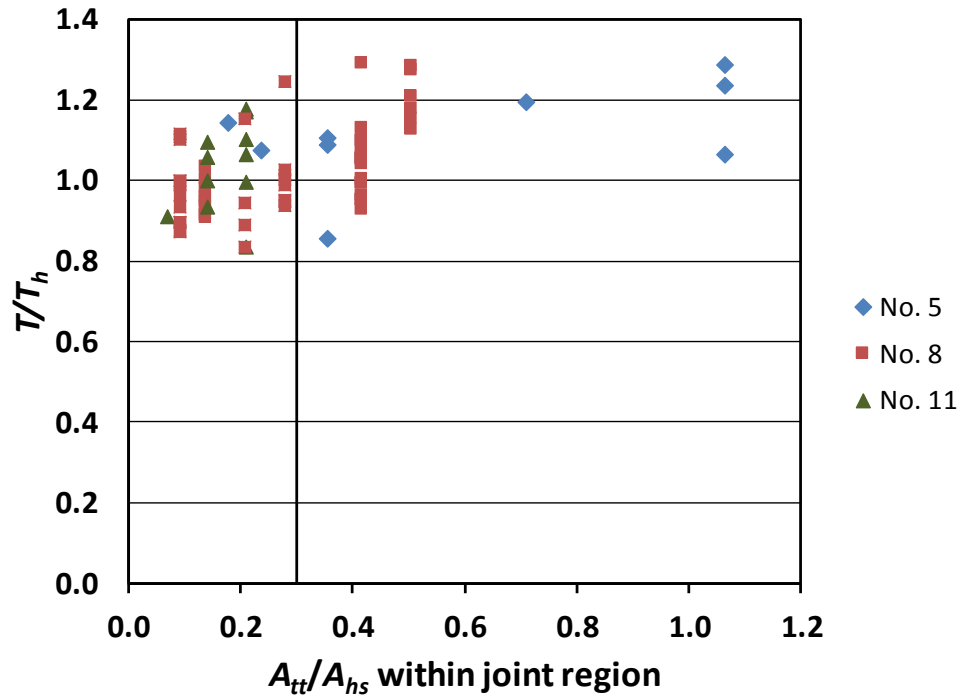
Figure 9.6 Ratio of T/T_h versus A_{tt}/A_{hs}, with T_h based on Eq. (7.9) with a limit on A_{tt}

A comparison of Figures 9.5 and 9.6 shows that, as expected, imposition of the 0.3 upper limit has the greatest effect on the specimens with the highest value of $A_{tt}/A_{hs.}$, three No. 5-bar

specimens with $A_{tt}/A_{hs} = 1.06$. These specimens experience the greatest increase in T/T_h, with an average $T/T_h = 1.19$, up from 0.95.

9.1.2.2 Confinement and spacing factor

The development length equation, Eq. (9.7), applies to widely-spaced bars. In practice, headed bars with a spacing of less than $8d_b$ are commonly used, especially in locations with congested reinforcement, such as beam-column joints. Therefore, it will be more convenient for designers to work with an equation for ℓ_{dt} based on closely spaced headed bars, allowing for a reduction in ℓ_{dt} for bars with wider spacing. As indicated by the trend line in Figure 9.3, without confining reinforcement, bars with a center-to-center spacing of $2d_b$ exhibit, on average, about one-half (51% by the trend line) of the anchorage strength of bars with a center-to-center spacing of $8d_b$ or greater. Based on this observation, Eq. (9.7) is multiplied by 2 to obtain an expression for bars spaced at $2d_b$, which accounts for the adverse effect of close spacing on the anchorage strength. For bars with a spacing greater than $2d_b$, a modification factor ψ_m is introduced in the development length equation.

$$\ell_{dt} = 0.002 \frac{f_y \psi_m \psi_r}{f_c'^{0.25}} d_b^{1.5} \tag{9.8}$$

where $\psi_m = \frac{1}{12}\left(14 - \frac{s}{d_b}\right) \geq 0.5$ for headed bars without confining reinforcement.

As shown by the trend line in Figure 9.4, the negative effect of close spacing is lower for headed bars with confining reinforcement than for bars without confining reinforcement. With confining reinforcement, bars with a center-to-center spacing of $2d_b$ exhibit, on average, about 65% of the anchorage strength of bars with a center-to-center spacing of $8d_b$ or greater. Since Eq. (9.8) is twice the value needed for bars with a spacing of $8d_b$, ψ_m must equal 0.5 for bars with confining reinforcement at $s = 8d_b$. In this case, ψ_m is approximated by

$\psi_m = \frac{1}{20}\left(18 - \frac{s}{d_b}\right) \geq 0.5$ for headed bars with confining reinforcement.

In cases where heads are placed in contact with adjacent bars (such as contact splices and staggered headed bars), the center-to-center spacing between the headed bars may be less than $2d_b$ (clear spacing less than $1d_b$). If the heads in contact with adjacent bars are round in shape and have

a net bearing area of $4A_b$ (minimum required area for HA heads), the center-to-center bar spacing will be about $1.62d_b$, corresponding to $\psi_m = 1.03$ without confining reinforcement. This value ($\psi_m = 1.03$) will decrease as head size increases. For simplification, ψ_m is taken as 1.0 in cases of $s < 2d_b$.

To simplify Eq. (9.8), the product of the modification factors $\psi_m\psi_r$ can be combined into a single modification factor ψ_{cs} that incorporates the effects of confining reinforcement and bar spacing, giving

$$\ell_{dt} = 0.002\frac{f_y\psi_{cs}}{f_c'^{0.25}}d_b^{1.5} \tag{9.9}$$

where ψ_{cs} is calculated using Eq. (9.10) for bars without confining reinforcement (in which case $\psi_r = 1.0$) and using Eq. (9.11) for bars with confining reinforcement.

$$\psi_{cs} = \psi_m = \frac{1}{12}\left(14 - \frac{s}{d_b}\right) \tag{9.10}$$

$$\psi_{cs} = \psi_m\psi_r = \frac{1}{20}\left(18 - \frac{s}{d_b}\right)\left(1 - \frac{48,000}{f_y}\frac{A_{tt}}{A_{hs}}d_b^{0.75}\right) \tag{9.11}$$

In Eq. (9.10) and (9.11), the limits on center-to-center spacing s ($s \leq 8d_b$, as set for ψ_m) and A_{tt}/A_{hs} ($A_{tt}/A_{hs} \leq 0.3$, as set for ψ_r) apply. To simplify ψ_{cs} for use in design, the value of d_b in the ψ_r term can be set to 1.0 (corresponding to a No. 8 bar). This simplification is slightly unconservative for bars smaller than No. 8, and slightly conservative for bars greater than No. 8. For No. 5 and No. 11 bars spaced at $2d_b$ with $f_y = 60$ ksi and $A_{tt}/A_{hs} = 0.3$, ψ_{cs} equals, respectively, 0.67 and 0.55, compared to $\psi_{cs} = 0.61$ for No. 8 bars. ℓ_{dt} will be about 10% shorter for No. 5 bars and about 10% longer for No. 11 bars than it would be without the simplification. These differences will decrease as bar spacing or yield strength (or both) increase. As will be demonstrated when the test results are compared with anchorage strengths corresponding to the final version of the design provisions, this simplification is safe. The values of ψ_{cs} based on Eq. (9.10) and (9.11), with $d_b = 1.0$ in the ψ_r term of Eq. (9.11), are shown in Table 9.2. In the table, values of ψ_{cs} for $f_y < 60,000$ psi are conservatively based on $f_y = 60,000$ psi.

213

Table 9.2 Modification factor ψ_{cs} for confining reinforcement and spacing[*]

Confinement level	f_y	s	
		$2d_b$	$\geq 8d_b$
$\dfrac{A_{tt}}{A_{hs}} \geq 0.3$	$\leq 60{,}000$	0.6	0.4
	$120{,}000$	0.7	0.45
No confining reinforcement	all	1.0	0.5

[*] ψ_{cs} is permitted to be linearly interpolated for values of A_{tt}/A_{hs} between 0 and 0.3 and for spacing s or yield strength of headed bar f_y intermediate to those in the table

9.1.2.3 Bar location factor

The beam-column joint specimens used to develop the descriptive (and design) equations had headed bars placed inside the column core, with a 2.5-in. minimum side cover to the bar. As suggested in Section 7.5, a 0.8 modification reduction factor is applied to the anchorage strength calculated based on the descriptive equations [Eq. (7.6) and (7.9)] except in cases where headed bars (1) terminate inside a confined column core with at least 2.5-in. side cover to the bar or (2) terminate in supporting members with at least $8d_b$ side cover to the bar.

For design, the 0.8 strength modification factor is converted to a development length modification factor ψ_o adding to the development length equation [Eq. (9.9)], giving

$$\ell_{dt} = 0.002 \frac{f_y \psi_{cs} \psi_o}{f_c'^{\,0.25}} d_b^{1.5} \tag{9.12}$$

ψ_o is taken as 1.0 for headed bars terminating inside a column core with clear side cover to the bar ≥ 2.5 in., or terminating in a supporting member with side cover to the bar $\geq 8d_b$; in other cases, ψ_o is taken as 1.25. The value $\psi_o = 1.25$ matches the findings by Sperry et al. (2015a) on hooked bars anchored in simulated beam-column joints, that "application of $\psi_o = 1.25$ results in values for hooked bars outside the column core that conservatively track the trend of those inside the column core."

9.1.2.4 Incorporation of strength reduction factor

Equation (9.12) for ℓ_{dt} is based on the simplified descriptive equation Eq. (9.3), with the incorporation of the effects of confining reinforcement, bar spacing and bar location. For use in

design, a strength reduction factor ϕ is needed to ensure a minimum probability of low strength. In the current case, the value of ϕ is selected so that not more than 5% of the specimens used to develop the equation will have a ratio of test-to-calculated failure load T/T_{calc} less than 1.0. Comparisons are made based on the data in Table B.1 in Appendix B. Using $\phi = 0.833$ gives

$$\ell_{dt} = 0.0024 \frac{f_y \Psi_{cs} \Psi_o}{f_c'^{0.25}} d_b^{1.5} \tag{9.13}$$

which results in 3.6% (five out of 138) of the comparisons with $T/T_{calc} < 1.0$.

Figures 9.7 and 9.8 show the ratio T/T_{calc} as a function of concrete compressive strength f_{cm} for the specimens used to develop the design equation. T is the peak load of a specimen divided by the number of headed bars. Figure 9.7 shows the results for the 64 specimens without confining reinforcement, with the statistical parameters (maximum, minimum, mean, STD, and COV) given in Table 9.3. The trend lines in Figure 9.7 are based on dummy variable analysis. The slightly downward sloping trend lines indicate that the effect of concrete compressive strength is slightly overestimated by the 0.25 power. The order of the lines shows that the design equation is more conservative for No. 5 bars than for No. 8 and No. 11 bars; however, no clear bias towards bar size is observed. The values of T/T_{calc} range from 0.85 to 1.61, with an average of 1.24 and a coefficient of variation of 0.130. Four out of 64 specimens had T/T_{calc} values below 1.0.
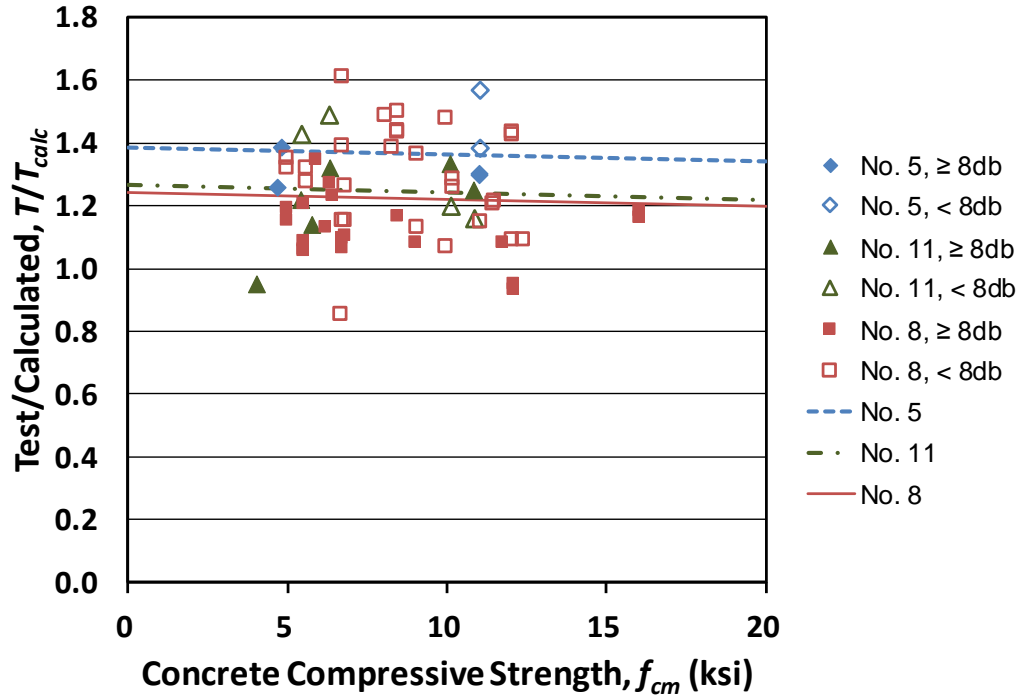
Figure 9.7 Ratio of test-to-calculated failure load T/T_{calc} for specimens without confining reinforcement versus concrete compressive strength f_{cm}, with T_{calc} based on Eq. (9.13) and Table 9.2

Table 9.3 Statistical parameters of T/T_{calc} for specimens without confining reinforcement, with T_{calc} based on Eq. (9.13) and Table 9.2

(Number of specimens)	All	Widely Spaced			Closely Spaced		
		No. 5	No. 8	No. 11	No. 5	No. 8	No. 11
	(64)	(4)	(20)	(6)	(2)	(28)	(4)
Max	1.61	1.39	1.35	1.33	1.57	1.61	1.49
Min	0.85	1.26	0.93	0.95	1.38	0.85	1.16
Mean	1.24	1.31	1.13	1.20	1.48	1.29	1.32
STD	0.161	0.053	0.099	0.142	0.130	0.167	0.164
COV	0.130	0.040	0.088	0.118	0.088	0.129	0.125
No. with $T/T_{calc} < 1.0$	4	0	2	1	0	1	0

Figure 9.8 shows the ratios of T/T_{calc} for the 74 specimens with confining reinforcement within the joint region, with statistical parameters (maximum, minimum, mean, STD, and COV) given in Table 9.4. In contrast to the results for the bars without confining reinforcement (Figure 9.7), the trend lines slope slightly upward in Figure 9.8, indicating that the effect of concrete compressive strength is slightly underestimated by the 0.25 power. The slightly downward and upward trend lines in Figures 9.7 and 9.8, however, indicate that the 0.25 power for concrete

216

compressive strength is suitable within the range of the test results. As seen in the results for the bars without confining reinforcement (Figure 9.7), the order of trend lines in Figure 9.8 (No. 5, No. 11, No. 8) indicates that the design equation is more conservative for No. 5 bars, but with no bar size bias. The values of T/T_{calc} range from 0.95 to 1.62, with an average of 1.28 and a coefficient of variation of 0.124. Only one out of 74 specimens had a T/T_{calc} value below 1.0 (T/T_{calc} = 0.95). Compared with the trend lines for $f_{su}/f_{s,ACI}$ shown in Figures 7.1 through 7.3, the trend lines for T/T_{calc} shown in Figures 7.7 and 7.8 are much less scattered and not in the order of bar size, indicating that the 1.5 power for d_b is more appropriate to characterize the effect of bar size on the anchorage strength of headed bars than the 1.0 power used in the development length equation in the current ACI Code.
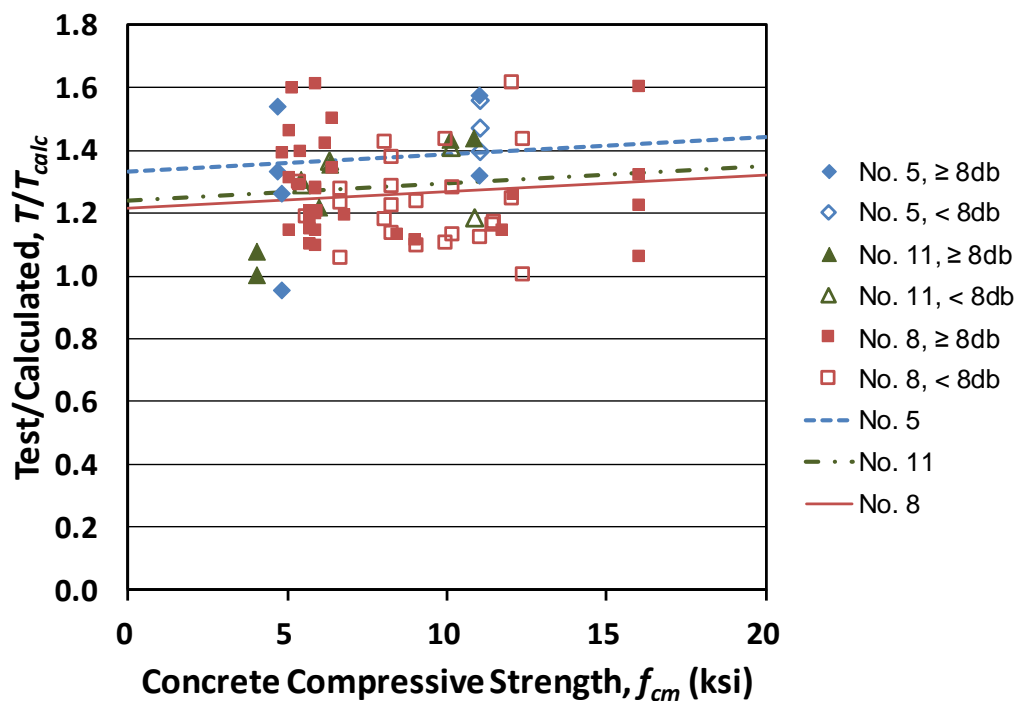
Figure 9.8 Ratio of test-to-calculated failure load T/T_{calc} for specimens with confining reinforcement versus concrete compressive strength f_{cm}, with T_{calc} based on Eq. (9.13) and Table 9.2

Table 9.4 Statistical parameters of T/T_{calc} for specimens with confining reinforcement, with T_{calc} based on Eq. (9.13) and Table 9.2

(Number of specimens)	All	Widely Spaced			Closely Spaced		
		No. 5	No. 8	No. 11	No. 5	No. 8	No. 11
	(74)	(6)	(30)	(7)	(3)	(24)	(4)
Max	1.62	1.58	1.61	1.44	1.56	1.62	1.41
Min	0.95	0.95	1.06	1.00	1.39	1.00	1.18
Mean	1.28	1.33	1.28	1.26	1.48	1.24	1.31
STD	0.158	0.224	0.158	0.170	0.081	0.142	0.098
COV	0.124	0.169	0.124	0.135	0.055	0.114	0.075
No. with $T/T_{calc} < 1.0$	1	1	0	0	0	0	0

Figure 9.9 compares the failure load T to the calculated load T_{calc} for the specimens used to develop the design equation. As shown in Tables 9.3 and 9.4, only five specimens out of 138 failed at lower loads than predicted by the design equation [Eq. (9.13)]. Overall, the average T/T_{calc} equals 1.26 for these 138 specimens used to develop the design equation.
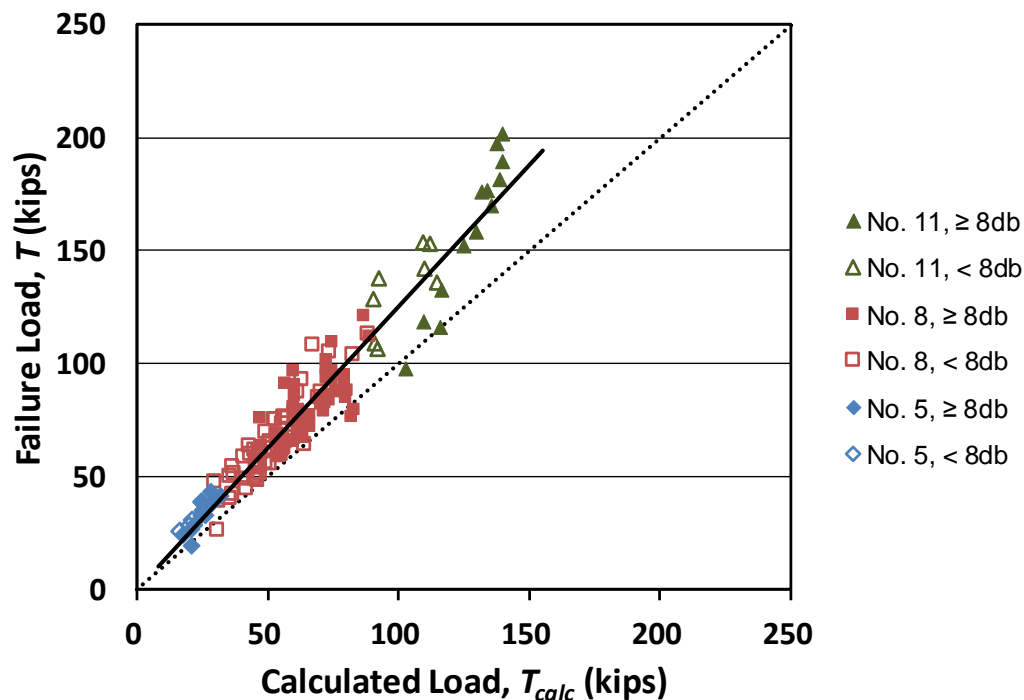
Figure 9.9 Test versus calculated failure load for the specimens used to develop design equation

9.1.2.5 Final equation

With ψ_e (for epoxy-coated or zinc and epoxy dual-coated bars) retained from the current Code provisions, the proposed development length equation for headed bars becomes:

$$\ell_{dt} = \left(0.0024 \frac{f_y \Psi_e \Psi_{cs} \Psi_o}{f_c'^{0.25}} \right) d_b^{1.5} \tag{9.1}$$

as described in Section 9.1

The proposed design equation is similar in form to that proposed for the development length of hooked bars by Sperry et al. (2015a).

$$\ell_{dh} = \left(\frac{f_y \Psi_e \Psi_r \Psi_m \Psi_o}{500 \lambda f_c'^{0.25}} \right) d_b^{1.5} \tag{9.14}$$

In both equations, the development length is a function of the yield strength of the bar f_y, f_c' raised to 0.25 power, and d_b raised to 1.5 power. This similarity is based on a strong similarity in the effects of these parameters on the strength of hooked and headed bars. In Eq. (9.14), λ is a modification factor for lightweight concrete retained from the current ACI 318-14 criteria for hooked bars. ψ_r is a modification factor for the effect of confining reinforcement, and ψ_m is a modification factor for the effect of bar spacing. In Eq. (9.1), the effects of confining reinforcement and bar spacing are represented by a single modification factor ψ_{cs}, with values given in Table 9.2 as a function of the specified yield strength f_y and the minimum center-to-center spacing s of the headed bars, and the ratio A_{tt}/A_{hs}. As noted in the table, values of ψ_{cs} may be interpolated for intermediate values of f_y, s, and A_{tt}/A_{hs}.

To evaluate the proposed design equation, the test results of beam-column joint, CCT node, shallow-embedment, and lap splice specimens in the current study and from previous studies, are compared with the design equation [Eq. (9.1)] in Sections 9.2 through 9.5. The same tests have been compared with the descriptive equations in Chapters 7 and 8. For each comparison, the anchorage strength predicted by the design equation T_{calc} is calculated using the measured values of concrete compressive strength and embedment length (or nominal values if measured values were not provided for previous studies), with the application of modification factors as appropriate. T_{calc} is derived from Eq. (9.1) and given by:

$$T_{calc} = \frac{\ell_{eh} f_{cm}^{0.25} A_b}{0.0024 \psi_e \psi_{cs} \psi_o d_b^{1.5}} \tag{9.15}$$

where ℓ_{eh} = embedment length (in.), f_{cm} = measured concrete compressive strength (psi); ψ_e = modification factor for epoxy-coated or zinc and epoxy dual-coated bars; ψ_{cs} = modification factor for confining reinforcement and bar spacing, in accordance with Table 9.2; ψ_o = modification factor for bar location; d_b = diameter of the headed bar (in.); and A_b = area of the headed bar (in.^{2}).

9.2 COMPARISON OF DESIGN EQUATION FOR BEAM-COLUMN JOINT TESTS

9.2.1 Beam-Column Joint Tests in Current Study

During the incorporation of strength reduction factor described in Section 9.1.2.4, the test results of the specimens used to develop the design equation are compared with the calculated failure loads based on Eq. (9.13). Equation (9.13) differs from the final version of the design equation [Eq. (9.1)] only in the absence of the modification factor ψ_e. As the headed bars tested in this study were uncoated, the factor ψ_e equals 1.0 and thus the comparisons presented in Section 9.1.2.4 will not be affected.

This section addresses the headed bars with large obstructions that were used to develop the design equation, and the headed bars with large heads (net bearing area $A_{brg} > 12A_b$) or with a large d_{eff}/ℓ_{eh} ratio, that were not used to develop the design equation.

9.2.1.1 Headed bars with large obstructions

The specimens used for the development of the design equation included headed bars with large obstructions (O4.5 and O9.1), based on the analysis in Section 7.4.3 that shows that headed bars with non-HA heads have similar anchorage strengths to those with HA heads. The O12.9 heads with both large obstruction and large head size were not included to develop the design equation and are discussed separately in Section 9.2.1.2. To determine if the non-HA heads could be safely used in design, the failure loads T for the specimens used to develop the design equation are compared with the calculated loads T_{calc} in Figure 9.10, with the data points for the non-HA heads represented by circles. Table 9.5 shows the comparisons with the design equation for the non-HA heads, along with the net bearing area expressed as a multiple of bar area, embedment

length ℓ_{eh} ($\ell_{eh,avg}$ in Table B.1 in Appendix B), and the measured concrete compressive strength f_{cm}.
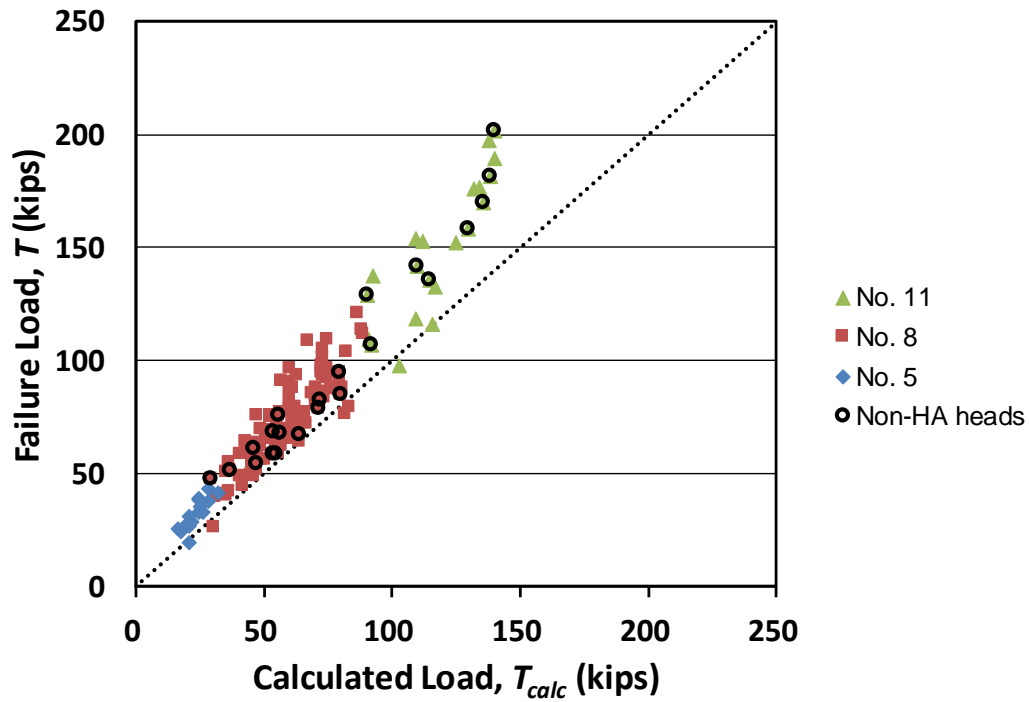
Figure 9.10 Test versus calculated failure load for the specimens with HA and non-HA heads that were used to develop design equation

In Figure 9.10, all of the non-HA heads exhibited higher anchorage strengths than predicted by the design equation. The values of T/T_{calc} for the non-HA heads shown in Table 9.5 range from 1.06 to 1.61, with an average of 1.24, virtually identical to the value of $T/T_{calc} = 1.26$ for the specimens used to develop the design equation. This indicates that the non-HA heads used in this study can be safely used with the proposed design provisions.

Table 9.5 Test results for non-HA heads and comparisons with design equation [Eq. (9.1)]

Specimen	Net Bearing Area[*]	ℓ_{eh} (in.)	f_{cm} (psi)	T (kips)	T/T_{calc}
(2@9)8-8-O4.5-0-i-2.5-3-9.5		9.00	6710	58.8	1.10
(2@7)8-8-O4.5-0-i-2.5-3-9.5		9.25	6710	54.5	1.15
(2@5)8-8-O4.5-0-i-2.5-3-9.5		9.00	6710	51.2	1.39
(2@3)8-8-O4.5-0-i-2.5-3-9.5		9.00	6710	47.7	1.61
8-5-O4.5-0-i-2.5-3-11.25		11.25	5500	67.4	1.06
8-5-O4.5-0-i-2.5-3-14.25	$4.5A_b$	14.13	5500	85.0	1.06
8-8-O4.5-0-i-2.5-3-9.5		9.19	6710	58.4	1.07
(3@5.35)11-12-O4.5-0-i-2.5-3-16.75		16.92	10860	106.8	1.16
(3@5.35)11-5-O4.5-0-i-2.5-3-19.25		19.50	5430	128.7	1.43
11-12-O4.5-0-i-2.5-3-16.75		17.13	10860	169.6	1.25
11-5-O4.5-0-i-2.5-3-19.25		19.44	5430	157.9	1.22
8-5-O9.1-0-i-2.5-3-14.5		14.38	4970	94.8	1.19
(3@5.5)8-5-O9.1-0-i-2.5-3-14.5	$9.1A_b$	14.35	4960	75.7	1.35
(4@3.7)8-5-O9.1-0-i-2.5-3-14.5		14.06	5570	61.2	1.32
8-5-O4.5-2#3-i-2.5-3-9.25		9.38	5750	67.9	1.20
8-5-O4.5-2#3-i-2.5-3-12.25		12.00	5750	78.5	1.10
8-5-O4.5-5#3-i-2.5-3-8.25		8.00	5900	68.4	1.28
8-5-O4.5-5#3-i-2.5-3-11.25		11.13	5900	82.2	1.14
(3@5.35)11-12-O4.5-6#3-i-2.5-3-16.75	$4.5A_b$	17.00	10860	135.8	1.18
(3@5.35)11-5-O4.5-6#3-i-2.5-3-19.25		19.38	5430	141.7	1.29
11-12-O4.5-6#3-i-2.5-3-16.75		16.81	10860	201.5	1.44
11-5-O4.5-6#3-i-2.5-3-19.25		19.63	5430	181.4	1.31
Mean					**1.24**

[*] Net bearing area is taken as the difference between the gross area of the head and the area of obstruction adjacent to the head. Refer to Table 2.1

9.2.1.2 Headed bars with large heads

In Section 7.4.2, the anchorage strengths of the headed bars with large heads (No. 5 F13.1, No. 8 S14.9, and No. 8 O12.9; $A_{brg} > 12A_b$) are compared with the descriptive equations, and it was found that the bars with large heads exhibited higher anchorage strengths on average than the strengths for the bars with smaller heads ($A_{brg} \leq 9.5A_b$). The test results for these large heads are compared with the design equation [Eq. (9.1)] in Figure 9.11 using circles. Figure 9.11 also includes the specimens that are used to develop Eq. (9.1) and a solid line that represents the best fit for the data for these specimens. Table 9.6 shows the comparisons for the large heads, along with the net bearing area, embedment length ℓ_{eh} ($\ell_{eh,avg}$ in Table B.1 in Appendix B), and the measured concrete compressive strength f_{cm}.
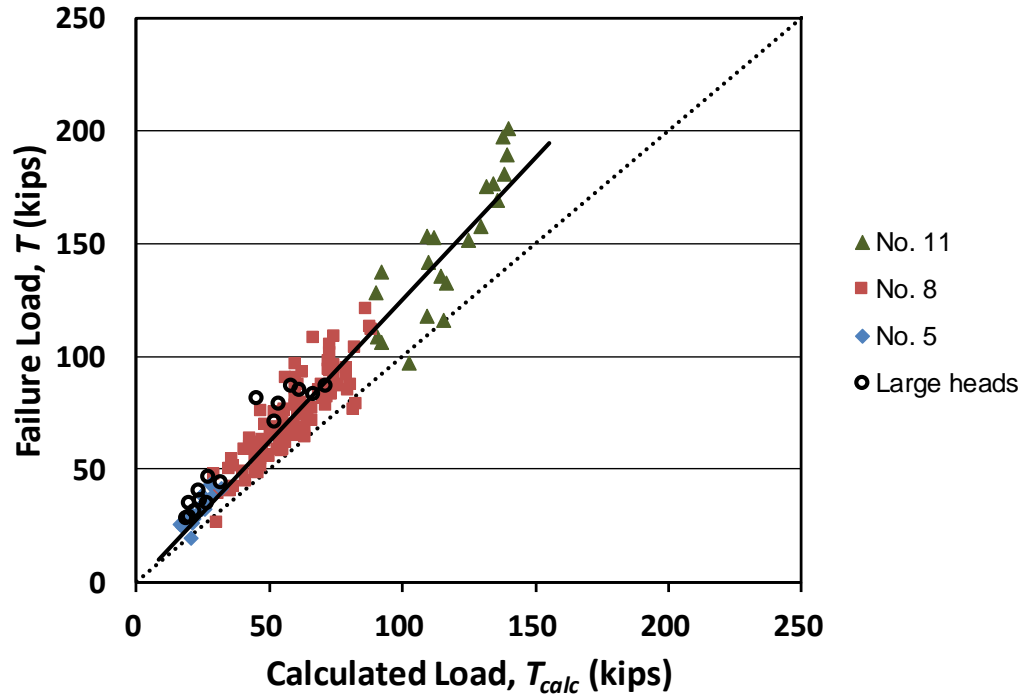
Figure 9.11 Test versus calculated failure load for specimens used to develop design equation and specimens with large heads

Table 9.6 Test results for large heads and comparisons with design equation [Eq. (9.1)]

Specimen	Net Bearing Area*	ℓ_{eh} (in.)	f_{cm} (psi)	T (kips)	T/T_{calc}
8-15-S14.9-0-i-2.5-3-9.5	$14.9A_b$	9.69	16030	87.1	1.21
8-8-O12.9-0-i-2.5-3-9.5	$12.9A_b$	9.69	8800	85.2	1.38
8-8-S14.9-0-i-2.5-3-8.25	$14.9A_b$	8.25	8800	70.9	1.35
5-5-F13.1-0-i-2.5-5-4	$13.1A_b$	4.41	4810	28.2	1.47
5-5-F13.1-0-i-2.5-3-6	$13.1A_b$	6.22	4690	35.3	1.31
5-12-F13.1-0-i-2.5-5-4	$13.1A_b$	4.13	11030	31.4	1.42
5-12-F13.1-0-i-2.5-3-6	$13.1A_b$	6.03	11030	44.2	1.37
8-15-S14.9-2#3-i-2.5-3-7	$14.9A_b$	7.00	16030	79.3	1.47
8-15-S14.9-5#3-i-2.5-3-5.5	$14.9A_b$	5.50	16030	81.4	1.78
8-8-O12.9-5#3-i-2.5-3-9.5	$12.9A_b$	9.38	8800	83.5	1.25
8-8-S14.9-5#3-i-2.5-3-8.25	$14.9A_b$	8.25	8800	87.0	1.49
5-5-F13.1-2#3-i-2.5-5-4	$13.1A_b$	4.09	4810	28.9	1.42
5-5-F13.1-5#3-i-2.5-5-4	$13.1A_b$	4.19	4690	35.2	1.75
5-5-F13.1-2#3-i-2.5-3-6	$13.1A_b$	5.94	4690	46.4	1.69
5-12-F13.1-2#3-i-2.5-5-4	$13.1A_b$	4.09	11030	36.3	1.50
5-12-F13.1-5#3-i-2.5-5-4	$13.1A_b$	4.13	11030	40.3	1.68
Mean					**1.47**

* Net bearing area of O12.9 is taken as the difference between the gross area of the head and the area of obstruction adjacent to the head. Refer to Table 2.1

Of the 16 data points for large heads shown in Figure 9.11, 14 are above the best-fit line for the data used to establish Eq. (9.1) and two are on the best-fit line, indicating that the anchorage strengths of the bars with large heads were generally higher than the anchorage strengths of the bars with smaller heads. The values of T/T_{calc} for the large heads shown in Table 9.6 range from 1.21 to 1.78, with an average of 1.47, about 17% greater than the average (1.26) for the data used to establish Eq. (9.1), and with a coefficient of variation of 0.117. To take advantage of additional strength obtained with larger head size, a 0.9 modification factor could be safely applied to the development length for headed bars with $A_{brg} > 12A_b$.

9.2.1.3 Headed bars with large h_{cl}/ℓ_{eh} ratio

As demonstrated in Section 7.4.4.1, the headed bars with $h_{cl}/\ell_{eh} \geq 1.33$ generally exhibit lower anchorage strengths than the headed bars with $h_{cl}/\ell_{eh} < 1.33$ when compared to the descriptive equations. The term h_{cl}/ℓ_{eh} is the ratio of the distance from the center of the bar to the top of bearing member to the embedment length. The ratio $h_{cl}/\ell_{eh} = 1.33$ corresponds to a ratio d_{eff}/ℓ_{eh} of approximately 1.5 (demonstrated in Section 7.4.4.2), a value matches the Commentary of ACI 318-14 regarding the potential of a breakout failure and the suggestion of use of strut-and-tie models for cases of $d/\ell_{dt} > 1.5$. For headed bars terminating at the far face of the column, a large h_{cl}/ℓ_{eh} (or d_{eff}/ℓ_{eh}) ratio indicates a deeper beam-column joint.

As described in Section 7.4.4.1, all but five specimens with $h_{cl}/\ell_{eh} \geq 1.33$ were excluded from the development of the descriptive equations (and thus the design equation). For the headed bars with $h_{cl}/\ell_{eh} \geq 1.33$ and not used to develop the design equation, the anchorage strengths T are compared with the calculated strengths T_{calc} in Figure 9.12, represented by open symbols. Table 9.7 shows these comparisons, along with the embedment length ℓ_{eh} ($\ell_{eh,avg}$ in Table B.1 in Appendix B), the ratio h_{cl}/ℓ_{eh}, and the measured concrete compressive strength f_{cm}.
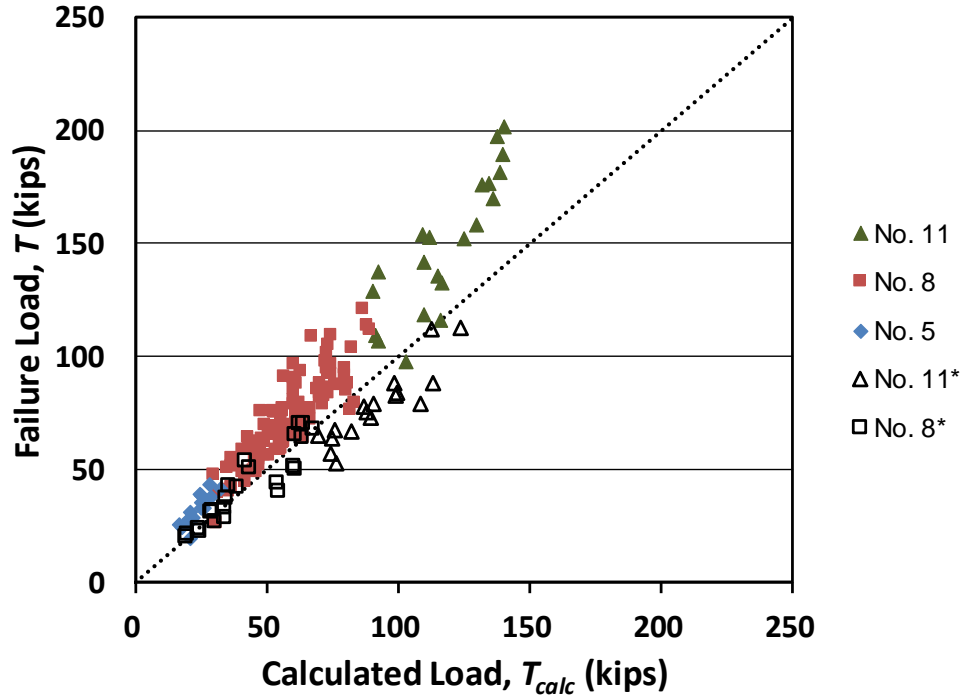
*Specimens with $h_{cl}/\ell_{eh} \geq 1.33$ and not used to develop the design equation

Figure 9.12 Test versus calculated failure load for specimens with $A_{brg} \leq 9.5A_b$

As shown in Figure 9.12, the 17 specimens containing No. 11 headed bars with $h_{cl}/\ell_{eh} \geq$ 1.33 (represented by open triangles) exhibited lower failure loads than predicted by the design equation, with only one specimen having $T/T_{calc} = 1.0$. Of the 23 specimens containing No. 8 headed bars with $h_{cl}/\ell_{eh} \geq 1.33$ (represented by open squares), eight specimens exhibited lower failure loads than predicted by Eq. (9.1). The data in Table 9.7 show that, of the 18 specimens without confining reinforcement, 15 specimens had $T/T_{calc} < 1.0$; of the 22 specimens with confining reinforcement, nine specimens had $T/T_{calc} < 1.0$. Overall, for the specimens without and with confining reinforcement, the values of T/T_{calc} equal 0.88 and 1.01, respectively. These values suggest that confining reinforcement improves the anchorage strength for headed bars with large h_{cl}/ℓ_{eh} (d_{eff}/ℓ_{eh}) ratios, and that use of the design equation [Eq. (9.1)] would be unconservative for these headed bars.

Table 9.7 Test results for specimens with $h_{cl}/\ell_{eh} \geq 1.33$ and not used to develop Eq. (9.1) and comparisons with Eq. (9.1)

	Specimen	ℓ_{eh} (in.)	h_{cl}/ℓ_{eh}	f_{cm} (psi)	T (kips)	T/T_{calc}
Group 12	(3@3)8-5-F4.1-0-i-2.5-7-6	6.19	1.62	4930	20.6	1.09
	(3@5)8-5-F4.1-0-i-2.5-7-6	6.33	1.58	4930	23.9	1.01
	(3@7)8-5-F4.1-0-i-2.5-7-6	6.25	1.60	4940	27.1	0.91
	(3@5.5)8-5-F9.1-0-i-2.5-7-6	6.21	1.61	5160	23.0	0.94
	(4@3.7)8-5-T9.5-0-i-2.5-7-6	6.13	1.63	5160	21.7	1.10
	8-5-F4.1-0-i-2.5-7-6	6.09	1.64	4930	28.7	0.85
	8-5-F9.1-0-i-2.5-7-6	6.13	1.63	4940	33.4	0.99
	(3@3)8-5-F4.1-5#3-i-2.5-7-6	6.00	1.67	4930	32.1	1.11
	(3@5)8-5-F4.1-5#3-i-2.5-7-6	6.29	1.59	4930	37.5	1.09
	(3@7)8-5-F4.1-5#3-i-2.5-7-6	6.10	1.64	4940	42.3	1.10
	(3@5.5)8-5-F9.1-5#3-i-2.5-7-6	6.25	1.60	5160	43.1	1.22
	(4@3.7)8-5-F9.1-5#3-i-2.5-7-6	6.03	1.66	5160	31.6	1.12
	8-5-F4.1-5#3-i-2.5-7-6	6.25	1.60	4930	50.7	1.18
	8-5-F9.1-5#3-i-2.5-7-6	6.16	1.62	4940	53.8	1.29
Group 15	11-5a-F3.8-0-i-2.5-3-12	12.00	1.63	3960	56.8	0.77
	11-5a-F8.6-0-i-2.5-3-12	12.13	1.61	3960	63.8	0.85
	11-5a-F3.8-2#3-i-2.5-3-12	12.00	1.63	3960	67.3	0.89
	11-5a-F3.8-6#3-i-2.5-3-12	12.09	1.61	3960	78.0	0.90
	11-5a-F8.6-6#3-i-2.5-3-12	12.56	1.55	4050	79.2	0.88
Group 16	8-8-F4.1-0-i-2.5-3-10-DB	9.88	1.97	7410	50.2	0.83
	8-8-F9.1-0-i-2.5-3-10-DB	9.81	1.99	7410	51.8	0.86
	8-5-F4.1-0-i-2.5-3-10-DB	9.88	1.97	4880	40.6	0.75
	8-5-F9.1-0-i-2.5-3-10-DB	9.75	2.00	4880	44.4	0.83
	8-8-F9.1-5#3-i-2.5-3-10-DB	9.63	2.03	7410	68.2	1.01
	8-5-F4.1-3#4-i-2.5-3-10-DB	10.13	1.93	4880	64.6	1.02
	8-5-F9.1-3#4-i-2.5-3-10-DB	9.75	2.00	4880	65.8	1.08
	8-5-F4.1-5#3-i-2.5-3-10-DB	10.19	1.91	4880	70.2	1.10
	8-5-F9.1-5#3-i-2.5-3-10-DB	9.94	1.96	4880	70.5	1.13
Group 17	11-8-F3.8-0-i-2.5-3-14.5	14.50	1.34	8660	79.1	0.73
	(3@5.35)11-8-F3.8-0-i-2.5-3-14.5	14.63	1.33	8720	52.9	0.69
	11-8-F3.8-2#3-i-2.5-3-14.5	14.69	1.33	8660	88.4	0.78
	(3@5.35)11-8-F3.8-2#3-i-2.5-3-14.5	14.54	1.34	8720	72.6	0.81
	11-8-F3.8-6#3-i-2.5-3-14.5	14.69	1.33	8660	112.7	0.91
	(3@5.35)11-8-F3.8-6#3-i-2.5-3-14.5	14.92	1.31	8720	83.7	0.84
Group 18	11-5-F3.8-0-i-2.5-3-12	12.13	1.61	5760	66.5	0.81
	11-5-F8.6-0-i-2.5-3-14.5	14.50	1.34	5970	82.8	0.84
	(3@5.35)11-5-F8.6-0-i-2.5-3-14.5	14.71	1.33	6240	65.1	0.94
	11-5-F3.8-6#3-i-2.5-3-12	12.50	1.56	5760	88.3	0.90
	11-5-F8.6-6#3-i-2.5-3-14.5	14.63	1.33	5970	112.3	1.00
	(3@5.35)11-5-F8.6-6#3-i-2.5-3-14.5	14.54	1.34	6240	75.6	0.86
Mean (without confining reinforcement)						**0.88**
Mean (with confining reinforcement)						**1.01**

As stated at the beginning of this section, d_{eff}/ℓ_{eh} approximates 1.5 for $h_{cl}/\ell_{eh} = 1.33$, while d_{eff}/ℓ_{eh} can be considered equivalent to d/ℓ_{dt} for design. For cases of $\ell_{dt} < d/1.5$, Commentary Section R25.4.4.2 of ACI 318-14 suggests that "providing reinforcement in the form of hoops and ties to establish a load path in accordance with strut-and-tie modeling principles"; in response to this suggestion, the anchorage strengths of the headed bars with confining reinforcement listed in Table 9.7 are examined using strut-and-tie modeling approach.

The headed bars in Table 9.7 had different amounts of confining reinforcement, from two No. 3 to six No. 3 hoops. For simplicity, it is assumed that all the hoops within the clear span between the headed bars and the top of the bearing member (not the effective confining reinforcement represented by A_{tt} shown in Table 9.2) serve as a single tie located in the middle of the joint. Thus a fraction of the total load (T_{total}) applied on the headed bars is transferred through a strut oriented at an angle θ from horizontal to the single tie assumed to be at mid-depth and, through a second diagonally oriented strut, to the bearing member, as shown in Figure 9.13. The fraction of the total load transferred through the joint equals the reaction from the bearing member R_1 (calculated based on a simply-supported model). In design of a joint, the tensile force in the headed bars would normally equal the compressive force in the compression zone of the beam; however, use of R_1 is more accurate for evaluating the specimens described herein because of the boundary conditions used for testing. Also, using R_1 rather than T_{total} produces a conservative result. With this approach, the anchorage strength of the headed bars is found to be controlled by the strength of the tie $f_{yt}A_v$ (f_{yt} is the yield strength of the hoops, and A_v is the total cross-sectional area of the single tie), rather than the strut or the nodal zone. Comparisons with strut-and-tie modeling for these specimens are shown in Table 9.8, including the reaction from the bearing member R_1, total cross-sectional area of the single tie A_v, failure load predicted by strut-and-tie modeling T_{STM} (equal to $f_{yt}A_v$), and the ratio of test-to-predicted failure load R_1/T_{STM}.
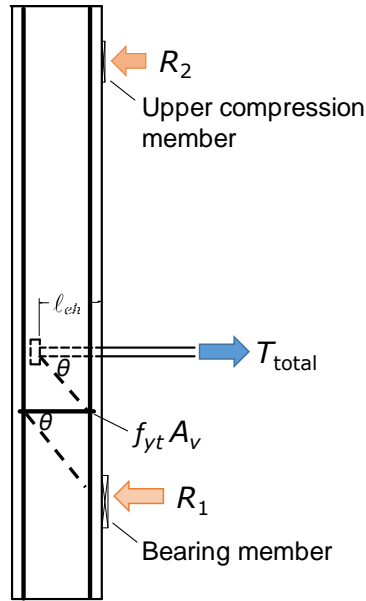
Figure 9.13 Load transfer through strut-and-tie mechanism

Table 9.8 Comparisons with strut-and-tie modeling for specimens with large h_{cl}/ℓ_{eh} ratio

Specimen	R_1 (kips)	A_v (in.²)	T_{STM} (kips)[*]	R_1/T_{STM}
(3@3)8-5-F4.1-5#3-i-2.5-7-6	57.5	0.66	45.1	1.27
(3@5)8-5-F4.1-5#3-i-2.5-7-6	67.2	0.66	45.1	1.49
(3@7)8-5-F4.1-5#3-i-2.5-7-6	75.7	0.66	45.1	1.68
(3@5.5)8-5-F9.1-5#3-i-2.5-7-6	77.3	0.66	45.1	1.71
(4@3.7)8-5-F9.1-5#3-i-2.5-7-6	75.5	0.66	45.1	1.67
8-5-F4.1-5#3-i-2.5-7-6	60.5	0.66	45.1	1.34
8-5-F9.1-5#3-i-2.5-7-6	64.3	0.66	45.1	1.42
11-5a-F3.8-2#3-i-2.5-3-12	89.1	0.44	30.1	2.96
11-5a-F3.8-6#3-i-2.5-3-12	103.3	1.1	75.2	1.37
11-5a-F8.6-6#3-i-2.5-3-12	104.9	1.1	75.2	1.39
8-8-F9.1-5#3-i-2.5-3-10-DB	90.4	0.88	60.2	1.50
8-5-F4.1-3#4-i-2.5-3-10-DB	85.5	0.8	54.7	1.56
8-5-F9.1-3#4-i-2.5-3-10-DB	87.1	0.8	54.7	1.59
8-5-F4.1-5#3-i-2.5-3-10-DB	92.9	0.88	60.2	1.54
8-5-F9.1-5#3-i-2.5-3-10-DB	93.3	0.88	60.2	1.55
11-8-F3.8-2#3-i-2.5-3-14.5	117.1	0.44	30.1	3.89
(3@5.35)11-8-F3.8-2#3-i-2.5-3-14.5	144.1	0.44	30.1	4.79
11-8-F3.8-6#3-i-2.5-3-14.5	149.2	1.1	75.2	1.98
(3@5.35)11-8-F3.8-6#3-i-2.5-3-14.5	166.2	1.1	75.2	2.21
11-5-F3.8-6#3-i-2.5-3-12	116.8	1.1	75.2	1.55
11-5-F8.6-6#3-i-2.5-3-14.5	148.7	1.1	75.2	1.98
(3@5.35)11-5-F8.6-6#3-i-2.5-3-14.5	150.2	1.1	75.2	2.00

[*] $T_{STM} = f_{yt}A_v$, with $f_{yt} = 68.4$ ksi

The ratios of R_1/T_{STM} shown in Table 9.8 range from 1.27 to 4.79, with an average of 1.93, indicating that the strut-and-tie modeling provides a conservative estimate of the anchorage strength of headed bars terminating in beam-column joints with $h_{cl}/\ell_{eh} \geq 1.33$ (or $\ell_{dt} \leq d/1.5$). As the design equation [Eq. (9.1)] is found to be unconservative dealing with the cases of $\ell_{dt} \leq d/1.5$, the design provisions are revised for use of headed bars in beam-column joints: If ℓ_{dt} calculated using Eq. (9.1) is less than or equal to $d/1.5$, transverse reinforcement in the form of hoops and ties should be provided to establish a load path in accordance with strut-and-tie modeling principles (as stated in Commentary Section R25.4.4.2 of ACI 318-14).

9.2.2 Bashandy (1996)

In Section 8.2.1, five specimens without confining reinforcement tested by Bashandy (1996) are compared with the descriptive equation [Eq. (7.6)], and it was found that Specimens T4 exhibited a low failure load possibly due to its large h_{cl}/ℓ_{eh} (d_{eff}/ℓ_{eh}) ratio. These five specimens are compared with the design equation in Table 9.9, along with the bar size, embedment length ℓ_{eh}, the ratios h_{cl}/ℓ_{eh} and d_{eff}/ℓ_{eh}, concrete compressive strength f_{cm}, and the center-to-center spacing in terms of bar diameter s/d_b.

Table 9.9 Test results for beam-column joint specimens tested by Bashandy (1996) and comparisons with design equation [Eq. (9.1)]

Specimen	Bar Size	ℓ_{eh}* (in.)	h_{cl}/ℓ_{eh}	d_{eff}/ℓ_{eh}	f_{cm}* (psi)	s/d_b	T* (kips)	T_{calc} (kips)	T/T_{calc}
T1	No. 11	11.0	1.00	1.27	3870	3.3	51.0	37.7	1.35
T2	No. 11	11.0	1.00	1.25	4260	3.3	49.9	38.6	1.29
T3	No. 11	11.2	0.98	1.24	4260	3.3	52.2	39.3	1.33
T4	No. 8	8.3	1.32	1.47	3870	5.0	21.1	28.8	0.73
T5	No. 11	11.0	1.00	1.23	3260	3.3	37.5	36.1	1.04

*Values are converted SI (1 in. = 25.4 mm; 1 psi = 1/145 MPa; and 1 kip = 4.44822 kN)

As expected, all specimens but T4 had higher failure loads than predicted by the design equation, with values of T/T_{calc} ranging from 1.04 to 1.35 with an average T/T_{calc} of 1.25. Specimen T4 with $d_{eff}/\ell_{eh} = 1.47$ exhibited only 73% of the predicted failure load. Although the ratio $d_{eff}/\ell_{eh} = 1.47$ is below the threshold value $d/\ell_{dt} = 1.5$ proposed for design, it matches the observation for the beam-column joint tests in this study that the value $d_{eff}/\ell_{eh} = 1.5$ is not precise and a somewhat

smaller value may be appropriate (Section 8.2.1). According to the discussion in Section 9.2.1.3, it is suggested that confining reinforcement is needed in Specimen T4 to ensure adequate anchorage strength and that strut-and-tie modeling is used to check this specimen with confining reinforcement provided.

9.2.3 Chun et al. (2009)

As discussed in Section 8.2.2, the 24 beam-column joint specimens with a single bar and no confining reinforcement tested by Chun et al. (2009) exhibited only 65% (on average) of the failure loads predicted by the descriptive equation [Eq. (7.6)]. Reasons for the low failure loads obtained with these specimens are most likely: (1) the heads used in the tests had obstructions that reduce the actual net bearing areas to approximately $2.8A_b$ (illustrated in Figure 8.1), though the heads met the current dimensional requirement for HA heads in ASTM A970; and (2) the descriptive equations, which are developed based on the test results of beam-column joint specimens containing at least two headed bars, along with the value of center-to-center bar spacing (s = column width) may not apply to these single-bar specimens.

The failure loads of these 24 beam-column joint specimens are compared with the design equation [Eq. (9.1)] in Table 9.10, along with the bar size, embedment length ℓ_{eh}, the ratios h_{cl}/ℓ_{eh} and d_{eff}/ℓ_{eh}, and the concrete compressive strength f_{cm}. For consistency, the center-to-center bar spacing s used to determine ψ_{cs} in Table 9.2 is taken as the column width $6d_b$. The comparisons shown in the table are within expectations: 20 specimens out of 24 had values of $T/T_{calc} < 1.0$. For the four specimens with $T/T_{calc} \geq 1.0$, the maximum value of T/T_{calc} equals 1.14 and the average value is 1.07, much lower than the average value (1.26) for the specimens used to develop the design equation. The values of T/T_{calc} do not appear much different for the specimens with $d_{eff}/\ell_{eh} > 1.5$ and those with $d_{eff}/\ell_{eh} < 1.5$, which is also as expected. Although these data suggest that the design equation predicts unconservative estimate of anchorage strengths for these headed bars, the type of heads used in the tests provide useful information for proposing a revision of HA head requirements in ASTM A970, which is discussed in Section 9.6.

Table 9.10 Test results for beam-column joint specimens tested by Chun et al. (2009) and comparisons with design equation [Eq. (9.1)]

Specimen	Bar Size	ℓ_{eh} (in.)	h_{cl}/ℓ_{eh}	d_{eff}/ℓ_{eh}	f_{cm} (psi)	T (kips)	T_{calc} (kips)	T/T_{calc}
No. 8-M-0.9L-(1)	No. 8	10.4	1.05	1.21	3640	27.9	39.9	0.70
No. 8-M-0.9L-(2)		10.4	1.05	1.22	3640	28.6	39.9	0.72
No. 8-M-0.7L-(1)		8.3	1.31	1.52	3640	27.4	31.8	0.86
No. 8-M-0.7L-(2)		8.3	1.31	1.53	3640	28.5	31.8	0.90
No. 8-M-0.7L-2R-(1)		8.3	1.31	1.53	3640	31.8	31.8	1.00
No. 8-M-0.7L-2R-(2)		8.3	1.31	1.53	3640	32.6	31.8	1.02
No. 8-M-0.5L-(1)		6.3	1.73	1.89	3640	16.4	24.2	0.68
No. 8-M-0.5L-(2)		6.3	1.73	1.94	3640	21.1	24.2	0.87
No. 11-M-0.9L-(1)	No. 11	14.6	0.99	1.15	3570	51.4	65.7	0.78
No. 11-M-0.9L-(2)		14.6	0.99	1.15	3570	52.4	65.7	0.80
No. 11-M-0.7L-(1)		11.6	1.25	1.42	3570	43.3	52.2	0.83
No. 11-M-0.7L-(2)		11.6	1.25	1.41	3570	41.6	52.2	0.80
No. 11-M-0.7L-2R-(1)		11.6	1.25	1.47	3570	59.1	52.2	1.13
No. 11-M-0.7L-2R-(2)		11.6	1.25	1.45	3570	51.1	52.2	0.98
No. 11-M-0.5L-(1)		8.5	1.71	1.94	3570	43.7	38.3	1.14
No. 11-M-0.5L-(2)		8.5	1.71	1.89	3570	34.3	38.3	0.90
No. 18-M-0.9L-(1)	No. 18	35.0	0.96	1.08	3510	157.7	198.6	0.79
No. 18-M-0.9L-(2)		35.0	0.96	1.08	3510	155.8	198.6	0.78
No. 18-M-0.7L-(1)		26.9	1.25	1.35	3510	97.6	152.7	0.64
No. 18-M-0.7L-(2)		26.9	1.25	1.35	3510	99.8	152.7	0.65
No. 18-M-0.7L-2R-(1)		26.9	1.25	1.37	3510	110.6	152.7	0.72
No. 18-M-0.7L-2R-(2)		26.9	1.25	1.37	3510	115.8	152.7	0.76
No. 18-M-0.5L-(1)		18.9	1.78	1.88	3510	69.6	107.3	0.65
No. 18-M-0.5L-(2)		18.9	1.78	1.88	3510	69.5	107.3	0.65

9.3 COMPARISON OF DESIGN EQUATION FOR CCT NODE TESTS

As demonstrated in Section 7.5.1 and Section 8.3, the headed bars in CCT node specimens both in the current study and from the previous study by Thompson et al. (2006a) exhibited higher anchorage strengths than predicted by the descriptive equation, even without the 0.8 strength modification factor. The 0.8 factor was not applied because in practice CCT nodes most often occur at the end of a beam within a confined column core. Therefore, the anchorage strengths for the CCT node specimens are compared with the design equation in this section, with ψ_o taken as 1.0 (rather than 1.25) in calculating T_{calc}.

9.3.1 CCT Node Tests in Current Study

The CCT node specimens in this study contained No. 8 bars with a 2.5 in. side cover to the bar, without confining reinforcement used in the nodal zone. The comparisons with the design equation are shown in Table 9.11, along with the embedment length ℓ_{eh} (distance from the bearing face of the head to the end of the extended nodal zone), measured concrete compressive strength f_{cm}, and the center-to-center bar spacing in terms of bar diameter s/d_b. As shown in the table, without the application of $\psi_o = 1.25$, the values of T/T_{calc} range from 1.29 to 2.81, with an average of 2.07. Compared to the values of T/T_{calc} for the beam-column joint specimens used to develop the design equation (range of 0.85 to 1.62; average of 1.26), it is obvious that the headed bars in the CCT node specimens exhibited higher anchorage strengths than the headed bars did in beam-column joint specimens, which is as expected.

Table 9.11 Test results for CCT node specimens in current study and comparisons with design equation [Eq. (9.1)]

Specimen	ℓ_{eh} (in.)	f_{cm} (psi)	s/d_b	T (kips)[†]	T_{calc} (kips)	T/T_{calc}
H-2-8-5-10.4-F4.1	10.4	4490	12	126.9	56.0	2.26
H-2-8-5-9-F4.1	9	5740	12	101.9	51.6	1.98
H-3-8-5-11.4-F4.1	11.4	5750	6	94.6	49.0	1.93
H-3-8-5-9-F4.1	9	5800	6	109.0	38.8	2.81
H-3-8-5-14-F4.1	14	5750	6	121.0	60.2	2.01
H-2-8-5-9-F4.1	9	4630	12	79.9	48.9	1.64
H-2-8-5-13-F4.1	13	4760	12	91.7	71.1	1.29
H-3-8-5-9-F4.1	9	4770	6	86.8	36.9	2.35
H-3-8-5-11-F4.1	11	4820	6	98.5	45.3	2.18
H-3-8-5-13-F4.1	13	4900	6	122.0	53.7	2.27

[†] T is based on strut-and-tie model

9.3.2 Thompson et al. (2006a)

The CCT node specimens tested by Thompson et al (2006a) contained a single bar with a $2.5d_b$ side cover to the bar. In the calculation of ψ_{cs} using Table 9.2, bar spacing s is taken as the width of the specimen ($6d_b$), same approach as used for the comparison with the descriptive equation in Section 8.3. For some specimens, No. 3 transverse stirrups were placed perpendicular to the bar within the nodal zone, which is not qualified as effective confining reinforcement in determining A_{tt}, and thus the calculation of ψ_{cs} is based on "no confinement reinforcement". The values of T/T_{calc} shown in Table 9.12 range from 1.74 to 2.14, with an average of 1.96, which is

similar in average but with less scatter compared to the values obtained with the CCT node specimens in the current study (ranging from 1.29 to 2.81, with an average of 2.07). The comparisons for the CCT node specimens from both sources indicate that the design equation can be safely used for headed bars in CCT node applications.

Table 9.12 Test results for CCT node specimens tested by Thompson et al. (2006a) and comparisons with design equation [Eq. (9.1)]

Specimen	Bar Size	ℓ_{eh} (in.)	f_{cm} (psi)	T (kips)[a]	T_{calc} (kips)	T/T_{calc}
CCT-08-55-04.70(H)-1[b d]		7	4000	54.0[b]	27.5	1.97
CCT-08-55-04.70(V)-1[d]		7	3900	54.0	27.3	1.98
CCT-08-55-10.39-1[b]		7	4000	54.0[b]	27.5	1.97
CCT-08-45-04.04-1[b]		7	4000	48.2[b]	27.5	1.75
CCT-08-45-04.70(V)-1[d]		7	3900	54.0	27.3	1.98
CCT-08-30-04.04-1[b]	No. 8	7	4100	48.2[b]	27.7	1.74
CCT-08-30-04.06-1[b]		7	4100	54.0[b]	27.7	1.95
CCT-08-30-10.39-1[b]		7	4100	54.0[b]	27.7	1.95
CCT-08-45-04.70(H)-1-S3[d]		7	3800	52.1	27.1	1.92
CCT-08-45-04.70(V)-1-C0.006[c d]		7	3800	50.6	27.1	1.87
CCT-08-45-04.70(V)-1-C0.012[c d]		7	3800	51.8	27.1	1.91
CCT-11-45-04.13(V)-1[d]		9.87	4000	88.9	45.7	1.95
CCT-11-45-06.69(H)-1[b d]	No. 11	9.87	4000	98.0[b]	45.7	2.14
CCT-11-45-06.69(V)-1[b d]		9.87	4000	98.0[b]	45.7	2.14
CCT-11-45-09.26-1[b]		9.87	4000	98.0[b]	45.7	2.14

[a] T is based on strain gauges located at $7d_b$ from the face of the head (the approximate location of the end of the extended nodal zone in most specimens)
[b] Specimen exhibited bar yielding before failure of the node
[c] Specimen had transverse stirrups perpendicular to the headed bars within the nodal zone
[d] "H" represents a rectangular head with the long side orientated horizontally; "V" represents a rectangular head with the long side orientated vertically

9.4 COMPARISON OF DESIGN EQUATION FOR SHALLOW EMBEDMENT PULLOUT TESTS

9.4.1 Shallow Embedment Pullout Tests in Current Study

The shallow embedment pullout specimens in the current study contained No. 8 headed bars without confining reinforcement. In Section 7.5.2, the comparisons of the failure loads for these specimens with the descriptive equation [Eq. (7.5)] show that a large h_{cl}/ℓ_{eh} ratio results in a low anchorage strength of headed bars with shallow embedment length in a manner similar to the ratio $h_{cl}/\ell_{eh} \geq 1.33$ found to cause low strengths for beam-column joint specimens in this study. It

is also suggested in Section 7.5.2 that the descriptive equations be used to provide an estimate for headed bars terminating in column-foundation connections with $d_{eff}/\ell_{eh} \leq 3$.

The anchorage strengths of the headed bars with shallow embedment T are compared with strengths T_{calc} calculated with the design equation [Eq. (9.1)] in Table 9.13, along with the measured embedment length ℓ_{eh}, the ratio d_{eff}/ℓ_{eh}, and the measured concrete compressive strength f_{cm}. As these headed bars had a high concrete cover – at least 23.5 in. ($23.5d_b$) to the side of bar, ψ_{cs} is taken as 0.5 for the case of $s \geq 8d_b$ without confining reinforcement in Table 9.2 and ψ_o is taken as 1.0 (satisfying the $8d_b$ side cover requirement) in calculating T_{calc}.

The ratios of T/T_{calc} in Table 9.13 show that, as expected, all but one specimen (8-5-F4.1-6#5-6 with $d_{eff}/\ell_{eh} = 5.73 > 3$), had higher anchorage strengths than predicted by the design equation. Excluding that specimen ($T/T_{calc} = 0.87$), the values of T/T_{calc} range from 1.21 to 2.28, with an average of 1.56, higher than the range of 0.85 to 1.62 and an average of 1.26 for the beam-column joint specimens used to develop the design equation. As the ratio d_{eff}/ℓ_{eh} is equivalent to d/ℓ_{dt} in design, it is suggested that for headed bars terminating in a foundation from a column, the development length ℓ_{dt} based on the design equation [Eq. (9.1)] satisfy $\ell_{dt} > d/3$.

Table 9.13 Test results for headed bars with shallow embedment in current study and comparisons with design equation [Eq. (9.1)]

Specimen	ℓ_{eh} (in.)	d_{eff}/ℓ_{eh}	f_{cm} (psi)	T (kips)	T_{calc} (kips)	T/T_{calc}
8-5-T9.5-8#5-6	8.0	1.48	7040	65.6	48.2	1.36
8-5-T9.5-8#5-6	8.3	1.44	7040	67.8	49.7	1.36
8-5-T4.0-8#5-6	8.5	1.38	7040	61.8	51.3	1.21
8-5-T4.0-8#5-6	7.5	1.55	7040	56.3	45.2	1.24
8-5-F4.1-8#5-6	7.4	1.63	5220	68.9	41.6	1.66
8-5-F4.1-8#5-6	7.4	1.63	5220	64.4	41.3	1.56
8-5-F9.1-8#5-6	7.1	1.71	5220	69.9	39.9	1.75
8-5-F9.1-8#5-6	7.0	1.69	5220	54.9	39.2	1.40
8-5-F4.1-2#8-6	6.0	1.96	7390	64.4	36.6	1.76
8-5-F9.1-2#8-6	6.0	1.96	7390	65.0	36.6	1.77
8-5-T4.0-2#8-6	6.1	1.93	7390	60.5	37.0	1.63
8-5-T9.5-2#8-6	6.1	1.90	7390	57.7	37.4	1.54
8-8-O12.9-6#5-6[*][‡]	6.3	1.79	8620	79.0	39.6	1.99
8-8-O9.1-6#5-6[*]	6.3	1.89	8620	70.9	39.6	1.79
8-8-S6.5-6#5-6	6.4	1.83	8620	92.4	40.4	2.28
8-8-O4.5-6#5-6[*]	6.5	1.86	8620	74.0	41.2	1.79
8-5-S14.9-6#5-6[‡]	6.5	1.84	4200	61.8	34.4	1.79
8-5-S6.5-6#5-6	6.5	1.75	4200	49.2	34.4	1.43
8-5-O12.9-6#5-6[*][‡]	6.6	1.73	4200	52.4	35.1	1.49
8-5-O4.5-6#5-6[*]	6.5	1.77	4200	50.1	34.4	1.45
8-5-S9.5-6#5-6	6.5	1.79	4200	48.9	34.4	1.42
8-5-S9.5-6#5-6	6.4	1.83	4200	54.5	33.8	1.61
8-5-F4.1-6#5-6	8.4	5.73	4200	39.1	44.7	0.87
8-5-F4.1-0-6	6.5	2.49	5180	50.5	36.3	1.39
8-5-F4.1-0-6	6.3	2.91	5180	48.9	34.9	1.40
8-5-F4.1-2#5-6	6.8	2.74	5180	61.5	37.7	1.63
8-5-F4.1-4#5-6	6.0	3.00	5180	53.4	33.5	1.59
8-5-F4.1-4#5-6	6.1	2.98	5180	52.4	34.2	1.53
8-5-F4.1-4#5-6	6.8	2.70	5460	53.5	38.2	1.40
8-5-F4.1-6#5-6	6.3	2.93	5460	47.3	35.4	1.34
8-5-F4.1-6#5-6	6.6	2.72	5460	55.9	37.5	1.49
8-5-F4.1-6#5-6	6.9	2.65	5460	52.6	38.9	1.35

[*] Headed bars with large obstructions exceeding the dimensional limits for HA heads in ASTM A970 (Figure 2.1)
[‡] Bars with large heads ($A_{brg} > 12A_b$)

9.4.2 DeVries et al. (1999)

Of the 18 headed bars with shallow embedment tested by DeVries at al. (1999), 14 were debonded by PVC sheathing placed over the straight length of the bar. As discussed in Section 8.4, the 18 headed bars with shallow embedment tested by DeVries at al. (1999) can be divided into

eight center bars, five edge bars, and five corner bars based on the location of the bar (or side cover to the bar). The values of side cover for the three groups of headed bars are noted in Table 9.14. Based on the side cover provided, the bar location factor ψ_o is taken as 1.25 for the edge and corner bars and 1.0 for center bars. In calculating ψ_{cs} using Table 9.2, the center-to-center bar spacing s is taken as twice of the minimum concrete cover to the center of the bar, which is consistent with the approach for the comparison with the descriptive equation [Eq. (7.6)] in Section 8.4. For the four specimens with transverse reinforcement placed perpendicular to the bar (T2B3, T2B4, T2B7, and T2B8), the ψ_{cs} values are determined based on "no confining reinforcement", as the transverse reinforcement is not considered as effective according to the definition of A_{tt}. The anchorage strengths T of these 18 headed bars are compared with the anchorage strengths T_{calc} predicted by the design equation Eq. (9.1) in Table 9.14, along with the bar diameter d_b, embedment length ℓ_{eh}, concrete compressive strength f_{cm}, and the bar spacing in terms of bar diameter s/d_b.

Table 9.14 Test results for headed bars with shallow embedment tested by DeVries et al. (1999) and comparisons with design equation [Eq. (9.1)]

Specimen	d_b (in.)[a]	ℓ_{eh} (in.)[a]	f_{cm} (psi)[a]	s/d_b[c]	T (kips)[a]	T_{calc} (kips)	T/T_{calc}	Note[e]
T1B1[b]	0.79	1.4	12040	45.7	17.3	8.6	2.01	
T1B2[b]	0.79	1.4	12040	45.7	13.9	8.6	1.62	
T1B3[b d]	0.79	4.4	12040	45.7	46.1[d]	27.1	1.70	
T1B4[b d]	0.79	4.4	12040	45.7	46.8[d]	27.1	1.73	Center bar
T1B5[b]	1.38	3.1	12040	26.1	48.3	25.3	1.91	
T1B6[b]	1.38	3.1	12040	26.1	50.6	25.3	2.00	
T1B7[b]	1.38	8.2	12040	26.1	110.2	66.2	1.66	
T3B11[b d]	0.79	9.0	3920	45.7	47.7[d]	41.4	1.15	
T2B1[b]	0.79	9.0	4790	5.1	41.4	23.5	1.76	
T2B2	0.79	9.0	4790	5.1	33.3	23.5	1.42	
T2B3[b f]	0.79	9.0	4790	5.1	36.0	23.5	1.53	Edge bar
T2B4[f]	0.79	9.0	4790	5.1	38.7	23.5	1.65	
T3B4[b]	0.79	9.0	3920	5.1	33.5	22.3	1.50	
T2B5[b]	0.79	9.0	4790	5.1	19.8	23.5	0.84	
T2B6	0.79	9.0	4790	5.1	27.4	23.5	1.17	
T2B7[b f]	0.79	9.0	4790	5.1	20.0	23.5	0.85	Corner bar
T2B8[f]	0.79	9.0	4790	5.1	28.1	23.5	1.20	
T3B8[b]	0.79	9.0	3920	5.1	12.8	22.3	0.57	

[a] Values are converted SI (1 in. = 25.4 mm; 1 psi = 1/145 MPa; and 1 kip = 4.44822 kN)
[b] Headed bar was covered with PVC sheathing to eliminate bond force along the bar; the actual embedment length rather than the bonded length was used to calculate T_{calc}
[c] Bar spacing s is taken as twice of the minimum concrete cover to the center of the bar
[d] Specimen failed with bar fracture
[e] Center bar: 18 in. from center of the bar to each edge; edge bar: 2 in. from center of the bar to the nearest edge and 18 in. to the orthogonal edge; corner bar: 2 in. from center of the bar to the nearest two edges
[f] Specimen had transverse reinforcement perpendicular to the headed bar

The values of T/T_{calc} in Table 9.14 show that of the 18 headed bars tested, only three debonded corner bars exhibited lower anchorage strengths than predicted by the design equation. This result is in accordance with the comparisons with the descriptive equation presented in Section 8.4, which show that all but those three debonded corners bars exhibited similar or higher anchorage strengths relative to the strengths observed for the beam-column joint specimens used to develop the descriptive equation. Excluding the bars debonded by the PVC sheathing, the four headed bars had values of T/T_{calc} ranging from 1.17 to 1.65, with an average of 1.36, indicating that the design equation produces conservative estimate for fully bonded headed bars with shallow embedment.

9.5 COMPARISON OF DESIGN EQUATION FOR LAP SPLICE TESTS

9.5.1 Lap Splice Tests in Current Study

The six lap splice specimens in the current study contained No. 6 headed bars with a 2-in. ($2.67d_b$) bottom and side clear cover to the bar, without confining reinforcement placed in the lap zone. As demonstrated in Section 7.6.3, the splice strengths of these spliced headed bars can be predicted with reasonable accuracy by the descriptive equation [Eq. (7.6)] with the application of the 0.8 modification factor to account for bar location. In Table 9.15, the splice strengths of these specimens T are compared with the strengths T_{calc} predicted by the design equation [Eq. (9.1)], along with the splice length ℓ_{st}, measured concrete compressive strength f_{cm}, and the smallest center-to-center spacing between adjacent bars in terms of bar diameter s/d_b. In calculating T_{calc}, the bar location factor ψ_o is taken as 1.25, as the provided $2.67d_b$ side cover is less than $8d_b$.

Table 9.15 Test results for headed bars in lap splice specimens in current study and comparisons with design equation [Eq. (9.1)]

Specimen	ℓ_{st} (in.)	f_{cm} (psi)	s/d_b	T (kips)[†]	T_{calc} (kips)	T/T_{calc}
(3)6-5-S4.0-12-0.5	12	6330	1.67	34.0	24.2	1.41
(3)6-5-S4.0-12-1.0	12	6380	2.33	36.8	24.9	1.48
(3)6-5-S4.0-12-1.9	12	6380	3.55	33.6	27.8	1.21
(3)6-12-S4.0-12-0.5	12	10890	1.67	36.1	27.7	1.30
(3)6-12-S4.0-12-1.0	12	10890	2.33	33.0	28.5	1.16
(3)6-12-S4.0-12-1.9	12	11070	3.55	36.4	31.9	1.14

[†] T based on moment-curvature method

As shown in Table 9.15, the values of T/T_{calc} for the six splice specimens range from 1.14 to 1.48, within the range of 0.85 to 1.62 for the beam-column joint specimens that were used to develop the design equation. The average of T/T_{calc} for the six specimens equals 1.28, slightly greater than the average value (1.26) for the beam-column joint specimens. These values suggest that, as expected, the proposed design equation predicts reasonably conservative strengths for the spliced headed bars in this study.

9.5.2 Thompson et al. (2006b)

The lap splice specimens tested by Thompson et al. (2006b) contained No. 8 headed bars with a 2-in. ($2d_b$) clear side cover to the bar for the majority of the specimens (only one specimen had a 1-in. clear cover). The clear top cover was 2 in. for all but one specimen, LS-08-04.04-14-10(N)-1-DB, which had a 4.5-in. top cover to the bar. This specimen also had a debonding sheath placed over the bar deformations in the lap zone. Because all of the specimens had top and side concrete clear cover less than $8d_b$, ψ_o is taken as 1.25 in the design equation [Eq. (9.1)]. Of the 15 specimens used for comparison, the last five specimens listed in Table 9.16 had confining reinforcement in the form of hairpins or transverse bars perpendicular to the headed bars (Figure 1.13). As demonstrated in Section 8.5.1, such confining reinforcement has a minimal effect on the splice strengths of the headed bars tested. The confining reinforcement placed perpendicular to the headed bars is also not considered as effective in calculating A_{tt} in Table 9.2. Thus, the modification factor ψ_{cs} in Table 9.2 is determined based on "no confining reinforcement" for these five specimens. The comparisons for the 15 splice specimens with the design equation are shown in Table 9.16, along with the splice length ℓ_{st}, concrete compressive strength f_{cm}, smallest center-to-center spacing between adjacent bars in terms of bar diameter s/d_b, and the clear side cover to the bar in terms of bar diameter c_{so}/d_b.

Table 9.16 Test results for lap splice specimens tested by Thompson et al. (2006b) and comparisons with design equation [Eq. (9.1)]

Specimen	ℓ_{st} (in.)	f_{cm} (psi)	s/d_b	c_{so}/d_b	T [b] (kips)	T_{calc} (kips)	T/T_{calc}
LS-08-04.70-03-06(N)-1	3	3200	3	1	14.7	6.5	2.27
LS-08-04.70-05-06(N)-1	5	3700	3	2	21.3	11.2	1.90
LS-08-04.70-05-10(N)-1	5	3200	5	2	19.0	13.2	1.44
LS-08-04.70-05-10(C)-1	5	3700	2	2	19.4	10.3	1.88
LS-08-04.70-08-10(N)-1	8	4000	5	2	34.4	22.3	1.54
LS-08-04.70-12-10(N)-1	12	4200	5	2	52.4	33.9	1.54
LS-08-04.04-08-10(N)-1	8	4000	5	2	35.1	22.3	1.57
LS-08-04.04-12-10(N)-1	12	3800	5	2	40.3	33.1	1.22
LS-08-04.04-14-10(N)-1	14	3500	5	2	51.4	37.8	1.36
LS-08-04.04-14-10(N)-1-DB[a]	14	3500	5	2	43.0	37.8	1.14
LS-08-04.70-08-10(N)-1-H0.25[c]	8	4200	5	2	43.3	22.6	1.91
LS-08-04.04-08-10(N)-1-H0.56[c]	8	3500	5	2	42.7	21.6	1.98
LS-08-04.04-08-10(N)-1-H1.01[c]	8	3500	5	2	44.8	21.6	2.07
LS-08-04.04-12-10(N)-1-H0.56[c]	12	3800	5	2	42.5	33.1	1.28
LS-08-04.04-12-10(N)-1-TTD[c]	12	3800	5	2	44.7	33.1	1.35

[a] Specimen had a debonding sheath placed over bar deformations in lap splice region
[b] T is based on strain gauge readings
[c] Specimen had confining reinforcement perpendicular to the headed bars

The values of T/T_{calc} in Table 9.16 show that all of the 15 specimens exhibited higher splice strengths than predicted by the design equation. T/T_{calc} ranges from 1.14 to 2.27, with an average of 1.63. As in Section 8.5.1, the lowest value $T/T_{calc} = 1.14$ is obtained for the specimen with debonded headed bars in the lap zone.

The comparisons with the design equation for the splice headed bars tested in the current and in previous study by Thompson et al. (2006b) suggest that the design equation, established based on the results of beam-column joint tests, is appropriate for use of headed bars in splice applications.

9.5.3 Chun (2015)

The 24 lap splice specimens tested by Chun (2015) contained No. 9 or No. 8 headed bars with a minimum of $1d_b$ clear side cover to the bar ($0.38d_b$ to the head). The specimens were tested with the spliced headed bars located at the bottom of the specimen, with a $2d_b$ clear bottom cover to the bar ($1.38d_b$ to the head). As discussed in Section 8.5.2, the headed bars with obstructions

similar to those used in the beam-column joint specimens by Chun et al. (2009) may have caused the low failure loads observed for the both specimen types (lap splices and beam-column joints). The use of $0.38d_b$ cover to the head (corresponding to 0.43 in. for 17 specimens and 0.37 in. for two specimens), which is even less than half of the maximum aggregate size 1 in.[5], may also have been responsible for the low splice strengths of these splice headed bars.

The splice strengths T for the 24 specimens tested by Chun (2015) are compared with the strengths T_{calc} predicted by the design equation in Table 9.17, along with the bar diameter d_b, splice length ℓ_{st}, concrete compressive strength f_{cm}, center-to-center spacing between adjacent spliced bars in terms of bar diameter s/d_b, side cover to the bar in terms of bar diameter c_{so}/d_b, and the transverse reinforcement index K_{tr}. In calculating T_{calc}, ψ_o is taken as 1.25 due to the low concrete cover provided ($1d_b$ to $3.5d_b$ to the bar, less than $8d_b$ needed for $\psi_o = 1.0$). The last eight specimens listed in Table 9.17 had transverse stirrups placed perpendicular to the spliced bars, which is not in accordance with the definition of A_{tt} for calculating ψ_{cs} in Table 9.2; thus, the values of ψ_{cs} are based on "no confining reinforcement."

As shown in Table 9.17, 15 specimens (out of 24) exhibited higher failure loads than predicted by Eq. (9.1), eight of which are those with confining reinforcement (transverse stirrups). Without confining reinforcement, the specimens had values of T/T_{calc} ranging from 0.80 to 1.30, with an average of 0.96. Compared to these values, the eight specimens with confining reinforcement and $1d_b$ side cover had values of T/T_{calc} relatively high, with a range of 1.21 to 1.85 and an average of 1.62. The difference in T/T_{calc} ratio between the splice specimens without and with confining reinforcement is expected, because the comparisons with the descriptive equation [Eq. (7.6), for the case of no confining reinforcement] presented in Section 8.5.2 already showed similar results. But as suggested in Section 8.5.2, the effectiveness of stirrups perpendicular to the headed bars needs be evaluated through additional lap splice tests where heads with an actual bearing area of at least $4A_b$ are used and more side cover is provided.

---

[5] Maximum aggregate size was provided by the author through personal communication.

Table 9.17 Test results for lap splice specimens tested by Chun (2015) and comparisons with design equation [Eq. (9.1)]

Specimen	d_b [a] (in.)	ℓ_{st} [a] (in.)	f_{cm} [a] (psi)	s/d_b	c_{so}/d_b	K_{tr}	T [b] (kips)	T_{calc} (kips)	T/T_{calc}
D29-S2-F42-L15	1.14	17.1	6000	2	1	-	45.0	41.0	1.10
D29-S2-F42-L20	1.14	22.8	6000	2	1	-	52.9	54.7	0.97
D29-S2-F42-L25	1.14	28.5	6000	2	1	-	62.6	68.4	0.92
D29-S2-F42-L30	1.14	34.3	5820	2	1	-	66.2	81.4	0.81
D29-S4-F42-L15	1.14	17.1	6000	3	2	-	48.4	44.7	1.08
D29-S4-F42-L20	1.14	22.8	6000	3	2	-	54.8	59.7	0.92
D29-S2-C3.5-F42-L15	1.14	17.1	5820	2	3.5	-	52.9	40.7	1.30
D29-S2-C3.5-F42-L20	1.14	22.8	5820	2	3.5	-	63.8	54.2	1.18
D29-S2-C3.5-F42-L25	1.14	28.5	5820	2	3.5	-	72.4	67.8	1.07
D25-S2-F42-L20	0.98	19.7	6000	2	1	-	37.1	46.5	0.80
D25-S2-F42-L25	0.98	24.6	6000	2	1	-	46.5	58.1	0.80
D29-S2-F21-L20	1.14	22.8	2940	2	1	-	34.0	45.8	0.74
D29-S2-F21-L25	1.14	28.5	2940	2	1	-	40.7	57.2	0.71
D29-S2-F70-L15	1.14	17.1	9120	2	1	-	49.8	45.5	1.09
D29-S2-F70-L20	1.14	22.8	9120	2	1	-	62.3	60.7	1.03
D29-S2-F70-L25	1.14	28.5	9120	2	1	-	67.0	75.9	0.88
D29-S2-F42-L15-Con.[c]	1.14	17.1	6000	2	1	1.51	69.9	41.0	1.70
D29-S2-F42-L20-Con.[c]	1.14	22.8	6000	2	1	1.51	84.4	54.7	1.54
D29-S2-F42-L20-LCon.[c]	1.14	22.8	6000	2	1	0.57	70.6	54.7	1.29
D29-S2-F42-L25-Lcon.[c]	1.14	28.5	5820	2	1	0.46	82.2	67.8	1.21
D29-S2-F42-L15-Con.2 [c]	1.14	17.1	5820	2	1	2.50	75.4	40.7	1.85
D29-S2-F42-L20-Con.2 [c]	1.14	22.8	5820	2	1	2.50	98.3	54.2	1.81
D29-S2-F70-L15-Con.[c]	1.14	17.1	9120	2	1	1.51	81.2	45.5	1.78
D29-S2-F70-L20-Con.[c d]	1.14	22.8	9120	2	1	1.51	105.4[d]	60.7	1.74

[a] Values are converted SI (1 in. = 25.4 mm; 1 psi = 0.006895 MPa)

[b] T is based on moment-curvature method

[c] Specimen were confined by transverse stirrups perpendicular to the spliced bars

[d] Specimen failed with yielding of spliced bars

9.6 DISCUSSION OF HEADS WITH OBSTRUCTIONS

As illustrated in Figure 2.1, three types of heads, O4.5, O9.1, and O12.9, had large obstructions that exceed the dimensional limits for the HA heads in the current ASTM A970, and thus have been referred to as non-HA heads throughout this study. During the data analysis for these non-HA heads in Chapters 7 and 9, an area based on the size of obstruction adjacent to head is used to represent the net bearing area A_{brg}, because examinations on these heads following the failure of the specimens most often showed that the concrete had remained on the full bearing face of the head, indicating that the taper of the obstructions at the face of the head may have helped to

bear more concrete. With this definition of net bearing area, the non-HA heads in this study have been demonstrated in Sections 7.4.3 and 7.6.2 to exhibit similar anchorage strengths to the HA heads in the beam-column joint and shallow embedment pullout tests. Therefore, the development of the design equation in this chapter includes the test results for the non-HA heads, and the inclusion has been justified to be appropriate in Section 9.2.1.1.

The comparisons for the headed bars used in the beam-column joint tests by Chun et al. (2009) and the lap splice tests by Chun (2015), as shown in Sections 8.2.2, 8.5.2, 9.2.3, and 9.5.3, however, reveal that low anchorage strengths can be obtained with a type of HA head that has the minimum required bearing area ($4A_b$) but has an obstruction with a diameter equal to the upper limit on diameter for HA heads ($1.5d_b$). In the current version of ASTM A970, the definition of net bearing area is the gross area of the head minus bar area, while ignoring the area of the obstructions if the obstructions are within the required dimensional limits. As discussed in Sections 8.2.2 and 8.5.2, taking full advantage of the definition of "net bearing area" results in an actual net bearing area of only about $2.8A_b$ for these $4A_b$ HA heads with a $1.5d_b$ diameter obstruction.

Based on the discussions for the "non-HA" heads used in this study and the "HA heads" used by Chun et al. (2009) and Chun (2015), it is suggested that the net bearing area A_{brg} for an acceptable head with an obstruction be defined as the difference between the gross area of the head and the area of the obstruction adjacent to the head and that A_{brg} shall be at least $4A_b$. In addition, the dimensions of the obstructions should be limited. Because the obstructions for the non-HA heads used in this study had a maximum length of $5.25d_b$ and a maximum diameter of $2d_b$ (the maximum values are obtained with No. 8 O4.5, O9.1, and O12.9), these values are selected as the upper dimensional limits for an acceptable obstruction. A proposal for recommended changes in requirements for class HA heads in ASTM A970 is presented in Section 9.7.2.

9.7 PROPOSED CODE PROVISIONS

9.7.1 Proposed Changes in ACI 318

Proposed design provisions for the development of headed bars presented in this section will be submitted for consideration for incorporation in the next edition of ACI 318. The following modified sections are recommended for Section 25.4. The recommendations address extending the

limits on f_c', f_y, bar spacing, and concrete cover; and modifying the development length equation in Section 25.4.4.2(a).

2.2—Notation
Add:

A_{hs} = total cross-sectional area of headed bars being developed, in.^{2}

A_{tt} = total cross-sectional area of all confining reinforcement parallel to ℓ_{dt} for headed bars being developed in beam-column joints and located within $8d_b$ of top (bottom) of the headed bars in direction of the interior of the joint for No. 3 through No. 8 headed bars or within $10d_b$ of the top (bottom) of the bar in direction of the interior of the joint for No. 9 through No. 11 headed bars; or minimum total cross-sectional area of all confining reinforcement parallel to headed bars being developed in members other than beam-column joints within $7\frac{1}{2}d_b$ on one side of the bar centerline for No. 3 through No. 8 headed bars or within $9\frac{1}{2}d_b$ on one side of the bar centerline for No. 9 through No. 11 headed bars, in.^{2}

s = minimum center-to-center spacing of headed bars being developed or spliced, in.

ψ_{cs} = factor used to modify development length based on confining reinforcement and bar spacing

ψ_o = factor used to modify development length based on bar location within member

15.4.4 Development of longitudinal reinforcement terminating in the joint shall be in accordance with **25.4**. If the effective depth d of any beam framing into the joint and generating shear exceeds **1.5** times the reinforcement anchorage length, analysis and design of the joint shall be based on the strut-and-tie method in accordance with **Chapter 23**.

16.3.5.5 Headed deformed bars shall be permitted to be anchored in tension in accordance with **25.4.4** if the effective depth d of the supported member is no more than **3** times the anchorage length.

25.4.1.4 The value of $\sqrt{f_c'}$ f_c' used to calculate development length shall not exceed ~~100~~ 10,000 psi, except as permitted in 25.4.4.2(a).

Replace **25.4.4** with:

25.4.4 *Development of standard headed bars in tension*

25.4.4.1 Use of heads to develop deformed bars in tension shall be permitted if conditions (a) through (d) are satisfied:
(a) Bar shall conform to 20.2.1.6
(b) Bar size shall not exceed No. 11
(c) Net bearing area of head A_{brg} shall be at least $4A_b$
(d) Concrete shall be normalweight

25.4.4.2 Development length ℓ_{dt} for headed deformed bars in tension shall be the greatest of (a) through (c).

(a) $\left(0.0024 \dfrac{f_y \Psi_e \Psi_{cs} \Psi_o}{f_c'^{0.25}} \right) d_b^{1.5}$ with ψ_e, ψ_{cs}, and ψ_o given in 25.4.4.3; the value of f_c' is permitted

to exceed 10,000 psi, but shall not exceed 16,000 psi.
  (b) $8d_b$
  (c) 6 in.

25.4.4.3 For the calculation of ℓ_{dt}, modification factors ψ_e and ψ_o shall be in accordance with Table 25.4.4.3a and modification factor ψ_{cs} shall be in accordance with Table 25.4.4.3b. Factor ψ_{cs} shall be permitted to be taken as 1.0.

Table 25.4.4.3a—Modification factors for development of headed bars in tension

Modification Factor	Condition	Value of Factor
Epoxy Ψ_e	Epoxy-coated or zinc and epoxy dual-coated reinforcement	1.2
	Uncoated or zinc-coated (galvanized) reinforcement	1.0
Location Ψ_o	For headed bars (1) terminating inside a column core with clear side cover to the bar $\geq$ 2.5 in., or (2) terminating in a supporting member with side cover to the bar $\geq$ $8d_b$	1.0
	Other	1.25

[1]d_b is the nominal diameter of the headed bar

Table 25.4.4.3b—Modification factor ψ_{cs} for confining reinforcement and spacing[1]

Confinement level	f_y	s	
		$2d_b$	$\geq 8d_b$
$\dfrac{A_{tt}}{A_{hs}} \geq 0.3$	$\leq$ 60,000	0.6	0.4
	120,000	0.7	0.45
No confining reinforcement	all	1.0	0.5

[1] ψ_{cs} is permitted to be linearly interpolated for values of A_{tt}/A_{hs} between 0 and 0.3 and for spacing s or yield strength of headed bar f_y intermediate to those in the table

9.7.2 Proposed Changes in ASTM A970

The recommended changes for the requirements for class HA head dimensions are proposed as follows. The proposed changes to Section A.1.1 of Annex A1 of ASTM A970/A970M-16 are shown using underline and strikeout.

A1.1 Replacement Requirements for 5.3
A1.1.1 Head dimensions for headed bars conforming to Class HA shall be provided by the purchaser in the purchase order.
A1.1.1.1 Head dimensions shall define the head geometry including thickness, diameter or height and width of the head (Fig. 1).
A1.1.1.2 Class HA head dimensions shall comply with A1.1.1.3 through A1.1.1.5.
A1.1.1.3 The net bearing area of the head shall not be less than four times the nominal cross-sectional area of the bar. The net bearing area of a bars without obstructions meeting the requirements of this annex is the gross area of the head minus the area of the deformed reinforcing bar. The net bearing area of a bar with obstructions meeting the requirements of this annex is the gross area of the head minus the area of the obstruction adjacent to the bearing face.
A1.1.1.4 The bearing face shall consist of a single, nominally flat surface that lies in a plane perpendicular to the longitudinal axis of the bar.
A1.1.1.5 Obstructions or interruptions of the bar deformations and non-planar features on the bearing face of the head shall not extend more than two 5.25 nominal bar diameters from the bearing face and shall not have a diameter greater than 1.5 2 nominal bar diameters (Fig. A1.1). Such obstructions shall not be considered to detract from the net bearing area of the head. Obstructions exceeding any of these limits are not permitted.
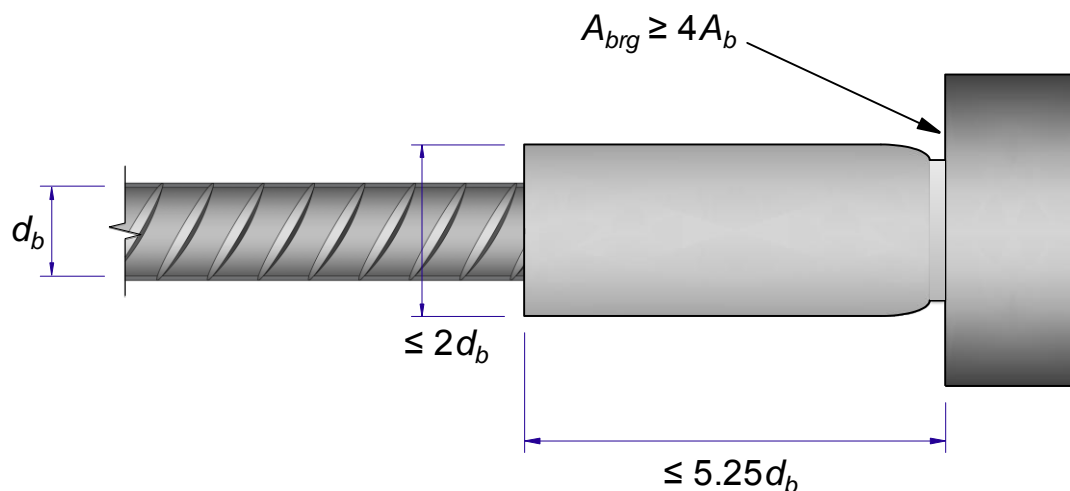
FIG. A1.1 Maximum Dimensions of Obstruction or Interruptions of Bar Deformations and Non-Planar Features of the Bearing Surface

CHAPTER 10: SUMMARY AND CONCLUSIONS

10.1 SUMMARY

This study evaluated the anchorage capacity of high-strength headed bars cast in normal and high-strength concrete. A total of 233 specimens were tested: 202 beam-column joint specimens, 10 CCT node specimens, 15 shallow embedment specimens (each containing one to three headed bars for a total of 32 tests), and 6 splice specimens. Bar stresses at failure ranged from 26,100 to 153,200 psi. Key variables included concrete compressive strength (3,960 to 16,030 psi), embedment length (4 to 19.25 in.), head size (3.8 to 14.9 times the bar area A_b), bar size (No. 5, No. 6, No. 8, and No. 11), number of headed bars tested simultaneously within a specimen (2, 3, or 4), center-to-center bar spacing (1.7 to 11.8 times the bar diameter d_b), and confining reinforcement within the joint region (ranging from none to six No. 3 bars (spaced at $3d_b$)). The headed bars, some meeting the requirements for HA heads in ASTM A970 and some with large obstructions that did not meet those requirements, were supplied by three manufacturers. Data available in the literature were included in the study. The test results were compared with the provision for development length in the ACI Building Code (ACI 318-14). Expressions were developed that characterize the anchorage capacity of headed bars as a function of embedment length, concrete compressive strength, bar diameter, bar spacing, and confining transverse reinforcement. These expressions were compared with the test results in the current and previous studies and used to develop design provisions for headed bar development length.

10.2 CONCLUSIONS

Based on the results of this research, the following conclusions can be drawn:

1. The provisions of ACI 318-14 overpredict the strength of headed bars with larger bar sizes and the effect of concrete compressive strength on the anchorage strength of headed bars in tension.

2. The effect of concrete compressive strength on the anchorage strength of headed bars can be represented by the compressive strength to the 0.25 power.

3. Anchorage strength is improved by confining reinforcement parallel to the headed bar; the increase in strength is proportional to the amount of confining reinforcement per headed bar, a factor that is not included in current design provisions.

4. The anchorage strength of headed bars decreases with center-to-center spacing as the center-to-center spacing decreases below eight bar diameters ($8d_b$).

5. The headed bars with large obstructions (exceeding the dimensional limits for HA heads in ASTM A970) used in this study have similar anchorage strengths to the headed bars with HA heads, and can be safely used with the proposed design provisions. At least one bar meeting the requirements of an HA head tested by others did not perform well, indicating that a change in the requirements in ASTM A970 is needed.

6. Headed bars with large bearing areas (12.9 to $14.9A_b$) exhibit greater anchorage strengths than the headed bars with smaller (3.8 to $9.5A_b$) bearing areas. The increase in strength, however, is not proportional to the bearing area.

7. The proposed Code provisions apply to headed reinforcing steel with yield strengths up to 120,000 psi and to concrete with compressive strengths up to 16,000 psi. The provisions account for the effects of confining reinforcement and bar spacing on anchorage strength of headed bars, safely reducing the current limit on bar clear spacing to $1d_b$, allowing for use of more closely spaced headed bars. This will benefit both nuclear power and building construction industries.

REFERENCES

AASHTO, 2012. "AASHTO LRFD Bridge Design Specifications," 6th edition, American Association of State Highway and Transportation Officials, 1672 pp.

ACI Committee 318, 1995. "Building Code Requirements for Structural Concrete (ACI 318-95) and Commentary," (ACI 318R-95), American Concrete Institute, Farmington Hills, Michigan, 369 pp.

ACI Committee 318, 2002. "Building Code Requirements for Structural Concrete (ACI 318-02) and Commentary," (ACI 318R-02), American Concrete Institute, Farmington Hills, Michigan, 443 pp.

ACI Committee 318, 2005. "Building Code Requirements for Structural Concrete (ACI 318-05) and Commentary," (ACI 318R-05), American Concrete Institute, Farmington Hills, Michigan, 430 pp.

ACI Committee 318, 2008. "Building Code Requirements for Structural Concrete (ACI 318-08) and Commentary," (ACI 318R-08), American Concrete Institute, Farmington Hills, Michigan, 465 pp.

ACI Committee 318, 2014. "Building Code Requirements for Structural Concrete (ACI 318-14) and Commentary," (ACI 318R-14), American Concrete Institute, Farmington Hills, Michigan, 520 pp.

ACI Committee 349, 2014. "Code Requirements for Nuclear Safety-Related Concrete Structures (ACI 349-13) and Commentary," (ACI 349-13), American Concrete Institute, Farmington Hills, Michigan, 196 pp.

ACI Committee 408, 2003. "Bond and Development of Straight Reinforcing Bars in Tension," (ACI 408R-3), American Concrete Institute, Farmington Hills, Michigan, 49 pp.

ACI Committee 352, 2002. "Recommendations for Design of Beam-Column Connections in Monolithic Reinforced Concrete Structures," (ACI 352R-02), American Concrete Institute, Farmington Hills, Michigan, 37 pp.

ASTM A615, 2014. "Standard Specification for Deformed and Plain Carbon-Steel Bars for Concrete Reinforcement," (ASTM A615/A615M-14), ASTM International, West Conshohocken, Pennsylvania, 7 pp.

ASTM A 706, 2015. "Standard Specification for Deformed and Plain Low-Alloy Steel Bars for Concrete Reinforcement," (ASTM A706/A706M-15), ASTM International, West Conshohocken, Pennsylvania, 7 pp.

ASTM A944, 1995. "Standard Test Method for Comparing Bond Strength of Steel Reinforcing Bars to Concrete Using Beam-End Specimens," (ASTM A944-95), ASTM International, West Conshohocken, Pennsylvania, 4 pp.

ASTM A970, 2016. "Standard Specification for Headed Steel Bars for Concrete Reinforcement," (ASTM A970/A970M-16), ASTM International, West Conshohocken, Pennsylvania, 9 pp.

ASTM 1035, 2015. "Standard Specification for Deformed and Plain, Low-Carbon, Chromium, Steel Bars for Concrete Reinforcement," (ASTM A1035/A1035M-14), ASTM International, West Conshohocken, Pennsylvania, 7 pp.

Bashandy, T. R., 1996. "Application of Headed Bars in Concrete Members," PhD dissertation, University of Texas at Austin, Dec., 303 pp.

Burguieres, S. T., 1974. "A Study of Mechanical Anchorages in Beam-Column Joints," Master of Engineering thesis, University of Texas at Austin, 234 pp.

Chun, S.-C., Oh, B., Lee, S.-H., and Naito, C. J., 2009. "Anchorage Strength and Behavior of Headed Bars in Exterior Beam-Column Joints," *ACI Structural Journal*, Vol. 106, No. 5, Sep.-Oct., pp. 579-590.

Chun, S.-C., 2015, "Lap Splice Tests Using High-Strength Headed Bars of 550 MPa (80 ksi) Yield Strength," *ACI Structural Journal*, Vol. 112, No. 6, Nov.-Dec., pp. 679-688.

Darwin, D., Zuo, J., Tholen, M. L., and Idun, E. K., 1996. "Development Length Criteria for Conventional and High Relative Rib Area Reinforcing Bars," *ACI Structural Journal*, Vol. 93, No. 3, May-June, pp. 1-13

Darwin, D., Barham, S., Kozul, R., and Luan, S., 2001, "Fracture Energy of High-Strength Concrete," *ACI Materials Journal*, Vol. 98, No. 5, Sep.-Oct., pp. 410-417

DeVries, R. A., 1996. "Anchorage of Headed Reinforcement in Concrete," PhD dissertation, University of Texas at Austin, Dec., 294 pp.

DeVries, R. A., Jirsa, J. O., and Bashandy, T., 1999, "Anchorage Capacity in Concrete of Headed Reinforcement with Shallow Embedments," *ACI Structural Journal*, Vol. 96, No. 5, Sep.-Oct., pp. 728-737.

Hamad, B. S., Jirsa, J. O., and D'Abreu de Paulo, N. I., 1993. "Anchorage Strength of Epoxy-Coated Hooked Bars," *ACI Structural Journal*, Vol. 90, No. 2, Mar.-Apr., pp. 210-217.

Hawkins, N. M., Kobayashi, A. S., and Fourney, M. E., 1975. "Reversed Cyclic Loading Bond Deterioration Tests," *Structures and Mechanics Report* No. SM75-5, Department of Civil Engineering, University of Washington, Seattle, Nov., 24 pp.

Hognestad, E., 1951, "A Study of Combined Bending and Axial Load in Reinforced Concrete Members," *Bulletin Series No. 399*, University of Illinois Engineering Experiment Station, Urbana, IL, Nov., 128pp.

Hong, S.-G., Chun, S.-C., Lee, S.-H., and Oh, B., 2007. "Strut-and-Tie Model for Development of Headed Bars in Exterior Beam-Column Joint," *ACI Structural Journal*, Vol. 104, No. 5, Sep.-Oct., pp. 590-600.

Kang, T. H.-K., Ha, S.-S., and Choi, D.-U., 2010. "Bar Pullout Tests and Seismic Tests of Small-Headed Bars in Beam-Column Joints," *ACI Structural Journal*, Vol. 107, No. 1, Jan.-Feb., pp. 32-42.

Kang, T. H.-K., Shin, M., Mitra, N., and Bonacci, J. F., 2009. "Seismic Design of Reinforced Concrete Beam-Column Joints with Headed Bars," *ACI Structural Journal*, Vol. 106, No. 6, Nov.-Dec., pp. 868-877.

Marques, J. L., and Jirsa, J. O., 1975. "A Study of Hooked Bar Anchorages in Beam-Column Joints," *ACI Journal*, Proceedings Vol. 72, No. 5, May-Jun., pp. 198-209.

McConnell, S. W., and Wallace, J. W., 1994. "Use of T-Headed Bars in Reinforced Concrete Knee-Joints Subjected to Cyclic Lateral Loading," *Report No*. CU/CEE-94/10, Department of Civil and Environmental Engineering, Clarkson University, Potsdam, New York, Jun., 44 pp.

McConnell, S. W., and Wallace, J. W., 1995. "Behavior of Reinforced Concrete Beam-Column Knee-Joints Subjected to Reversed Cyclic Loading," *Report No*. CU/CEE-95/07, Department of Civil and Environmental Engineering, Clarkson University, Potsdam, New York, Jun., 197 pp.

Peckover, J., Darwin, D., 2013. "Anchorage of High-Strength Reinforcing Bars with Standard Hooks: Initial Tests" *SL Report* No. 13-1, University of Kansas Center for Research, Lawrence, KS, 47 pp.

Pinc, R. L., Watkins, M. D., and Jirsa, J. O., 1977. "The Strength of Hooked Bar Anchorages in Beam-Column Joints," *CESRL Report No*. 77-3, Department of Civil Engineering-Structures Research Laboratory, University of Texas, Austin, Texas, 67 pp.

Sperry, J., Al-Yasso, S., Searle, N., DeRubeis, M., Darwin, D., O'Reilly, M., Matamoros, A., Feldman, L., Lepage, A., Lequesne, R., Ajaam, A., 2015a. "Anchorage of High-Strength Reinforcing Bars with Standard Hooks," *SM Report* No. 111, University of Kansas Center for Research, Inc., Lawrence, Kansas, Jun., 243 pp.

Sperry, J., Darwin, D., O'Reilly, M., and Lequesne, R., 2015b, "Anchorage Strength of Conventional and High-Strength Hooked Bars in Concrete," *SM Report* No. 115, University of Kansas Center for Research, Lawrence, KS, Dec., 266 pp.

Thompson, M. K., 2002. "The Anchorage Behavior of Headed Reinforcement in CCT Nodes and Lap Splices," PhD dissertation, University of Texas at Austin, May, 502 pp.

Thompson, M. K., Ziehl, M. J., Jirsa, J. O., and Breen, J. E., 2005. "CCT Nodes Anchored by Headed Bars-Part 1: Behavior of Nodes," *ACI Structural Journal*, Vol. 102, No. 6, Nov.-Dec., pp. 808-815.

Thompson, M. K., Jirsa, J. O., and Breen, J. E., 2006a. "CCT Nodes Anchored by Headed Bars-Part 2: Capacity of Nodes," *ACI Structural Journal*, Vol. 103, No. 1, Jan.-Feb., pp. 65-73.

Thompson, M. K., Ledesma, A., Jirsa, J. O., and Breen, J. E., 2006b. "Lap Splices Anchored by Headed Bars," *ACI Structural Journal*, Vol. 103, No. 2, Mar.-Apr., pp. 271-279.

Wallace, J. W., McConnell, S. W., Gupta, P., and Cote, P. A., 1998. "Use of Headed Reinforcement in Beam-Column Joints Subjected to Earthquake Loads," *ACI Structural Journal*, Vol. 95, No. 5, Sep.-Oct., pp. 590-606.

Wright, J. L., and McCabe, S. L., 1997. "The Development Length and Anchorage Behavior of Headed Reinforcing Bars," *SM Report No*. 44, University of Kansas Center for Research, Inc., Lawrence, Kansas, Sep., 147 pp.

Zuo, J., and Darwin, D., 1998. "Bond Strength of High Relative Rib Area Reinforcing Bars," *SM Report* No. 46, University of Kansas Center for Research, Inc., Lawrence, Kansas, Jan., 350 pp.

Zuo, J., and Darwin, D., 2000. "Splice Strength of Conventional and High Relative Rib Area Bars in Normal and High-Strength Concrete," *ACI Structural Journal*, Vol. 97, No. 4, July-Aug., pp. 630-641

APPENDIX A: NOTATION

a depth of equivalent rectangular compressive stress block

A_{ab} Total cross-sectional area of all confining reinforcement parallel to ℓ_{dt} for headed bars being developed in beam-column joints and located within $8d_b$ of the bottom (top) of the headed bars in direction of the outside of the joint for No. 3 through No. 8 headed bars or within $10d_b$ of the bottom (top) of the bar in direction of the outside of the joint for No. 9 through No. 11 headed bars (see Figures 7.20 and 7.21)

A_b Area of an individual headed bar

A_{brg} Net bearing area of the head of headed deformed bar

A_{cs} Cross-sectional area at one end of a strut in a strut-and-tie model, taken perpendicular to the axis of the strut

A_{hs} Total cross-sectional area of headed bars being developed

$A_{tr,l}$ Area of single leg of confining reinforcement within joint region

A_{tt} Total cross-sectional area of all confining reinforcement parallel to ℓ_{dt} for headed bars being developed in beam-column joints and located within $8d_b$ of the top (bottom) of the headed bars in direction of the interior of the joint for No. 3 through No. 8 headed bars or within $10d_b$ of the top (bottom) of the bar in direction of the interior of the joint for No. 9 through No. 11 headed bars; or minimum total cross-sectional area of all confining reinforcement parallel to headed bars being developed in members other than beam-column joints within $7\frac{1}{2}d_b$ on one side of the bar centerline for No. 3 through No. 8 headed bars or within $9\frac{1}{2}d_b$ on one side of the bar centerline for No. 9 through No. 11 headed bars

A_v Area of confining reinforcement located between the headed bar and the top of the bearing member

b Width of column

c Effective depth of neutral axis from the assumed extreme compression fiber for beam-column joint and shallow embedment pullout specimens

c_{bc} Clear cover measured from the back of the head to the back of the member

c_h Clear spacing between adjacent headed bars

c_o Clear cover measured from the head to the side of the column

c_{sb} Clear cover measured from the bottom of the beam to the headed bar

c_{so} Clear cover measured from the side of the headed bar to the side of the member

$c_{so,avg}$ Average clear side cover of the headed bars

d Distance from the centroid of the tension bar to the extreme compression fiber of the beam

d_b Nominal diameter of bar

d_{eff} Effective value of d for beam-column joint and shallow embedment pullout specimens

d_{tr} Nominal bar diameter of confining reinforcement within joint region

d_{tro} Nominal bar diameter of confining reinforcement outside joint region

f_c' Specified compressive strength of concrete

f_{cm} Measured concrete compressive strength

f_N Stress in a headed bar at failure normalized with respect to 5,000-psi compressive strength of concrete

$f_{s,ACI}$ Stress in headed bar as calculated by Section 25.4.4.2 of ACI 318-14

f_{su} Average stress in headed bars at failure

$f_{su,max}$ Maximum stress in individual headed bar

f_y Specified yield strength of headed bar

f_{yt}	Yield strength of transverse reinforcement
h	Depth of column
h_{cl}	Height measured from the center of the headed bar to the top of the bearing member (see Figure 2.13)
h_{cu}	Height measured from the center of the headed bar to the bottom of the upper compression member (see Figure 2.13)
K_{tr}	Transverse reinforcement index
ℓ_{dh}	Development length in tension of deformed bar or deformed wire with a standard hook, measured from outside end of hook, point of tangency, toward critical section
ℓ_{dt}	Development length in tension of headed deformed bar, measured from the critical section to the bearing face of the head
ℓ_{eh}	Embedment length measured from the bearing face of the head to the face of the member (or the end of the extended nodal zone, for CCT node specimens)
$\ell_{eh,\text{avg}}$	Average embedment length of headed bars
ℓ_{st}	Lap length of headed spliced bars (not including head thickness)
n	Number of headed bars loaded simultaneously
N	Number of legs of confining reinforcement in joint region
P	Peak load on applied to a beam (CCT node or splice) specimen
R_1	Reaction from the bearing member for beam-column joint specimens in current study
T	Test failure load on a headed bar; average load on headed bars at failure
T_c	Contribution of concrete to anchorage strength of a headed bar
T_{calc}	Calculated failure load on a headed bar
T_h	Anchorage strength of a headed bar
T_{ind}	Peak load on individual headed bar at failure
T_{max}	Maximum load on individual headed bar
T_N	Load on a headed bar at failure normalized with respect to 5,000-psi compressive strength of concrete
T_s	Contribution of confining reinforcement to anchorage strength of a headed bar
T_{STM}	Calculated load on headed bars at anchorage failure based on strut-and-tie model
T_{total}	Sum of loads on headed bars at failure
s	Center-to-center spacing between adjacent headed bars
s_{tr}	Center-to-center spacing of confining reinforcement (hoops) within joint region
s_{tro}	Center-to-center spacing of hoops outside joint region
β_s	Factor used to account for the effect of cracking and confining reinforcement on the effective compressive strength of the concrete in a strut (see Section 4.6.2)
β_1	Factor relating depth of equivalent rectangular compressive stress block to neutral axis depth
ϕ	Strength reduction factor (see Section 9.1.2.4)
ψ_{cs}	Factor used to modify development length based on confining reinforcement and bar spacing
ψ_e	Factor used to modify development length based on reinforcement coating
ψ_m	Factor used to modify development length based on bar spacing
ψ_o	Factor used to modify development length based on bar location within member

ψ_r Factor used to modify development length based on confining reinforcement

λ Modification factor to reflect the reduced mechanical properties of lightweight concrete relative to normalweight concrete of the same compressive strength

Acronym list

AASHTO   American Association of State Highway Transportation Officials
ACI   American Concrete Institute
ASTM   American Society of the International Association for Testing and Materials
BSG   Bulk Specific Gravity
CCT   Compression-compression-tension
HA   Class HA head dimensions shall satisfy (1) $A_{brg} \geq 4A_b$ and (2) Obstructions or interruptions of the bar deformations and non-planar features on the bearing face of the head shall not extend more than two nominal bar diameters from the bearing face and shall not have a diameter greater than 1.5 nominal bar diameters (Figure 1.2); Class HA also requires the development of the minimum specified tensile strength of the reinforcing bar
SG   Specific Gravity
SSD   Saturated Surface Dry
STM   Strut-and-tie model

Failure types (described in Section 3.2)
CB   Concrete breakout
SB   Side blowout
FP   Local front pullout (secondary failure)
BS   Back cover spalling (secondary failure)
Y   Yield of headed bars

APPENDIX B: DETAILED BEAM-COLUMN JOINT SPECIMEN RESULTS

B.1 LONGITUDINAL COLUMN STEEL LAYOUTS

The longitudinal column reinforcement layouts (Figures B.1 – B.17) shown below may not reflect the real size, number, and location of headed bars. Confining reinforcement is omitted in the layouts for clarity.
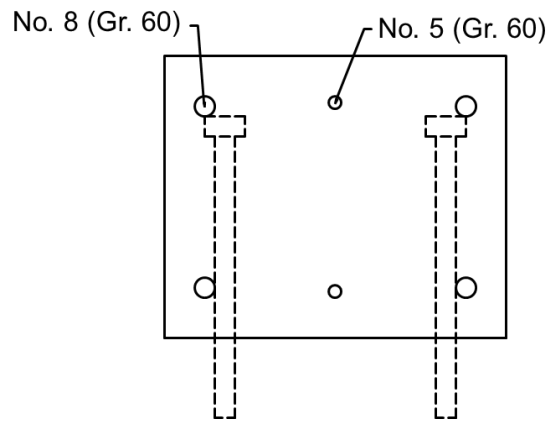
Figure B.1 Layout B1: 4 No. 8 + 2 No. 5 (Gr. 60)
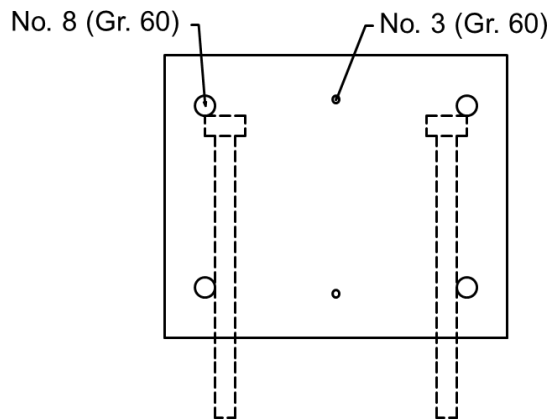
Figure B.2 Layout B2: 4 No. 8 + 2 No. 3 (Gr. 60)
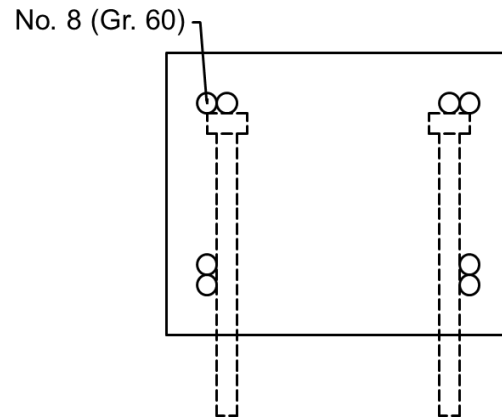
No. 8 (Gr. 60)

Figure B.3 Layout B3: 8 No. 8 (Gr. 60), bundled at corner
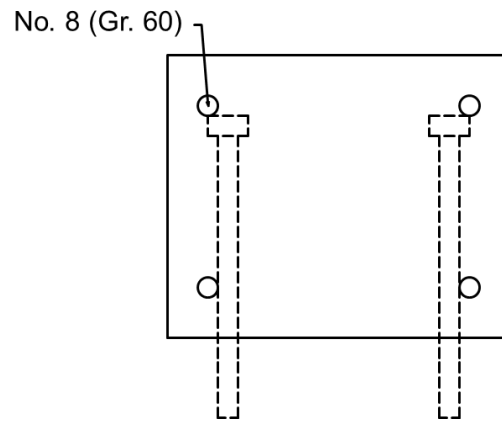
No. 8 (Gr. 60)

Figure B.4 Layout B4: 4 No. 8 (Gr. 60)
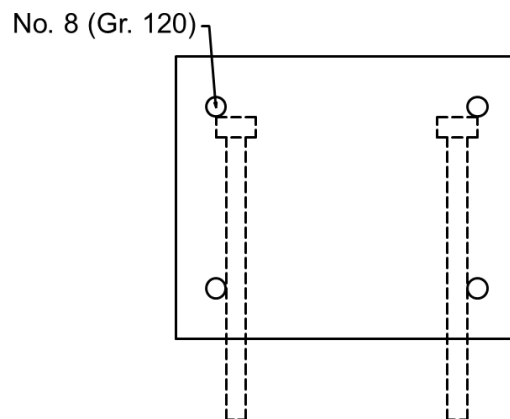
No. 8 (Gr. 120)

Figure B.5 Layout B5: 4 No. 8 (Gr. 120)
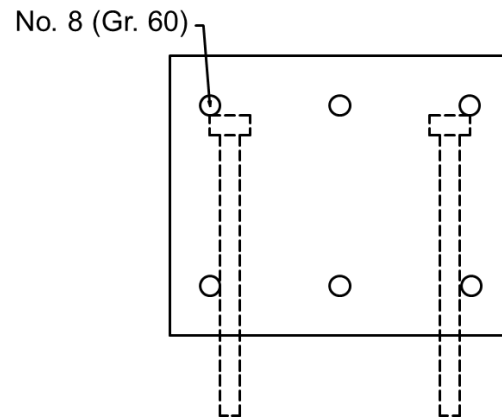
No. 8 (Gr. 60)

Figure B.6 Layout B6: 6 No. 8 (Gr. 60)
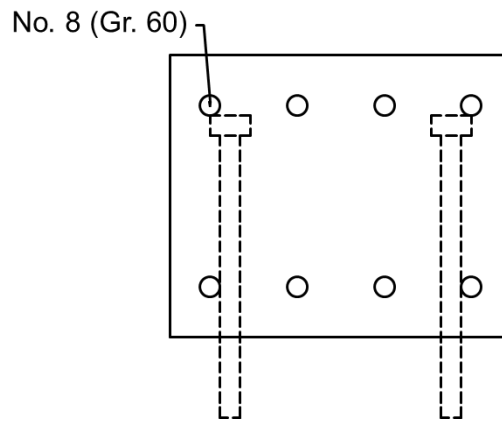
No. 8 (Gr. 60)

Figure B.7 Layout B7: 8 No. 8 (Gr. 60)
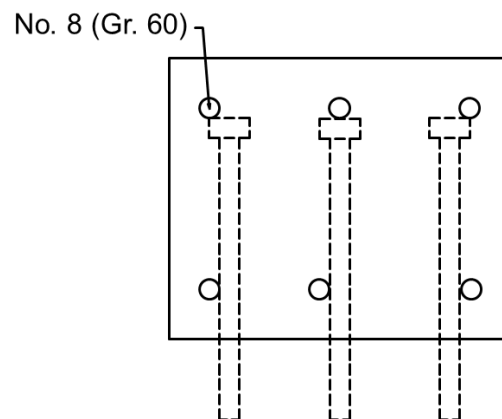
No. 8 (Gr. 60)

Figure B.8 Layout B8: 6 No. 8 (Gr. 60), non-symmetric

257
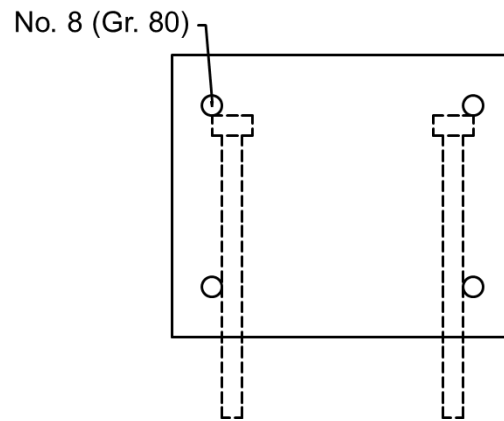
Figure B.9 Layout B9: 4 No. 8 (Gr. 80)
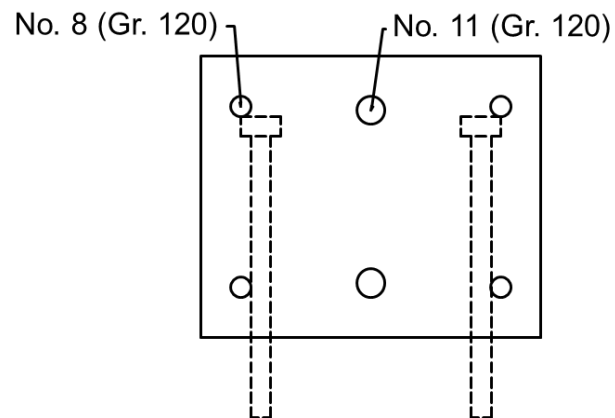
Figure B.10 Layout B10: 4 No. 8 + 2 No. 11 (Gr. 120)
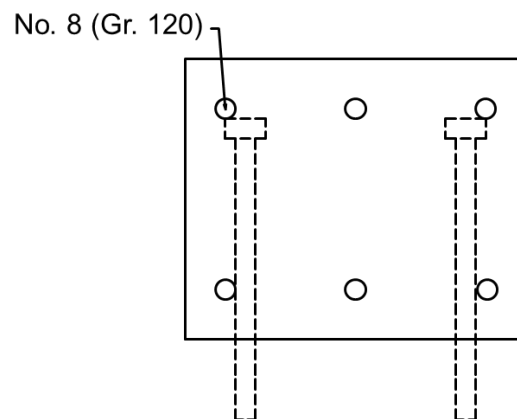
Figure B.11 Layout B11: 6 No. 8 (Gr. 120)
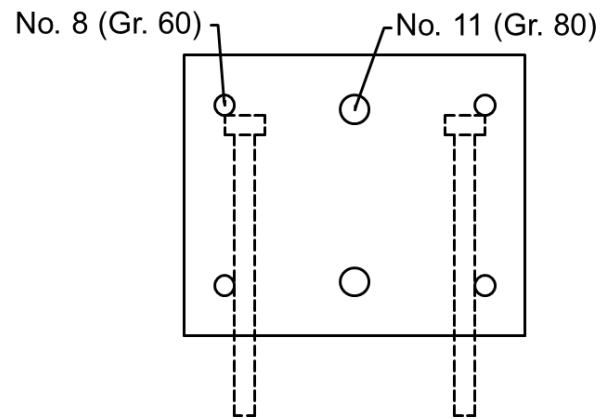
No. 8 (Gr. 60)　　　　No. 11 (Gr. 80)

Figure B.12 Layout B12: 4 No. 8 (Gr. 60) + 2 No. 11 (Gr. 80)
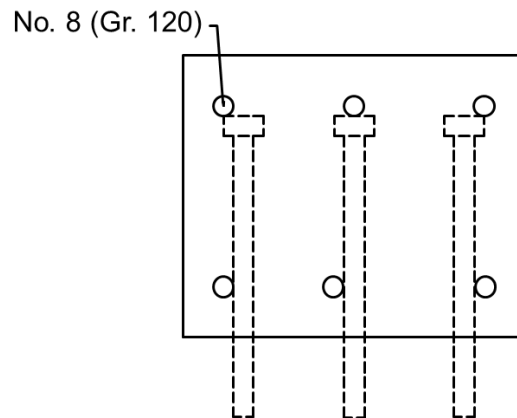
No. 8 (Gr. 120)

Figure B.13 Layout B13: 6 No. 8 (Gr. 120), non-symmetric
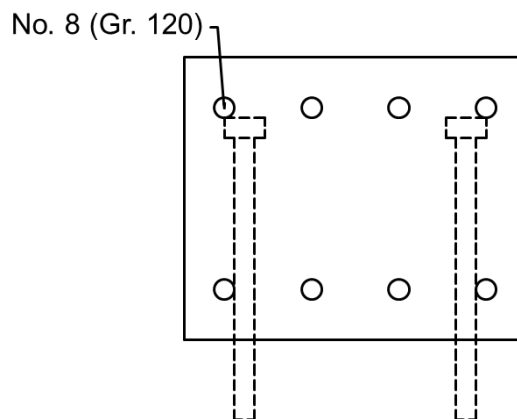
No. 8 (Gr. 120)

Figure B.14 Layout B14: 8 No. 8 (Gr. 120)
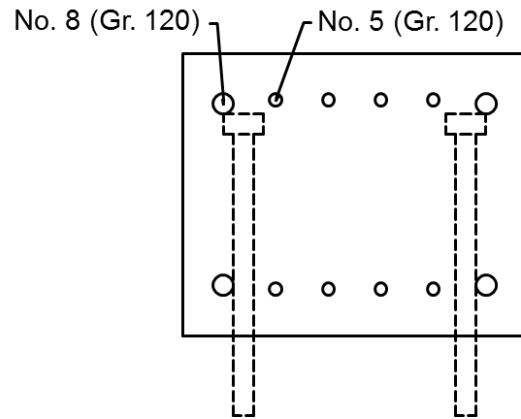
No. 8 (Gr. 120)　　　No. 5 (Gr. 120)

Figure B.15 Layout B15: 4 No. 8 +8 No. 5 (Gr. 120)
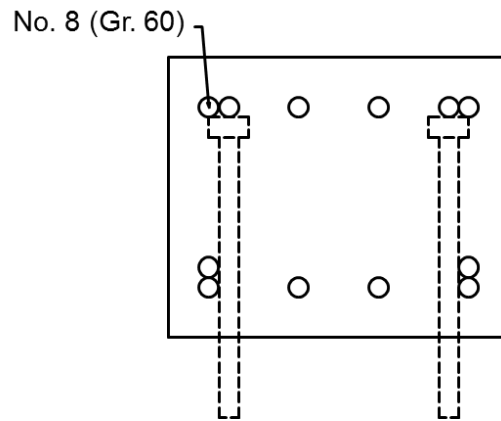
No. 8 (Gr. 60)

Figure B.16 Layout B16: 12 No. 8 (Gr. 60)

No. 8 (Gr. 60)　　　No. 3 (Gr. 60)
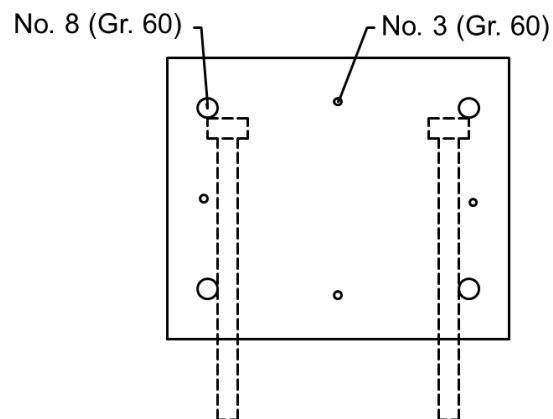
Figure B.17 Layout B17: 4 No. 8 + 4 No. 3 (Gr. 60)

260

B.2 STRESS-STRAIN CURVES
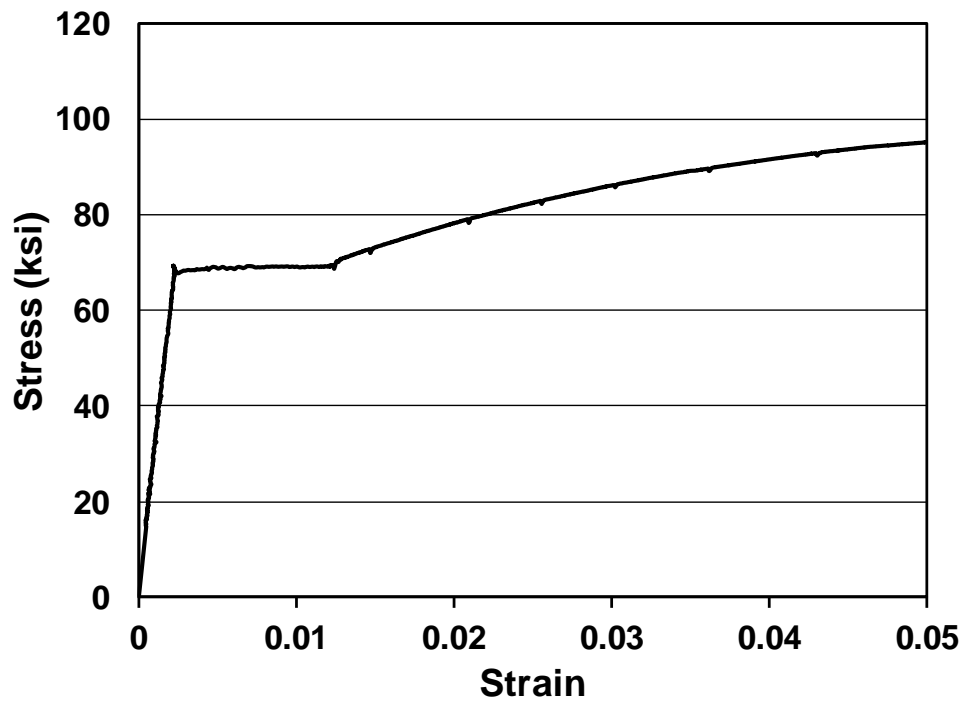
Figure B.18 Stress-strain curve for No. 3 reinforcing steel
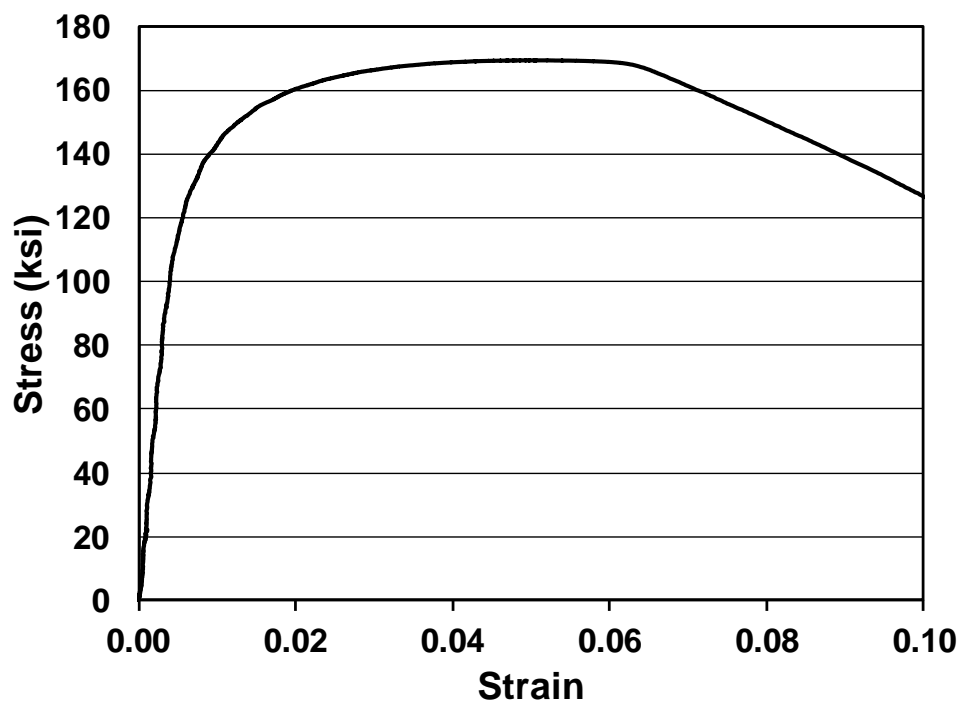
Figure B.19 Stress-strain curve for No. 8 reinforcing steel
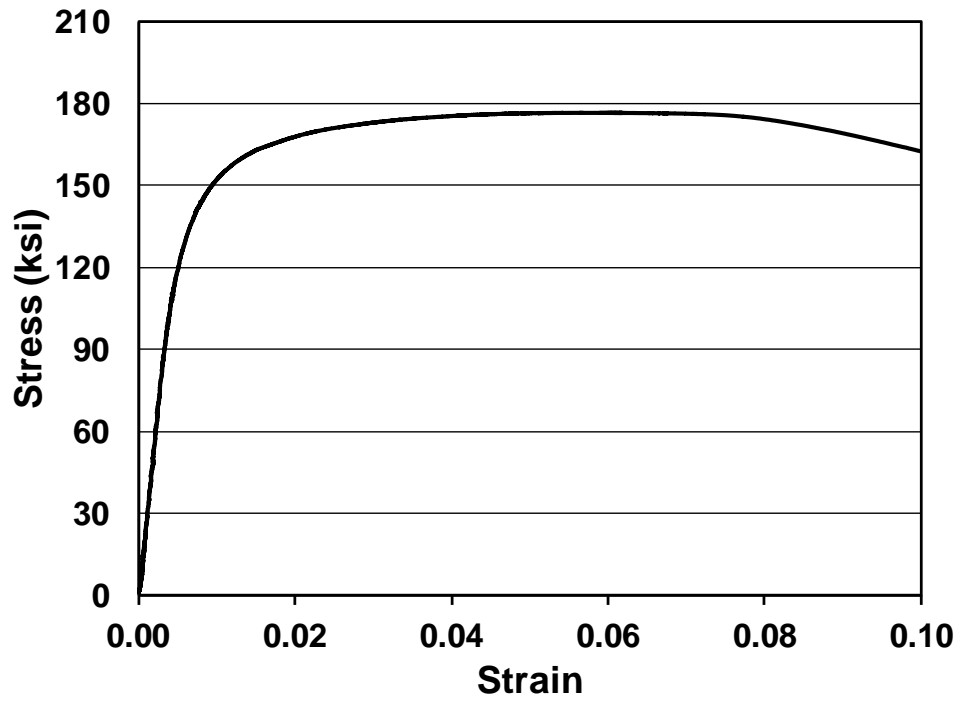
Figure B.20 Stress-strain curve for No. 11 reinforcing steel

B.3 COMPREHENSIVE TEST RESULTS

Table B.1 Comprehensive test results and data for beam-column joint specimens

	Specimen	Head	c_o in.	A_{brg}	ℓ_{eh} in.	$\ell_{eh,avg}$ in.	f_{cm} psi	Age days	d_b in.	A_b in.²
Group 1	8-5-T4.0-0-i-3-3-15.5[a][b]	A B	2.4	$4.0A_b$	15.50 16.00	15.75	4850	7	1	0.79
	8-5-T4.0-0-i-4-3-15.5[a][b]	A B	3.4	$4.0A_b$	15.50 15.06	15.28	5070	8	1	0.79
	8-5-T4.0-4#3-i-3-3-12.5[a]	A B	2.4	$4.0A_b$	12.06 12.69	12.38	5070	8	1	0.79
	8-5-T4.0-4#3-i-4-3-12.5[a]	A B	3.4	$4.0A_b$	11.94 12.19	12.06	5380	11	1	0.79
	8-5-T4.0-4#4-i-3-3-12.5[a]	A B	2.4	$4.0A_b$	12.56 12.31	12.44	5070	8	1	0.79
	8-5-T4.0-4#4-i-4-3-12.5[a]	A B	3.4	$4.0A_b$	12.06 12.31	12.19	4850	7	1	0.79
Group 2	8-5g-T4.0-0-i-2.5-3-12.5[a]	A B	1.9	$4.0A_b$	12.69 12.44	12.56	5910	14	1	0.79
	8-5g-T4.0-0-i-3.5-3-12.5[a]	A B	2.9	$4.0A_b$	12.44 12.56	12.50	6320	15	1	0.79
	8-5g-T4.0-5#3-i-2.5-3-9.5[a]	A B	1.9	$4.0A_b$	9.44 9.69	9.56	5090	7	1	0.79
	8-5g-T4.0-5#3-i-3.5-3-9.5[a]	A B	2.9	$4.0A_b$	9.69 9.44	9.56	5910	14	1	0.79
	8-5g-T4.0-4#4-i-2.5-3-9.5[a]	A B	1.9	$4.0A_b$	9.44 8.94	9.19	5180	8	1	0.79
	8-5g-T4.0-4#4-i-3.5-3-9.5[a]	A B	2.9	$4.0A_b$	9.31 9.69	9.50	5910	14	1	0.79
Group 3	8-5-T4.0-0-i-2.5-3-12.5[a]	A B	1.9	$4.0A_b$	12.69 12.50	12.59	6210	8	1	0.79
	8-5-T4.0-0-i-3.5-3-12.5[a]	A B	2.9	$4.0A_b$	12.81 12.50	12.66	6440	9	1	0.79
	8-5-T4.0-5#3-i-2.5-3-9.5[a]	A B	1.9	$4.0A_b$	9.44 9.19	9.31	5960	7	1	0.79
	8-5-T4.0-5#3-i-3.5-3-9.5[a]	A B	2.9	$4.0A_b$	9.06 9.06	9.06	6440	9	1	0.79
	8-5-T4.0-4#4-i-2.5-3-9.5[a]	A B	1.9	$4.0A_b$	9.19 9.31	9.25	6440	9	1	0.79
	8-5-T4.0-4#4-i-3.5-3-9.5[a]	A B	2.9	$4.0A_b$	9.56 8.94	9.25	6210	8	1	0.79
Group 4	8-8-F4.1-0-i-2.5-3-10.5	A B	2.0	$4.1A_b$	10.25 10.75	10.50	8450	9	1	0.79
	8-8-F4.1-2#3-i-2.5-3-10	A B	2.0	$4.1A_b$	9.75 10.00	9.88	8450	9	1	0.79
	(3@3)8-8-F4.1-0-i-2.5-3-10.5	A B C	2.0	$4.1A_b$	10.63 10.75 10.38	10.58	8450	9	1	0.79

[a] Specimen contained crossties within joint region (see Figure 2.4)
[b] Specimen had no confining reinforcement above joint region

263

Table B.1 Cont. Comprehensive test results and data for beam-column joint specimens

	Specimen	Head	b in.	h in.	h_{cl} in.	d_{eff} in.	c_{so} in.	$c_{so,avg}$ in.	c_{bc} in.	s in.	d_{tr} in.	$A_{tr,l}$ in.^{2}
Group 1	8-5-T4.0-0-i-3-3-15.5[a b]	A B	17.9	20.3	10.25	12.94	3.0 2.9	3.0	3.3 2.8	11.0	-	-
	8-5-T4.0-0-i-4-3-15.5[a b]	A B	19.6	20.3	10.25	13.03	3.8 3.9	3.8	3.3 3.7	10.9	-	-
	8-5-T4.0-4#3-i-3-3-12.5[a]	A B	17.6	17.4	10.25	13.08	2.9 2.9	2.9	3.8 3.2	10.9	0.375	0.11
	8-5-T4.0-4#3-i-4-3-12.5[a]	A B	20.0	17.3	10.25	12.94	3.9 4.1	4.0	3.9 3.6	11.0	0.375	0.11
	8-5-T4.0-4#4-i-3-3-12.5[a]	A B	17.5	17.3	10.25	13.78	2.9 3.0	2.9	3.2 3.4	10.6	0.5	0.2
	8-5-T4.0-4#4-i-4-3-12.5[a]	A B	20.1	17.3	10.25	13.30	3.9 4.1	4.0	3.7 3.4	11.1	0.5	0.2
Group 2	8-5g-T4.0-0-i-2.5-3-12.5[a]	A B	16.8	17.2	10.25	13.28	2.5 2.5	2.5	3.0 3.3	10.8	-	-
	8-5g-T4.0-0-i-3.5-3-12.5[a]	A B	18.7	17.1	10.25	12.74	3.3 3.4	3.3	3.2 3.1	11.1	-	-
	8-5g-T4.0-5#3-i-2.5-3-9.5[a]	A B	17.3	14.1	10.25	12.94	2.8 2.8	2.8	3.2 2.9	10.8	0.375	0.11
	8-5g-T4.0-5#3-i-3.5-3-9.5[a]	A B	18.9	14.2	10.25	12.46	3.3 3.4	3.3	3.0 3.3	11.3	0.375	0.11
	8-5g-T4.0-4#4-i-2.5-3-9.5[a]	A B	16.5	14.1	10.25	13.32	2.5 2.5	2.5	3.2 3.7	10.5	0.5	0.2
	8-5g-T4.0-4#4-i-3.5-3-9.5[a]	A B	19.0	14.3	10.25	12.94	4.0 3.8	3.9	3.4 3.1	10.3	0.5	0.2
Group 3	8-5-T4.0-0-i-2.5-3-12.5[a]	A B	16.6	17.2	10.25	12.76	2.4 2.5	2.4	3.0 3.2	10.8	-	-
	8-5-T4.0-0-i-3.5-3-12.5[a]	A B	18.5	17.2	10.25	12.68	3.5 3.6	3.6	2.9 3.2	10.4	-	-
	8-5-T4.0-5#3-i-2.5-3-9.5[a]	A B	16.5	14.3	10.25	12.54	2.5 2.5	2.5	3.3 3.6	10.5	0.375	0.11
	8-5-T4.0-5#3-i-3.5-3-9.5[a]	A B	18.6	14.3	10.25	12.38	3.1 3.8	3.4	3.7 3.7	10.8	0.375	0.11
	8-5-T4.0-4#4-i-2.5-3-9.5[a]	A B	16.6	14.1	10.25	12.92	2.6 2.5	2.6	3.4 3.3	10.5	0.5	0.2
	8-5-T4.0-4#4-i-3.5-3-9.5[a]	A B	18.6	14.2	10.25	12.56	3.5 3.4	3.4	3.1 3.8	10.8	0.5	0.2
Group 4	8-8-F4.1-0-i-2.5-3-10.5	A B	16.8	14.8	10.25	12.19	2.4 2.5	2.4	3.5 3.0	10.9	-	-
	8-8-F4.1-2#3-i-2.5-3-10	A B	17.0	14.1	10.25	12.10	2.5 2.4	2.4	3.3 3.1	11.1	0.375	0.11
	(3@3)8-8-F4.1-0-i-2.5-3-10.5	A B C	11.9	14.6	10.25	13.18	2.5 - 2.4	2.4	3.0 2.8 3.2	3.0 3.0	-	-

[a] Specimen contained crossties within joint region (see Figure 2.4)
[b] Specimen had no confining reinforcement above joint region

Table B.1 Cont. Comprehensive test results and data for beam-column joint specimens

Specimen	Head	N	s_{tr}[c] in.	A_{tt} in.^{2}	d_{tro} in.	s_{tro}[c] in.	A_{ab} in.^{2}	n	A_{hs} in.^{2}	Long. Reinf. Layout
Group 1 8-5-T4.0-0-i-3-3-15.5[a b]	A B	-	-	-	-	-	-	2	1.58	B1
8-5-T4.0-0-i-4-3-15.5[a b]	A B	-	-	-	-	-	-	2	1.58	B1
8-5-T4.0-4#3-i-3-3-12.5[a]	A B	8	3 (1.5)	0.66	0.375	3 (1.5)	0.66	2	1.58	B2
8-5-T4.0-4#3-i-4-3-12.5[a]	A B	8	3 (1.5)	0.66	0.375	3 (1.5)	0.66	2	1.58	B2
8-5-T4.0-4#4-i-3-3-12.5[a]	A B	8	4 (2)	0.80	0.5	4 (2)	0.80	2	1.58	B17
8-5-T4.0-4#4-i-4-3-12.5[a]	A B	8	4 (2)	0.80	0.5	4 (2)	0.80	2	1.58	B17
Group 2 8-5g-T4.0-0-i-2.5-3-12.5[a]	A B	-	-	-	0.375	3.5 (1.75)	0.44	2	1.58	B2
8-5g-T4.0-0-i-3.5-3-12.5[a]	A B	-	-	-	0.375	3.5 (1.75)	0.44	2	1.58	B2
8-5g-T4.0-5#3-i-2.5-3-9.5[a]	A B	10	3 (1.5)	0.66	0.375	3.5 (1.75)	0.44	2	1.58	B2
8-5g-T4.0-5#3-i-3.5-3-9.5[a]	A B	10	3 (1.5)	0.66	0.375	3.5 (1.75)	0.44	2	1.58	B2
8-5g-T4.0-4#4-i-2.5-3-9.5[a]	A B	8	4 (2)	0.80	0.5	3.5 (1.75)	0.80	2	1.58	B17
8-5g-T4.0-4#4-i-3.5-3-9.5[a]	A B	8	4 (2)	0.80	0.5	3.5 (1.75)	0.80	2	1.58	B17
Group 3 8-5-T4.0-0-i-2.5-3-12.5[a]	A B	-	-	-	0.375	3.5 (1.75)	0.44	2	1.58	B2
8-5-T4.0-0-i-3.5-3-12.5[a]	A B	-	-	-	0.375	3.5 (1.75)	0.44	2	1.58	B2
8-5-T4.0-5#3-i-2.5-3-9.5[a]	A B	10	3 (1.5)	0.66	0.375	3.5 (1.75)	0.44	2	1.58	B2
8-5-T4.0-5#3-i-3.5-3-9.5[a]	A B	10	3 (1.5)	0.66	0.375	3.5 (1.75)	0.44	2	1.58	B2
8-5-T4.0-4#4-i-2.5-3-9.5[a]	A B	8	4 (2)	0.80	0.5	3.5 (1.75)	0.80	2	1.58	B17
8-5-T4.0-4#4-i-3.5-3-9.5[a]	A B	8	4 (2)	0.80	0.5	3.5 (1.75)	0.80	2	1.58	B17
Group 4 8-8-F4.1-0-i-2.5-3-10.5	A B	-	-	-	0.375	4 (2)	0.44	2	1.58	B1
8-8-F4.1-2#3-i-2.5-3-10	A B	4	5 (5.5)	0.22	0.375	4 (2)	0.44	2	1.58	B1
(3@3)8-8-F4.1-0-i-2.5-3-10.5	A B C	-	-	-	0.375	3.5 (1.75)	0.44	3	2.37	B3

[a] Specimen contained crossties within joint region (see Figure 2.4)
[b] Specimen had no confining reinforcement above joint region
[c] Value in parenthesis is the spacing between the first hoop and the center of the headed bar

265

Table B.1 Cont. Comprehensive test results and data for beam-column joint specimens

	Specimen	Head	Failure Type	Lead (Head) Slip in.	T_{max} kips	$f_{su,max}$ ksi	T_{ind} kips	T_{total} kips	T kips	f_{su} ksi
Group 1	8-5-T4.0-0-i-3-3-15.5[a b]	A	SB/FP	0.019	81.6	103.3	81.6	160.9	80.4	101.8
		B		-	92.2	116.7	79.3			
	8-5-T4.0-0-i-4-3-15.5[a b]	A	SB/FP	0.308	92.5	117.1	92.5	190.9	95.4	120.8
		B		-	98.5	124.7	98.4			
	8-5-T4.0-4#3-i-3-3-12.5[a c]	A	SB/FP	0.227	87.9	111.3	87.9	175.0	87.5	110.8
		B		-	-[ǂ]	-[ǂ]	87.1			
	8-5-T4.0-4#3-i-4-3-12.5[a]	A	SB/FP	-	110.8	140.3	97.2	192.3	96.2	121.7
		B		0.239	95.2	120.5	95.1			
	8-5-T4.0-4#4-i-3-3-12.5[a]	A	SB/FP	0.049	109.5	138.6	109.4	218.1	109.0	138.0
		B		-	111.0	140.5	108.6			
	8-5-T4.0-4#4-i-4-3-12.5[a]	A	SB/FP	0.228	102.5	129.7	102.5	203.0	101.5	128.5
		B		0.350	103.4	130.9	100.5			
Group 2	8-5g-T4.0-0-i-2.5-3-12.5[a]	A	SB/FP	-	117.6	148.9	99.3	195.4	97.7	123.7
		B		0.022 (0.008)	96.1	121.6	96.1			
	8-5g-T4.0-0-i-3.5-3-12.5[a]	A	SB/FP	0.427	104.6	132.4	93.2	186.8	93.4	118.2
		B		(0.025)	93.6	118.5	93.6			
	8-5g-T4.0-5#3-i-2.5-3-9.5[a]	A	SB	0.190	78.9	99.9	78.9	157.4	78.7	99.6
		B		0.545	92.6	117.2	78.5			
	8-5g-T4.0-5#3-i-3.5-3-9.5[a]	A	SB	0.599	88.4	111.9	80.3	159.0	79.5	100.6
		B		0.193	78.7	99.6	78.7			
	8-5g-T4.0-4#4-i-2.5-3-9.5[a]	A	SB	0.187	92.2	116.7	92.2	181.5	90.7	114.8
		B		0.498 (0.032)	102.2	129.4	89.3			
	8-5g-T4.0-4#4-i-3.5-3-9.5[a]	A	SB	-	112.0	141.8	97.6	193.4	96.7	122.4
		B		(0.056)	95.8	121.3	95.8			
Group 3	8-5-T4.0-0-i-2.5-3-12.5[a]	A	SB/FP	-	84.0	106.3	84.0	166.6	83.3	105.4
		B		-	95.0	120.3	82.6			
	8-5-T4.0-0-i-3.5-3-12.5[a]	A	SB/FP	0.013	92.1	116.6	92.1	183.7	91.9	116.3
		B		-	100.1	126.7	91.6			
	8-5-T4.0-5#3-i-2.5-3-9.5[a]	A	SB	0.185	74.5	94.3	74.5	148.5	74.2	93.9
		B		0.163	74.0	93.7	74.0			
	8-5-T4.0-5#3-i-3.5-3-9.5[a]	A	SB/FP	-	80.7	102.2	80.7	161.1	80.6	102.0
		B		0.570	96.1	121.6	80.4			
	8-5-T4.0-4#4-i-2.5-3-9.5[a]	A	SB/FP	-	94.9	120.1	91.6	181.1	90.5	114.6
		B		(0.005)	89.5	113.3	89.5			
	8-5-T4.0-4#4-i-3.5-3-9.5[a]	A	SB/FP	0.186	86.6	109.6	86.6	171.1	85.6	108.4
		B		-	89.0	112.7	84.6			
Group 4	8-8-F4.1-0-i-2.5-3-10.5	A	CB	-	77.8	98.5	77.8	154.1	77.1	97.6
		B		-	76.3	96.6	76.3			
	8-8-F4.1-2#3-i-2.5-3-10	A	CB	0.107	73.5	93.0	73.5	146.8	73.4	92.9
		B		0.168	73.3	92.8	73.3			
	(3@3)8-8-F4.1-0-i-2.5-3-10.5	A	CB	0.170	49.0	62.0	49.0	164.3	54.8	69.4
		B		0.212	56.2	71.1	56.2			
		C		0.162	59.1	74.8	59.1			

[a] Specimen contained crossties within joint region (see Figure 2.4)
[b] Specimen had no confining reinforcement above joint region
[ǂ] No anchorage failure on the bar

266

Table B.1 Cont. Comprehensive test results and data for beam-column joint specimens

	Specimen	Head	c_o in.	A_{brg}	ℓ_{eh} in.	$\ell_{eh,avg}$ in.	f_{cm} psi	Age days	d_b in.	A_b in.^{2}
	(3@3)8-8-F4.1-0-i-2.5-3-10.5-HP	A B C	2.0	4.1A_b	10.13 10.13 10.75	10.33	8450	9	1	0.79
	(3@3)8-8-F4.1-2#3-i-2.5-3-10	A B C	2.0	4.1A_b	10.13 10.00 10.13	10.08	8260	8	1	0.79
	(3@3)8-8-F4.1-2#3-i-2.5-3-10-HP	A B C	2.0	4.1A_b	10.25 10.13 10.50	10.29	8260	8	1	0.79
	(3@4)8-8-F4.1-0-i-2.5-3-10.5	A B C	2.0	4.1A_b	10.88 10.75 10.88	10.83	8450	9	1	0.79
	(3@4)8-8-F4.1-2#3-i-2.5-3-10	A B C	2.0	4.1A_b	9.75 9.63 10.25	9.88	8050	7	1	0.79
Group 4	(3@4)8-8-F4.1-2#3-i-2.5-3-10-HP	A B C	2.0	4.1A_b	10.00 10.75 10.25	10.33	8050	7	1	0.79
	(3@5)8-8-F4.1-0-i-2.5-3-10.5	A B C	2.0	4.1A_b	10.50 10.38 10.19	10.35	8050	7	1	0.79
	(3@5)8-8-F4.1-0-i-2.5-3-10.5-HP	A B C	2.0	4.1A_b	9.75 10.50 10.50	10.25	8260	8	1	0.79
	(3@5)8-8-F4.1-2#3-i-2.5-3-10.5	A B C	2.0	4.1A_b	9.63 9.75 10.00	9.79	8260	8	1	0.79
	(3@5)8-8-F4.1-2#3-i-2.5-3-10.5-HP	A B C	2.0	4.1A_b	9.88 10.00 10.13	10.00	8260	8	1	0.79
	8-12-F4.1-0-i-2.5-3-10	A B	2.0	4.1A_b	9.63 9.75	9.69	11760	34	1	0.79
	8-12-F4.1-5#3-i-2.5-3-10	A B	2.0	4.1A_b	10.00 10.00	10.00	11760	34	1	0.79
Group 5	(3@3)8-12-F4.1-0-i-2.5-3-10	A B C	2.0	4.1A_b	9.81 10.00 9.88	9.90	11040	31	1	0.79
	(3@3)8-12-F4.1-5#3-i-2.5-3-10	A B C	2.0	4.1A_b	10.00 10.13 9.88	10.00	11040	31	1	0.79
	(3@4)8-12-F4.1-0-i-2.5-3-10	A B C	2.0	4.1A_b	10.00 9.75 10.00	9.92	11440	32	1	0.79

Table B.1 Cont. Comprehensive test results and data for beam-column joint specimens

Group	Specimen	Head	b in.	h in.	h_{cl} in.	d_{eff} in.	c_{so} in.	$c_{so,avg}$ in.	c_{bc} in.	s in.	d_{tr} in.	$A_{tr,l}$ in.^{2}
Group 4	(3@3)8-8-F4.1-0-i-2.5-3-10.5-HP	A					2.5		3.4	3.0		
		B	11.8	14.6	10.25	12.95	-	2.5	3.4		-	-
		C					2.5		2.8	2.8		
	(3@3)8-8-F4.1-2#3-i-2.5-3-10	A					2.5		3.1	2.9		
		B	11.8	14.2	10.25	13.64	-	2.4	3.2		0.375	0.11
		C					2.4		3.1	3.0		
	(3@3)8-8-F4.1-2#3-i-2.5-3-10-HP	A					2.5		2.8	3.0		
		B	12.1	14.0	10.25	13.36	-	2.6	2.9		0.375	0.11
		C					2.6		2.5	3.0		
	(3@4)8-8-F4.1-0-i-2.5-3-10.5	A					2.5		2.8	3.9		
		B	13.9	14.7	10.25	12.94	-	2.5	3.0		-	-
		C					2.5		2.8	4.0		
	(3@4)8-8-F4.1-2#3-i-2.5-3-10	A					2.4		3.4	4.0		
		B	13.8	14.2	10.25	12.92	-	2.4	3.5		0.375	0.11
		C					2.4		2.9	4.0		
	(3@4)8-8-F4.1-2#3-i-2.5-3-10-HP	A					2.5		3.8	4.0		
		B	14.3	14.8	10.25	13.61	-	2.5	3.0		0.375	0.11
		C					2.5		3.5	4.3		
	(3@5)8-8-F4.1-0-i-2.5-3-10.5	A					2.5		3.2	4.9		
		B	15.9	14.7	10.25	12.95	-	2.5	3.3		-	-
		C					2.4		3.5	5.1		
	(3@5)8-8-F4.1-0-i-2.5-3-10.5-HP	A					2.4		4.0	5.1		
		B	16.0	14.8	10.25	12.71	-	2.4	3.3		-	-
		C					2.5		3.3	5.0		
	(3@5)8-8-F4.1-2#3-i-2.5-3-10.5	A					2.4		3.6	4.8		
		B	15.3	14.2	10.25	12.55	-	2.4	3.4		0.375	0.11
		C					2.4		3.2	4.8		
	(3@5)8-8-F4.1-2#3-i-2.5-3-10.5-HP	A					2.4		3.2	5.0		
		B	16.0	14.1	10.25	12.94	-	2.4	3.1		0.375	0.11
		C					2.5		2.9	5.1		
Group 5	8-12-F4.1-0-i-2.5-3-10	A					2.4		3.5			
		B	16.9	14.2	10.25	11.55	2.6	2.5	3.4	10.9	0.375	-
	8-12-F4.1-5#3-i-2.5-3-10	A					2.5		3.2			
		B	17.0	14.2	10.25	11.83	2.5	2.5	3.2	11.0	0.375	0.11
	(3@3)8-12-F4.1-0-i-2.5-3-10	A					2.5		3.3	3.1		
		B	12.0	14.2	10.25	11.98	-	2.4	3.2		0.375	-
		C					2.4		3.3	3.0		
	(3@3)8-12-F4.1-5#3-i-2.5-3-10	A					2.4		2.9	3.0		
		B	12.0	13.9	10.25	12.81	-	2.4	2.8		0.375	0.11
		C					2.4		3.1	3.1		
	(3@4)8-12-F4.1-0-i-2.5-3-10	A					2.5		3.0	4.0		
		B	14.0	14.0	10.25	11.91	-	2.5	3.3		0.375	-
		C					2.5		3.0	4.0		

Table B.1 Cont. Comprehensive test results and data for beam-column joint specimens

	Specimen	Head	N	s_{tr}* in.	A_{tt} in.²	d_{tro} in.	s_{tro}* in.	A_{ab} in.²	n	A_{hs} in.²	Long. Reinf. Layout
Group 4	(3@3)8-8-F4.1-0-i-2.5-3-10.5-HP	A B C	-	-	-	0.375	3.5 (1.75)	0.44	3	2.37	B3
	(3@3)8-8-F4.1-2#3-i-2.5-3-10	A B C	4	5 (5.5)	0.22	0.375	3 (1.5)	0.66	3	2.37	B3
	(3@3)8-8-F4.1-2#3-i-2.5-3-10-HP	A B C	4	5 (5.5)	0.22	0.375	3 (1.5)	0.66	3	2.37	B3
	(3@4)8-8-F4.1-0-i-2.5-3-10.5	A B C	-	-	-	0.375	4 (2)	0.44	3	2.37	B3
	(3@4)8-8-F4.1-2#3-i-2.5-3-10	A B C	4	5 (5.5)	0.22	0.375	3.5 (1.75)	0.44	3	2.37	B3
	(3@4)8-8-F4.1-2#3-i-2.5-3-10-HP	A B C	4	5 (5.5)	0.22	0.375	3.5 (1.75)	0.44	3	2.37	B3
	(3@5)8-8-F4.1-0-i-2.5-3-10.5	A B C	-	-	-	0.375	4 (2)	0.44	3	2.37	B3
	(3@5)8-8-F4.1-0-i-2.5-3-10.5-HP	A B C	-	-	-	0.375	4 (2)	0.44	3	2.37	B3
	(3@5)8-8-F4.1-2#3-i-2.5-3-10.5	A B C	4	5 (5.5)	0.22	0.375	4 (2)	0.44	3	2.37	B3
	(3@5)8-8-F4.1-2#3-i-2.5-3-10.5-HP	A B C	4	5 (5.5)	0.22	0.375	4 (2)	0.44	3	2.37	B3
Group 5	8-12-F4.1-0-i-2.5-3-10	A B	-	-	-	0.375	4 (2)	0.44	2	1.58	B4
	8-12-F4.1-5#3-i-2.5-3-10	A B	10	3 (1.5)	0.66	0.375	4 (2)	0.44	2	1.58	B5
	(3@3)8-12-F4.1-0-i-2.5-3-10	A B C	-	-	-	0.375	3 (1.5)	0.66	3	2.37	B5
	(3@3)8-12-F4.1-5#3-i-2.5-3-10	A B C	10	3 (1.5)	0.66	0.375	3 (1.5)	0.66	3	2.37	B5
	(3@4)8-12-F4.1-0-i-2.5-3-10	A B C	-	-	-	0.375	3 (1.5)	0.66	3	2.37	B5

* Value in parenthesis is the spacing between the first hoop and the center of the headed bar

Table B.1 Cont. Comprehensive test results and data for beam-column joint specimens

	Specimen	Head	Failure Type	Lead (Head) Slip in.	T_{max} kips	$f_{su,max}$ ksi	T_{ind} kips	T_{total} kips	T kips	f_{su} ksi
Group 4	(3@3)8-8-F4.1-0-i-2.5-3-10.5-HP	A	CB/FP	0.399	55.3	70.0	55.3	151.4	50.5	63.9
		B		0.448	50.2	63.5	50.2			
		C		0.075	46.0	58.2	46.0			
	(3@3)8-8-F4.1-2#3-i-2.5-3-10	A	CB	0.097	53.2	67.3	53.2	185.8	61.9	78.4
		B		0.202	65.3	82.7	65.3			
		C		0.127	67.3	85.2	67.3			
	(3@3)8-8-F4.1-2#3-i-2.5-3-10-HP	A	CB	0.100	51.4	65.1	51.4	170.1	56.7	71.8
		B		0.150	58.7	74.3	58.7			
		C		0.151	60.0	75.9	60.0			
	(3@4)8-8-F4.1-0-i-2.5-3-10.5	A	CB	0.117	62.8	79.5	62.8	176.1	58.7	74.3
		B		0.339	62.3	78.9	62.3			
		C		0.146	51.4	65.1	51.0			
	(3@4)8-8-F4.1-2#3-i-2.5-3-10	A	CB	0.113	61.7	78.1	61.7	166.4	55.5	70.3
		B		0.213	52.9	67.0	52.9			
		C		0.203	51.8	65.6	51.8			
	(3@4)8-8-F4.1-2#3-i-2.5-3-10-HP	A	CB	0.143	70.6	89.4	70.5	209.5	69.8	88.4
		B		0.338	70.2	88.9	70.2			
		C		-	68.8	87.1	68.8			
	(3@5)8-8-F4.1-0-i-2.5-3-10.5	A	CB	0.255	67.9	85.9	67.9	192.0	64.0	81.0
		B		0.172	65.7	83.2	65.7			
		C		0.237	58.4	73.9	58.4			
	(3@5)8-8-F4.1-0-i-2.5-3-10.5-HP	A	CB	0.113	62.9	79.6	62.9	179.6	59.9	75.8
		B		-	60.8	77.0	60.8			
		C		-	55.9	70.8	55.9			
	(3@5)8-8-F4.1-2#3-i-2.5-3-10.5	A	CB	-	61.4	77.7	61.4	168.2	56.1	71.0
		B		0.388	56.1	71.0	50.1			
		C		0.217	56.7	71.8	56.7			
	(3@5)8-8-F4.1-2#3-i-2.5-3-10.5-HP	A	CB	0.036	62.0	78.5	62.0	196.4	65.5	82.9
		B		0.171	70.8	89.6	70.8			
		C		0.168	63.6	80.5	63.6			
Group 5	8-12-F4.1-0-i-2.5-3-10	A	CB	0.110	72.5	91.8	72.5	143.6	71.8	90.9
		B		0.099 (0.079)	71.1	90.0	71.1			
	8-12-F4.1-5#3-i-2.5-3-10	A	SB/FP	-	88.4	111.9	88.4	174.3	87.2	110.4
		B		(0.006)	86.0	108.9	86.0			
	(3@3)8-12-F4.1-0-i-2.5-3-10	A	CB	-	38.5	48.7	38.5	126.5	42.2	53.4
		B		-	42.3	53.5	40.3			
		C		-	47.7	60.4	47.7			
	(3@3)8-12-F4.1-5#3-i-2.5-3-10	A	CB	0.230	65.7	83.2	65.7	187.4	61.6	78.0
		B		0.252	63.9	80.9	63.9			
		C		0.123	55.1	69.7	55.1			
	(3@4)8-12-F4.1-0-i-2.5-3-10	A	CB	0.120	49.1	62.2	49.1	146.6	48.9	61.9
		B		0.069	55.1	69.7	55.0			
		C		0.118 (0.043)	42.5	53.8	42.5			

Table B.1 Cont. Comprehensive test results and data for beam-column joint specimens

	Specimen	Head	c_o	A_{brg}	ℓ_{eh}	$\ell_{eh,\text{avg}}$	f_{cm}	Age	d_b	A_b
			in.		in.	in.	psi	days	in.	in.^{2}
Group 5	(3@4)8-12-F4.1-5#3-i-2.5-3-10	A B C	2.0	$4.1A_b$	9.81 9.88 9.63	9.77	11440	32	1	0.79
	(3@5)8-12-F4.1-0-i-2.5-3-10	A B C	2.0	$4.1A_b$	9.88 10.13 9.75	9.92	11460	33	1	0.79
	(3@5)8-12-F4.1-5#3-i-2.5-3-10	A B C	2.0	$4.1A_b$	9.75 9.38 9.69	9.60	11460	33	1	0.79
Group 6	8-5-S6.5-0-i-2.5-3-11.25	A B	1.8	$6.5A_b$	11.00 11.13	11.06	5500	6	1	0.79
	8-5-S6.5-0-i-2.5-3-14.25	A B	1.8	$6.5A_b$	14.38 14.13	14.25	5500	6	1	0.79
	8-5-O4.5-0-i-2.5-3-11.25	A B	1.6	$4.5A_b$	11.00 11.50	11.25	5500	6	1	0.79
	8-5-O4.5-0-i-2.5-3-14.25	A B	1.6	$4.5A_b$	14.38 13.88	14.13	5500	6	1	0.79
	8-5-S6.5-2#3-i-2.5-3-9.25	A B	1.8	$6.5A_b$	9.25 9.00	9.13	5750	7	1	0.79
	8-5-S6.5-2#3-i-2.5-3-12.25	A B	1.8	$6.5A_b$	12.50 12.13	12.31	5750	7	1	0.79
	8-5-O4.5-2#3-i-2.5-3-9.25	A B	1.6	$4.5A_b$	9.38 9.38	9.38	5750	7	1	0.79
	8-5-O4.5-2#3-i-2.5-3-12.25	A B	1.6	$4.5A_b$	12.00 12.00	12.00	5750	7	1	0.79
	8-5-S6.5-5#3-i-2.5-3-8.25	A B	1.8	$6.5A_b$	8.38 8.25	8.31	5900	8	1	0.79
	8-5-S6.5-5#3-i-2.5-3-11.25	A B	1.8	$6.5A_b$	10.88 11.00	10.94	5900	8	1	0.79
	8-5-O4.5-5#3-i-2.5-3-8.25	A B	1.6	$4.5A_b$	8.13 7.88	8.00	5900	8	1	0.79
	8-5-O4.5-5#3-i-2.5-3-11.25	A B	1.6	$4.5A_b$	11.38 10.88	11.13	5900	8	1	0.79
Group 7	8-5-T9.5-0-i-2.5-3-14.5	A B	1.4	$9.5A_b$	14.25 14.50	14.38	4970	8	1	0.79
	8-5-O9.1-0-i-2.5-3-14.5	A B	1.3	$9.1A_b$	14.38 14.38	14.38	4970	8	1	0.79
	8-5-T9.5-5#3-i-2.5-3-14.5	A B	1.4	$9.5A_b$	14.50 14.25	14.38	5420	13	1	0.79
	8-5-O9.1-5#3-i-2.5-3-14.5	A B	1.3	$9.1A_b$	14.06 14.13	14.09	4970	8	1	0.79
	(3@5.5)8-5-T9.5-0-i-2.5-3-14.5	A B C	1.4	$9.5A_b$	14.25 14.25 14.25	14.25	4960	9	1	0.79

Table B.1 Cont. Comprehensive test results and data for beam-column joint specimens

	Specimen	Head	b in.	h in.	h_{cl} in.	d_{eff} in.	c_{so} in.	$c_{so,\text{avg}}$ in.	c_{bc} in.	s in.	d_{tr} in.	$A_{tr,l}$ in.^{2}
Group 5	(3@4)8-12-F4.1-5#3-i-2.5-3-10	A B C	13.8	14.0	10.25	12.48	2.4 - 2.5	2.4	3.2 3.1 3.3	3.9 4.0	0.375	0.11
	(3@5)8-12-F4.1-0-i-2.5-3-10	A B C	16.1	14.1	10.25	11.88	2.5 - 2.5	2.5	3.2 3.0 3.3	5.0 5.1	0.375	-
	(3@5)8-12-F4.1-5#3-i-2.5-3-10	A B C	16.3	14.3	10.25	12.31	2.5 - 2.5	2.5	3.5 3.9 3.6	5.1 5.2	0.375	0.11
Group 6	8-5-S6.5-0-i-2.5-3-11.25	A B	16.8	16.1	10.25	12.70	2.5 2.5	2.5	3.4 3.3	10.8	0.375	-
	8-5-S6.5-0-i-2.5-3-14.25	A B	16.3	19.1	10.25	13.10	2.3 2.4	2.3	3.0 3.3	10.6	0.375	-
	8-5-O4.5-0-i-2.5-3-11.25	A B	16.9	16.1	10.25	12.44	2.5 2.5	2.5	3.5 3.0	10.9	0.375	-
	8-5-O4.5-0-i-2.5-3-14.25	A B	17.0	19.1	10.25	13.01	2.5 2.5	2.5	3.1 3.6	11.0	0.375	-
	8-5-S6.5-2#3-i-2.5-3-9.25	A B	17.5	14.0	10.25	12.25	2.8 2.5	2.6	3.0 3.3	11.3	0.375	0.11
	8-5-S6.5-2#3-i-2.5-3-12.25	A B	16.9	17.1	10.25	12.96	2.4 2.5	2.5	2.8 3.2	11.0	0.375	0.11
	8-5-O4.5-2#3-i-2.5-3-9.25	A B	17.0	14.1	10.25	12.39	2.5 2.5	2.5	3.1 3.1	11.0	0.375	0.11
	8-5-O4.5-2#3-i-2.5-3-12.25	A B	16.6	16.9	10.25	12.73	2.4 2.5	2.4	3.3 3.3	10.8	0.375	0.11
	8-5-S6.5-5#3-i-2.5-3-8.25	A B	16.9	13.1	10.25	12.18	2.5 2.4	2.4	3.0 3.1	11.0	0.375	0.11
	8-5-S6.5-5#3-i-2.5-3-11.25	A B	17.6	16.0	10.25	12.87	2.5 2.4	2.4	3.4 3.3	11.8	0.375	0.11
	8-5-O4.5-5#3-i-2.5-3-8.25	A B	17.3	13.0	10.25	12.37	2.5 2.8	2.6	3.3 3.5	11.0	0.375	0.11
	8-5-O4.5-5#3-i-2.5-3-11.25	A B	16.6	15.9	10.25	12.81	2.5 2.4	2.4	2.9 3.4	10.8	0.375	0.11
Group 7	8-5-T9.5-0-i-2.5-3-14.5	A B	17.0	19.1	10.25	13.43	2.6 2.5	2.6	3.4 3.1	10.9	0.375	-
	8-5-O9.1-0-i-2.5-3-14.5	A B	17.3	19.2	10.25	13.54	2.5 2.8	2.6	3.2 3.2	11.0	0.375	-
	8-5-T9.5-5#3-i-2.5-3-14.5	A B	17.1	19.2	10.25	14.22	2.5 2.6	2.6	3.2 3.5	11.0	0.375	0.11
	8-5-O9.1-5#3-i-2.5-3-14.5	A B	17.0	19.2	10.25	-‡	2.5 2.5	2.5	3.5 3.4	11.0	0.375	0.11
	(3@5.5)8-5-T9.5-0-i-2.5-3-14.5	A B C	16.9	19.2	10.25	14.08	2.4 - 2.5	2.4	3.4 3.4 3.4	5.5 5.5	0.375	-

‡ d_{eff} was not calculated for specimen with bar yielding

	Specimen	Head	N	s_{tr}* in.	A_{tt} in.²	d_{tro} in.	s_{tro}* in.	A_{ab} in.²	n	A_{hs} in.²	Long. Reinf. Layout
Group 5	(3@4)8-12-F4.1-5#3-i-2.5-3-10	A B C	10	3 (1.5)	0.66	0.375	3 (1.5)	0.66	3	2.37	B5
	(3@5)8-12-F4.1-0-i-2.5-3-10	A B C	-	-	-	0.375	3 (1.5)	0.66	3	2.37	B5
	(3@5)8-12-F4.1-5#3-i-2.5-3-10	A B C	10	3 (1.5)	0.66	0.375	3 (1.5)	0.66	3	2.37	B5
Group 6	8-5-S6.5-0-i-2.5-3-11.25	A B	-	-	-	0.5	3.5 (1.75)	0.80	2	1.58	B4
	8-5-S6.5-0-i-2.5-3-14.25	A B	-	-	-	0.5	3.5 (1.75)	0.80	2	1.58	B4
	8-5-O4.5-0-i-2.5-3-11.25	A B	-	-	-	0.5	3.5 (1.75)	0.80	2	1.58	B4
	8-5-O4.5-0-i-2.5-3-14.25	A B	-	-	-	0.5	3.5 (1.75)	0.80	2	1.58	B4
	8-5-S6.5-2#3-i-2.5-3-9.25	A B	4	5.5 (5)	0.22	0.5	3 (1.5)	1.20	2	1.58	B4
	8-5-S6.5-2#3-i-2.5-3-12.25	A B	4	5.5 (5)	0.22	0.5	3 (1.5)	1.20	2	1.58	B4
	8-5-O4.5-2#3-i-2.5-3-9.25	A B	4	5.5 (5)	0.22	0.5	3 (1.5)	1.20	2	1.58	B4
	8-5-O4.5-2#3-i-2.5-3-12.25	A B	4	5.5 (5)	0.22	0.5	3 (1.5)	1.20	2	1.58	B4
	8-5-S6.5-5#3-i-2.5-3-8.25	A B	10	3 (1.5)	0.66	0.5	2.5 (1.25)	1.20	2	1.58	B4
	8-5-S6.5-5#3-i-2.5-3-11.25	A B	10	3 (1.5)	0.66	0.5	3 (1.5)	1.20	2	1.58	B4
	8-5-O4.5-5#3-i-2.5-3-8.25	A B	10	3 (1.5)	0.66	0.5	2.5 (1.25)	1.20	2	1.58	B4
	8-5-O4.5-5#3-i-2.5-3-11.25	A B	10	3 (1.5)	0.66	0.5	3 (1.5)	1.20	2	1.58	B4
Group 7	8-5-T9.5-0-i-2.5-3-14.5	A B	-	-	-	0.375	4 (2)	0.44	2	1.58	B4
	8-5-O9.1-0-i-2.5-3-14.5	A B	-	-	-	0.375	4 (2)	0.44	2	1.58	B4
	8-5-T9.5-5#3-i-2.5-3-14.5	A B	10	3 (1.5)	0.66	0.375	4 (2)	0.44	2	1.58	B6
	8-5-O9.1-5#3-i-2.5-3-14.5	A B	10	3 (1.5)	0.66	0.375	4 (2)	0.28	2	1.58	B6
	(3@5.5)8-5-T9.5-0-i-2.5-3-14.5	A B C	-	-	-	0.375	4 (2)	0.44	3	2.37	B5

* Value in parenthesis is the spacing between the first hoop and the center of the headed bar

Table B.1 Cont. Comprehensive test results and data for beam-column joint specimens

	Specimen	Head	Failure Type	Lead (Head) Slip in.	T_{max} kips	$f_{su,max}$ ksi	T_{ind} kips	T_{total} kips	T kips	f_{su} ksi
Group 5	(3@4)8-12-F4.1-5#3-i-2.5-3-10	A	CB/FP	0.138	64.0	81.0	64.0	197.1	65.7	83.2
		B		0.240	66.5	84.2	66.5			
		C		0.260	66.7	84.4	66.6			
	(3@5)8-12-F4.1-0-i-2.5-3-10	A	CB	0.079	57.1	72.3	57.1	165.4	55.1	69.7
		B		0.177	55.3	70.0	55.3			
		C		0.249 (0.081)	53.0	67.1	53.0			
	(3@5)8-12-F4.1-5#3-i-2.5-3-10	A	CB/FP	0.164	77.2	97.7	77.2	209.1	69.7	88.2
		B		0.123	65.4	82.8	65.4			
		C		0.122	66.7	84.4	66.6			
Group 6	8-5-S6.5-0-i-2.5-3-11.25	A	SB/FP	0.161	74.9	94.8	74.9	151.1	75.6	95.6
		B		-	76.2	96.5	76.2			
	8-5-S6.5-0-i-2.5-3-14.25	A	SB/FP	(0.054)	87.5	110.8	87.5	175.4	87.7	111.0
		B		-	103.4	130.9	88.0			
	8-5-O4.5-0-i-2.5-3-11.25	A	SB/FP	0.037	67.6	85.6	67.6	134.8	67.4	85.3
		B		0.198	67.2	85.0	67.2			
	8-5-O4.5-0-i-2.5-3-14.25	A	SB/FP	0.214 (0.023)	103.5	131.0	84.2	170.0	85.0	107.6
		B		0.113	85.8	108.6	85.8			
	8-5-S6.5-2#3-i-2.5-3-9.25	A	CB	(0.012)	62.6	79.2	62.6	126.7	63.4	80.2
		B		-	64.1	81.2	64.1			
	8-5-S6.5-2#3-i-2.5-3-12.25	A	SB/FP	0.340	84.6	107.1	84.6	171.9	86.0	108.8
		B		0.254	89.3	113.0	87.3			
	8-5-O4.5-2#3-i-2.5-3-9.25	A	SB/FP	0.309	67.6	85.6	67.1	135.8	67.9	86.0
		B		0.205	68.7	86.9	68.7			
	8-5-O4.5-2#3-i-2.5-3-12.25	A	SB/FP	0.305	82.8	104.8	77.4	157.0	78.5	99.4
		B		0.220	79.6	100.8	79.6			
	8-5-S6.5-5#3-i-2.5-3-8.25	A	CB/FP	0.363	61.9	78.4	61.9	124.1	62.0	78.5
		B		0.500	62.2	78.7	62.2			
	8-5-S6.5-5#3-i-2.5-3-11.25	A	SB/FP	-	100.8	127.6	84.2	169.0	84.5	106.9
		B		0.046	84.7	107.2	84.7			
	8-5-O4.5-5#3-i-2.5-3-8.25	A	SB/FP	0.457	68.3	86.5	68.3	136.8	68.4	86.6
		B		0.383	68.5	86.7	68.5			
	8-5-O4.5-5#3-i-2.5-3-11.25	A	SB/FP	0.171	85.0	107.6	82.1	164.5	82.2	104.1
		B		-	82.4	104.3	82.4			
Group 7	8-5-T9.5-0-i-2.5-3-14.5	A	SB/FP	0.130	91.5	115.8	91.5	183.3	91.7	116.0
		B		0.312	115.9	146.7	91.8			
	8-5-O9.1-0-i-2.5-3-14.5	A	SB/FP	0.060	94.6	119.7	94.6	189.6	94.8	120.0
		B		0.186	95.2	120.5	95.0			
	8-5-T9.5-5#3-i-2.5-3-14.5	A	SB/FP	-	120.7[‡]	152.8[‡]	120.6	242.0	121.0	153.2
		B		-	121.4	153.7	121.4			
	8-5-O9.1-5#3-i-2.5-3-14.5	A	Y	0.050	118.8	150.4	118.8	238.5	119.3	150.9
		B		-	119.7	151.5	119.7			
	(3@5.5)8-5-T9.5-0-i-2.5-3-14.5	A	CB	0.156	68.7	87.0	68.7	220.2	73.4	92.9
		B		0.138	78.8	99.7	78.8			
		C		0.217	72.6	91.9	72.6			

[‡] No anchorage failure on the bar

274

Table B.1 Cont. Comprehensive test results and data for beam-column joint specimens

	Specimen	Head	c_o in.	A_{brg}	ℓ_{eh} in.	$\ell_{eh,avg}$ in.	f_{cm} psi	Age days	d_b in.	A_b in.^{2}
Group 7	(3@5.5)8-5-O9.1-0-i-2.5-3-14.5	A B C	1.3	$9.1A_b$	14.31 14.50 14.25	14.35	4960	9	1	0.79
	(3@5.5)8-5-T9.5-5#3-i-2.5-3-14.5	A B C	1.4	$9.5A_b$	14.50 14.38 14.38	14.42	5370	10	1	0.79
	(3@5.5)8-5-O9.1-5#3-i-2.5-3-14.5	A B C	1.3	$9.1A_b$	14.06 14.44 14.31	14.27	5420	13	1	0.79
	(4@3.7)8-5-T9.5-0-i-2.5-3-14.5	A B C D	1.4	$9.5A_b$	14.25 14.38 14.25 14.19	14.30	5570	14	1	0.79
	(4@3.7)8-5-O9.1-0-i-2.5-3-14.5	A B C D	1.3	$9.1A_b$	14.06 14.06 14.06 14.06	14.06	5570	14	1	0.79
	(4@3.7)8-5-T9.5-5#3-i-2.5-3-14.5	A B C D	1.4	$9.5A_b$	14.44 14.38 14.63 14.50	14.50	5570	14	1	0.79
	(4@3.7)8-5-O9.1-5#3-i-2.5-3-14.5	A B C D	1.3	$9.1A_b$	14.44 14.44 14.63 14.44	14.50	5570	14	1	0.79
Group 8	8-15-T4.0-0-i-2.5-4.5-9.5	A B	1.9	$4.0A_b$	9.50 9.50	9.50	16030	88	1	0.79
	8-15-S9.5-0-i-2.5-3-9.5	A B	1.4	$9.5A_b$	9.50 9.50	9.50	16030	88	1	0.79
	8-15-S14.9-0-i-2.5-3-9.5	A B	1.0	$14.9A_b$	9.63 9.75	9.69	16030	88	1	0.79
	8-15-T4.0-2#3-i-2.5-4.5-7	A B	1.9	$4.0A_b$	7.13 7.00	7.06	16030	87	1	0.79
	8-15-S9.5-2#3-i-2.5-3-7	A B	1.4	$9.5A_b$	7.13 7.00	7.06	16030	87	1	0.79
	8-15-S14.9-2#3-i-2.5-3-7	A B	1.0	$14.9A_b$	7.00 7.00	7.00	16030	87	1	0.79
	8-15-T4.0-5#3-i-2.5-4.5-5.5	A B	1.9	$4.0A_b$	5.50 5.50	5.50	16030	88	1	0.79
	8-15-S9.5-5#3-i-2.5-3-5.5	A B	1.4	$9.5A_b$	5.75 5.50	5.63	16030	88	1	0.79
	8-15-S14.9-5#3-i-2.5-3-5.5	A B	1.0	$14.9A_b$	5.50 5.50	5.50	16030	88	1	0.79

Table B.1 Cont. Comprehensive test results and data for beam-column joint specimens

	Specimen	Head	b in.	h in.	h_{cl} in.	d_{eff} in.	c_{so} in.	$c_{so,avg}$ in.	c_{bc} in.	s in.	d_{tr} in.	$A_{tr,l}$ in.^{2}
Group 7	(3@5.5)8-5-O9.1-0-i-2.5-3-14.5	A					2.4		3.3	5.5		
		B	16.9	19.2	10.25	14.20	-	2.4	3.1		0.375	-
		C					2.5		3.3	5.5		
	(3@5.5)8-5-T9.5-5#3-i-2.5-3-14.5	A					2.5		3.1	5.6		
		B	17.4	19.1	10.25	14.93	-	2.6	3.2		0.375	0.11
		C					2.8		3.2	5.5		
	(3@5.5)8-5-O9.1-5#3-i-2.5-3-14.5	A					2.5		3.5	5.8		
		B	17.3	19.2	10.25	-‡	-	2.5	3.2		0.375	0.11
		C					2.5		3.3	5.5		
	(4@3.7)8-5-T9.5-0-i-2.5-3-14.5	A					2.5		3.5	3.8		
		B	17.3	19.2	10.25	14.17	-	2.5	3.3	3.8	0.375	-
		C					-		3.5			
		D					2.5		3.5	3.8		
	(4@3.7)8-5-O9.1-0-i-2.5-3-14.5	A					2.5		3.4	3.6		
		B	16.8	19.1	10.25	14.19	-	2.4	3.4	3.8	0.375	-
		C					-		3.4			
		D					2.4		3.4	3.5		
	(4@3.7)8-5-T9.5-5#3-i-2.5-3-14.5	A					2.4		3.2	3.8		
		B	17.1	19.1	10.25	15.20	-	2.4	3.2	3.8	0.375	0.11
		C					-		3.0			
		D					2.5		3.1	3.8		
	(4@3.7)8-5-O9.1-5#3-i-2.5-3-14.5	A					2.5		3.1	3.6		
		B	16.9	19.1	10.25	-‡	-	2.5	3.1	3.6	0.375	0.11
		C					-		2.9			
		D					2.5		3.1	3.6		
Group 8	8-15-T4.0-0-i-2.5-4.5-9.5	A	17.0	15.5	10.25	11.36	2.5	2.5	4.5	11.0	0.375	-
		B					2.5		4.5			
	8-15-S9.5-0-i-2.5-3-9.5	A	17.3	15.2	10.25	11.33	2.8	2.6	2.9	11.0	0.375	-
		B					2.5		2.9			
	8-15-S14.9-0-i-2.5-3-9.5	A	16.8	15.3	10.25	11.41	2.5	2.5	2.9	10.8	0.375	-
		B					2.5		2.8			
	8-15-T4.0-2#3-i-2.5-4.5-7	A	17.0	13.1	10.25	11.03	2.5	2.5	4.5	11.0	0.375	0.11
		B					2.5		4.6			
	8-15-S9.5-2#3-i-2.5-3-7	A	16.9	13.1	10.25	11.14	2.5	2.5	3.2	10.9	0.375	0.11
		B					2.5		3.3			
	8-15-S14.9-2#3-i-2.5-3-7	A	17.6	13.1	10.25	11.30	2.8	2.8	3.3	11.0	0.375	0.11
		B					2.9		3.3			
	8-15-T4.0-5#3-i-2.5-4.5-5.5	A	16.9	11.7	10.25	11.09	2.4	2.4	4.7	11.0	0.375	0.11
		B					2.5		4.7			
	8-15-S9.5-5#3-i-2.5-3-5.5	A	16.8	11.5	10.25	11.26	2.3	2.4	3.0	11.0	0.375	0.11
		B					2.5		3.3			
	8-15-S14.9-5#3-i-2.5-3-5.5	A	17.0	12.0	10.25	11.33	2.5	2.5	3.8	11.0	0.375	0.11
		B					2.5		3.8			

‡ d_{eff} was not calculated for specimen with bar yielding

	Specimen	Head	N	s_{tr}* in.	A_{tt} in.²	d_{tro} in.	s_{tro}* in.	A_{ab} in.²	n	A_{hs} in.²	Long. Reinf. Layout
Group 7	(3@5.5)8-5-O9.1-0-i-2.5-3-14.5	A B C	-	-	-	0.375	4 (2)	0.44	3	2.37	B5
	(3@5.5)8-5-T9.5-5#3-i-2.5-3-14.5	A B C	10	3 (1.5)	0.66	0.375	4 (2)	0.44	3	2.37	B5
	(3@5.5)8-5-O9.1-5#3-i-2.5-3-14.5	A B C	10	3 (1.5)	0.66	0.375	4 (2)	0.19	3	2.37	B5
	(4@3.7)8-5-T9.5-0-i-2.5-3-14.5	A B C D	-	-	-	0.375	4 (2)	0.44	4	3.16	B5
	(4@3.7)8-5-O9.1-0-i-2.5-3-14.5	A B C D	-	-	-	0.375	4 (2)	0.44	4	3.16	B5
	(4@3.7)8-5-T9.5-5#3-i-2.5-3-14.5	A B C D	10	3 (1.5)	0.66	0.375	3 (1.5)	0.66	4	3.16	B5
	(4@3.7)8-5-O9.1-5#3-i-2.5-3-14.5	A B C D	10	3 (1.5)	0.66	0.375	3 (1.5)	0.21	4	3.16	B5
Group 8	8-15-T4.0-0-i-2.5-4.5-9.5	A B	-	-	-	0.5	4 (2)	0.80	2	1.58	B6
	8-15-S9.5-0-i-2.5-3-9.5	A B	-	-	-	0.5	4 (2)	0.80	2	1.58	B6
	8-15-S14.9-0-i-2.5-3-9.5	A B	-	-	-	0.5	4 (2)	0.80	2	1.58	B6
	8-15-T4.0-2#3-i-2.5-4.5-7	A B	4	5.5 (5)	0.22	0.5	4 (2)	0.80	2	1.58	B6
	8-15-S9.5-2#3-i-2.5-3-7	A B	4	5.5 (5)	0.22	0.5	4 (2)	0.80	2	1.58	B6
	8-15-S14.9-2#3-i-2.5-3-7	A B	4	5.5 (5)	0.22	0.5	4 (2)	0.80	2	1.58	B6
	8-15-T4.0-5#3-i-2.5-4.5-5.5	A B	10	3 (1.5)	0.66	0.5	4 (2)	0.80	2	1.58	B7
	8-15-S9.5-5#3-i-2.5-3-5.5	A B	10	3 (1.5)	0.66	0.5	4 (2)	0.80	2	1.58	B7
	8-15-S14.9-5#3-i-2.5-3-5.5	A B	10	3 (1.5)	0.66	0.5	4 (2)	0.80	2	1.58	B7

* Value in parenthesis is the spacing between the first hoop and the center of the headed bar

	Specimen	Head	Failure Type	Lead (Head) Slip in.	T_{max} kips	$f_{su,max}$ ksi	T_{ind} kips	T_{total} kips	T kips	f_{su} ksi
Group 7	(3@5.5)8-5-O9.1-0-i-2.5-3-14.5	A		0.081 (0.043)	91.0	115.2	91.0			
		B	CB	0.085	76.2	96.5	76.2	227.1	75.7	95.8
		C		0.055	59.9	75.8	59.9			
	(3@5.5)8-5-T9.5-5#3-i-2.5-3-14.5	A		0.121	91.5	115.8	91.5			
		B	CB	0.086	91.5	115.8	91.5	283.8	94.6	119.7
		C		0.223	100.8	127.6	100.8			
	(3@5.5)8-5-O9.1-5#3-i-2.5-3-14.5	A		-	115.4	146.1	102.9			
		B	Y	-	104.4	132.2	100.4	306.6	102.2	129.4
		C		-	103.3	130.8	103.3			
	(4@3.7)8-5-T9.5-0-i-2.5-3-14.5	A		0.159	89.7	113.5	89.7			
		B	CB	0.236	46.9	59.4	46.9	243.3	60.8	77.0
		C		-	57.6	72.9	57.6			
		D		0.168	49.1	62.2	49.1			
	(4@3.7)8-5-O9.1-0-i-2.5-3-14.5	A		0.088	67.9	85.9	67.9			
		B	CB	-	69.7	88.2	69.7	244.9	61.2	77.5
		C		-	56.6	71.6	56.6			
		D		0.114 (0.085)	50.8	64.3	50.8			
	(4@3.7)8-5-T9.5-5#3-i-2.5-3-14.5	A		0.320	-†	-†	-			
		B	CB	-	82.2	104.1	82.2	-†	76.9†	97.3
		C		-	74.6	94.4	74.6			
		D		0.161	73.8	93.4	73.8			
	(4@3.7)8-5-O9.1-5#3-i-2.5-3-14.5	A		0.087	-†	-†	-			
		B	Y	0.016	97.1	122.9	96.8	-†	89.1†	112.8
		C		-	88.9	112.5	88.9			
		D		0.033	81.4	103.0	81.4			
Group 8	8-15-T4.0-0-i-2.5-4.5-9.5	A	CB	-	83.2	105.3	83.2	166.6	83.3	105.4
		B		0.237	83.4	105.6	83.4			
	8-15-S9.5-0-i-2.5-3-9.5	A	CB	-	83.5	105.7	83.5	163.3	81.7	103.4
		B		-	79.9	101.1	79.9			
	8-15-S14.9-0-i-2.5-3-9.5	A	CB	-	88.2	111.6	88.2	174.2	87.1	110.3
		B		-	86.1	109.0	86.1			
	8-15-T4.0-2#3-i-2.5-4.5-7	A	CB	-	59.1	74.8	59.1	118.0	59.0	74.7
		B		-	58.9	74.6	58.9			
	8-15-S9.5-2#3-i-2.5-3-7	A	CB	-	66.4	84.1	66.4	134.3	67.1	84.9
		B		-	67.9	85.9	67.9			
	8-15-S14.9-2#3-i-2.5-3-7	A	CB	-	79.7	100.9	79.7	158.7	79.3	100.4
		B		-	78.9	99.9	78.9			
	8-15-T4.0-5#3-i-2.5-4.5-5.5	A	CB	-	64.0	81.0	64.0	126.6	63.3	80.1
		B		-	62.6	79.2	62.6			
	8-15-S9.5-5#3-i-2.5-3-5.5	A	CB	-	76.6	97.0	76.6	151.6	75.8	95.9
		B		-	75.0	94.9	75.0			
	8-15-S14.9-5#3-i-2.5-3-5.5	A	CB	-	80.7	102.2	80.7	162.7	81.4	103.0
		B		-	82.0	103.8	82.0			

† Load on headed bar A was not recorded due to a malfunction of load cell; T taken as the average load of the other three bars.

Table B.1 Cont. Comprehensive test results and data for beam-column joint specimens

	Specimen	Head	c_o in.	A_{brg}	ℓ_{eh} in.	$\ell_{eh,\text{avg}}$ in.	f_{cm} psi	Age days	d_b in.	A_b in.^{2}
Group 9	8-8-T9.5-0-i-2.5-3-9.5	A B	1.4	$9.5A_b$	9.50 9.25	9.38	9040	12	1	0.79
	8-8-T9.5-2#3-i-2.5-3-9.5	A B	1.4	$9.5A_b$	9.00 9.38	9.19	9040	12	1	0.79
	(3@4)8-8-T9.5-0-i-2.5-3-9.5	A B C	1.4	$9.5A_b$	9.00 9.50 9.25	9.25	9040	12	1	0.79
	(3@4)8-8-T9.5-2#3-i-2.5-3-9.5	A B C	1.4	$9.5A_b$	9.75 9.50 9.50	9.58	9040	12	1	0.79
	(3@5)8-8-T9.5-0-i-2.5-3-9.5	A B C	1.4	$9.5A_b$	9.50 9.75 9.25	9.50	9940	11	1	0.79
	(3@5)8-8-T9.5-2#3-i-2.5-3-9.5	A B C	1.4	$9.5A_b$	9.50 9.50 9.25	9.42	9940	11	1	0.79
	(3@7)8-8-T9.5-0-i-2.5-3-9.5	A B C	1.4	$9.5A_b$	9.50 9.63 9.38	9.50	10180	10	1	0.79
	(3@7)8-8-T9.5-2#3-i-2.5-3-9.5	A B C	1.4	$9.5A_b$	9.50 9.75 9.50	9.58	10180	10	1	0.79
	8-8-T9.5-0-i-2.5-3-14.5	A B	1.4	$9.5A_b$	14.50 14.25	14.38	10180	10	1	0.79
	(3@4)8-8-T9.5-0-i-2.5-3-14.5	A B C	1.4	$9.5A_b$	14.25 14.75 14.75	14.58	9040	12	1	0.79
	(3@4)8-8-T9.5-2#3-i-2.5-3-14.5	A B C	1.4	$9.5A_b$	14.50 14.50 14.25	14.42	9040	12	1	0.79
	(3@5)8-8-T9.5-0-i-2.5-3-14.5	A B C	1.4	$9.5A_b$	14.75 14.50 14.50	14.58	9940	11	1	0.79
	(3@5)8-8-T9.5-2#3-i-2.5-3-14.5	A B C	1.4	$9.5A_b$	14.00 14.25 14.00	14.08	9940	11	1	0.79
	(3@7)8-8-T9.5-0-i-2.5-3-14.5	A B C	1.4	$9.5A_b$	14.44 14.56 14.63	14.54	10180	10	1	0.79
	(3@7)8-8-T9.5-2#3-i-2.5-3-14.5	A B C	1.4	$9.5A_b$	14.50 14.63 14.50	14.54	10180	10	1	0.79

Table B.1 Cont. Comprehensive test results and data for beam-column joint specimens

	Specimen	Head	b in.	h in.	h_{cl} in.	d_{eff} in.	c_{so} in.	$c_{so,avg}$ in.	c_{bc} in.	s in.	d_{tr} in.	$A_{tr,l}$ in.²
Group 9	8-8-T9.5-0-i-2.5-3-9.5	A B	17.0	14.3	10.25	11.79	2.5 2.5	2.5	3.3 3.5	11.0	0.375	-
	8-8-T9.5-2#3-i-2.5-3-9.5	A B	17.0	14.0	10.25	11.87	2.8 2.5	2.6	3.5 3.1	10.8	0.375	0.11
	(3@4)8-8-T9.5-0-i-2.5-3-9.5	A B C	14.0	14.0	10.25	11.98	2.5 - 2.5	2.5	3.5 3.0 3.3	4.0 4.0	0.375	-
	(3@4)8-8-T9.5-2#3-i-2.5-3-9.5	A B C	14.0	14.3	10.25	12.47	2.5 - 2.5	2.5	3.0 3.3 3.3	4.0 4.0	0.375	0.11
	(3@5)8-8-T9.5-0-i-2.5-3-9.5	A B C	16.0	14.3	10.25	11.77	2.5 - 2.5	2.5	3.3 3.0 3.5	5.0 5.0	0.375	-
	(3@5)8-8-T9.5-2#3-i-2.5-3-9.5	A B C	16.0	14.3	10.25	12.16	2.5 - 2.5	2.5	3.3 3.3 3.5	5.0 5.0	0.375	0.11
	(3@7)8-8-T9.5-0-i-2.5-3-9.5	A B C	19.9	14.1	10.25	12.08	2.5 - 2.5	2.5	3.1 2.9 3.2	7.0 6.9	0.375	-
	(3@7)8-8-T9.5-2#3-i-2.5-3-9.5	A B C	20.1	14.3	10.25	12.05	2.5 - 2.5	2.5	3.3 3.0 3.3	7.0 7.1	0.375	0.11
	8-8-T9.5-0-i-2.5-3-14.5	A B	17.1	19.3	10.25	-‡	2.5 2.5	2.5	3.3 3.6	11.1	0.375	-
	(3@4)8-8-T9.5-0-i-2.5-3-14.5	A B C	14.0	19.0	10.25	13.54	2.5 - 2.5	2.5	3.3 2.8 2.8	4.0 4.0	0.375	-
	(3@4)8-8-T9.5-2#3-i-2.5-3-14.5	A B C	14.0	19.0	10.25	13.92	2.5 - 2.5	2.5	3.0 3.0 3.3	4.0 4.0	0.375	0.11
	(3@5)8-8-T9.5-0-i-2.5-3-14.5	A B C	15.8	19.1	10.25	13.43	2.5 - 2.5	2.5	2.9 3.1 3.1	4.8 5.0	0.375	-
	(3@5)8-8-T9.5-2#3-i-2.5-3-14.5	A B C	15.5	19.3	10.25	13.84	2.3 - 2.3	2.3	3.8 3.5 3.8	5.0 5.0	0.375	0.11
	(3@7)8-8-T9.5-0-i-2.5-3-14.5	A B C	20.0	19.1	10.25	13.02	2.5 - 2.5	2.5	3.1 3.0 2.9	7.0 7.0	0.375	-
	(3@7)8-8-T9.5-2#3-i-2.5-3-14.5	A B C	20.0	19.1	10.25	13.28	2.5 - 2.5	2.5	3.1 2.9 3.1	7.0 7.0	0.375	0.11

‡ d_{eff} was not calculated for specimen with bar yielding

Table B.1 Cont. Comprehensive test results and data for beam-column joint specimens

	Specimen	Head	N	s_{tr}* in.	A_{tt} in.^{2}	d_{tro} in.	s_{tro}* in.	A_{ab} in.^{2}	n	A_{hs} in.^{2}	Long. Reinf. Layout
Group 9	8-8-T9.5-0-i-2.5-3-9.5	A B	-	-	-	0.375	3 (1.5)	0.66	2	1.58	B6
	8-8-T9.5-2#3-i-2.5-3-9.5	A B	4	6 (4.5)	0.22	0.375	3 (1.5)	0.66	2	1.58	B6
	(3@4)8-8-T9.5-0-i-2.5-3-9.5	A B C	-	-	-	0.375	3 (1.5)	0.66	3	2.37	B5
	(3@4)8-8-T9.5-2#3-i-2.5-3-9.5	A B C	4	6 (4.5)	0.22	0.375	3 (1.5)	0.66	3	2.37	B5
	(3@5)8-8-T9.5-0-i-2.5-3-9.5	A B C	-	-	-	0.375	3 (1.5)	0.66	3	2.37	B5
	(3@5)8-8-T9.5-2#3-i-2.5-3-9.5	A B C	4	6 (4.5)	0.22	0.375	3 (1.5)	0.66	3	2.37	B5
	(3@7)8-8-T9.5-0-i-2.5-3-9.5	A B C	-	-	-	0.5	4.5 (2.25)	0.80	3	2.37	B7
	(3@7)8-8-T9.5-2#3-i-2.5-3-9.5	A B C	4	6 (4.5)	0.22	0.5	4.5 (2.25)	0.80	3	2.37	B7
	8-8-T9.5-0-i-2.5-3-14.5	A B	-	-	-	0.375	4 (2)	0.28	2	1.58	B6
	(3@4)8-8-T9.5-0-i-2.5-3-14.5	A B C	-	-	-	0.375	4 (2)	0.44	3	2.37	B5
	(3@4)8-8-T9.5-2#3-i-2.5-3-14.5	A B C	4	6 (4.5)	0.22	0.375	4 (2)	0.44	3	2.37	B5
	(3@5)8-8-T9.5-0-i-2.5-3-14.5	A B C	-	-	-	0.375	3.5 (1.75)	0.44	3	2.37	B8
	(3@5)8-8-T9.5-2#3-i-2.5-3-14.5	A B C	4	6 (4.5)	0.22	0.375	3.5 (1.75)	0.44	3	2.37	B8
	(3@7)8-8-T9.5-0-i-2.5-3-14.5	A B C	-	-	-	0.5	4.5 (2.25)	0.80	3	2.37	B8
	(3@7)8-8-T9.5-2#3-i-2.5-3-14.5	A B C	4	6 (4.5)	0.22	0.5	4.5 (2.25)	0.80	3	2.37	B8

* Value in parenthesis is the spacing between the first hoop and the center of the headed bar

Table B.1 Cont. Comprehensive test results and data for beam-column joint specimens

	Specimen	Head	Failure Type	Lead (Head) Slip in.	T_{max} kips	$f_{su,max}$ ksi	T_{ind} kips	T_{total} kips	T kips	f_{su} ksi
Group 9	8-8-T9.5-0-i-2.5-3-9.5	A	CB	0.168	65.0	82.3	65.0	130.5	65.2	82.5
		B		0.127	65.5	82.9	65.5			
	8-8-T9.5-2#3-i-2.5-3-9.5	A	CB	-	69.0	87.3	69.0	137.5	68.7	87.0
		B		0.103 (0.003)	68.5	86.7	68.5			
	(3@4)8-8-T9.5-0-i-2.5-3-9.5	A	CB	0.421	33.5	42.4	33.5	120.8	40.3	51.0
		B		0.232	43.2	54.7	43.2			
		C		0.356 (0.098)	44.2	55.9	44.1			
	(3@4)8-8-T9.5-2#3-i-2.5-3-9.5	A	CB	0.440	51.5	65.2	51.5	155.3	51.8	65.6
		B		0.293	54.5	69.0	54.5			
		C		0.230 (0.051)	49.3	62.4	49.3			
	(3@5)8-8-T9.5-0-i-2.5-3-9.5	A	CB	-	54.5	69.0	54.5	133.5	44.5	56.3
		B		-	27.9	35.3	27.9			
		C		0.015 (0.055)	51.0	64.6	51.0			
	(3@5)8-8-T9.5-2#3-i-2.5-3-9.5	A	CB	0.373	55.7	70.5	55.2	167.8	55.9	70.8
		B		0.430	60.6	76.7	60.6			
		C		0.342 (0.001)	52.0	65.8	52.0			
	(3@7)8-8-T9.5-0-i-2.5-3-9.5	A	CB	-	54.2	68.6	54.2	206.1	68.7	87.0
		B		0.180	66.3	83.9	66.3			
		C		0.094 (0.008)	85.6	108.4	85.6			
	(3@7)8-8-T9.5-2#3-i-2.5-3-9.5	A	CB	0.469	65.7	83.2	65.2	202.9	67.6	85.6
		B		0.124	62.6	79.2	62.6			
		C		0.145 (0.011)	75.1	95.1	75.1			
	8-8-T9.5-0-i-2.5-3-14.5	A	Y	-	117.3	148.5	117.3	237.6	118.8	150.4
		B		0.038	120.3	152.3	120.3			
	(3@4)8-8-T9.5-0-i-2.5-3-14.5	A	CB	-	80.9	102.4	80.9	229.7	76.6	97.0
		B		-	79.2	100.3	79.2			
		C		0.073	75.0	94.9	69.7			
	(3@4)8-8-T9.5-2#3-i-2.5-3-14.5	A	CB	0.122	79.5	100.6	79.5	256.3	85.4	108.1
		B		-	89.3	113.0	89.3			
		C		0.165 (0.016)	87.5	110.8	87.5			
	(3@5)8-8-T9.5-0-i-2.5-3-14.5	A	CB	0.086	87.3	110.5	87.0	279.6	93.2	118.0
		B		-	104.0	131.6	104.0			
		C		0.090 (0.031)	88.5	112.0	88.5			
	(3@5)8-8-T9.5-2#3-i-2.5-3-14.5	A	CB	0.144	93.8	118.7	93.7	315.5	105.2	133.2
		B		-	99.3	125.7	99.3			
		C		0.083	122.5	155.1	122.5			
	(3@7)8-8-T9.5-0-i-2.5-3-14.5	A	CB/BS	0.138	104.4	132.2	104.4	311.9	104.0	131.6
		B		0.166	99.2	125.6	99.2			
		C		0.130	108.3	137.1	108.3			
	(3@7)8-8-T9.5-2#3-i-2.5-3-14.5	A	CB	-	105.8	133.9	105.8	340.3	113.4	143.5
		B		-	98.7	124.9	97.9			
		C		(0.027)	136.6	172.9	136.6			

Table B.1 Cont. Comprehensive test results and data for beam-column joint specimens

	Specimen	Head	c_o in.	A_{brg}	ℓ_{eh} in.	$\ell_{eh,\text{avg}}$ in.	f_{cm} psi	Age days	d_b in.	A_b in.^{2}
Group 10	(2@9)8-12-F4.1-0-i-2.5-3-12	A B	2.0	4.1A_b	12.13 12.00	12.06	12080	57	1	0.79
	(2@9)8-12-F9.1-0-i-2.5-3-12	A B	2.0	9.1A_b	11.75 12.00	11.88	12080	57	1	0.79
	(2@9)8-12-F4.1-5#3-i-2.5-3-12	A B	2.0	4.1A_b	11.94 12.00	11.97	12080	57	1	0.79
	(2@9)8-12-F9.1-5#3-i-2.5-3-12	A B	2.0	9.1A_b	12.13 12.13	12.13	12080	57	1	0.79
	(3@4.5)8-12-F4.1-0-i-2.5-3-12	A B C	2.0	4.1A_b	12.13 12.25 12.25	12.21	12040	58	1	0.79
	(3@4.5)8-12-F9.1-0-i-2.5-3-12	A B C	2.0	9.1A_b	12.00 12.13 12.00	12.04	12040	58	1	0.79
	(3@4.5)8-12-F4.1-5#3-i-2.5-3-12	A B C	2.0	4.1A_b	12.13 12.19 12.19	12.17	12040	58	1	0.79
	(3@4.5)8-12-F9.1-5#3-i-2.5-3-12	A B C	2.0	9.1A_b	11.94 11.88 11.88	11.90	12040	58	1	0.79
	(4@3)8-12-F4.1-0-i-2.5-3-12	A B C D	2.0	4.1A_b	12.00 12.00 12.00 12.00	12.00	12040	58	1	0.79
	(4@3)8-12-F9.1-0-i-2.5-3-12	A B C D	2.0	9.1A_b	12.06 12.13 12.25 12.25	12.17	12360	61	1	0.79
	(4@3)8-12-F4.1-5#3-i-2.5-3-12	A B C D	2.0	4.1A_b	12.00 12.00 12.13 12.00	12.03	12360	61	1	0.79
	(4@3)8-12-F9.1-5#3-i-2.5-3-12	A B C D	2.0	9.1A_b	12.00 12.00 12.00 11.81	11.95	12360	61	1	0.79
Group 11	8-8-O4.5-0-i-2.5-3-9.5	A B	1.6	4.5A_b	9.13 9.25	9.19	6710	16	1	0.79
	(2@9)8-8-O4.5-0-i-2.5-3-9.5	A B	1.6	4.5A_b	9.13 8.88	9.00	6710	16	1	0.79
	(2@7)8-8-O4.5-0-i-2.5-3-9.5	A B	1.6	4.5A_b	9.38 9.13	9.25	6710	16	1	0.79
	(2@5)8-8-O4.5-0-i-2.5-3-9.5	A B	1.6	4.5A_b	9.13 8.88	9.00	6710	16	1	0.79

	Specimen	Head	b in.	h in.	h_{cl} in.	d_{eff} in.	c_{so} in.	$c_{so,avg}$ in.	c_{bc} in.	s in.	d_{tr} in.	$A_{tr,l}$ in.^{2}
Group 10	(2@9)8-12-F4.1-0-i-2.5-3-12	A B	15.0	16.1	10.25	11.83	2.5 2.5	2.5	2.9 3.1	9.0	0.375	-
	(2@9)8-12-F9.1-0-i-2.5-3-12	A B	14.9	16.0	10.25	11.78	2.5 2.5	2.5	3.3 3.0	8.9	0.375	-
	(2@9)8-12-F4.1-5#3-i-2.5-3-12	A B	14.9	16.1	10.25	12.49	2.5 2.4	2.5	3.2 3.1	9.0	0.375	0.11
	(2@9)8-12-F9.1-5#3-i-2.5-3-12	A B	14.9	17.7	10.25	-‡	2.4 2.5	2.4	4.5 4.5	9.0	0.375	0.11
	(3@4.5)8-12-F4.1-0-i-2.5-3-12	A B C	14.8	16.1	10.25	12.51	2.5 - 2.5	2.5	2.9 2.8 2.8	4.5 4.3	0.375	-
	(3@4.5)8-12-F9.1-0-i-2.5-3-12	A B C	14.8	16.1	10.25	12.52	2.4 - 2.4	2.4	3.1 2.9 3.1	4.5 4.5	0.375	-
	(3@4.5)8-12-F4.1-5#3-i-2.5-3-12	A B C	15.2	16.1	10.25	12.89	2.6 - 2.6	2.6	2.9 2.9 2.9	4.4 4.5	0.375	0.11
	(3@4.5)8-12-F9.1-5#3-i-2.5-3-12	A B C	15.0	16.0	10.25	13.51	2.5 - 2.5	2.5	3.1 3.1 3.1	4.5 4.5	0.375	0.11
	(4@3)8-12-F4.1-0-i-2.5-3-12	A B C D	14.9	16.0	10.25	12.23	2.4 - - 2.5	2.4	3.0 3.0 3.0 3.0	3.0 3.0 3.0	0.375	-
	(4@3)8-12-F9.1-0-i-2.5-3-12	A B C D	15.0	16.2	10.25	12.22	2.5 - - 2.5	2.5	3.1 3.0 2.9 2.9	3.0 3.0 3.0	0.375	-
	(4@3)8-12-F4.1-5#3-i-2.5-3-12	A B C D	15.1	16.2	10.25	12.76	2.4 - - 2.5	2.5	3.2 3.2 3.0 3.2	3.1 3.0 3.0	0.375	0.11
	(4@3)8-12-F9.1-5#3-i-2.5-3-12	A B C D	14.9	16.0	10.25	13.68	2.4 - - 2.5	2.5	3.0 3.0 3.0 3.2	3.0 3.0 3.0	0.375	0.11
Group 11	8-8-O4.5-0-i-2.5-3-9.5	A B	17.3	14.1	10.25	11.93	2.8 2.4	2.6	3.3 3.2	11.1	0.375	-
	(2@9)8-8-O4.5-0-i-2.5-3-9.5	A B	15.3	14.1	10.25	12.17	2.6 2.5	2.6	3.3 3.6	9.1	0.375	-
	(2@7)8-8-O4.5-0-i-2.5-3-9.5	A B	13.1	14.1	10.25	12.31	2.5 2.6	2.6	3.1 3.3	7.0	0.375	-
	(2@5)8-8-O4.5-0-i-2.5-3-9.5	A B	11.3	14.2	10.25	12.53	2.5 2.5	2.5	3.4 3.7	5.3	0.375	-

‡ d_{eff} was not calculated for specimen with bar yielding

	Specimen	Head	N	s_{tr}* in.	A_{tt} in.^{2}	d_{tro} in.	s_{tro}* in.	A_{ab} in.^{2}	n	A_{hs} in.^{2}	Long. Reinf. Layout
Group 10	(2@9)8-12-F4.1-0-i-2.5-3-12	A B	-	-	-	0.5	3 (1.5)	1.20	2	1.58	B5
	(2@9)8-12-F9.1-0-i-2.5-3-12	A B	-	-	-	0.5	3 (1.5)	1.20	2	1.58	B5
	(2@9)8-12-F4.1-5#3-i-2.5-3-12	A B	10	3 (1.5)	0.66	0.5	3 (1.5)	1.20	2	1.58	B5
	(2@9)8-12-F9.1-5#3-i-2.5-3-12	A B	10	3 (1.5)	0.66	0.5	3 (1.5)	0.76	2	1.58	B5
	(3@4.5)8-12-F4.1-0-i-2.5-3-12	A B C	-	-	-	0.5	3 (1.5)	1.20	3	2.37	B5
	(3@4.5)8-12-F9.1-0-i-2.5-3-12	A B C	-	-	-	0.5	3 (1.5)	1.20	3	2.37	B5
	(3@4.5)8-12-F4.1-5#3-i-2.5-3-12	A B C	10	3 (1.5)	0.66	0.5	3 (1.5)	1.20	3	2.37	B5
	(3@4.5)8-12-F9.1-5#3-i-2.5-3-12	A B C	10	3 (1.5)	0.66	0.5	3 (1.5)	1.20	3	2.37	B5
	(4@3)8-12-F4.1-0-i-2.5-3-12	A B C D	-	-	-	0.5	3 (1.5)	1.20	4	3.16	B5
	(4@3)8-12-F9.1-0-i-2.5-3-12	A B C D	-	-	-	0.5	3 (1.5)	1.20	4	3.16	B5
	(4@3)8-12-F4.1-5#3-i-2.5-3-12	A B C D	10	3 (1.5)	0.66	0.5	3 (1.5)	1.20	4	3.16	B5
	(4@3)8-12-F9.1-5#3-i-2.5-3-12	A B C D	10	3 (1.5)	0.66	0.5	3 (1.5)	1.20	4	3.16	B5
Group 11	8-8-O4.5-0-i-2.5-3-9.5	A B	-	-	-	0.375	4 (2)	0.44	2	1.58	B4
	(2@9)8-8-O4.5-0-i-2.5-3-9.5	A B	-	-	-	0.375	4 (2)	0.44	2	1.58	B4
	(2@7)8-8-O4.5-0-i-2.5-3-9.5	A B	-	-	-	0.375	4 (2)	0.44	2	1.58	B4
	(2@5)8-8-O4.5-0-i-2.5-3-9.5	A B	-	-	-	0.375	4 (2)	0.44	2	1.58	B4

* Value in parenthesis is the spacing between the first hoop and the center of the headed bar

Table B.1 Cont. Comprehensive test results and data for beam-column joint specimens

	Specimen	Head	Failure Type	Lead (Head) Slip in.	T_{max} kips	$f_{su,max}$ ksi	T_{ind} kips	T_{total} kips	T kips	f_{su} ksi
Group 10	(2@9)8-12-F4.1-0-i-2.5-3-12	A	CB/FP	-	79.8	101.0	79.8	158.1	79.1	100.1
		B		-	78.3	99.1	78.3			
	(2@9)8-12-F9.1-0-i-2.5-3-12	A	CB/BS	0.048	76.1	96.3	76.1	153.0	76.5	96.8
		B		-	76.9	97.3	76.9			
	(2@9)8-12-F4.1-5#3-i-2.5-3-12	A	SB/FP	0.126	112.5[ǂ]	142.4[ǂ]	112.5	223.8	111.9	141.6
		B		0.126	111.3	140.9	111.3			
	(2@9)8-12-F9.1-5#3-i-2.5-3-12	A	Y	0.200	125.2	158.5	125.2	242.3	121.2	153.4
		B		0.025	117.1	148.2	117.1			
	(3@4.5)8-12-F4.1-0-i-2.5-3-12	A	CB	0.133	79.1	100.1	79.1	225.7	75.2	95.2
		B		0.037	75.8	95.9	75.8			
		C		0.089	70.7	89.5	70.7			
	(3@4.5)8-12-F9.1-0-i-2.5-3-12	A	CB	(0.046)	77.8	98.5	77.8	226.2	75.4	95.4
		B		-	63.3	80.1	63.3			
		C		0.117	85.1	107.7	85.1			
	(3@4.5)8-12-F4.1-5#3-i-2.5-3-12	A	CB	0.170	83.8	106.1	83.8	263.1	87.7	111.0
		B		0.094	86.0	108.9	86.0			
		C		0.169	93.2	118.0	93.2			
	(3@4.5)8-12-F9.1-5#3-i-2.5-3-12	A	CB	0.250	108.1	136.8	108.1	325.7	108.6	137.4
		B		0.096	110.7	140.1	110.7			
		C		0.234	106.9	135.3	106.9			
	(4@3)8-12-F4.1-0-i-2.5-3-12	A	CB	-	41.7	52.8	41.7	197.2	49.3	62.4
		B		-	49.5	62.7	49.5			
		C		0.135	66.8	84.6	66.8			
		D		0.032	39.4	49.9	39.4			
	(4@3)8-12-F9.1-0-i-2.5-3-12	A	CB	-	49.2	62.3	49.2	201.3	50.3	63.7
		B		-	45.7	57.8	45.7			
		C		-	53.2	67.3	53.2			
		D		-	53.1	67.2	53.1			
	(4@3)8-12-F4.1-5#3-i-2.5-3-12	A	CB	0.030	73.8	93.4	73.8	256.7	64.2	81.2
		B		-	63.3	80.1	63.3			
		C		0.101	48.2	61.0	48.2			
		D		0.093	71.5	90.5	71.5			
	(4@3)8-12-F9.1-5#3-i-2.5-3-12	A	CB	-	85.2	107.8	85.2	351.3	87.8	111.1
		B		-	72.8	92.2	72.8			
		C		-	111.1	140.6	111.1			
		D		-	82.1	103.9	82.1			
Group 11	8-8-O4.5-0-i-2.5-3-9.5	A	CB/FP	0.002	61.9	78.4	61.8	116.7	58.4	73.9
		B		0.002	54.9	69.5	54.9			
	(2@9)8-8-O4.5-0-i-2.5-3-9.5	A	CB	0.014	57.5	72.8	57.5	117.6	58.8	74.4
		B		0.019	60.1	76.1	60.1			
	(2@7)8-8-O4.5-0-i-2.5-3-9.5	A	CB	0.010	57.2	72.4	57.2	109.0	54.5	69.0
		B		0.030	51.8	65.6	51.8			
	(2@5)8-8-O4.5-0-i-2.5-3-9.5	A	CB	0.035	45.7	57.8	45.7	102.4	51.2	64.8
		B		0.041	56.7	71.8	56.7			

[ǂ] No anchorage failure on the bar

Table B.1 Cont. Comprehensive test results and data for beam-column joint specimens

	Specimen	Head	c_o in.	A_{brg}	ℓ_{eh} in.	$\ell_{eh,avg}$ in.	f_{cm} psi	Age days	d_b in.	A_b in.^{2}
Group 11	(2@3)8-8-O4.5-0-i-2.5-3-9.5	A B	1.6	4.5A_b	9.13 8.88	9.00	6710	16	1	0.79
	(2@9)8-8-T4.0-0-i-2.5-3-9.5	A B	1.9	4.0A_b	9.25 9.50	9.38	6790	17	1	0.79
	(2@9)8-8-T4.0-5#3-i-2.5-3-9.5	A B	1.9	4.0A_b	9.50 9.50	9.50	6790	17	1	0.79
	(3@4.5)8-8-T4.0-0-i-2.5-3-9.5	A B C	1.9	4.0A_b	9.25 9.50 9.25	9.33	6790	17	1	0.79
	(3@4.5)8-8-T4.0-5#3-i-2.5-3-9.5	A B C	1.9	4.0A_b	9.13 9.25 9.13	9.17	6650	20	1	0.79
	(4@3)8-8-T4.0-0-i-2.5-3-9.5	A B C D	1.9	4.0A_b	9.63 9.63 9.25 9.38	9.47	6650	20	1	0.79
	(4@3)8-8-T4.0-5#3-i-2.5-3-9.5	A B C D	1.9	4.0A_b	9.75 9.63 9.88 9.38	9.66	6650	20	1	0.79
	(3@3)8-8-T4.0-0-i-2.5-3-9.5	A B C	1.9	4.0A_b	9.25 9.63 9.50	9.46	6790	17	1	0.79
	(3@3)8-8-T4.0-5#3-i-2.5-3-9.5	A B C	1.9	4.0A_b	9.25 9.38 9.38	9.33	6650	20	1	0.79
Group 12	8-5-F4.1-0-i-2.5-7-6	A B	2.0	4.1A_b	6.06 6.13	6.09	4930	14	1	0.79
	8-5-F4.1-5#3-i-2.5-7-6	A B	2.0	4.1A_b	6.25 6.25	6.25	4930	14	1	0.79
	(3@3)8-5-F4.1-0-i-2.5-7-6	A B C	2.0	4.1A_b	6.06 6.25 6.25	6.19	4930	14	1	0.79
	(3@3)8-5-F4.1-5#3-i-2.5-7-6	A B C	2.0	4.1A_b	6.00 6.00 6.00	6.00	4930	14	1	0.79
	(3@5)8-5-F4.1-0-i-2.5-7-6	A B C	2.0	4.1A_b	6.50 6.25 6.25	6.33	4930	14	1	0.79
	(3@5)8-5-F4.1-5#3-i-2.5-7-6	A B C	2.0	4.1A_b	6.25 6.13 6.50	6.29	4930	14	1	0.79
	(3@7)8-5-F4.1-0-i-2.5-7-6	A B C	2.0	4.1A_b	6.25 6.25 6.25	6.25	4940	15	1	0.79

Table B.1 Cont. Comprehensive test results and data for beam-column joint specimens

	Specimen	Head	b in.	h in.	h_{cl} in.	d_{eff} in.	c_{so} in.	$c_{so,avg}$ in.	c_{bc} in.	s in.	d_{tr} in.	$A_{tr,l}$ in.^{2}
Group 11	(2@3)8-8-O4.5-0-i-2.5-3-9.5	A B	9.1	14.1	10.25	12.85	2.4 2.6	2.5	3.4 3.6	3.1	0.375	-
	(2@9)8-8-T4.0-0-i-2.5-3-9.5	A B	15.1	14.1	10.25	12.26	2.5 2.5	2.5	3.4 3.1	9.1	0.375	-
	(2@9)8-8-T4.0-5#3-i-2.5-3-9.5	A B	15.1	14.0	10.25	12.74	2.5 2.5	2.5	3.0 3.0	9.1	0.375	0.11
	(3@4.5)8-8-T4.0-0-i-2.5-3-9.5	A B C	15.1	14.1	10.25	12.23	2.6 - 2.5	2.6	3.4 3.1 3.4	4.5 4.5	0.375	-
	(3@4.5)8-8-T4.0-5#3-i-2.5-3-9.5	A B C	15.3	14.2	10.25	13.33	2.4 - 2.5	2.4	3.6 3.4 3.6	4.8 4.6	0.375	0.11
	(4@3)8-8-T4.0-0-i-2.5-3-9.5	A B C D	14.8	14.2	10.25	11.97	2.4 - - 2.5	2.4	3.1 3.1 3.4 3.3	3.0 2.9 3.0	0.375	-
	(4@3)8-8-T4.0-5#3-i-2.5-3-9.5	A B C D	15.3	14.1	10.25	13.45	2.6 - - 2.5	2.6	2.9 3.0 2.8 3.3	3.0 3.1 3.0	0.375	0.11
	(3@3)8-8-T4.0-0-i-2.5-3-9.5	A B C	12.3	14.0	10.25	12.65	2.5 - 2.5	2.5	3.3 2.9 3.0	3.1 3.1	0.375	-
	(3@3)8-8-T4.0-5#3-i-2.5-3-9.5	A B C	12.1	14.1	10.25	13.73	2.6 - 2.4	2.5	3.3 3.2 3.2	3.0 3.1	0.375	0.11
Group 12	8-5-F4.1-0-i-2.5-7-6	A B	17.3	14.2	10.25	11.25	2.5 2.8	2.6	7.2 7.1	11.0	0.375	-
	8-5-F4.1-5#3-i-2.5-7-6	A B	17.1	14.0	10.25	12.02	2.5 2.6	2.6	6.8 6.8	11.0	0.375	0.11
	(3@3)8-5-F4.1-0-i-2.5-7-6	A B C	12.6	13.7	10.25	11.78	2.8 - 2.5	2.6	6.6 6.4 6.4	3.3 3.1	0.375	-
	(3@3)8-5-F4.1-5#3-i-2.5-7-6	A B C	12.5	14.0	10.25	12.63	2.5 - 2.6	2.6	7.0 7.0 7.0	3.3 3.1	0.375	0.11
	(3@5)8-5-F4.1-0-i-2.5-7-6	A B C	16.9	14.2	10.25	11.58	2.8 - 2.8	2.8	6.7 6.9 6.9	5.1 5.3	0.375	-
	(3@5)8-5-F4.1-5#3-i-2.5-7-6	A B C	16.8	14.3	10.25	12.34	2.8 - 2.8	2.8	7.0 7.1 6.8	5.3 5.0	0.375	0.11
	(3@7)8-5-F4.1-0-i-2.5-7-6	A B C	20.5	14.3	10.25	11.45	2.8 - 2.6	2.7	7.0 7.0 7.0	7.1 7.0	0.375	-

288

Table B.1 Cont. Comprehensive test results and data for beam-column joint specimens

	Specimen	Head	N	s_{tr}* in.	A_{tt} in.²	d_{tro} in.	s_{tro}* in.	A_{ab} in.²	n	A_{hs} in.²	Long. Reinf. Layout
Group 11	(2@3)8-8-O4.5-0-i-2.5-3-9.5	A B	-	-	-	0.375	4 (2)	0.44	2	1.58	B4
	(2@9)8-8-T4.0-0-i-2.5-3-9.5	A B	-	-	-	0.5	4 (2)	0.80	2	1.58	B9
	(2@9)8-8-T4.0-5#3-i-2.5-3-9.5	A B	10	3 (1.5)	0.66	0.5	4 (2)	0.80	2	1.58	B5
	(3@4.5)8-8-T4.0-0-i-2.5-3-9.5	A B C	-	-	-	0.5	4 (2)	0.80	3	2.37	B9
	(3@4.5)8-8-T4.0-5#3-i-2.5-3-9.5	A B C	10	3 (1.5)	0.66	0.5	4 (2)	0.80	3	2.37	B5
	(4@3)8-8-T4.0-0-i-2.5-3-9.5	A B C D	-	-	-	0.5	4 (2)	0.80	4	3.16	B9
	(4@3)8-8-T4.0-5#3-i-2.5-3-9.5	A B C D	10	3 (1.5)	0.66	0.5	4 (2)	0.80	4	3.16	B5
	(3@3)8-8-T4.0-0-i-2.5-3-9.5	A B C	-	-	-	0.375	3 (1.5)	0.66	3	2.37	B5
	(3@3)8-8-T4.0-5#3-i-2.5-3-9.5	A B C	10	3 (1.5)	0.66	0.375	3 (1.5)	0.66	3	2.37	B5
Group 12	8-5-F4.1-0-i-2.5-7-6	A B	-	-	-	0.375	3 (1.5)	0.66	2	1.58	B4
	8-5-F4.1-5#3-i-2.5-7-6	A B	10	3 (1.5)	0.66	0.375	3 (1.5)	0.66	2	1.58	B4
	(3@3)8-5-F4.1-0-i-2.5-7-6	A B C	-	-	-	0.375	3 (1.5)	0.66	3	2.37	B4
	(3@3)8-5-F4.1-5#3-i-2.5-7-6	A B C	10	3 (1.5)	0.66	0.375	3 (1.5)	0.66	3	2.37	B5
	(3@5)8-5-F4.1-0-i-2.5-7-6	A B C	-	-	-	0.375	3 (1.5)	0.66	3	2.37	B5
	(3@5)8-5-F4.1-5#3-i-2.5-7-6	A B C	10	3 (1.5)	0.66	0.375	3 (1.5)	0.66	3	2.37	B5
	(3@7)8-5-F4.1-0-i-2.5-7-6	A B C	-	-	-	0.375	3 (1.5)	0.66	3	2.37	B8

* Value in parenthesis is the spacing between the first hoop and the center of the headed bar

Comprehensive test results and data for beam-column joint specimens

	Specimen	Head	Failure Type	Lead (Head) Slip in.	T_{max} kips	$f_{su,max}$ ksi	T_{ind} kips	T_{total} kips	T kips	f_{su} ksi
Group 11	(2@3)8-8-O4.5-0-i-2.5-3-9.5	A	CB	0.037	51.9	65.7	51.9	95.5	47.7	60.4
		B		0.021	43.6	55.2	43.6			
	(2@9)8-8-T4.0-0-i-2.5-3-9.5	A	CB	0.015	65.0	82.3	65.0	123.7	61.8	78.2
		B		0.016	58.7	74.3	58.7			
	(2@9)8-8-T4.0-5#3-i-2.5-3-9.5	A	SB/FP	0.078	70.7	89.5	70.7	153.3	76.7	97.1
		B		0.035	87.5	110.8	82.6			
	(3@4.5)8-8-T4.0-0-i-2.5-3-9.5	A	CB	0.013	43.9	55.6	43.9	122.1	40.7	51.5
		B		0.013	27.9	35.3	27.9			
		C		0.013	50.3	63.7	50.3			
	(3@4.5)8-8-T4.0-5#3-i-2.5-3-9.5	A	CB/FP	0.015	56.5	71.5	55.3	187.4	62.5	79.1
		B		0.558	68.6	86.8	65.8			
		C		0.003	66.4	84.1	66.3			
	(4@3)8-8-T4.0-0-i-2.5-3-9.5	A	CB	-	25.2	31.9	25.2	104.6	26.2	33.1
		B		-	31.2	39.5	31.2			
		C		-	31.7	40.1	31.7			
		D		0.005	16.6	21.0	16.5			
	(4@3)8-8-T4.0-5#3-i-2.5-3-9.5	A	CB	0.005	57.7	73.0	57.7	194.6	48.6	61.5
		B		-	30.1	38.1	30.1			
		C		-	52.3	66.2	52.3			
		D		0.015	54.4	68.9	54.4			
	(3@3)8-8-T4.0-0-i-2.5-3-9.5	A	CB	0.014	39.9	50.5	39.9	118.1	39.4	49.8
		B		0.016	44.3	56.1	44.3			
		C		0.014	33.9	42.9	33.9			
	(3@3)8-8-T4.0-5#3-i-2.5-3-9.5	A	CB	0.003	56.9	72.0	56.8	169.6	56.5	71.6
		B		-	63.6	80.5	63.6			
		C		0.007	49.3	62.4	49.2			
Group 12	8-5-F4.1-0-i-2.5-7-6	A	CB	0.005	30.2	38.2	27.7	57.3	28.7	36.3
		B		0.027	29.7	37.6	29.7			
	8-5-F4.1-5#3-i-2.5-7-6	A	CB	0.027	51.6	65.3	48.8	101.3	50.7	64.1
		B		0.023	52.7	66.7	52.5			
	(3@3)8-5-F4.1-0-i-2.5-7-6	A	CB	-	15.5	19.6	14.9	61.8	20.6	26.1
		B		-	24.3	30.8	24.3			
		C		-	22.7	28.7	22.7			
	(3@3)8-5-F4.1-5#3-i-2.5-7-6	A	CB	-	32.2	40.8	32.2	96.3	32.1	40.6
		B		-	30.8	39.0	30.8			
		C		-	33.3	42.2	33.3			
	(3@5)8-5-F4.1-0-i-2.5-7-6	A	CB	0.026	24.1	30.5	24.0	71.8	23.9	30.3
		B		-	23.8	30.1	23.3			
		C		0.002	24.5	31.0	24.5			
	(3@5)8-5-F4.1-5#3-i-2.5-7-6	A	CB	0.007	31.3	39.6	30.9	112.6	37.5	47.5
		B		0.014	38.3	48.5	38.3			
		C		0.014	43.8	55.5	43.4			
	(3@7)8-5-F4.1-0-i-2.5-7-6	A	CB	0.001	31.1	39.4	31.1	81.2	27.1	34.3
		B		-	19.1	24.2	19.0			
		C		0.013	31.1	39.4	31.1			

Table B.1 Cont. Comprehensive test results and data for beam-column joint specimens

	Specimen	Head	c_o in.	A_{brg}	ℓ_{eh} in.	$\ell_{eh,\text{avg}}$ in.	f_{cm} psi	Age days	d_b in.	A_b in.²
Group 12	(3@7)8-5-F4.1-5#3-i-2.5-7-6	A B C	2.0	4.1A_b	6.00 6.19 6.13	6.10	4940	15	1	0.79
	8-5-F9.1-0-i-2.5-7-6	A B	2.0	9.1A_b	6.13 6.13	6.13	4940	15	1	0.79
	8-5-F9.1-5#3-i-2.5-7-6	A B	2.0	9.1A_b	6.19 6.13	6.16	4940	15	1	0.79
	(3@5.5)8-5-F9.1-0-i-2.5-7-6	A B C	2.0	9.1A_b	6.25 6.13 6.25	6.21	5160	16	1	0.79
	(3@5.5)8-5-F9.1-5#3-i-2.5-7-6	A B C	2.0	9.1A_b	6.13 6.25 6.38	6.25	5160	16	1	0.79
	(4@3.7)8-5-T9.5-0-i-2.5-6.5-6	A B C D	1.4	9.5A_b	6.19 6.13 6.19 6.00	6.13	5160	16	1	0.79
	(4@3.7)8-5-F9.1-5#3-i-2.5-7-6	A B C D	2.0	9.1A_b	6.00 6.00 6.00 6.13	6.03	5160	16	1	0.79
Group 13	5-5-F4.0-0-i-2.5-5-4	A B	2.2	4.0A_b	4.00 4.13	4.06	4810	8	0.625	0.31
	5-5-F13.1-0-i-2.5-5-4	A B	2.2	13.1A_b	4.25 4.56	4.41	4810	8	0.625	0.31
	5-5-F4.0-2#3-i-2.5-5-4	A B	2.2	4.0A_b	3.88 3.75	3.81	4810	8	0.625	0.31
	5-5-F13.1-2#3-i-2.5-5-4	A B	2.2	13.1A_b	4.25 3.94	4.09	4810	8	0.625	0.31
	5-5-F4.0-5#3-i-2.5-5-4	A B	2.2	4.0A_b	3.94 4.38	4.16	4810	8	0.625	0.31
	5-5-F13.1-5#3-i-2.5-5-4	A B	2.2	13.1A_b	4.13 4.25	4.19	4690	7	0.625	0.31
	5-5-F4.0-0-i-2.5-3-6	A B	2.2	4.0A_b	6.00 6.00	6.00	4690	7	0.625	0.31
	5-5-F13.1-0-i-2.5-3-6	A B	2.2	13.1A_b	6.13 6.31	6.22	4690	7	0.625	0.31
	5-5-F4.0-2#3-i-2.5-3-6	A B	2.2	4.0A_b	6.00 6.00	6.00	4690	7	0.625	0.31
	5-5-F13.1-2#3-i-2.5-3-6	A B	2.2	13.1A_b	5.88 6.00	5.94	4690	7	0.625	0.31
	5-5-F4.0-5#3-i-2.5-3-6	A B	2.2	4.0A_b	6.00 6.13	6.06	4690	7	0.625	0.31

Table B.1 Cont. Comprehensive test results and data for beam-column joint specimens

	Specimen	Head	b in.	h in.	h_{cl} in.	d_{eff} in.	c_{so} in.	$c_{so,avg}$ in.	c_{bc} in.	s in.	d_{tr} in.	$A_{tr,l}$ in.^{2}
Group 12	(3@7)8-5-F4.1-5#3-i-2.5-7-6	A B C	20.5	14.1	10.25	12.13	2.6 - 2.8	2.7	7.1 6.9 7.0	7.1 7.0	0.375	0.11
	8-5-F9.1-0-i-2.5-7-6	A B	17.3	14.2	10.25	11.42	2.8 2.8	2.8	7.0 7.0	10.8	0.375	-
	8-5-F9.1-5#3-i-2.5-7-6	A B	17.0	14.1	10.25	12.13	2.5 2.5	2.5	6.9 7.0	11.0	0.375	0.11
	(3@5.5)8-5-F9.1-0-i-2.5-7-6	A B C	17.3	14.4	10.25	11.42	2.5 - 2.8	2.6	7.1 7.3 7.1	5.5 5.5	0.375	-
	(3@5.5)8-5-F9.1-5#3-i-2.5-7-6	A B C	17.3	14.4	10.25	12.44	2.5 - 2.8	2.6	7.3 7.1 7.0	5.5 5.5	0.375	0.11
	(4@3.7)8-5-T9.5-0-i-2.5-6.5-6	A B C D	17.0	14.2	10.25	11.72	2.8 - - 2.5	2.6	6.5 6.6 6.5 6.7	3.5 3.6 3.6	0.375	-
	(4@3.7)8-5-F9.1-5#3-i-2.5-7-6	A B C D	17.4	14.3	10.25	12.39	2.5 - - 2.6	2.6	7.3 7.3 7.3 7.1	3.8 3.8 3.8	0.375	0.11
Group 13	5-5-F4.0-0-i-2.5-5-4	A B	12.9	9.8	5.25	6.39	2.5 2.5	2.5	5.3 5.1	7.3	-	-
	5-5-F13.1-0-i-2.5-5-4	A B	13.1	9.6	5.25	6.56	2.5 2.5	2.5	4.8 4.5	7.5	-	-
	5-5-F4.0-2#3-i-2.5-5-4	A B	13.0	9.6	5.25	6.16	2.5 2.5	2.5	5.3 5.4	7.4	0.375	0.11
	5-5-F13.1-2#3-i-2.5-5-4	A B	13.1	9.8	5.25	6.59	2.6 2.6	2.6	5.1 5.4	7.3	0.375	0.11
	5-5-F4.0-5#3-i-2.5-5-4	A B	13.1	9.8	5.25	6.48	2.6 2.5	2.6	5.3 4.9	7.4	0.375	0.11
	5-5-F13.1-5#3-i-2.5-5-4	A B	13.0	9.8	5.25	6.92	2.5 2.5	2.5	5.1 5.0	7.4	0.375	0.11
	5-5-F4.0-0-i-2.5-3-6	A B	13.1	9.8	5.25	6.80	2.5 2.6	2.6	3.3 3.3	7.3	-	-
	5-5-F13.1-0-i-2.5-3-6	A B	13.3	9.7	5.25	6.92	2.5 2.6	2.6	3.1 2.9	7.5	-	-
	5-5-F4.0-2#3-i-2.5-3-6	A B	13.1	9.7	5.25	7.04	2.6 2.5	2.6	3.2 3.2	7.4	0.375	0.11
	5-5-F13.1-2#3-i-2.5-3-6	A B	12.9	9.7	5.25	7.45	2.5 2.6	2.5	3.3 3.2	7.3	0.375	0.11
	5-5-F4.0-5#3-i-2.5-3-6	A B	13.1	9.7	5.25	7.31	2.5 2.6	2.6	3.2 3.1	7.4	0.375	0.11

Table B.1 Cont. Comprehensive test results and data for beam-column joint specimens

	Specimen	Head	N	s_{tr}* in.	A_{tt} in.²	d_{tro} in.	s_{tro}* in.	A_{ab} in.²	n	A_{hs} in.²	Long. Reinf. Layout
Group 12	(3@7)8-5-F4.1-5#3-i-2.5-7-6	A B C	10	3 (1.5)	0.66	0.5	4 (2)	0.80	3	2.37	B8
	8-5-F9.1-0-i-2.5-7-6	A B	-	-	-	0.375	3 (1.5)	0.66	2	1.58	B4
	8-5-F9.1-5#3-i-2.5-7-6	A B	10	3 (1.5)	0.66	0.375	3 (1.5)	0.66	2	1.58	B9
	(3@5.5)8-5-F9.1-0-i-2.5-7-6	A B C	-	-	-	0.375	3 (1.5)	0.66	3	2.37	B5
	(3@5.5)8-5-F9.1-5#3-i-2.5-7-6	A B C	10	3 (1.5)	0.66	0.5	4 (2)	0.80	3	2.37	B5
	(4@3.7)8-5-T9.5-0-i-2.5-6.5-6	A B C D	-	-	-	0.375	3 (1.5)	0.66	4	3.16	B5
	(4@3.7)8-5-F9.1-5#3-i-2.5-7-6	A B C D	10	3 (1.5)	0.66	0.5	3 (1.5)	1.20	4	3.16	B5
Group 13	5-5-F4.0-0-i-2.5-5-4	A B	-	-	-	0.375	3.5 (1.75)	0.22	2	0.62	B4
	5-5-F13.1-0-i-2.5-5-4	A B	-	-	-	0.375	3.5 (1.75)	0.22	2	0.62	B4
	5-5-F4.0-2#3-i-2.5-5-4	A B	4	3.5 (2.625)	0.22	0.375	3.5 (1.75)	0.22	2	0.62	B4
	5-5-F13.1-2#3-i-2.5-5-4	A B	4	3.5 (2.625)	0.22	0.375	3.5 (1.75)	0.22	2	0.62	B4
	5-5-F4.0-5#3-i-2.5-5-4	A B	10	1.75 (0.875)	0.66	0.375	3.5 (1.75)	0.22	2	0.62	B4
	5-5-F13.1-5#3-i-2.5-5-4	A B	10	1.75 (0.875)	0.66	0.375	3.5 (1.75)	0.22	2	0.62	B4
	5-5-F4.0-0-i-2.5-3-6	A B	-	-	-	0.375	3.5 (1.75)	0.22	2	0.62	B4
	5-5-F13.1-0-i-2.5-3-6	A B	-	-	-	0.375	3.5 (1.75)	0.22	2	0.62	B4
	5-5-F4.0-2#3-i-2.5-3-6	A B	4	3.5 (2.625)	0.22	0.375	3.5 (1.75)	0.22	2	0.62	B4
	5-5-F13.1-2#3-i-2.5-3-6	A B	4	3.5 (2.625)	0.22	0.375	3.5 (1.75)	0.22	2	0.62	B4
	5-5-F4.0-5#3-i-2.5-3-6	A B	10	1.75 (0.875)	0.66	0.375	3.5 (1.75)	0.22	2	0.62	B4

* Value in parenthesis is the spacing between the first hoop and the center of the headed bar

Table B.1 Cont. Comprehensive test results and data for beam-column joint specimens

	Specimen	Head	Failure Type	Lead (Head) Slip in.	T_{max} kips	$f_{su,max}$ ksi	T_{ind} kips	T_{total} kips	T kips	f_{su} ksi
Group 12	(3@7)8-5-F4.1-5#3-i-2.5-7-6	A	CB	-	44.1	55.8	44.1			
		B		-	35.2	44.6	35.2	126.8	42.3	53.5
		C		-	47.5	60.1	47.5			
	8-5-F9.1-0-i-2.5-7-6	A	CB	0.001	32.4	41.0	32.0	66.8	33.4	42.3
		B		-	34.8	44.1	34.8			
	8-5-F9.1-5#3-i-2.5-7-6	A	CB	0.017	53.4	67.6	53.4	107.6	53.8	68.1
		B		0.033	54.3	68.7	54.2			
	(3@5.5)8-5-F9.1-0-i-2.5-7-6	A	CB	0.014	28.6	36.2	28.6			
		B		-	13.9	17.6	13.9	68.9	23.0	29.1
		C		0.015	26.4	33.4	26.4			
	(3@5.5)8-5-F9.1-5#3-i-2.5-7-6	A	CB	0.025	40.5	51.3	39.9			
		B		-	46.5	58.9	46.5	129.4	43.1	54.6
		C		0.022	43.0	54.4	43.0			
	(4@3.7)8-5-T9.5-0-i-2.5-6.5-6	A	CB	0.001	25.9	32.8	25.9			
		B		0.016	14.6	18.5	14.6	86.9	21.7	27.5
		C		-	17.8	22.5	17.8			
		D		0.024	28.8	36.5	28.6			
	(4@3.7)8-5-F9.1-5#3-i-2.5-7-6	A	CB	-	39.5	50.0	39.5			
		B		-	31.5	39.9	31.5	126.5	31.6	40.0
		C		-	20.4	25.8	20.4			
		D		0.023	35.1	44.4	35.1			
Group 13	5-5-F4.0-0-i-2.5-5-4	A	CB	-	25.9	83.5	25.9	49.1	24.5	79.0
		B		-	23.1	74.5	23.1			
	5-5-F13.1-0-i-2.5-5-4	A	CB	-	26.6	85.8	26.5	56.4	28.2	91.0
		B		-	30.2	97.4	29.9			
	5-5-F4.0-2#3-i-2.5-5-4	A	CB	-	20.1	64.8	20.1	39.3	19.7	63.5
		B		-	19.2	61.9	19.2			
	5-5-F13.1-2#3-i-2.5-5-4	A	CB	-	28.6	92.3	27.9	57.7	28.9	93.2
		B		-	30.1	97.1	29.8			
	5-5-F4.0-5#3-i-2.5-5-4	A	CB	-	27.0	87.1	27.0	53.0	26.5	85.5
		B		-	26.1[‡]	84.2[‡]	26.0			
	5-5-F13.1-5#3-i-2.5-5-4	A	CB	-	35.5	114.5	35.5	70.4	35.2	113.5
		B		-	34.8	112.3	34.8			
	5-5-F4.0-0-i-2.5-3-6	A	SB	-	34.6[‡]	111.6[‡]	32.9	65.5	32.7	105.5
		B		-	33.0	106.5	32.6			
	5-5-F13.1-0-i-2.5-3-6	A	SB/FP	-	33.2[‡]	107.1[‡]	33.1	70.6	35.3	113.9
		B		-	37.6	121.3	37.5			
	5-5-F4.0-2#3-i-2.5-3-6	A	SB/FP	-	40.0	129.0	35.5	75.7	37.9	122.3
		B		-	40.3	130.0	40.3			
	5-5-F13.1-2#3-i-2.5-3-6	A	SB/FP	-	46.3[‡]	149.4[‡]	46.3	92.8	46.4	149.7
		B		-	46.6	150.3	46.5			
	5-5-F4.0-5#3-i-2.5-3-6	A	SB/FP	-	42.4	136.8	42.4	86.9	43.5	140.3
		B		-	44.6	143.9	44.6			

[‡] No anchorage failure on the bar

Table B.1 Cont. Comprehensive test results and data for beam-column joint specimens

	Specimen	Head	c_o in.	A_{brg}	ℓ_{eh} in.	$\ell_{eh,avg}$ in.	f_{cm} psi	Age days	d_b in.	A_b in.^{2}
Group 14	5-12-F4.0-0-i-2.5-5-4	A B	2.2	$4.0A_b$	4.13 4.00	4.06	11030	35	0.625	0.31
	5-12-F13.1-0-i-2.5-5-4	A B	2.2	$13.1A_b$	4.13 4.13	4.13	11030	35	0.625	0.31
	5-12-F4.0-2#3-i-2.5-5-4	A B	2.2	$4.0A_b$	4.13 4.13	4.13	11030	35	0.625	0.31
	5-12-F13.1-2#3-i-2.5-5-4	A B	2.2	$13.1A_b$	4.06 4.13	4.09	11030	35	0.625	0.31
	5-12-F4.0-5#3-i-2.5-5-4	A B	2.2	$4.0A_b$	4.19 4.25	4.22	11030	35	0.625	0.31
	5-12-F13.1-5#3-i-2.5-5-4	A B	2.2	$13.1A_b$	4.13 4.13	4.13	11030	35	0.625	0.31
	5-12-F4.0-0-i-2.5-3-6	A B	2.2	$4.0A_b$	6.00 6.00	6.00	11030	36	0.625	0.31
	5-12-F13.1-0-i-2.5-3-6	A B	2.2	$13.1A_b$	6.00 6.06	6.03	11030	36	0.625	0.31
	(3@5.9)5-12-F4.0-0-i-2.5-4-5	A B C	2.2	$4.0A_b$	5.06 5.06 5.00	5.04	11030	36	0.625	0.31
	(3@5.9)5-12-F4.0-2#3-i-2.5-4-5	A B C	2.2	$4.0A_b$	5.13 5.13 5.19	5.15	11030	36	0.625	0.31
	(3@5.9)5-12-F4.0-5#3-i-2.5-4-5	A B C	2.2	$4.0A_b$	5.19 4.88 5.00	5.02	11030	36	0.625	0.31
	(4@3.9)5-12-F4.0-0-i-2.5-4-5	A B C D	2.2	$4.0A_b$	5.19 5.13 5.25 5.19	5.19	11030	39	0.625	0.31
	(4@3.9)5-12-F4.0-2#3-i-2.5-4-5	A B C D	2.2	$4.0A_b$	5.00 5.00 5.13 5.00	5.03	11030	39	0.625	0.31
	(4@3.9)5-12-F4.0-5#3-i-2.5-4-5	A B C D	2.2	$4.0A_b$	5.25 5.13 5.19 5.19	5.19	11030	39	0.625	0.31
Group 15	11-5a-F3.8-0-i-2.5-3-17	A B	2.0	$3.8A_b$	16.38 16.75	16.56	4050	36	1.41	1.56
	11-5a-F3.8-2#3-i-2.5-3-17	A B	2.0	$3.8A_b$	17.44 17.44	17.44	4050	36	1.41	1.56
	11-5a-F3.8-6#3-i-2.5-3-17	A B	2.0	$3.8A_b$	16.75 16.69	16.72	4050	36	1.41	1.56

Table B.1 Cont. Comprehensive test results and data for beam-column joint specimens

	Specimen	Head	b in.	h in.	h_{cl} in.	d_{eff} in.	c_{so} in.	$c_{so,avg}$ in.	c_{bc} in.	s in.	d_{tr} in.	$A_{tr,l}$ in.^{2}
Group 14	5-12-F4.0-0-i-2.5-5-4	A	13.1	9.8	5.25	5.96	2.6	2.6	5.1	7.3	-	-
		B					2.6		5.3			
	5-12-F13.1-0-i-2.5-5-4	A	13.0	9.6	5.25	6.04	2.5	2.5	4.9	7.4	-	-
		B					2.5		4.9			
	5-12-F4.0-2#3-i-2.5-5-4	A	13.1	9.6	5.25	6.08	2.8	2.6	5.0	7.3	0.375	0.11
		B					2.5		5.0			
	5-12-F13.1-2#3-i-2.5-5-4	A	13.1	9.7	5.25	6.17	2.3	2.6	5.2	7.4	0.375	0.11
		B					2.9		5.1			
	5-12-F4.0-5#3-i-2.5-5-4	A	13.1	9.5	5.25	6.23	2.5	2.6	4.8	7.4	0.375	0.11
		B					2.6		4.8			
	5-12-F13.1-5#3-i-2.5-5-4	A	13.1	9.7	5.25	6.27	2.5	2.5	5.0	7.4	0.375	0.11
		B					2.6		5.0			
	5-12-F4.0-0-i-2.5-3-6	A	13.1	9.6	5.25	6.30	2.6	2.6	3.1	7.4	-	-
		B					2.5		3.1			
	5-12-F13.1-0-i-2.5-3-6	A	13.0	9.7	5.25	6.36	2.5	2.6	3.2	7.3	-	-
		B					2.6		3.1			
	(3@5.9)5-12-F4.0-0-i-2.5-4-5	A	13.1	9.8	5.25	6.31	2.5	2.5	4.2	3.8	-	-
		B					-		4.2			
		C					2.5		4.3	3.8		
	(3@5.9)5-12-F4.0-2#3-i-2.5-4-5	A	13.1	9.7	5.25	6.58	2.5	2.5	4.1	3.8	0.375	0.11
		B					-		4.1			
		C					2.5		4.0	3.8		
	(3@5.9)5-12-F4.0-5#3-i-2.5-4-5	A	12.9	9.6	5.25	6.71	2.4	2.5	3.9	3.8	0.375	0.11
		B					-		4.3			
		C					2.6		4.1	3.6		
	(4@3.9)5-12-F4.0-0-i-2.5-4-5	A	12.8	9.6	5.25	6.54	2.5	2.5	3.9	2.3	-	-
		B					-		4.0	2.5		
		C					-		3.8			
		D					2.5		3.9	2.4		
	(4@3.9)5-12-F4.0-2#3-i-2.5-4-5	A	13.0	9.6	5.25	6.81	2.5	2.5	4.1	2.5	0.375	0.11
		B					-		4.1	2.4		
		C					-		3.9			
		D					2.5		4.1	2.5		
	(4@3.9)5-12-F4.0-5#3-i-2.5-4-5	A	13.3	9.5	5.25	-‡	2.5	2.5	3.8	2.6	0.375	0.11
		B					-		3.9	2.5		
		C					-		3.8			
		D					2.5		3.8	2.5		
Group 15	11-5a-F3.8-0-i-2.5-3-17	A	21.9	22.0	20	23.11	2.6	2.5	4.2	15.5	-	-
		B					2.4		3.8			
	11-5a-F3.8-2#3-i-2.5-3-17	A	21.7	21.8	20	23.77	2.6	2.6	3.0	15.1	0.375	0.11
		B					2.6		3.0			
	11-5a-F3.8-6#3-i-2.5-3-17	A	21.4	21.9	20	23.70	2.4	2.5	3.8	15.0	0.375	0.11
		B					2.6		3.8			

‡ d_{eff} was not calculated for specimen with bar yielding

Table B.1 Cont. Comprehensive test results and data for beam-column joint specimens

	Specimen	Head	N	s_{tr}* in.	A_{tt} in.²	d_{tro} in.	s_{tro}* in.	A_{ab} in.²	n	A_{hs} in.²	Long. Reinf. Layout
Group 14	5-12-F4.0-0-i-2.5-5-4	A B	-	-	-	0.375	3.5 (1.75)	0.22	2	0.62	B4
	5-12-F13.1-0-i-2.5-5-4	A B	-	-	-	0.375	3.5 (1.75)	0.22	2	0.62	B4
	5-12-F4.0-2#3-i-2.5-5-4	A B	4	3.5 (2.625)	0.22	0.375	3.5 (1.75)	0.22	2	0.62	B4
	5-12-F13.1-2#3-i-2.5-5-4	A B	4	3.5 (2.625)	0.22	0.375	3.5 (1.75)	0.22	2	0.62	B4
	5-12-F4.0-5#3-i-2.5-5-4	A B	10	1.75 (0.875)	0.66	0.375	3.5 (1.75)	0.22	2	0.62	B4
	5-12-F13.1-5#3-i-2.5-5-4	A B	10	1.75 (0.875)	0.66	0.375	3.5 (1.75)	0.22	2	0.62	B4
	5-12-F4.0-0-i-2.5-3-6	A B	-	-	-	0.375	3.5 (1.75)	0.22	2	0.62	B4
	5-12-F13.1-0-i-2.5-3-6	A B	-	-	-	0.375	3.5 (1.75)	0.22	2	0.62	B4
	(3@5.9)5-12-F4.0-0-i-2.5-4-5	A B C	-	-	-	0.375	3.5 (1.75)	0.22	3	0.93	B5
	(3@5.9)5-12-F4.0-2#3-i-2.5-4-5	A B C	4	3.5 (2.625)	0.22	0.375	3.5 (1.75)	0.22	3	0.93	B5
	(3@5.9)5-12-F4.0-5#3-i-2.5-4-5	A B C	10	1.75 (0.875)	0.66	0.375	3.5 (1.75)	0.22	3	0.93	B5
	(4@3.9)5-12-F4.0-0-i-2.5-4-5	A B C D	-	-	-	0.375	3.5 (1.75)	0.22	4	1.24	B5
	(4@3.9)5-12-F4.0-2#3-i-2.5-4-5	A B C D	4	3.5 (2.625)	0.22	0.375	3.5 (1.75)	0.22	4	1.24	B5
	(4@3.9)5-12-F4.0-5#3-i-2.5-4-5	A B C D	10	1.75 (0.875)	0.22	0.375	3.5 (1.75)	0.18	4	1.24	B5
Group 15	11-5a-F3.8-0-i-2.5-3-17	A B	-	-	-	0.5	4 (2)	1.20	2	3.12	B10
	11-5a-F3.8-2#3-i-2.5-3-17	A B	4	8 (6)	0.22	0.5	4 (2)	1.20	2	3.12	B10
	11-5a-F3.8-6#3-i-2.5-3-17	A B	12	4 (2)	0.66	0.5	4 (2)	1.20	2	3.12	B10

* Value in parenthesis is the spacing between the first hoop and the center of the headed bar

Table B.1 Cont. Comprehensive test results and data for beam-column joint specimens

	Specimen	Head	Failure Type	Lead (Head) Slip in.	T_{max} kips	$f_{su,max}$ ksi	T_{ind} kips	T_{total} kips	T kips	f_{su} ksi
Group 14	5-12-F4.0-0-i-2.5-5-4	A	CB	0.123	28.9	93.2	28.9	56.6	28.3	91.3
		B		0.055	27.7	89.4	27.7			
	5-12-F13.1-0-i-2.5-5-4	A	CB	0.179	32.6	105.2	32.5	62.7	31.4	101.3
		B		0.116	30.2	97.4	30.2			
	5-12-F4.0-2#3-i-2.5-5-4	A	CB	0.072	33.7	108.7	33.7	65.4	32.7	105.5
		B		0.015	31.7	102.3	31.7			
	5-12-F13.1-2#3-i-2.5-5-4	A	CB	0.136	34.4	111.0	34.4	72.5	36.3	117.1
		B		0.025	38.2	123.2	38.2			
	5-12-F4.0-5#3-i-2.5-5-4	A	CB	0.196	40.2	129.7	40.2	77.7	38.9	125.5
		B		0.308	37.5	121.0	37.5			
	5-12-F13.1-5#3-i-2.5-5-4	A	CB	0.172	40.8	131.6	40.8	80.6	40.3	130.0
		B		0.269	39.8	128.4	39.8			
	5-12-F4.0-0-i-2.5-3-6	A	SB	0.136	43.9	141.6	41.8	83.5	41.7	134.5
		B		0.226	41.6	134.2	41.6			
	5-12-F13.1-0-i-2.5-3-6	A	CB	0.081	44.7	144.2	44.5	88.3	44.2	142.6
		B		0.327	43.8	141.3	43.8			
	(3@5.9)5-12-F4.0-0-i-2.5-4-5	A	CB	-	27.1	87.4	27.0	84.1	28.0	90.4
		B		0.100	28.9	93.2	28.8			
		C		-	28.2	91.0	28.2			
	(3@5.9)5-12-F4.0-2#3-i-2.5-4-5	A	CB	0.169	34.5	111.3	34.5	105.4	35.1	113.3
		B		-	35.3	113.9	35.3			
		C		-	35.6	114.8	35.6			
	(3@5.9)5-12-F4.0-5#3-i-2.5-4-5	A	CB	0.266	42.5	137.1	42.3	115.9	38.6	124.6
		B		0.216	33.3	107.4	32.7			
		C		-	41.3	133.2	40.9			
	(4@3.9)5-12-F4.0-0-i-2.5-4-5	A	CB	0.099	28.3	91.3	28.3	-†	25.6†	82.7
		B		-	-†	-†	-			
		C		0.109	24.5	79.0	24.5			
		D		-	24.1	77.7	24.1			
	(4@3.9)5-12-F4.0-2#3-i-2.5-4-5	A	CB	0.123	33.5	108.1	33.3	-†	30.9†	99.7
		B		-	-†	-†	-			
		C		0.228	30.7	99.0	30.7			
		D		-	28.7	92.6	28.7			
	(4@3.9)5-12-F4.0-5#3-i-2.5-4-5	A	Y	-	48.9	157.7	48.0	-†	48.1†	155.2
		B		-	-†	-†	-			
		C		-	51.3	165.5	49.4			
		D		-	46.9	151.3	46.8			
Group 15	11-5a-F3.8-0-i-2.5-3-17	A	CB/FP	0.106	97.1	62.2	97.1	195.1	97.5	62.5
		B		0.043	98.0	62.8	98.0			
	11-5a-F3.8-2#3-i-2.5-3-17	A	SB/FP	0.337	117.7	75.4	117.7	236.5	118.2	75.8
		B		0.235	133.4	85.5	118.8			
	11-5a-F3.8-6#3-i-2.5-3-17	A	SB/FP	0.130	119.9	76.9	114.5	232.4	116.2	74.5
		B		0.041	118.0	75.6	118.0			

† Load on headed bar B was not recorded due to a malfunction of load cell; T taken as the average load of the other three bars.

Table B.1 Cont. Comprehensive test results and data for beam-column joint specimens

	Specimen	Head	c_o in.	A_{brg}	ℓ_{eh} in.	$\ell_{eh,avg}$ in.	f_{cm} psi	Age days	d_b in.	A_b in.^{2}
Group 15	11-5a-F3.8-0-i-2.5-3-12	A B	2.0	3.8A_b	12.19 11.81	12.00	3960	35	1.41	1.56
	11-5a-F3.8-2#3-i-2.5-3-12	A B	2.0	3.8A_b	11.81 12.19	12.00	3960	35	1.41	1.56
	11-5a-F3.8-6#3-i-2.5-3-12	A B	2.0	3.8A_b	12.13 12.06	12.09	3960	35	1.41	1.56
	11-5a-F8.6-0-i-2.5-3-12	A B	2.0	8.6A_b	12.13 12.13	12.13	3960	35	1.41	1.56
	11-5a- F8.6-6#3-i-2.5-3-12	A B	2.0	8.6A_b	12.69 12.44	12.56	4050	36	1.41	1.56
Group 16	8-8-F4.1-0-i-2.5-3-10-DB	A B	2.0	4.1A_b	9.88 9.88	9.88	7410	49	1	0.79
	8-8-F9.1-0-i-2.5-3-10-DB	A B	2.0	9.1A_b	9.88 9.75	9.81	7410	49	1	0.79
	8-8-F9.1-5#3-i-2.5-3-10-DB	A B	2.0	9.1A_b	9.63 9.63	9.63	7410	49	1	0.79
	8-5-F4.1-0-i-2.5-3-10-DB	A B	2.0	4.1A_b	9.88 9.88	9.88	4880	19	1	0.79
	8-5-F9.1-0-i-2.5-3-10-DB	A B	2.0	9.1A_b	9.63 9.88	9.75	4880	19	1	0.79
	8-5-F4.1-3#4-i-2.5-3-10-DB	A B	2.0	4.1A_b	10.00 10.25	10.13	4880	19	1	0.79
	8-5-F9.1-3#4-i-2.5-3-10-DB	A B	2.0	9.1A_b	9.75 9.75	9.75	4880	20	1	0.79
	8-5-F4.1-5#3-i-2.5-3-10-DB	A B	2.0	4.1A_b	10.25 10.13	10.19	4880	20	1	0.79
	8-5-F9.1-5#3-i-2.5-3-10-DB	A B	2.0	9.1A_b	10.00 9.88	9.94	4880	20	1	0.79
Group 17	11-8-F3.8-0-i-2.5-3-14.5	A B	2.0	3.8A_b	14.50 14.50	14.50	8660	19	1.41	1.56
	11-8-F3.8-2#3-i-2.5-3-14.5	A B	2.0	3.8A_b	14.63 14.75	14.69	8660	19	1.41	1.56
	11-8-F3.8-6#3-i-2.5-3-14.5	A B	2.0	3.8A_b	14.88 14.50	14.69	8660	19	1.41	1.56
	(3@5.35)11-8-F3.8-0-i-2.5-3-14.5	A B C	2.0	3.8A_b	14.38 14.75 14.75	14.63	8720	20	1.41	1.56
	(3@5.35)11-8-F3.8-2#3-i-2.5-3-14.5	A B C	2.0	3.8A_b	14.50 14.63 14.50	14.54	8720	20	1.41	1.56
	(3@5.35)11-8-F3.8-6#3-i-2.5-3-14.5	A B C	2.0	3.8A_b	15.13 14.88 14.75	14.92	8720	20	1.41	1.56

	Specimen	Head	b in.	h in.	h_{cl} in.	d_{eff} in.	c_{so} in.	$c_{so,\text{avg}}$ in.	c_{bc} in.	s in.	d_{tr} in.	$A_{tr,l}$ in.^{2}
Group 15	11-5a-F3.8-0-i-2.5-3-12	A B	21.7	16.5	20	21.84	2.6 2.8	2.7	2.9 3.3	14.9	-	-
	11-5a-F3.8-2#3-i-2.5-3-12	A B	21.4	17.1	20	22.18	2.4 2.4	2.4	3.9 3.5	15.3	0.375	0.11
	11-5a-F3.8-6#3-i-2.5-3-12	A B	21.6	17.0	20	22.53	2.8 2.5	2.7	3.5 3.6	14.9	0.375	0.11
	11-5a- F8.6-0-i-2.5-3-12	A B	21.7	16.8	20	22.07	2.8 2.5	2.6	3.3 3.3	15.0	-	-
	11-5a- F8.6-6#3-i-2.5-3-12	A B	22.0	17.3	20	22.53	2.8 2.7	2.7	3.3 3.5	15.2	0.375	0.11
Group 16	8-8-F4.1-0-i-2.5-3-10-DB	A B	17.1	14.3	20	21.38	2.5 2.6	2.6	3.4 3.4	11.0	-	-
	8-8-F9.1-0-i-2.5-3-10-DB	A B	17.3	14.2	20	21.42	2.6 2.6	2.6	3.3 3.4	11.0	-	-
	8-8-F9.1-5#3-i-2.5-3-10-DB	A B	17.4	14.2	20	21.88	2.5 2.8	2.6	3.6 3.6	11.1	0.375	0.11
	8-5-F4.1-0-i-2.5-3-10-DB	A B	17.4	14.1	20	21.43	2.5 2.6	2.6	3.3 3.3	11.3	-	-
	8-5-F9.1-0-i-2.5-3-10-DB	A B	17.5	14.3	20	21.56	2.6 2.6	2.6	3.6 3.4	11.3	-	-
	8-5-F4.1-3#4-i-2.5-3-10-DB	A B	17.3	14.1	20	22.27	2.5 2.5	2.5	3.1 2.9	11.3	0.5	0.2
	8-5-F9.1-3#4-i-2.5-3-10-DB	A B	17.3	14.4	20	22.31	2.6 2.6	2.6	3.6 3.6	11.0	0.5	0.2
	8-5-F4.1-5#3-i-2.5-3-10-DB	A B	17.5	14.3	20	22.47	2.6 2.8	2.7	3.1 3.2	11.1	0.375	0.11
	8-5-F9.1-5#3-i-2.5-3-10-DB	A B	17.3	14.2	20	22.48	2.6 2.6	2.6	3.2 3.3	11.0	0.375	0.11
Group 17	11-8-F3.8-0-i-2.5-3-14.5	A B	21.8	19.3	20	21.54	2.8 2.5	2.6	3.4 3.4	15.1	-	-
	11-8-F3.8-2#3-i-2.5-3-14.5	A B	21.8	19.3	20	21.72	2.5 2.6	2.6	3.3 3.1	15.3	0.375	0.11
	11-8-F3.8-6#3-i-2.5-3-14.5	A B	21.7	19.4	20	22.19	2.4 2.5	2.4	3.2 3.6	15.4	0.375	0.11
	(3@5.35)11-8-F3.8-0-i-2.5-3-14.5	A B C	22.0	19.3	20	21.53	2.8 - 2.8	2.8	3.6 3.2 3.2	7.5 7.6	-	-
	(3@5.35)11-8-F3.8-2#3-i-2.5-3-14.5	A B C	21.8	19.2	20	22.10	2.5 - 2.6	2.6	3.3 3.2 3.3	7.5 7.8	0.375	0.11
	(3@5.35)11-8-F3.8-6#3-i-2.5-3-14.5	A B C	22.2	19.6	20	22.42	2.8 - 2.8	2.8	3.1 3.4 3.5	7.6 7.6	0.375	0.11

300

Table B.1 Cont. Comprehensive test results and data for beam-column joint specimens

	Specimen	Head	N	s_{tr}^{*} in.	A_{tt} in.²	d_{tro} in.	s_{tro}^{*} in.	A_{ab} in.²	n	A_{hs} in.²	Long. Reinf. Layout
Group 15	11-5a-F3.8-0-i-2.5-3-12	A B	-	-	-	0.5	5 (2.5)	1.20	2	3.12	B11
	11-5a-F3.8-2#3-i-2.5-3-12	A B	4	8 (6)	0.22	0.5	5 (2.5)	1.20	2	3.12	B11
	11-5a-F3.8-6#3-i-2.5-3-12	A B	12	4 (2)	0.66	0.5	5 (2.5)	1.20	2	3.12	B11
	11-5a- F8.6-0-i-2.5-3-12	A B	-	-	-	0.5	5 (2.5)	1.20	2	3.12	B11
	11-5a- F8.6-6#3-i-2.5-3-12	A B	12	4 (2)	0.66	0.5	5 (2.5)	1.20	2	3.12	B11
Group 16	8-8-F4.1-0-i-2.5-3-10-DB	A B	-	-	-	0.5	5 (2.5)	0.80	2	1.58	B12
	8-8-F9.1-0-i-2.5-3-10-DB	A B	-	-	-	0.5	5 (2.5)	0.80	2	1.58	B12
	8-8-F9.1-5#3-i-2.5-3-10-DB	A B	10	5 (2.5)	0.44	0.5	5 (2.5)	0.80	2	1.58	B12
	8-5-F4.1-0-i-2.5-3-10-DB	A B	-	-	-	0.5	5 (2.5)	0.80	2	1.58	B12
	8-5-F9.1-0-i-2.5-3-10-DB	A B	-	-	-	0.5	5 (2.5)	0.80	2	1.58	B12
	8-5-F4.1-3#4-i-2.5-3-10-DB	A B	6	7.5 (6)	0.40	0.5	5 (2.5)	0.80	2	1.58	B12
	8-5-F9.1-3#4-i-2.5-3-10-DB	A B	6	7.5 (6)	0.40	0.5	5 (2.5)	0.80	2	1.58	B12
	8-5-F4.1-5#3-i-2.5-3-10-DB	A B	10	5 (2.5)	0.44	0.5	5 (2.5)	0.80	2	1.58	B12
	8-5-F9.1-5#3-i-2.5-3-10-DB	A B	10	5 (2.5)	0.44	0.5	5 (2.5)	0.80	2	1.58	B12
Group 17	11-8-F3.8-0-i-2.5-3-14.5	A B	-	-	-	0.5	5 (2.5)	1.20	2	3.12	B12
	11-8-F3.8-2#3-i-2.5-3-14.5	A B	4	8 (6)	0.22	0.5	5 (2.5)	1.20	2	3.12	B12
	11-8-F3.8-6#3-i-2.5-3-14.5	A B	12	4 (2)	0.66	0.5	5 (2.5)	1.20	2	3.12	B12
	(3@5.35)11-8-F3.8-0-i-2.5-3-14.5	A B C	-	-	-	0.5	5 (2.5)	1.20	3	4.68	B13
	(3@5.35)11-8-F3.8-2#3-i-2.5-3-14.5	A B C	4	8 (6)	0.22	0.5	5 (2.5)	1.20	3	4.68	B14
	(3@5.35)11-8-F3.8-6#3-i-2.5-3-14.5	A B C	12	4 (2)	0.66	0.5	5 (2.5)	1.20	3	4.68	B14

* Value in parenthesis is the spacing between the first hoop and the center of the headed bar

Table B.1 Cont. Comprehensive test results and data for beam-column joint specimens

	Specimen	Head	Failure Type	Lead (Head) Slip in.	T_{max} kips	$f_{su,max}$ ksi	T_{ind} kips	T_{total} kips	T kips	f_{su} ksi
Group 15	11-5a-F3.8-0-i-2.5-3-12	A	CB	0.025	54.2	34.7	54.2	113.7	56.8	36.4
		B		0.006	59.5	38.1	59.5			
	11-5a-F3.8-2#3-i-2.5-3-12	A	CB	0.231	67.2	43.1	67.2	134.6	67.3	43.1
		B		0.007	67.4	43.2	67.4			
	11-5a-F3.8-6#3-i-2.5-3-12	A	CB/FP	0.007	77.4	49.6	77.4	156.0	78.0	50.0
		B		0.429	82.3	52.8	78.6			
	11-5a- F8.6-0-i-2.5-3-12	A	CB	0.202	63.7	40.8	63.7	127.7	63.8	40.9
		B		0.145	75.4	48.3	64.0			
	11-5a- F8.6-6#3-i-2.5-3-12	A	CB	0.237	78.3	50.2	78.3	158.4	79.2	50.8
		B		0.250	80.2	51.4	80.2			
Group 16	8-8-F4.1-0-i-2.5-3-10-DB	A	CB	0.129	49.9	63.2	49.9	100.3	50.2	63.5
		B		0.065	50.5	63.9	50.5			
	8-8-F9.1-0-i-2.5-3-10-DB	A	CB	0.010	47.4	60.0	47.4	103.6	51.8	65.6
		B		0.036	56.2	71.1	56.2			
	8-8-F9.1-5#3-i-2.5-3-10-DB	A	CB	0.012	65.5	82.9	65.5	136.5	68.2	86.3
		B		0.102	71.0	89.9	71.0			
	8-5-F4.1-0-i-2.5-3-10-DB	A	CB/FP	0.188	37.4	47.3	37.4	81.3	40.6	51.4
		B		0.322	44.4	56.2	43.9			
	8-5-F9.1-0-i-2.5-3-10-DB	A	CB	0.061	42.6	53.9	39.0	88.7	44.4	56.2
		B		0.008	49.7	62.9	49.7			
	8-5-F4.1-3#4-i-2.5-3-10-DB	A	CB	0.081	60.6	76.7	60.6	129.2	64.6	81.8
		B		0.180	68.7	87.0	68.7			
	8-5-F9.1-3#4-i-2.5-3-10-DB	A	CB	0.017	62.4	79.0	62.4	131.5	65.8	83.3
		B		0.258	69.1	87.5	69.1			
	8-5-F4.1-5#3-i-2.5-3-10-DB	A	CB	0.019	63.2	80.0	63.2	140.4	70.2	88.9
		B		0.120	77.2	97.7	77.2			
	8-5-F9.1-5#3-i-2.5-3-10-DB	A	CB	0.120	66.8	84.6	66.8	141.0	70.5	89.2
		B		0.248	74.2	93.9	74.2			
Group 17	11-8-F3.8-0-i-2.5-3-14.5	A	CB	0.123	79.4	50.9	79.4	158.1	79.1	50.7
		B		0.008	78.7	50.4	78.7			
	11-8-F3.8-2#3-i-2.5-3-14.5	A	CB	0.591	87.8	56.3	87.8	176.9	88.4	56.7
		B		0.008	89.1	57.1	89.1			
	11-8-F3.8-6#3-i-2.5-3-14.5	A	CB	0.140	112.4	72.1	112.4	225.3	112.7	72.2
		B		0.178	112.9	72.4	112.9			
	(3@5.35)11-8-F3.8-0-i-2.5-3-14.5	A	CB	-	51.9	33.3	51.9	158.7	52.9	33.9
		B		0.040	54.9	35.2	54.9			
		C		-	51.9	33.3	51.9			
	(3@5.35)11-8-F3.8-2#3-i-2.5-3-14.5	A	CB	-	74.0	47.4	74.0	217.7	72.6	46.5
		B		0.260	72.1	46.2	72.1			
		C		-	71.6	45.9	71.6			
	(3@5.35)11-8-F3.8-6#3-i-2.5-3-14.5	A	CB	-	93.2	59.7	93.2	251.0	83.7	53.7
		B		0.211	85.3	54.7	85.3			
		C		0.292	72.4	46.4	72.4			

Table B.1 Cont. Comprehensive test results and data for beam-column joint specimens

	Specimen	Head	c_o in.	A_{brg}	ℓ_{eh} in.	$\ell_{eh,avg}$ in.	f_{cm} psi	Age days	d_b in.	A_b in.^{2}
Group 17	8-8-O12.9-0-i-2.5-3-9.5	A B	1.0	12.9A_b	9.75 9.63	9.69	8800	21	1	0.79
	8-8-S14.9-0-i-2.5-3-8.25	A B	1.0	14.9A_b	8.25 8.25	8.25	8800	21	1	0.79
	8-8-O12.9-5#3-i-2.5-3-9.5	A B	1.0	12.9A_b	9.50 9.25	9.38	8800	21	1	0.79
	8-8-S14.9-5#3-i-2.5-3-8.25	A B	1.0	14.9A_b	8.25 8.25	8.25	8800	21	1	0.79
Group 18	11-5-F3.8-0-i-2.5-3-12	A B	2.0	3.8A_b	12.13 12.13	12.13	5760	6	1.41	1.56
	11-5-F3.8-6#3-i-2.5-3-12	A B	2.0	3.8A_b	12.50 12.50	12.50	5760	6	1.41	1.56
	11-5-F3.8-0-i-2.5-3-17	A B	2.0	3.8A_b	17.50 17.00	17.25	5760	6	1.41	1.56
	11-5-F3.8-6#3-i-2.5-3-17	A B	2.0	3.8A_b	16.88 17.00	16.94	5970	7	1.41	1.56
	11-5- F8.6-0-i-2.5-3-14.5	A B	2.0	8.6A_b	14.50 14.50	14.50	5970	7	1.41	1.56
	11-5- F8.6-6#3-i-2.5-3-14.5	A B	2.0	8.6A_b	14.50 14.75	14.63	5970	7	1.41	1.56
	(3@5.35)11-5- F8.6-0-i-2.5-3-14.5	A B C	2.0	8.6A_b	14.38 15.25 14.50	14.71	6240	8	1.41	1.56
	(3@5.35)11-5- F8.6-6#3-i-2.5-3-14.5	A B C	2.0	8.6A_b	14.75 14.50 14.38	14.54	6240	8	1.41	1.56
Group 19	11-12-O4.5-0-i-2.5-3-16.75	A B	1.3	4.5A_b	17.13 17.13	17.13	10860	36	1.41	1.56
	11-12-S5.5-0-i-2.5-3-16.75	A B	1.5	5.5A_b	16.75 17.13	16.94	10120	37	1.41	1.56
	11-12-O4.5-6#3-i-2.5-3-16.75	A B	1.3	4.5A_b	16.75 16.88	16.81	10860	37	1.41	1.56
	11-12-S5.5-6#3-i-2.5-3-16.75	A B	1.5	5.5A_b	16.63 17.00	16.81	10120	38	1.41	1.56
	(3@5.35)11-12-O4.5-0-i-2.5-3-16.75	A B C	1.3	4.5A_b	16.88 17.13 16.75	16.92	10860	36	1.41	1.56
	(3@5.35)11-12-S5.5-0-i-2.5-3-16.75	A B C	1.5	5.5A_b	16.88 17.00 16.88	16.92	10120	38	1.41	1.56
	(3@5.35)11-12-O4.5-6#3-i-2.5-3-16.75	A B C	1.3	4.5A_b	16.88 17.13 17.00	17.00	10860	37	1.41	1.56
	(3@5.35)11-12-S5.5-6#3-i-2.5-3-16.75	A B C	1.5	5.5A_b	16.75 17.00 16.50	16.75	10120	38	1.41	1.56

Table B.1 Cont. Comprehensive test results and data for beam-column joint specimens

	Specimen	Head	b in.	h in.	h_{cl} in.	d_{eff} in.	c_{so} in.	$c_{so,avg}$ in.	c_{bc} in.	s in.	d_{tr} in.	$A_{tr,l}$ in.^{2}
Group 17	8-8-O12.9-0-i-2.5-3-9.5	A B	16.9	14.3	10.25	12.31	2.5 2.5	2.5	2.9 3.0	10.9	-	-
	8-8-S14.9-0-i-2.5-3-8.25	A B	17.3	14.3	10.25	11.97	2.6 2.6	2.6	3.3 3.3	11.0	-	-
	8-8-O12.9-5#3-i-2.5-3-9.5	A B	17.1	14.2	10.25	12.27	2.5 2.6	2.6	3.1 3.3	11.0	0.375	0.11
	8-8-S14.9-5#3-i-2.5-3-8.25	A B	17.3	14.1	10.25	12.36	2.8 2.5	2.6	3.1 3.1	11.0	0.375	0.11
Group 18	11-5-F3.8-0-i-2.5-3-12	A B	21.7	17.0	20	21.66	2.8 2.5	2.6	3.5 3.5	15.0	-	-
	11-5-F3.8-6#3-i-2.5-3-12	A B	21.8	16.9	20	22.20	2.6 2.8	2.7	3.1 3.1	15.0	0.375	0.11
	11-5-F3.8-0-i-2.5-3-17	A B	21.9	21.9	20	23.31	2.5 3.0	2.8	3.0 3.5	15.0	-	-
	11-5-F3.8-6#3-i-2.5-3-17	A B	21.5	22.0	20	23.70	2.6 2.5	2.6	3.8 3.6	15.0	0.375	0.11
	11-5- F8.6-0-i-2.5-3-14.5	A B	21.7	19.1	20	22.02	2.5 2.6	2.6	3.3 3.3	15.1	-	-
	11-5- F8.6-6#3-i-2.5-3-14.5	A B	21.5	19.5	20	22.74	2.6 2.6	2.6	3.6 3.4	14.9	0.375	0.11
	(3@5.35)11-5- F8.6-0-i-2.5-3-14.5	A B C	21.3	19.2	20	22.32	2.6 - 2.5	2.6	3.4 2.6 3.3	7.3 7.5	-	-
	(3@5.35)11-5- F8.6-6#3-i-2.5-3-14.5	A B C	21.4	19.1	20	22.70	2.5 - 2.8	2.6	3.0 3.3 3.4	7.4 7.4	0.375	0.11
Group 19	11-12-O4.5-0-i-2.5-3-16.75	A B	21.9	23.1	20	22.63	2.8 2.8	2.8	3.9 3.9	15.0	-	-
	11-12-S5.5-0-i-2.5-3-16.75	A B	22.3	23.1	20	22.93	2.8 2.9	2.8	3.6 3.2	15.3	-	-
	11-12-O4.5-6#3-i-2.5-3-16.75	A B	21.7	23.1	20	23.12	2.5 2.8	2.6	4.3 4.1	15.0	0.375	0.11
	11-12-S5.5-6#3-i-2.5-3-16.75	A B	22.4	22.7	20	23.28	2.6 3.0	2.8	3.3 2.9	15.4	0.375	0.11
	(3@5.35)11-12-O4.5-0-i-2.5-3-16.75	A B C	21.8	22.9	20	22.48	3.0 - 2.5	2.8	3.9 3.6 4.0	7.5 7.4	-	-
	(3@5.35)11-12-S5.5-0-i-2.5-3-16.75	A B C	21.9	23.1	20	22.72	2.8 - 2.8	2.8	3.5 3.4 3.5	7.5 7.5	-	-
	(3@5.35)11-12-O4.5-6#3-i-2.5-3-16.75	A B C	21.8	22.9	20	23.16	2.5 - 2.8	2.6	3.9 3.7 3.8	7.5 7.6	0.375	0.11
	(3@5.35)11-12-S5.5-6#3-i-2.5-3-16.75	A B C	21.9	22.8	20	23.84	2.6 - 3.0	2.8	3.3 3.0 3.5	7.4 7.5	0.375	0.11

	Specimen	Head	N	s_{tr}* in.	A_{tt} in.²	d_{tro} in.	s_{tro}* in.	A_{ab} in.²	n	A_{hs} in.²	Long. Reinf. Layout
Group 17	8-8-O12.9-0-i-2.5-3-9.5	A B	-	-	-	0.5	4.5 (2.25)	0.80	2	1.58	B6
	8-8-S14.9-0-i-2.5-3-8.25	A B	-	-	-	0.5	4.5 (2.25)	0.80	2	1.58	B6
	8-8-O12.9-5#3-i-2.5-3-9.5	A B	10	3 (1.5)	0.66	0.5	4.5 (2.25)	0.80	2	1.58	B6
	8-8-S14.9-5#3-i-2.5-3-8.25	A B	10	3 (1.5)	0.66	0.5	4.5 (2.25)	0.80	2	1.58	B6
Group 18	11-5-F3.8-0-i-2.5-3-12	A B	-	-	-	0.5	5 (2.5)	1.20	2	3.12	B6
	11-5-F3.8-6#3-i-2.5-3-12	A B	12	4 (2)	0.66	0.5	5 (2.5)	1.20	2	3.12	B12
	11-5-F3.8-0-i-2.5-3-17	A B	-	-	-	0.5	6 (3)	0.80	2	3.12	B7
	11-5-F3.8-6#3-i-2.5-3-17	A B	12	4 (2)	0.66	0.5	6 (3)	0.80	2	3.12	B7
	11-5- F8.6-0-i-2.5-3-14.5	A B	-	-	-	0.5	5 (2.5)	1.20	2	3.12	B12
	11-5- F8.6-6#3-i-2.5-3-14.5	A B	12	4 (2)	0.66	0.5	5 (2.5)	1.20	2	3.12	B12
	(3@5.35)11-5- F8.6-0-i-2.5-3-14.5	A B C	-	-	-	0.5	5 (2.5)	1.20	3	4.68	B15
	(3@5.35)11-5- F8.6-6#3-i-2.5-3-14.5	A B C	12	4 (2)	0.66	0.5	4.5 (2.25)	1.20	3	4.68	B15
Group 19	11-12-O4.5-0-i-2.5-3-16.75	A B	-	-	-	0.5	4 (2)	1.20	2	3.12	B16
	11-12-S5.5-0-i-2.5-3-16.75	A B	-	-	-	0.5	4 (2)	1.20	2	3.12	B16
	11-12-O4.5-6#3-i-2.5-3-16.75	A B	12	4 (2)	0.66	0.5	4 (2)	1.20	2	3.12	B16
	11-12-S5.5-6#3-i-2.5-3-16.75	A B	12	4 (2)	0.66	0.5	4 (2)	1.20	2	3.12	B16
	(3@5.35)11-12-O4.5-0-i-2.5-3-16.75	A B C	-	-	-	0.5	4 (2)	1.20	3	4.68	B16
	(3@5.35)11-12-S5.5-0-i-2.5-3-16.75	A B C	-	-	-	0.5	4 (2)	1.20	3	4.68	B16
	(3@5.35)11-12-O4.5-6#3-i-2.5-3-16.75	A B C	12	4 (2)	0.66	0.5	4 (2)	1.20	3	4.68	B16
	(3@5.35)11-12-S5.5-6#3-i-2.5-3-16.75	A B C	12	4 (2)	0.66	0.5	4 (2)	1.20	3	4.68	B16

* Value in parenthesis is the spacing between the first hoop and the center of the headed bar

Table B.1 Cont. Comprehensive test results and data for beam-column joint specimens

	Specimen	Head	Failure Type	Lead (Head) Slip in.	T_{max} kips	$f_{su,max}$ ksi	T_{ind} kips	T_{total} kips	T kips	f_{su} ksi
Group 17	8-8-O12.9-0-i-2.5-3-9.5	A	CB	-	85.5	108.2	85.5	170.5	85.2	107.8
		B		-	84.9	107.5	84.9			
	8-8-S14.9-0-i-2.5-3-8.25	A	CB	0.010	70.8	89.6	70.8	141.8	70.9	89.7
		B		0.187	71.0	89.9	71.0			
	8-8-O12.9-5#3-i-2.5-3-9.5	A	CB	0.237	84.4	106.8	84.4	166.9	83.5	105.7
		B		0.198	82.5	104.4	82.5			
	8-8-S14.9-5#3-i-2.5-3-8.25	A	CB	0.197	87.2	110.4	87.2	174.0	87.0	110.1
		B		0.022	86.8	109.9	86.8			
Group 18	11-5-F3.8-0-i-2.5-3-12	A	CB	0.140	68.7	44.0	68.7	132.9	66.5	42.6
		B		0.262	64.3	41.2	64.3			
	11-5-F3.8-6#3-i-2.5-3-12	A	CB	0.041	88.2	56.5	88.2	176.5	88.3	56.6
		B		0.008	88.3	56.6	88.3			
	11-5-F3.8-0-i-2.5-3-17	A	CB/FP	0.115	132.6	85.0	132.6	265.5	132.7	85.1
		B		0.015	132.9	85.2	132.9			
	11-5-F3.8-6#3-i-2.5-3-17	A	CB	0.157	154.9	99.3	154.9	303.7	151.9	97.4
		B		0.051	148.9	95.4	148.9			
	11-5- F8.6-0-i-2.5-3-14.5	A	CB	0.005	83.6	53.6	83.6	165.7	82.8	53.1
		B		0.783	82.1	52.6	82.1			
	11-5- F8.6-6#3-i-2.5-3-14.5	A	CB	0.144	113.9	73.0	113.9	224.6	112.3	72.0
		B		0.010	110.7	71.0	110.7			
	(3@5.35)11-5- F8.6-0-i-2.5-3-14.5	A	CB	-	66.5	42.6	66.5	195.4	65.1	41.7
		B		0.013	61.7	39.6	61.7			
		C		0.068	67.1	43.0	67.1			
	(3@5.35)11-5- F8.6-6#3-i-2.5-3-14.5	A	CB	-	68.8	44.1	68.8	226.9	75.6	48.5
		B		0.287	83.3	53.4	83.2			
		C		0.016	74.9	48.0	74.9			
Group 19	11-12-O4.5-0-i-2.5-3-16.75	A	CB	0.032	168.4	107.9	168.3	339.3	169.6	108.7
		B		0.029	171.0	109.6	171.0			
	11-12-S5.5-0-i-2.5-3-16.75	A	CB	0.091	179.1	114.8	179.1	351.9	175.9	112.8
		B		0.215	172.7	110.7	172.7			
	11-12-O4.5-6#3-i-2.5-3-16.75	A	SB/FP	0.024	202.5	129.8	202.5	403.0	201.5	129.2
		B		0.022	200.7[‡]	128.7[‡]	200.5			
	11-12-S5.5-6#3-i-2.5-3-16.75	A	CB	0.028	206.1	132.1	206.1	394.8	197.4	126.5
		B		0.025	188.7	121.0	188.7			
	(3@5.35)11-12-O4.5-0-i-2.5-3-16.75	A	CB	-	109.3	70.1	107.6	320.4	106.8	68.5
		B		0.003	114.1	73.1	114.1			
		C		0.003	98.7	63.3	98.7			
	(3@5.35)11-12-S5.5-0-i-2.5-3-16.75	A	CB	-	117.1	75.1	117.1	327.0	109.0	69.9
		B		-	93.8	60.1	93.8			
		C		-	116.1	74.4	116.1			
	(3@5.35)11-12-O4.5-6#3-i-2.5-3-16.75	A	CB	-	131.7	84.4	131.7	407.4	135.8	87.1
		B		0.213	131.8	84.5	131.8			
		C		0.145	143.9	92.2	143.9			
	(3@5.35)11-12-S5.5-6#3-i-2.5-3-16.75	A	CB	-	155.9	99.9	155.9	461.3	153.8	98.6
		B		0.095	154.9	99.3	154.9			
		C		-	150.6	96.5	150.6			

[‡] No anchorage failure on the bar

Table B.1 Cont. Comprehensive test results and data for beam-column joint specimens

	Specimen	Head	c_o in.	A_{brg}	ℓ_{eh} in.	$\ell_{eh,avg}$ in.	f_{cm} psi	Age days	d_b in.	A_b in.^{2}
Group 20	11-5-O4.5-0-i-2.5-3-19.25	A B	1.3	$4.5A_b$	19.63 19.25	19.44	5430	12	1.41	1.56
	11-5-S5.5-0-i-2.5-3-19.25	A B	1.5	$5.5A_b$	19.38 19.38	19.38	6320	11	1.41	1.56
	11-5-O4.5-6#3-i-2.5-3-19.25	A B	1.3	$4.5A_b$	19.50 19.75	19.63	5430	12	1.41	1.56
	11-5-S5.5-6#3-i-2.5-3-19.25	A B	1.5	$5.5A_b$	19.13 19.13	19.13	6320	13	1.41	1.56
	(3@5.35)11-5-O4.5-0-i-2.5-3-19.25	A B C	1.3	$4.5A_b$	19.50 19.63 19.38	19.50	5430	12	1.41	1.56
	(3@5.35)11-5-S5.5-0-i-2.5-3-19.25	A B C	1.5	$5.5A_b$	19.25 19.38 19.25	19.29	6320	11	1.41	1.56
	(3@5.35)11-5-O4.5-6#3-i-2.5-3-19.25	A B C	1.3	$4.5A_b$	19.38 19.63 19.13	19.38	5430	13	1.41	1.56
	(3@5.35)11-5-S5.5-6#3-i-2.5-3-19.25	A B C	1.5	$5.5A_b$	19.00 19.38 19.38	19.25	6320	13	1.41	1.56

Table B.1 Cont. Comprehensive test results and data for beam-column joint specimens

	Specimen	Head	b in.	h in.	h_{cl} in.	d_{eff} in.	c_{so} in.	$c_{so,avg}$ in.	c_{bc} in.	s in.	d_{tr} in.	$A_{tr,l}$ in.^{2}
Group 20	11-5-O4.5-0-i-2.5-3-19.25	A B	21.9	25.6	20	24.09	2.6 2.8	2.7	3.9 4.3	15.1	-	-
	11-5-S5.5-0-i-2.5-3-19.25	A B	22.0	25.4	20	24.17	2.5 3.0	2.8	3.3 3.3	15.1	-	-
	11-5-O4.5-6#3-i-2.5-3-19.25	A B	21.7	25.6	20	24.70	2.5 2.8	2.6	3.9 3.7	15.0	0.375	0.11
	11-5-S5.5-6#3-i-2.5-3-19.25	A B	22.2	25.3	20	24.47	2.8 2.8	2.8	3.4 3.4	15.3	0.375	0.11
	(3@5.35)11-5-O4.5-0-i-2.5-3-19.25	A B C	22.0	25.4	20	25.00	2.8 - 2.8	2.8	3.8 3.6 3.9	7.6 7.5	-	-
	(3@5.35)11-5-S5.5-0-i-2.5-3-19.25	A B C	21.9	25.5	20	24.86	2.8 - 2.8	2.8	3.5 3.4 3.5	7.5 7.5	-	-
	(3@5.35)11-5-O4.5-6#3-i-2.5-3-19.25	A B C	21.8	25.4	20	25.50	2.5 - 2.6	2.6	3.9 3.6 4.1	7.6 7.6	0.375	0.11
	(3@5.35)11-5-S5.5-6#3-i-2.5-3-19.25	A B C	21.8	25.4	20	25.41	2.6 - 2.8	2.7	3.6 3.3 3.3	7.3 7.8	0.375	0.11

Table B.1 Cont. Comprehensive test results and data for beam-column joint specimens

	Specimen	Head	N	s_{tr}* in.	A_{tt} in.^{2}	d_{tro} in.	s_{tro}* in.	A_{ab} in.^{2}	n	A_{hs} in.^{2}	Long. Reinf. Layout
Group 20	11-5-O4.5-0-i-2.5-3-19.25	A B	-	-	-	-	0.5	4 (2)	1.20	2	3.12	B16
	11-5-S5.5-0-i-2.5-3-19.25	A B	-	-	-	-	0.5	4 (2)	1.20	2	3.12	B16
	11-5-O4.5-6#3-i-2.5-3-19.25	A B	12	4 (2)	0.66	0.5	4 (2)	1.20	2	3.12	B16
	11-5-S5.5-6#3-i-2.5-3-19.25	A B	12	4 (2)	0.66	0.5	4 (2)	1.20	2	3.12	B16
	(3@5.35)11-5-O4.5-0-i-2.5-3-19.25	A B C	-	-	-	-	0.5	4 (2)	1.20	3	4.68	B16
	(3@5.35)11-5-S5.5-0-i-2.5-3-19.25	A B C	-	-	-	-	0.5	4 (2)	1.20	3	4.68	B16
	(3@5.35)11-5-O4.5-6#3-i-2.5-3-19.25	A B C	12	4 (2)	0.66	0.5	4 (2)	1.20	3	4.68	B16
	(3@5.35)11-5-S5.5-6#3-i-2.5-3-19.25	A B C	12	4 (2)	0.66	0.5	4 (2)	1.20	3	4.68	B16

* Value in parenthesis is the spacing between the first hoop and the center of the headed bar

Table B.1 Cont. Comprehensive test results and data for beam-column joint specimens

	Specimen	Head	Failure Type	Lead (Head) Slip in.	T_{max} kips	$f_{su,max}$ ksi	T_{ind} kips	T_{total} kips	T kips	f_{su} ksi
Group 20	11-5-O4.5-0-i-2.5-3-19.25	A B	SB/FP	0.021 0.128	161.4 154.4	103.5 99.0	161.4 154.3	315.7	157.9	101.2
	11-5-S5.5-0-i-2.5-3-19.25	A B	SB/FP	0.117 0.095	176.9 176.8‡	113.4 113.3‡	176.9 176.7	353.6	176.8	113.3
	11-5-O4.5-6#3-i-2.5-3-19.25	A B	SB/FP	0.012 0.036	180.4‡ 182.6	115.6‡ 117.1	180.3 182.6	362.9	181.4	116.3
	11-5-S5.5-6#3-i-2.5-3-19.25	A B	SB/FP	0.316 0.147	191.5‡ 187.7	122.8‡ 120.3	191.5 187.7	379.2	189.6	121.5
	(3@5.35)11-5-O4.5-0-i-2.5-3-19.25	A B C	CB	0.001 - -	132.5 127.5 126.0	84.9 81.7 80.8	132.5 127.5 126.0	386.0	128.7	82.5
	(3@5.35)11-5-S5.5-0-i-2.5-3-19.25	A B C	CB/BS	- 0.321 0.105	137.3 140.5 134.9	88.0 90.1 86.5	137.3 140.4 134.5	412.2	137.4	88.1
	(3@5.35)11-5-O4.5-6#3-i-2.5-3-19.25	A B C	CB	- - 0.042	137.4 137.1 150.7	88.1 87.9 96.6	137.4 137.1 150.7	425.1	141.7	90.8
	(3@5.35)11-5-S5.5-6#3-i-2.5-3-19.25	A B C	CB	- - 0.020	151.6 157.4 149.5	97.2 100.9 95.8	151.6 157.4 149.5	458.6	152.9	98.0

‡ No anchorage failure on the bar

APPENDIX C: DETAILED CCT NODE SPECIMEN RESULTS
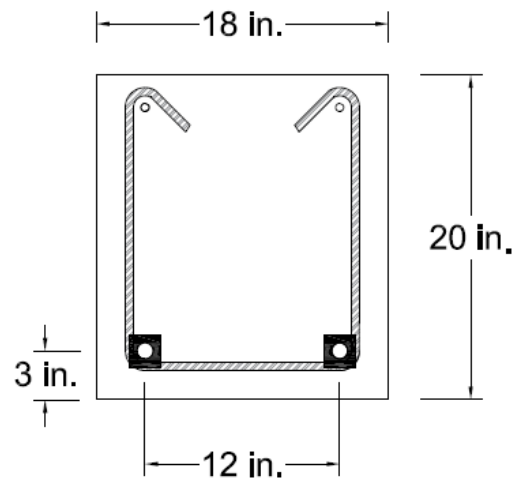
Figure C.1 Cross-section of the specimens with two headed bars
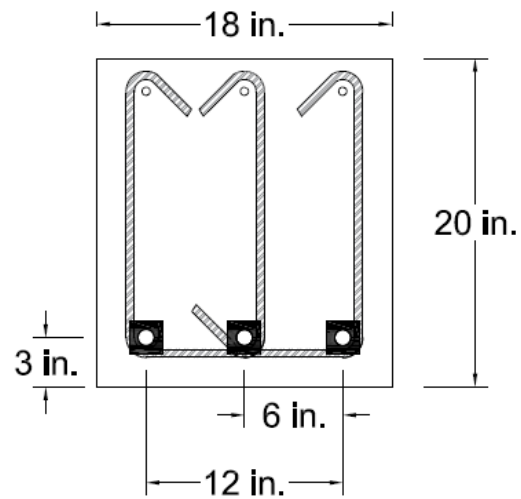
Figure C.2 Cross-section of the specimens with three headed bars

Table C.1 Details of the CCT node specimens

	Beam Type	ℓ_{eh} in.	f_{cm} psi	d_b in.	b in.	h in.	n	c_{so} in.	c_{sb} in.	c_{bc} in.
	Series 1 / Headed end									
1	H-2-8-5-9-F4.1-I	9	5740	1	18.0	20.0	2	2.5	2.5	2
2	H-2-8-5-10.4-F4.1-I	10.4	4490	1	18.1	20.3	2	2.5	2.5	2
3	H-3-8-5-9-F4.1-I	9	5800	1	18.3	20.1	3	2.5	2.5	2
4	H-3-8-5-11.4-F4.1-I	11.4	5750	1	18.0	20.1	3	2.5	2.5	2
5	H-3-8-5-14-F4.1-I	14	5750	1	18.1	20.0	3	2.5	2.5	2
	Series 1 / Non-headed end									
6	NH-2-8-5-9-F4.1-I	9	5740	1	18.0	20.0	2	2.5	2.5	2
7	NH-2-8-5-10.4-F4.1-I	10.4	5330	1	18.3	20.0	2	2.5	2.5	2
8	NH-3-8-5-9-F4.1-I	9	5800	1	18.0	20.1	3	2.5	2.5	2
9	NH-3-8-5-11.4-F4.1-I	11.4	5750	1	18.0	20.1	3	2.5	2.5	2
10	NH-3-8-5-14-F4.1-I	14	5750	1	18.0	20.0	3	2.5	2.5	2
	Series 2 / Headed end									
2	H-2-8-5-9-F4.1-II	9	4630	1	18.3	20.3	2	2.5	2.5	2
2	H-2-8-5-13-F4.1-II	13	4760	1	18.4	20.1	2	2.5	2.5	2
2	H-3-8-5-9-F4.1-II	9	4770	1	18.3	20.0	3	2.5	2.5	2
2	H-3-8-5-11-F4.1-II	11	4820	1	18.3	20.3	3	2.5	2.5	2
15	H-3-8-5-13-F4.1-II	13	4900	1	18.4	20.0	3	2.5	2.5	2
	Series 2 / Non-headed end									
16	NH-2-8-5-9-F4.1-II	9	4630	1	18.4	20.3	2	2.5	2.5	2
17	NH-2-8-5-13-F4.1-II	13	4760	1	18.4	20.1	2	2.5	2.5	2
18	NH-3-8-5-9-F4.1-II	9	4770	1	18.3	20.0	3	2.5	2.5	2
19	NH-3-8-5-11-F4.1-II	11	4820	1	18.3	20.3	3	2.5	2.5	2
20	NH-3-8-5-13-F4.1-II	13	4900	1	18.4	20.0	3	2.5	2.5	2

Table C.1 Cont. Details of the CCT node specimens

	Beam Type	A_h in²	s in.	Bearing Plate Width in.	P kips	Deflection at Peak Load in.	Failure Type
			Series 1 / Headed end				
1	H-2-8-5-9-F4.1-I	$4A_b$	12	6	278	0.2	Side blowout
2	H-2-8-5-10.4-F4.1-I	$4A_b$	12	6	346	0.3	Side blowout
3	H-3-8-5-9-F4.1-I	$4A_b$	6	6	446	*	Side blowout
4	H-3-8-5-11.4-F4.1-I	$4A_b$	6	6	386	0.33	Side blowout
5	H-3-8-5-14-F4.1-I	$4A_b$	6	6	495	*	Side blowout
			Series 1 / Non-headed end				
6	NH-2-8-5-9-F4.1-I	$4A_b$	12	6	158	0.05	Pullout
7	NH-2-8-5-10.4-F4.1-I	$4A_b$	12	6	236	0.13	Pullout
8	NH-3-8-5-9-F4.1-I	$4A_b$	6	6	255	0.1	Pullout
9	NH-3-8-5-11.4-F4.1-I	$4A_b$	6	6	245	*	Pullout
10	NH-3-8-5-14-F4.1-I	$4A_b$	6	6	356	0.18	Pullout
			Series 2 / Headed end				
11	H-2-8-5-9-F4.1-II	$4A_b$	12	6	218	0.1	Side blowout
12	H-2-8-5-13-F4.1-II	$4A_b$	12	6	250	0.11	Side blowout
13	H-3-8-5-9-F4.1-II	$4A_b$	6	6	355	0.14	Concrete crushing
14	H-3-8-5-11-F4.1-II	$4A_b$	6	6	403	0.19	Side blowout
15	H-3-8-5-13-F4.1-II	$4A_b$	6	6	499	0.37	Side blowout
			Series 2 / Non-headed end				
16	NH-2-8-5-9-F4.1-II	$4A_b$	12	6	218	*	Pullout
17	NH-2-8-5-13-F4.1-II	$4A_b$	12	6	234	0.08	Pullout
18	NH-3-8-5-9-F4.1-II	$4A_b$	6	6	205	0.08	Pullout
19	NH-3-8-5-11-F4.1-II	$4A_b$	6	6	316	0.13	Pullout
20	NH-3-8-5-13-F4.1-II	$4A_b$	6	6	365	0.14	Pullout

*Data not available

APPENDIX D: DETAILED SHALLOW EMBEDMENT SPECIMEN RESULTS
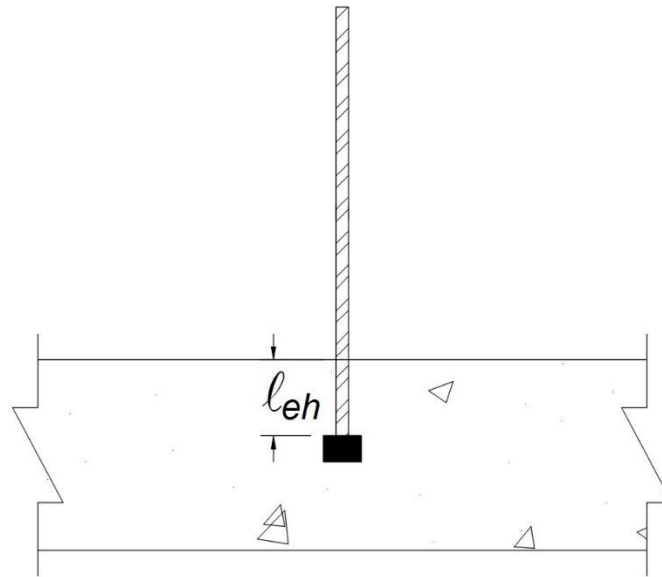
Figure D.1 Cross-section view of shallow embedment specimen with no flexural reinforcement.
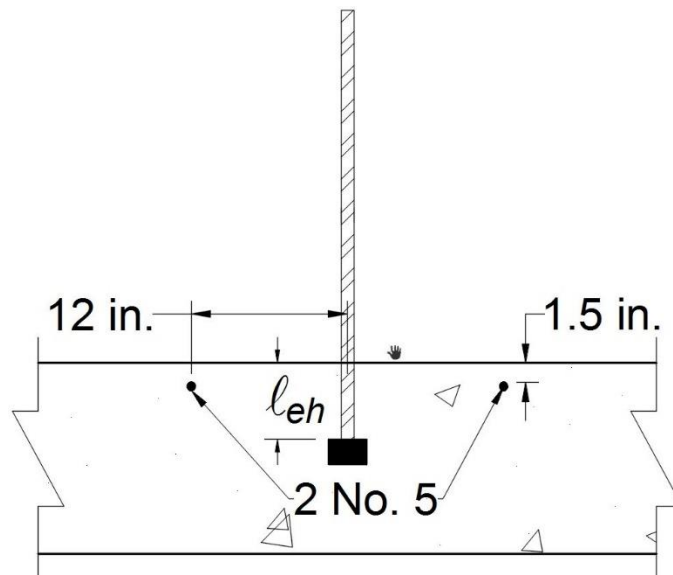
Figure D.2 Cross-section view of shallow embedment specimen with 2 No. 5 bars as flexural reinforcement.
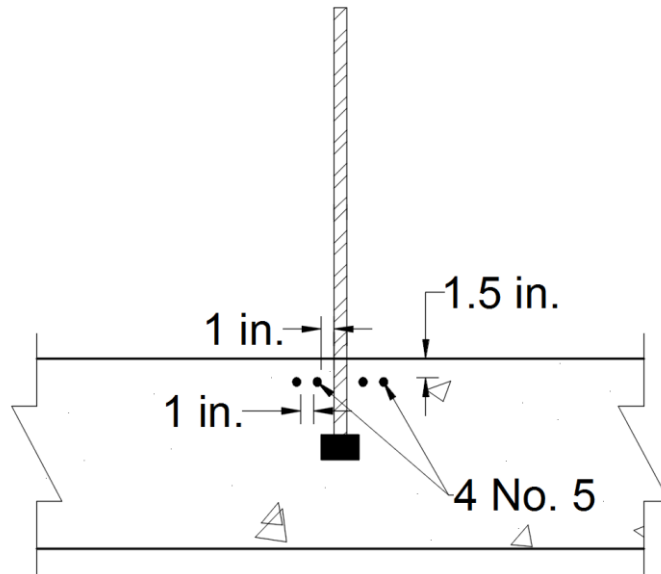
Figure D.3 Cross-section view of shallow embedment specimen with 4 No. 5 bars as flexural reinforcement.
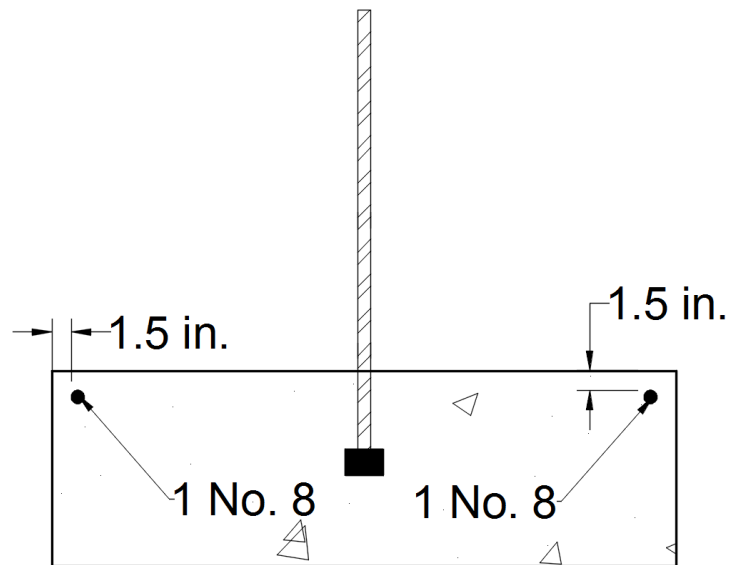
Figure D.4 End view of shallow embedment specimen with 2 No. 8 bars as flexural reinforcement.
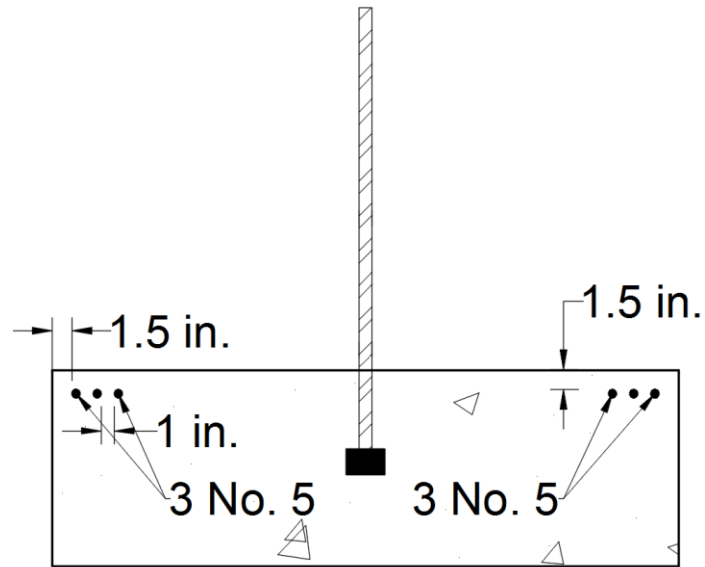
Figure D.5 End view of shallow embedment specimen with 6 No. 5 bars as flexural reinforcement.
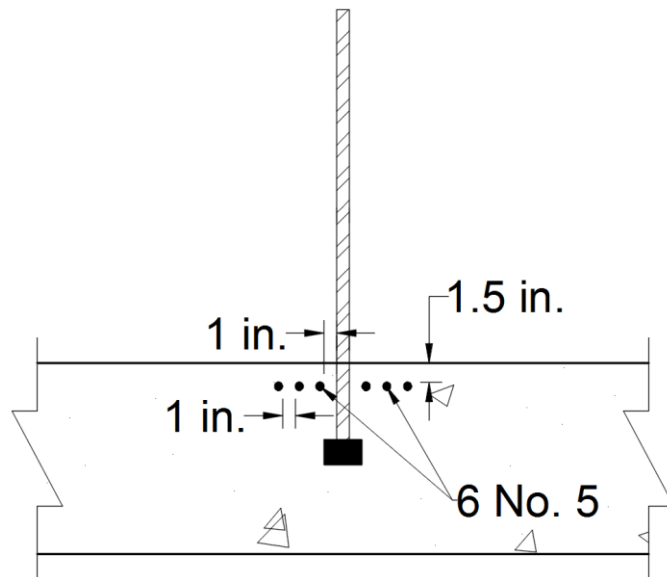
Figure D.6 Cross-section view of shallow embedment specimen with 6 No. 5 bars as flexural reinforcement.
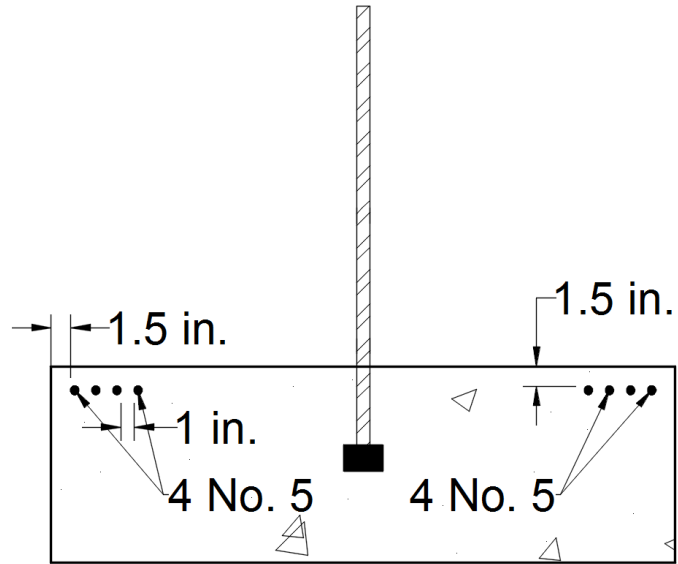
Figure D.7 End view of shallow embedment specimen with 8 No. 5 bars as flexural reinforcement.
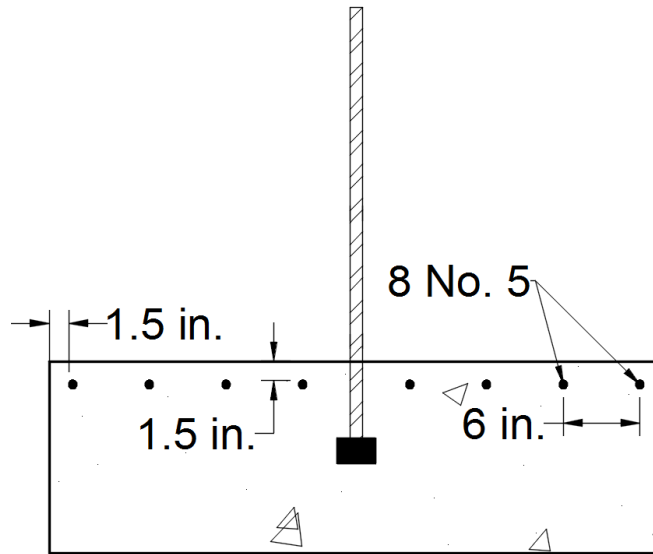
Figure D.8 End view of shallow embedment specimen with 8 No. 5 bars as flexural reinforcement.

Table D.1 Detail of shallow embedment pullout specimens[1]

Specimen[2]			ℓ_{eh} in.	f_{cm} psi	b in.	h in.	h_{cl} in.	c_{so} in.	c_{th} in.	A_{brg}/A_b	A_{st} in.[2]	T kips	f_{su} ksi	Reinf. Layout[4]
	SN	Designation	Head											
Series 1	1	8-5-T9.5-8#5-6	A	8.0	7040	48	15	10.5	23.5	7.0	9.5	2.48	65.6	83.0	D8
		8-5-T9.5-8#5-6	B	8.3	7040	48	15	10.5	23.5	6.8	9.5	2.48	67.8	85.8	D7
	2	8-5-T4.0-8#5-6	A	8.5	7040	48	15	10.5	23.5	6.5	4.0	2.48	61.8	78.2	D7
		8-5-T4.0-8#5-6	B	7.5	7040	48	15	10.5	23.5	7.5	4.0	2.48	56.3	71.3	D7
Series 2	3	8-5-F4.1-8#5-6	A	7.4	5220	48	15	10.5	23.5	7.6	4.1	2.48	68.9	87.2	D7
		8-5-F4.1-8#5-6	B	7.4	5220	48	15	10.5	23.5	7.6	4.1	2.48	64.4	81.5	D7
	4	8-5-F9.1-8#5-6	A	7.1	5220	48	15	10.5	23.5	7.9	9.1	2.48	69.9	88.5	D7
		8-5-F9.1-8#5-6	B	7.0	5220	48	15	10.5	23.5	8.0	9.1	2.48	54.9	69.5	D7
Series 3	5	8-5-F4.1-2#8-6	A	6.0	7390	48	15	10.5	23.5	9.0	4.1	1.58	64.4	81.5	D4
		8-5-F9.1-2#8-6	B	6.0	7390	48	15	10.5	23.5	9.0	9.1	1.58	65.0	82.3	D4
	6	8-5-T4.0-2#8-6	A	6.1	7390	48	15	10.5	23.5	8.9	4.0	1.58	60.5	76.6	D4
		8-5-T9.5-2#8-6	B	6.1	7390	48	15	10.5	23.5	8.9	9.5	1.58	57.7	73.0	D4
Series 4	7	8-8-O12.9-6#5-6	A	6.3	8620	48	15	9.8	23.5	8.8	12.9	1.86	79.0	100.0	D5
		8-8-O9.1-6#5-6	B	6.3	8620	48	15	10.5	23.5	8.8	9.1	1.86	70.9	89.7	D5
	8	8-8-S6.5-6#5-6	A	6.4	8620	48	15	10.0	23.5	8.6	6.5	1.86	92.4	117.0	D5
		8-8-O4.5-6#5-6	B	6.5	8620	48	15	10.8	23.5	8.5	4.5	1.86	74.0	93.7	D5
Series 5	9	8-5-S14.9-6#5-6	A	6.5	4200	48	15	10.3	23.5	8.5	14.0	1.86	61.8	78.2	D5
		8-5-S6.5-6#5-6	B	6.5	4200	48	15	10.0	23.5	8.5	6.5	1.86	49.2	62.3	D5
	10	8-5-O12.9-6#5-6	A	6.6	4200	48	15	10.0	23.5	8.4	12.9	1.86	52.4	66.3	D5
		8-5-O4.5-6#5-6	B	6.5	4200	48	15	10.1	23.5	8.5	4.5	1.86	50.1	63.4	D5
	11	8-5-S9.5-6#5-6	A	6.5	4200	48	15	10.3	23.5	8.5	9.5	1.86	48.9	61.9	D5
		8-5-S9.5-6#5-6	B	6.4	4200	48	15	10.1	23.5	8.6	9.5	1.86	54.5	69.0	D5
	12	8-5-F4.1-6#5-6[3]	-	8.4	4200	48	15	47.3	23.5	6.6	4.1	1.86	39.1	49.5	D5
Series 6	13	8-5-F4.1-0-6	A	6.5	5180	60	19	15.0	30.3	12.0	4.1	0	50.5	63.9	D1
		8-5-F4.1-0-6	B	6.3	5180	60	19	17.0	30.5	12.0	4.1	0	48.9	61.9	D1
		8-5-F4.1-2#5-6	C	6.8	5180	60	19	17.0	30.3	12.0	4.1	0.62	61.5	77.8	D2
	14	8-5-F4.1-4#5-6	A	6.0	5180	60	19	16.8	30.0	12.0	4.1	1.24	53.4	67.6	D3
		8-5-F4.1-4#5-6	B	6.1	5180	60	19	17.0	30.3	12.0	4.1	1.24	52.4	66.3	D3
		8-5-F4.1-4#5-6	C	6.8	5460	60	19	17.0	30.3	12.0	4.1	1.24	53.5	67.7	D3
	15	8-5-F4.1-6#5-6	A	6.3	5460	60	19	17.3	30.5	12.0	4.1	1.86	47.3	59.8	D6
		8-5-F4.1-6#5-6	B	6.6	5460	60	19	16.8	30.0	12.0	4.1	1.86	55.9	70.8	D6
		8-5-F4.1-6#5-6	C	6.9	5460	60	19	17.0	30.3	12.0	4.1	1.86	52.6	66.6	D6

[1] SN = specimen number; ℓ_{eh} = embedment length; b and h_{slab} = width and height of slab, respectively; h_{cl} = clear distance between the center of headed bar to the inner face of the nearest support plate; c_{so} = clear side concrete cover to the headed bar; c_{th} = bottom clear concrete cover to the head; A_{brg} = net bearing area of head; A_b = area of bar; A_{st} = total area of flexural reinforcement; T = peak tensile load; f_{su} = peak stress on headed bar

[2] Multiple headed bars in a single specimen are denoted by letters A, B, and C.

[3] Specimen contained a single headed bar at the middle.

[4] Detail of reinforcement in a plane perpendicular to the headed bar shown in Appendix D, Figures D1-D8.

APPENDIX E: DETAILED SPLICE SPECIMEN RESULTS
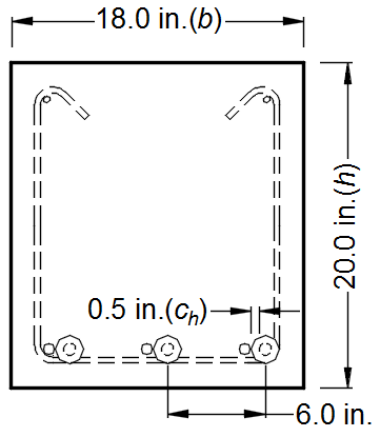
Figure E.1 Lapped bars with clear spacing of 0.5 in.
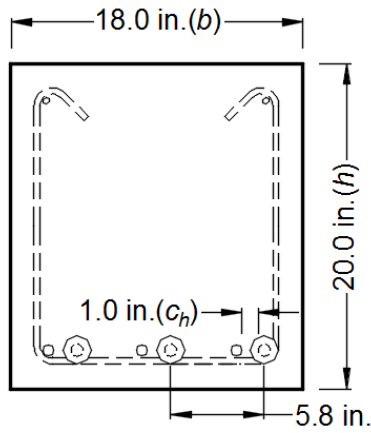
Figure E.2 Lapped bars with clear spacing of 1 in.
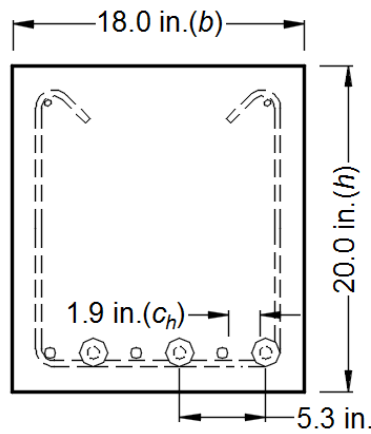
Figure E.3 Lapped bars with clear spacing of 1.9 in.

Table E.1 Detail of headed bar splice specimens[1]

Specimen	N	d_b in.	A_b in²	f_{cm} psi	ℓ_{st} in.	c_h in.	b in.	h in.	L_1 in.	L_2 in.	f_{su} ksi	P kips	M kip-in	Section Detail[2]
(3) 6-5-S4.0-12-0.5	3	0.75	0.44	6330	12	$^1/_2$	18.0	20.3	40.1	64.0	77.2	83.2	1669.2	E1
(3) 6-5-S4.0-12-1.0	3	0.75	0.44	6380	12	1	18.1	20.3	40.1	64.0	83.6	90.1	1804.8	E2
(3) 6-5-S4.0-12-1.9	3	0.75	0.44	6380	12	$1^7/_8$	18.0	20.1	40.1	64.0	76.3	82.2	1649.1	E3
(3) 6-12-S4.0-12-0.5	3	0.75	0.44	10890	12	$^1/_2$	18.0	20.1	40.0	64.1	81.9	89.1	1782.8	E1
(3) 6-12-S4.0-12-1.0	3	0.75	0.44	10890	12	1	18.0	20.5	40.1	64.0	75.0	81.5	1635.9	E2
(3) 6-12-S4.0-12-1.9	3	0.75	0.44	11070	12	$1^7/_8$	18.0	20.5	40.0	64.0	82.8	90.1	1802.4	E3

[1]N = number of lapped bars; A_b = cross-sectional area of lapped bar; b and h = width and depth of specimen, respectively; L_1 = average distance between loading points and the nearest supports; L_2 = distance between two supports (span length); f_{su} = stress on lapped bar at failure calculated from moment-curvature analysis; P = total load applied on specimen; M = average bending moment in splice region.

[2]Reinforcement detail at splice region shown in Appendix E, Figures E1-E3

APPENDIX F: TEST-TO-CALCULATED RATIOS[6]

Table F.1 Test-to-calculated ratios for beam-column joint specimens with widely-spaced headed bars and no confining reinforcement[*]

	Specimen	T kips	Descriptive Equation[a]		Design Equation[b]	
			T_c kips	T/T_c	T_{calc} kips	T/T_{calc}
1	8-5g-T4.0-0-i-2.5-3-12.5	97.7	85.1	1.15	72.5	1.35
2	8-5g-T4.0-0-i-3.5-3-12.5	93.4	86.0	1.09	73.4	1.27
3	8-5-T4.0-0-i-2.5-3-12.5	83.3	86.3	0.96	73.6	1.13
4	8-5-T4.0-0-i-3.5-3-12.5	91.9	87.5	1.05	74.6	1.23
5	8-8-F4.1-0-i-2.5-3-10.5	77.1	77.1	1.00	66.3	1.16
6	8-12-F4.1-0-i-2.5-3-10	71.8	76.8	0.93	66.4	1.08
7	8-5-S6.5-0-i-2.5-3-11.25	75.6	73.4	1.03	62.7	1.20
8	8-5-S6.5-0-i-2.5-3-14.25	87.7	95.2	0.92	80.8	1.09
9	8-5-O4.5-0-i-2.5-3-11.25	67.4	74.6	0.90	63.8	1.06
10	8-5-O4.5-0-i-2.5-3-14.25	85.0	94.4	0.90	80.1	1.06
11	8-5-T9.5-0-i-2.5-3-14.5	91.7	93.8	0.98	79.5	1.15
12	8-5-O9.1-0-i-2.5-3-14.5	94.8	93.8	1.01	79.5	1.19
13	8-15-T4.0-0-i-2.5-4.5-9.5	83.3	81.1	1.03	70.4	1.18
14	8-15-S9.5-0-i-2.5-3-9.5	81.7	81.1	1.01	70.4	1.16
15	8-8-T9.5-0-i-2.5-3-9.5	65.2	69.7	0.94	60.2	1.08
16	(2@9)8-12-F4.1-0-i-2.5-3-12	79.1	96.9	0.82	83.3	0.95
17	(2@9)8-12-F9.1-0-i-2.5-3-12	76.5	95.3	0.80	82.0	0.93
18	8-8-O4.5-0-i-2.5-3-9.5	58.4	63.6	0.92	54.7	1.07
19	(2@9)8-8-O4.5-0-i-2.5-3-9.5	58.8	62.2	0.94	53.6	1.10
20	(2@9)8-8-T4.0-0-i-2.5-3-9.5	61.8	65.1	0.95	56.0	1.10
21	5-5-F4.0-0-i-2.5-5-4	24.5	21.5	1.14	17.7	1.39
22	5-5-F4.0-0-i-2.5-3-6	32.7	31.9	1.03	26.0	1.26
23	5-12-F4.0-0-i-2.5-5-4	28.3	26.2	1.08	21.8	1.30
24	5-12-F4.0-0-i-2.5-3-6	41.7	39.2	1.06	32.1	1.30
25	11-5a-F3.8-0-i-2.5-3-17	97.5	116.5	0.84	102.6	0.95
26	11-5-F3.8-0-i-2.5-3-17	132.7	132.2	1.00	116.7	1.14
27	11-12-O4.5-0-i-2.5-3-16.75	169.6	152.8	1.11	135.7	1.25
28	11-12-S5.5-0-i-2.5-3-16.75	175.9	148.5	1.18	131.9	1.33
29	11-5-O4.5-0-i-2.5-3-19.25	157.9	147.4	1.07	129.6	1.22
30	11-5-S5.5-0-i-2.5-3-19.25	176.8	152.4	1.16	134.1	1.32

[*] Specimens used to develop descriptive equations
[a] T_c based on Eq. (7.6)
[b] T_{calc} based on Eq. (9.15)

---

[6] Six beam-column joint specimens in this study exhibiting bar yielding rather than anchorage failure are not included.

Table F.2 Test-to-calculated ratios for beam-column joint specimens with closely-spaced headed bars and no confining reinforcement[*]

	Specimen	T kips	Descriptive Equation[a]		Design Equation[b]	
			T_c kips	T/T_c	T_{calc} kips	T/T_{calc}
31	(3@3)8-8-F4.1-0-i-2.5-3-10.5	54.8	46.3	1.18	36.4	1.50
32	(3@3)8-8-F4.1-0-i-2.5-3-10.5-HP	50.5	44.3	1.14	35.2	1.44
33	(3@4)8-8-F4.1-0-i-2.5-3-10.5	58.7	53.6	1.09	40.8	1.44
34	(3@5)8-8-F4.1-0-i-2.5-3-10.5	64.0	57.3	1.12	43.0	1.49
35	(3@5)8-8-F4.1-0-i-2.5-3-10.5-HP	59.9	57.4	1.04	43.2	1.39
36	(3@3)8-12-F4.1-0-i-2.5-3-10	42.2	46.4	0.91	36.6	1.15
37	(3@4)8-12-F4.1-0-i-2.5-3-10	48.9	53.0	0.92	40.5	1.21
38	(3@5)8-12-F4.1-0-i-2.5-3-10	55.1	60.0	0.92	45.3	1.22
39	(3@5.5)8-5-T9.5-0-i-2.5-3-14.5	73.4	74.7	0.98	55.6	1.32
40	(3@5.5)8-5-O9.1-0-i-2.5-3-14.5	75.7	75.3	1.01	56.0	1.35
41	(4@3.7)8-5-T9.5-0-i-2.5-3-14.5	60.8	63.1	0.96	47.6	1.28
42	(4@3.7)8-5-O9.1-0-i-2.5-3-14.5	61.2	61.0	1.00	46.3	1.32
43	(3@4)8-8-T9.5-0-i-2.5-3-9.5	40.3	46.7	0.86	35.6	1.13
44	(3@5)8-8-T9.5-0-i-2.5-3-9.5	44.5	55.1	0.81	41.6	1.07
45	(3@7)8-8-T9.5-0-i-2.5-3-9.5	68.7	67.2	1.02	53.4	1.29
46	(3@4)8-8-T9.5-0-i-2.5-3-14.5	76.6	74.6	1.03	56.2	1.36
47	(3@5)8-8-T9.5-0-i-2.5-3-14.5	93.2	84.5	1.10	63.0	1.48
48	(3@7)8-8-T9.5-0-i-2.5-3-14.5	104.0	104.8	0.99	82.4	1.26
49	(3@4.5)8-12-F4.1-0-i-2.5-3-12	75.2	69.9	1.08	52.7	1.43
50	(3@4.5)8-12-F9.1-0-i-2.5-3-12	75.4	69.6	1.08	52.4	1.44
51	(4@3)8-12-F4.1-0-i-2.5-3-12	49.3	57.3	0.86	45.1	1.09
52	(4@3)8-12-F9.1-0-i-2.5-3-12	50.3	58.5	0.86	46.1	1.09
53	(2@7)8-8-O4.5-0-i-2.5-3-9.5	54.5	59.5	0.92	47.2	1.15
54	(2@5)8-8-O4.5-0-i-2.5-3-9.5	51.2	48.7	1.05	36.8	1.39
55	(2@3)8-8-O4.5-0-i-2.5-3-9.5	47.7	37.7	1.27	29.6	1.61
56	(3@4.5)8-8-T4.0-0-i-2.5-3-9.5	40.7	46.7	0.87	35.2	1.16
57	(4@3)8-8-T4.0-0-i-2.5-3-9.5	26.2	38.7	0.68	30.6	0.85
58	(3@3)8-8-T4.0-0-i-2.5-3-9.5	39.4	39.8	0.99	31.2	1.26
59	(3@5.9)5-12-F4.0-0-i-2.5-4-5	28.0	27.7	1.01	20.3	1.38
60	(4@3.9)5-12-F4.0-0-i-2.5-4-5	25.6	22.3	1.15	16.3	1.57
61	(3@5.35)11-12-O4.5-0-i-2.5-3-16.75	106.8	118.5	0.90	92.2	1.16
62	(3@5.35)11-12-S5.5-0-i-2.5-3-16.75	109.0	117.1	0.93	91.1	1.20
63	(3@5.35)11-5-O4.5-0-i-2.5-3-19.25	128.7	117.3	1.10	90.3	1.43
64	(3@5.35)11-5-S5.5-0-i-2.5-3-19.25	137.4	119.7	1.15	92.3	1.49

[*] Specimens used to develop descriptive equations
[a] T_c based on Eq. (7.6)
[b] T_{calc} based on Eq. (9.15)

Table F.3 Test-to-calculated ratios for beam-column joint specimens with widely-spaced headed bars with confining reinforcement[*]

	Specimen	T kips	Descriptive Equation[a]		Design Equation[b]	
			T_h kips	T/T_h	T_{calc} kips	T/T_{calc}
65	8-5-T4.0-4#3-i-3-3-12.5	87.5	96.9	0.90	76.4	1.15
66	8-5-T4.0-4#3-i-4-3-12.5	96.2	95.9	1.00	74.6	1.29
67	8-5-T4.0-4#4-i-3-3-12.5	109.0	100.7	1.08	74.6	1.46
68	8-5-T4.0-4#4-i-4-3-12.5	101.5	98.2	1.03	72.9	1.39
69	8-5g-T4.0-5#3-i-2.5-3-9.5	78.7	78.1	1.01	60.1	1.31
70	8-5g-T4.0-5#3-i-3.5-3-9.5	79.5	80.3	0.99	62.3	1.28
71	8-5g-T4.0-4#4-i-2.5-3-9.5	90.7	79.2	1.14	56.7	1.60
72	8-5g-T4.0-4#4-i-3.5-3-9.5	96.7	83.3	1.16	60.1	1.61
73	8-5-T4.0-5#3-i-2.5-3-9.5	74.2	78.7	0.94	61.5	1.21
74	8-5-T4.0-5#3-i-3.5-3-9.5	80.6	78.2	1.03	60.1	1.34
75	8-5-T4.0-4#4-i-2.5-3-9.5	90.5	82.9	1.09	60.3	1.50
76	8-5-T4.0-4#4-i-3.5-3-9.5	85.6	82.3	1.04	60.3	1.42
77	8-8-F4.1-2#3-i-2.5-3-10	73.4	77.7	0.94	65.0	1.13
78	8-12-F4.1-5#3-i-2.5-3-10	87.2	95.5	0.91	76.2	1.14
79	8-5-S6.5-2#3-i-2.5-3-9.25	63.4	66.2	0.96	55.2	1.15
80	8-5-S6.5-2#3-i-2.5-3-12.25	86.0	88.2	0.97	72.8	1.18
81	8-5-O4.5-2#3-i-2.5-3-9.25	67.9	67.9	1.00	56.4	1.20
82	8-5-O4.5-2#3-i-2.5-3-12.25	78.5	86.0	0.91	71.4	1.10
83	8-5-S6.5-5#3-i-2.5-3-8.25	62.0	71.7	0.87	56.7	1.09
84	8-5-S6.5-5#3-i-2.5-3-11.25	84.5	89.9	0.94	70.5	1.20
85	8-5-O4.5-5#3-i-2.5-3-8.25	68.4	69.5	0.98	53.5	1.28
86	8-5-O4.5-5#3-i-2.5-3-11.25	82.2	91.2	0.90	72.0	1.14
87	8-5-T9.5-5#3-i-2.5-3-14.5	121.0	111.9	1.08	86.7	1.40
88	8-15-T4.0-2#3-i-2.5-4.5-7	59.0	65.1	0.91	55.6	1.06
89	8-15-S9.5-2#3-i-2.5-3-7	67.1	65.1	1.03	55.0	1.22
90	8-15-T4.0-5#3-i-2.5-4.5-5.5	63.3	62.3	1.02	48.0	1.32
91	8-15-S9.5-5#3-i-2.5-3-5.5	75.8	63.4	1.20	47.4	1.60
92	8-8-T9.5-2#3-i-2.5-3-9.5	68.7	73.6	0.93	61.8	1.11
93	(2@9)8-12-F4.1-5#3-i-2.5-3-12	111.9	112.2	1.00	89.0	1.26
94	(2@9)8-8-T4.0-5#3-i-2.5-3-9.5	76.7	82.1	0.93	64.4	1.19
95	5-5-F4.0-2#3-i-2.5-5-4	19.7	23.7	0.83	20.7	0.95
96	5-5-F4.0-5#3-i-2.5-5-4	26.5	32.6	0.81	21.0	1.26
97	5-5-F4.0-2#3-i-2.5-3-6	37.9	35.4	1.07	28.5	1.33
98	5-5-F4.0-5#3-i-2.5-3-6	43.5	42.9	1.01	28.3	1.54
99	5-12-F4.0-2#3-i-2.5-5-4	32.7	30.2	1.08	24.7	1.32
100	5-12-F4.0-5#3-i-2.5-5-4	38.9	37.9	1.03	24.7	1.58
101	11-5a-F3.8-2#3-i-2.5-3-17	118.2	130.1	0.91	109.5	1.08
102	11-5a-F3.8-6#3-i-2.5-3-17	116.2	139.4	0.83	115.9	1.00
103	11-5-F3.8-6#3-i-2.5-3-17	151.9	152.7	1.00	124.9	1.22
104	11-12-O4.5-6#3-i-2.5-3-16.75	201.5	171.7	1.17	140.0	1.44
105	11-12-S5.5-6#3-i-2.5-3-16.75	197.4	169.2	1.17	137.8	1.43
106	11-5-O4.5-6#3-i-2.5-3-19.25	181.4	170.7	1.06	138.7	1.31
107	11-5-S5.5-6#3-i-2.5-3-19.25	189.6	172.1	1.10	139.8	1.36

[*] Specimens used to develop descriptive equations
[a] T_h based on Eq. (7.9)
[b] T_{calc} based on Eq. (9.15)

Table F.4 Test-to-calculated ratios for beam-column joint specimens with closely-spaced headed bars with confining reinforcement[*]

	Specimen	T kips	Descriptive Equation[a]		Design Equation[b]	
			T_h kips	T/T_h	T_{calc} kips	T/T_{calc}
108	(3@3)8-8-F4.1-2#3-i-2.5-3-10	61.9	55.9	1.11	44.9	1.38
109	(3@3)8-8-F4.1-2#3-i-2.5-3-10-HP	56.7	57.4	0.99	46.2	1.23
110	(3@4)8-8-F4.1-2#3-i-2.5-3-10	55.5	59.4	0.93	47.0	1.18
111	(3@4)8-8-F4.1-2#3-i-2.5-3-10-HP	69.8	62.8	1.11	48.9	1.43
112	(3@5)8-8-F4.1-2#3-i-2.5-3-10.5	56.1	62.8	0.89	49.3	1.14
113	(3@5)8-8-F4.1-2#3-i-2.5-3-10.5-HP	65.5	65.6	1.00	51.0	1.28
114	(3@3)8-12-F4.1-5#3-i-2.5-3-10	61.6	65.2	0.95	54.7	1.13
115	(3@4)8-12-F4.1-5#3-i-2.5-3-10	65.7	69.3	0.95	56.4	1.16
116	(3@5)8-12-F4.1-5#3-i-2.5-3-10	69.7	74.6	0.93	59.5	1.17
117	(3@5.5)8-5-T9.5-5#3-i-2.5-3-14.5	94.6	94.7	1.00	72.8	1.30
118	(4@3.7)8-5-T9.5-5#3-i-2.5-3-14.5	76.9	81.7	0.94	64.6	1.19
119	(3@4)8-8-T9.5-2#3-i-2.5-3-9.5	51.8	59.3	0.87	47.2	1.10
120	(3@5)8-8-T9.5-2#3-i-2.5-3-9.5	55.9	64.2	0.87	50.5	1.11
121	(3@7)8-8-T9.5-2#3-i-2.5-3-9.5	67.6	75.6	0.89	59.8	1.13
122	(3@4)8-8-T9.5-2#3-i-2.5-3-14.5	85.4	88.8	0.96	69.0	1.24
123	(3@5)8-8-T9.5-2#3-i-2.5-3-14.5	105.2	95.6	1.10	73.3	1.43
124	(3@7)8-8-T9.5-2#3-i-2.5-3-14.5	113.4	113.8	1.00	88.3	1.28
125	(3@4.5)8-12-F4.1-5#3-i-2.5-3-12	87.7	89.0	0.99	70.3	1.25
126	(3@4.5)8-12-F9.1-5#3-i-2.5-3-12	108.6	87.3	1.24	67.1	1.62
127	(4@3)8-12-F4.1-5#3-i-2.5-3-12	64.2	77.0	0.83	64.0	1.00
128	(4@3)8-12-F9.1-5#3-i-2.5-3-12	87.8	76.3	1.15	61.2	1.44
129	(3@4.5)8-8-T4.0-5#3-i-2.5-3-9.5	62.5	61.7	1.01	49.0	1.28
130	(4@3)8-8-T4.0-5#3-i-2.5-3-9.5	48.6	54.8	0.89	46.0	1.06
131	(3@3)8-8-T4.0-5#3-i-2.5-3-9.5	56.5	55.1	1.03	45.8	1.23
132	(3@5.9)5-12-F4.0-2#3-i-2.5-4-5	35.1	32.8	1.07	25.2	1.39
133	(3@5.9)5-12-F4.0-5#3-i-2.5-4-5	38.6	36.1	1.07	24.8	1.56
134	(4@3.9)5-12-F4.0-2#3-i-2.5-4-5	30.9	27.1	1.14	21.0	1.47
135	(3@5.35)11-12-O4.5-6#3-i-2.5-3-16.75	135.8	145.6	0.93	114.7	1.18
136	(3@5.35)11-12-S5.5-6#3-i-2.5-3-16.75	153.8	140.5	1.09	109.2	1.41
137	(3@5.35)11-5-O4.5-6#3-i-2.5-3-19.25	141.7	141.9	1.00	109.9	1.29
138	(3@5.35)11-5-S5.5-6#3-i-2.5-3-19.25	152.9	144.9	1.06	112.0	1.37

[*] Specimens used to develop descriptive equations
[a] T_h based on Eq. (7.9)
[b] T_{calc} based on Eq. (9.15)

Table F.5 Test-to-calculated ratios for beam-column joint specimens without confining reinforcement above joint region[*]

	Specimen	T	Descriptive Equation[a]		Design Equation[b]	
			T_c	T/T_c	T_{calc}	T/T_{calc}
		kips	kips		kips	
139	8-5-T4.0-0-i-3-3-15.5	80.4	102.4	0.79	86.5	0.93
140	8-5-T4.0-0-i-4-3-15.5	95.4	100.4	0.95	84.9	1.12

[*] Specimens not used to develop descriptive equations
[a] T_c based on Eq. (7.6)
[b] T_{calc} based on Eq. (9.15)

Table F.6 Test-to-calculated ratios for beam-column joint specimens with large heads $(A_{brg} > 12A_b)$[*]

	Specimen	T	Descriptive Equation[a]		Design Equation[b]	
			T_c or T_h	T/T_c T/T_h	T_{calc}	T/T_{calc}
		kips	kips		kips	
141	8-15-S14.9-0-i-2.5-3-9.5	87.1	82.7	1.05	71.8	1.21
142	8-15-S14.9-2#3-i-2.5-3-7	79.3	64.6	1.23	53.8	1.47
143	8-15-S14.9-5#3-i-2.5-3-5.5	81.4	62.3	1.31	45.8	1.78
144	5-5-F13.1-0-i-2.5-5-4	28.2	23.4	1.21	19.2	1.47
145	5-5-F13.1-2#3-i-2.5-5-4	28.9	25.2	1.15	20.4	1.42
146	5-5-F13.1-5#3-i-2.5-5-4	35.2	32.7	1.08	20.1	1.75
147	5-5-F13.1-0-i-2.5-3-6	35.3	33.1	1.07	26.9	1.31
148	5-5-F13.1-2#3-i-2.5-3-6	46.4	35.1	1.32	27.5	1.69
149	5-12-F13.1-0-i-2.5-5-4	31.4	26.6	1.18	22.1	1.42
150	5-12-F13.1-2#3-i-2.5-5-4	36.3	30.0	1.21	24.2	1.50
151	5-12-F13.1-5#3-i-2.5-5-4	40.3	37.3	1.08	24.0	1.68
152	5-12-F13.1-0-i-2.5-3-6	44.2	39.4	1.12	32.3	1.37
153	8-8-O12.9-0-i-2.5-3-9.5	85.2	71.6	1.19	61.8	1.38
154	8-8-S14.9-0-i-2.5-3-8.25	70.9	60.7	1.17	52.6	1.35
155	8-8-O12.9-5#3-i-2.5-3-9.5	83.5	85.4	0.98	66.9	1.25
156	8-8-S14.9-5#3-i-2.5-3-8.25	87.0	76.8	1.13	58.5	1.49

[*] Specimens not used to develop descriptive equations
[a] T_c based on Eq. (7.6) for specimens without confining reinforcement; T_h based on Eq. (7.9) for specimens with confining reinforcement
[b] T_{calc} based on Eq. (9.15)

Table F.7 Test-to-calculated ratios for beam-column joint specimens with large h_{cl}/ℓ_{eh} ratio[*]

	Specimen	T kips	Descriptive Equation[a]		Design Equation[b]	
			T_c or T_h kips	T/T_c T/T_h	T_{calc} kips	T/T_{calc}
157	8-5-F4.1-0-i-2.5-7-6	28.7	38.7	0.74	33.6	0.85
158	8-5-F4.1-5#3-i-2.5-7-6	50.7	55.8	0.91	42.9	1.18
159	(3@3)8-5-F4.1-0-i-2.5-7-6	20.6	24.0	0.86	18.9	1.09
160	(3@3)8-5-F4.1-5#3-i-2.5-7-6	32.1	36.2	0.89	28.8	1.11
161	(3@5)8-5-F4.1-0-i-2.5-7-6	23.9	31.3	0.76	23.8	1.01
162	(3@5)8-5-F4.1-5#3-i-2.5-7-6	37.5	43.7	0.86	34.3	1.09
163	(3@7)8-5-F4.1-0-i-2.5-7-6	27.1	37.1	0.73	29.8	0.91
164	(3@7)8-5-F4.1-5#3-i-2.5-7-6	42.3	48.6	0.87	38.6	1.10
165	8-5-F9.1-0-i-2.5-7-6	33.4	38.9	0.86	33.8	0.99
166	8-5-F9.1-5#3-i-2.5-7-6	53.8	55.2	0.97	41.6	1.29
167	(3@5.5)8-5-F9.1-0-i-2.5-7-6	23.0	32.0	0.72	24.5	0.94
168	(3@5.5)8-5-F9.1-5#3-i-2.5-7-6	43.1	45.0	0.96	35.4	1.22
169	(4@3.7)8-5-T9.5-0-i-2.5-6.5-6	21.7	25.3	0.86	19.7	1.10
170	(4@3.7)8-5-F9.1-5#3-i-2.5-7-6	31.6	36.3	0.87	28.4	1.12
171	11-5a-F3.8-0-i-2.5-3-12	56.8	83.2	0.68	73.9	0.77
172	11-5a-F3.8-2#3-i-2.5-3-12	67.3	90.4	0.74	75.9	0.89
173	11-5a-F3.8-6#3-i-2.5-3-12	78.0	105.6	0.74	86.6	0.90
174	11-5a-F8.6-0-i-2.5-3-12	63.8	84.0	0.76	74.7	0.85
175	11-5a-F8.6-6#3-i-2.5-3-12	79.2	109.4	0.72	90.5	0.88
176	8-8-F4.1-0-i-2.5-3-10-DB	50.2	70.1	0.72	60.3	0.83
177	8-8-F9.1-0-i-2.5-3-10-DB	51.8	69.7	0.74	59.9	0.86
178	8-8-F9.1-5#3-i-2.5-3-10-DB	68.2	79.0	0.86	67.2	1.01
179	8-5-F4.1-0-i-2.5-3-10-DB	40.6	63.4	0.64	54.3	0.75
180	8-5-F9.1-0-i-2.5-3-10-DB	44.4	62.6	0.71	53.6	0.83
181	8-5-F4.1-3#4-i-2.5-3-10-DB	64.6	74.8	0.86	63.2	1.02
182	8-5-F9.1-3#4-i-2.5-3-10-DB	65.8	72.4	0.91	60.7	1.08
183	8-5-F4.1-5#3-i-2.5-3-10-DB	70.2	76.2	0.92	63.8	1.10
184	8-5-F9.1-5#3-i-2.5-3-10-DB	70.5	74.6	0.95	62.1	1.13
185	11-8-F3.8-0-i-2.5-3-14.5	79.1	121.9	0.65	108.6	0.73
186	11-8-F3.8-2#3-i-2.5-3-14.5	88.4	130.8	0.68	112.9	0.78
187	11-8-F3.8-6#3-i-2.5-3-14.5	112.7	145.3	0.78	123.7	0.91
188	(3@5.35)11-8-F3.8-0-i-2.5-3-14.5	52.9	97.7	0.54	76.2	0.69
189	(3@5.35)11-8-F3.8-2#3-i-2.5-3-14.5	72.6	111.9	0.65	89.3	0.81
190	(3@5.35)11-8-F3.8-6#3-i-2.5-3-14.5	83.7	123.3	0.68	99.2	0.84
191	11-5-F3.8-0-i-2.5-3-12	66.5	92.0	0.72	82.0	0.81
192	11-5-F3.8-6#3-i-2.5-3-12	88.3	116.7	0.76	98.3	0.90
193	11-5-F8.6-0-i-2.5-3-14.5	82.8	111.5	0.74	99.0	0.84
194	11-5-F8.6-6#3-i-2.5-3-14.5	112.3	134.3	0.84	112.3	1.00
195	(3@5.35)11-5-F8.6-0-i-2.5-3-14.5	65.1	89.4	0.73	69.4	0.94
196	(3@5.35)11-5-F8.6-6#3-i-2.5-3-14.5	75.6	110.7	0.68	87.9	0.86

[*] Specimens not used to develop descriptive equations

[a] T_c based on Eq. (7.6) for specimens without confining reinforcement; T_h based on Eq. (7.9) for specimens with confining reinforcement

[b] T_{calc} based on Eq. (9.15)

Table F.8 Beam-column joint specimens in current study with bar yielding[*]

	Specimen	T kips	Descriptive Equation		Design Equation	
			T_c or T_h kips	T/T_c T/T_h	T_c or T_h kips	T/T_c T/T_h
197	8-5-O9.1-5#3-i-2.5-3-14.5	119.3	*	*	*	*
198	(3@5.5)8-5-O9.1-5#3-i-2.5-3-14.5	102.2	*	*	*	*
199	(4@3.7)8-5-O9.1-5#3-i-2.5-3-14.5	89.1	*	*	*	*
200	8-8-T9.5-0-i-2.5-3-14.5	118.8	*	*	*	*
201	(2@9)8-12-F9.1-5#3-i-2.5-3-12	121.2	*	*	*	*
202	(4@3.9)5-12-F4.0-5#3-i-2.5-4-5	48.1	*	*	*	*

[*] Specimens did not exhibit a bond failure and were not compared against descriptive or design equations

Table F.9 Test-to-calculated ratios for CCT node specimens in current study

	Specimen	T kips	Descriptive Equation[a]		Design Equation[b]	
			T_c kips	T/T_c	T_{calc} kips	T/T_{calc}
203	H-2-8-5-10.4-F4.1	126.9	65.6	1.93	56.0	2.26
204	H-2-8-5-9-F4.1	101.9	59.9	1.70	51.6	1.98
205	H-3-8-5-11.4-F4.1	94.6	64.7	1.46	49.0	1.93
206	H-3-8-5-9-F4.1	109.0	50.8	2.14	38.8	2.81
207	H-3-8-5-14-F4.1	121.0	80.0	1.51	60.2	2.01
208	H-2-8-5-9-F4.1	79.9	56.9	1.40	48.9	1.64
209	H-2-8-5-13-F4.1	91.7	83.7	1.10	71.1	1.29
210	H-3-8-5-9-F4.1	86.8	48.5	1.79	36.9	2.35
211	H-3-8-5-11-F4.1	98.5	59.8	1.65	45.3	2.18
212	H-3-8-5-13-F4.1	122.0	71.3	1.71	53.7	2.27

[a] T_c based on Eq. (7.6)
[b] T_{calc} based on Eq. (9.15), with $\psi_o = 1.0$

Table F.10 Test-to-calculated ratios for shallow embedment pullout specimens in current study

	Specimen	T kips	Descriptive Equation[a]		Design Equation[b]	
			T_c kips	T/T_c	T_{calc} kips	T/T_{calc}
213	8-5-T9.5-8#5-6	65.6	55.8	1.18	48.2	1.36
214	8-5-T9.5-8#5-6	67.8	57.5	1.18	49.7	1.36
215	8-5-T4.0-8#5-6	61.8	59.3	1.04	51.3	1.21
216	8-5-T4.0-8#5-6	56.3	52.2	1.08	45.2	1.24
217	8-5-F4.1-8#5-6	68.9	48.1	1.43	41.6	1.66
218	8-5-F4.1-8#5-6	64.4	47.7	1.35	41.3	1.56
219	8-5-F9.1-8#5-6	69.9	46.1	1.52	39.9	1.75
220	8-5-F9.1-8#5-6	54.9	45.2	1.21	39.2	1.40
221	8-5-F4.1-2#8-6	64.4	41.9	1.54	36.6	1.76
222	8-5-F9.1-2#8-6	65.0	41.9	1.55	36.6	1.77
223	8-5-T4.0-2#8-6	60.5	42.4	1.43	37.0	1.63
224	8-5-T9.5-2#8-6	57.7	42.8	1.35	37.4	1.54
225	8-8-O12.9-6#5-6[c][d]	79.0	45.4	1.74	39.6	1.99
226	8-8-O9.1-6#5-6[c]	70.9	45.4	1.56	39.6	1.79
227	8-8-S6.5-6#5-6	92.4	46.3	1.99	40.4	2.28
228	8-8-O4.5-6#5-6[c]	74.0	47.3	1.57	41.2	1.79
229	8-5-S14.9-6#5-6[d]	61.8	39.8	1.55	34.4	1.79
230	8-5-S6.5-6#5-6	49.2	39.8	1.24	34.4	1.43
231	8-5-O12.9-6#5-6[c][d]	52.4	40.6	1.29	35.1	1.49
232	8-5-O4.5-6#5-6[c]	50.1	39.8	1.26	34.4	1.45
233	8-5-S9.5-6#5-6	48.9	39.8	1.23	34.4	1.42
234	8-5-S9.5-6#5-6	54.5	39.0	1.40	33.8	1.61
235	8-5-F4.1-6#5-6	39.1	52.0	0.75	44.7	0.87
236	8-5-F4.1-0-6	50.5	41.8	1.21	36.3	1.39
237	8-5-F4.1-0-6	48.9	40.2	1.22	34.9	1.40
238	8-5-F4.1-2#5-6	61.5	43.5	1.41	37.7	1.63
239	8-5-F4.1-4#5-6	53.4	38.5	1.39	33.5	1.59
240	8-5-F4.1-4#5-6	52.4	39.3	1.33	34.2	1.53
241	8-5-F4.1-4#5-6	53.5	44.0	1.21	38.2	1.40
242	8-5-F4.1-6#5-6	47.3	40.7	1.16	35.4	1.34
243	8-5-F4.1-6#5-6	55.9	43.2	1.29	37.5	1.49
244	8-5-F4.1-6#5-6	52.6	44.9	1.17	38.9	1.35

[a] T_c based on Eq. (7.5)
[b] T_{calc} based on Eq. (9.15)
[c] Headed bars with large obstructions exceeding the dimensional limits for HA heads in ASTM A970
[d] Bars with large heads ($A_{brg} > 12A_b$)

Table F.11 Test-to-calculated ratios for lap splice specimens in current study

	Specimen	T kips	Descriptive Equation[a]		Design Equation[b]	
			T_c kips	T/T_c	T_{calc} kips	T/T_{calc}
245	(3)6-5-S4.0-12-0.5	34.0	28.9	1.18	24.2	1.41
246	(3)6-5-S4.0-12-1.0	36.8	32.3	1.14	24.9	1.48
247	(3)6-5-S4.0-12-1.9	33.6	38.3	0.88	27.8	1.21
248	(3)6-12-S4.0-12-0.5	36.1	32.9	1.10	27.7	1.30
249	(3)6-12-S4.0-12-1.0	33.0	36.7	0.90	28.5	1.16
250	(3)6-12-S4.0-12-1.9	36.4	43.7	0.83	31.9	1.14

[a] T_c based on Eq. (7.6) with 0.8 reduction factor
[b] T_{calc} based on Eq. (9.15)

Table F.12 Test-to-calculated ratios for beam-column joint specimens by Bashandy (1996)

Specimen	d_b in.	ℓ_{eh}[*] in.	h_{cl}/ℓ_{eh}	d_{eff}/ℓ_{eh}	f_{cm}[*] psi	s/d_b	T[*] kips	Descriptive Equation[a]		Design Equation[b]	
								T_c kips	T/T_c	T_{calc} kips	T/T_{calc}
T1	1.41	11.0	1.00	1.27	3870	3.3	51.0	46.7	1.09	37.7	1.35
T2	1.41	11.0	1.00	1.25	4260	3.3	49.9	47.8	1.04	38.6	1.29
T3	1.41	11.2	0.98	1.24	4260	3.3	52.2	48.7	1.07	39.3	1.33
T4	1.0	8.3	1.32	1.47	3870	5.0	21.1	38.3	0.55	28.8	0.73
T5	1.41	11.0	1.00	1.23	3260	3.3	37.5	44.8	0.84	36.1	1.04

[*] Values are converted from SI (1 in. = 25.4 mm; 1 psi = 1/145 MPa; and 1 kip = 4.44822 kN)
[a] T_c based on Eq. (7.6)
[b] T_{calc} based on Eq. (9.15)

Table F.13 Test-to-calculated ratios for beam-column joint specimens by Chun et al. (2009)

Specimen	d_b in.	ℓ_{eh} in.	h_{cl}/ℓ_{eh}	d_{eff}/ℓ_{eh}	f_{cm} psi	T kips	Descriptive Equation[a] T_c kips	T/T_c	Design Equation[b] T_{calc} kips	T/T_{calc}
No. 8-M-0.9L-(1)	1.0	10.4	1.05	1.21	3640	27.9	52.8	0.53	39.9	0.70
No. 8-M-0.9L-(2)	1.0	10.4	1.05	1.22	3640	28.6	52.8	0.54	39.9	0.72
No. 8-M-0.7L-(1)	1.0	8.3	1.31	1.52	3640	27.4	41.8	0.66	31.8	0.86
No. 8-M-0.7L-(2)	1.0	8.3	1.31	1.53	3640	28.5	41.8	0.68	31.8	0.90
No. 8-M-0.7L-2R-(1)	1.0	8.3	1.31	1.53	3640	31.8	41.8	0.76	31.8	1.00
No. 8-M-0.7L-2R-(2)	1.0	8.3	1.31	1.53	3640	32.6	41.8	0.78	31.8	1.02
No. 8-M-0.5L-(1)	1.0	6.3	1.73	1.89	3640	16.4	31.5	0.52	24.2	0.68
No. 8-M-0.5L-(2)	1.0	6.3	1.73	1.94	3640	21.1	31.5	0.67	24.2	0.87
No. 11-M-0.9L-(1)	1.41	14.6	0.99	1.15	3570	51.4	84.0	0.61	65.7	0.78
No. 11-M-0.9L-(2)	1.41	14.6	0.99	1.15	3570	52.4	84.0	0.62	65.7	0.80
No. 11-M-0.7L-(1)	1.41	11.6	1.25	1.42	3570	43.3	66.3	0.65	52.2	0.83
No. 11-M-0.7L-(2)	1.41	11.6	1.25	1.41	3570	41.6	66.3	0.63	52.2	0.80
No. 11-M-0.7L-2R-(1)	1.41	11.6	1.25	1.47	3570	59.1	66.3	0.89	52.2	1.13
No. 11-M-0.7L-2R-(2)	1.41	11.6	1.25	1.45	3570	51.1	66.3	0.77	52.2	0.98
No. 11-M-0.5L-(1)	1.41	8.5	1.71	1.94	3570	43.7	48.1	0.91	38.3	1.14
No. 11-M-0.5L-(2)	1.41	8.5	1.71	1.89	3570	34.3	48.1	0.71	38.3	0.90
No. 18-M-0.9L-(1)	2.26	35.0	0.96	1.08	3510	157.7	242.7	0.65	198.6	0.79
No. 18-M-0.9L-(2)	2.26	35.0	0.96	1.08	3510	155.8	242.7	0.64	198.6	0.78
No. 18-M-0.7L-(1)	2.26	26.9	1.25	1.35	3510	97.6	185.0	0.53	152.7	0.64
No. 18-M-0.7L-(2)	2.26	26.9	1.25	1.35	3510	99.8	185.0	0.54	152.7	0.65
No. 18-M-0.7L-2R-(1)	2.26	26.9	1.25	1.37	3510	110.6	185.0	0.60	152.7	0.72
No. 18-M-0.7L-2R-(2)	2.26	26.9	1.25	1.37	3510	115.8	185.0	0.63	152.7	0.76
No. 18-M-0.5L-(1)	2.26	18.9	1.78	1.88	3510	69.6	128.6	0.54	107.3	0.65
No. 18-M-0.5L-(2)	2.26	18.9	1.78	1.88	3510	69.5	128.6	0.54	107.3	0.65

[a] T_c based on Eq. (7.6), with s = column width ($6d_b$)
[b] T_{calc} based on Eq. (9.15), with s = column width ($6d_b$) for calculating ψ_{cs}

Table F.14 Test-to-calculated ratios for CCT node specimens by Thompson et al. (2006a)

Specimen	d_b	ℓ_{eh}	f_{cm}	T	Descriptive Equation[a]		Design Equation[b]	
					T_c	T/T_c	T_{calc}	T/T_{calc}
	in.	in.	psi	kips	kips		kips	
CCT-08-55-04.70(H)-1[c e]	1.0	7.0	4000	54.0[c]	35.9	1.51	27.5	1.97
CCT-08-55-04.70(V)-1 [e]	1.0	7.0	3900	54.0	35.7	1.51	27.3	1.98
CCT-08-55-10.39-1[c]	1.0	7.0	4000	54.0[c]	35.9	1.51	27.5	1.97
CCT-08-45-04.04-1[c]	1.0	7.0	4000	48.2[c]	35.9	1.34	27.5	1.75
CCT-08-45-04.70(V)-1 [e]	1.0	7.0	3900	54.0	35.7	1.51	27.3	1.98
CCT-08-30-04.04-1[c]	1.0	7.0	4100	48.2[c]	36.1	1.33	27.7	1.74
CCT-08-30-04.06-1[c]	1.0	7.0	4100	54.0[c]	36.1	1.50	27.7	1.95
CCT-08-30-10.39-1[c]	1.0	7.0	4100	54.0[c]	36.1	1.50	27.7	1.95
CCT-08-45-04.70(H)-1-S3 [e]	1.0	7.0	3800	52.1	35.5	1.47	27.1	1.92
CCT-08-45-04.70(V)-1-C0.006[d e]	1.0	7.0	3800	50.6	35.5	1.43	27.1	1.87
CCT-08-45-04.70(V)-1-C0.012[d e]	1.0	7.0	3800	51.8	35.5	1.46	27.1	1.91
CCT-11-45-04.13(V)-1 [e]	1.41	9.87	4000	88.9	57.7	1.54	45.7	1.95
CCT-11-45-06.69(H)-1[c e]	1.41	9.87	4000	98.0[c]	57.7	1.70	45.7	2.14
CCT-11-45-06.69(V)-1[c e]	1.41	9.87	4000	98.0[c]	57.7	1.70	45.7	2.14
CCT-11-45-09.26-1[c]	1.41	9.87	4000	98.0[c]	57.7	1.70	45.7	2.14

[a] T_c based on Eq. (7.6), with s = column width ($6d_b$)
[b] T_{calc} based on Eq. (9.15), with s = column width ($6d_b$) for calculating ψ_{cs}
[c] Specimen exhibited bar yielding
[d] Specimen had transverse stirrups perpendicular to the headed bars within the nodal zone
[e] "H" represents a rectangular head with the long side orientated horizontally; "V" represents a rectangular head with the long side orientated vertically

Table F.15 Test-to-calculated ratios for shallow embedment pullout specimens by DeVries et al. (1999)

Specimen	$d_b{}^*$ in.	$\ell_{eh}{}^*$ in.	$f_{cm}{}^*$ psi	$s/d_b{}^c$	T^* kips	Descriptive Equation[a] T_c kips	T/T_c	Design Equation[b] T_{calc} kips	T/T_{calc}
T1B1[d]	0.79	1.4	12040	45.7	17.3	9.8	1.76	8.6	2.01
T1B2[d]	0.79	1.4	12040	45.7	13.9	9.8	1.42	8.6	1.62
T1B3[d e]	0.79	4.4	12040	45.7	46.1[d]	31.9	1.45	27.1	1.70
T1B4[d e]	0.79	4.4	12040	45.7	46.8[d]	31.9	1.47	27.1	1.73
T1B5[d]	1.38	3.1	12040	26.1	48.3	27.2	1.78	25.3	1.91
T1B6[d]	1.38	3.1	12040	26.1	50.6	27.2	1.86	25.3	2.00
T1B7[d]	1.38	8.2	12040	26.1	110.2	73.0	1.51	66.2	1.66
T3B11[d e]	0.79	9.0	3920	45.7	47.7[d]	50.4	0.95	41.4	1.15
T2B1[d]	0.79	9.0	4790	5.1	41.4	32.6	1.27	23.5	1.76
T2B2	0.79	9.0	4790	5.1	33.3	32.6	1.02	23.5	1.42
T2B3[d f]	0.79	9.0	4790	5.1	36.0	32.6	1.10	23.5	1.53
T2B4[f]	0.79	9.0	4790	5.1	38.7	32.6	1.19	23.5	1.65
T3B4[d]	0.79	9.0	3920	5.1	33.5	31.1	1.08	22.3	1.50
T2B5[d]	0.79	9.0	4790	5.1	19.8	32.6	0.61	23.5	0.84
T2B6	0.79	9.0	4790	5.1	27.4	32.6	0.84	23.5	1.17
T2B7[d f]	0.79	9.0	4790	5.1	20.0	32.6	0.61	23.5	0.85
T2B8[f]	0.79	9.0	4790	5.1	28.1	32.6	0.86	23.5	1.20
T3B8[d]	0.79	9.0	3920	5.1	12.8	31.1	0.41	22.3	0.57

[*] Values are converted from SI (1 in. = 25.4 mm; 1 psi = 1/145 MPa; and 1 kip = 4.44822 kN)

[a] T_c based on Eq. (7.6) with 0.8 reduction factor applied as appropriate

[b] T_{calc} based on Eq. (9.15)

[c] s = twice of the minimum concrete cover to the center of the bar

[d] Headed bar debonded by PVC sheathing

[e] Specimen failed with bar fracture

[f] Specimen had transverse reinforcement placed perpendicular to the headed bar

Table F.16 Test-to-calculated ratios for lap splice specimens by Thompson et al. (2006b)

Specimen	d_b in.	ℓ_{st} in.	f_{cm} psi	s/d_b	c_{so}/d_b	T kips	Descriptive Equation[a]		Design Equation[b]	
							T_c kips	T/T_c	T_{calc} kips	T/T_{calc}
LS-08-04.70-03-06(N)-1	1.0	3	3200	3	1	14.7	8.0	1.84	6.5	2.27
LS-08-04.70-05-06(N)-1	1.0	5	3700	3	2	21.3	14.0	1.52	11.2	1.90
LS-08-04.70-05-10(N)-1	1.0	5	3200	5	2	19.0	17.3	1.10	13.2	1.44
LS-08-04.70-05-10(C)-1	1.0	5	3700	2	2	19.4	12.0	1.61	10.3	1.88
LS-08-04.70-08-10(N)-1	1.0	8	4000	5	2	34.4	29.7	1.16	22.3	1.54
LS-08-04.70-12-10(N)-1	1.0	12	4200	5	2	52.4	45.6	1.15	33.9	1.54
LS-08-04.04-08-10(N)-1	1.0	8	4000	5	2	35.1	29.7	1.18	22.3	1.57
LS-08-04.04-12-10(N)-1	1.0	12	3800	5	2	40.3	44.5	0.90	33.1	1.22
LS-08-04.04-14-10(N)-1	1.0	14	3500	5	2	51.4	51.2	1.00	37.8	1.36
LS-08-04.04-14-10(N)-1-DB[c]	1.0	14	3500	5	2	43.0	51.2	0.84	37.8	1.14
LS-08-04.70-08-10(N)-1-H0.25[d]	1.0	8	4200	5	2	43.3	30.0	1.44	22.6	1.91
LS-08-04.04-08-10(N)-1-H0.56[d]	1.0	8	3500	5	2	42.7	28.8	1.49	21.6	1.98
LS-08-04.04-08-10(N)-1-H1.01[d]	1.0	8	3500	5	2	44.8	28.8	1.56	21.6	2.07
LS-08-04.04-12-10(N)-1-H0.56[d]	1.0	12	3800	5	2	42.5	44.5	0.95	33.1	1.28
LS-08-04.04-12-10(N)-1-TTD[d]	1.0	12	3800	5	2	44.7	44.5	1.00	33.1	1.35

[a] T_c based on Eq. (7.6) with 0.8 reduction factor applied

[b] T_{calc} based on Eq. (9.15)

[c] Debonding sheathing was placed over straight portion of headed bars in the lap zone

[d] Specimen had confining reinforcement perpendicular to the headed bar

Table F.17 Test-to-calculated ratios for lap splice specimens by Chun (2015)

Specimen	$d_b{}^*$ in.	$\ell_{st}{}^*$ in.	$f_{cm}{}^*$ psi	s/d_b	c_{so}/d_b	$T^{\,e}$ kips	Descriptive Equation[a] T_c kips	T/T_c	Design Equation[b] T_{calc} kips	T/T_{calc}
D29-S2-F42-L15	1.14	17.1	6000	2	1	45.0	50.4	0.89	41.0	1.10
D29-S2-F42-L20	1.14	22.8	6000	2	1	52.9	67.8	0.78	54.7	0.97
D29-S2-F42-L25	1.14	28.5	6000	2	1	62.6	85.3	0.73	68.4	0.92
D29-S2-F42-L30	1.14	34.3	5820	2	1	66.2	102.1	0.65	81.4	0.81
D29-S4-F42-L15	1.14	17.1	6000	3	2	48.4	58.6	0.83	44.7	1.08
D29-S4-F42-L20	1.14	22.8	6000	3	2	54.8	78.8	0.69	59.7	0.92
D29-S2-C3.5-F42-L15	1.14	17.1	5820	2	3.5	52.9	50.0	1.06	40.7	1.30
D29-S2-C3.5-F42-L20	1.14	22.8	5820	2	3.5	63.8	67.2	0.95	54.2	1.18
D29-S2-C3.5-F42-L25	1.14	28.5	5820	2	3.5	72.4	84.6	0.86	67.8	1.07
D25-S2-F42-L20	0.98	19.7	6000	2	1	37.1	55.2	0.67	46.5	0.80
D25-S2-F42-L25	0.98	24.6	6000	2	1	46.5	69.5	0.67	58.1	0.80
D29-S2-F21-L20	1.14	22.8	2940	2	1	34.0	57.1	0.59	45.8	0.74
D29-S2-F21-L25	1.14	28.5	2940	2	1	40.7	71.9	0.57	57.2	0.71
D29-S2-F70-L15	1.14	17.1	9120	2	1	49.8	55.7	0.89	45.5	1.09
D29-S2-F70-L20	1.14	22.8	9120	2	1	62.3	74.9	0.83	60.7	1.03
D29-S2-F70-L25	1.14	28.5	9120	2	1	67.0	94.3	0.71	75.9	0.88
D29-S2-F42-L15-Con.[c]	1.14	17.1	6000	2	1	69.9	50.4	1.39	41.0	1.70
D29-S2-F42-L20-Con.[c]	1.14	22.8	6000	2	1	84.4	67.8	1.25	54.7	1.54
D29-S2-F42-L20-LCon.[c]	1.14	22.8	6000	2	1	70.6	67.8	1.04	54.7	1.29
D29-S2-F42-L25-Lcon.[c]	1.14	28.5	5820	2	1	82.2	84.6	0.97	67.8	1.21
D29-S2-F42-L15-Con.2[c]	1.14	17.1	5820	2	1	75.4	50.0	1.51	40.7	1.85
D29-S2-F42-L20-Con.2[c]	1.14	22.8	5820	2	1	98.3	67.2	1.46	54.2	1.81
D29-S2-F70-L15-Con.[c]	1.14	17.1	9120	2	1	81.2	55.7	1.46	45.5	1.78
D29-S2-F70-L20-Con.[c d]	1.14	22.8	9120	2	1	105.4	74.9	1.41	60.7	1.74

[*] Values are converted from SI (1 in. = 25.4 mm; 1 psi = 1/145 MPa; and 1 kip = 4.44822 kN)

[a] T_c based on Eq. (7.6) with 0.8 reduction factor applied

[b] T_{calc} based on Eq. (9.15)

[c] Specimen were confined by transverse stirrups perpendicular to the spliced bars

[d] Specimen failed with yielding of spliced bars

[e] T based on moment-curvature method calculated by Chun (2015)

APPENDIX G: SPECIMEN IDENTIFICATION FOR DATA POINTS PRESENTED IN FIGURES

Table G.1 Specimen identification for data points presented in figures[*]

Figure	Specimen Number
Figure 4.21	203-212
Figure 5.3	213-244
Figure 5.4	213-244
Figure 5.6	213-244
Figure 6.2	245-250
Figure 6.3	245-250
Figure 6.7	245-250
Figure 7.1	1-30, 139-140, 141, 144, 147, 149, 152-154, 157, 165, 171, 174, 185, 191, 193
Figure 7.2	77, 79-82, 88-89, 92, 95, 97, 99, 101, 142, 145, 148, 150, 172, 186
Figure 7.3	69-70, 73-74, 78, 83-87, 90-91, 93-94, 96, 98, 100, 102-107, 143, 146, 151, 155-156, 158, 166, 173, 175, 187, 192, 194
Figure 7.4	5-6, 11-12, 15-17, 20, 23-24, 27-52, 56-64, 157, 159,161, 163, 165, 167, 169, 185, 188, 193, 195
Figure 7.5	77, 92, 99, 108-113, 119-124, 132, 134, 186, 189
Figure 7.6	78, 87, 93-94, 100, 104-107, 114-118, 125-131, 133, 135-138, 158, 160, 162, 164, 166, 168, 170, 187, 190, 194, 196
Figure 7.7	1-20, 139-141, 153-154, 157, 165
Figure 7.8	69-70, 73-74, 78, 83-87, 90-91, 93-94, 143, 155-156, 158, 166
Figure 7.9	1-30
Figure 7.10	31-64
Figure 7.11	1-64
Figure 7.12	1-64
Figure 7.14	65-107
Figure 7.15	108-138
Figure 7.16	65-138
Figure 7.17	65-138
Figure 7.18	1-138
Figure 7.19	65-138
Figure 7.20	65-138
Figure 7.21	1-64
Figure 7.22	1-64, 157, 159, 161, 163, 165, 167, 169, 171, 174, 176-177, 179-180, 185, 188, 191, 193, 195
Figure 7.23	65-138, 158, 160, 162, 164, 166, 168, 170, 172-173, 175, 178, 181-184, 186-187, 189-190, 192, 194, 196
Figure 7.24	158, 160, 162, 164, 166, 168, 170, 172-173, 175, 178, 181-184, 186-187, 189-190, 192, 194, 196

[*] Specimens identification only for specimens in current study. Refer to Tables F.1 to F.11

Table G.1 Cont. Specimen identification for data points presented in figures[*]

Figure 7.25	1-64, 157, 159, 161, 163, 165, 167, 169, 171, 174, 176-177, 179-180, 185, 188, 191, 193, 195
Figure 7.26	65-138, 158, 160, 162, 164, 166, 168, 170, 172-173, 175, 178, 181-184, 186-187, 189-190, 192, 194, 196
Figure 7.31	207-238
Figure 9.1	1-30
Figure 9.2	65-107
Figure 9.3	31-64
Figure 9.4	108-138
Figure 9.5	65-138
Figure 9.6	65-138
Figure 9.7	1-64
Figure 9.8	65-138
Figure 9.9	1-138
Figure 9.10	1-138
Figure 9.11	1-138, 141-156
Figure 9.12	1-138, 157-196

[*] Specimens identification only for specimens in current study. Refer to Tables F.1 to F.11